

# Design of Reinforced Concrete Halls

By

DIPL. ING. **M. HILAL** DR. SC. TECHN.  
PROFESSOR, FACULTY OF ENGINEERING  
CAIRO UNIVERSITY, GIZA

**2005**

## P R E F A C E

The contents of this edition are mainly the same as those of the previous one with the necessary corrections and the addition of one of the biggest structures designed by the author, namely the bulk urea store shown in Fig. VIII-9.

It has further been found more convenient to replace chapter XI on Foundations by a new chapter, published for the first time, on Folded Plate Structures. A simple systematic method of design, based on the fundamentals of mechanics and theory of plane structures has been shown. To illustrate the application of the method, the design and details of three different folded-plate structures worked out by the author are included in this chapter. The chapter on Foundations is in the author's textbook on "Fundamentals of Reinforced and Prestressed Concretes".

The author hopes that this book remains of benefit to structural engineers, graduate and undergraduate students of the engineering faculties and higher institutes in the design of reinforced concrete structures of common use.

March 1978

M. Hilal

## C O N T E N T S

	Page
I- Introduction	1
Different types of reinforced concrete roof structures dealt with in the book	
II- Simple Girders	13
Details (14); New trends (15); Conclusions (19)	
III- Continuous Girders	21
Internal forces in continuous beams of variable moment of inertia (22); Representation of influence lines as elastic lines (26); Influence lines for bending moments and shearing forces (28); Absolute bending moment and shearing force diagrams (28); Recommendations (29); Examples (34)	
IV- Frames	37
Three-hinged frames (41); Two-hinged frames (42); Two hinged frames with a tie;(57); Fixed frames (60); Internal forces in two-hinged and fixed simple frames (64) Continuous frames (72); Bending moments in continuous frames with two, three and four equal spans (90); Examples of framed structures (98).	
V- Vierendeel Girders	111
Simplified theory (111); Examples (119).	
VI- Trusses	121
Simplified theory(123); Examples (124).	
VII- Saw-tooth Roof structures	131
Slab type (132); Girder type (138); Saw-tooth roofs covering big span halls (143).	

VIII- Arched Slabs and Girders

Three-hinged arches (150); Two-hinged arches (159); Two-hinged arch with a tie (164); Two-hinged arch with polygonal tie (167); Fixed arches (168); Continuous arches (169); Tables of internal forces in two-hinged and fixed parabolic arches (173).

IX- Constructional Details

Insulation and isolation of roofs (177); Secondary beams (177); Short cantilevers (179); Expansion joints (179); End gables (179).

X- Hinged and Free Bearings

A- Hinged bearings: Steel bearings (181); Ménager hinges (182); Considère hinges (184); Lead hinges (189); concrete hinges (188).

B- Free bearings: Steel bearings (189); Rocker bearings (189); Rubber bearings (190).

XI- Folded-plate Structures

Definition and types (197); Assumptions and structural behavior (200); Slab and beam action (200); Ridge and plate loads (201); Free edge stresses and compatibility at the ridges (202);

Determination of edge shears and final stresses: Theorem of three edge shears (203); Stress distribution method (203); Shear stresses in folded plates (204); Illustrative examples (206); Design of diaphragms (225); Illustrative example (226); Multiple folded-plate structures (230); Illustrative example (231).

XII- Thin Shell Structures

Introduction (247); Loading (249);

Surfaces of revolution (250); Membrane theory (251);

Analytical method (251); Graphical method (255);

Application to popular surfaces of revolution (256);

Spherical shells (256); Conical shells (260); Edge forces and transition curves (261); Tables of membrane forces in popular shells of revolution (261); Examples (268); Circular beams (269).

Cylindrical shells (275); Introduction (275); Membrane theory (276); Beam theory (288); Analysis of beam action of symmetrical circular cylindrical shells (290); Examples (296); Analysis of arch action of symmetrical circular cylindrical shells (299); External and internal forces acting on end diaphragms (309); Constructional details (311); Examples (312).

Cross-supported cylindrical shell (314); Example (317).

Saw-tooth shells (320); Example (327).

Short shell (328); Examples (331).

Membrane theory of shells of general shape (334):  
 Basic idea (334); Conditions of equilibrium (337);  
 Pucher differential equation (340).

Illustrative examples (341): Paraboloid shell of revolution with an equilateral triangular plan (341); Example (343); Membrane shells with rectangular ground plan (347) Examples (351); Conoid shells (359); Examples (362);  
 The hyperbolic paraboloid (366); Examples (372).

## I. - I N T R O D U C T I O N

The object of a hall is to cover a limited area that has to be utilised for a certain purpose such as meetings, sports, storage, exhibitions, industry, ... etc.

Reinforced concrete halls and their supporting elements must satisfy the following conditions:

a) The disposition, layout, lighting, ventilation, drainage and in general the architectural composition must satisfy the requirements of the owner for an economic, efficient and good-looking structure.

b) The structure and its structural members should be so designed and constructed that they are able, with appropriate safety, to withstand all the loads, superimposed loads and other actions ( such as: differential settlements and temperature changes ) liable to occur during construction and in use.

The object of the design calculations is to guarantee sufficient safety against the structure being rendered 'unfit' for service.

A structure is considered to have become 'unfit' when one or more of its members ceases to perform the function for which it was designed, owing to failure , buckling due to elastic, plastic or dynamic instability, excessive cracking, excessive elastic or plastic deformations... etc.

c) The structural supporting elements must be so chosen that they give the most economic solution within the available possible means.

d) The initial and maintenance cost must be the minimum possible.

e) The structure should preferably show clearly the statical system adopted and it is generally recommended not to hide the supporting elements. The proportions and dimensions chosen according to a convenient statical system are generally the most convenient and best looking.

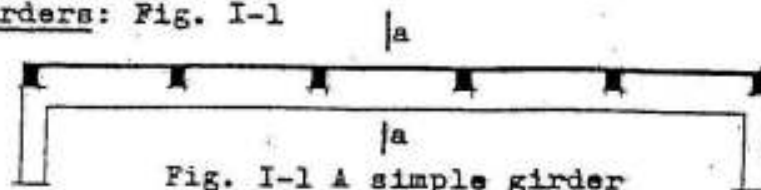
The structures dealt with in the following chapters are supposed to be of reinforced concrete. The general principles given here cannot be applied directly to prestressed concrete structures without the necessary adaptation.

The main supporting elements of big span halls can be classified, regarding their statical systems, as follows:

1) Girder Types

Under these systems, we understand girders or trusses giving vertical reactions for vertical loads such as:

a) Simple girders: Fig. I-1



In this system, the maximum bending moment takes place at one section only (section a-a) and is relatively high. The design of the girder is governed by the extreme fiber stress of the same section and hence, uneconomic!

b) Cantilever girders: Fig. I-2

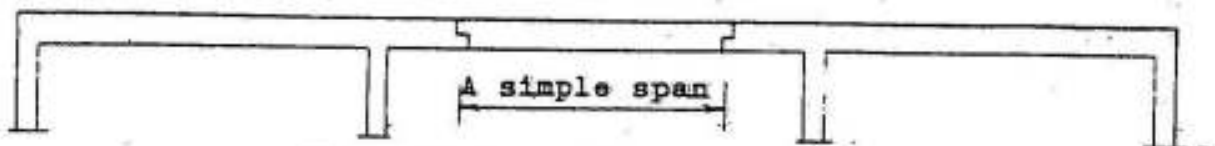


Fig. I-2 A cantilever girder

This statically determinate system is generally used in long girders or where differential settlements are expected.

c) Continuous girders: Fig. I-3

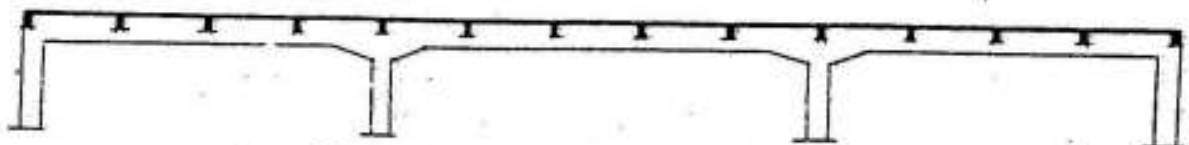


Fig. I-3 A continuous girder

Such statically indeterminate systems are generally used in girders shorter than about 45 m and where differential settlements do not give high internal forces.

In reinforced concrete structures, it is generally not possible to construct the knife edge hinges allowing the full rotation or the rollers allowing the displacement and rotation assumed in such ideal statical systems.

Girders supported on reinforced concrete columns possess generally some sort of fixation.

For girders monolithically cast with the columns, if no exact cal-

culuation as a building frame is done, it is allowed to consider them as freely supported on the interior columns and rigidly connected to the exterior columns. The fixing moment may approximately be estimated in the following manner: Fig. I-4

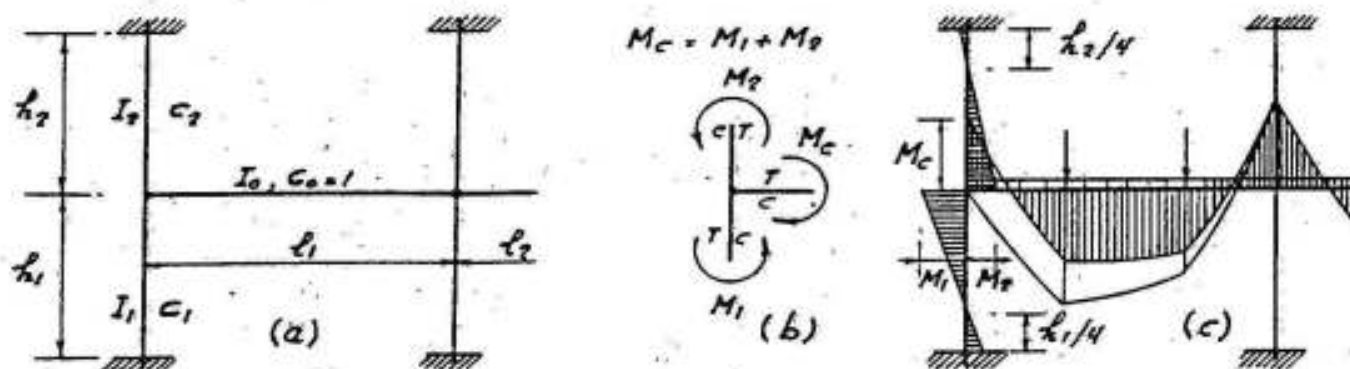


Fig. I-4 Moment distribution in a building frame

Assume  $I_0$ ,  $I_1$  and  $I_2$  to be the moments of inertia of the girder of span  $l$ , the lower column of height  $h_1$ , and the upper column of height  $h_2$ . Their relative rigidity can be given by the factors:

$$c_0 = \frac{I_0}{l} \cdot \frac{l}{I_0} = 1 \quad \text{reference value}$$

$$c_1 = \frac{I_1}{h_1} \cdot \frac{l}{I_0} \quad \text{relative rigidity of lower column}$$

$$c_2 = \frac{I_2}{h_2} \cdot \frac{l}{I_0} \quad \text{relative rigidity of upper column}$$

Then, the fixing moment  $M_c$  at the exterior columns is given by:

$$M_c = \bar{M} \cdot \frac{c_1 + c_2}{1 + c_1 + c_2}$$

in which  $\bar{M}$  is the fixed-end-moment of the loaded span  $l_1$ . This moment will be distributed on the columns in proportion to their relative rigidity  $c$ . Thus

$$M_1 = M_c \cdot \frac{c_1}{c_1 + c_2} \quad \text{and} \quad M_2 = M_c \cdot \frac{c_2}{c_1 + c_2}$$

For girders of top floor  $c_2 = 0$  and  $M_1 = M_c$

The sense of the bending moments can be adjusted by the system



of arrows shown in Fig. I-4 b.

The exterior columns are to be designed for the induced bending moments shown in Fig. I-4 c plus the maximum axial loads, whereas the interior columns may be calculated for the maximum axial loads only.

d) Vierendeel girders: Fig. I-5

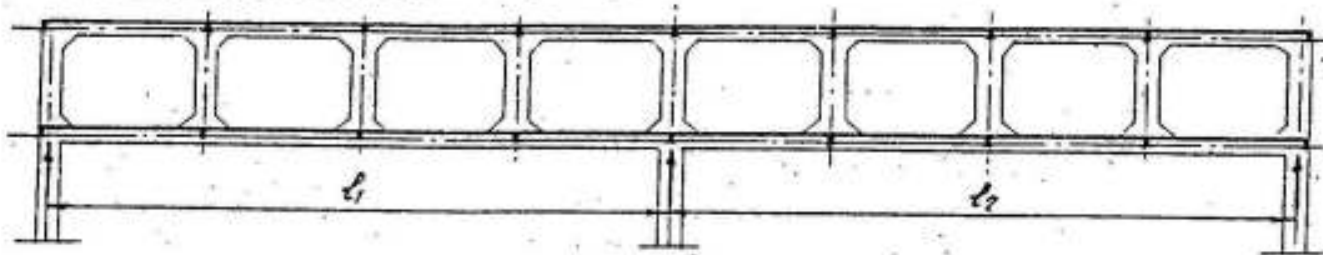


Fig. I-5 A Vierendeel girder

Vierendeel girders are composed of a top chord, a bottom chord and verticals. This system is internally high grade statically indeterminate while externally, it might be statically determinate as in freely supported simple and cantilever spans or indeterminate as in continuous spans.

e) Trusses: Fig. I-6

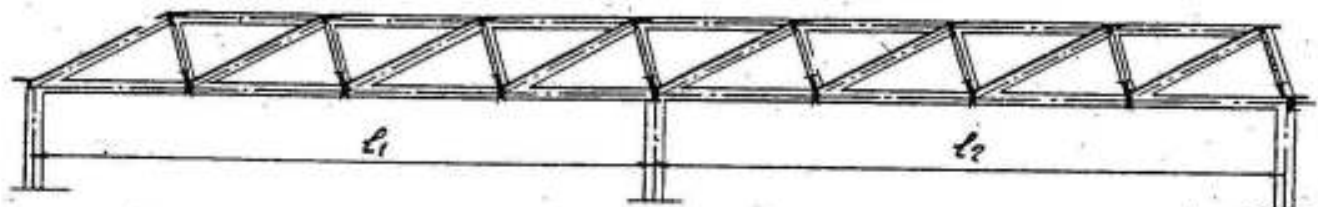


Fig. I-6 A Continuous truss

Trusses may, in some cases, give a convenient solution for the main supporting element of the hall. They may be simple, externally statically determinate, or continuous, externally statically indeterminate.

The joints being monolithically cast and rigidly connected, the induced bending moments may, in some cases, be of considerable values and in order to have trusses free from corner cracks, such moments must be considered in the design.

2) Sheds

These are polygonal or curved slabs (or girders) with ties giving vertical reactions for vertical loads. As typical examples, we give the following types:

a) Saw-tooth slab and girder types: Fig. I-7

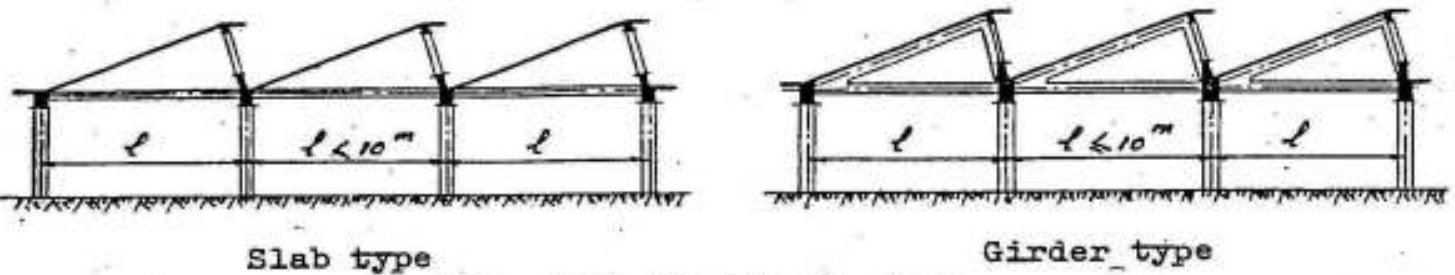


Fig. I-7 Saw-tooth sheds

b) Polygonal sheds with a tie: Fig. I-8

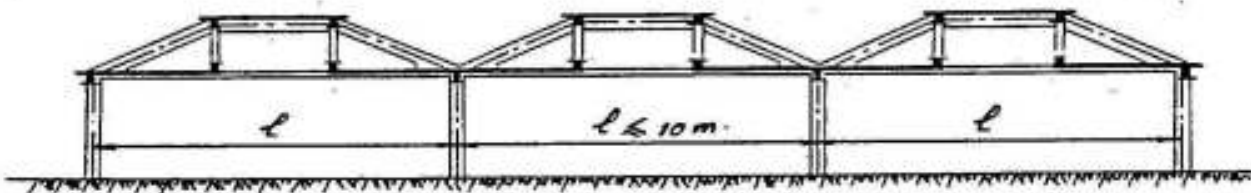


Fig. I-8 A Polygonal shed with a tie

In these two types, the elongation of the tie for spans  $l < 10$  m is generally small and can be neglected. Hence, we get vertical reactions for vertical loads.

c) Arched slabs (or girders) with a tie: Fig. I-9

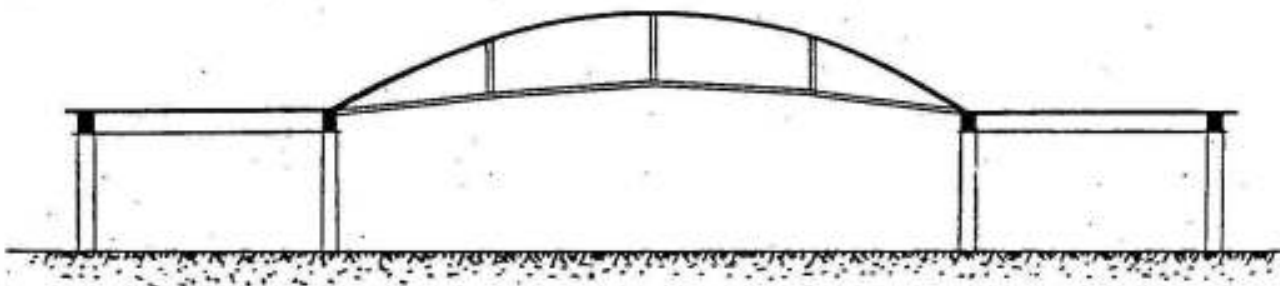


Fig. I-9 Arched-slab roof

### 3) Frames

The main feature of a frame is the continuity and rigid connection of the horizontal, inclined or curved members of the roof with the vertical or inclined supporting members. The continuity gives inclined reactions for vertical loads, and the bending moments due to the loads will be distributed on the different members of the frame.

Frames may be classified to the following systems:

a) Statically determinate frames: Fig. I-10

One may recognize here: cantilever frames (Fig. I-10a), simple frames (Fig. I-10b) and three hinged frames (Fig. I-10c).

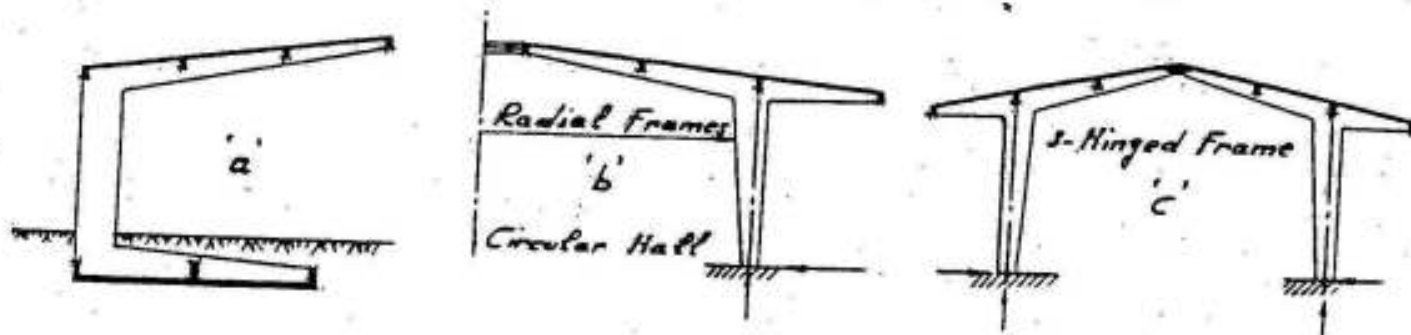


Fig. I-10 Statically determinate frames

b) Once statically indeterminate frames with or without ties:

(Fig. I-11)

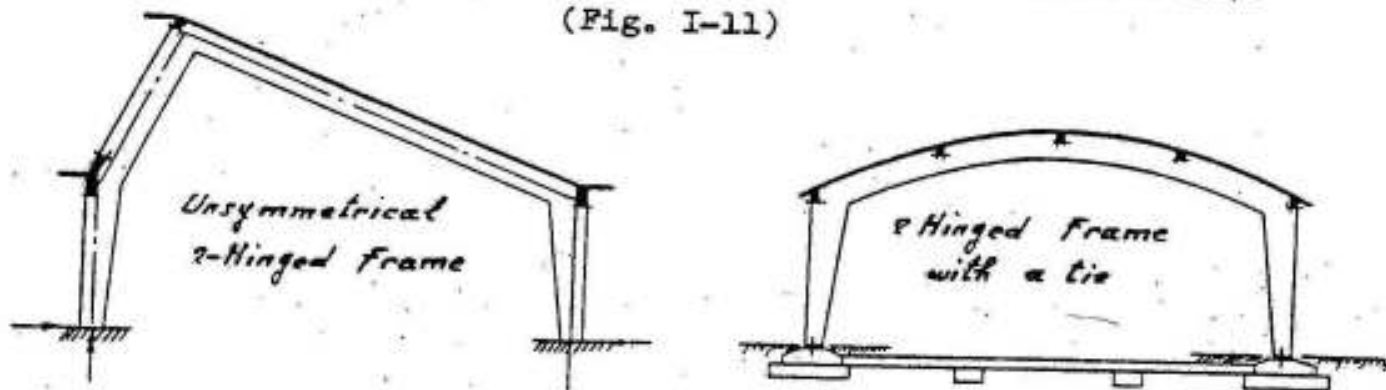


Fig. I-11 Once statically indeterminate frames with or without ties

c) Twice statically indeterminate two-hinged frames with ties:

(Fig. I-12)



Fig. I-12

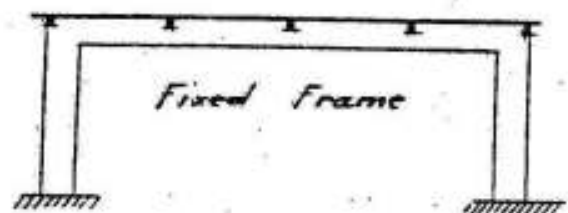


Fig. I-13

d) Three times statically indeterminate frames: Fig. I-13

e) Continuous and multiple frames: Fig. I-14 a and b.

Such frames are generally high grade statically indeterminate and need much time to determine the statically indeterminate values and the internal forces. The solution can however be much simplified for

symmetrical frames generally used in structures.

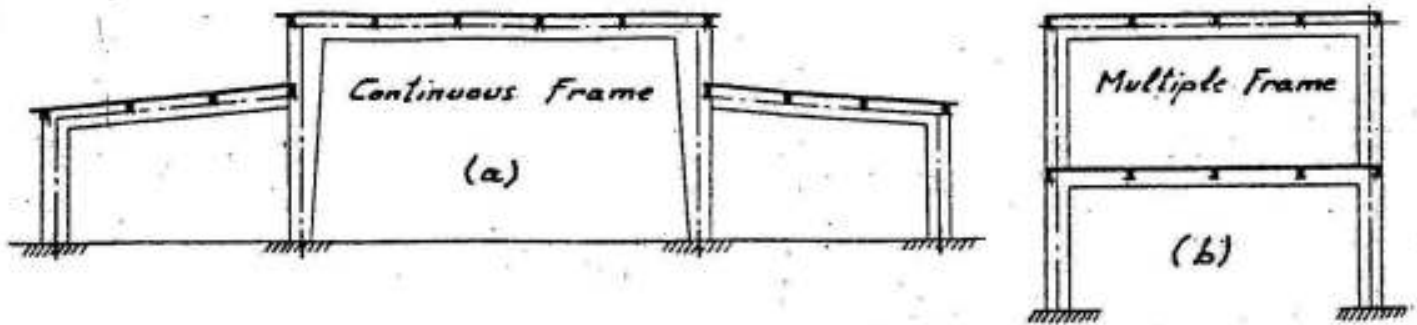


Fig. I-14 Continuous and multiple frames

#### 4) Arched Roofs

Structures covering long spans and large areas without intermediate supports using the minimum amount of building materials have always been one of the main aims of structural engineers. When a plane roof surface is not necessary to meet the functional requirements of the structure, an arched roof conveniently formed is normally found to give the least amount of building materials because here, the external loads are mainly resisted by internal compressive forces plus small bending moments and shearing forces. Arches may be constructed in different systems as shown in Fig. I-15 a to f.

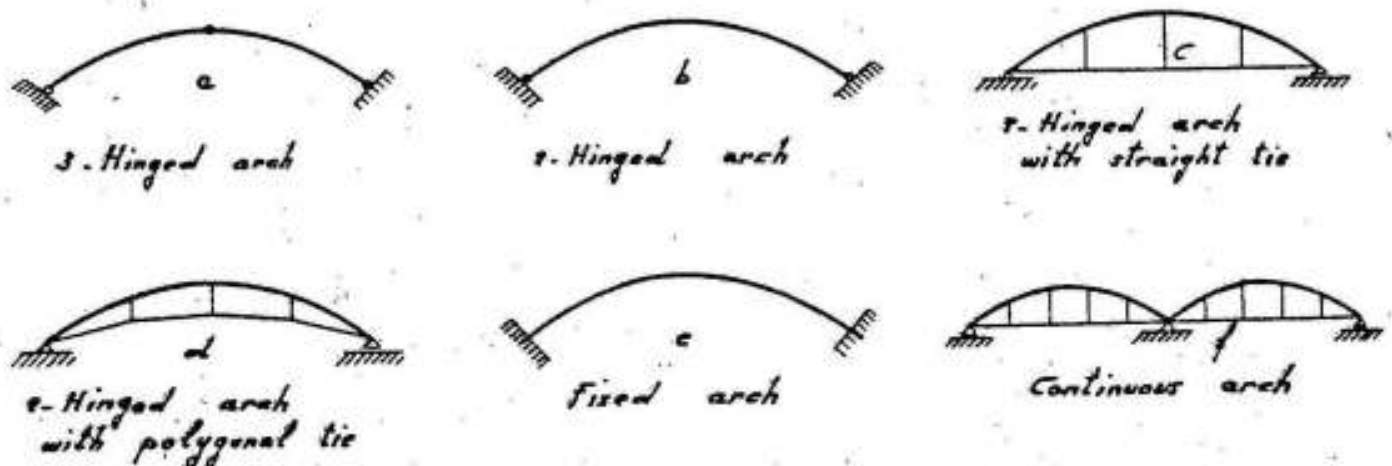


Fig. I-15 Different types of arched girders

#### 5) Shell Roofs

As a further development of the arch principle, shell surfaces provide structurally efficient solution to the problem of carrying roof loads over long spans. They owe their efficiency to the translation of the applied loads into compressive, tensile and shear stresses in the plane of their surface generally termed as the membrane stresses. We recognize: Surfaces of revolution, cylindrical shells, and double curved shells.

a) Surfaces of revolution: e.g. domes and cones. Fig. I-16

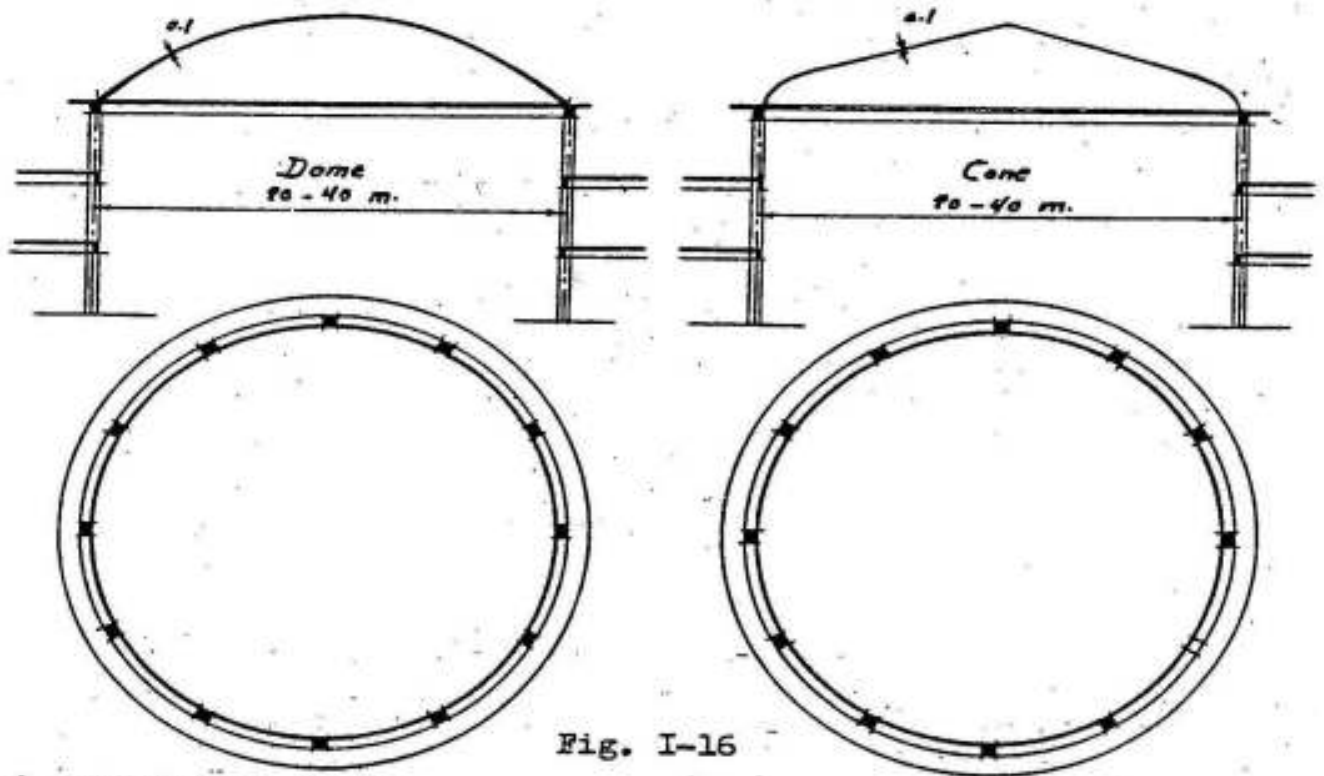


Fig. I-16

c) Cylindrical shells

The behavior of a shell is completely different from that of the arch. The arch is a plane structure resisting the external loads by plane forces; whereas the shell is a space structure supported on the diaphragms and resists the external loads by membrane stresses in its surface.

Shells may be long as for example, the barrel vault shown in Fig. I-17 and the saw-tooth shell roof shown in Fig. I-18. Such shells may

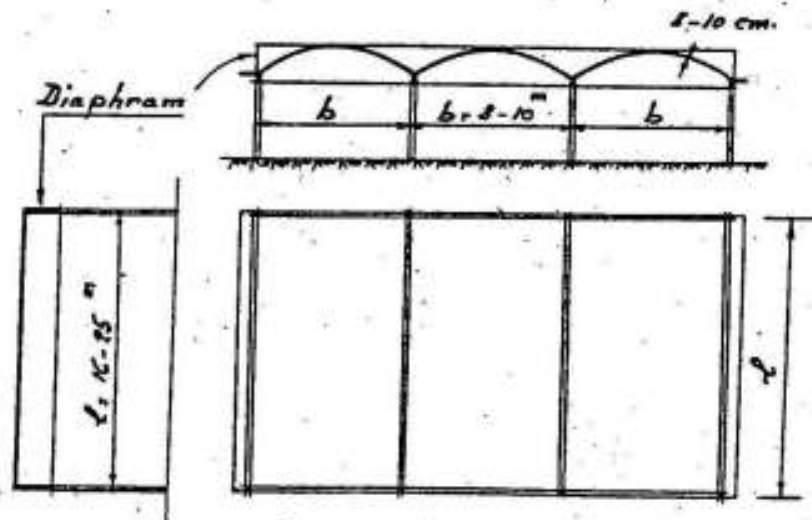


Fig. I-17 A long cylindrical barrel-vault shell roof

be considered as beams of span  $l$  and breadth  $b$ .

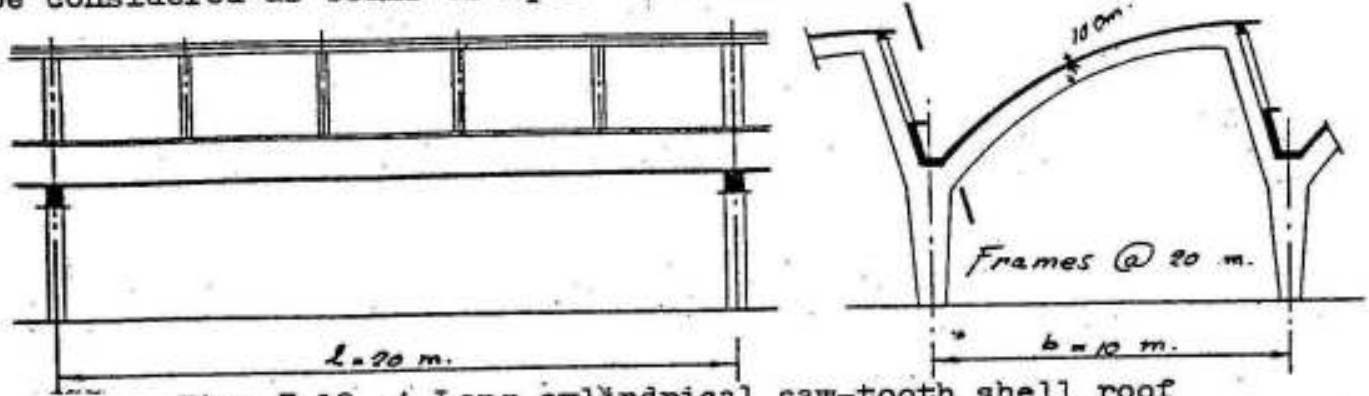


Fig. I-18 A Long cylindrical saw-tooth shell roof

They may also be short as for example the shell roof shown in Fig. I-19. Such a shell may be treated as a curved membrane supported on the diaphragms.

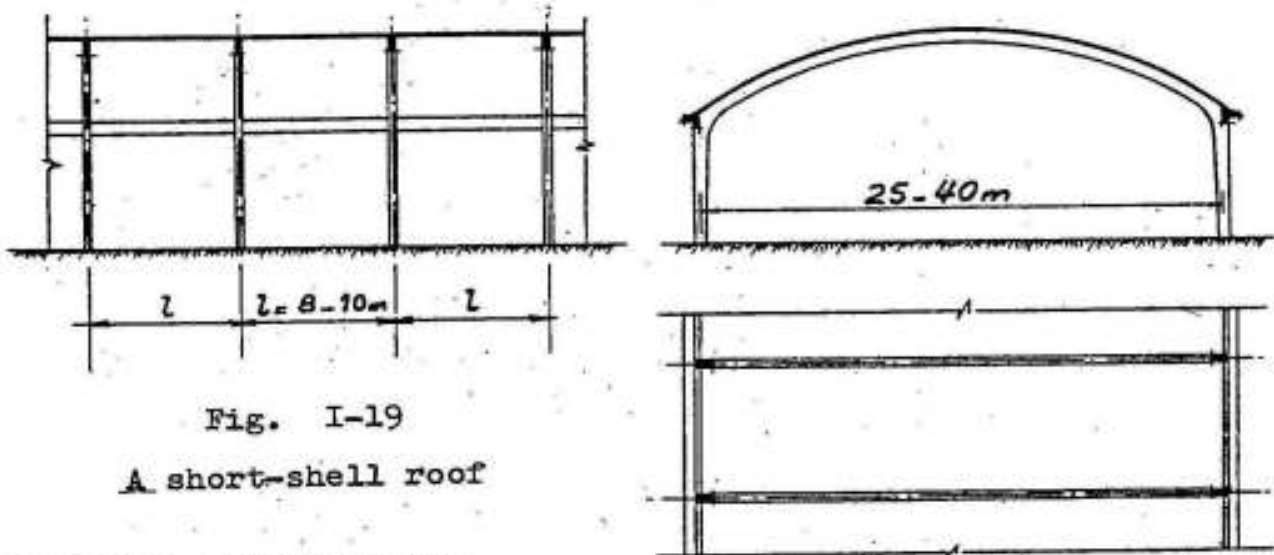


Fig. I-19  
A short-shell roof

c) Double curved shells

Double curved shells have been recently extensively used in modern structural architecture to cover relatively big areas with the least possible building materials. Some of the simple forms are shown in Fig. I-20 a to d.

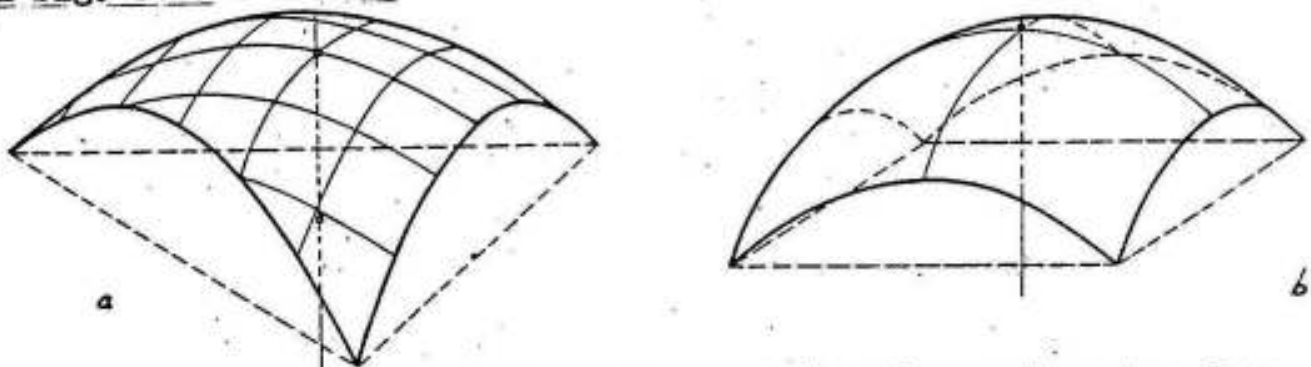


Fig. I-20 Double curved shells on triangular and rectangular ground plan

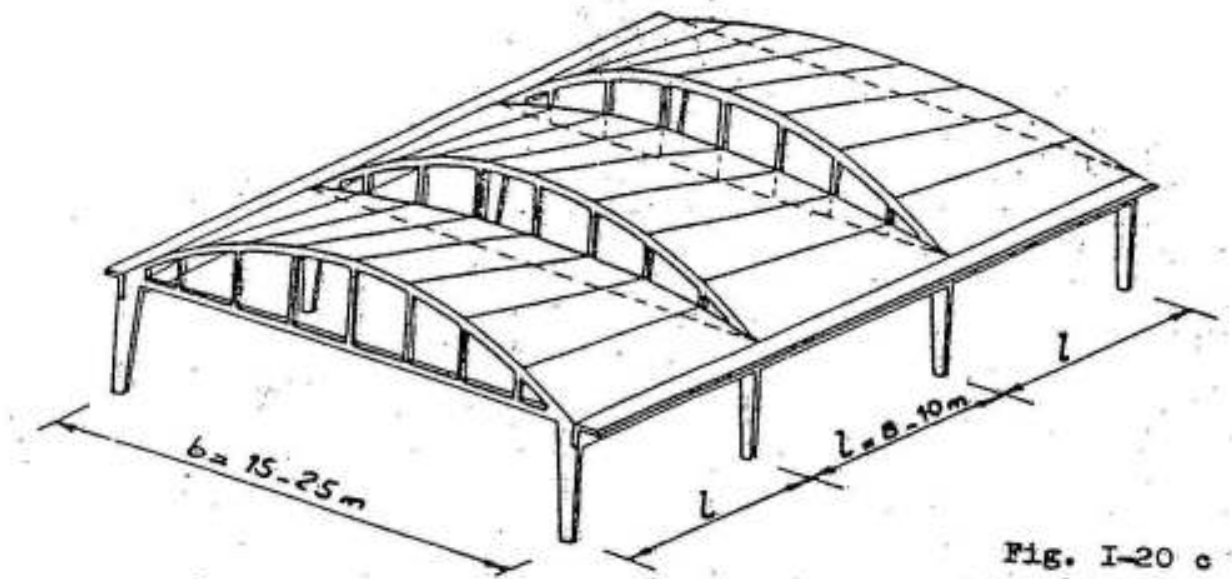


Fig. I-20 c  
A Conoid roof

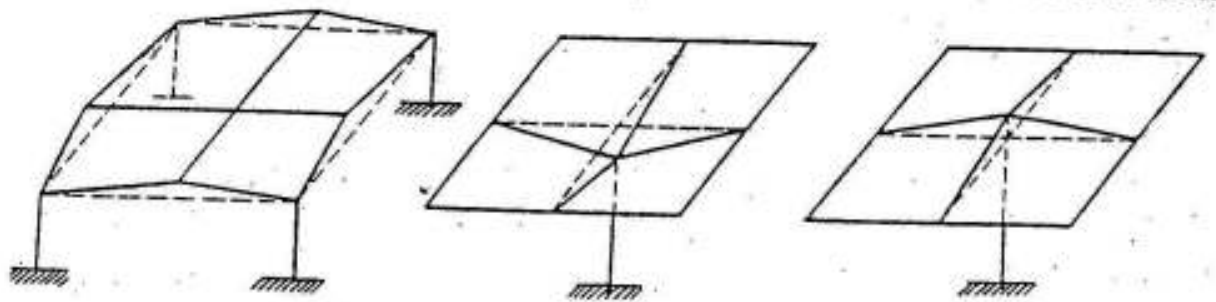


Fig. I-20 d Some simple forms of hyperbolic paraboloid roofs

6) Folded-plate roofs: Fig. I-21

In an attempt to simplify formwork and yet retain many of the ad-

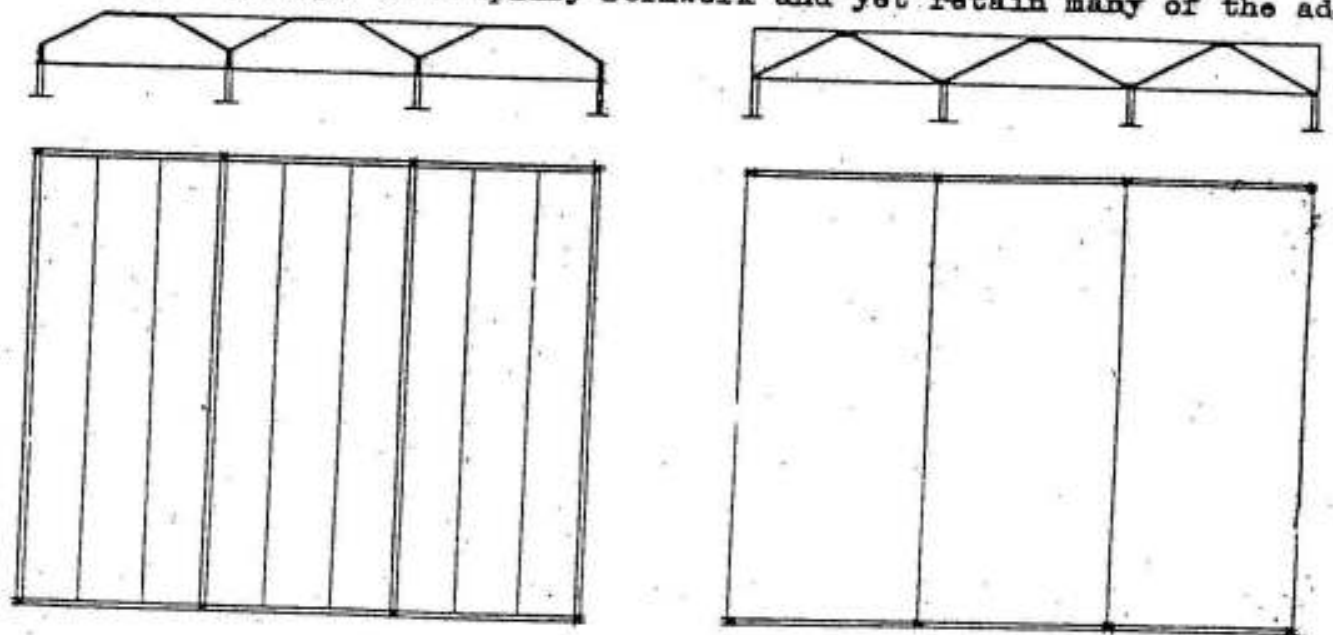


Fig. I-21 Folded-plate roofs

vantage characteristics of cylindrical shells, the folded-plate structure is evolved. These surfaces have a deep corrugated form similar to that of cylindrical shells, except that plane elements are used, intersecting in fold lines parallel to the span direction as shown in Fig. I-21.

The following 7 chapters, II to IIIIV, include the theory, design and construction of the classic basic systems of the main supporting elements of plane structures namely: simple girders, continuous girders, frames, Vierendeel girders, trusses, saw-tooth structures and arched roofs.

In chapter IX some constructional details, necessary for the design are treated.

In order to reduce the internal forces due to temperature changes, shrinkage displacement of the supports, hinged and eventually free bearings are extensively introduced at the supports of the main supporting elements. Chapter X has been devoted for the theory, design and constructional details of such bearings.

The analysis of folded-plate structures, followed by detailed design examples is presented in chapter XI.

It has been found, as stated before, that big spans with the least possible amount of building materials can be achieved by the use of shell structures. The exact analysis of such structures is generally very complicated, but due to the remarkable reserve strength of shell construction, which makes it practically impossible for a shell structure to collapse, it has been possible, without detailed mathematical analysis, to use simplified methods of calculation based on the qualitative understanding of the fundamental nature of the behavior of some forms of shells.

Some simple basic forms of shell structures, treated in a clear, simple manner are given in chapter XII.



## II - S I M P L E G I R D E R S

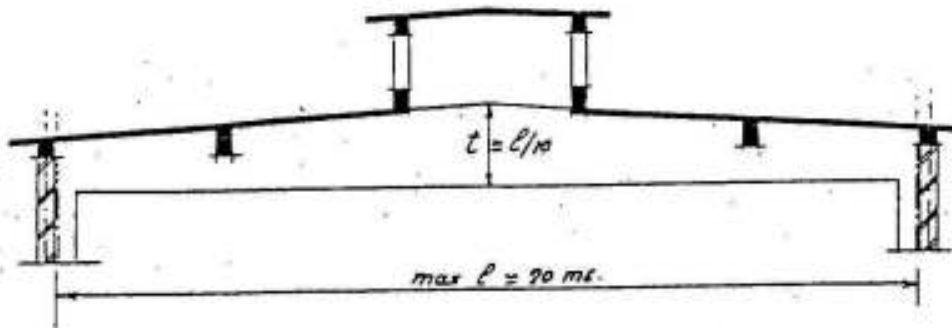


Fig. II-1 A simple girder

Simple girders as the main supporting element of a roof of a hall (fig II-1) may be used when differential settlements are liable to take place or in special cases e.g. when a new roof is to be constructed on existing bearing masonry walls or if the columns used to support the girders are relatively slender ... etc.

If the span of a simple girder is bigger than 10 meters, it is recommended to make one of the supports hinged and the other sliding to allow for the free movement of the girder. In this case a clear horizontal joint between the reinforced concrete roof and the walls is to be arranged allowing the necessary rotation and displacement of the roof to take place without creating cracks in the wall.

In case of girders supported on slender columns, it is recommended to join the columns supporting the girders and lying in masonry walls by horizontal beams arranged at convenient distances (3-5 ms). In this manner, the columns and the outside walls, as one plane, can follow the deformation of the roof without creating vertical cracks between the columns and the walls or horizontal cracks between the roof wall beams and the walls.

In masonry or brick walls, it is however a good practice to arrange reinforced concrete connecting members - vertical columns and horizontal beams - every 16 to 20 m<sup>2</sup>. Accordingly, if the

SIMPLY SUPPORTED GIRDER

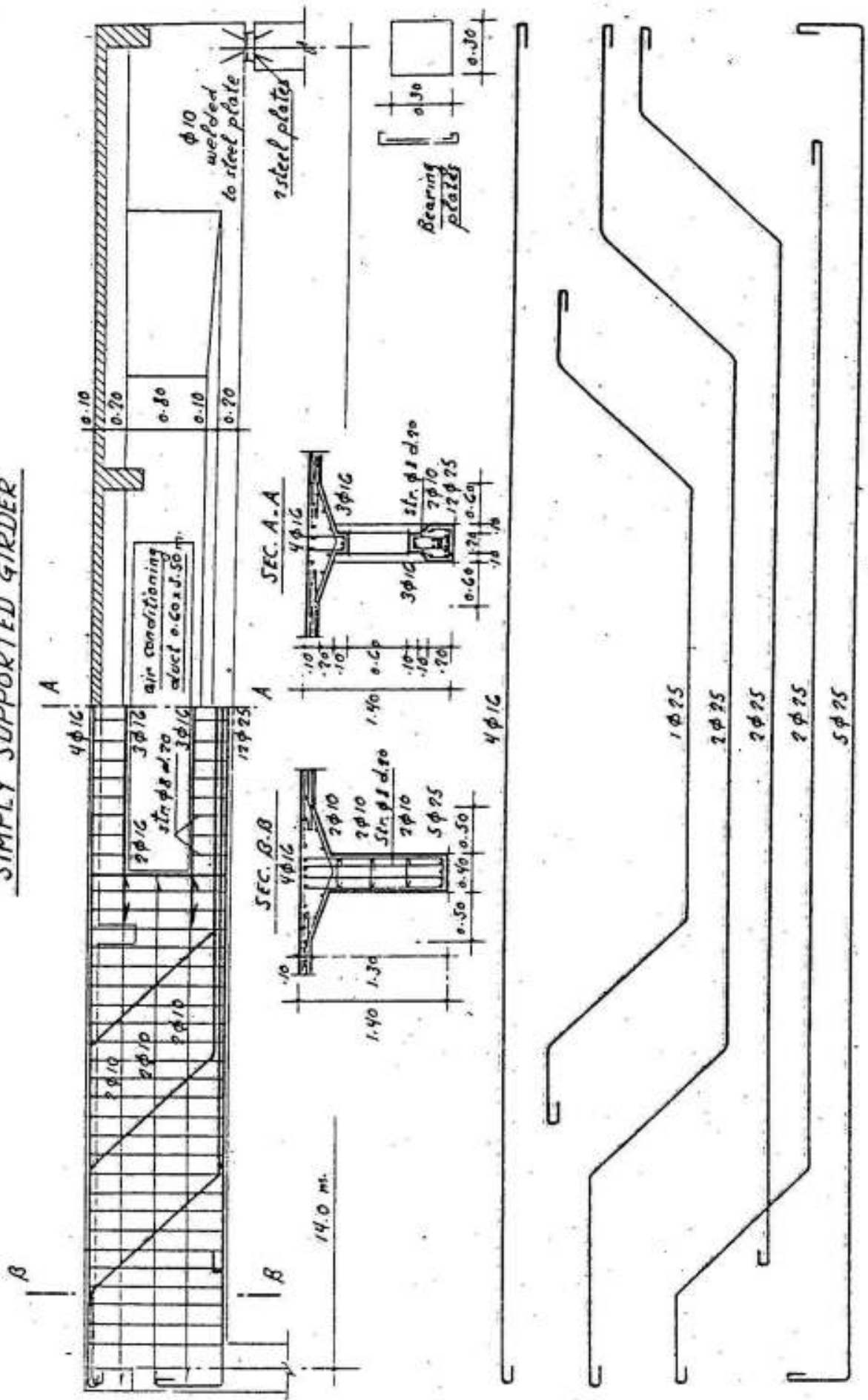


Fig. II-2 Details of reinforcements of a simple girder

vertical columns in the outside walls of a building are arranged every 6 ms, it is recommended to arrange horizontal connecting beams in the wall every 3-3.5 ms.

Figure II-2 shows the details of the roof - main girder of an air-conditioned hall 14 ms span.

In order to reduce the own weight of the 140 cms deep main girder, the breadth of 80 cms from the web is shosen 20 cms and an opening 60 x 350 cms for the air-conditioning duct is arranged at the middle of the span.

The opening has been chosen in the tension zone, which is statically not acting and, at the middle of the beam where the shear stresses are minnum. Its height is to be chosen such that there is sufficient concrete area at the top to resist the compressive stresses in the girder and ample cover for the tension reinforcements at the bottom.

The bottom enlarged part of the web is arranged in order to give adequate space for the tension reinforcements of the main girder.

In order to resist the shear stresses safely, the breadth of the web has been increased gradually from 20 to 40 cms on the two sides of the girder at zones of high shear stresses. For the same reason, it is not recommended to arrange the air-conditioning ducts near the supports at the inner surface of the outside walls.

The steel reinforcement shown in figure II-2 gives the classic known arrangement in which the diagonal tension of the beam is mainly resisted by the combined action of the bent bars and the stirrups.

In order to avoid the formation of vertical shrinkage cracks along the web, shrinkage reinforcements  $\phi$  10 mms arranged at distances of about 35 cms along the outside surface of the beam are provided. The relatively heavy bars arranged around the air-conditioning opening are recommended.

The haunches introduced between the roof slab and the web of the main girder increase the moment of resistance of the girder because in this manner, the effective breadth of the flange is increased.

We give in the following some new trends in the design of reinforced concrete girders :

1) The use of deformed high grade or cold twisted (e.g. Tor or Tentor) steel for the main reinforcement is preferred due to bigger bond

and higher resistance. If the bond between the steel reinforcement and the concrete is increased the tension cracks are increased in number and decreased in width. Due to higher resistance the area of the steel reinforcement is reduced and the girder under consideration is generally more economic. In the shown example, the main steel of  $12 \phi 25$  mm may be replaced by  $12 \phi 22$  high grade steel or  $11 \phi 22$  cold twisted steel.

2) It has been proved by tests that the use of high grade reinforcements of small diameters distributed on the tension zone of the girder gives a better distribution of the cracks. Figure II-3 shows the cross-sections of two beams designed for the same span and loading, and having the same moment of resistance. At failure, the number of tension cracks in the beam b reinforced by high grade steel was three times as much and much narrower than those of beam a in spite of the higher stresses in steel.

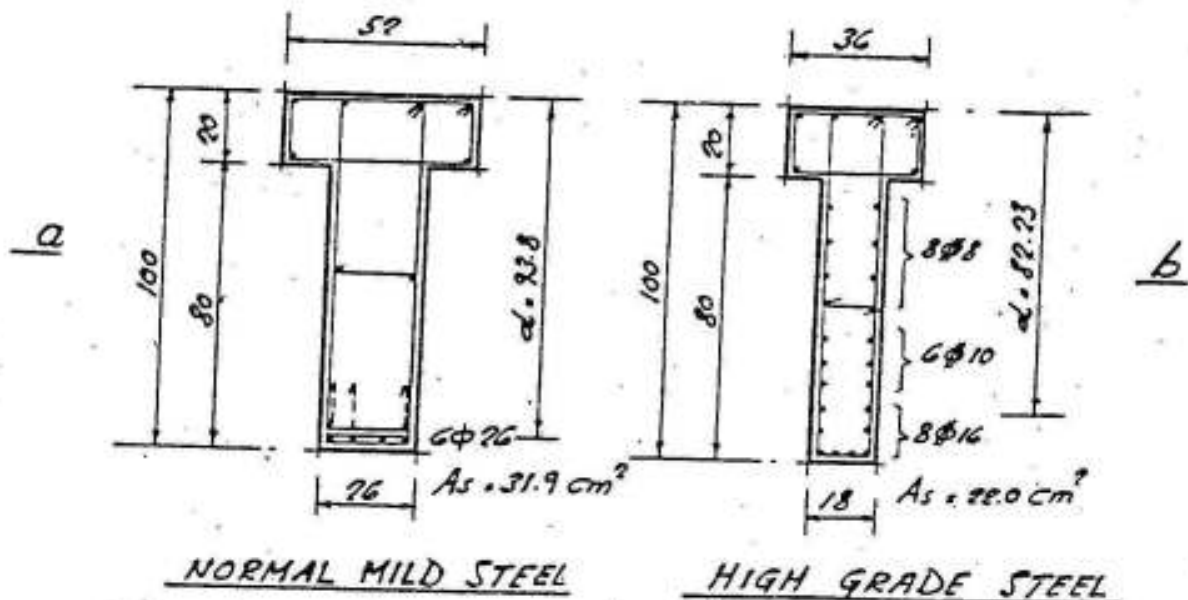


Fig. II-3 Sections of the same moment of resistance

3) When tension cracks are developed at the central part of a beam, the bond between the steel and concrete is broken at the position of the cracks. Under heavy loads, the width and number of tension cracks is increased and the beam may collapse as the bar is pulled through the concrete. To prevent this occurrence, end anchorage is essential, fig II-4. If the anchorage is adequate, such a beam will not collapse even if the bond is broken over the entire length between anchorages. This is so because the beam acts as an arch with a tie as shown in figure II-4, in which the shaded uncracked concrete represents the arch and the tension reinforcements the tie. In this

base, the force in the tension steel, over the entire unbonded length, is constant and equal to  $T = M_{max} / y_{ct}$ . In consequence, the total steel elongation in such beams is larger than in those in which bond is preserved, resulting in larger deflections and larger widths of cracks.

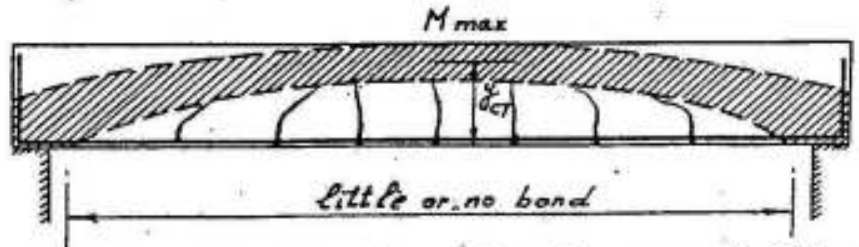


Fig. II-4 Tied-arch action in a cracked beam

In this manner, one can easily imagine that the cutting off of the longitudinal tension bars weakens the tie and reduces the bearing capacity of the beam. The shearing forces can however be resisted by the inclined compressive forces of the arch.

It is consequently recommended to use for the tension reinforcements deformed bars giving high bond resistance and, to introduce at least one third of such reinforcements to the supports and to anchor them well beyond the center line of the supports.

4) The width of the diagonal tension cracks depends on the type of the web reinforcements used, as can be seen from the following test results which show that the use of inclined stirrups arranged at small distances gives the best result. (Fig. II-5).

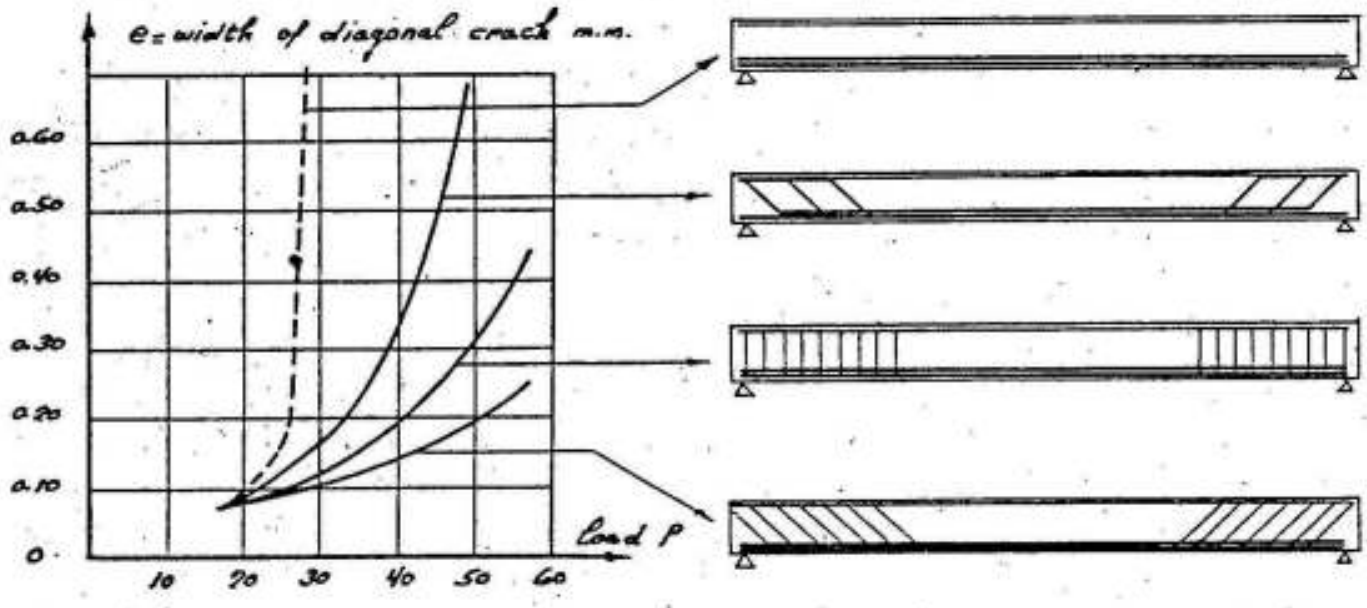


Fig. II-5 Effect of type of web reinforcements on width of cracks

5) A reinforced concrete simple beam can however be considered as a complex truss (Fig. II-6) with the tension steel reinforcement as the bottom chord, the top concrete - the flange - as the top chord, comp-

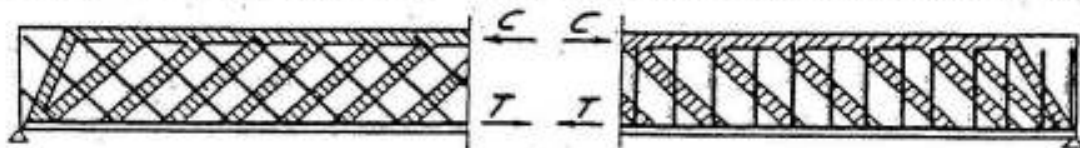


Fig. II-6 Action of a simple reinforced concrete beam as a complex truss

ression concrete diagonals and tension steel vertical or diagonal stirrups.

6) It has been found that the tension in the longitudinal reinforcement of a cracked simple beam is not equal to zero at the supports, but there exists a value  $T_0$  equal to  $1 - 1.6 Q$  where  $Q$  is the shearing force in the bottom chord of a truss with inclined compression diagonals as shown in Fig. II-7.

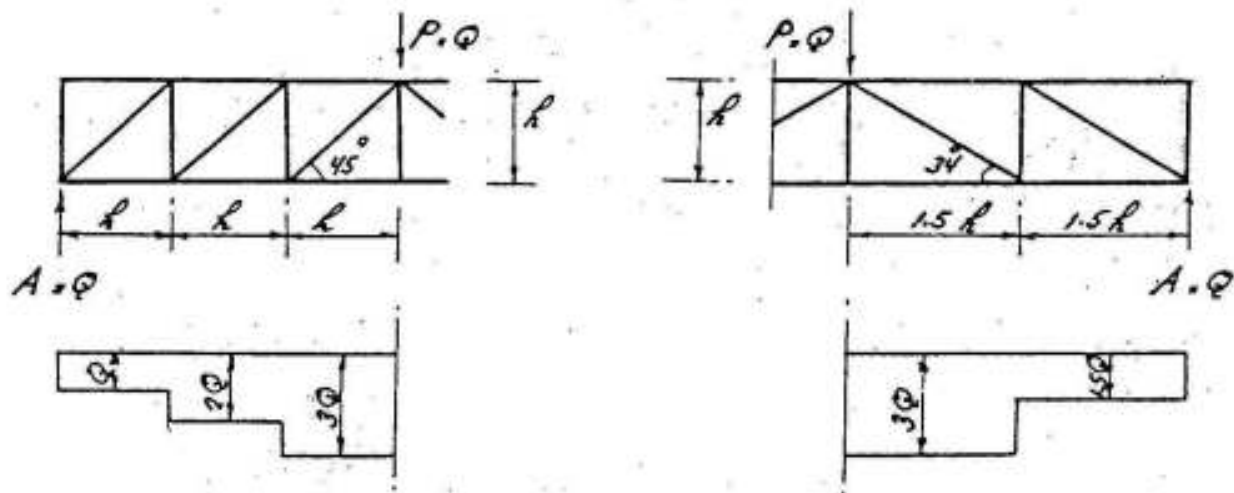


Fig. II-7 Tension in bottom chord of trusses with different inclined diagonals

7) The checking of the anchorage conditions at the ends of the longitudinal reinforcing bars should be based on the bending moment ( or the tension ) diagram, which should be suitably displaced to take account of the need to absorb the horizontal components of the forces in the 'struts' (compression members) of the fictitious lattice system of the complex truss.

This displaced diagram (see Fig. II-8), which serves as the basis for designing the longitudinal reinforcement, is obtained by shifting the enveloping curve of the bending moments (or the tensions) parallel to the center-line of the member in the most unfavourable direction by

by an amount equal to the effective depth  $d$  of the section. The longitudinal bars should be anchored outside the 'displaced' diagram.'

The amount of displacement actually required may vary between  $\frac{d}{2}$  and  $d$ , according to the efficiency of the transverse reinforcement: the value of  $d$  is thus certainly on the safe side.

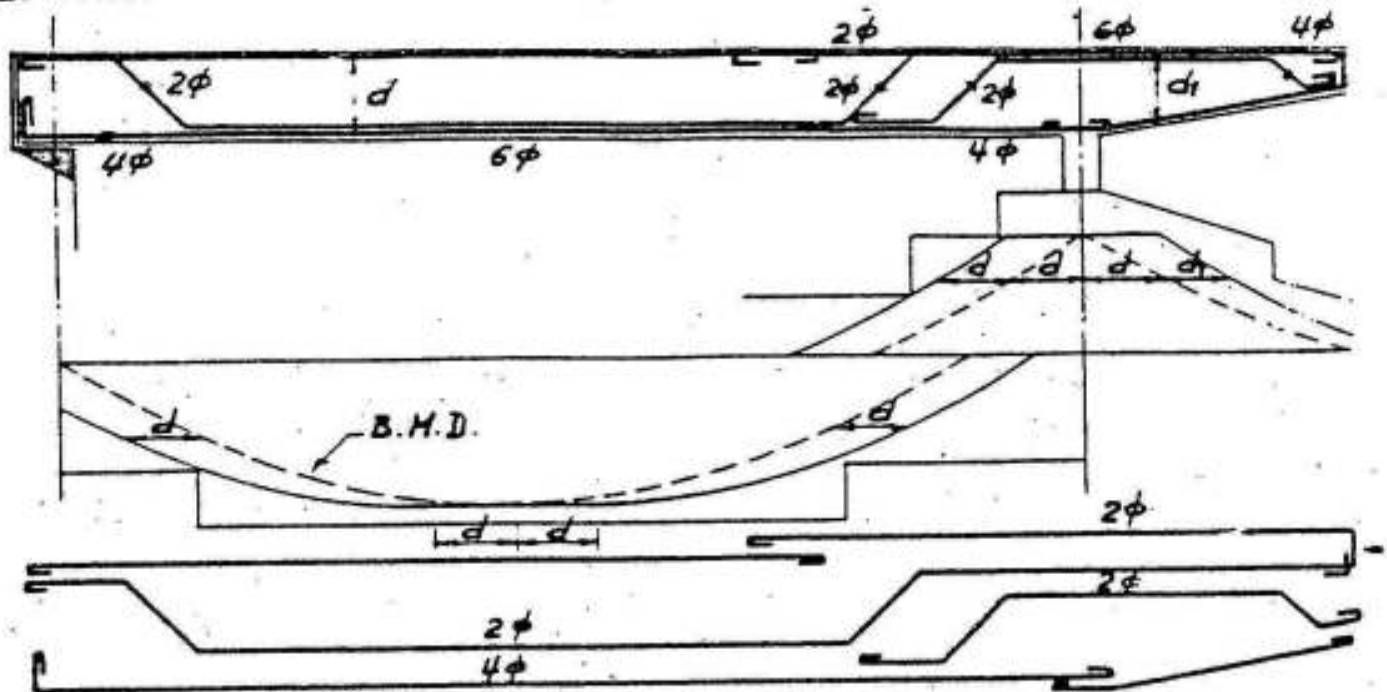


Fig. II-8 Displaced bending moment and moment of resistance diagrams

#### Conclusions

From the previous investigations, we arrive to the following conclusions:

- 1) The use of high grade or cold treated steels as tension reinforcement is preferred especially for bigger diameters.
- 2) The use of longitudinal reinforcements of relatively small diameters 8-10 mm. distributed over the two surfaces of the web and at small distances (15 - 20 cms) reduce the width of the cracks and can be considered as resisting a part of the tension in the section relative to the distance of the bars from the neutral axis.
- 3) The maximum possible part of the tension reinforcement is to be introduced to the supports and well anchored there.
- 4) The anchorage conditions at the ends of the longitudinal tension bars should be based on the shifted bending moment diagram i.e., the ends of the bars determined according to the classic moment of resistance diagram must be shifted a distance  $d$  in the most unfavourable direction.
- 5) The use of inclined stirrups at small distances (15 - 20 cms) to resist relatively high diagonal tension is most effective.

### III - CONTINUOUS GIRDERS

Continuous girders of constant and variable moment of inertia give in many cases a convenient solution for big spans. If the choice of the spans is free and the magnitude of the loads on the different spans is the same, it is recommended to choose the inner spans somewhat bigger than the outer ones in order to have field moments of nearly the same order (fig III-1).

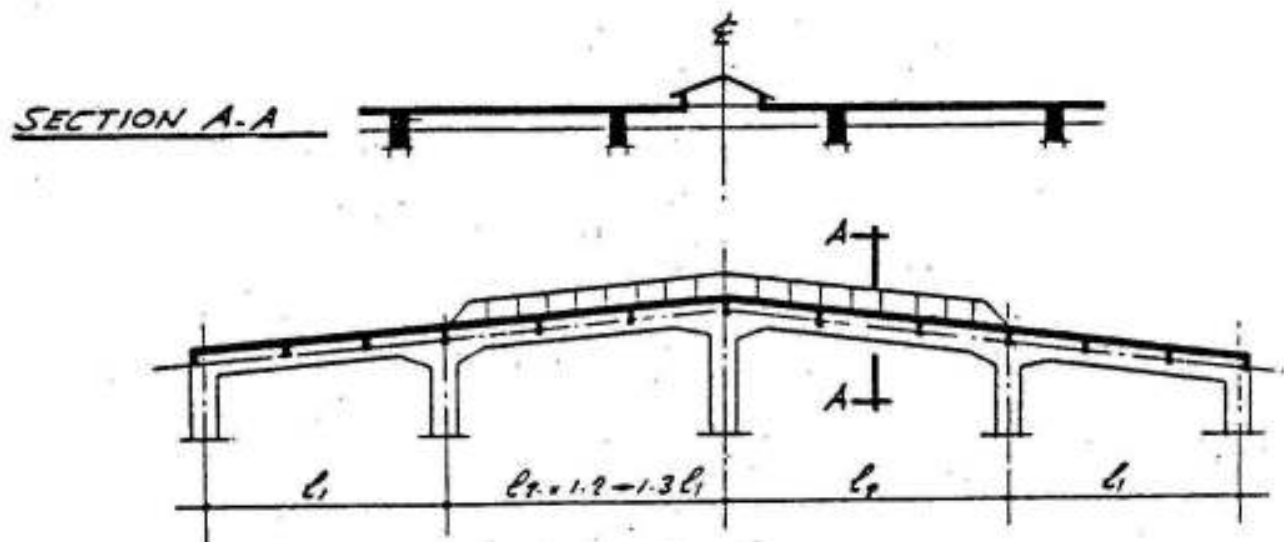


Fig. III-1 A continuous girder

The increase of the depth of the girder towards the supports affects the bending moment diagram increasing the connecting moments by 10 - 20% and decreasing the field moments by the corresponding values. For spans bigger than  $10^{ms}$  such effects must be taken in consideration as shown in the following example of a crane girder subject to uniform dead loads and concentrated rolling loads. (Fig III-2,A)

To reduce the amount of work included in the problem, the girder is chosen symmetrical and composed of three spans only.

---

Refer to "Theory of Elastically Restrained Beams" by M. Hilal .  
Published 1945.



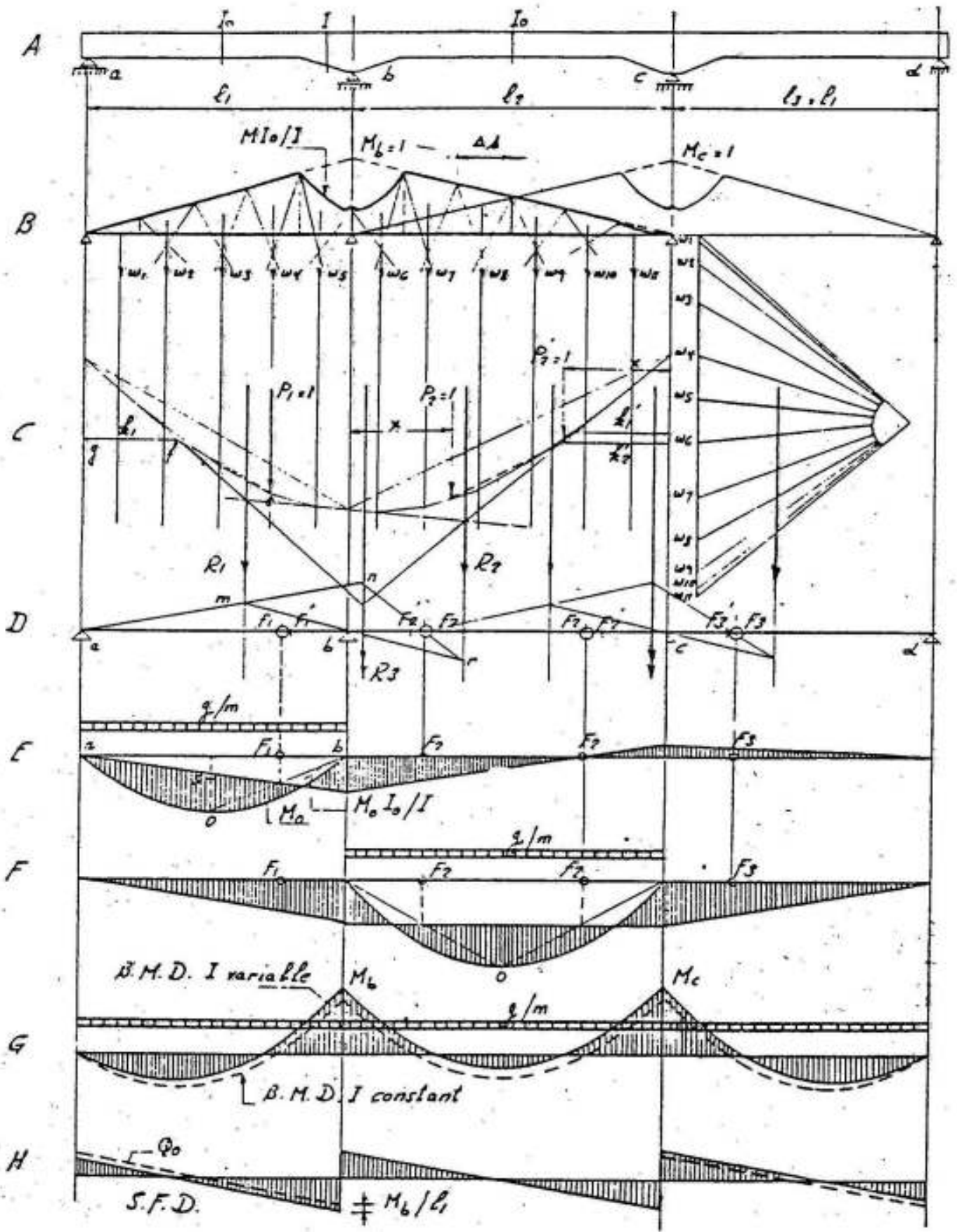


Fig. III-2. Fixed points, moments and shears in a continuous girder of variable moment of inertia

We give in the following the main steps required to determine the internal forces using the graphical fixed - points - method.

The internal forces due to the permanent uniformly distributed dead loads will be determined by superposition of uniform loads on the different spans. The increase of the dead load due to the variation of the depth of the main girder near the supports may be neglected without making an appreciable error.

The internal forces due to the rolling loads will be determined by the influence lines. It is generally not recommended to use the influence lines for determining the internal forces due to permanent dead loads, the use of the direct method of loading of the different spans gives much better results.

### 1) Determination of the Fixed Points

(Fig III-2 B,C and D)

In order to find out the left fixed point  $F_2$  of span  $l_2$ , one has to determine the position of the resultant elastic weights  $R_1$ ,  $R_2$  and  $R_3$ ; where

$R_1$  = resultant of elastic weights  $w = \Delta s MI_0/I$  due to  $M_b = 1$  acting on  $l_1$

$R_2$  = resultant of elastic weights  $w = \Delta s MI_0/I$  due to  $M_b = 1$  acting on  $l_2$

$R_3$  = resultant of  $R_1$  and  $R_2$

These positions can be determined graphically in the following manner: For ab and bc as simple beams, draw the bending moment diagrams (B.M.D.) due to  $M_b = 1$ , then determine the reduced B.M.D. by multiplying the ordinates of the B.M.D. by  $I_0/I$ . Divide the reduced B.M.D. into convenient number of strips  $\Delta s$ . Determine the magnitude of the elastic weights  $w = \Delta s MI_0/I$  (fig III-2B) and draw their force and link polygons. (Fig III-2C).

$R_1$  &  $R_2$  lie at the point of intersection of the first and last rays of the link polygon of the elastic weights on  $l_1$  and  $l_2$  respectively and  $R_3$  is the resultant of  $R_1$  and  $R_2$ .

If the beam were of constant moment of inertia, then  $R_1$  and  $R_2$  lie at the third points of  $l_1$  and  $l_2$  respectively whereas  $R_3$  lies at the inverted third point.

Having determined  $R_1$ ,  $R_2$  and  $R_3$ , the left fixed point  $F_2$  of

span  $l_2$  can be determined using the known normal construction of beams of constant moment of inertia (fig. III-2D) by drawing a line  $m n$  passing through the left fixed point of span  $l_1$  ( in our case, point  $a$  ), meeting  $R_1$  in  $m$  and  $R_3$  in  $n$  , through  $m$  draw line  $m b$  and extend it to meet  $R_2$  in  $r$  , line  $n r$  intersects  $b c$  at the position of  $F_2$  .

Repeating the same construction for spans  $l_2$  and  $l_3$  as simple beams due to  $M_c = 1$  , one can determine the left fixed point  $F_3$  of span  $l_3$  .

Due to the increase of the moment of inertia of the girder towards the supports, one can easily notice that the position of the fixed points  $F$  moves towards the center-lines of the spans relative to the fixed points  $F'$  of the same girder if it were of constant moment of inertia. (Fig. III-2D)

## 2) Bending Moments and Shearing Forces due to Uniform Loads

### a) Unsymmetrical exterior span loaded by $g t/m'$ .

For such a span of unsymmetrical variation of moment of inertia, the bending moment diagram can be determined as follows (Fig III-2E).

Draw the  $M_o$  - diagram (shown full) and the reduced,  $M_o I_o / I$  diagram (shown dotted). Determine the center of gravity  $S$  of the reduced diagram by dividing it into convenient vertical strips, assuming the area of each strip as an elastic weight acting in its center of gravity, and drawing a force and the corresponding link polygons. Through  $S$  draw a vertical line to meet the  $M_o$  - diagram in  $O$  . The closing line of the B.M.D. passes through the point of intersection of the crossing line  $b O$  and the vertical through  $F_1$  .

### b) Symmetrical intermediate span loaded by $g t/m'$ .

This span has a symmetrical variation of the moment of inertia and hence  $O$  lies at the middle of the  $M_o$  - diagram and the normal construction of the B.M.D. applies. (Fig III-2F).

The final B.M.D. due to a dead load  $g/m$  acting on all spans (fig III-2G) shows that , due to the increase of  $I$  at the supports , the connecting moments are increased and the field moments are decreased compared to beams of constant  $I$  .

As the depth and reinforcements of the girder along the spans are generally governed by the field moments, then a beam of variable  $I$  is supposed to be more economic than a beam of constant  $I$  .

The shearing force in any panel can be determined from the

General equation :

$$Q = Q_0 + \frac{M_R - M_L}{l}$$

where

$Q_0$  = the shearing force of the simple beam

$M_R$  and  $M_L$  = the connecting moments at the right and left supports of the span under consideration.

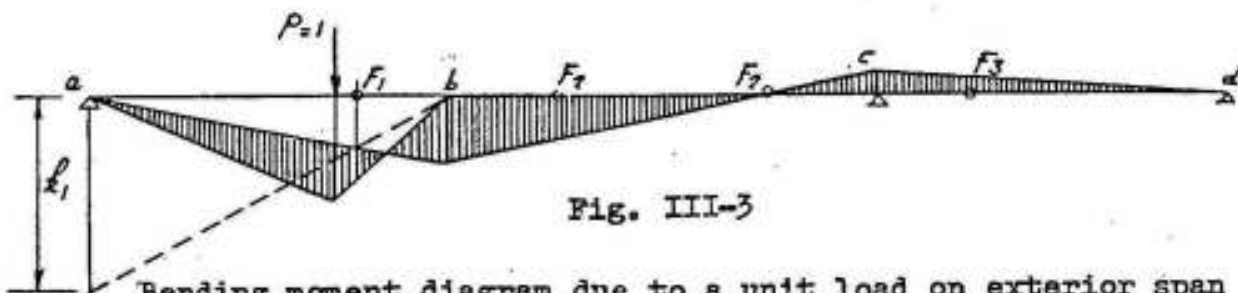
### 3) Bending Moments due to a Concentrated Unit Load

The internal forces ( B.M<sup>s</sup> , S.F<sup>s</sup> ... etc) and reactions of a continuous beam due to rolling loads can be determined by the influence-lines-method.

The influence line of a force acting in any section of a beam represents the value of the force in the section due to a simple unit load moving over the beam, the ordinates being drawn at the position of the load.

In order to determine the influence lines of the bending moments of the different sections, one has to draw the B.M.D. due to a concentrated load  $P = 1$  at a series of sections. For beams of variable moment of inertia, this can be done as follows:

For a load  $P = 1$  acting on span  $l_1$ , draw a vertical through the point of application of  $P$  to meet the link polygon of the elastic weights  $w$  due to  $M_D = 1$  in  $e$  ( fig. III-2C ), then draw the line  $e f$ , parallel to the closing line to meet the first ray of the link polygon in  $f$ ; the horizontal distance  $f g$  gives the crossing distance  $k_1$  used for determining the B.M.D. as shown in figure III-3.



For a load  $P_2 = 1$  acting on span  $l_2$  at a distance  $x$  from the left support  $b$ , the crossing distances  $k'_1$  and  $k'_2$  can be determined by assuming  $P_2$  once at  $x$  from the left support  $b$  and once at the same distance  $x$  from the right support  $c$ . (Fig III-2C). The B.M.D. is drawn by plotting the smaller of the crossing distances  $k'$  at the nearer support as shown in figure III-4.



in which

$\delta_{mn}$  = deflection at point m of main system, due to  $M_n = 1$  .

So that

$$M_n = -\alpha_{nm} / \alpha_{nn} = -\delta_{mn} / \alpha_{nn}$$

or

$$M_n = \delta_{mn} \times \text{constant}$$

In the same way , for the influence line of the bending moment at b ,  $M_b$  , choose a main system in which  $M_b = 0$  by introducing a hinge in the beam at b , the elastic line of this main system due to  $M_b$  gives the form of the required influence line of  $M_b$  (Fig III-5B).

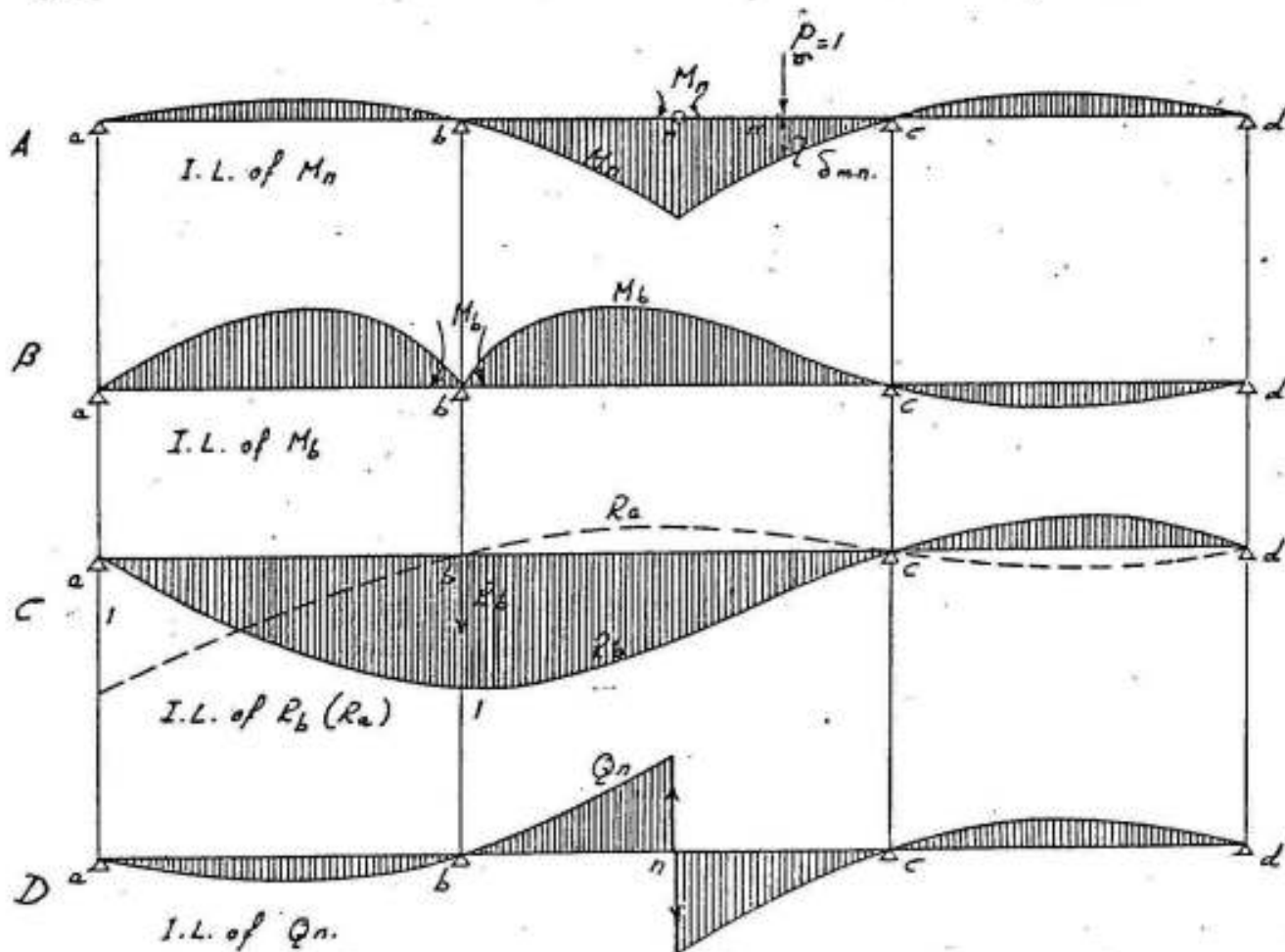


Fig.III-5 Representation of influence lines as elastic lines

The same principle can be used for determining the form of the influence line of the reactions, that is, for the influence line of the reaction  $R_b$  (or  $R_a$ ) choose a main system in which  $R_b$  (or  $R_a$ ) = 0,

this can be done by removing the support at b (or a), the elastic line of the chosen main system due to  $R_b$  (or  $R_a$ ) as a load gives the form of the influence line of  $R_b$  (or  $R_a$ ). (Fig III-5C).

The form of the influence line of the shearing force at any section can be determined by cutting the continuous beam at the section and applying two equal and opposite forces. (Fig III-5D).

This method is generally not used for determining the ordinates of the influence lines but as check for their form.

### 5) Influence Lines for Bending Moments and Shearing Forces

The ordinates of the influence lines of the bending moments are generally determined from the ordinates of the B.M.D. due to  $P = 1$  acting at the different sections, but the influence lines of the shearing forces in all sections of any span can be done in one process as follows : (Fig III-6).

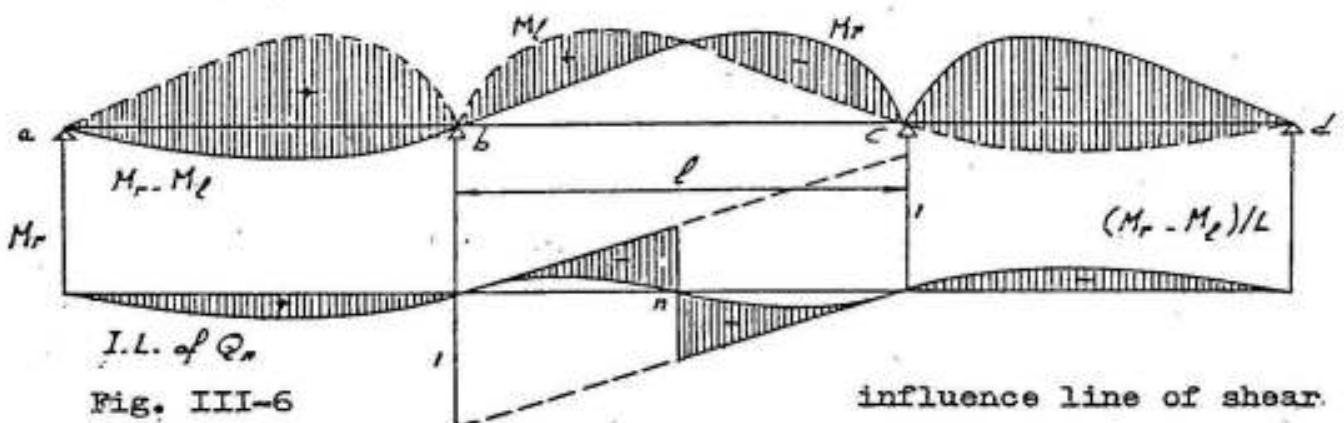


Fig. III-6

The shearing force at any section is given by:

$$Q = Q_0 + \frac{M_2 - M_1}{l}$$

The influence line of  $Q_0$  for any section in span bc is given by 2 triangles bounded by the two parallel lines with ordinates equal to 1 at b and c. It varies from section to section. The effect of  $(M_2 - M_1)/l$  is given by the curve shown in figure III-6, whose ordinates are constant for all sections in bc.

### 6) Absolute Bending Moments and Shearing Forces

The maximum bending moments and shearing forces due to rolling loads will be as shown in figure III-7A & B. Adding the B.M.<sup>s</sup> and S.F.<sup>s</sup> due to dead loads given in figure III-2G & H to those due to rolling loads, we get the absolute maximum diagrams given in figure III-7C & D.

It has to be noted that for heavy live or rolling loads, negative field moments  $M_m$  at the middle of intermediate spans are liable to take place, in which case, the necessary top steel reinforcement must be arranged.

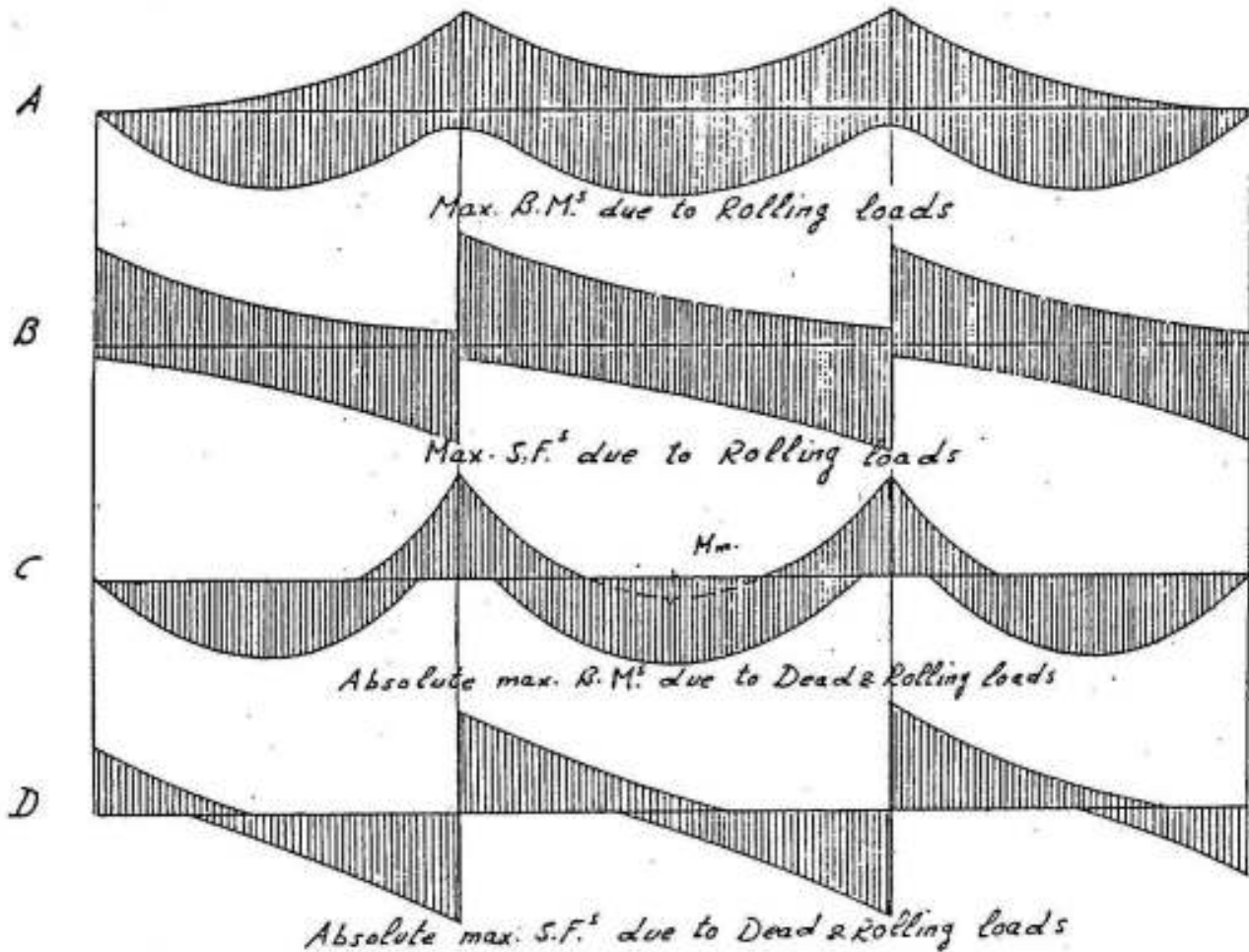


Fig. III-7 Absolute maximum bending moments and shearing forces

#### Recommendations

- 1) The arrangement of the tension reinforcement is to be done according to the tension line shifted a distance  $d$  from the  $M/y_{CT}$  - line as shown in figure III-8.
- 2) The tension reinforcement over the supports is not to be concentrated in the rib, a better distribution of the cracks will be attained if a part of the reinforcement is distributed in the flange, if any, as shown in section B-B of figure III-8.
- 3) The maximum shearing force occurs immediately adjacent to the supports but the maximum shear stress to be considered in the design is that at a section  $d$  from the face of the support because adjacent to the supports, the additional local stresses caused by reactions



counteract crack formation . For this reason , it is generally recommended, in cases where bent bars are arranged to resist diagonal tension , to make the interior bent at a convenient distance from the face of the support so that the top horizontal part of the bent bar can share effectively in resisting the connecting moment. (Refer to figure III-8 in which the first bent at the intermediate support is arranged at the top end of a line drawn from the face of the support and making  $60^\circ$  with the horizontal).

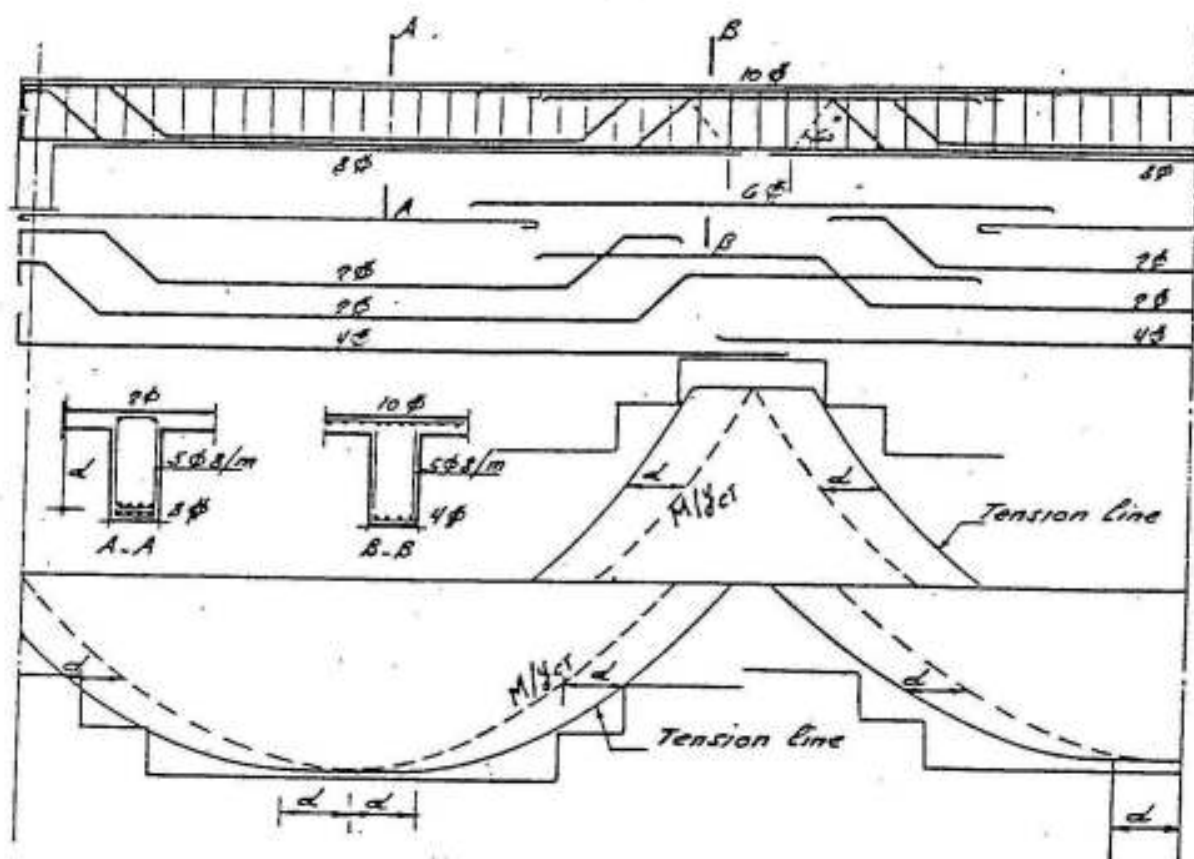


Fig. III-8 Details of reinforcements of a continuous girder

- 4) Some new tests have shown that the best distribution and minimum width of cracks can be attained by using inclined (or vertical) stirrups at zones of high shear stresses as was shown in figure II-6. Accordingly the use of straight bars only for reinforcing continuous (or simple) beams may be the convenient solution. Fig III-9
- 5) The slope of the effective haunch must not be more than 3:1, otherwise , the principal normal compressive stress  $\sigma_1$  parallel to the outer surface of the haunch is excessive relative to the

horizontal normal stress  $\sigma_c$

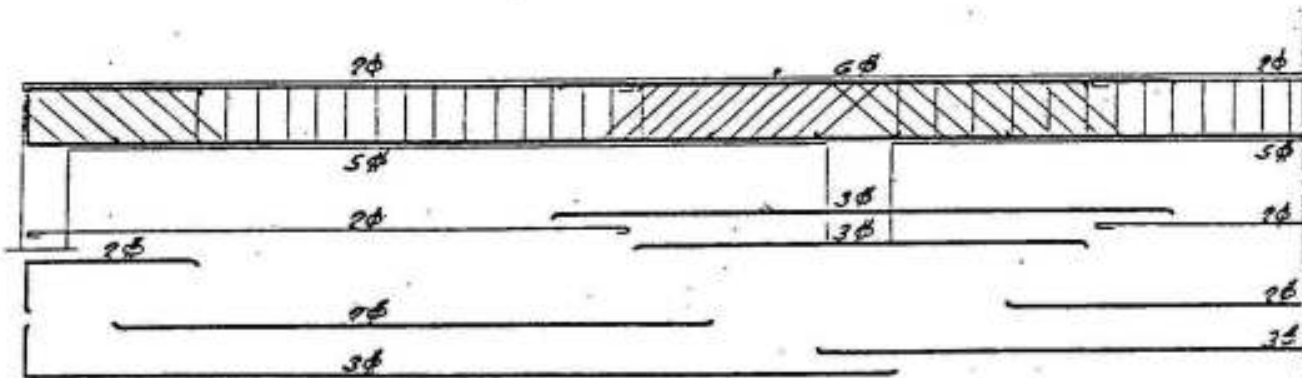


Fig. III-9 Use of straight steel bars and inclined stirrups in continuous girders

According to figure III-10, we have :

$$(\sigma_1 ds \cos \alpha) \cos \alpha = \sigma_c ds$$

So that

$$\sigma_1 = \sigma_c / \cos^2 \alpha$$

For a slope 1:1

$$\cos^2 \alpha = \frac{1}{2} \quad \text{and} \quad \sigma_1 = 2 \sigma_c \quad \text{not allowed!}$$

" " " 3:1

$$\cos^2 \alpha = 9/10 \quad \sigma_1 = 1.11 \sigma_c \quad \text{accepted.}$$

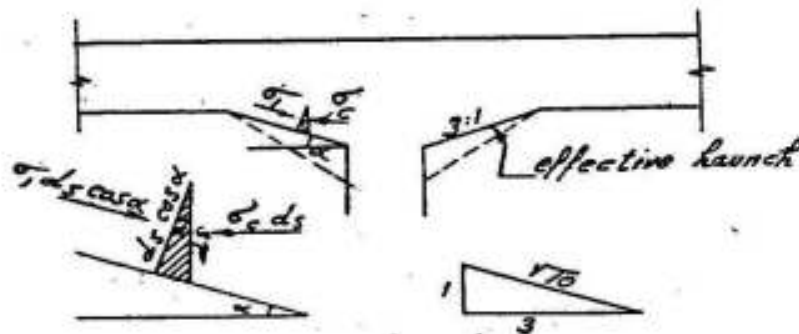


Fig. III-10 Principal compressive stresses in haunches

6) The maximum moment that can be resisted by a section is that which causes a stress in tension steel equal to its yield stress; so that, if in a continuous beam, the moment in any of the critical sections - sections of maximum connecting and field moments - is bigger than the mentioned maximum value, the increase will be resisted by the other critical sections on condition that the equilibrium of the beam is maintained. A statically indeterminate beam remains in equilibrium until the stress in steel of all critical sections (max three in number) reaches the yield stress, at which moment collapse is liable to

take place.

Accordingly, a redistribution of the bending moments determined according to the theory of elasticity is possible; any of the critical values may be changed within a range of  $\pm 16\%$  of  $M_0$  ( $M_0$  = the max. B.M. of the simple beam) on condition that the tension reinforcement is not chosen smaller than half the value required according to the theory of elasticity. Fig III-11.

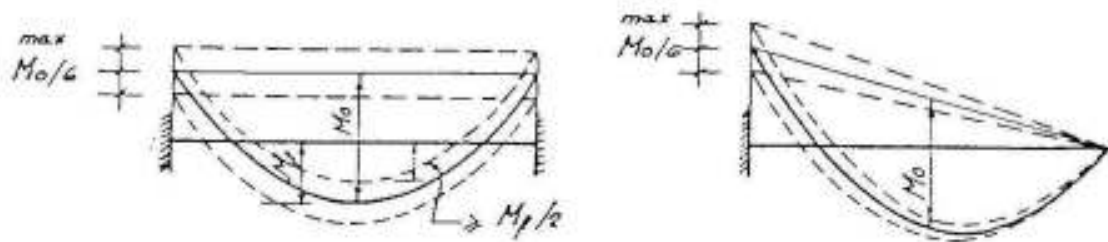


Fig. III-11 Limits of redistribution of bending moments

In order to avoid visible cracks in the lower surface of beams (and slabs) and to have convenient depths - in case of beams of small breadth - and reinforcements, it is generally advantageous to reduce the connecting moments and to increase the field moments by the corresponding values.

Example:

A continuous beam of 2 equal spans is subject to a dead load  $g = 1$  t/m and a live load  $p = 1$  t/m. Determine the extreme values of the bending moments for the minimum possible design connecting moment. The span of the beam is 8 m.

Solution: (Fig III-12)

Connecting moment for one span only loaded by  $g = 1$  t/m

$$M_B = gl^2 / 16 = 1 \times 8^2 / 16 = 4 \text{ mt}$$

Max. connecting moment for the 2 spans loaded by  $g + p = 2$  t/m

$$\text{max. } \bar{M}_B = 4 \times 4 = 16 \text{ mt}$$

Allowed reduction of connecting moment:

$$\bar{M}_B = 0.16 \times 16 = 2.56 \text{ mt}$$

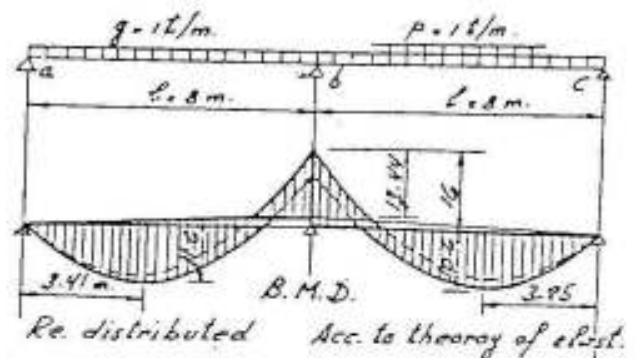


Fig. III-12

Design connecting moment =  $16 - 2.56 = \underline{13.44}$  mt

For max. field moment, the two spans will be loaded by  $g$  and one span only by  $p$ , in which case

$$M_b = 3 \times 4 = 12 \text{ mt}$$

$$\text{Outer reaction of loaded span : } R = 2 \times 8/2 - 12/8 = 6.5t$$

Max. field moment lies at point of zero shear which is assumed to be a distance  $x$  from the exterior support, where

$$x = R/w = 6.5 / 2 = 3.25 \text{ m}$$

$$\text{Max. field moment } M_f = wx^2 / 2 = 2 \times 3.25^2 / 2 = 10.6 \text{ mt}$$

After re-distribution, the connecting moment for one span loaded is given by:

$$M_b = 12 - \bar{M}_b = 12 - 2.56 = 9.44 \text{ mt}$$

$$\text{Outer reaction of loaded span : } R = 2 \times 8/2 - 9.44/8 = 6.84 \text{ t}$$

$$\text{Max. field moment lies at } x = 6.82/2 = 3.41 \text{ m}$$

$$\text{Max. field moment } M_f = wx^2 / 2 = 2 \times 3.41^2 / 2 = \underline{11.64} \text{ mt}$$

We give in the following some examples of continuous reinforced concrete girders:

The example shown in figure III-13 gives a continuous girder with a relatively short span between long spans. In this case, the short span will be subject to negative connecting moment over its whole length; the reinforcements can be arranged as shown.

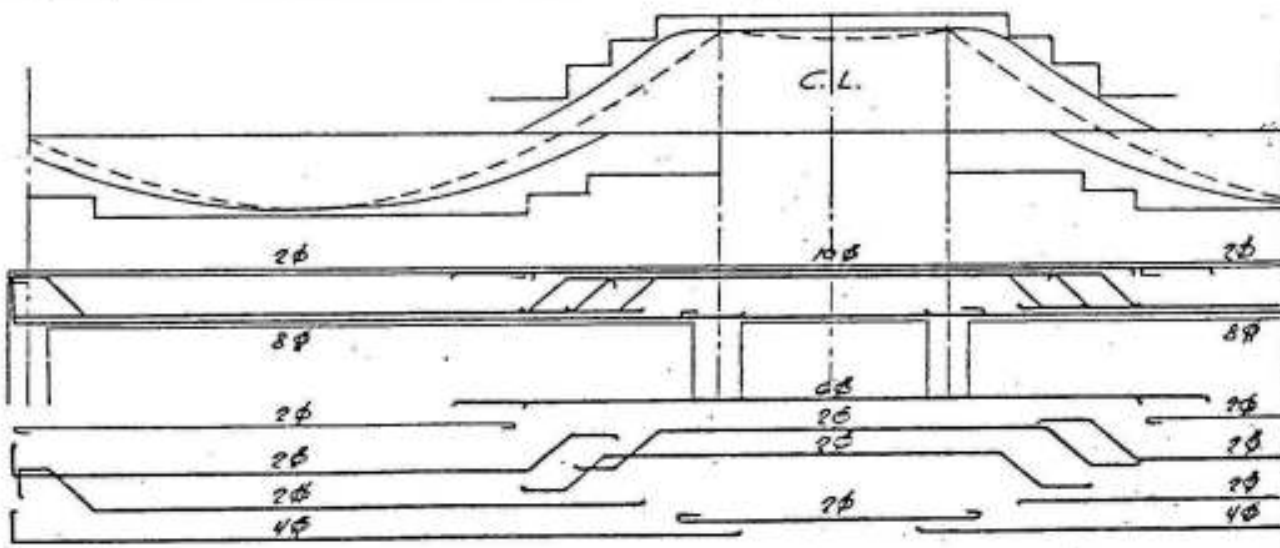


Fig. III-13 Details of a continuous girder with a short span between long spans

If the shorter span is an outside one , the details can be as shown in figure III-14.

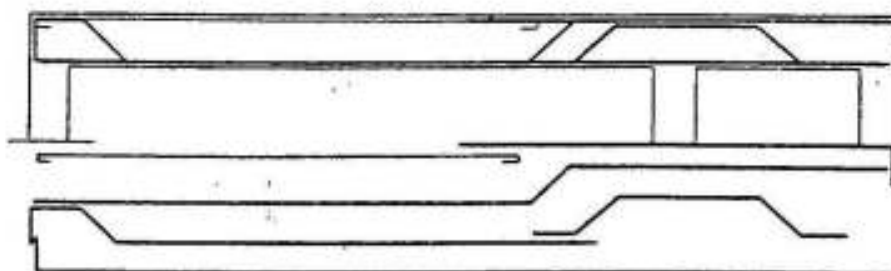


Fig. III-14 Continuous girder with an outside short span

Fig III-15 shows a "continuous" girder 15 ms span supporting a 10 m saw tooth roof in factory 135 at Helwan.

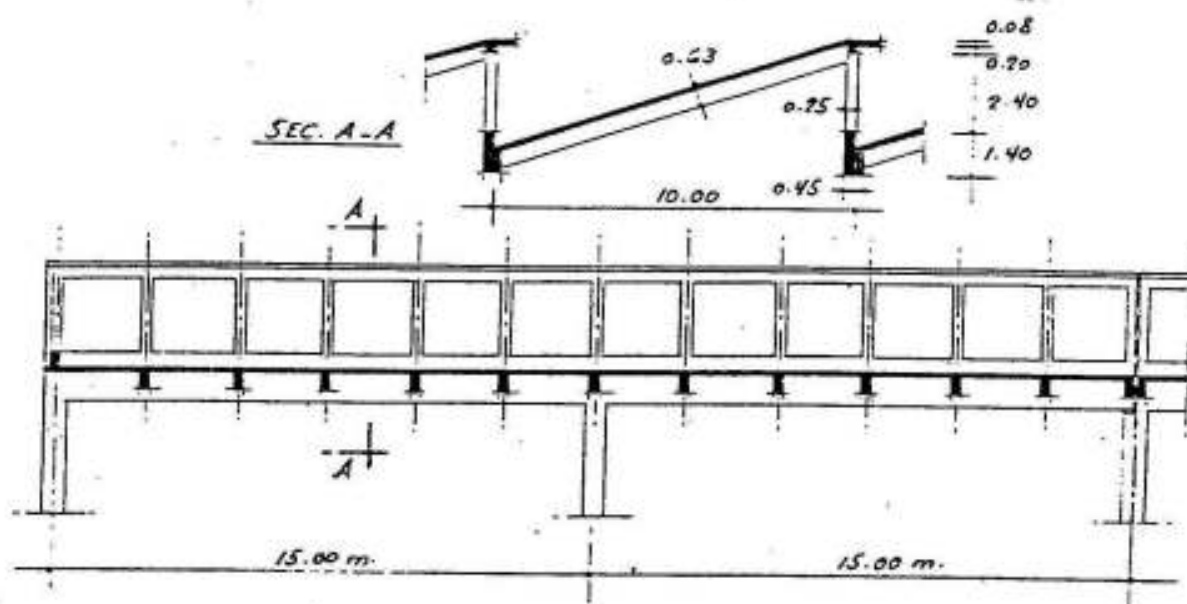
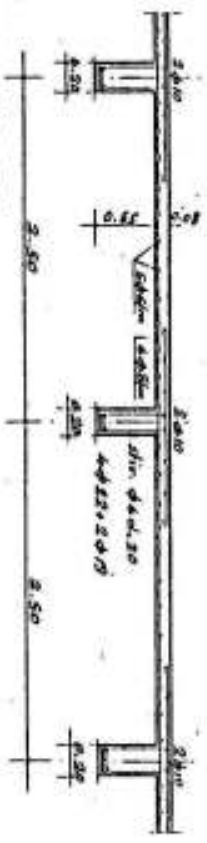
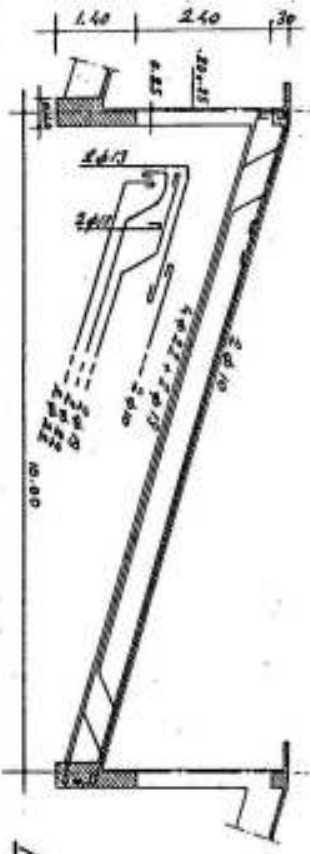
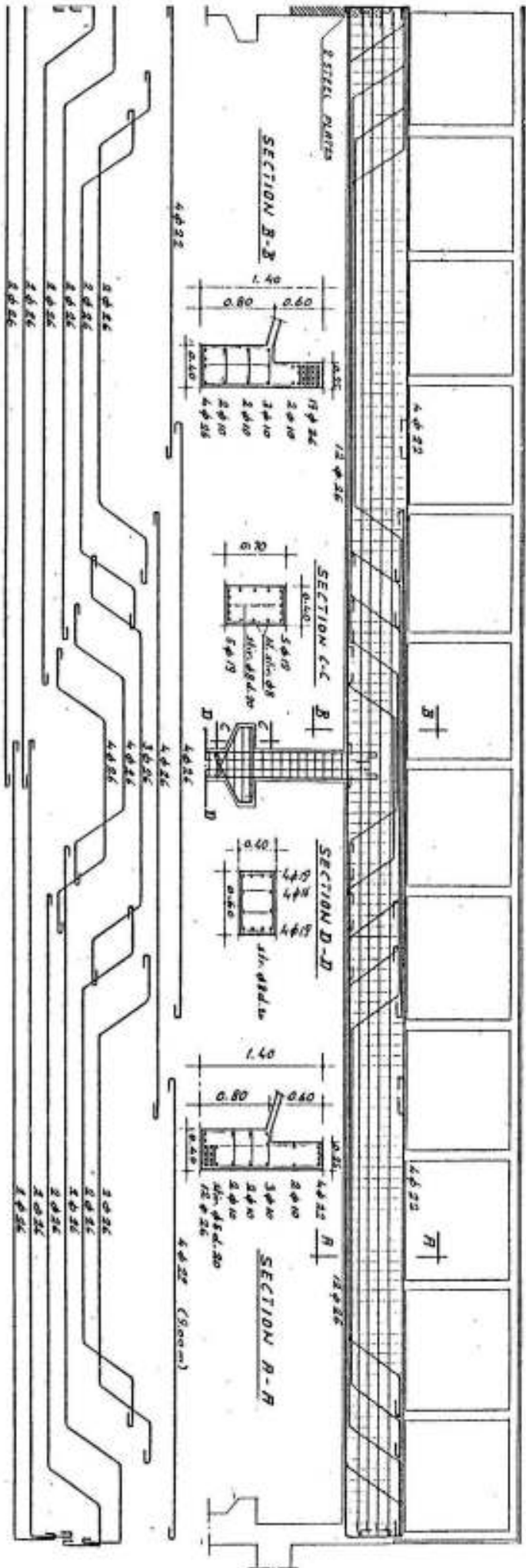


Fig. III-15 Cross and longitudinal sections of factory 135 at Helwan

The details of reinforcements of the roof slab and secondary beams as well as the details of the main girder are shown in fig III-16.

Due to constructional requirements , the bearing area of some continuous girders on the supporting columns is relatively small - e.g. the bearing at the right support of the girder shown in figure III-15; if the cross reinforcements of the head of the column are not sufficient to resist the tension due to friction and splitting a crack, which may endanger the safety of the whole girder, is liable to be developed.



FACTORY 135- HELWRN  
 PLS. III-16

The required cross reinforcement can be calculated as follows: (fig III-17).

Assuming that the frictional force resulting from the possible resistance to shrinkage is  $H = \mu A$

in which

$\mu = 0.2$  to  $1$  according to condition and type of bearing plates, and the cross tensile splitting force due to the concentration of  $A$  is  $T \approx \frac{A}{3}$

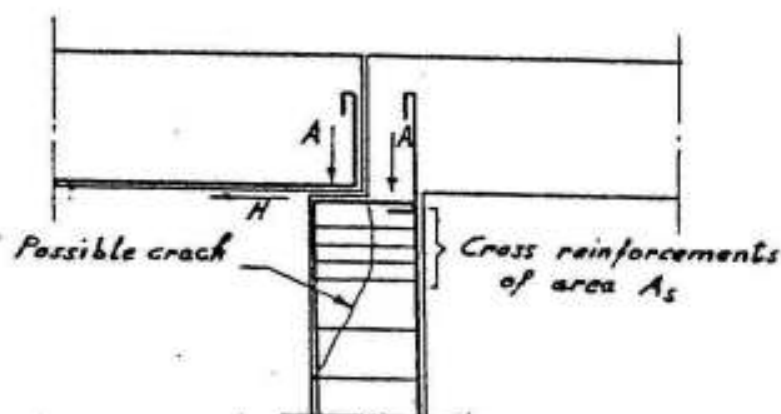


Fig. III-17 Horizontal forces and cross reinforcements at the head of a supporting column

Then the total cross tensile force is  $H + T$ , and the required cross reinforcement is given by

$$A_s = (H + T) / \sigma_s = (0.55 \text{ to } 1.3) A / \sigma_s$$

Fig III-18 shows the roof slab and the main girders of an air conditioned wollen textile factory. The air-conditioning ducts, 10 meters apart, have a trapezoidal section 1.5 ms clear depth, their clear width is 1.00 m at top and 0.80 m at bottom. The supporting columns are arranged below the ducts at distances of 24 ms.

The walls, top and bottom slabs of the duct have been chosen 20 cms thick, so that it was possible to use the 1.90 ms high trapezoidal section of the ducts as continuous main girders 24 ms span to support a ribbed roof slab 8.6 ms clear span.

The ribbed slab is one way and 30 cms thick. It is composed of a solid slab 6 cms thick and ribs arranged every 50 cms. The ribs have a trapezoidal section 24 cms deep and 8/10 cms wide. In order to distribute the load over the ribs and to assure their combined

action , two stiffening ribs having the same section as the main ribs are arranged in the longitudinal direction parallel to the ducts. In order to have adequate space for resisting the connecting moments two, 40 cms long, solid parts are arranged adjacent to the ducts.

The reinforcement of the solid slab is  $5\phi 8/m$  normal to the ribs and  $4\phi 6/m$  parallel to the ribs.

The main ribs are reinforced by  $2\phi 16$  at the bottom in the span and at the top over the supports. The stiffening ribs have  $2\phi 16$  at bottom and  $2\phi 13$  at top.

The reinforcement of the main girders is placed in the lower slab at the middle of the spans and in the top slab over the supports. The bent bars are placed in the walls. In order to avoid splicing of the reinforcements, special long bars of length  $\leq 32$  ms are used.

In continuous girders of equal spans which are of common use in buildings, the connecting moments over the supports are generally bigger than the field moments. If the slabs are arranged at the upper fibers of the girder, then the sections of bigger moments at the supports behave as rectangular and require big depths, whereas the sections of smaller moments at mid-span behave as T-sections and require relatively smaller depth.

In case a girder of constant depth is required, it is recommended:

- a) to redistribute the bending moments by reducing the connecting moments by an amount  $\leq M_o/6$ . The reduction may however vary from support to support to give a simplified distribution of the reinforcements,
- b) to reduce the connecting moments over the supports according to a parabolic curve due to the distribution of the reaction over the width of the support, and,
- c) to design the section of maximum connecting moment for the minimum depth and the maximum allowed compression reinforcement which must be  $\leq \sim 0.4$  the tension reinforcement.





#### IV- FRAMES

A frame is a structure in which the rigid connections between the girders and the supporting columns are utilized so that the internal forces due to the loads are resisted by the combined action of the girders and the columns i.e. the bending moment  $M_o$  is distributed on both of them. (Fig IV-1).

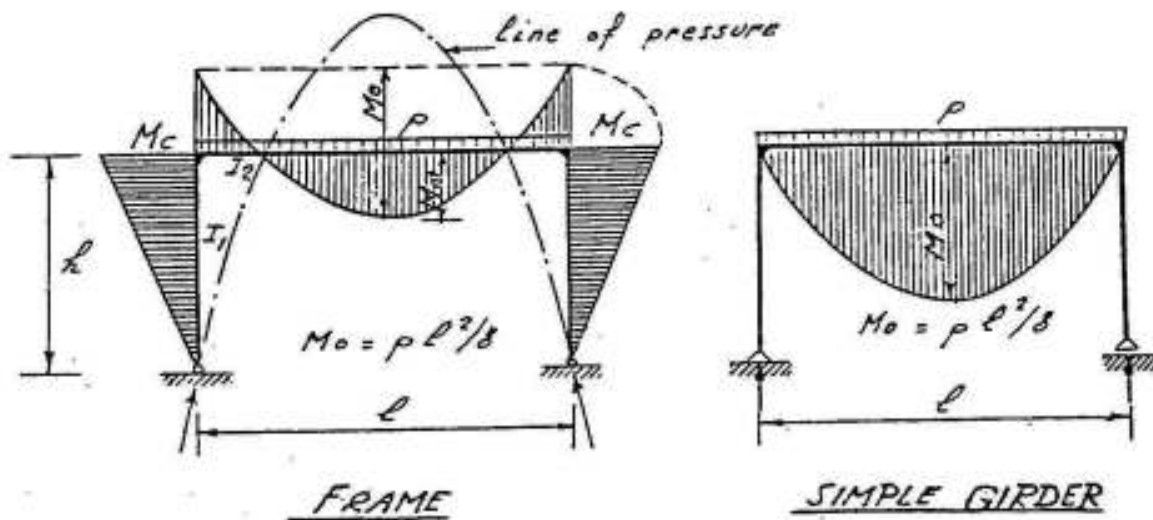


Fig. IV-1 Frames and simple girders

In a simple girder, we get for vertical loads vertical reactions while in a frame, vertical loads give inclined reactions.

The magnitude of the bending moments resisted by the columns depends on the relative stiffness  $\chi$  of the girder with respect to the columns, where

$$\chi = \frac{h}{l} \cdot \frac{I_2}{I_1}$$

For constant  $I_1$  and  $I_2$  and uniform load  $p$ , the connecting moment  $M_c$  of a rectangular frame is given by:

$$M_c = - \frac{pl^2}{4(3 + 2\chi)} = - \frac{pl^2}{\frac{4}{\chi}}$$

The field moment is therefore:

$$M_m = \frac{pl^2}{8} - M_c = + \frac{pl^2}{k_2}$$

We give in the following table the values of  $k_1$  and  $k_2$  for different  $h/l$  and  $I_2 / I_1$  values

$h/l$	$I_2/I_1$	$\chi$	$k_1$	$k_2$
0.4	1.5	0.60	16.8	15.3
0.5		0.75	18.0	14.4
0.6		0.90	19.2	13.7
0.4	2.0	0.80	18.4	14.0
0.5		1.00	20.0	13.3
0.6		1.20	21.6	12.7
0.4	2.5	1.00	20.0	13.3
0.5		1.25	22.0	12.6
0.6		1.50	24.0	12.0

The table shows that the bigger the value of  $\chi$ , the smaller is the moment resisted by the columns. This moment depends also on the variation of the moment of inertia in such a way that the portions of bigger moment of inertia resist bigger moments as shown in fig IV-2 which shows three two-hinged frames of the same span subject to uniform loads. Case a shows a frame with a stiff girder and a slender column; the bending moment  $M_o = pl^2/8$  is mainly resisted by the girder and a small bending moment is resisted by the columns. In case b the girder and columns are approximately of the same stiffness, the

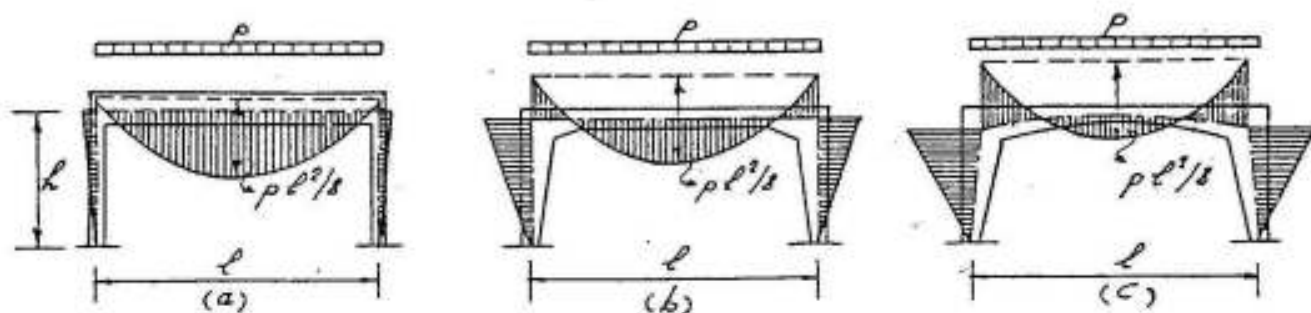


Fig. IV-2 Distribution of moments between girder and columns

field and corner connecting moments are nearly of the same order. Case c shows a frame of relatively big moment of inertia at the corners causing big connecting moments and small field moments.

The minimum bending moments in a frame take place if its axis coincides on the line of pressure of the loads. The axis of a reinforced concrete frame may be assumed as the line connecting the centers of gravity of the plain concrete sections; the width of flange to be considered in T-sections is  $B = 6t_s + b_o$ , where  $t_s$  = thickness of flange and  $b_o$  = breadth of web. The line of pressure gives the position of the resultant of the loads and reactions in any section. (Refer to fig IV-1).

Accordingly, if the form of the frame is not specified, the economic frames are those in which the axis coincides on the line of pressure of the loads i.e for a single concentrated load choose a triangular frame, for a series of concentrated loads,, choose a polygonal frame and for a uniform load a parabolic frame is most convenient (Fig IV-3).

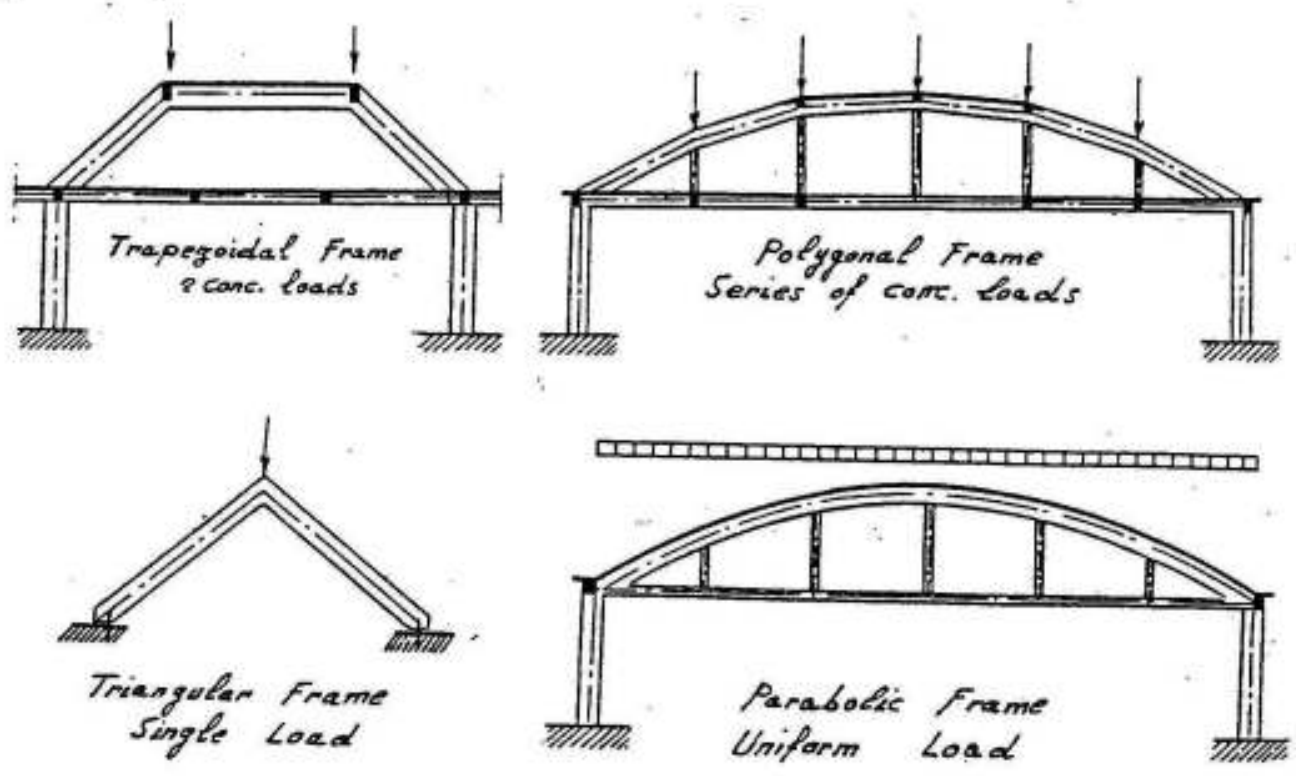


Fig. IV-3 Line of pressure and axis of frame

The choice of the form of a frame is generally governed by the external and internal architectural considerations as well as the purpose for which it is used. The structural system depends on the conditions at the supports.

Statically determinate three hinged frames are used on weak soils that may be subject to small horizontal or vertical movements of the bearing hinges. (Fig IV-4).

Two hinged frames are generally used on medium soils as they are not very sensitive to displacements of the supports.

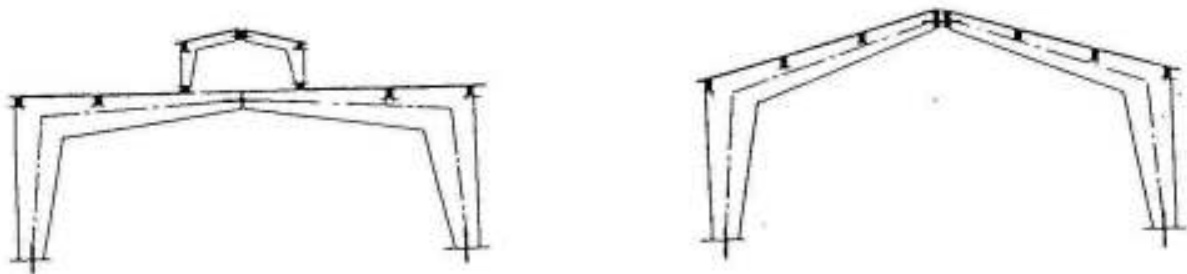


Fig. IV-4 Three-hinged frames

Temperature changes and shrinkage cause moderate stresses that can be easily resisted. Fig IV-5 shows some of the forms extensively used in reinforced concrete structures.

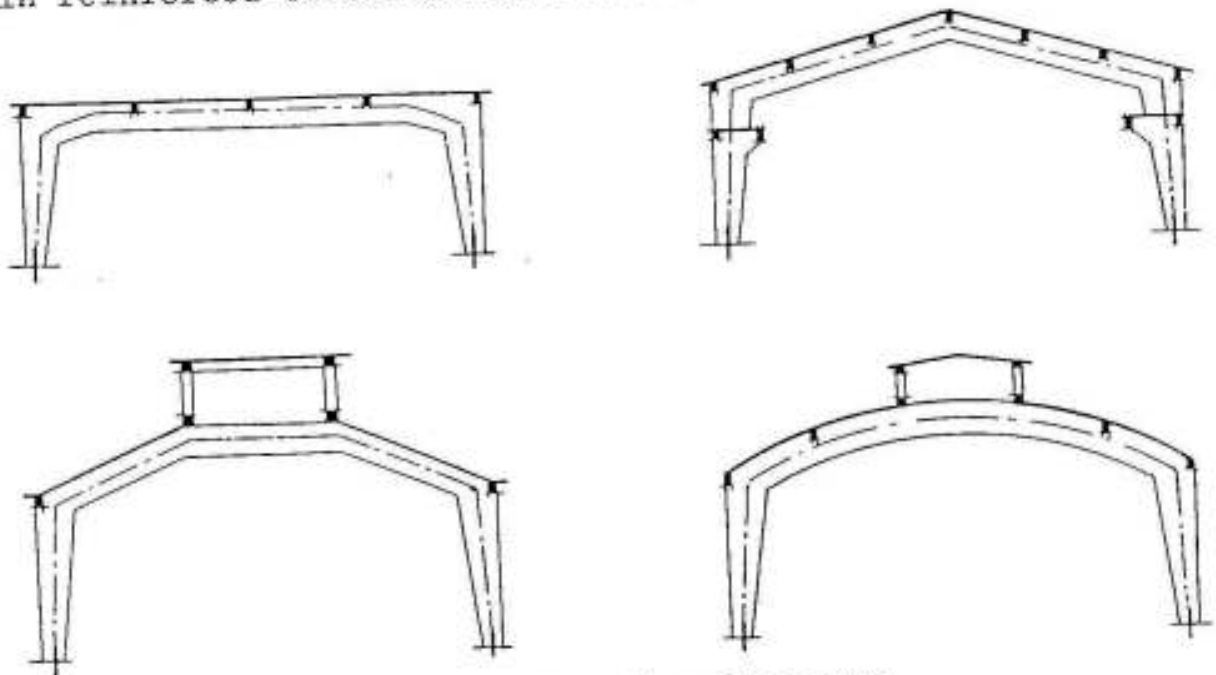


Fig. IV-5 Two-hinged frames

On good firm soils, fixed frames may be used. In this system, the internal stresses due to horizontal or vertical displacement of the supports as those due to temperature changes and shrinkage are relatively high and must be considered.

Three Hinged Frames

A three hinged frame is statically determinate. The external reactions can be determined from the conditions:

$$\sum X = 0, \sum Y = 0, \sum M = 0 \text{ and } M_c = 0$$

The example shown in fig. IV-6 gives the reactions, the connecting moments at d and e and the line of pressure of a three hinged polygonal frame.

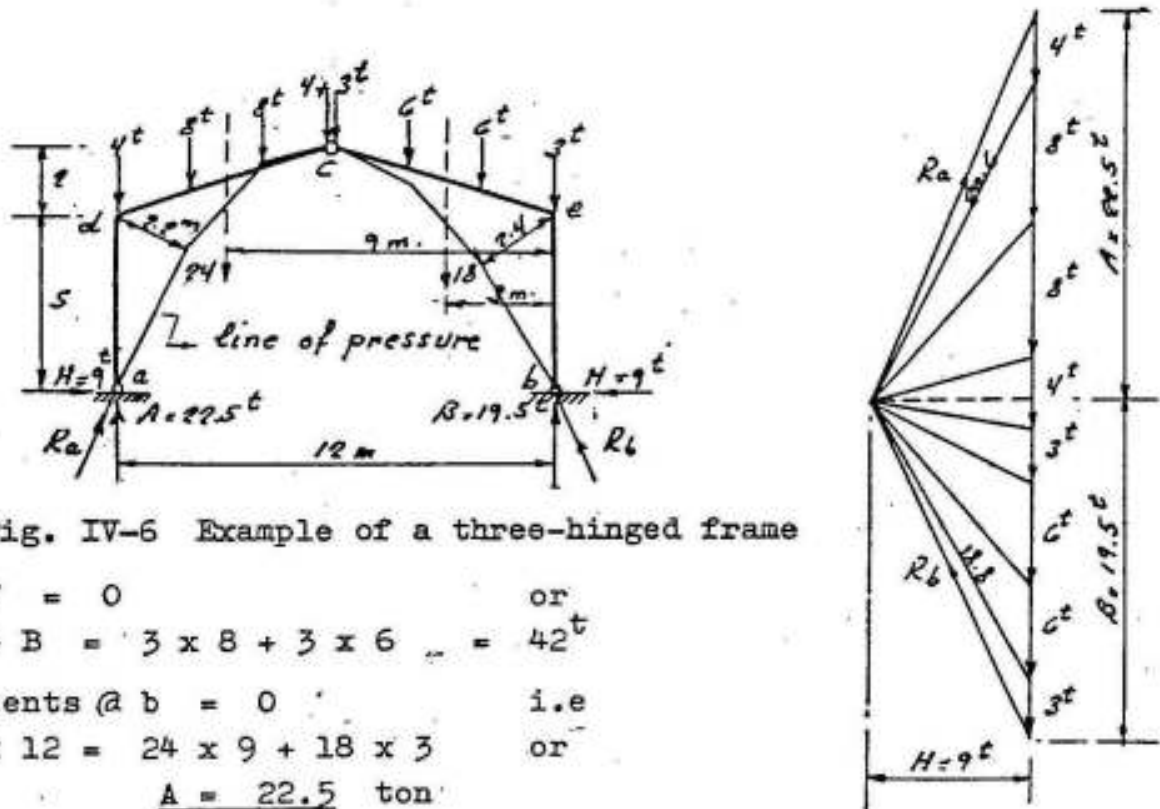


Fig. IV-6 Example of a three-hinged frame

$$\begin{aligned} \sum Y &= 0 && \text{or} \\ A + B &= 3 \times 8 + 3 \times 6 = 42^t \\ \text{Moments @ } b &= 0 && \text{i.e.} \\ A \times 12 &= 24 \times 9 + 18 \times 3 && \text{or} \\ &A = 22.5 \text{ ton} \end{aligned}$$

Therefore

$$B = 19.5 \text{ ton}$$

$$\begin{aligned} \text{Moments about } c &= 0 && \text{i.e.} \\ 22.5 \times 6 - H \times 7 - 24 \times 3 &= 0 && \text{or} \end{aligned}$$

$$H = 9.0 \text{ ton}$$

$$\text{Therefore } M_d = M_c = 9 \times 5 = 45 \text{ mt}$$

The line of pressure is the link polygon of the loads and reactions with  $R_a$  as the first ray at  $a$  and  $R_b$  as the last ray at  $b$ , it



in which

$M_0$ ,  $N_0$  &  $Q_0$  are the bending moment, normal force and shearing force of the main system due to the given loads, and  $M_1$ ,  $N_1$  and  $Q_1$  are the B.M., N.F. and S.F. of the main system due to  $H = 1$

$\alpha t l$  = horiz. displ. of main system at b due to a temperature increase of  $t$  if  $\alpha$  is the coef. of linear expansion.

The displacements  $\delta_0$  and  $\delta_1$  due to shear stresses are very small compared to those due to normal stresses and are generally neglected; furthermore, only in structures where the normal forces are relatively big and govern the design (e.g. in arches), the bending moments only are considered when calculating  $\delta_0$  and  $\delta_1$  so that

$$1 \cdot \delta_0 = \int \frac{M_0 M_1 ds}{EI} + \alpha t l$$

and

$$1 \cdot \delta_1 = \int \frac{M_1^2 ds}{EI}$$









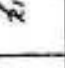



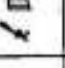


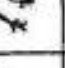

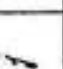

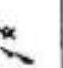



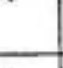

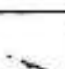


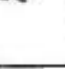
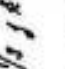









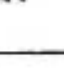

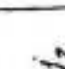
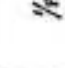
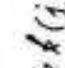
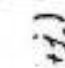

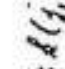
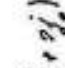

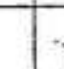



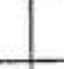
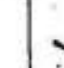
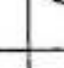




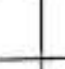
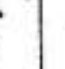

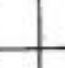

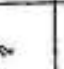

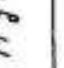


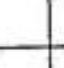
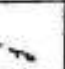

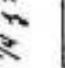
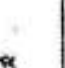
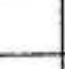

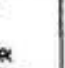
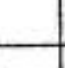


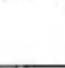



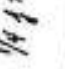



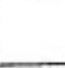

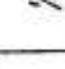
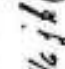
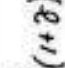


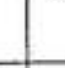
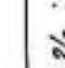

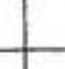
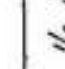
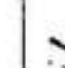
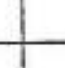
So that

$$H = - \frac{\delta_0}{\delta_1} = - \frac{\int \frac{M_0 M_1 ds}{I} + E \alpha t l}{\int \frac{M_1^2 ds}{I}}$$

When using this method of virtual work, it has to be noted that  $H$  is to be chosen in the direction satisfying the condition of elasticity. It can however be chosen in any direction (inwards or outwards), in this case the bending moments  $M_0$  and  $M_1$  are to be drawn on the tension side taking the sense of  $H$  in consideration.  $\int M_1^2 ds/I$  is always positive and  $\int M_0 M_1 ds/I$  is to be assumed positive if the  $M_0$  and the corresponding  $M_1$  diagrams are on the same side of the axis of the frame and negative if the two diagrams are on opposite sides. If the sign of  $H$  according to the previous equation is positive, then the assumed direction is correct and if it is negative, the assumed direction is to be reversed.  $\int M_0 M_1 ds$  is the area of the  $M_0$  diagram along a certain element multiplied by the ordinate of the corresponding  $M_1$  diagram at the position of the center of gravity of the  $M_0$  diagram, that is  $\int M_0 M_1 ds$  for the inclined member of length  $s$  (fig. IV-7) is given by  $A_0 y$ , whereas  $\int M_1^2 ds$  for the same element is equal to the area of the trapezoidal  $M_1$  - diagram multiplied by the ordinate of the same diagram lying at its center of gravity.



Values of  $\int M_j M_k ds = s$  terms given in table

No										$s_1$	$s_2$								$\int_j^2 ds$	
1										$\frac{1}{2} j$	$\frac{1}{2} j$	$\frac{1}{2} j$	$\frac{1}{2} j$	$\frac{1}{2} j$	$\frac{1}{2} j$	$\frac{1}{2} j$	$\frac{1}{2} j$	$\frac{1}{2} j$	$\frac{1}{2} j$	$\frac{1}{2} j$
2										$\frac{1}{2} j$	$\frac{1}{2} j$	$\frac{1}{2} j$	$\frac{1}{2} j$	$\frac{1}{2} j$	$\frac{1}{2} j$	$\frac{1}{2} j$	$\frac{1}{2} j$	$\frac{1}{2} j$	$\frac{1}{2} j$	$\frac{1}{2} j$
3										$\frac{1}{2} j$	$\frac{1}{2} j$	$\frac{1}{2} j$	$\frac{1}{2} j$	$\frac{1}{2} j$	$\frac{1}{2} j$	$\frac{1}{2} j$	$\frac{1}{2} j$	$\frac{1}{2} j$	$\frac{1}{2} j$	$\frac{1}{2} j$
4										$\frac{1}{2} j$	$\frac{1}{2} j$	$\frac{1}{2} j$	$\frac{1}{2} j$	$\frac{1}{2} j$	$\frac{1}{2} j$	$\frac{1}{2} j$	$\frac{1}{2} j$	$\frac{1}{2} j$	$\frac{1}{2} j$	$\frac{1}{2} j$
5										$\frac{1}{2} j$	$\frac{1}{2} j$	$\frac{1}{2} j$	$\frac{1}{2} j$	$\frac{1}{2} j$	$\frac{1}{2} j$	$\frac{1}{2} j$	$\frac{1}{2} j$	$\frac{1}{2} j$	$\frac{1}{2} j$	$\frac{1}{2} j$
6										$\frac{1}{2} j$	$\frac{1}{2} j$	$\frac{1}{2} j$	$\frac{1}{2} j$	$\frac{1}{2} j$	$\frac{1}{2} j$	$\frac{1}{2} j$	$\frac{1}{2} j$	$\frac{1}{2} j$	$\frac{1}{2} j$	$\frac{1}{2} j$
7										$\frac{1}{2} j$	$\frac{1}{2} j$	$\frac{1}{2} j$	$\frac{1}{2} j$	$\frac{1}{2} j$	$\frac{1}{2} j$	$\frac{1}{2} j$	$\frac{1}{2} j$	$\frac{1}{2} j$	$\frac{1}{2} j$	$\frac{1}{2} j$
8										$\frac{1}{2} j$	$\frac{1}{2} j$	$\frac{1}{2} j$	$\frac{1}{2} j$	$\frac{1}{2} j$	$\frac{1}{2} j$	$\frac{1}{2} j$	$\frac{1}{2} j$	$\frac{1}{2} j$	$\frac{1}{2} j$	$\frac{1}{2} j$
9										$\frac{1}{2} j$	$\frac{1}{2} j$	$\frac{1}{2} j$	$\frac{1}{2} j$	$\frac{1}{2} j$	$\frac{1}{2} j$	$\frac{1}{2} j$	$\frac{1}{2} j$	$\frac{1}{2} j$	$\frac{1}{2} j$	$\frac{1}{2} j$
10										$\frac{1}{2} j$	$\frac{1}{2} j$	$\frac{1}{2} j$	$\frac{1}{2} j$	$\frac{1}{2} j$	$\frac{1}{2} j$	$\frac{1}{2} j$	$\frac{1}{2} j$	$\frac{1}{2} j$	$\frac{1}{2} j$	$\frac{1}{2} j$
11										$\frac{1}{2} j$	$\frac{1}{2} j$	$\frac{1}{2} j$	$\frac{1}{2} j$	$\frac{1}{2} j$	$\frac{1}{2} j$	$\frac{1}{2} j$	$\frac{1}{2} j$	$\frac{1}{2} j$	$\frac{1}{2} j$	$\frac{1}{2} j$



Tables on page 44 & 45 give the values of  $\int M_j M_k ds$  as a general form for  $\int M_0 M_1 ds$  and  $\int M_1^2 ds$  along an element of length  $s$  for constant moment of inertia and different diagrams of  $M_j$  and  $M_k$ .

The magnitude of the horizontal thrust  $H$  and the corresponding internal forces depend on the exact form of the axis of the frame and the moment of inertia of the different sections; both depend on the dimensions of the sections which in turn depend on the internal forces. This means that the final dimensions of a frame depend on the preliminary dimensions for which the axis and the moments of inertia have been determined. The solution can be assumed correct when the final results are the same as the preliminary. Such a coincidence can be achieved if we proceed as follows: (Fig IV-8).

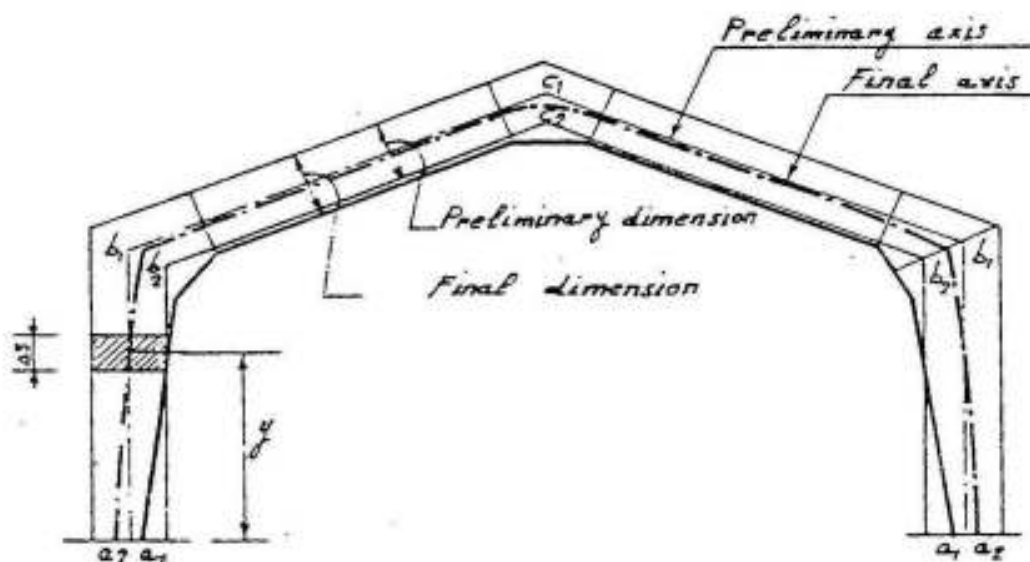
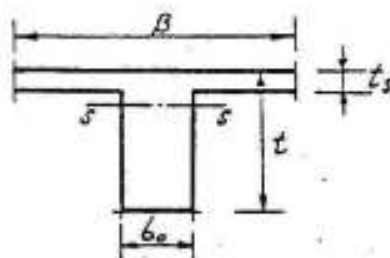


Fig. IV-8 Axis of a two-hinged frame

- 1) For any frame of general layout assume preliminary dimensions and axis based on previous experience or similar structures.
- 2) Calculate the own weight of the different elements and determine the dead and live loads.
- 3) Compute the moments of inertia of the elements of the frame for the assumed dimensions. The moment of inertia of girders monolithically cast with the slabs may be calculated for a plain concrete T-section with breadth of flange  $B = 6t_s + b_0$ . Such values are given in the following table:

Moment of Inertia of T-Sections

$$I_s = \mu B t^3$$



Values of  $10^4 \mu$

$\frac{b_e}{t}$ B	$t_s/t$										
	.05	.10	.15	.20	.25	.30	.35	.40	.50	.55	.60
.05	97	109	111	111	112	115	122	132	169	196	231
.06	110	125	129	129	129	132	137	147	181	207	241
.07	122	140	145	146	146	148	152	161	193	218	251
.08	133	154	161	162	162	163	167	175	205	229	260
.09	143	167	176	178	178	182	182	189	217	240	270
.10	154	179	190	192	192	193	196	202	228	250	279
.11	164	192	203	206	207	207	209	215	240	260	288
.12	173	204	216	220	221	221	223	227	251	271	298
.13	182	215	229	233	234	234	236	240	262	281	307
.14	191	226	241	246	247	247	248	252	272	290	316
.15	200	236	252	258	260	260	261	264	283	300	324
.16	209	245	263	270	272	272	273	276	293	310	333
.17	217	255	273	282	284	284	285	287	304	319	342
.18	225	265	284	293	296	296	295	298	314	329	350
.19	234	274	295	304	307	308	307	309	324	338	359
.20	242	283	304	314	318	319	319	320	333	347	367
.22	258	301	323	334	339	340	340	341	353	365	384
.24	275	318	342	354	359	360	360	361	371	382	400
.26	291	334	360	373	378	380	380	381	389	399	417
.28	306	350	376	390	397	399	399	400	407	416	431
.30	320	366	392	407	415	417	418	418	424	432	446
.32	336	380	408	424	432	435	435	435	441	448	461
.34	352	396	424	440	448	452	452	452	457	464	475
.36	367	410	438	455	464	468	468	469	473	479	490
.38	382	426	453	470	480	484	485	485	488	497	504
.40	397	441	468	485	495	499	500	500	503	508	517
.42	412	454	482	499	509	514	515	515	518	522	530
.44	427	468	496	513	523	528	530	530	532	536	544
.46	441	482	509	527	537	542	544	544	546	549	557
.48	456	496	523	540	551	556	558	558	560	563	569
.50	470	509	533	553	564	569	571	572	573	576	582
.55	505	544	567	585	596	601	604	604	605	607	612
.60	544	575	599	616	626	631	634	635	636	637	641
.65	581	609	630	645	655	660	663	664	664	665	668
.70	616	642	660	674	683	688	691	691	692	692	695
.75	652	675	691	702	709	714	717	718	718	718	720
.80	689	706	720	729	736	740	742	743	743	743	744
.90	761	770	779	782	786	788	789	790	790	790	791
1.0	833	833	833	833	833	833	833	833	833	833	833

- 4) Calculate the statically indeterminate value and the corresponding internal forces. The results of some simple forms of frames are given at the end of this chapter; they simplify these calculations.
- 5) Determine the dimensions required to resist the calculated internal forces, which may be modified to suit the expected final form of the frame.
- 6) For the new dimensions draw the new axis and calculate the moment of inertia of the different sections. In this stage, it is recommended to divide the frame to a convenient number of strips of length  $\Delta s$  and to determine H from the relation:

$$H = - \frac{\sum \frac{M_o M_1 \Delta s}{I} + E a t l}{\sum \frac{M_1^2 \Delta s}{I}} = - \frac{\sum \frac{M_o y \Delta s}{I} + E a t l}{\sum \frac{y^2 \Delta s}{I}}$$

The calculations may be put in table form as follows:

Element No	$\Delta s$	b or B	t	I	y	$y^2$	$y^2 \Delta s / I$	$M_o$	$M_o y \Delta s / I$
1									
2									
3									
4									
.									
.									
.									
							$\Sigma = \dots$		$\Sigma = \dots$

- 7) The calculations are to be repeated until the final dimensions are the same as the preliminary. After some experience, each step can be done once only.

In big frames, the real axis and the variation of the moment of inertia are to be considered in the calculations, otherwise big errors are liable to take place as shown in fig IV-9 in which the corner moments will be increased by values that may amount to 25%, in which case the field moments are decreased by about 20% due to the increase of I towards the corners. (Fig IV-9).

The steps of the design will be shown in the following simple example.

It is required to design the main supporting element of a hall which is to be covered by a reinforced concrete flat roof, if it is 20 ms wide, 40 ms long and 20 ms clear height.

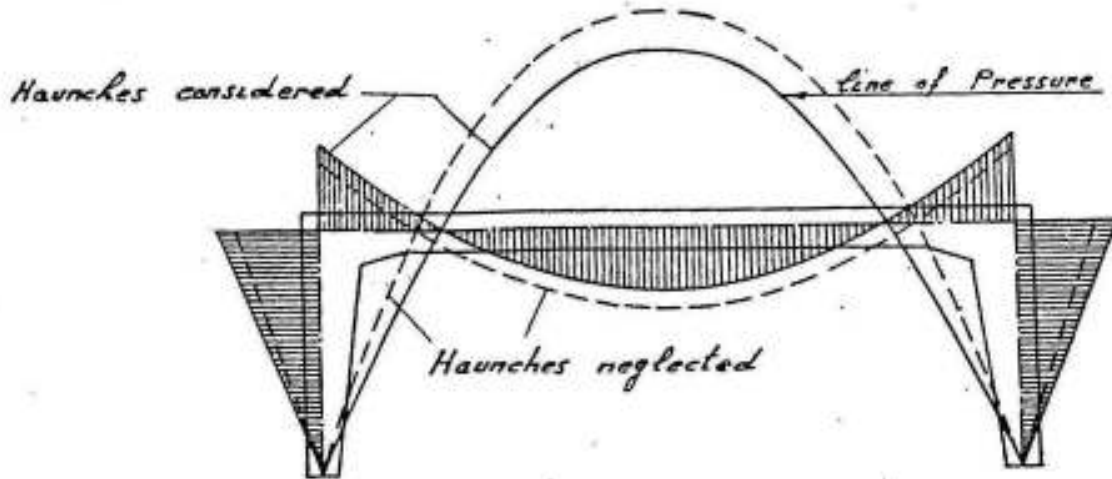


Fig. IV-9 Effect of haunches on internal forces

The main supporting element can be chosen as a rectangular frame, 20 ms span arranged every 5.0 ms. In order to get a reasonable slab  $\sim 10$  cms thick, secondary beams 20 x 40 cms will be arranged every  $\sim 4.0$  ms. Accordingly, the general layout of the different supporting elements will be as shown in fig IV-10.

As a first estimate, assume the depth of the main girder of the frame  $\sim 1/14$  of the span i.e.  $\sim 1.40$  ms, the column may also be assumed 1.40 m at the top and 0.6 m at the bottom. The breadth of both girder and columns  $b_0$  can be chosen = 0.4 m. For the preliminary calculations, the load on the frame from the roof may be assumed as uniformly distributed.

$$\begin{aligned} \text{Slab load} &= \text{own weight} + \text{roof cover} + \text{live load} \\ &= 250 + 150 + 100 = 500 \text{ kg/m}^2 \end{aligned}$$

$$\begin{aligned} \text{Equivalent uniform load due to own weight of secondary beams} \\ &= 0.2 \times 0.3 \times 2500/4 = 150/4 = 38 \text{ "} \end{aligned}$$

$$\text{Roof load} = (500 + 38) \times 5 = 538 \times 5 = 2700 \text{ kg/m}$$

$$\text{Own weight} = 0.4 \times 1.3 \times 2500 = 1300 \text{ "}$$

$$\text{total} = 4000 \text{ "}$$

$$\begin{aligned} \text{Breadth of flange of main girder } B &= 6 t_s + b_0 = 6 \times 10 + 40 = 100 \text{ cm} \\ \text{Area of cross-section " " } A &= 100 \times 10 + 40 \times 130 = 6200 \text{ cm}^2 \end{aligned}$$

Arm of center of gravity from bottom  $y_o = \frac{1000 \times 135 + 40 \times 130 \times 65}{6200} = 76 \text{ cms}$

The moment of inertia  $I_2$  can be determined according to table given on page 47, hence

for  $b_o/B = \frac{40}{100} = 0.4$ ,  $t_s/t = 10/140 = 0.071$   $\mu = 0.0415$

Therefore

$$I_2 = \mu B t^3 = 0.0415 \times 1.0 \times 1.4^3 = 0.114 \text{ m}^4$$

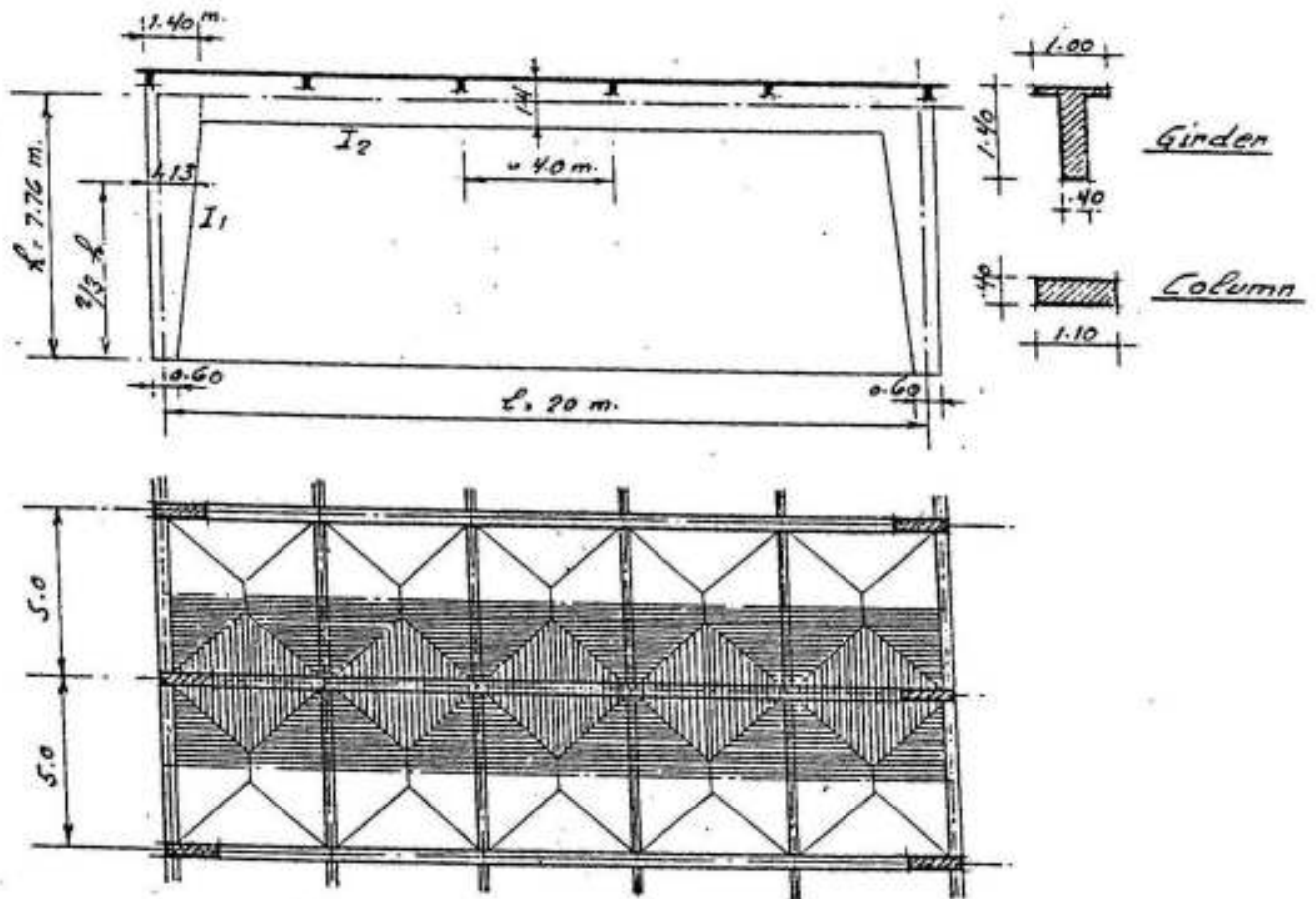


Fig. IV-10 Example of a two-hinged frame

For the preliminary calculations, one may assume the moment of inertia of the column as constant and compute it for an average section at  $2/3 h$  i.e.  $0.40 \times 1.13^3$ , thus

$$I_1 = b t^3/12 = 0.4 \times 1.13^3/12 = 0.048 \text{ m}^4$$

The relative stiffness is therefore given by

$$\kappa = \frac{h}{l} \cdot \frac{I_2}{I_1} = \frac{7.76}{20} \times \frac{0.114}{0.048} = 0.925$$

The connecting moment  $M_c$  is therefore given by:

$$M_c = - \frac{pl^2}{4(3+2\kappa)} = - \frac{pl^2}{4(3+2 \times 0.925)} = - \frac{pl^2}{19.4} = - \frac{4 \times 20^2}{19.4} = - 82.5 \text{ mt}$$

Due to the increase of the depth of the columns towards the upper corner,  $M_c$  will be increased by say 10%. Such an increase is however allowed due to the possible redistribution of the maximum moments. Hence  $M_c = 1.1 \times 82.5 = 90 \text{ mt}$

The horizontal thrust  $H$  is therefore given by:

$$H = M_c / h = \frac{90}{7.76} = 11.6 \text{ tons}$$

The field moment  $M_m$  is :

$$M_m = \frac{pl^2}{8} - M_c = \frac{4 \times 20^2}{8} - 90 = 110 \text{ mt}$$

The final check will be done for the dimensions computed to resist the following internal forces:

- |                             |                        |  |
|-----------------------------|------------------------|--|
| 1) Middle section of girder | $M_m = 110 \text{ mt}$ | $N = 11.6^t \text{ (comp.)}$           |
| 2) Sections at sup. " "     | $M_c = 90 \text{ mt}$  | $N = 11.6^t \text{ "}$                 |
| 3) Top section of column    | $M_c = 90 \text{ mt}$  | $N = 4 \times 10 = 40^t \text{ comp.}$ |

The chosen dimensions are just sufficient.

For the final calculations of the internal forces, the dimensions, the reinforcements, the stresses ... etc will be done for the real axis taking the variation of the moment of inertia in consideration.  $M_o$  is to be calculated for the direct uniform load from the slab plus its own weight and the concentrated reactions of the secondary beams. (Fig IV-10&11). It is preferable to divide the frame into strips of

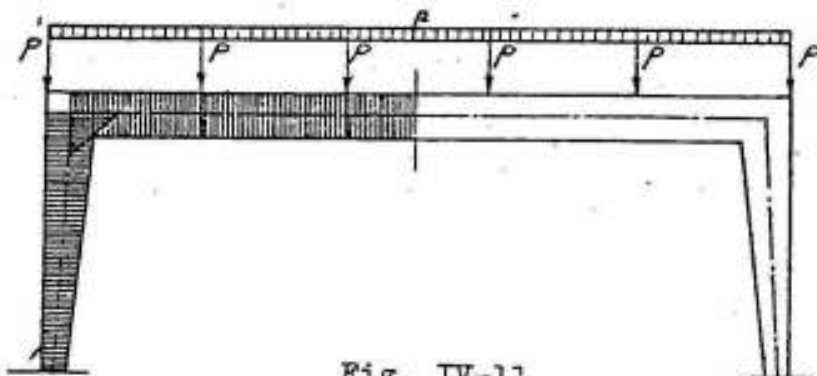


Fig. IV-11

convenient length and to tabulate the results as shown on page 48



The direct uniform load is given by:

$$p = 0.5 \times 4 \times 500 + 0.4 \times 1.3 \times 2500 = 1000 + 1300 = 2300 \text{ kg/m}$$

The average load breadth on the secondary beams is  $\frac{1}{2} \times \frac{5}{5} = 2.4 \text{ ms}$

So that the concentrated loads are given by :

$$P = (2.4 \times 500 + 0.2 \times 0.3 \times 2500) \times 5 = (1200 + 150) \times 5 = 1350 \times 5 = 6750 \text{ kgs}$$

The moments of inertia of the girder and columns at the corner can be computed for the enlarged section shown in fig IV-11.

Assuming that the required tension reinforcement at the middle of the girder is  $10\phi 25$  and at the corner is  $7\phi 25$  then , the typical details can be done as shown in fig IV-12.

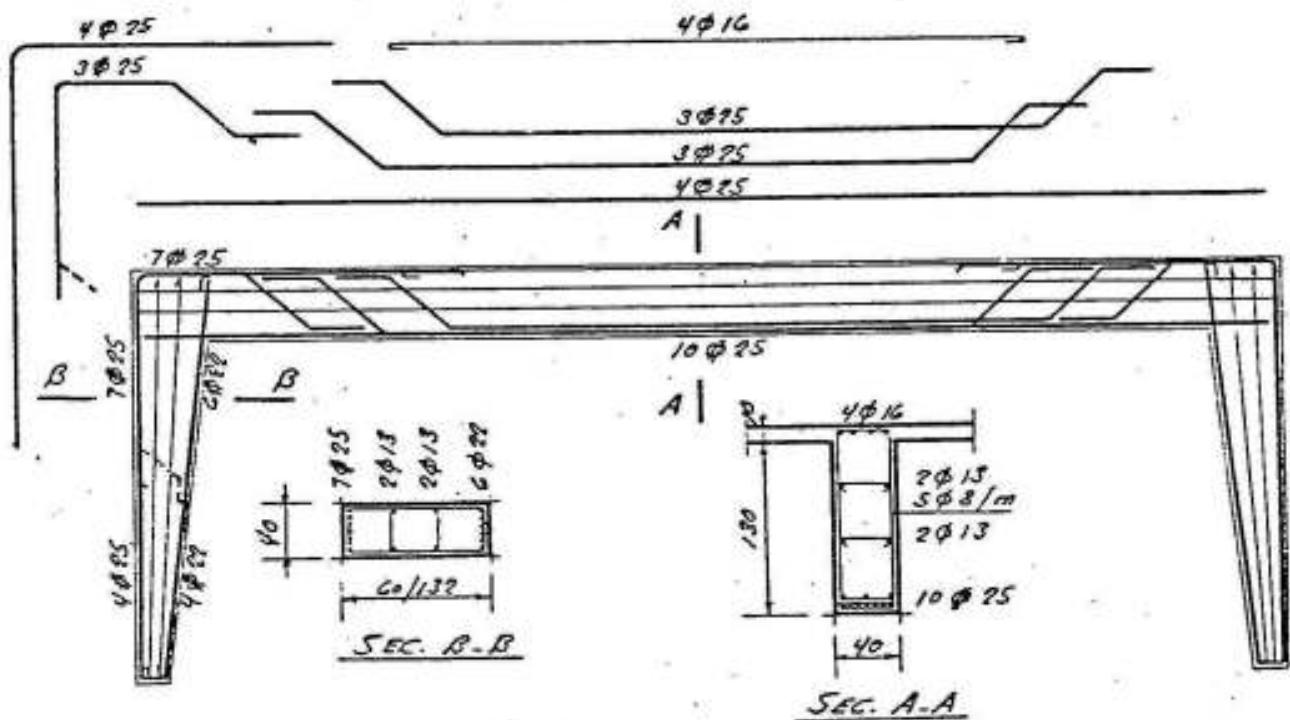
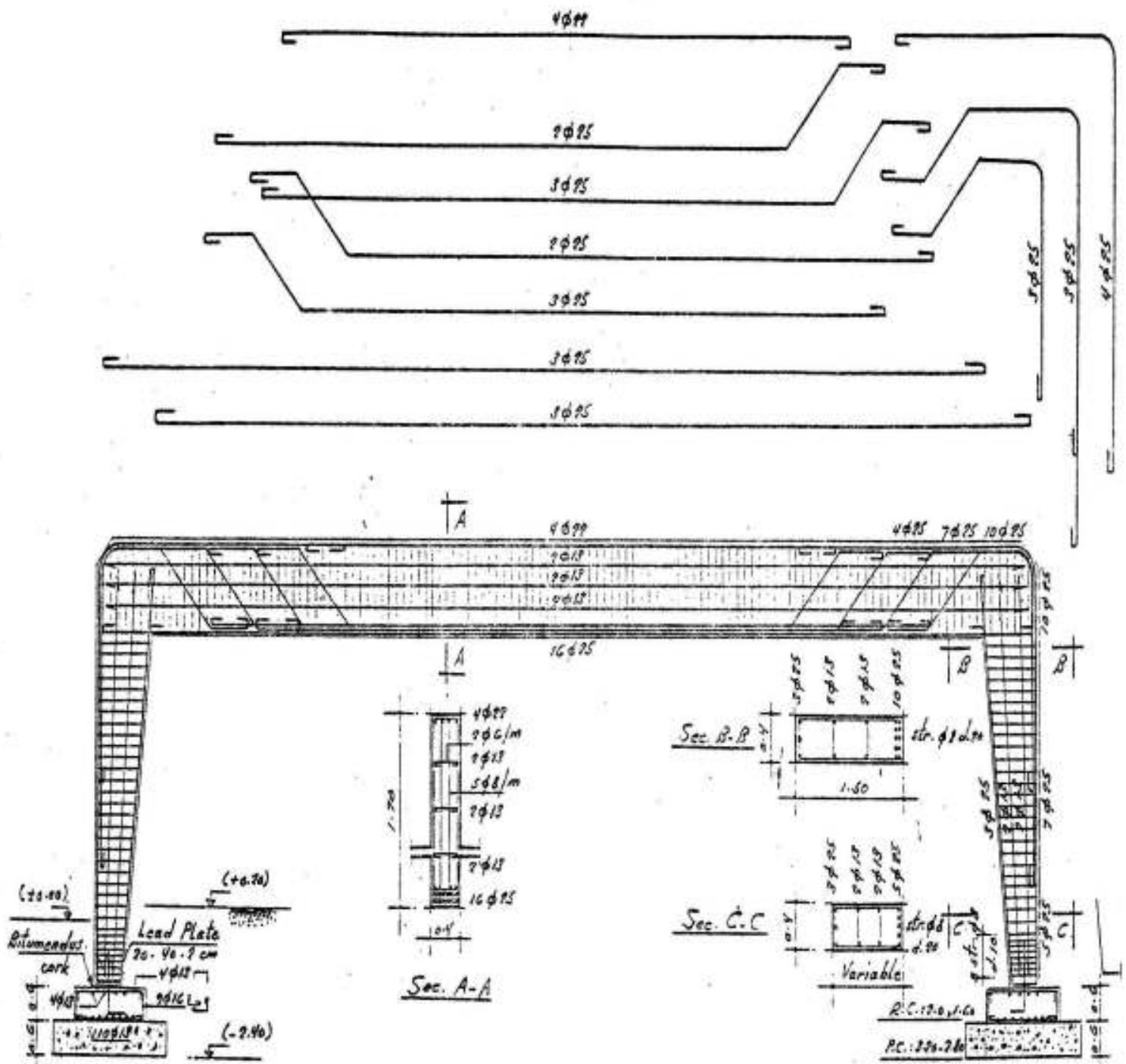


Fig. IV-12 Reinforcements of a two-hinged frame

It is recommended to resist the corner moment of the frame by the tension reinforcements of the column and not to introduce the bent bars of the girder in the columns. It is also not necessary to bend the tension reinforcements in the columns - shown dotted - because the normal and diagonal tensile stresses are generally low, due to the existence of big normal compressive forces, moreover, such an arrangement causes undesirable movements which may loosen the reinforcement



PAINTS AND CHEMICAL INDUSTRIES Co.

Details of reinforcement of main frames

Fig. IV-13



**Curing** concreting operations.

Shrinkage reinforcements  $\phi 10$  mm @ 30 cms or  $\phi 13$  mm @ 40 cms are essential to prevent the formation of vertical cracks between the stirrups.

The stirrups at the hinges in a height equal to the depth of the column foot are to be doubled\* to resist the tensile horizontal splitting force due to the concentration of the reaction in the hinge.

We give in the following, examples of some frames used as main supporting elements in relatively big halls:

1) The rectangular frame of the main factory hall of the "Paints and Chemical Industries at Matariah", shown in figure IV-13.

The frames are 24 ms. span spaced every 4 ms. and support a saw tooth roof in the form shown in figure VII-16. In order to have a convenient slope for the roof slab and sufficient height for the windows the depth of the main girder was chosen 2.0 ms. which is much bigger than 1/16 of the span. Such a choice led to relatively thin columns due to small connecting moments.

2) The main frames supporting the roof of the main studio at the T.V. building, Cairo, (fig IV-14); the span and spacing are 36.0 and 4.9 ms respectively. The columns of the frames were designed to support the vertical reactions of a simple roof steel truss, for this reason, they were 0.5 x 1.6 m only and no special provisions were made to resist big horizontal forces. After executing the cast in place plain concrete mechanical pile foundations for the previous condition, it was decided to cover the studio by a reinforced concrete roof. The space available for the main girders was 3.40 ms which is the height between the upper two floors. It was also required to make the necessary provisions for constructing a suspended ceiling at the level of the lower floor to be used for lighting mounting and control purposes. Provisions for big air conditioning ducts were specified.

Due to these special conditions, the girders were assumed as partially fixed to the columns. The connecting moments were limited by the maximum moment of resistance of the columns and the maximum moment and horizontal forces that can be resisted by the existing pile foundations.

The span being relatively big, all possible provisions were taken to

---

\* The determination of the required area will be given later.

reduce the dead loads of the roof slab and the own weight of the main girders. For this purpose, the main girders were chosen such that they give maximum resistance and minimum weight by choosing a web 25 cms thick; the enlarged width at the bottom was necessary to have sufficient space for the tension steel. The openings at the middle of the span are arranged for the air-conditioning ducts and to reduce the internal forces due to the own weight of the girder. The big haunches between the web and the roof slab were necessary to resist the compressive stresses of the girder. Due to the big moment of inertia of the roof slab at the girders, its field moments were very small and it was possible to construct it as one way slab, 8 cms thick. In order to prevent the lateral buckling of the web vertical stiffeners were arranged. The breadth of the main girder is increased on the two sides at the zones of high shear stresses and to have a smooth gradual transition from column to girder. The lower connecting cross-beams are arranged to simplify the construction of the required suspended ceiling.

The fixing moments of the girder are resisted by the tension column reinforcements; these being  $20 \Phi 25$  mm then: (See fig IV-15).

$$A_s = 100 \text{ cm}^2 \quad \sigma_s = 2 \text{ t/cm}^2$$

$$T = A_s \sigma_s = 100 \times 2 = 200 \text{ t}$$

Resultant  $F$  is given by:

$$F = T\sqrt{2} = 200\sqrt{2} = 282 \text{ t}$$

This value is relatively big and acts on a length  $= 1/4(2\pi r)$ , the smaller the radius  $r$ , the higher is the concentration of the force  $F$  and the bigger the splitting tensile stresses  $\sigma_{sp}$ . In order to resist  $\sigma_{sp}$ , the diagonal corner bars shown in fig IV-14 are arranged.

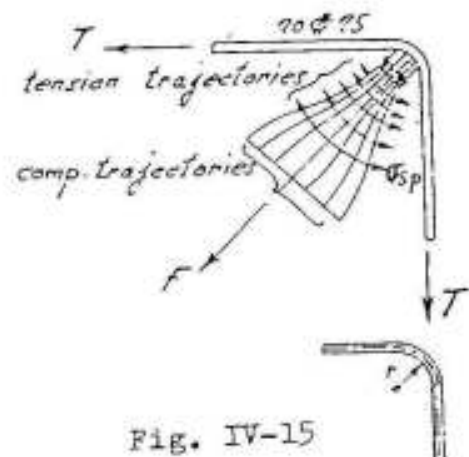


Fig. IV-15

2) Fig IV-16 shows the details of a polygonal frame used as the main supporting element of a factory at Helwan. The arrangement of the reinforcements follows the same general simple principles stated before, that is, the tension in the outside fiber of the corners between the column and the girder is resisted by the reinforcements of the column and no reinforcements are introduced from the girder in the columns.

The maximum field moment of this frame takes place at the crown

causing maximum tensile stresses at the lower fiber of the section. These tensile stresses are resisted by the main tension reinforcements c, d, e and f which must be sufficiently anchored in the compression zone with a minimum anchorage length of  $40\phi$ .

Fig IV-17 shows that if the tension reinforcements are continuous over a sharp corner as shown in (a), failure of the lower cover will

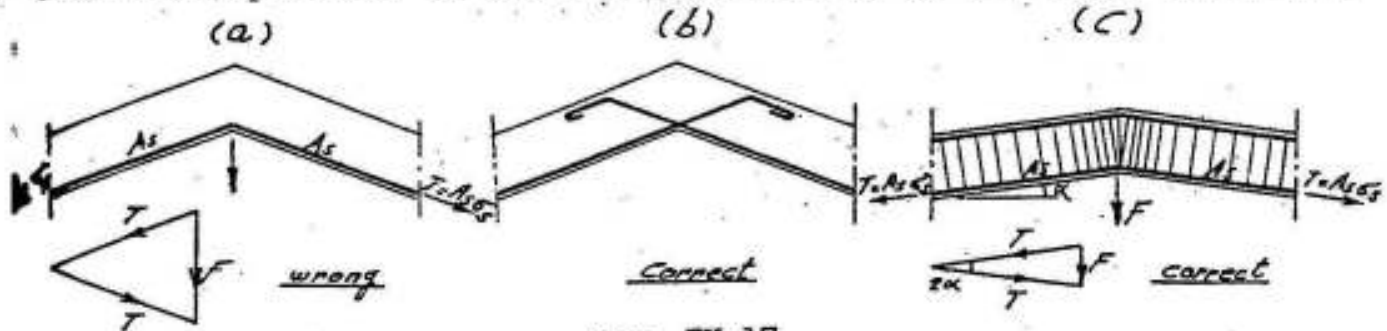


Fig. IV-17

take place due to the action of the resultant force  $F$ . If  $\alpha$  is small as in (c), then  $F$  is small and can be resisted by additional stirrups placed at the crown of the girder. Their area of cross-section  $A_{st}$  can be calculated as follows:

$$F = 2 T \sin \alpha = 2 A_s \sigma_s \sin \alpha$$

If the allowable tensile stress in the stirrups is  $\sigma_{st}$ , then

$$A_{st} \sigma_{st} = 2 A_s \sigma_s \sin \alpha$$

or

$$A_{st} = A_s \cdot 2 \frac{\sigma_s}{\sigma_{st}} \sin \alpha$$

However, if the tension reinforcements change their direction on an arc of a circle with radius  $r$ , then every stirrup must be able to resist a tensile force  $F$  due to this change. Assuming that  $\sin \alpha \approx \tan \alpha$ , then, according to fig IV-18, we get

$$F/T = s/r \quad \text{but} \quad T = A_s \sigma_s$$

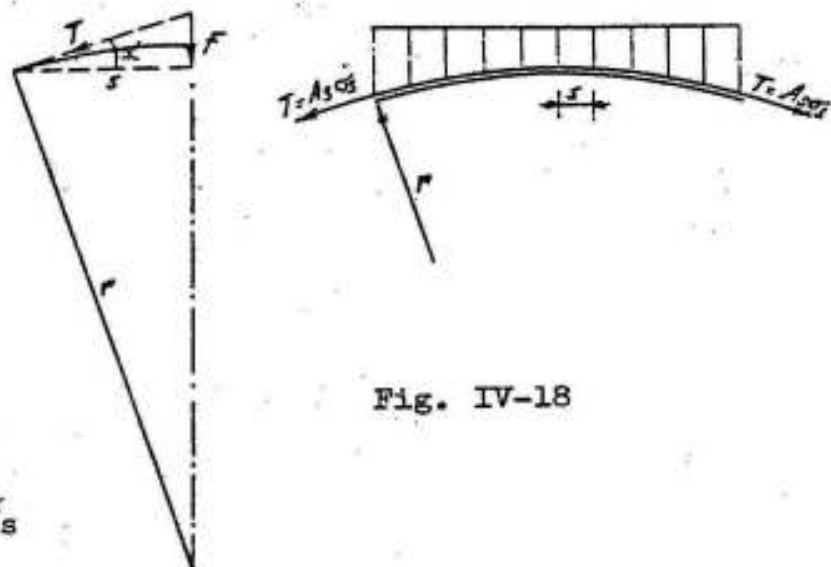
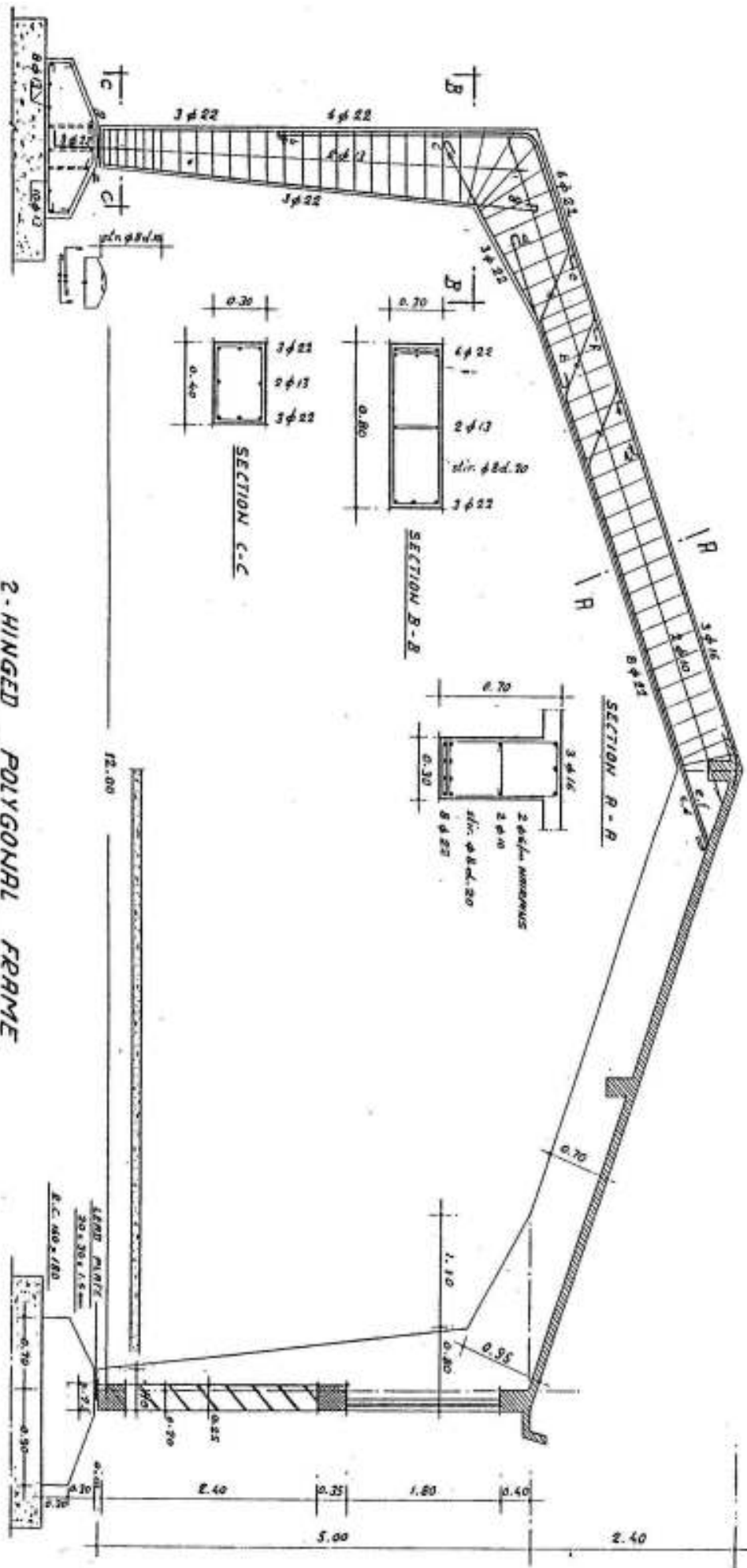


Fig. IV-18



**2-HINGED POLYGONAL FRAME**

PLF. IV-16

then

$$F = A_{st} \sigma_{st} = A_s \sigma_s s/r$$

$$\text{and } A_{st} = \frac{A_s s}{r} \cdot \frac{\sigma_s}{\sigma_{st}}$$

In frames with sharp corners at positions of maximum field moment for example point c of figure IV-19, many designers arrange a haunch c that shown in figure IV-19, but as the moments at points c' have nearly

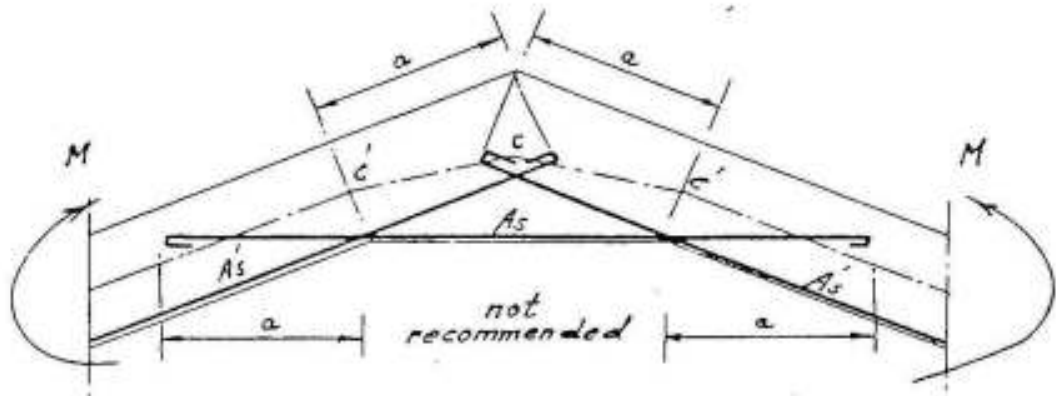


Fig. IV-19

the same magnitude as that at c, then the horizontal and the inclined reinforcements  $A_s$  and  $A_s'$  will be of the same order and need sufficient anchorage lengths  $a$  as shown. Such an arrangement includes a big waste in the reinforcements and therefore not recommended. A simple corner as that shown in figure IV-17b is more convenient.

However, in corners where the internal compressive forces  $C$  give an outward resultant  $F$ , special stirrups of area  $A_{st}$  must be arranged to resist it. Assuming the allowable stress of the stirrups  $\sigma_{st}$ , then according to figure IV-20, we get

$$A_{st} = A_s \cdot 2 \frac{\sigma_s}{\sigma_{st}} \sin \alpha$$

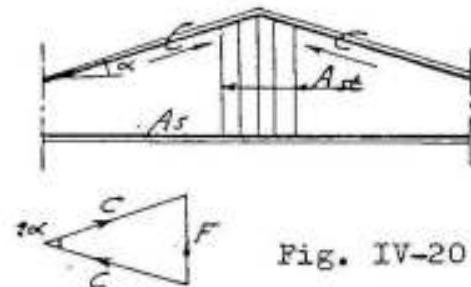


Fig. IV-20



## Two Hinged Frame With A Tie

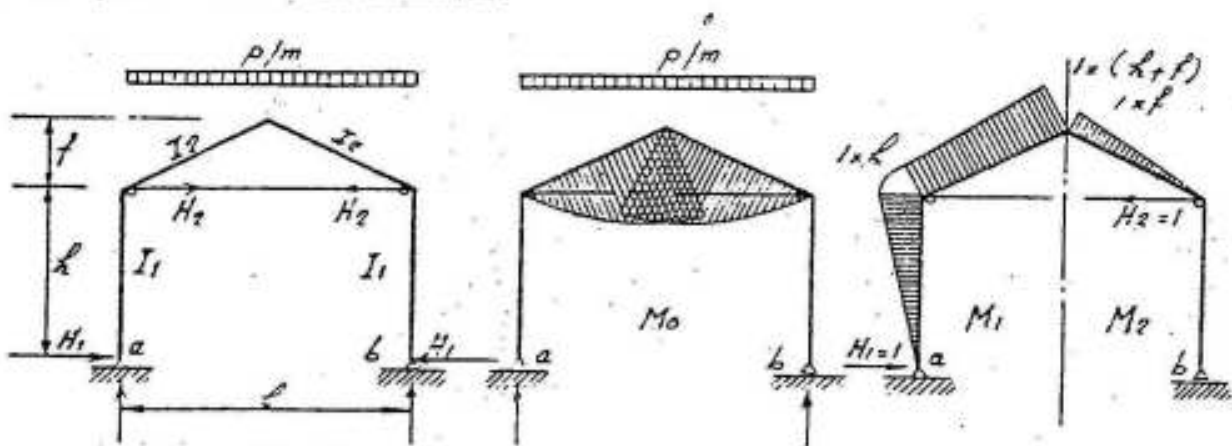


Fig. IV-21 Analysis of a two-hinged frame with a tie

A two hinged frame with a tie as shown in figure IV-21 is twice statically indeterminate. If the statically determinate simple frame with a roller at b and tie cut is chosen as main system, the conditions of elasticity will be:

- 1) The horizontal displacement  $\delta_1$  of point b equals zero, or

$$\delta_1 = 0$$

- 2) The relative horizontal displacement of the two ends at the cut section of the tie  $\delta_2$  must be equal to the elongation of the tie under the effect of the load  $H_2$ , or

$$\delta_2 = -H_2 l / A_t E_t$$

in which  $A_t$  and  $E_t$  are the effective area of cross-section and modulus of elasticity of the tie. If the tie is made of reinforced concrete and is subject to tensile stresses that cause cracks in the concrete, then  $A_t$  and  $E_t$  are the area of cross-section and the modulus of elasticity of the steel in the tie. The negative sign is introduced in the equation because  $H_2$  acts in a direction opposite to  $\delta_2$ .

The statically indeterminate values are  $H_1$  at the lower hinges and  $H_2$  in the tie.

The equations of elasticity are therefore:

$$\delta_1 = 0 = \delta_{10} + H_1 \delta_{11} + H_2 \delta_{12}$$

$$\delta_2 = -H_2 l / A_t E_t = \delta_{20} + H_1 \delta_{21} + H_2 \delta_{22} \quad \text{or}$$

$$0 = \delta_{20} + H_1 \delta_{21} + H_2 (\delta_{22} + l / A_t E_t)$$

in which

$$\delta_{10} = \int M_0 M_1 ds / EI$$

= the horizontal displacement of the main system at the level of the lower hinges due to load

$$\delta_{20} = \int M_0 M_2 ds / EI$$

= the horiz. displ. of the main system at the level of the tie due to load

$$\delta_{11} = \int M_1^2 ds / EI$$

= the horiz. displ. of the main system at the level of the lower hinge due to  $H_1 = 1$

$$\delta_{22} = \int M_2^2 ds / EI$$

= the horiz. displ. of the main system at the level of the tie due to  $H_2 = 1$

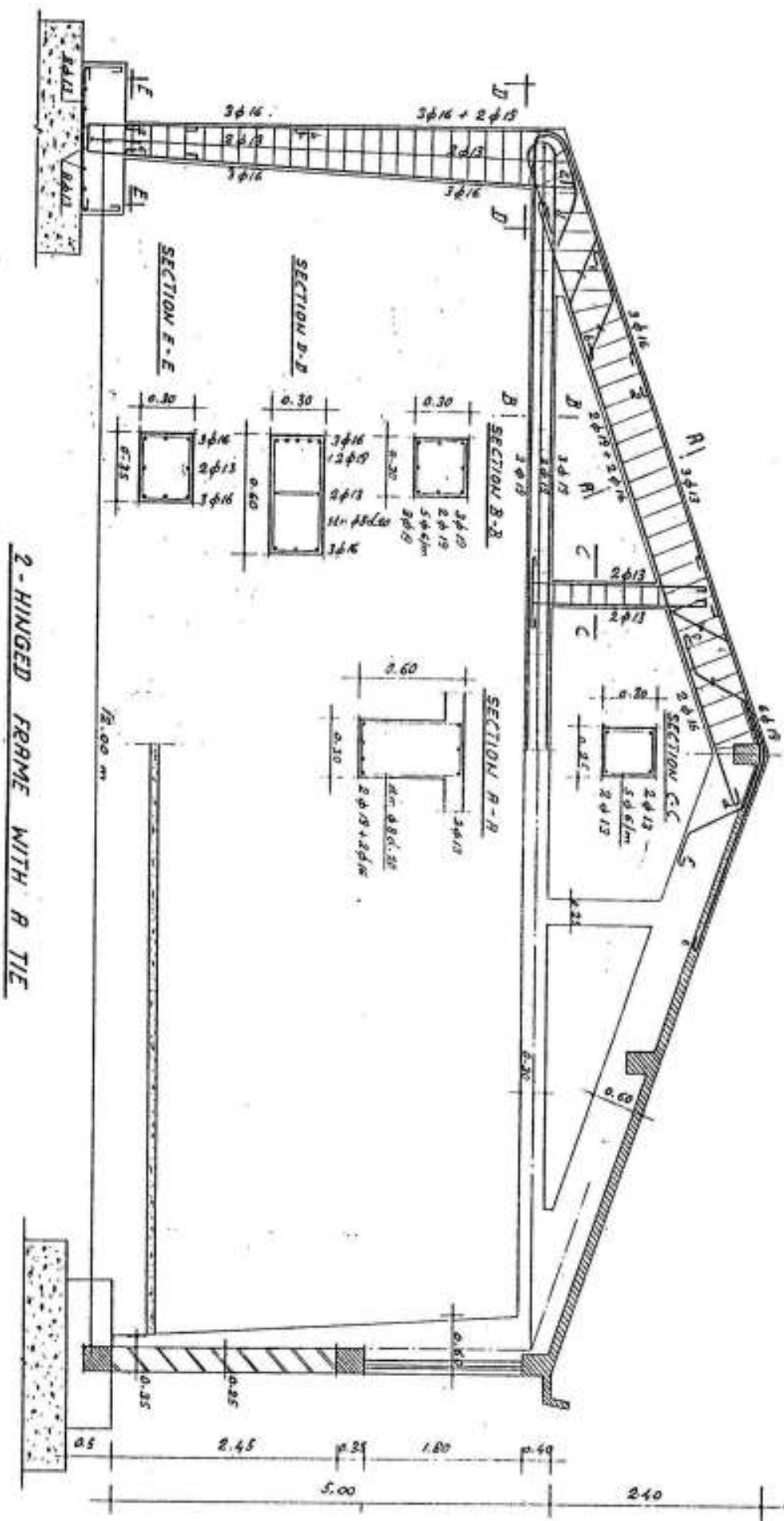
$$\delta_{12} = \delta_{21} = \int M_1 M_2 ds / EI$$

= the horiz. displ. of the main system at the level of the lower hinges due to  $H_2 = 1$

= the horiz. displ. of the main system at the level of the tie due to  $H_1 = 1$

The values of the elastic displacements  $\delta$  are very small and the magnitude of  $H_1$  and  $H_2$  may be subject to serious errors if the values of  $\delta$  are not exactly calculated and if the equations of elasticity are solved by approximate methods (e.g. by the slide rule).

In a frame adceb hinged at a & b and with a rigid tie de, figure IV-22, the elastic deformation  $\delta_2$  of the tie is equal to zero and  $H_2$  is much bigger than  $H_1$ . Moreover, if the elastic deformation of dc and ce is neglected, then c will be fixed in space relative to d and e. In this manner, the frame adceb with the rigid tie de subject to symmetrical load can be considered as a continuous beam of spans  $ad = h$ ,  $dc = ce = s$  and  $eb = h$  in which the two spans dc and ce are loaded. The bending moments at corners d, c and e are negative and the magnitude of the maximum moments is much smaller than in a frame without tie. Fig IV-22 shows the limiting cases of the horizontal thrusts and bending moments of a polygonal frame; case a shows the bending moments and line of pressure of a frame without a tie, whereas case b shows a frame with a rigid tie. Bending moments of frames with elastic ties lie between the shown two limiting cases.



2-HINGED FRAME WITH R TIE

Fig IV-23 shows the details of a frame with a tie. The reinforcements of the tie must be carefully anchored to the corner of the frame; the anchorage length, measured beyond the point of intersection of column, girder and tie, must satisfy the requirements of the code (min.  $40\phi$ ). In order to prevent the sagging of the tie, hangers at convenient distances ( $3-4ms$ ) must be arranged.

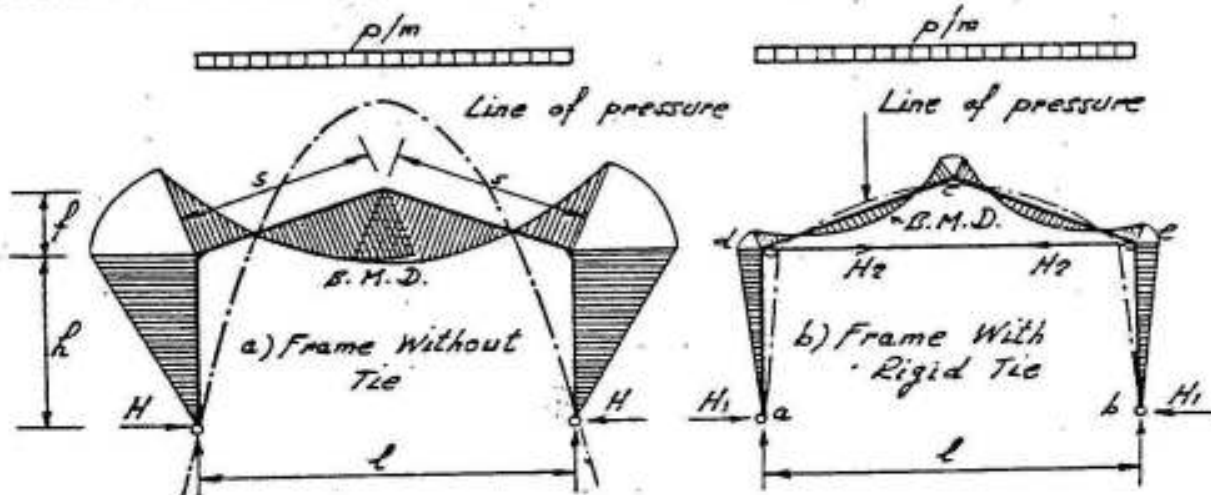


Fig. IV-22 Effect of ties on two-hinged frames

Because of the small horizontal thrust at the lower hinges, the columns may be directly connected to their footing.

A rigid tie at the top of the columns gives a better distribution of the internal forces in the columns and the girder although this does not necessarily mean a more economic solution because of the complicated form work and the big amount of steel in the tie and hangers. It gives however a smaller horizontal thrust on the foundations.

A frame without a tie is simpler and architecturally more acceptable than a frame with a tie and hangers.

If the foundations of a frame cannot resist its horiz. thrust, a tie may be arranged at the bottom hinges to resist the thrust. (Fig IV-24). In this case, the frame is once statically, indeterminate and the horizontal thrust  $H$  can be determined from the equation of elasticity:

$$\delta = - Hl / A_t E_t = \delta_0 + H \delta_1$$

so that

$$H = - \frac{\delta_0}{\delta_1 + l / A_t E_t} = - \frac{\int \frac{M_0 M_1}{EI} ds}{\int \frac{M_1^2}{EI} ds + \frac{l}{A_t E_t}}$$

For elastic ties at foundation level,  $H$  is smaller than that of two hinged frames without ties or with rigid ties, the result is that the corner moment is smaller and the field moment is bigger.

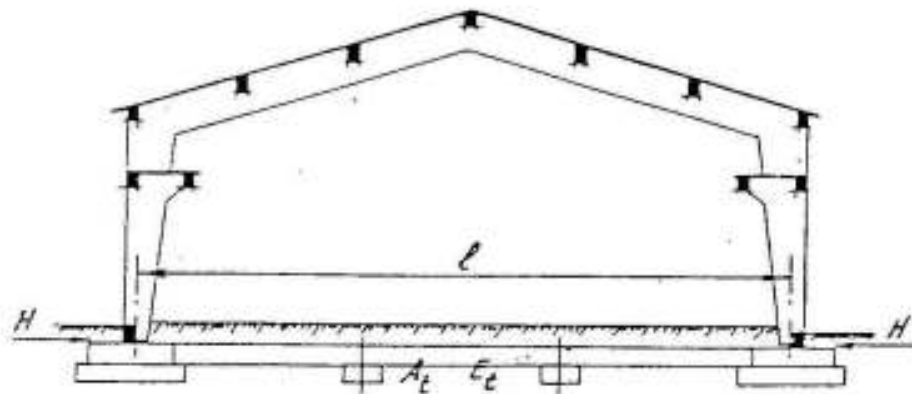


Fig. IV-24 Two-hinged frame with a tie at foundation level

#### Fixed Frames

In a fixed frame (fig IV-25), the horizontal displacement, the vertical displacement and the angles of rotation at the points of supports  $a$  and  $b$  are equal to zero.

It is three times statically indeterminate. The nature and sense of the statically indeterminate values satisfying the conditions of elasticity depend on the main system which may be a cantilever, double cantilevers, a simple beam, a three hinged frame ... etc. The conditions of elasticity and the statically

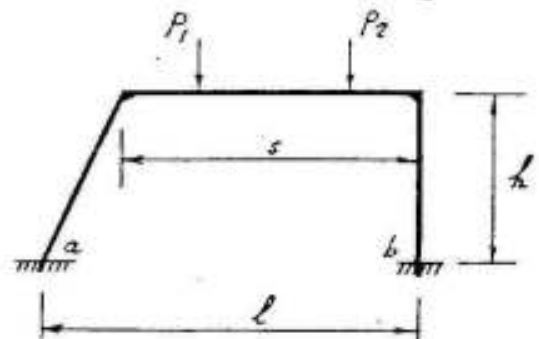


Fig. IV-25 Fixed frame

indeterminate values for three different main systems of a rectangular frame are shown in figure IV-26.

The equations of elasticity in the three cases are:

$$\delta_1 = 0 = \delta_{10} + X_1 \delta_{11} + X_2 \delta_{12} + X_3 \delta_{13}$$

$$\delta_2 = 0 = \delta_{20} + X_1 \delta_{21} + X_2 \delta_{22} + X_3 \delta_{23}$$

$$\delta_3 = 0 = \delta_{30} + X_1 \delta_{31} + X_2 \delta_{32} + X_3 \delta_{33}$$

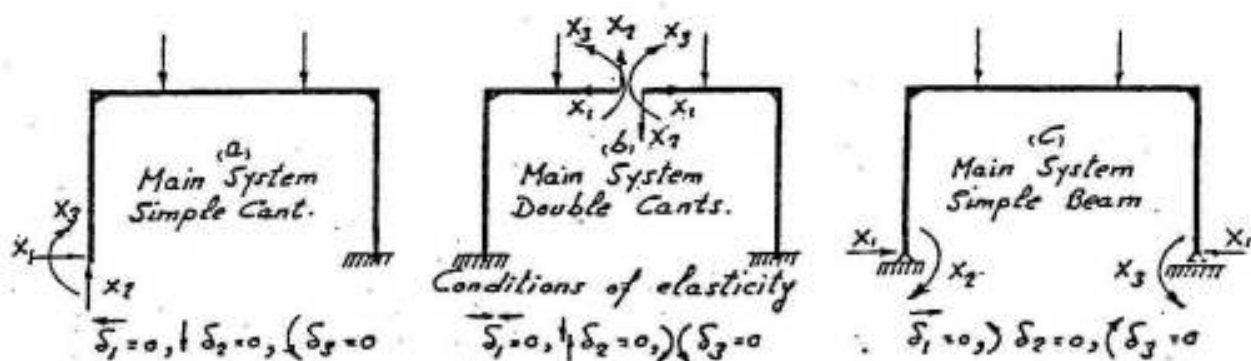


Fig. IV-26 Different main systems of a fixed frame

In order to explain the problem, we discuss the solution using the simple cantilever shown in "a" as main system. In this case, the displacements  $\delta_1$ ,  $\delta_2$  and  $\delta_3$  with single indices give the three components of the movement at the free end due to the loading namely:

$\delta_1$  = horizontal displacement,

$\delta_2$  = vertical " " ,

$\delta_3$  = angle of rotation .

While in the displacements with double indices, the first index indicates the sense and the second the cause, e.g.

$\delta_{10}$  = horiz. displ. of free end of main system due to load

$\delta_{22}$  = vert. " " " " " " " " " "  $X_2 = 1$

$\delta_{31}$  = angle of rot. " " " " " " " " " "  $X_1 = 1$  and so on

According to figure IV-27, the theory of virtual work gives:

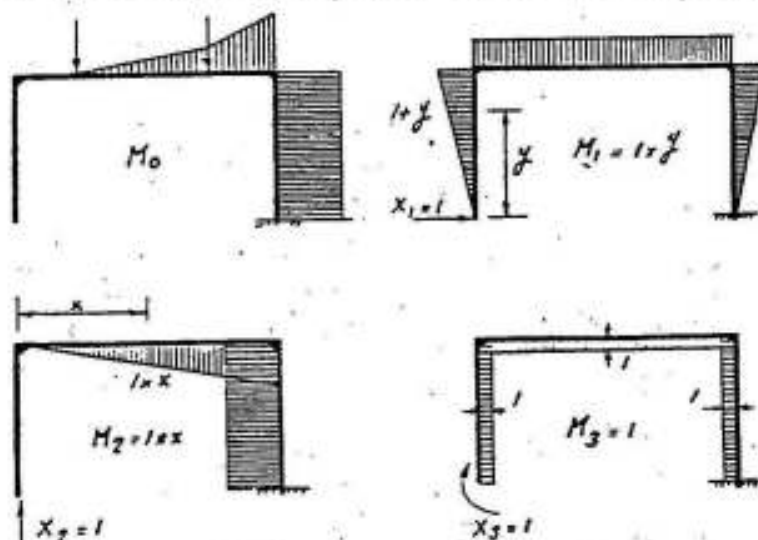


Fig. IV-27 Analysis of a fixed frame

$$E \delta_{10} = \int M_0 y \, ds/I, \quad E \delta_{20} = \int M_0 x \, ds/I, \quad E \delta_{30} = \int M_0 \, ds/I$$

$$E \delta_{11} = \int y^2 \, ds/I, \quad E \delta_{22} = \int x^2 \, ds/I, \quad E \delta_{33} = \int ds/I$$

$$E \delta_{12} = E \delta_{21} = \int xy \, ds/I, \quad E \delta_{23} = E \delta_{32} = \int x \, ds/I, \quad E \delta_{31} = E \delta_{13} = \int y \, ds/I$$

If the free end of the main system is connected to a rigid member with its other end at a point O which is chosen such that: (Fig. IV-28).

$$\int xy \, ds/I = 0, \quad \int x \, ds/I = 0 \quad \text{and} \quad \int y \, ds/I = 0$$

then, the displacements of the edge at O will be identical with those of the free end and if the statically indeterminate forces  $X_1 (= H)$

and  $X_2 (= V)$  and  $X_3 (= M)$  are assumed acting at point O (called the center of elasticity of the frame) then the displacements

$$\delta_{12} = \delta_{21} = \frac{1}{E} \int xy \, ds/I,$$

$$\delta_{13} = \delta_{31} = \frac{1}{E} \int y \, ds/I \quad \text{and}$$

$$\delta_{23} = \delta_{32} = \frac{1}{E} \int x \, ds/I \quad \text{are all equal to zero, and the equations}$$

of elasticity will be reduced to :

$$0 = \delta_{10} + X_1 \delta_{11} \quad \text{or} \quad X_1 = - \delta_{10} / \delta_{11}$$

$$0 = \delta_{20} + X_2 \delta_{22} \quad \text{or} \quad X_2 = - \delta_{20} / \delta_{22}$$

$$0 = \delta_{30} + X_3 \delta_{33} \quad \text{or} \quad X_3 = - \delta_{30} / \delta_{33}$$

So that

$$X_1 = H = - \frac{\int M_0 y \, ds/I}{\int y^2 \, ds/I}$$

$$X_2 = V = - \frac{\int M_0 x \, ds/I}{\int x^2 \, ds/I}$$

$$X_3 = M = - \frac{\int M_0 \, ds/I}{\int ds/I}$$

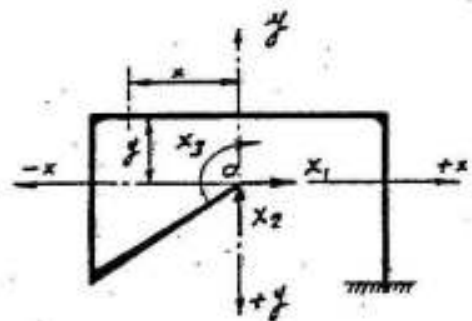


Fig. IV-28

The  $M_0$ ,  $M_1 (= 1 \cdot y)$ ,  $M_2 (= 1 \cdot x)$  and  $M_3$  (due to  $X_3 = 1$ ) diagrams drawn on the tension side are shown in their final form in fig IV-29.

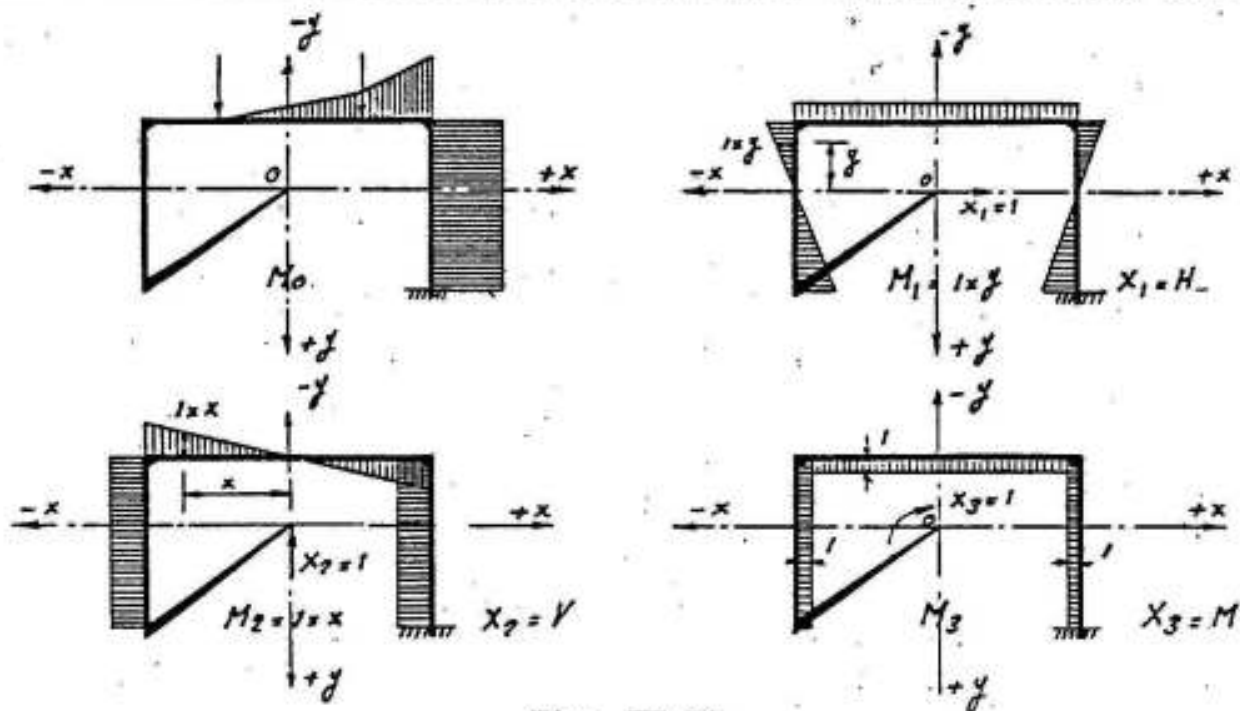


Fig. IV-29

In this manner, the determination of the statically indeterminate values is much simplified. The bending moment in any section of the frame at  $x$  and  $y$  from the principal axes of elasticity passing through  $O$  is given by :

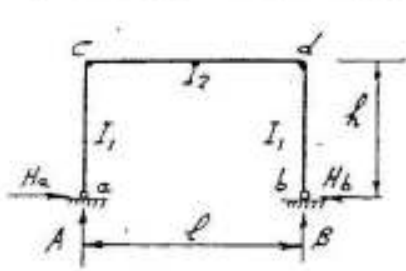
$$\begin{aligned}
 M_{x,y} &= M_0 + X_1 M_1 + X_2 M_2 + X_3 M_3 \\
 &= M_0 + X_1 y + X_2 x + X_3 \\
 &= M_0 + H y + V x + M
 \end{aligned}$$

In order to simplify the determination of the internal forces, we give in the following, the reactions of 6 types of frames of extensive use in reinforced concrete, namely:

- 1) Two hinged symmetrical rectangular frames.
- 2) " " " frames with parabolic girder.
- 3) " " " polygonal frames without & with ties.
- 4) Fixed symmetrical rectangular frames.
- 5) " " frames with parabolic girders.
- 6) " " polygonal frames.



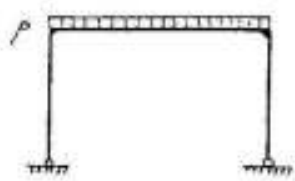
# 1- TWO HINGED SYMMETRICAL RECTANGULAR FRAMES



$$\alpha = \frac{I_2}{I_1} \cdot \frac{l}{h} \quad \mu = 7\alpha + 3$$

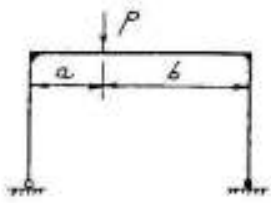
in case of unloaded columns

$$M_C = -H_a \cdot h \quad M_D = -H_b \cdot h$$



$$H_a = H_b = \frac{pl^2}{4h\mu}$$

$$A = B = pl/2$$



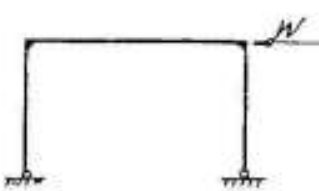
$$H_a = H_b = \frac{3}{2} \frac{Pab}{h\ell\mu}$$

$$A = Pb/l \quad B = Pa/l$$



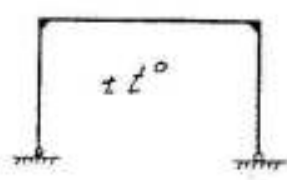
$$H_a = \frac{wl}{8} \cdot \frac{5\alpha + 6}{\mu} \quad H_b = -\frac{wl}{8} \cdot \frac{11\alpha + 13}{\mu}$$

$$A = B = wl^2/2$$



$$H_a = -H_b = W/2$$

$$A = B = Wl/l$$



Temperature change of  $t^\circ$

$$H_a = H_b = \frac{3\alpha t}{\mu} \frac{EI_2}{h^2}$$

$$A = B = 0$$

$\alpha = \text{coeff. of linear expansion} = 0.00001$

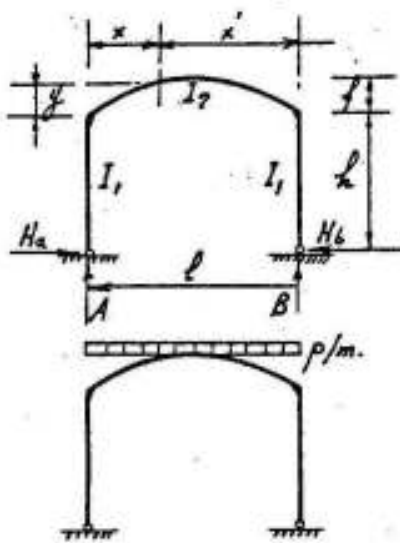


Horizontal displacement of support  $\delta$

$$H_a = H_b = -\frac{3\delta EI_2}{h^2 l \mu}$$

$$A = B = 0$$

2-TWO HINGED SYMMETRICAL FRAME WITH PARABOLIC GIRDER



Equation of Parabola

$$\xi = x/l \quad \xi' = x'/l$$

$$\alpha = \frac{I_2}{I_1} \cdot \frac{l}{l}$$

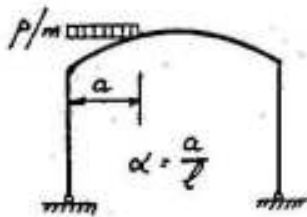
$$y = 4f \xi \xi'$$

$$f = l/l$$

$$\mu = 5(2\alpha + 3) + 42(5 + 2\alpha)$$

$$H_a = H_b = \frac{pl^2}{4h} \cdot \frac{5 + 4\alpha}{\mu}$$

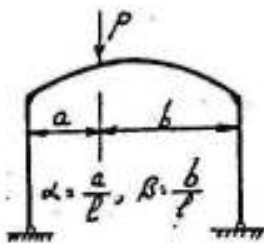
$$A = B = pl/l$$



$$H_a = H_b = \frac{pa^2}{4h} \cdot \frac{5(3 - 2\alpha) + 27(5 - 5\alpha^2 + 2\alpha^3)}{\mu}$$

$$A = pa(2 - \alpha)^2$$

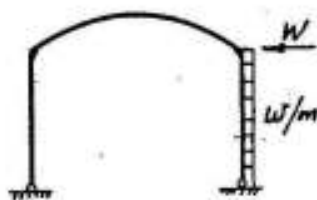
$$B = pa\alpha/l$$



$$H_a = H_b = \frac{5Pa b}{2l h} \cdot \frac{3 + 27(1 + \alpha\beta)}{\mu}$$

$$A = P\beta$$

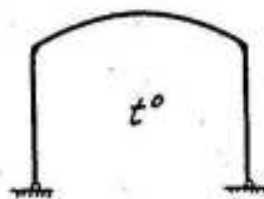
$$B = P\alpha$$



$$H_a = \left[ \frac{5wh}{2} \cdot \frac{52\alpha + 6 + 42}{\mu} \right] + \left[ \frac{5W}{2} \cdot \frac{2\alpha + 3 + 27}{\mu} \right]$$

$$H_b = wh + W - H_a$$

$$A - B = \frac{wh^2}{2l} + \frac{Wl}{2}$$

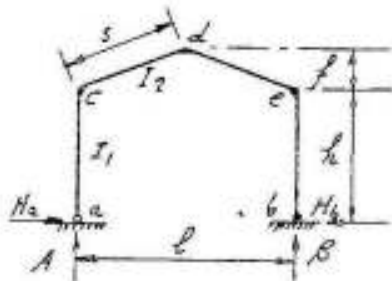


Temperature change of  $t^\circ$

$$H_a = H_b = \pm \frac{15\alpha t E I_2}{h^2 \mu}$$

$$A = B = 0$$

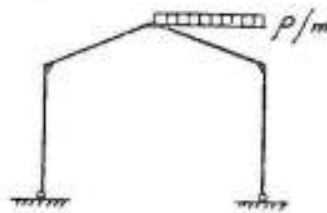
### 3-TWO HINGED SYMMETRICAL POLYGONAL FRAME



$$\alpha = \frac{I_2}{I_1} \cdot \frac{l}{s} \quad \eta = f/h \quad \mu = (\alpha + 3) + 2(2 + 3)$$

In case of unloaded columns

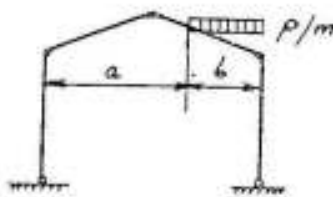
$$M_c = -H_a \cdot h, \quad M_e = -H_b \cdot h, \quad M_d = M_o - H_a(h + f)$$



$$H_a = H_b = \frac{pl^2}{64h} \cdot \frac{5\eta + 8}{\mu}$$

$$A = pl/8$$

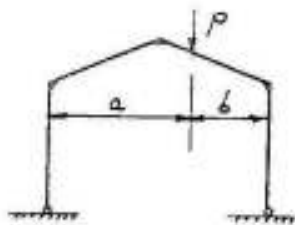
$$B = 3pl/8$$



$$H_a = H_b = \frac{pb^2}{8h} \cdot \frac{2l(3l - 2b) + 7(3l^2 - 2b^2)}{l^2 \mu}$$

$$A = pb^2/2l$$

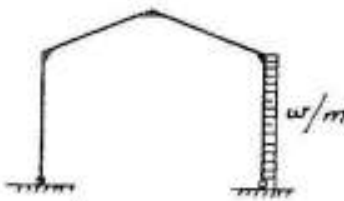
$$B = \frac{pb}{2}(l + 5b)$$



$$H_a = H_b = \frac{Pb}{4h} \cdot \frac{6a \cdot l + 7(3l^2 - 4b^2)}{l^2 \mu}$$

$$A = Pb/l$$

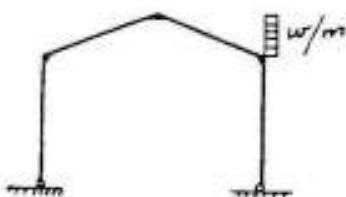
$$B = Pa/l$$



$$H_a = \frac{wh}{16} \cdot \frac{5\alpha + 6(2 + 2)}{\mu}$$

$$H_b = H_a - wh$$

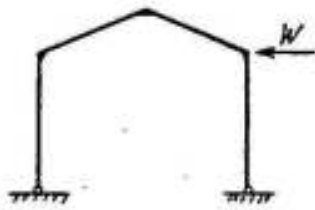
$$A = -B = wh^2/2l$$



$$H_a = \frac{wf}{16} \cdot \frac{2(\alpha + 3) + 52(2 + 4)}{\mu}$$

$$H_b = H_a - wf$$

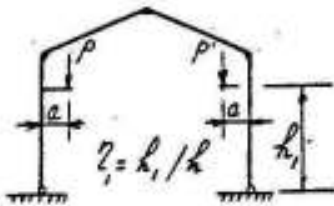
$$A = -B = wf(2h + f)/2l$$



$$H_a = \frac{W}{4} \cdot \frac{2x + 3(2+2)}{\mu}$$

$$H_b = H_a - W$$

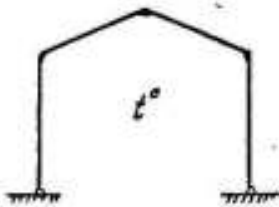
$$A = -B = Wl/l$$



$$H = H_a = H_b = \frac{3a}{4h} (P + P') \cdot \frac{x(1-z^2) + (2+2)}{\mu}$$

$$A = P \frac{a}{l} + P' \frac{l-a}{l}$$

$$B = P \frac{a}{l} + P' \frac{l-a}{l}$$



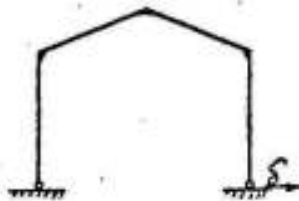
Temp. change of  $t^\circ$

$$H_a = H_b = \frac{3\alpha t l}{2\mu} \cdot \frac{EI_c}{h^2 I_s}$$

$$A = B = 0$$

$\alpha = \text{coeff. of linear expansion}$

$$= 0.00001$$



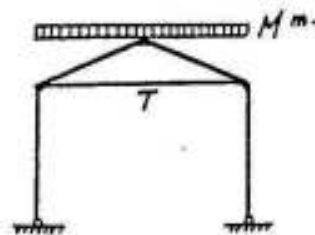
Horizontal displacement of support  $\delta$

$$H_a = H_b = -\frac{3\delta}{2\mu} \cdot \frac{EI_c}{h^2 I_s}$$

$$A = B = 0$$

Frame with rigid tie

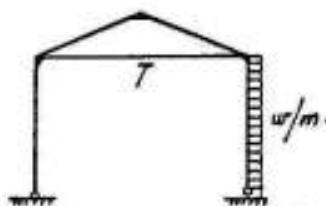
$$4x + 3 = \mu$$



$$H = H_a = H_b = \frac{pl^2}{16h\mu}$$

$$A = B = \frac{wl}{2}$$

$$T = \frac{pl^2}{16h} \cdot \frac{10x + 6 - 2}{2\mu}$$



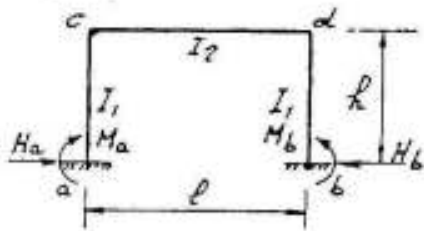
$$H_a = wh \cdot \frac{x + \mu}{4\mu}$$

$$H_b = wh - H_a$$

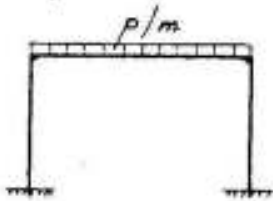
$$T = wh \cdot \frac{(3+x) + 22(x+\mu)}{8\mu^2}$$

$$A = -B = wh^2/2l$$

#### 4. FIXED SYMMETRICAL RECTANGULAR FRAME



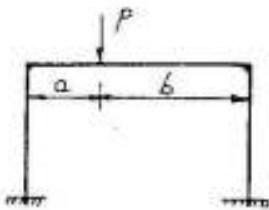
$$\alpha = \frac{I_2}{I_1} \cdot \frac{h}{l} \quad \mu_1 = \alpha + 2 \quad \mu_2 = 6\alpha + 1$$



$$H = H_a = H_b = \frac{p l^2}{4 h \mu_1} \quad A = B = \frac{p l}{12}$$

$$M_a = M_b = \frac{p l^2}{12 \mu_1} = H \cdot h / 3$$

$$M_c = M_d = \frac{p l^2}{6 \mu_1} = -2 H \cdot h / 3$$

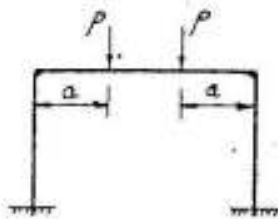


$$\alpha = \frac{a}{l}, \beta = \frac{b}{l}$$

$$H = H_a = H_b = \frac{3 P l \alpha \beta}{2 h \mu_1}; A = P \beta \left[ 1 + \frac{\alpha (B - \alpha)}{\mu_2} \right]; B = P - A$$

$$M_a = \frac{P l \alpha \beta}{2} \cdot \frac{5\alpha - 1 + 2\alpha \mu_1}{\mu_1 \mu_2}; M_c = M_a - H \cdot h$$

$$M_b = \frac{P l \alpha \beta}{2} \cdot \frac{7\alpha + 3 - 2\alpha \mu_1}{\mu_1 \mu_2}; M_d = M_b - H \cdot h$$



$$\alpha = \frac{a}{l}$$

$$H = H_a = H_b = \frac{3 P l \alpha \beta}{h \mu_1} \quad A = B = P$$

$$M_a = M_b = \frac{P l \alpha \beta}{\mu_1} = H \cdot h / 3$$

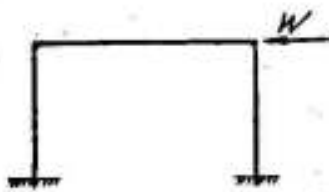
$$M_c = M_d = -\frac{2 P l \alpha \beta}{\mu_1} = -2 H \cdot h / 3$$



$$H_a = \frac{w h^2}{3} \cdot \frac{2\alpha + 3}{\mu_1}; H_b = H_a - w h \quad A = -B = \frac{w h^2 \alpha}{2 \mu_2}$$

$$M_a = \frac{w h^2}{24} \left( \frac{5\alpha + 9}{\mu_1} - \frac{12\alpha}{\mu_2} \right); M_c = M_a - H_a \cdot h$$

$$M_b = -\frac{w h^2}{24} \left( \frac{12 - 5\alpha + 9}{\mu_1} - \frac{12\alpha}{\mu_2} \right); M_d = M_b - H_b \cdot h + \frac{w h^2}{2}$$

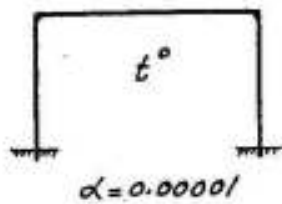


$$H_a = -H_b = W/l$$

$$A = -B = \frac{3Wl^2 \alpha}{2\mu_2}$$

$$M_a = -M_b = \frac{Wl}{2} \cdot \frac{3\alpha + 1}{\mu_2}$$

$$M_c = -M_d = -\frac{Wl}{2} \cdot \frac{3\alpha}{\mu_2}$$



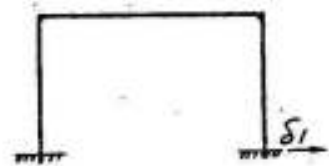
Temp. change  $t^\circ$

$$H = H_a = H_b = 3\alpha t \frac{EI_2}{l^2} \cdot \frac{2\alpha + 1}{\alpha \mu_1}$$

$$A = B = 0$$

$$M_a = M_b = H \frac{l \alpha + 1}{2\alpha + 1}$$

$$M_c = M_d = -H \frac{l \alpha}{2\alpha + 1}$$



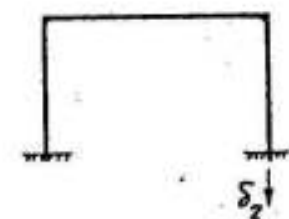
Horizontal displacement  $\delta_1$

$$H = H_a = H_b = -3\delta_1 \frac{EI_2}{l^2} \cdot \frac{2\alpha + 1}{\alpha \mu_1}$$

$$A = B = 0$$

$$M_a = M_b = H \cdot l \frac{1 + \alpha}{\mu_1}$$

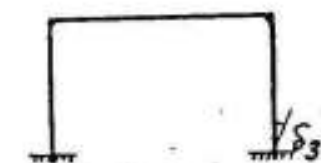
$$M_c = M_d = -H \frac{l}{\mu_1}$$



Vertical displacement  $\delta_2$

$$H_a = H_b = 0 \quad A = -B = 6\delta_2 \frac{EI_2}{l^2 \mu_2}$$

$$M_a = M_c = -M_b = -M_d = -3\delta_2 \frac{EI_2}{l \mu_2} = -A \cdot l/2$$



Rotation of support  $\delta_3$

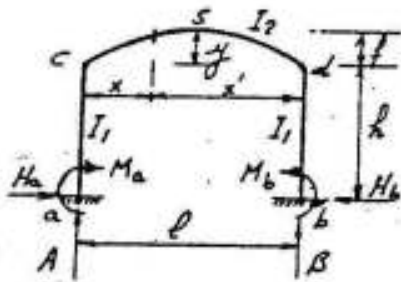
$$H = H_a = H_b = \frac{3\delta_3 EI_2}{2kl \mu_1}$$

$$A = -B = \frac{6\delta_3 EI_2}{l^2 \mu_2}$$

$$M_a = \frac{3\delta_3 EI_2}{l} \left( -\frac{1}{\mu_2} + \frac{1}{2\alpha} + \frac{1}{6\mu_1} \right)$$

$$M_b = \frac{3\delta_3 EI_2}{l} \left( \frac{1}{\mu_2} + \frac{1}{2\alpha} - \frac{1}{6\mu_1} \right)$$

## 5. FIXED SYMMETRICAL FRAME WITH PARABOLIC GIRDER

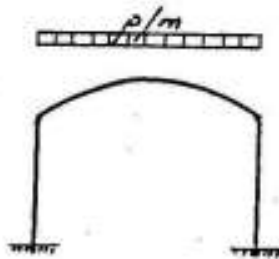


Equation of parabolic girder  $y = 4f \xi \xi'$

$$\xi = x/l \quad \xi' = x'/l \quad \eta = f/l$$

$$\alpha = \frac{I_2}{I_1} \cdot \frac{h}{l} \quad \mu_2 = 6\alpha + 1$$

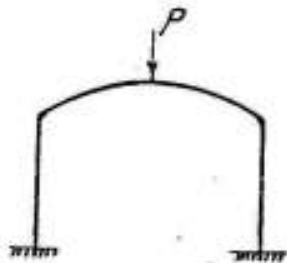
$$\mu_1 = 15\alpha(\alpha + 2) + 19\alpha^2(5 + 4\eta^2) + 4\eta^2$$



$$H_a = H_b = \frac{p l^2}{4h} \cdot \frac{7(12\alpha + 1) + 15\alpha}{\mu_1} \quad A = B = p l / 2$$

$$M_a = M_b = \frac{p l^2}{4} \cdot \frac{7\mu_2 + 5\alpha}{\mu_1}$$

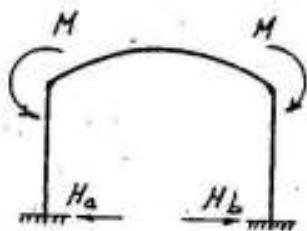
$$M_c = M_d = -H \cdot h + M_a \quad M_s = \frac{p l^2}{8} - H(l + h) + M_a$$



$$H_a = H_b = \frac{15 P l}{16 h} \cdot \frac{7(10\alpha + 1) + 6\alpha}{\mu_1} \quad A = B = P / 2$$

$$M_a = M_b = \frac{P l}{16} \cdot \frac{7(7 + 15) + 15\alpha(5\eta^2 + 2)}{\mu_1}$$

$$M_c = M_d = -H \cdot h + M_a \quad M_s = \frac{P l}{4} - H(l + h) + M_a$$

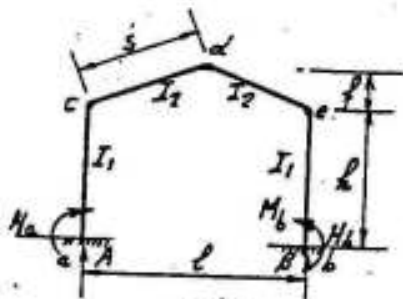


$$H_a = H_b = \frac{15 M \alpha}{h} \cdot \frac{3 + 4\eta^2}{\mu_1} \quad A = B = 0$$

$$M_a = M_b = -M \frac{15\alpha(1 + 2\eta^2) - 4\eta^2}{\mu_1}$$

$$M_c = M_d = H h + M_a \quad M_s = -M + H(l + h) + M_a$$

## 6- FIXED SYMMETRICAL POLYGONAL FRAME

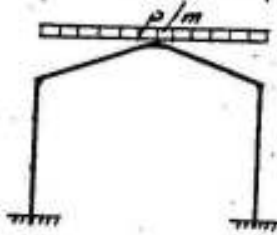


$$\alpha = \frac{I_2}{I_1} \cdot \frac{l}{s}$$

$$\gamma = l/h$$

$$\mu_1 = \alpha(\alpha+4) + 2\alpha^2(3+2\gamma) + \gamma^2$$

$$\mu_2 = 3\alpha + 1$$



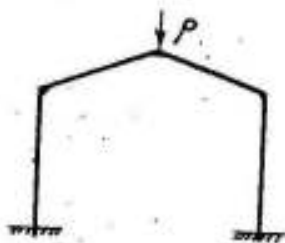
$$H_a = H_b = \frac{p l^2}{3h} \cdot \frac{4\alpha + 5\alpha\gamma + \gamma^2}{\mu_1}$$

$$A = B = p l / 2$$

$$M_a = M_b = \frac{p l^2}{48} \cdot \frac{\alpha(8+15\gamma) + \gamma(6-\gamma)}{\mu_1}$$

$$M_c = M_e = -H_a \cdot h + M_a$$

$$M_d = p \frac{l^2}{8} + M_a - H_a(h+l)$$



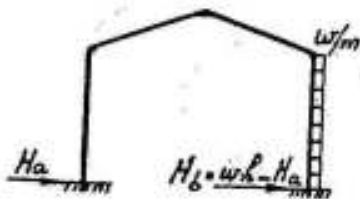
$$H_a = H_b = \frac{P l}{4h} \cdot \frac{3\alpha + 4\alpha\gamma + \gamma^2}{\mu_1}$$

$$A = B = P / 2$$

$$M_a = M_b = \frac{P l}{4} \cdot \frac{\alpha + 2\alpha\gamma + \gamma^2}{\mu_1}$$

$$M_c = M_e = -H_a \cdot h + M_a$$

$$M_d = \frac{P l}{4} + M_a - H_a(h+l)$$



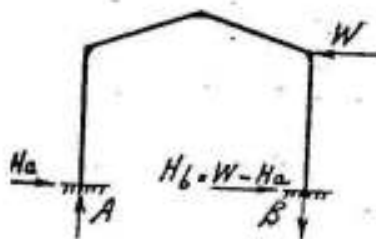
$$H_a = \frac{w l \alpha}{4} \cdot \frac{\alpha + \gamma + \gamma^2}{\mu_1}$$

$$A = -B = \frac{w l^2}{2l} \cdot \frac{M_b - M_a}{l}$$

$$\frac{M_a}{M_b} = \frac{w l^2}{24} \left[ \frac{-\alpha(\alpha+\gamma) + \alpha^2(15+16\gamma) + \gamma^2}{\mu_1} + \frac{6(2\alpha+1)}{\mu_2} \right]$$

$$M_c = -H_a h + M_a$$

$$M_e = \frac{w l^2}{2} + M_a - H_b h$$



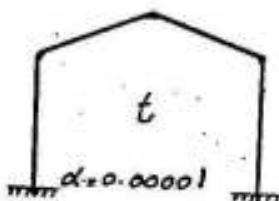
$$H_a = \frac{P \alpha}{2} \cdot \frac{\alpha + 4 + 3\gamma}{\mu_1}$$

$$A = -B = \frac{3 P l \alpha}{2 l \mu_2}$$

$$\frac{M_a}{M_b} = \frac{P l}{4} \left[ \frac{-2\gamma(\alpha + 2\alpha\gamma + \gamma^2) + 3\alpha + \gamma}{\mu_1} \right]$$

$$M_c = -H_a h + M_a$$

$$M_e = H_b h + M_a$$



$$H = \frac{6 E I_2 \alpha t l}{5 h^2} \cdot \frac{\alpha + 1}{\mu_1}$$

$$A = B = 0$$

$$M_a = M_b = + \frac{3 E I_2 \alpha t l}{5 h} \cdot \frac{\alpha + \gamma + \gamma^2}{\mu_1}$$

$$M_c = M_e = M_a - H \cdot h$$

$$M_d = M_a - H \cdot (h+l)$$



### Continuous Frames

Continuous frames are generally high grade statically indeterminate. The degree of indeterminacy depends on the number and type of supports. Using the method of virtual work, the determination of the internal forces in the continuous frame shown in fig IV-30 can be done in the following manner :

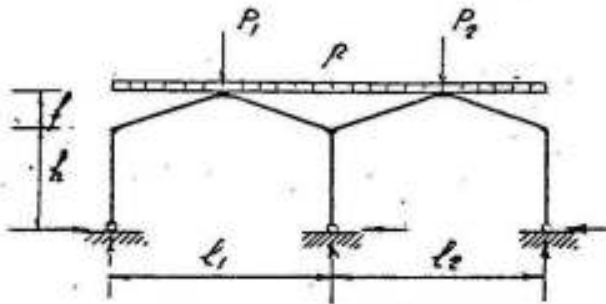


Fig. IV-30 Continuous frame

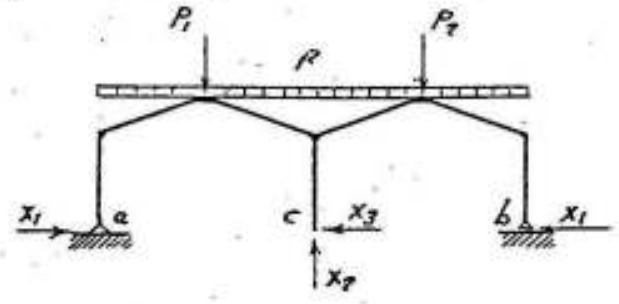


Fig. IV-31 Main system

This frame has 6 reaction components, the conditions of equilibrium being 3, then the frame is 3 times statically indeterminate. Choosing the statically determinate frame, hinged at a and supported on a roller at b as a main system, fig IV-31 then, due to the loading, support b moves horizontally a distance  $\delta_1$  while point c moves vertically a distance  $\delta_2$  and horizontally a distance  $\delta_3$ . The conditions of elasticity are therefore:  $\delta_1 = 0$   $\delta_2 = 0$  and  $\delta_3 = 0$

To satisfy these conditions, 3 statically indeterminate values  $X_1$ ,  $X_2$  and  $X_3$  are required.

The equations of elasticity are given by:

$$\delta_1 = 0 = \delta_{10} + X_1 \delta_{11} + X_2 \delta_{12} + X_3 \delta_{13}$$

$$\delta_2 = 0 = \delta_{20} + X_1 \delta_{21} + X_2 \delta_{22} + X_3 \delta_{23}$$

$$\delta_3 = 0 = \delta_{30} + X_1 \delta_{31} + X_2 \delta_{32} + X_3 \delta_{33}$$

in which

$$EI \delta_{10} = \int M_0 M_1 ds \quad , \quad EI \delta_{20} = \int M_0 M_2 ds \quad , \quad EI \delta_{30} = \int M_0 M_3 ds$$

The  $M_0$ ,  $M_1$ ,  $M_2$  and  $M_3$  diagrams drawn on the tension side and taking the assumed sense of the statically indeterminate values  $X_1$ ,  $X_2$  and  $X_3$  in consideration are shown in fig IV-32.

If the frame is symmetrical in shape and loading, as is generally the case in roof structures, then  $X_3$  equals zero and the intermediate column is subject to axial forces only. In such a case the frame may

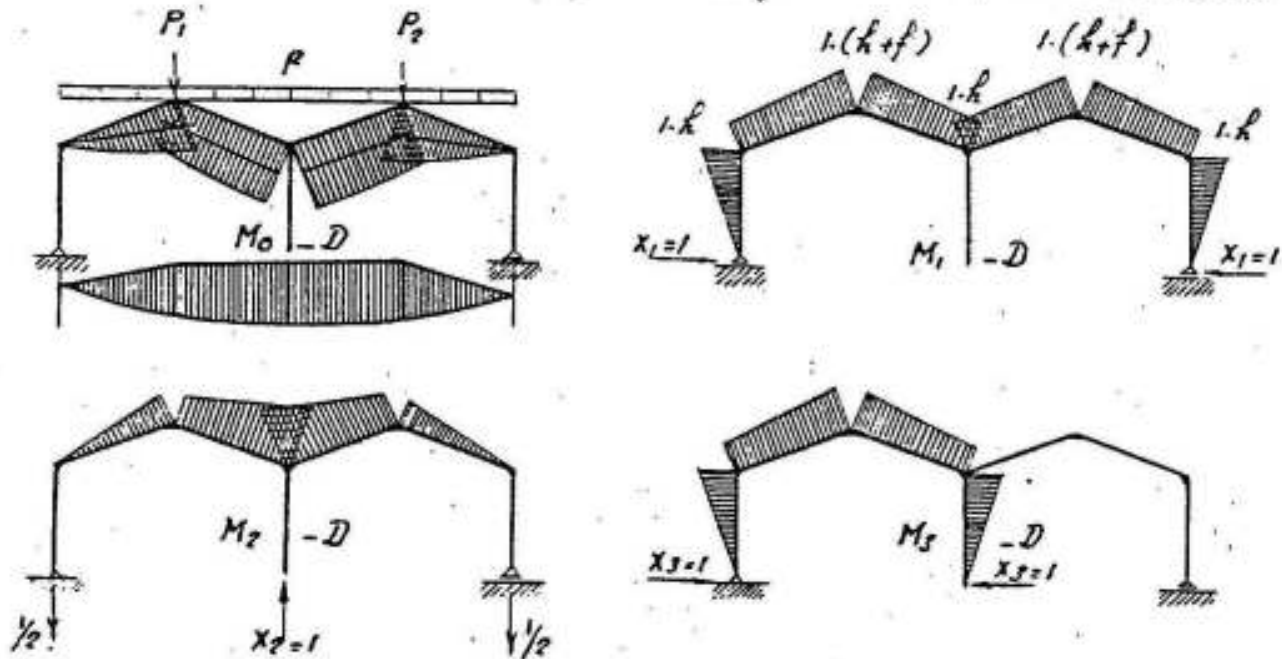


Fig. IV-32 Analysis of a continuous frame

be constructed with a slender intermediate column which can be assumed as a pendulum. The system in this form is only twice statically indeterminate. (Fig IV-33).

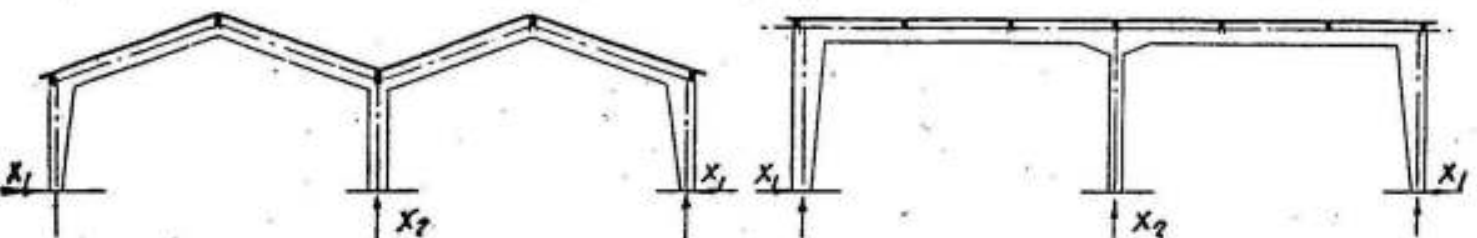


Fig. IV-33 Continuous frames with a central pendulum

Assuming the same main system (as shown in fig IV-31), the equations of elasticity will be reduced to:

$$\begin{aligned} \delta_1 = 0 &= \delta_{10} + X_1 \delta_{11} + X_2 \delta_{12} \\ \delta_2 = 0 &= \delta_{20} + X_1 \delta_{21} + X_2 \delta_{22} \end{aligned}$$

Figs IV-34 and IV-35 give the general layout, main dimensions and details of the main continuous frames of the printing, dyeing and bleaching halls of the Misr spinning and weaving company at Mehalla.

As a result of the various industrial processes accomplished in these halls, a big amount of hot chemicals evaporate. This hot vapour must find its way outside the hall. It is absolutely essential to take the necessary provisions so that the vapour does not accumulate or condensate inside the hall. In order to satisfy this requirement and to facilitate the movement of the vapour, the roof slab below the top windows was chosen circular and arranged at the inner side of the main girders. The vapour being hot it moves upwards and, due to the cross ventilation created by the upper windows, it is driven outwards without having the possibility to accumulate or condensate.

During construction, the main tension reinforcements were replaced by the equivalent amount of cold twisted steel.

The upper monitor of the frame has been cancelled in the end panels of the halls at the end gables to get a better side view.

#### The Slope - Deflection Method

This method is one of the oldest known methods used for determining the connecting moments of statically indeterminate beams and frames composed of a series of straight members. The study of one single span elastically restrained at both ends is evidently of prime importance. (Fig IV-36).

The deformation angles  $\alpha$  and  $\beta$  can be determined according to law of superposition from the following relations:

$$\alpha = \alpha_0 + M_1 \alpha_1 + M_2 \alpha_2$$

$$\beta = \beta_0 + M_1 \beta_1 + M_2 \beta_2 \quad \text{in which}$$

$\alpha_0$  and  $\beta_0$  = deformation angles of main system due to given loads

$\alpha_1$  "  $\beta_1$  = " " " " " "  $M_1 = 1$

$\alpha_2$  "  $\beta_2$  = " " " " " "  $M_2 = 1$ , hence

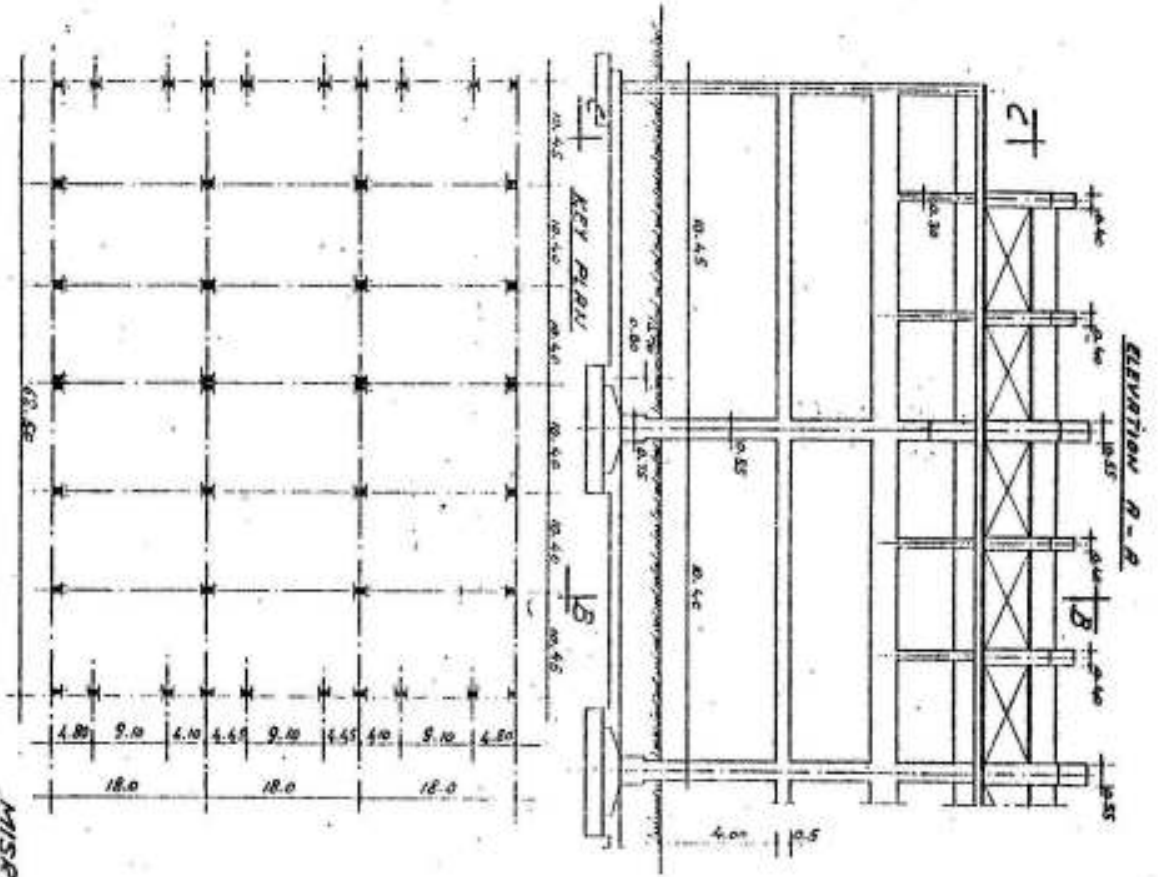
$$\alpha_1 = \int_0^l \frac{x'^2}{l^2} \frac{dx}{EI} \quad \text{for } I = \text{constant} \quad \alpha_1 = \frac{l}{3EI}$$

$$\alpha_2 = \int_0^l \frac{xx'}{l^2} \frac{dx}{EI} = 1 \quad \alpha_2 = \frac{l}{6EI} = \beta_1$$

$$\beta_2 = \int_0^l \frac{x^2}{l^2} \frac{dx}{EI} \quad \beta_2 = \frac{l}{3EI}$$

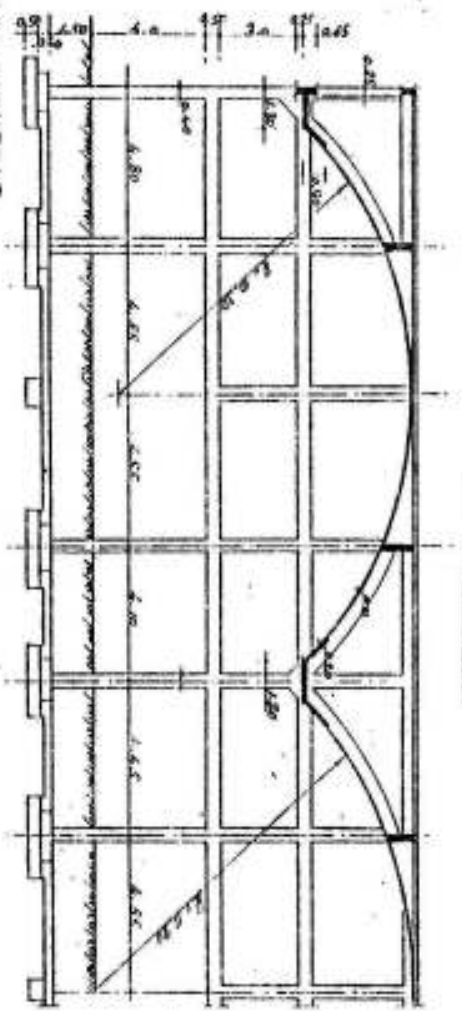
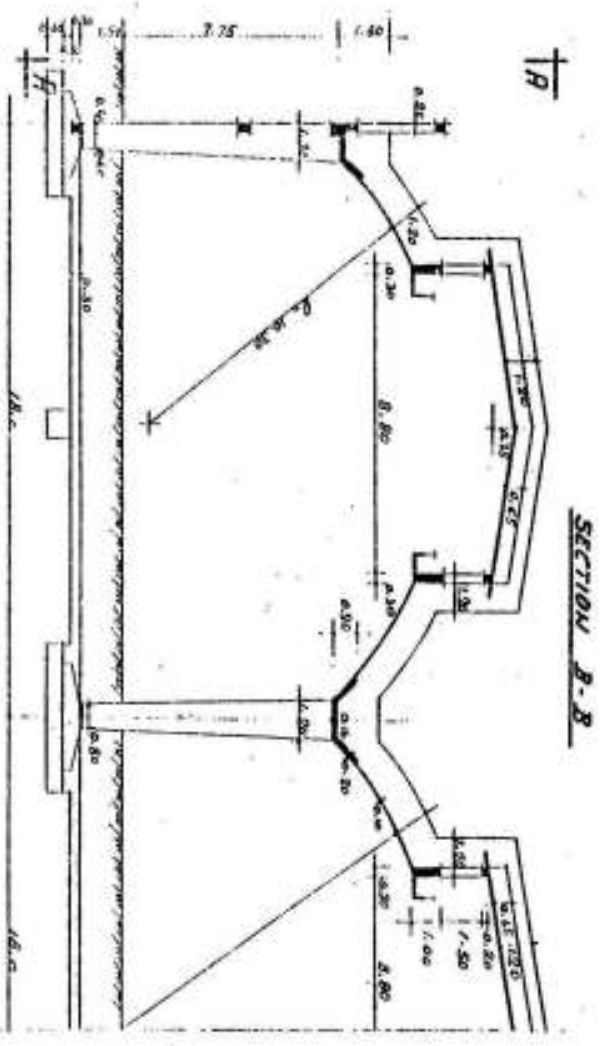
---

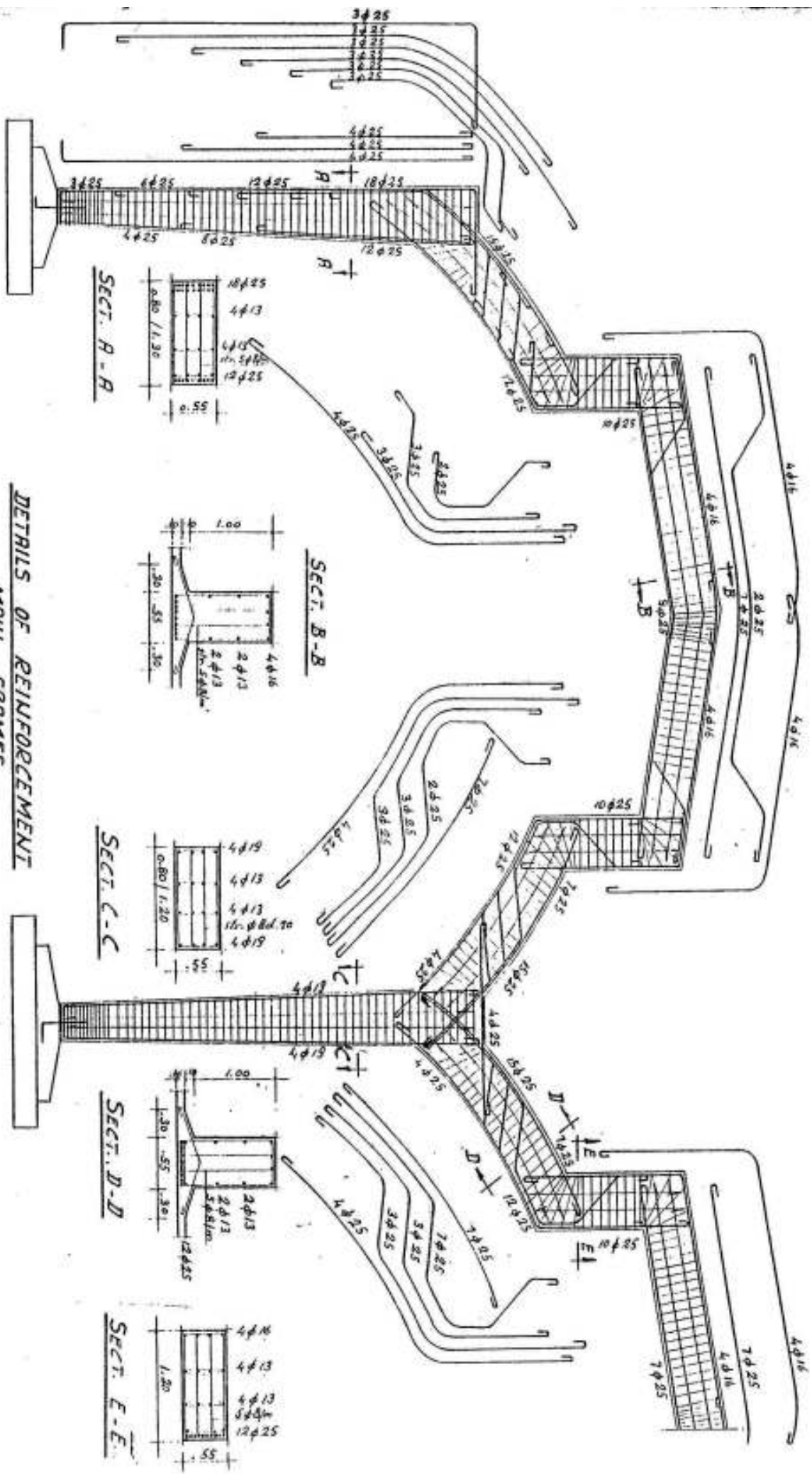
Refer to "Theory of Elastically Restrained Beams" by M.Hilal.



MISR S.P.W. - MEHRILLI  
DYING PLANT

PLG. IV-34





**DETAILS OF REINFORCEMENT**

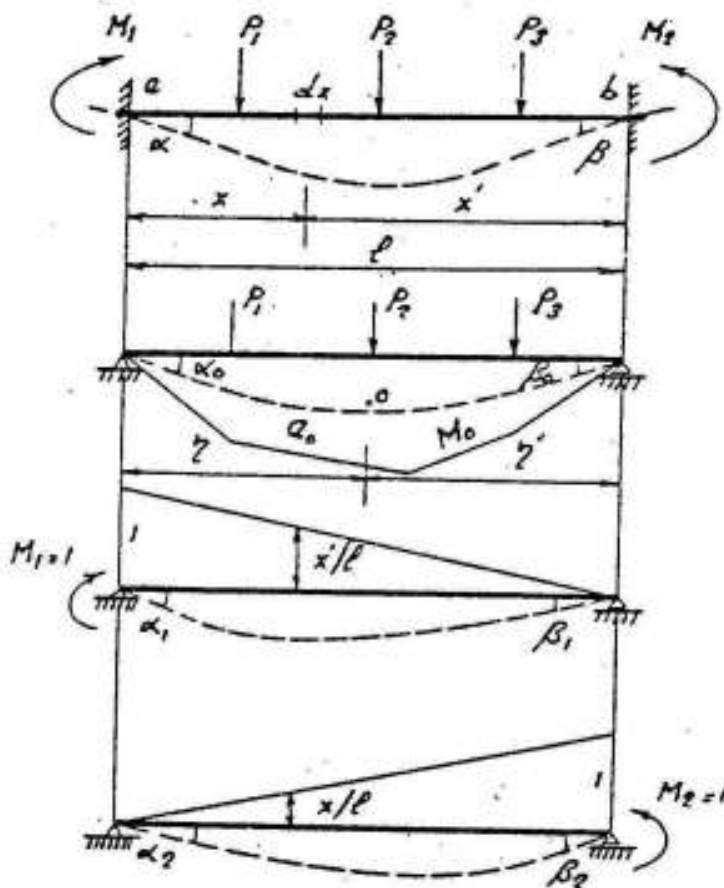
**MAIN FRAMES**

**FIG. IV-35**

According to theory of Maxwell, we have

$$\alpha_0 = \int_0^l \frac{M_0 x'}{l} \frac{dx}{EI} \quad \text{for } I = \text{constant} \quad \alpha_0 = \frac{A_0 \eta'}{EI}$$

$$\beta_0 = \int_0^l \frac{M_0 x}{l} \frac{dx}{EI} \quad \text{" " " " " " " " } \beta_0 = \frac{A_0 \eta}{EI}$$



- Fig. IV-36

where

$A_0$  = area of B.M.D. of main system due to given loads

$\eta$  &  $\eta'$  = the distances of the center of gravity O of the  $M_0$  - diagram from the verticals through a and b

We consider in the following (fig. IV-37) a frame 1-2-3 with a rigid joint at 2.

The condition of elasticity at joint 2 is :  $\beta = -\alpha'$

So that

$$\beta + \alpha' = 0 = \beta_0 + M_1 \beta_1 + M_2 \beta_2 + \alpha'_0 + M_2 \alpha'_1 + M_3 \alpha'_2$$

or  $0 = M_1 \beta_1 + M_2 (\beta_2 + \alpha'_1) + M_3 \alpha'_2 + (\beta_0 + \alpha'_0)$

For constant moments of inertia  $I$  and  $I'$ , we get

$$M_1 \frac{s}{6EI} + M_2 \left( \frac{s}{3EI} + \frac{s'}{3EI'} \right) + M_3 \frac{s'}{6EI'} = - \left( \frac{Q_0 \eta}{sEI} + \frac{Q'_0 \eta'}{s'EI'} \right)$$

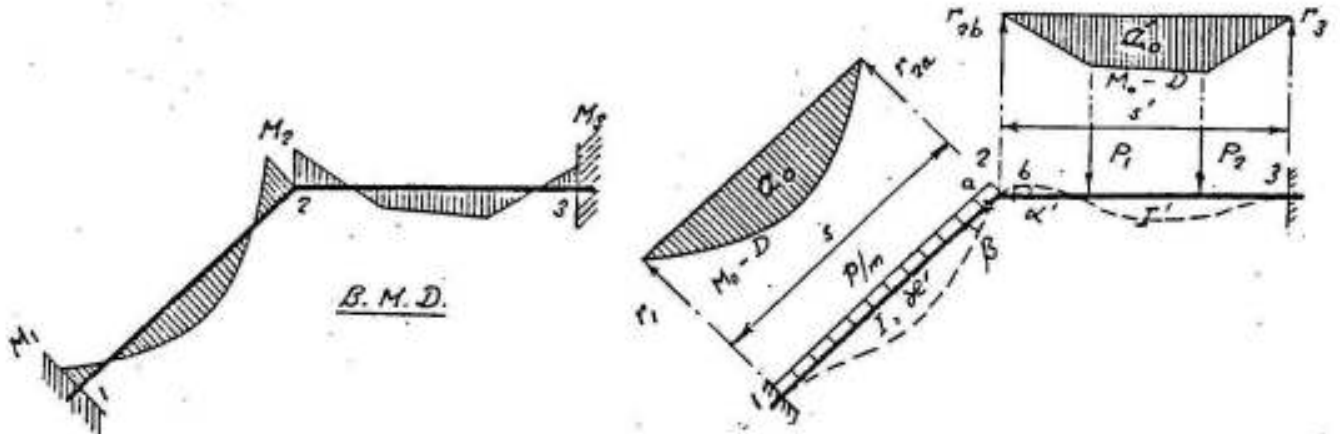


Fig. IV-37

Assuming

$$\chi = \frac{I'}{s'} \cdot \frac{s}{I}$$

$$r_{2a} = Q_0 \eta / s$$

$$r_{2b} = Q'_0 \eta' / s'$$

and multiplying the two sides of the equation by  $\frac{6EI'}{s'}$ , we get -

$$M_1 \chi + 2M_2 (\chi + 1) + M_3 = -6 \left( \frac{r_{2a}}{s} \chi + \frac{r_{2b}}{s'} \right)$$

This equation of three moments can be used for determining the moments at the corners of two hinged and fixed frames with unmovable joints.

The following system of equations can be written for the frame shown in fig. IV-37.

$$1 - 2 \quad 2M_1 \chi + M_2 \chi = -6 \frac{r_1}{s} \chi$$

$$1 - 2 - 3 \quad M_1 \chi + 2M_2 (\chi + 1) + M_3 = -6 \left( \frac{r_{2a}}{s} \chi + \frac{r_{2b}}{s'} \right)$$

$$2 - 3 \quad M_2 + 2M_3 = -6 \frac{r_3}{s'}$$

They are sufficient to determine the moments  $M_1$ ,  $M_2$  and  $M_3$ .

Frames symmetrical in shape and loading have generally unmovable joints and the connecting moments can be determined by the given equation of three moments if the members in any rigid joint are not more than two.

### Examples

1) Closed frame subject to internal pressure  $p/m$  as shown in fig IV-38.

$$\chi = \frac{I}{l} \cdot \frac{h}{I_1}$$

The connecting moment  $M$  can be determined from the equation

$$M\chi + 2M(\chi + 1) + M = -6 \left( \frac{r_1}{h} \chi + \frac{r}{l} \right) = -6 \left( p \frac{h^2}{24} \chi + p \frac{l^2}{24} \right)$$

$$M = -p \frac{(h^2 \chi + l^2)}{12(\chi + 1)}$$

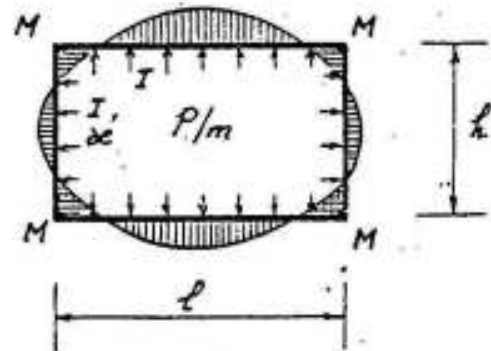


Fig. IV-38

2) Two-vent closed frame subject to external pressure  $p$  as shown in fig. IV-39.

$$\chi = \frac{I}{l} \cdot \frac{h}{I_1}$$

Due to symmetry, the intermediate wall will not be subject to any moments and the only unknown values are the connecting moments  $M_1$  and  $M_2$ . Thus

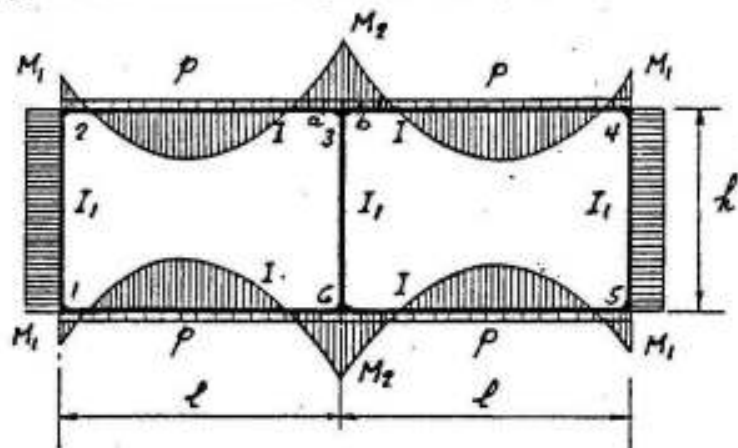


Fig. IV-39

$$1 - 2 - 3 \quad M_1 \chi + 2M_1(\chi + 1) + M_2 = -6 \frac{r_2}{l}$$

$$\text{or} \quad M_1(3\chi + 2) + M_2 = -p \frac{l^2}{4}$$

$$2 - 3 - 4 \quad M_1 + 2M_2 + 2M_2 + M_1 = -6 \left( \frac{r_{3a}}{l} + \frac{r_{3b}}{l} \right)$$

$$\text{or} \quad 2M_1 + 4M_2 = -p \frac{l^2}{2}$$



These two equations give

$$M_1 = -p \frac{l^2}{12(2\chi + 1)} \quad M_2 = -p \frac{l^2}{12} \frac{3\chi + 1}{2\chi + 1}$$

3) Fixed frame subject to uniform load  $p/m$  (fig IV-40). Due to symmetry, the corners  $c$  and  $d$  will not move horizontally; hence :

$$a - c \quad 2M_a \chi + M_c \chi = 0 \quad \chi = \frac{I}{l} \cdot \frac{h}{I_1}$$

$$\text{or} \quad M_a = -\frac{1}{2} M_c \quad (\text{a})$$

$$a-c-d \quad M_a \chi + 2M_c (\chi + 1) + M_d = -6 r_c / l$$

$$\text{but} \quad M_c = M_d \quad \text{and} \quad r_c = p l^2 / 24$$

$$M_a \chi + M_c (2\chi + 3) = -p l^2 / 4 \quad (\text{b})$$

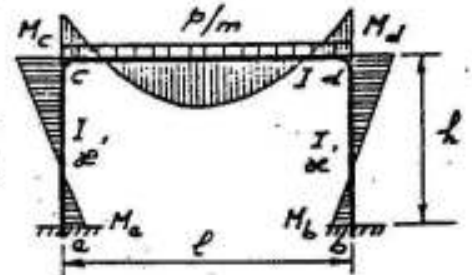


Fig. IV-40

then,

Equations a and b give

$$M_a = M_b = p \frac{l^2}{12(\chi + 2)} \quad M_c = M_d = -p \frac{l^2}{6(\chi + 2)}$$

Continuous frames with unmovable joints can be treated in a similar manner as follows: (Fig IV-41).

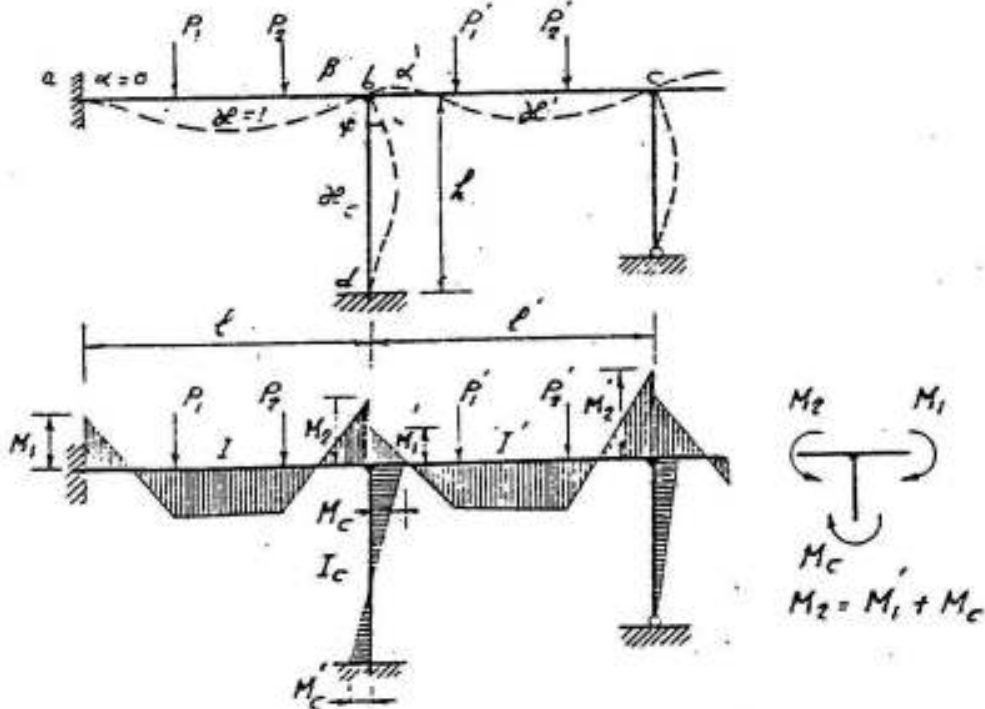


Fig. IV-41

Consider two successive spans  $l$  and  $l'$  subject to the loads  $P_1, P_2 \dots$  and  $P_1', P_2' \dots$  etc. The elastic line and the bending moments will be as shown in figure IV-41.

The condition of elasticity at the middle support is

$$\alpha' = -\beta = \psi$$

According to the law of superposition, the angles of rotation  $\beta, \alpha'$  and  $\psi$  can be expressed as follows:

$$\beta = \beta_0 + M_1 \beta_1 + M_2 \beta_2$$

$$\alpha' = \alpha'_0 + M_1' \alpha'_1 + M_2' \alpha'_2$$

$$\psi = \psi_0 + M_c' \psi_1 + M_c \psi_2$$

Due to the equilibrium of the middle joint, we must have :

$$M_2 = M_1' + M_c$$

Therefore, we get

$$\alpha' + \beta = 0 = \beta_0 + \alpha'_0 + M_1 \beta_1 + M_2 \beta_2 + M_1' \alpha'_1 + M_2' \alpha'_2$$

$$\psi + \beta = 0 = \beta_0 + \psi_0 + M_1 \beta_1 + M_2 \beta_2 + M_c \psi_1 + M_c' \psi_2$$

This system of equations gives a number of equations equal to that of the unknown fixing moments.

Assuming that the moment of inertia of each span or column is constant, and introducing the factors  $\chi$  such that

$$\chi = \frac{I}{l} \cdot \frac{l}{I} = 1 \quad \chi' = \frac{I}{l} \cdot \frac{l'}{I'} \quad \chi_c = \frac{I}{l} \cdot \frac{h}{I_c}$$

we get:

$$\text{for a-b-c} \quad M_1 + 2M_2 + 2M_1' \chi + M_2' \chi = -6 \left( \frac{F}{l} + \frac{F'}{l'} \chi' \right)$$

$$\text{" a-b-d} \quad M_1 + 2M_2 + 2M_c \chi_c + M_c' \chi_c = -6 \left( \frac{F}{l} + \frac{F_c}{h} \chi_c \right)$$

This system of equations of four moments is sufficient for determining the values of the unknown moments as can be seen in the following examples.

Examples

1) It is required to determine the corner moments in the continuous frame shown in figure IV-42 due to a uniform load  $p$  acting on  $l_1$ .

Assume:

$$\kappa_c = -\frac{I}{l} \cdot \frac{h}{I_c} \quad \text{and} \quad l_1 = l_2 = l \quad \text{so that} \quad \kappa_1 = \kappa_2 = 1$$

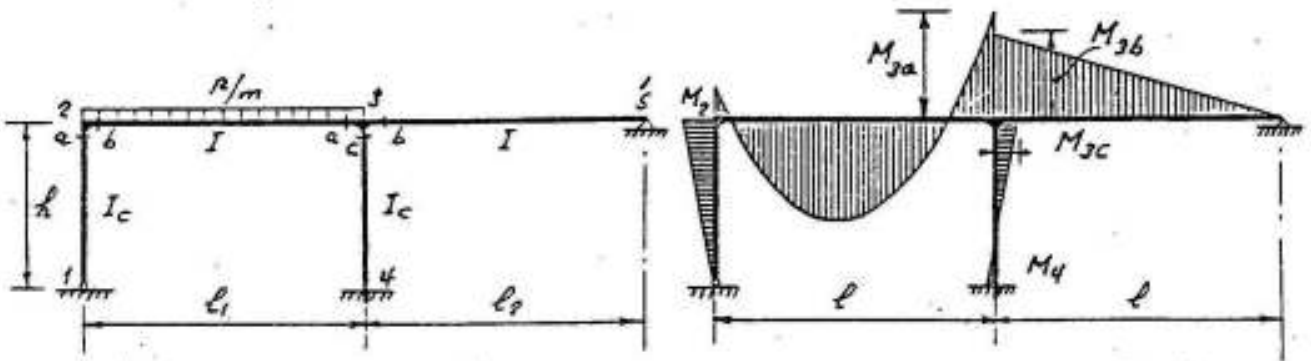


Fig. IV-42

As the girder is hinged at 5, no vertical or horizontal movement of the supports will take place, hence the equation of four moments can be applied in the form given before as follows:

$$1-2-3 \quad 2M_{2a} \kappa_c + 2M_{2b} + M_{3a} = -6 r_{2b}/l = -pl^2/4$$

$$2-3-4 \quad M_{2b} + 2M_{3a} + (2M_{3c} + M_4)\kappa_c = -6 r_{3a}/l = -pl^2/4$$

$$2-3-5 \quad M_{2b} + 2M_{3a} + 2M_{3b} = -6 r_{3a}/l = -pl^2/4$$

in which  $r_{2b} = r_{3a} = pl^3/24$

We have further:

$$M_{2a} = M_{2b} = M_2 \quad \text{and} \quad M_{3a} - M_{3b} = M_{3c}$$

The column 3-4 being fixed at its base, then the fixed point lies at  $h/3$  as shown in figure IV-42 and  $M_4 = -M_{3c}/2$ .

These equations are sufficient to determine the unknown moments; they give

$$M_2 = -0.019 pl^2, \quad M_{3a} = -0.0662 pl^2, \quad M_{3b} = -0.0496 pl^2$$

$$M_{3c} = M_{3a} - M_{3b} = -0.0166 pl^2 \quad \text{and} \quad M_4 = -M_{3c}/2 = +0.0083 pl^2$$

The bending moment diagram, drawn on the tension side, is shown in figure IV-42.

2) The multiple frame shown in figure IV-43 is symmetrical and symmetrically loaded. If the change in length due to normal forces and temperature changes are neglected, the joints can be assumed to remain in position; and the equation of four moments can be applied.

Assuming:

$$\kappa = \frac{I}{l} \cdot \frac{l}{I} = 1$$

$$\kappa_1 = \frac{I}{l} \cdot \frac{h_1}{I_1}$$

$$\kappa_2 = \frac{I}{l} \cdot \frac{h_2}{I_2}$$

$$\text{and } \kappa_3 = \frac{I}{l} \cdot \frac{l}{I_3}$$

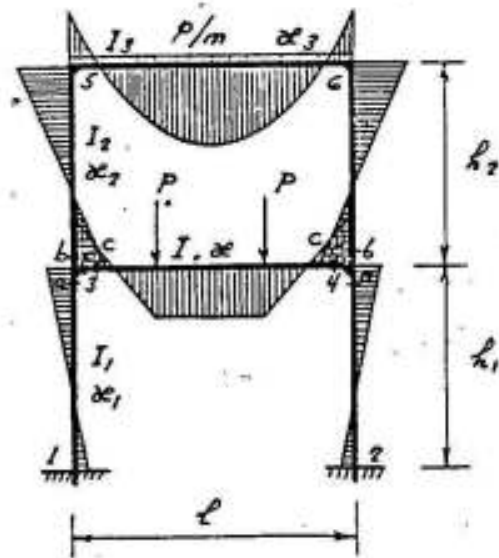


Fig. IV-43

then the equations required to determine the unknown corner moments are:

$$1-3 \quad 2M_1 \kappa_1 + M_{3a} \kappa_1 = 0 \quad \text{or} \quad M_1 = -M_{3a} / 2$$

$$1-3-5 \quad M_1 \kappa_1 + 2M_{3a} \kappa_1 + 2M_{3b} \kappa_2 + M_5 \kappa_2 = 0$$

$$1-3-4 \quad M_1 \kappa_1 + 2M_{3a} \kappa_1 + 2M_{3c} + M_{4c} = -6 r_{3c} / l$$

$$3-5-6 \quad M_{3b} \kappa_2 + 2M_5 (\kappa_2 + \kappa_3) + M_6 \kappa_3 = -6 r_5 \cdot \kappa_3 / l$$

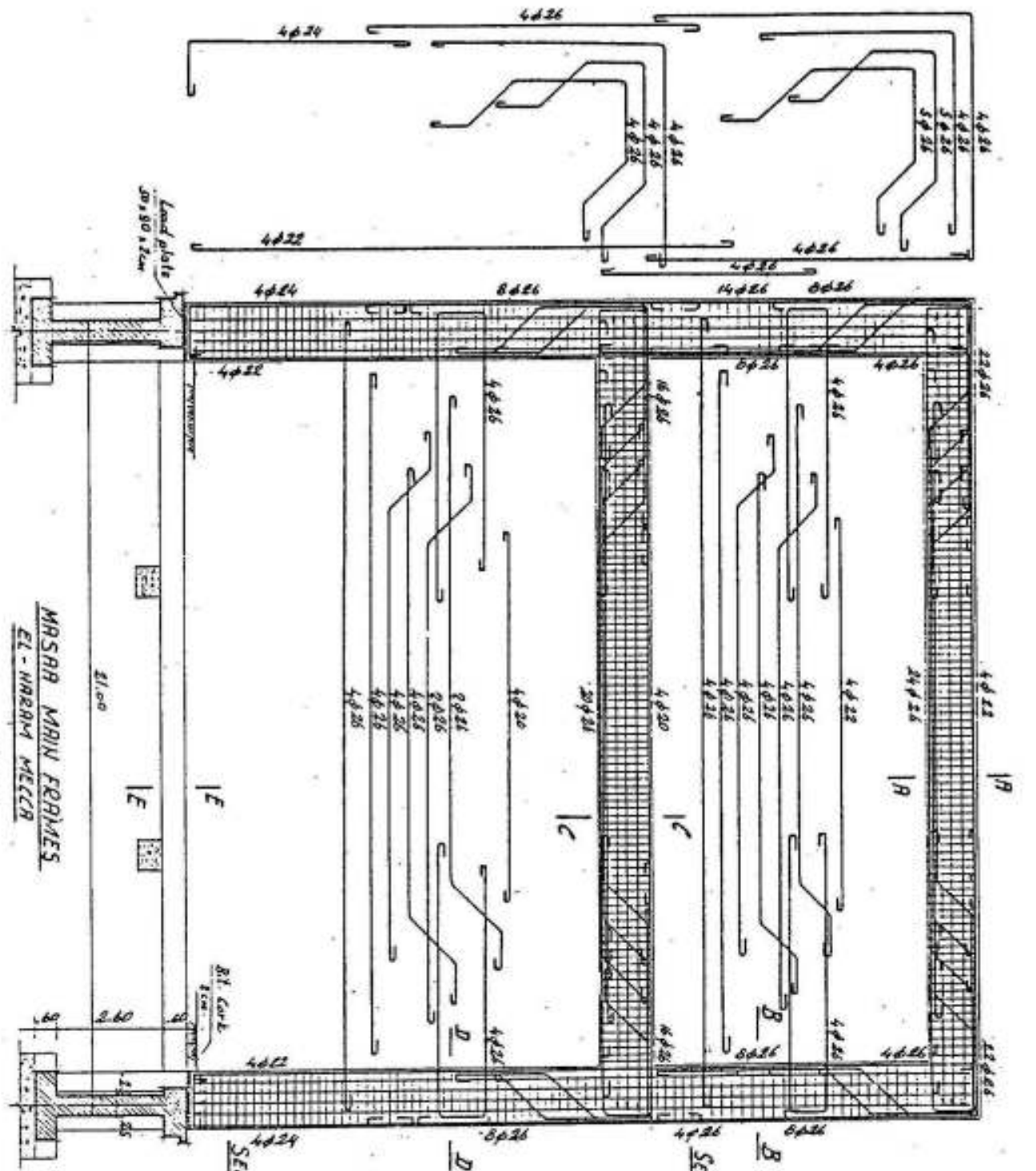
$$\text{joint 3} \quad M_{3a} - M_{3b} - M_{3c} = 0$$

$$\text{Due to symmetry } M_{3c} = M_{4c} \quad \text{and} \quad M_5 = M_6$$

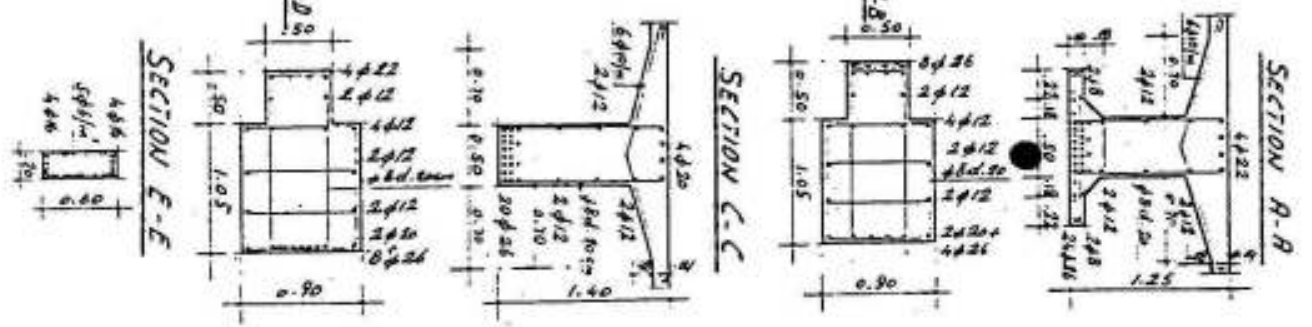
Figure IV-44 shows the details of reinforcements of El Masaa supporting multiple main frames at Mecca; it can be considered as a typical example for this system.

#### Equation of three moments for frames with moving joints

The corners of frames are generally not subject to horizontal or vertical movements if there are fixed supports to prevent this movement or if they are symmetrical and symmetrically loaded, otherwise.



MRSRR MRIN FERRES  
 EL - MRARRA MECCN  
 FIG. IV-14



the corners move from their position. Such frames can be treated as follows: (Fig IV-45).

$$\chi = \frac{I_0}{s_0} \cdot \frac{s}{I}$$

$$\chi' = \frac{I_0}{s_0} \cdot \frac{s'}{I'}$$

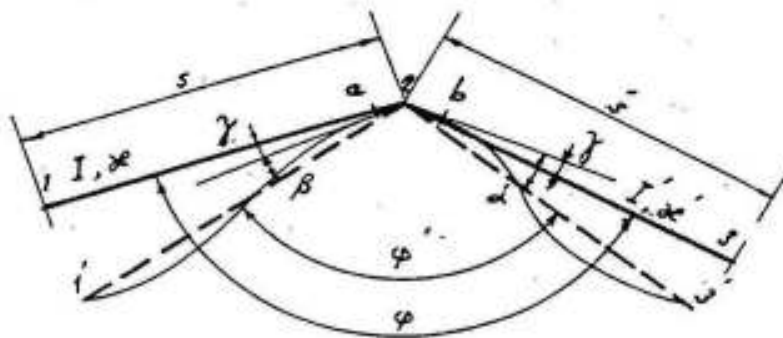


Fig. IV-45

Assume that the two members 1-2 of length  $s$  and 2-3 of length  $s'$  of a frame are rigidly connected at 2, and that the angle between their axes is  $\varphi$ . After deformation, joints 1 and 3 move to 1' and 3'; the angle between the new positions 1'-2 and 2-3' is  $\varphi'$ . Due to the rigidity of the joint, the angle between the tangents to the elastic line at 2 does not change before and after deformation so that:

$$\varphi' = \varphi - \beta - \gamma + \gamma' - \alpha'$$

$$\text{or } \varphi - \varphi' = \overline{\Delta\varphi} = \beta + \alpha'$$

Hence, according to the law of superposition, we get:

$$\overline{\Delta\varphi} = \beta + \alpha' = \beta_0 + M_1 \beta_1 + M_2 \beta_2 + \alpha'_0 + M_2 \alpha'_1 + M_3 \alpha'_2$$

$$\text{or } \overline{\Delta\varphi} = M_1 \beta_1 + M_2 (\beta_2 + \alpha'_1) + M_3 \alpha'_2 + (\beta_0 + \alpha'_0)$$

The right side of this equation has the same general form of the equation of three moments given before.

If we assume further, that the moments of inertia  $I$  and  $I'$  of the members  $s$  and  $s'$  are constant, and

$$\chi = \frac{I_0}{s_0} \cdot \frac{s}{I} \qquad \chi' = \frac{I_0}{s_0} \cdot \frac{s'}{I'}$$

where  $s_0$  and  $I_0$  are the length and moment of inertia of a reference member, we get

$$\frac{6EI_0}{s_0} \cdot \overline{\Delta\varphi} = M_1 \chi + 2M_2 (\chi + \chi') + M_3 \chi' + 6 \left( \frac{r_{2a}}{s} \chi + \frac{r_{2b}}{s'} \chi' \right)$$

Calling  $\frac{6EI_0}{s_0} \overline{\Delta\varphi} = \Delta\varphi$ , then

$$\Delta\varphi = M_1 \chi + 2M_2 (\chi + \chi') + M_3 \chi' + 6 \left( \frac{r_2 b}{s} \chi + \frac{r_2 b}{s'} \chi' \right)$$

This equation gives the modified form of the equation of three moments for frames with moving joints.

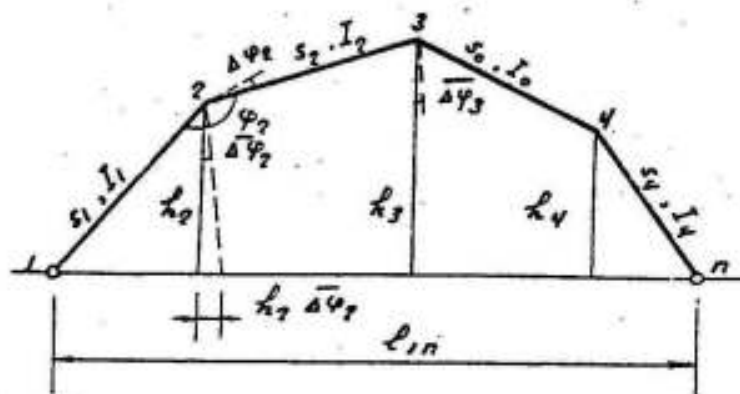


Fig. IV-46

Figure IV-46 shows a frame with rigid moving joints, the change  $\overline{\Delta\varphi}$  of the angles  $\varphi$  can be determined from the given general equation of three moments. Due to  $\overline{\Delta\varphi_2}$ , we get a change in the span  $l_{1-n}$  equal to  $h_2 \overline{\Delta\varphi_2}$ ; so that the change in  $l_{1n}$  due to the change in the angles of all the joints is given by

$$\Delta l_{1n} = h_2 \overline{\Delta\varphi_2} + h_3 \overline{\Delta\varphi_3} + h_4 \overline{\Delta\varphi_4} \dots$$

Multiplying both sides of the equation by  $6EI_0/s_0$ , we get

$$\frac{6EI_0}{s_0} \Delta l_{1n} = h_2 \Delta\varphi_2 + h_3 \Delta\varphi_3 + h_4 \Delta\varphi_4 = \sum h \Delta\varphi$$

If 1 and n are fixed in position, then  $\Delta l_{1n} = 0$ , and

$$\sum h \Delta\varphi = 0$$

If h is also constant, then

$$\sum \Delta\varphi = 0$$

The application of the method will be shown when solving the rectangular frame subject to wind pressure shown in figure IV-47a.

$$\sum \Delta \psi = 0 \quad \text{or} \quad \Delta \psi_c + \Delta \psi_d = 0$$

hence :

$$\left[ 2M_c (\chi + 1) + M_d + \frac{wh^2}{4} \chi \right] + \left[ M_c + 2M_d (\chi + 1) \right] = 0$$

So that

$$M_c + M_d = - \frac{wh^2 \chi}{4(2\chi + 3)}$$

But  $M_c = \frac{wh^2}{2} - Hh$  and  $M_d = -Hh$

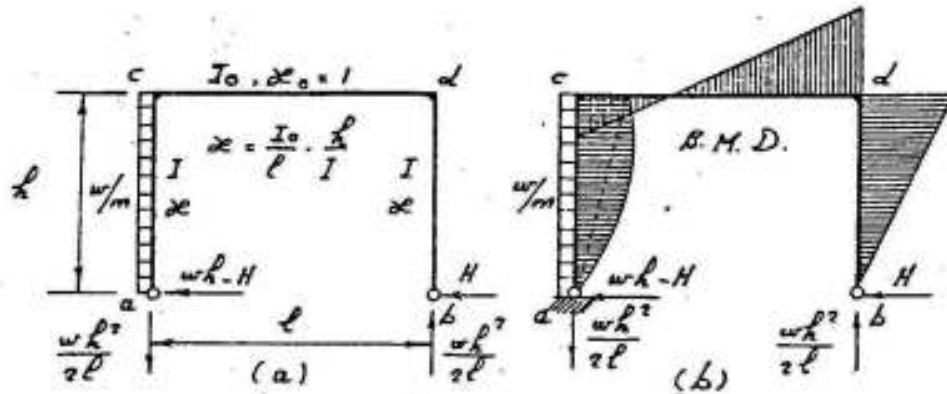


Fig. IV-47

Therefore

$$\frac{wh^2}{2} - 2Hh = - \frac{wh^2 \chi}{4(2\chi + 3)} \quad \text{and}$$

$$H = \frac{wh}{8} \cdot \frac{5\chi + 6}{2\chi + 3}$$

Further;  $M_d = -Hh = - \frac{wh^2}{8} \cdot \frac{5\chi + 6}{2\chi + 3}$

and  $M_c = \frac{wh^2}{2} - Hh = \frac{3wh^2}{8} \cdot \frac{\chi + 2}{2\chi + 3}$

The bending moment diagram is shown in figure IV-47b.

If the unsymmetrical wind load  $w$  is replaced by symmetrical and anti-symmetrical loads  $w/2$  as shown in fig IV-48b & c, the frame can be solved as follows:

For casel: Symmetrical load  $w/2$  , hence  $M_c = M_d$



$$2M_c (\chi + 1) + M_c = - \frac{w}{2} \frac{h^2}{4} \chi \quad \text{or} \quad M_c = - \frac{wh^2 \chi}{8(2\chi + 3)}$$

For case 2 ; Anti-symmetrical load  $w/2$ , hence  $H = wh/2$ , and

$$M_c = -M_d = \pm \frac{wh}{4}$$

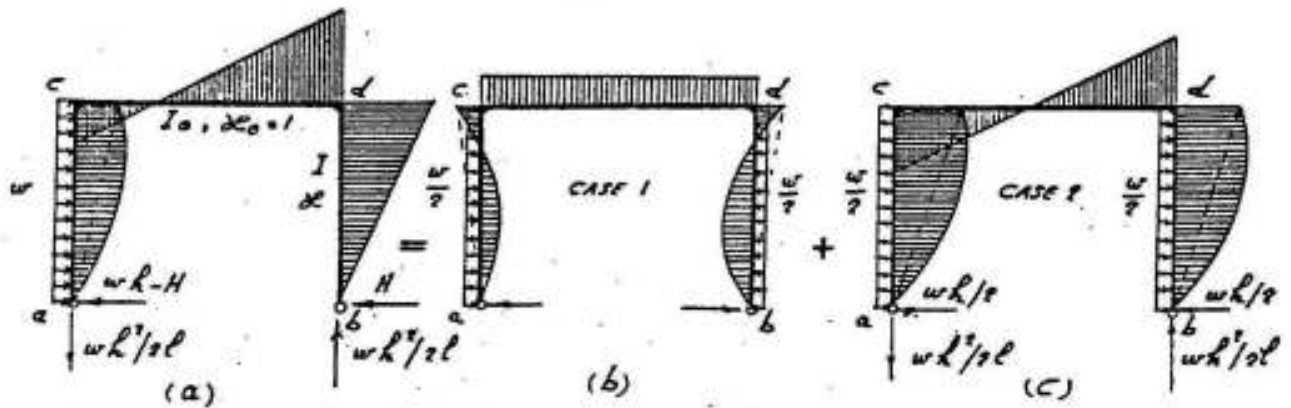


Fig. IV-48

By superposition, we get

$$M_d = - \frac{wh^2 \chi}{8(2\chi + 3)} - \frac{wh^2}{4} = - \frac{wh^2}{8} \cdot \frac{5\chi + 6}{2\chi + 3} \quad \text{and}$$

$$M_c = - \frac{wh^2 \chi}{8(2\chi + 3)} + \frac{wh^2}{4} = \frac{3wh^2}{8} \cdot \frac{\chi + 2}{2\chi + 3}$$

#### Continuous frames with moving joints

The same principles can be applied to continuous frames with moving joints using a modified four moment equation. The solution can be much simplified if unsymmetrical loads can be replaced by symmetrical and antisymmetrical loads as shown in the following example of a continuous frame subject to wind pressure. Fig IV-49.

$$\chi_1 = \frac{I}{l} \cdot \frac{h}{I_1}$$

$$\chi_2 = \frac{I}{l} \cdot \frac{h}{I_2}$$

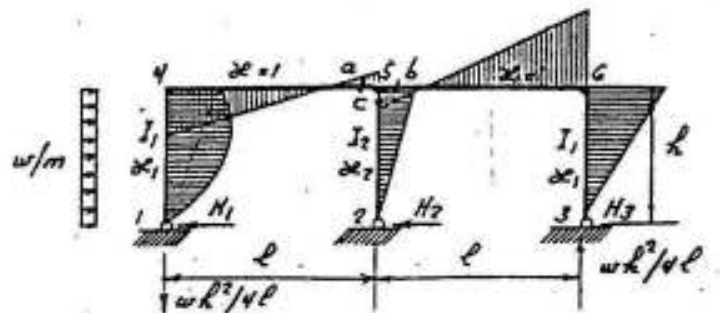


Fig. IV-49

This case of loading can be replaced by the symmetrical case shown in figure IV-50 and the antisymmetrical case shown in figure IV-51.

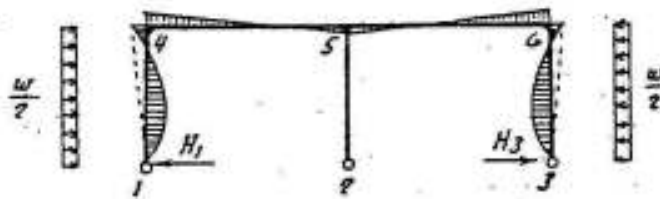


Fig. IV-50

Case 1 ; Symmetrical case. Fig IV-50

Due to symmetry  $M_{5c} = 0$  ,  $M_{5a} = M_{5b} = M_5$

$$M_4 = M_6 \quad , \quad H_1 = H_3 \quad \& \quad H_2 = 0$$

Hence

$$1-4-5 \quad 2M_4 (\chi_1 + 1) + M_5 = -\frac{w}{2} \frac{h^2}{4} \chi_1 \quad (a)$$

$$4-5-6 \quad M_4 + 4M_5 + M_6 = 0 \quad \text{or} \quad M_4 = -2M_5 \quad (b)$$

Equations (a) and (b) give :

$$M_4 = -\frac{wh^2\chi_1}{4(4\chi_1 + 3)} \quad \text{and} \quad M_5 = +\frac{wh^2\chi_1}{8(4\chi_1 + 3)}$$

But  $H_1 h - wh^2/4 = M_4$  so that  $H_1 = M_4/h + wh/4$

and 
$$H_1 = H_3 = \frac{3wh}{4} \cdot \frac{\chi_1 + 1}{4\chi_1 + 3}$$

Case 2 : Anti-symmetrical case of loading : Fig IV-51.

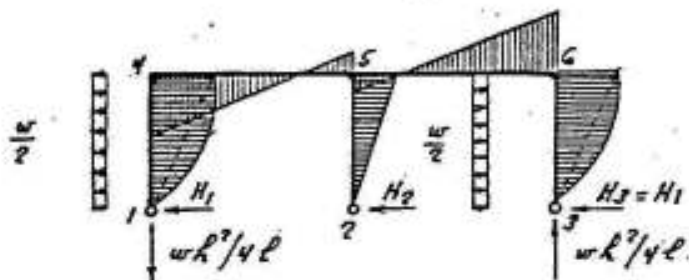


Fig. IV-51

Due to anti-symmetry:  $M_6 = -M_4$  ,  $M_{5a} = -M_{5b}$  ,  $M_{5a} - M_{5b} - M_{5c} = 0$

$$\text{So that } M_{5c} = 2M_{5a}$$

$$\text{Further } H_1 = H_3 \text{ and } H_2 = wh - 2H_1$$

We have

$$\Delta \varphi_4 + \Delta \varphi_{5(a-c)} = 0 \quad \text{hence}$$

$$\left[ 2M_4 (\kappa_1 + 1) + M_{5a} + \frac{w}{2} - \frac{h^2}{4} \kappa_1 \right] + \left[ (M_4 + 2M_{5a} + 2M_{5c} \kappa_2) \right] = 0 \quad (a)$$

Replacing  $M_{5a}$  by  $\frac{1}{2} M_{5c}$  , equation a can be given in the form:

$$2M_4 (2\kappa_1 + 3) + M_{5c} (4\kappa_2 + 3) + \frac{wh^2}{4} \kappa_1 = 0 \quad (b)$$

Referring to figure IV-51 , we find that

$$M_4 = H_1 h - wh^2 / 4 \quad , \quad M_{5c} = -H_2 h = -(wh - 2H_1) h$$

Substituting these values in equation b , we get

$$H_1 = \frac{wh}{16} \cdot \frac{3\kappa_1 + 16\kappa_2 + 18}{\kappa_1 + 2\kappa_2 + 3}$$

As  $H_2 = wh - 2H_1$  , we get further

$$H_2 = \frac{wh}{8} \cdot \frac{5\kappa_1 + 6}{\kappa_1 + 2\kappa_2 + 3}$$

By superposition of cases 1 and 2 , we get

$$H_1 = \frac{wh}{16} \left[ \frac{3\kappa_1 + 16\kappa_2 + 18}{\kappa_1 + 2\kappa_2 + 3} + \frac{12(\kappa_1 + 1)}{4\kappa_1 + 3} \right]$$

$$H_2 = \frac{wh}{8} \cdot \frac{5\kappa_1 + 6}{\kappa_1 + 2\kappa_2 + 3}$$

$$H_3 = \frac{wh}{16} \left[ \frac{3\kappa_1 + 16\kappa_2 + 18}{\kappa_1 + 2\kappa_2 + 3} - \frac{12(\kappa_1 + 1)}{4\kappa_1 + 3} \right]$$

Assuming  $I = 2I_1 = 8I_2$  and  $l = 2h$  then

$$\kappa_1 = 1 \quad , \quad \kappa_2 = 4 \quad \text{and}$$

$$H_1 = 0.658 wh \quad , \quad H_2 = 0.115 wh \quad \text{and} \quad H_3 = 0.227 wh$$

The bending moment diagrams are shown in figures IV-49, 50 & 51.

The following tables give the values of the bending moments at the corners of continuous frames having two, three and four equal spans subject to uniform and wind loads. The moments of inertia of the girder ( $I_0$ ) and of the columns ( $I$ ) are assumed to be constant. The relative stiffness  $\kappa$  is given by:

$$\kappa = \frac{I_0}{I} \cdot \frac{h}{l}$$

The bending moments are given in the form:

$$M = \alpha ( \pm pl^2/4 ) \quad \text{for uniform vertical load } p/m ,$$

$$M = \alpha ( \pm wh^2 ) \quad \text{for horizontal wind load } w/m, \text{ and}$$

$$M = \alpha ( \pm Wh ) \quad \text{for concentrated wind load } W .$$

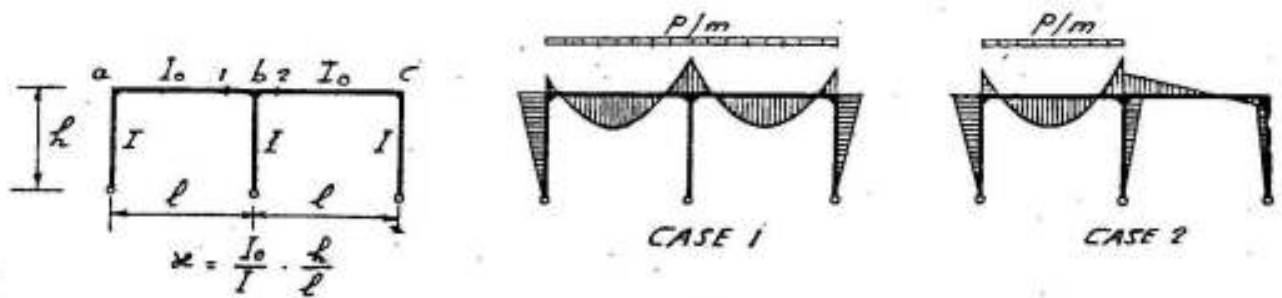
It has to be noticed here that

In case of roofs supported on continuous frames of the form shown in the following tables, the live and wind loads are generally small relative to the dead loads so that for the main vertical superimposed loads, the frames are symmetrical and symmetrically loaded and the bending moments on the intermediate columns are either null or nil. In such cases, the intermediate columns may be chosen slender and act as pendulums capable of resisting vertical reactions only as shown in figure IV-33.

Symmetrical cases of loading can however be calculated by the equation of three moments given on page 79 , while unsymmetrical cases can be replaced by symmetrical and antisymmetrical cases.

Intermediate rigid columns are to be used in cases of unsymmetrical frames, heavy live or wind loads.

Bending Moments in Continuous Frames With Two Equal Spans



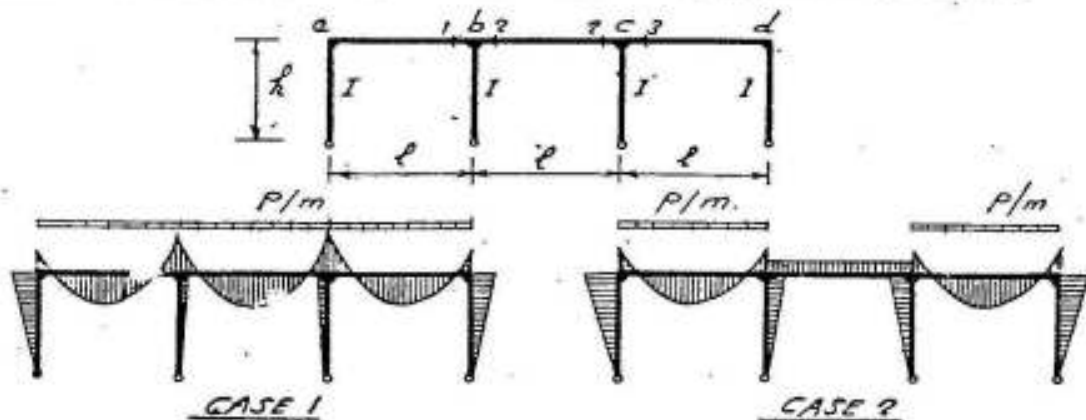
$\kappa$	Case 1		Case 2			
	$M_a = M_c$	$M_{b1} = M_{b2}$	$M_a$	$M_{b1}$	$M_{b2}$	$M_c$
0.05	0.3125	0.3438	0.3150	0.3306	0.0132	0.0025
0.10	0.2941	0.3529	0.2986	0.3280	0.0250	0.0045
0.20	0.2632	0.3684	0.2705	0.3231	0.0453	0.0073
0.30	0.2381	0.3810	0.2473	0.3187	0.0623	0.0092
0.33	0.2315	0.3843	0.2411	0.3174	0.0668	0.0096
0.40	0.2174	0.3913	0.2277	0.3147	0.0766	0.0104
0.50	0.2000	0.4000	0.2111	0.3111	0.0889	0.0111
0.60	0.1452	0.4074	0.1968	0.3079	0.0995	0.0116
0.75	0.1667	0.4167	0.1786	0.3036	0.1131	0.0119
1.00	0.1429	0.4286	0.1548	0.2976	0.1310	0.0119
1.25	0.1250	0.4375	0.1366	0.2928	0.1447	0.0116
1.50	0.1111	0.4444	0.1222	0.2889	0.1556	0.0111
2.00	0.0909	0.4545	0.1010	0.2828	0.1717	0.0101
2.50	0.0769	0.4615	0.0861	0.2784	0.1832	0.0092
3.00	0.0667	0.4667	0.0750	0.2750	0.1917	0.0083
3.50	0.0588	0.4706	0.0665	0.2723	0.1983	0.0076
4.00	0.0526	0.4737	0.0597	0.2702	0.2035	0.0070
5.00	0.0435	0.4783	0.0495	0.2669	0.2114	0.0060
6.00	0.0370	0.4815	0.0423	0.1646	0.2169	0.0053
Multiplier: $p l^2 / 4$						

Bending Moments in Continuous Frames With Two Equal Spans



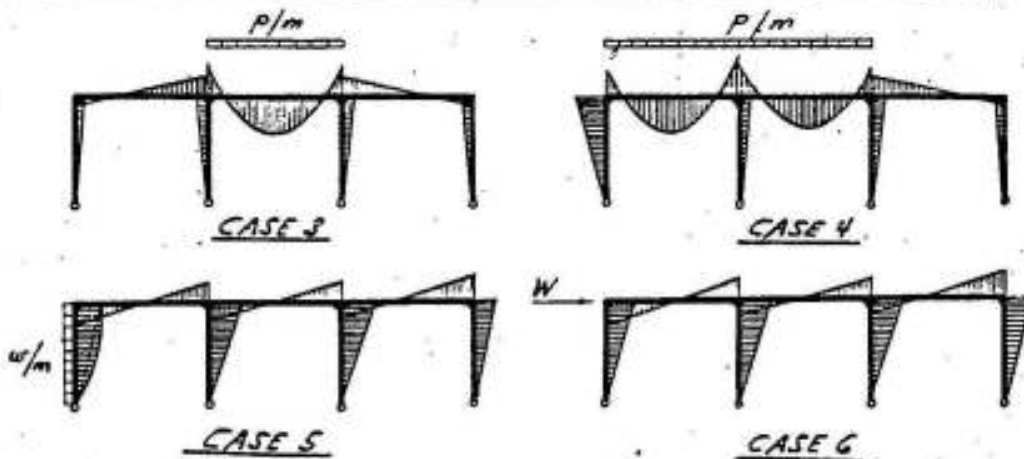
$\kappa$	Case 3				Case 4	
	$M_a$	$M_{b1}$	$M_{b2}$	$M_c$	$M_a = -M_c$	$M_{b1} = -M_{b2}$
0.05	0.1221	0.1221	0.1260	0.1299	0.2540	0.2460
0.10	0.1196	0.1194	0.1268	0.1343	0.2576	0.2424
0.20	0.1153	0.1149	0.1281	0.1417	0.2639	0.2361
0.30	0.1120	0.1113	0.1291	0.1477	0.2692	0.2308
0.33	0.1111	0.1103	0.1294	0.1488	0.2707	0.2293
0.40	0.1093	0.1081	0.1299	0.1527	0.2737	0.2262
0.50	0.1069	0.1056	0.1306	0.1569	0.2778	0.2222
0.60	0.1050	0.1033	0.1311	0.1606	0.2813	0.2188
0.75	0.1027	0.1004	0.1317	0.1652	0.2857	0.2143
1.00	0.0997	0.0967	0.1324	0.1711	0.2917	0.2083
1.25	0.0975	0.0939	0.1329	0.1757	0.2963	0.2037
1.50	0.0958	0.0917	0.1333	0.1792	0.3000	0.2000
2.00	0.0934	0.0884	0.1338	0.1844	0.3056	0.1944
2.50	0.0918	0.0861	0.1341	0.1880	0.3095	0.1905
3.00	0.0906	0.0844	0.1344	0.1906	0.3125	0.1875
3.50	0.0897	0.0831	0.1345	0.1927	0.3148	0.1852
4.00	0.0891	0.0820	0.1346	0.1943	0.3167	0.1831
5.00	0.0880	0.0805	0.1348	0.1967	0.3194	0.1806
6.00	0.0872	0.0793	0.1349	0.1984	0.3214	0.1786
	Multiplier $w h^2$				$W h$	

Bending Moments in Continuous Frames with Three Equal Spans



$\kappa = \frac{I_0}{I} \cdot \frac{h}{l}$		0.05	0.10	0.20	0.30	0.33	0.40	0.50	0.60	0.75
Case 1	$M_a = M_d$	.313	.295	.266	.242	.236	.223	.207	.193	.175
	$M_{b1} = M_{c3}$	.343	.351	.362	.370	.372	.375	.376	.383	.386
	$M_{b2} = M_{c2}$	.334	.334	.337	.339	.340	.342	.345	.347	.351
Case 2	$M_a = M_d$	.322	.312	.291	.273	.268	.256	.241	.228	.211
	$M_{b1} = M_{c3}$	.323	.315	.301	.291	.288	.283	.276	.167	.263
	$M_{b2} = M_{c2}$	.010	.020	.035	.049	.052	.060	.069	.077	.088
Case 3	$M_a = M_d$	.009	.016	.025	.030	.031	.033	.035	.035	.035
	$M_{b1} = M_{c3}$	.020	.036	.061	.079	.083	.093	.104	.112	.122
	$M_{b2} = M_{c2}$	.323	.315	.301	.291	.288	.283	.276	.270	.263
Case 4	$M_{b1}$	.348	.360	.378	.391	.394	.401	.408	.414	.421
	$M_{b2}$	.339	.344	.352	.363	.365	.371	.377	.383	.390
Case 5	$M_a$	.080	.077	.073	.069	.068	.066	.064	.061	.059
	$M_{b1}$	.082	.080	.078	.077	.076	.075	.075	.074	.073
	$M_{b2}$	.083	.083	.082	.082	.082	.081	.081	.081	.081
	$M_{c2}$	.083	.082	.081	.079	.079	.078	.077	.076	.075
	$M_{c3}$	.085	.087	.089	.090	.091	.091	.092	.093	.093
	$M_d$	.088	.092	.098	.103	.105	.108	.111	.114	.118
Case 6	$M_a = -M_d$	.172	.177	.184	.191	.192	.196	.200	.204	.208
	$M_{b1} = -M_{c3}$	.167	.167	.167	.167	.167	.167	.167	.167	.167
	$M_{b2} = -M_{c2}$	.162	.157	.149	.143	.141	.138	.133	.130	.125

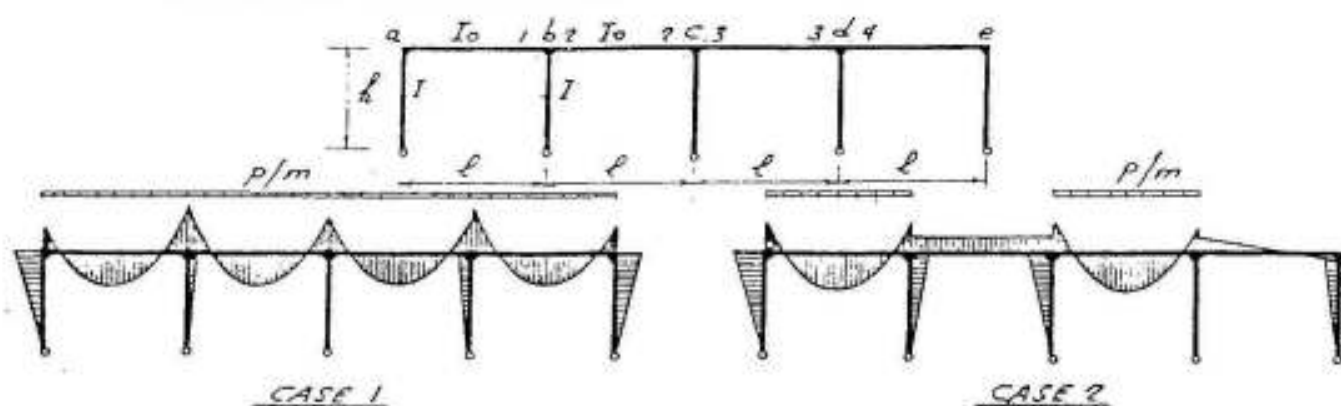
Bending Moments in Continuous Frames with Three Equal Spans



1.00	1.25	1.50	2.00	2.50	3.00	3.50	4.00	5.00	6.00	Multiplica- tor
.153	.135	.121	.101	.086	.075	.067	.060	.050	.043	$pl^2/4$
.390	.392	.394	.396	.397	.398	.398	.399	.399	.399	
.356	.360	.364	.369	.373	.376	.379	.380	.384	.386	
.186	.167	.152	.128	.110	.097	.086	.078	.065	.056	"
.254	.248	.242	.235	.230	.226	.223	.221	.217	.215	
.102	.113	.121	.134	.144	.151	.156	.160	.167	.172	
.034	.032	.030	.027	.024	.022	.020	.018	.015	.013	"
.136	.145	.152	.161	.168	.172	.176	.178	.182	.185	
.254	.248	.242	.235	.227	.226	.223	.221	.217	.215	
.429	.435	.439	.445	.449	.452	.454	.455	.457	.459	"
.400	.408	.414	.423	.430	.434	.438	.441	.445	.449	
.055	.053	.051	.047	.045	.043	.042	.041	.039	.038	$wh^2$
.073	.072	.072	.072	.071	.071	.071	.071	.071	.071	
.082	.082	.082	.083	.083	.083	.083	.084	.084	.084	
.073	.072	.071	.069	.068	.067	.066	.066	.065	.064	
.094	.094	.095	.095	.095	.095	.096	.096	.096	.096	
.123	.127	.130	.135	.138	.140	.142	.143	.146	.147	
.214	.219	.222	.227	.231	.233	.235	.237	.239	.241	$Wh$
.167	.167	.167	.167	.167	.167	.167	.167	.167	.167	
.119	.115	.111	.106	.103	.100	.098	.097	.094	.093	

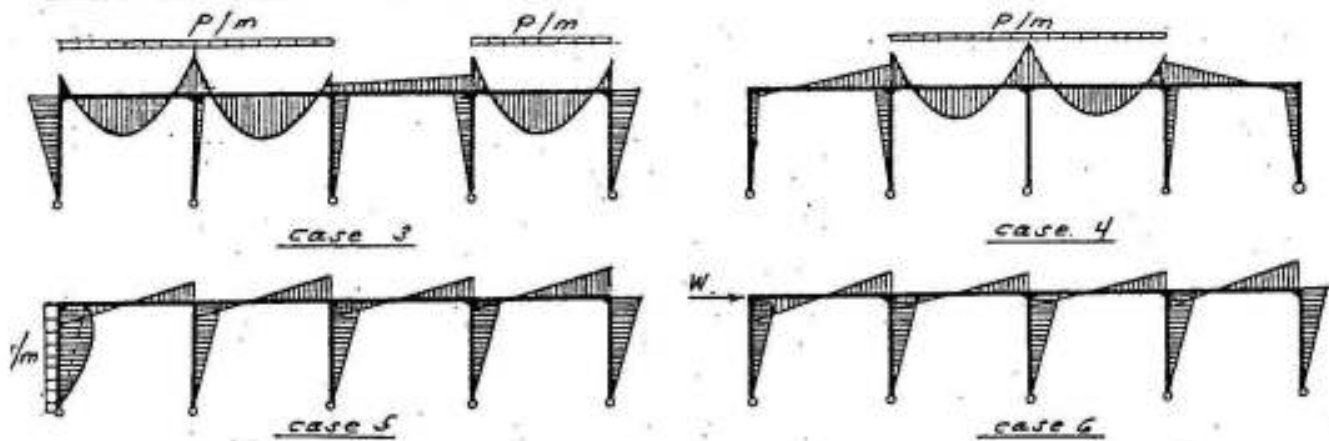


Bending Moments in Continuous Frames with Four Equal Spans



$\kappa = \frac{I_c}{I_b} \cdot \frac{h}{l}$		0.50	0.10	0.20	0.30	0.33	0.40	0.50	0.60	0.75
Case 1	$M_a = M_e$	.313	.295	.266	.242	.236	.222	.206	.192	.174
	$M_{b1} = M_{d4}$	.343	.351	.363	.371	.373	.377	.383	.386	.391
	$M_{b2} = M_{d3}$	.334	.335	.339	.344	.346	.349	.353	.357	.363
	$M_{c2} = M_{c3}$	.333	.332	.330	.328	.327	.326	.324	.322	.319
Case 2	$M_a$	.319	.305	.281	.261	.255	.243	.227	.213	.195
	$M_{b1}$	.327	.321	.310	.302	.300	.295	.289	.283	.277
	$M_{b2}$	.007	.014	.028	.040	.044	.051	.061	.070	.082
	$M_{c2}$	.014	.025	.043	.055	.059	.065	.073	.080	.087
	$M_{c3}$	.319	.307	.288	.273	.269	.260	.250	.242	.232
	$M_{d3}$	.327	.321	.312	.304	.302	.297	.292	.287	.281
	$M_{d4}$	.016	.030	.052	.069	.074	.083	.094	.103	.115
	$M_b$	.006	.010	.016	.019	.019	.020	.021	.021	.021
Case 3	$M_{b1}$	.344	.353	.367	.379	.382	.388	.396	.402	.410
	$M_{b2}$	.344	.352	.367	.378	.381	.387	.395	.401	.409
Case 4	$M_{c2} = M_{c3}$	.343	.351	.363	.371	.373	.377	.382	.387	.391
Case 5	$M_a$	.059	.055	.050	.045	.044	.042	.039	.036	.033
	$M_{b1}$	.061	.059	.057	.055	.055	.054	.053	.053	.052
	$M_{b2}$	.063	.063	.064	.065	.065	.065	.066	.067	.068
	$M_{c2}$	.063	.063	.063	.064	.064	.064	.064	.065	.065
	$M_{c3}$	.062	.062	.062	.062	.061	.061	.061	.060	.060
	$M_{d3}$	.062	.062	.061	.061	.060	.060	.059	.058	.057
	$M_{d4}$	.064	.066	.068	.070	.070	.071	.072	.073	.073
	$M_e$	.066	.070	.075	.080	.081	.083	.086	.089	.092
Case 6	$M_a = -M_e$	.130	.134	.141	.147	.148	.151	.155	.158	.162
	$M_{b1} = -M_{d4}$	.126	.127	.127	.128	.128	.128	.128	.128	.128
	$M_{b2} = -M_{d3}$	.122	.120	.113	.112	.111	.109	.106	.104	.101
	$M_{c2} = -M_{c3}$	.122	.120	.117	.114	.113	.112	.111	.110	.108

Bending Moments in Continuous Frames with Four Equal Spans



1.00	1.25	1.50	2.00	2.50	3.00	3.50	4.00	5.00	6.00	Multiplica- tor
.151	.133	.119	.099	.084	.073	.065	.058	.049	.041	$pl^2/4$
.397	.402	.405	.409	.412	.415	.416	.418	.420	.421	
.370	.376	.381	.389	.394	.398	.402	.404	.408	.411	
.315	.312	.310	.306	.303	.301	.299	.298	.296	.294	
.171	.152	.137	.114	.098	.086	.076	.069	.057	.049	"
.268	.262	.257	.249	.244	.240	.237	.235	.231	.229	
.098	.111	.121	.136	.147	.156	.162	.167	.175	.181	
.097	.103	.108	.115	.120	.123	.126	.128	.130	.132	
.218	.209	.201	.191	.183	.178	.174	.170	.166	.162	
.272	.265	.260	.253	.247	.243	.240	.237	.233	.231	
.129	.140	.148	.160	.168	.175	.179	.183	.188	.192	
.020	.019	.018	.016	.014	.013	.011	.010	.009	.008	
.421	.428	.434	.443	.449	.453	.457	.459	.463	.466	"
.419	.427	.433	.442	.448	.452	.456	.459	.463	.465	"
.397	.402	.405	.409	.412	.415	.416	.418	.420	.421	"
.028	.025	.022	.019	.016	.014	.012	.011	.009	.008	$wh^2$
.051	.050	.049	.048	.048	.047	.047	.047	.046	.046	
.069	.071	.071	.073	.074	.075	.075	.076	.077	.077	
.066	.067	.067	.068	.068	.069	.069	.069	.070	.070	
.059	.059	.058	.057	.057	.056	.056	.056	.056	.055	
.056	.055	.054	.052	.051	.050	.050	.050	.048	.048	
.075	.075	.076	.077	.077	.078	.078	.078	.079	.079	
.097	.100	.103	.107	.109	.111	.113	.114	.116	.117	
.167	.171	.174	.179	.182	.184	.186	.188	.190	.191	$wh$
.128	.128	.128	.128	.127	.127	.127	.127	.126	.126	
.098	.095	.093	.090	.088	.086	.085	.084	.082	.081	
.107	.105	.105	.104	.103	.103	.102	.102	.102	.101	

Multiple frames with moving joints

Joints of multiple frames subject to unsymmetrical loads (e.g. wind pressure) move horizontally. The equations of elasticity are : (Fig IV-52a).

$$\Delta\psi_1 + \Delta\psi_2 = 0 \quad , \quad \Delta\psi_1 + \Delta\psi_{3ac} = 0 \quad , \quad \Delta\psi_2 + \Delta\psi_{4ac} = 0 \quad \dots \text{etc.}$$

Their number is 10 and are sufficient to determine the 10 unknown moments although they need a lot of time.

The solution can be much simplified, if the unsymmetrical wind load shown in 'a' is replaced by the symmetrical load shown in 'b' and the anti-symmetrical load shown in 'c' .

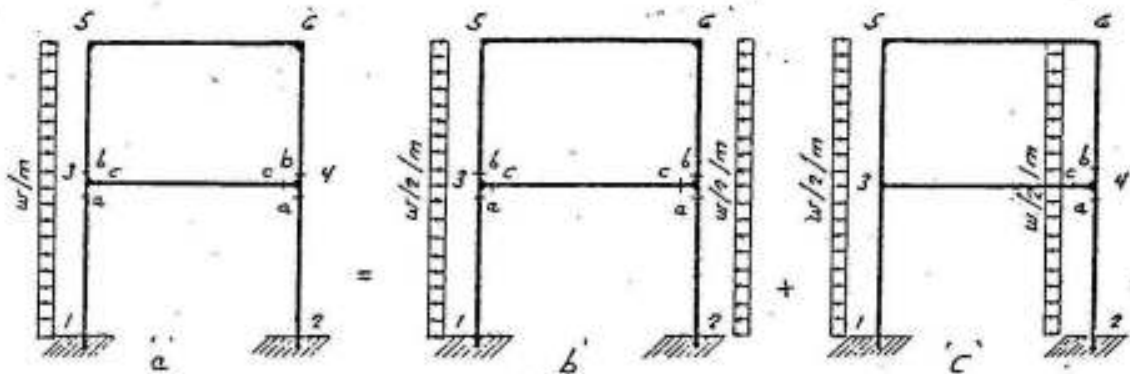


Fig. IV-52

Due to symmetry of case b, we have:

$$M_1 = M_2 \quad , \quad M_{3a} = M_{4a} \quad , \quad M_{3b} = M_{4b}$$

$$M_{3c} = M_{4c} \quad \text{and} \quad M_5 = M_6 ;$$

whereas due to anti-symmetry of case c, we have:

$$M_1 = -M_2 \quad , \quad M_{3a} = -M_{4a} \quad , \quad M_{3b} = -M_{4b}$$

$$M_{3c} = -M_{4c} \quad \text{and} \quad M_5 = -M_6$$

The bending moment diagram is shown in figure IV-53.

The distribution of the bending moments in building frames depends mainly on the relative stiffness of the members\* as shown in figure IV-54.

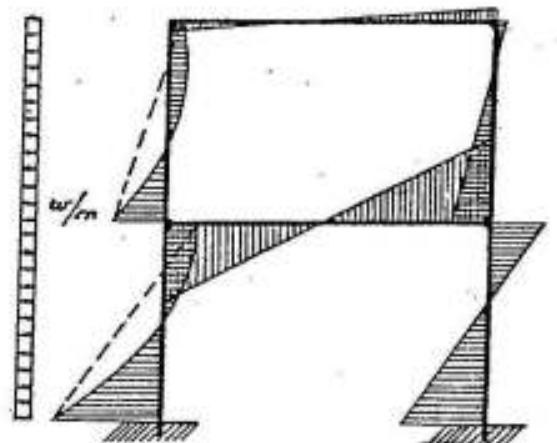


Fig. IV-53

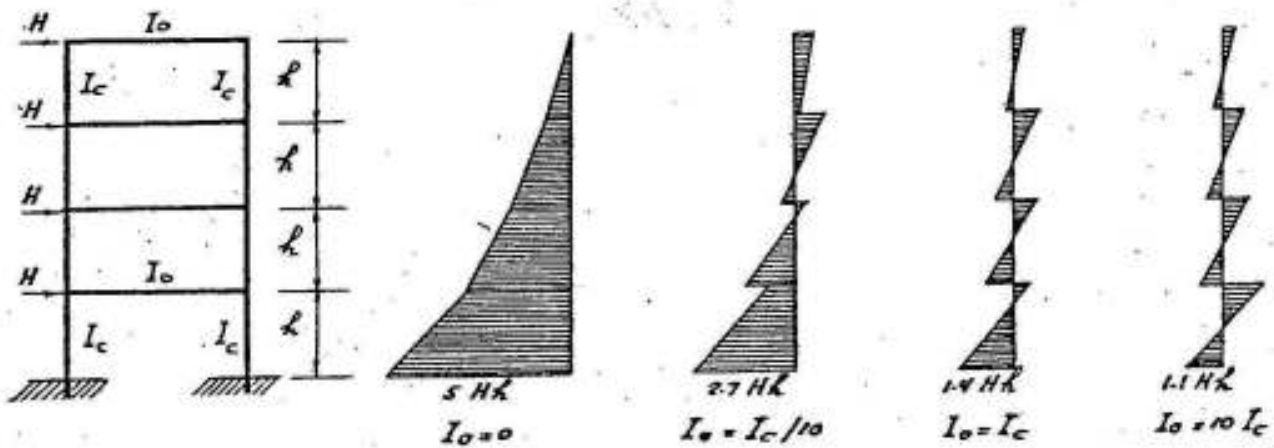


Fig. IV-54

In practical cases of building frames, the bending moments can be estimated in the manner shown in figure IV-55.

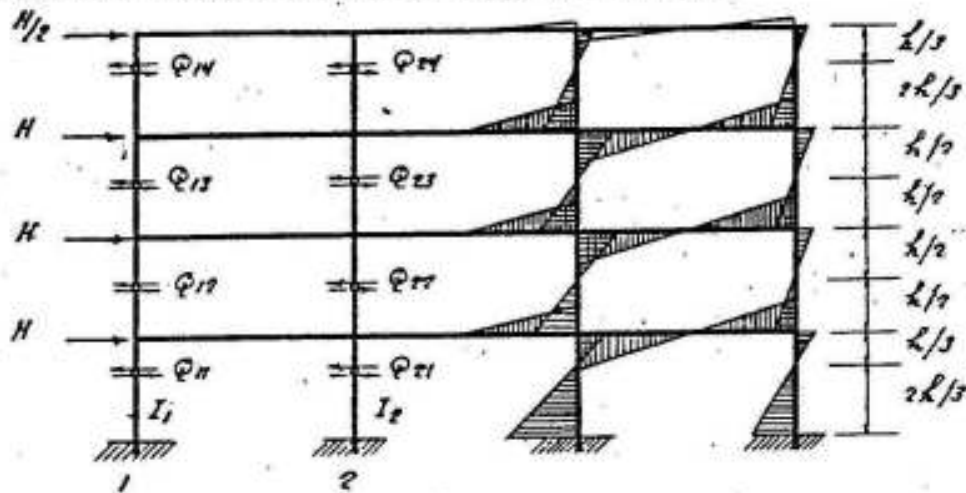


Fig. IV-55

One may assume that the total shearing force  $\sum H$  acting on any of the floors is distributed on the columns in proportion to their moment of inertia\*. Hence

$$Q_1 = \sum H \frac{I_1}{2(I_1 + I_2)} \quad ; \quad Q_2 = \sum H \frac{I_2}{2(I_1 + I_2)}$$

The bending moments in the girders at inner supports may be assumed equal; they must keep the equilibrium of the joints as shown in fig. IV-56 which shows the equilibrium of the joints at exterior and

\* G. Franz. Konstruktionslehre des Stahlbetons. Springer-Verlag Berlin

interior columns.

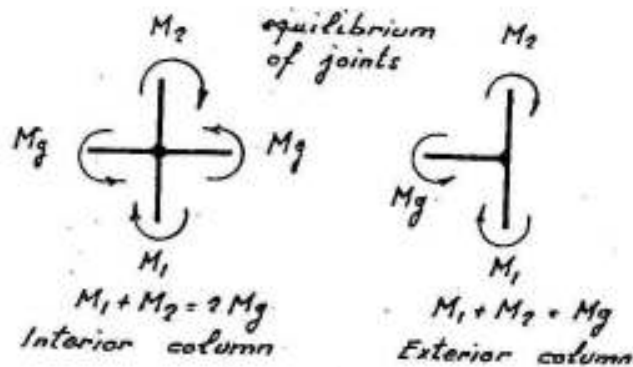


Fig. IV-56

### Cantilever Frames

Cantilever frames are extensively used in simple statically determinate plane forms as shown in figures IV-57 , 58 and 59.

Figure IV-57 shows the cross-section of an exhibition hall at Munich. The hall is 40 ms wide and 12 ms high, each of the main supporting elements is composed of two, double-cantilever statically determinate frames. The upper cantilever arm is 15 ms long while the intermediate one is 10 ms only. The intermediate 10 ms in the roof are covered by crystal glass windows. The soil being rocky it was possible to use isolated footings of the form shown in figure.

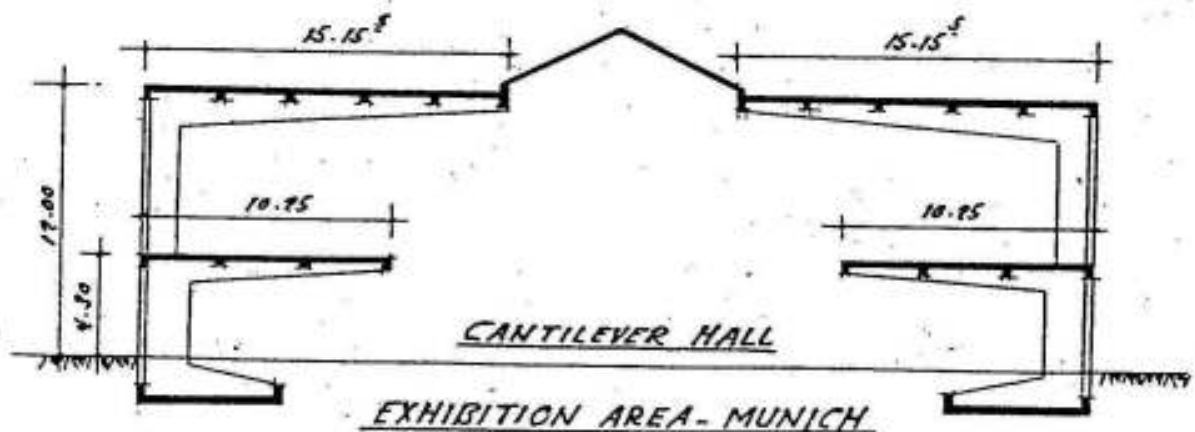
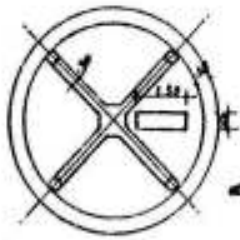
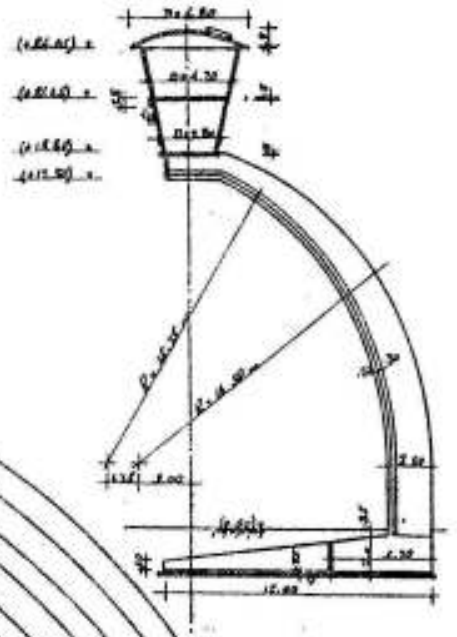


Fig. IV-57

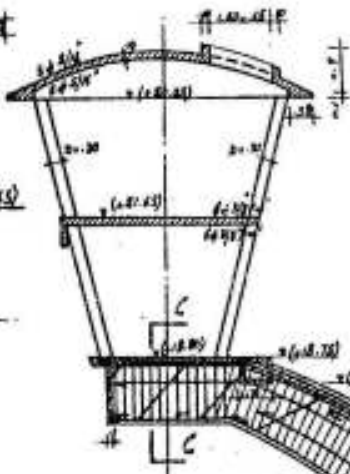
Figure IV-58 shows the main stand of the parade area at Cairo . The main cantilevers are 21.5 ms long and 3.0 ms between centers. Due to the architectural and structural requirements, the folded slab of the roof is located at the bottom of the main cantilever girders which have a maximum depth of 2.87 ms and a breadth of 30 cms (Sec. 2-2) Due to the big amount of tension steel required in the outside fiber

UPPER FLOOR

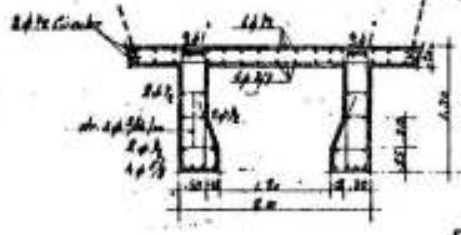
TELEVISION AND BROADCASTING CABIN  
AT THE PARADE AREA  
EL-NASR CITY BRID



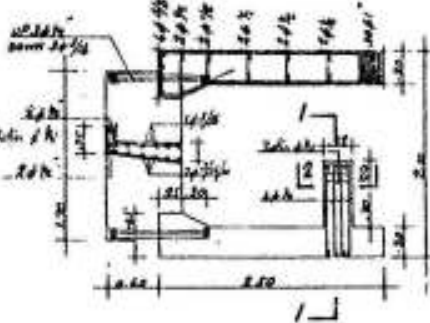
MIDDLE FLOOR (CROSS)



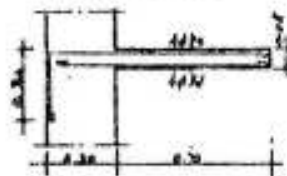
SECTION C-C



SECTION R-R



SECTION 1-1



SECTION 2-2



SECTION D-D

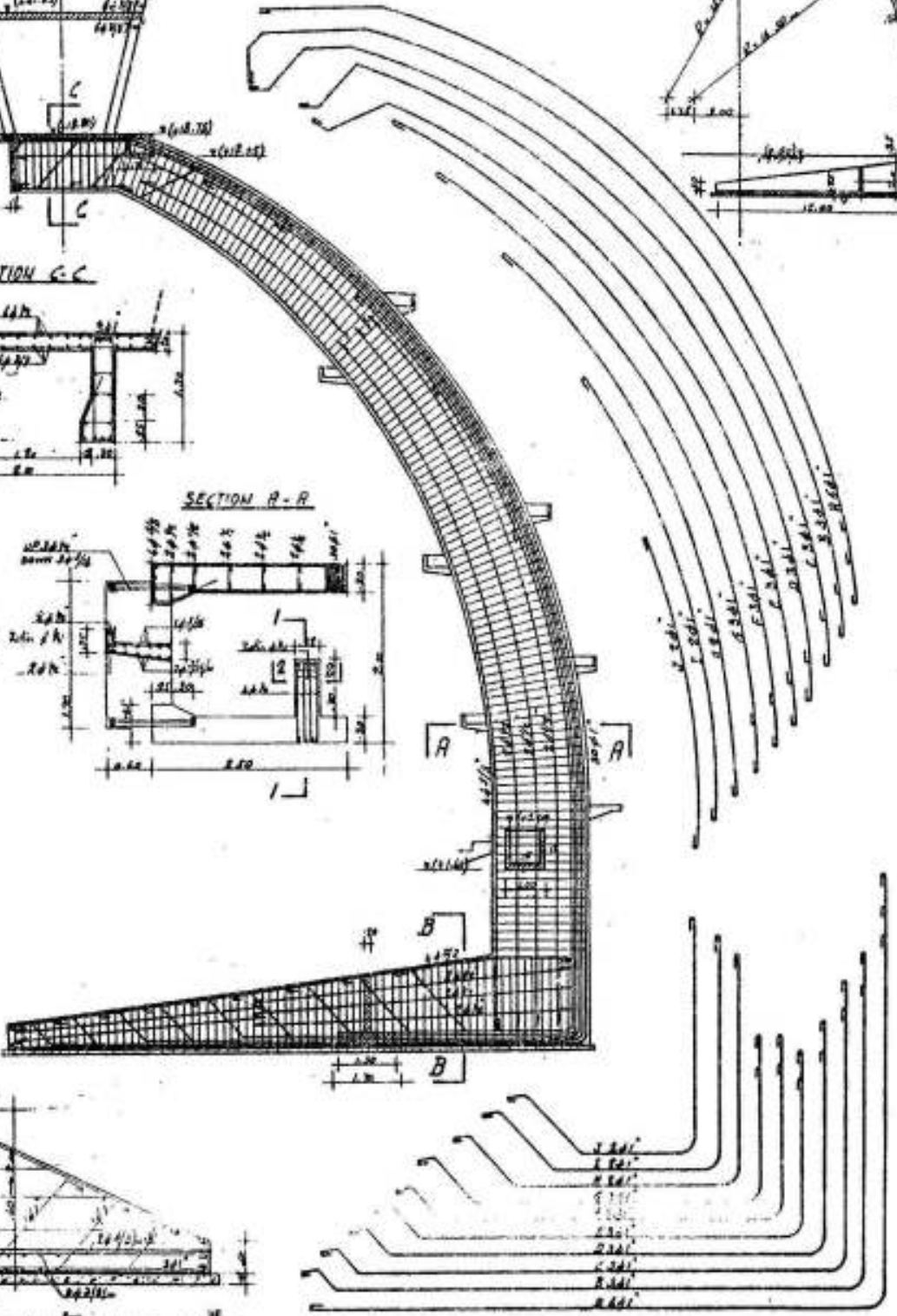
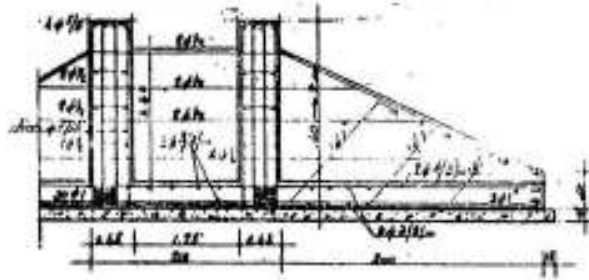


Fig. IV 5C

at the joint between the cantilever and the main column, it was necessary to add diagonal corner bars of the form shown in figure IV-14 to resist the possible splitting tensile stresses.

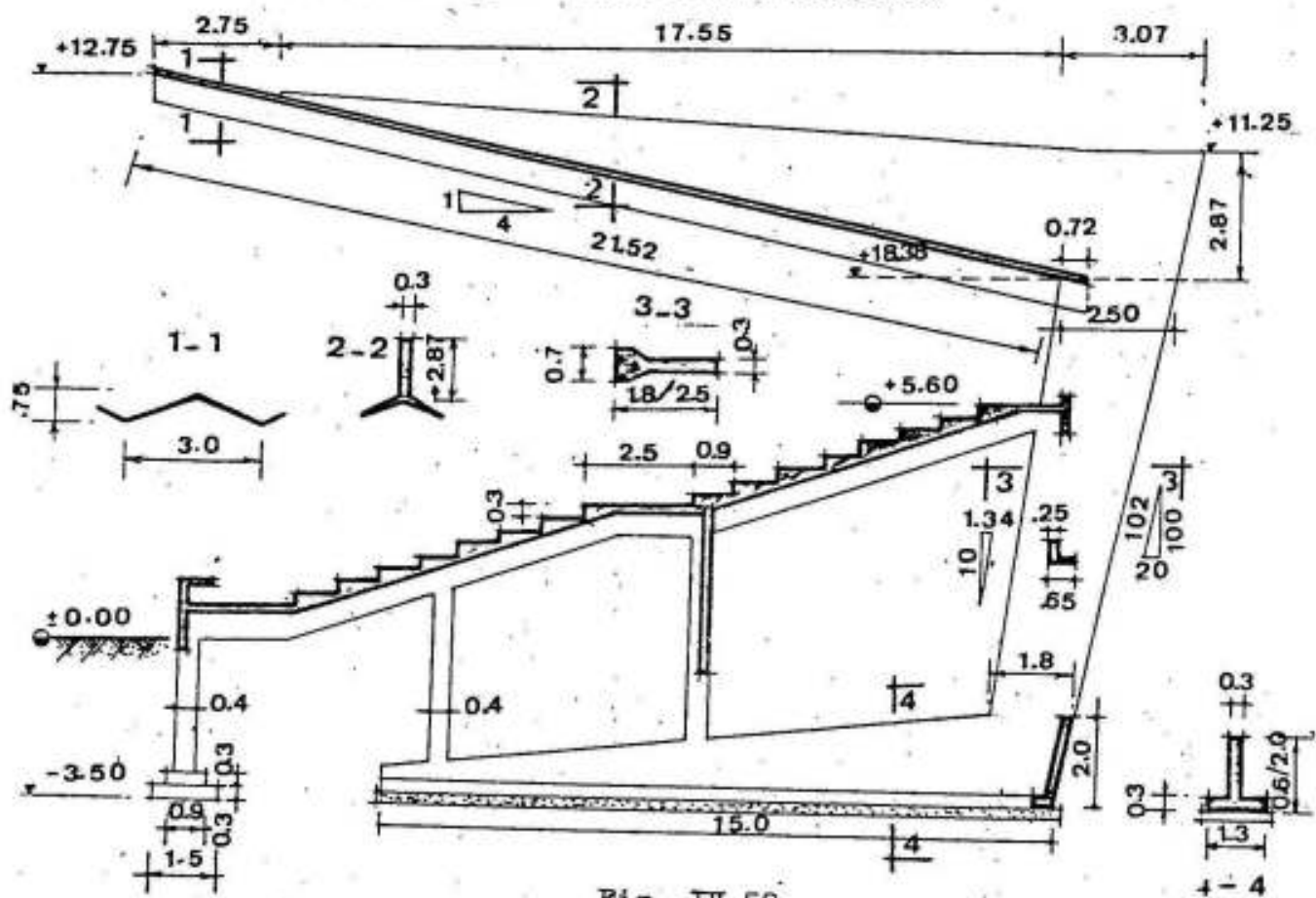


Fig. IV-58

Figure IV-59 shows the layout, main dimensions and details of reinforcements of the television and broadcasting cabin in the parade area at Cairo. The main supporting element of the cabin is composed of two curved simple cantilever frames at 1.7 ms between centers. The max. cross-section of each frame is 30x250 cms reinforced by 30  $\phi$  1" on the tension side. During construction, the main tension reinforcement was replaced by 21  $\Phi$  25 mm cold-twisted tor-steel of which, not more than two bars were spliced in any section. Due to the high compressive stresses in the girders, each one was provided with an unsymmetrical compression flange as shown in figure. The reinforced concrete landings of the staircase together with the foundation slab and cross-rib, and the top slab at level 18.75 join the two girders and prevent any lateral buckling. Due to the concentration of the main loads in the cabin, it was necessary to extend the combined footing of the frames to 15. ms. The breadth of the footing, necessary to limit the stress on the sandy layers in the site to 1.5 kg/cm<sup>2</sup> was 8. ms.

## Special Forms of Frames

Simple and continuous frames can further be used in various forms to satisfy certain requirements as shown in the following structures:

1) Unsymmetrical simple or continuous saw-tooth frames as shown in figure IV-60.

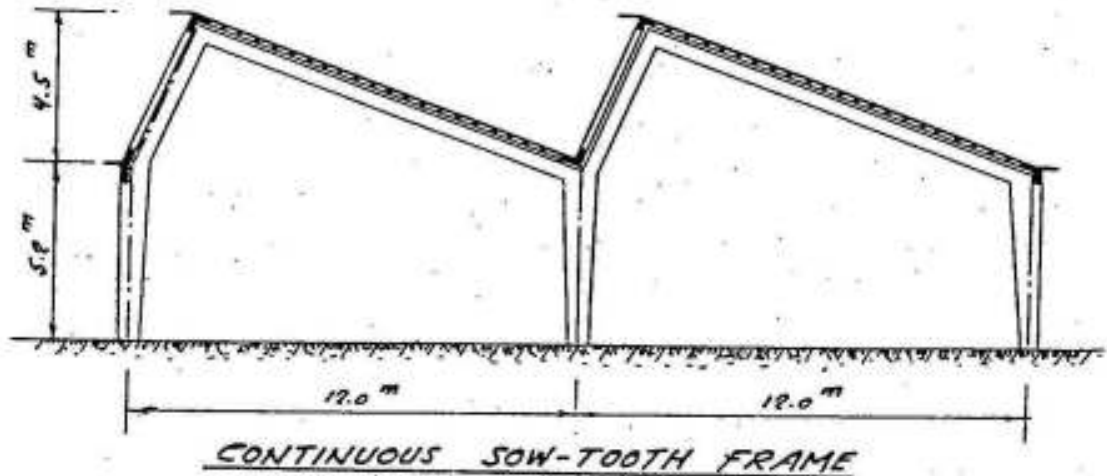


Fig. IV-60

2) Continuous frames as shown in figure IV-61

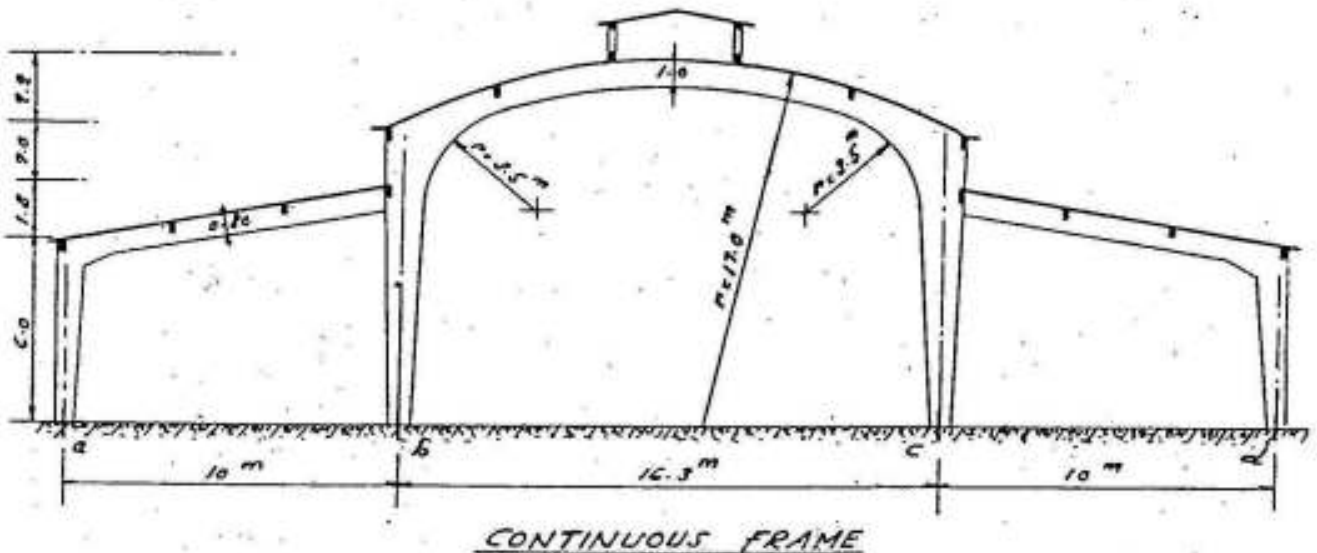


Fig. IV-61

The system shown in figure is provided with hinges at the foot of the columns and hence it is five times statically indeterminate for general cases of loading and three times statically indeterminate for symmetrical cases of loading if the main system is chosen statically



determinate; for example, by removing the hinges at a & d and replacing the hinge at c by a roller.

The statically indeterminate values and the required equations of elasticity for both cases are as follows:

a) General case of loading: e.g. wind loads. (Fig. IV-62).

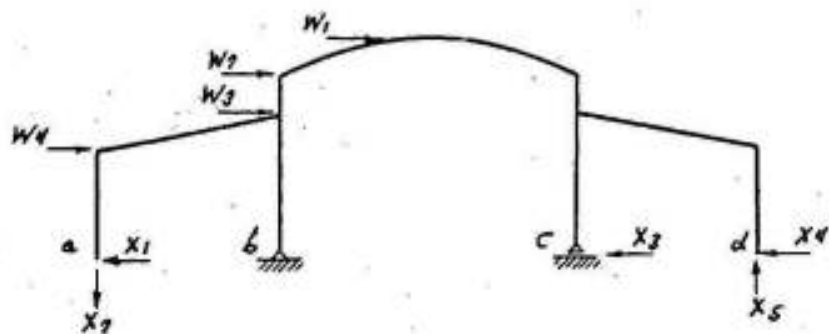


Fig. IV-62

$$\begin{aligned}
 -\delta_1 = 0 &= \delta_{10} + X_1 \delta_{11} + X_2 \delta_{12} + X_3 \delta_{13} + X_4 \delta_{14} + X_5 \delta_{15} \\
 \delta_2 = 0 &= \delta_{20} + X_1 \delta_{21} + X_2 \delta_{22} + X_3 \delta_{23} + X_4 \delta_{24} + X_5 \delta_{25} \\
 \delta_3 = 0 &= \delta_{30} + X_1 \delta_{31} + X_2 \delta_{32} + X_3 \delta_{33} + X_4 \delta_{34} + X_5 \delta_{35} \\
 &\dots \text{ etc.}
 \end{aligned}$$

b) Symmetrical case of loading: e.g. dead loads. (Fig. IV-63).

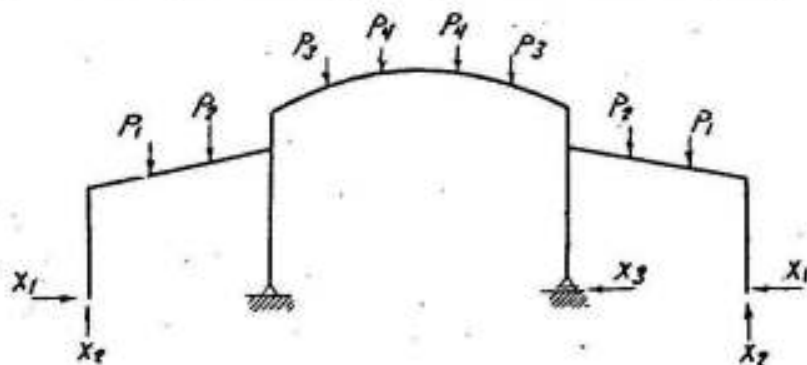


Fig. IV-63

$$\begin{aligned}
 \delta_1 = 0 &= \delta_{10} + X_1 \delta_{11} + X_2 \delta_{12} + X_3 \delta_{13} \\
 \delta_2 = 0 &= \delta_{20} + X_2 \delta_{21} + X_2 \delta_{22} + X_3 \delta_{23} \\
 \delta_3 = 0 &= \delta_{30} + X_1 \delta_{31} + X_3 \delta_{32} + X_3 \delta_{33}
 \end{aligned}$$

The displacements with double indices  $\delta_{jk}$  can be determined acco-

rding to the theory of virtual work from the general equation

$$1 \cdot \delta_{jk} = \int M_j M_k ds / EI$$

The general case of loading given under "a" can however be simplified if it is replaced by a symmetrical case of loading and an antisymmetrical case of loading.

For the symmetrical case, figure IV-64, we have:

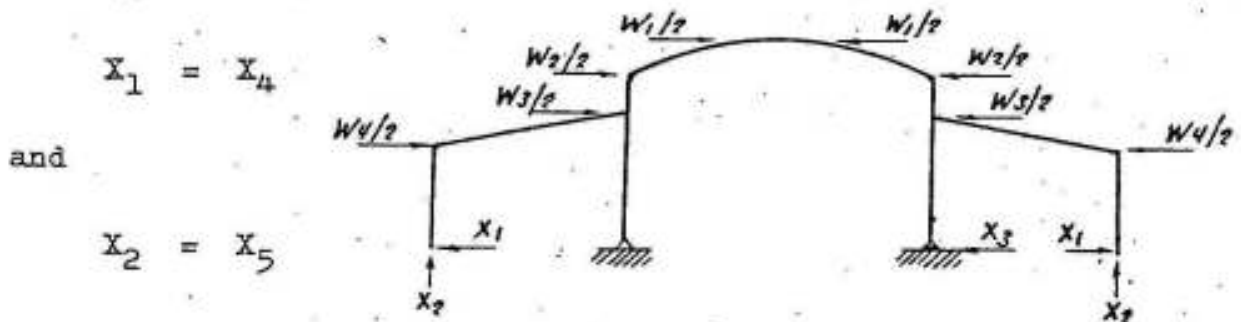


Fig. IV-64

Whereas, for the antisymmetrical case, figure IV-65, we have:

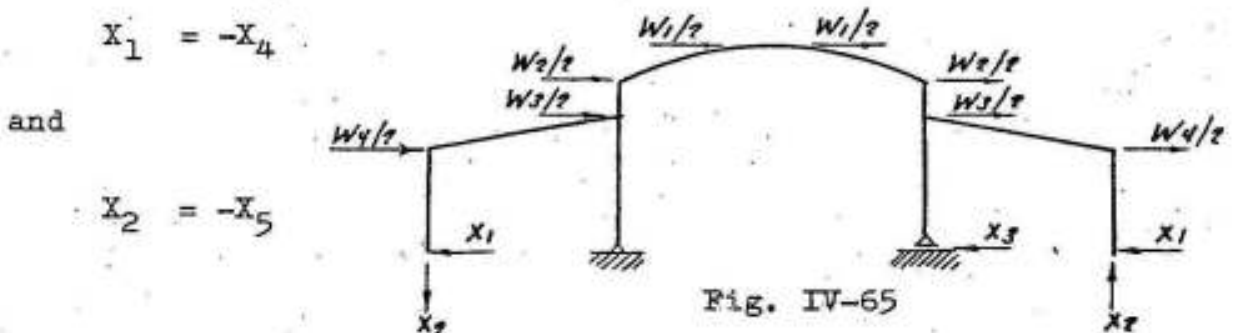


Fig. IV-65

It is also possible to choose a statically indeterminate main system by dividing the frame into three units and introducing rollers at the joints of the side halls with the intermediate columns as shown in figure IV-66.

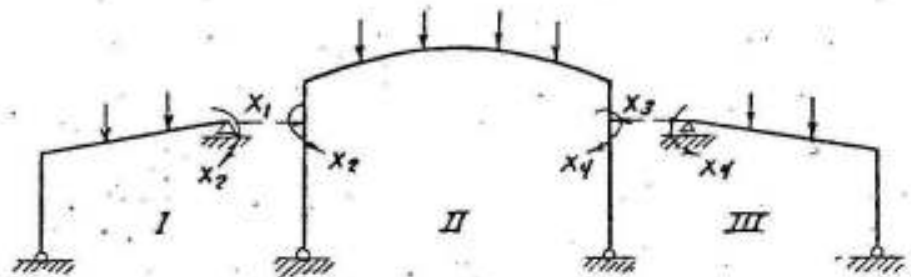


Fig. IV-66

In this manner, the main system of the two units I and III is statically determinate while that of unit II is once statically indeterminate.

For general unsymmetrical cases of loading the unknowns are  $X_1$ ,  $X_2$ ,  $X_3$  and  $X_4$ . For symmetrical frames symmetrically loaded,  $X_1 = X_3$  and  $X_2 = X_4$ , while for antisymmetrical cases of loading  $X_1 = -X_3$  and  $X_2 = -X_4$ . If unsymmetrical loads are replaced by symmetrical and antisymmetrical loads, the unknowns are generally not more than two and the problem is much simplified.

If a tie is allowed at the foot of the arched girder, the system shown in figure IV-67 may be used.

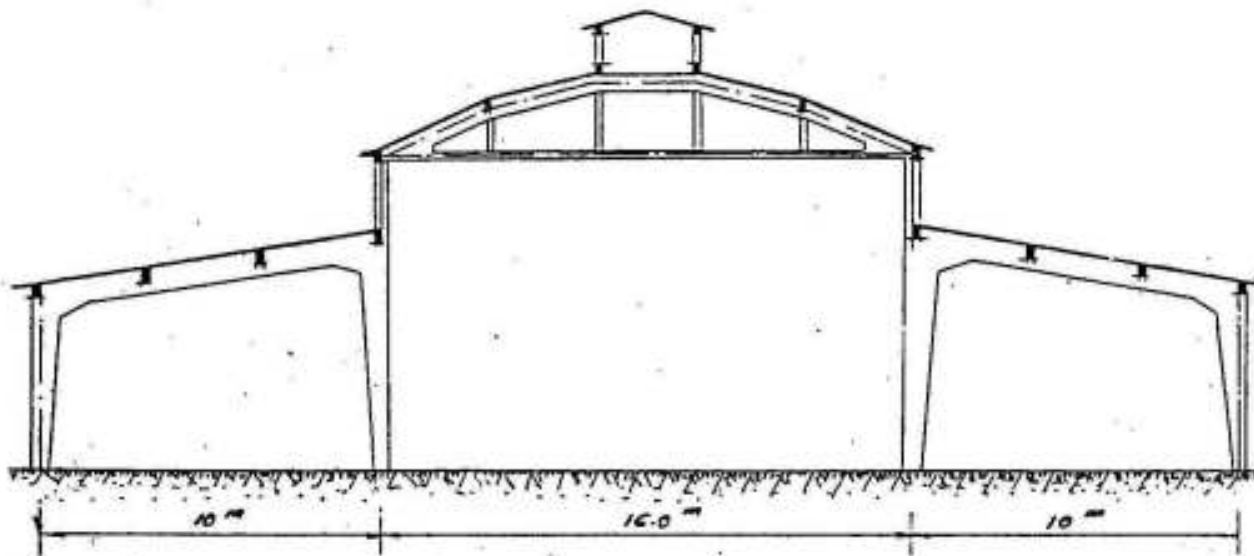


Fig. IV-67

Each of the two main side elements may be considered as a two hinged frame while the intermediate polygonal girder with its tie may be considered as freely supported on the two upper slender columns.

3) Frames supporting sports stands as shown in figure IV-68.

It is recommended in such a simple two-hinged frame to choose its form such that the bending moment along "d-e" is partly negative at "d" and "e" and partly positive at "m" and that the maximum positive and negative bending moments are approximately equal.

Figures IV-69 and 70 give the general layout and details of reinforcement of the arena at the Cairo International Fair-city. It shows an ingenious application of a simple idea to give a masterpiece in the

in the field of structural engineering. In order to give the required form for the main girders, it was necessary to increase their breadth at the outside support as shown.

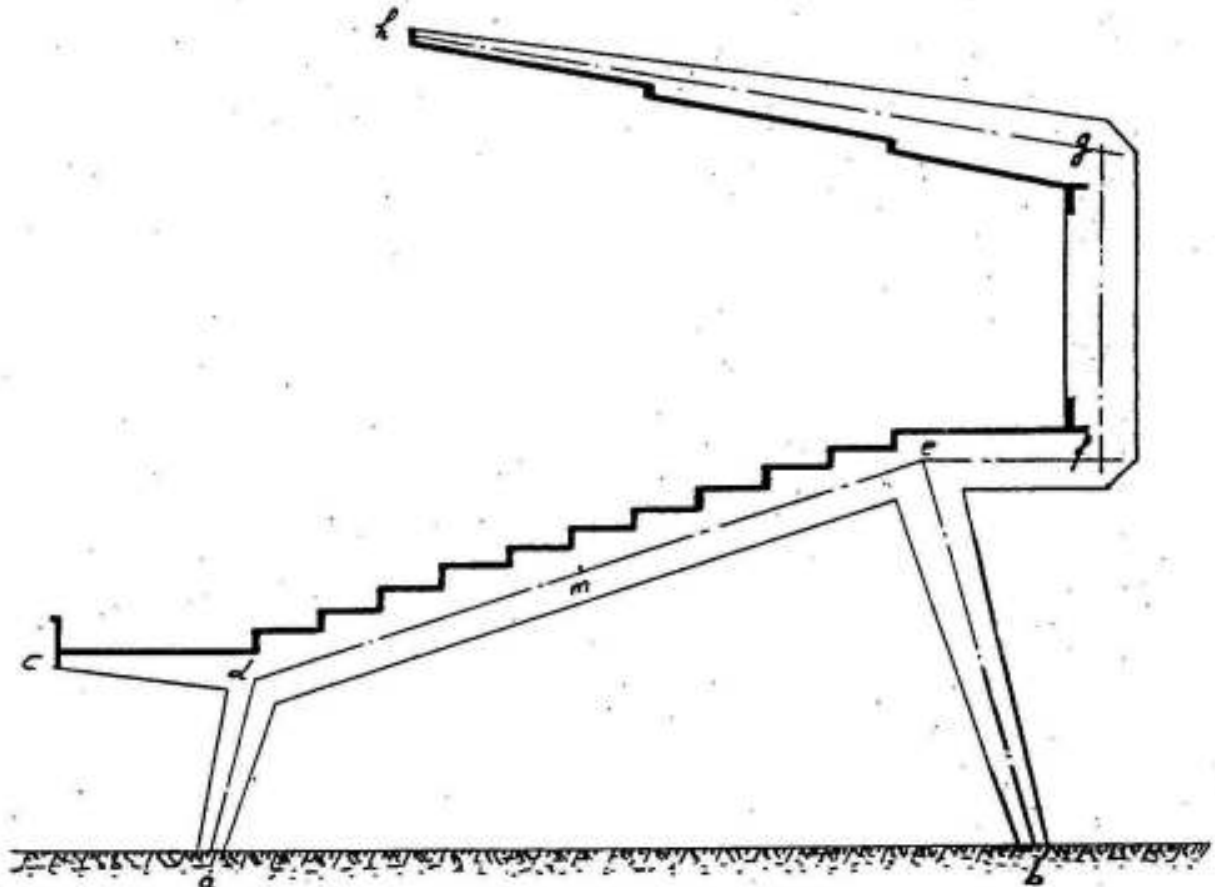
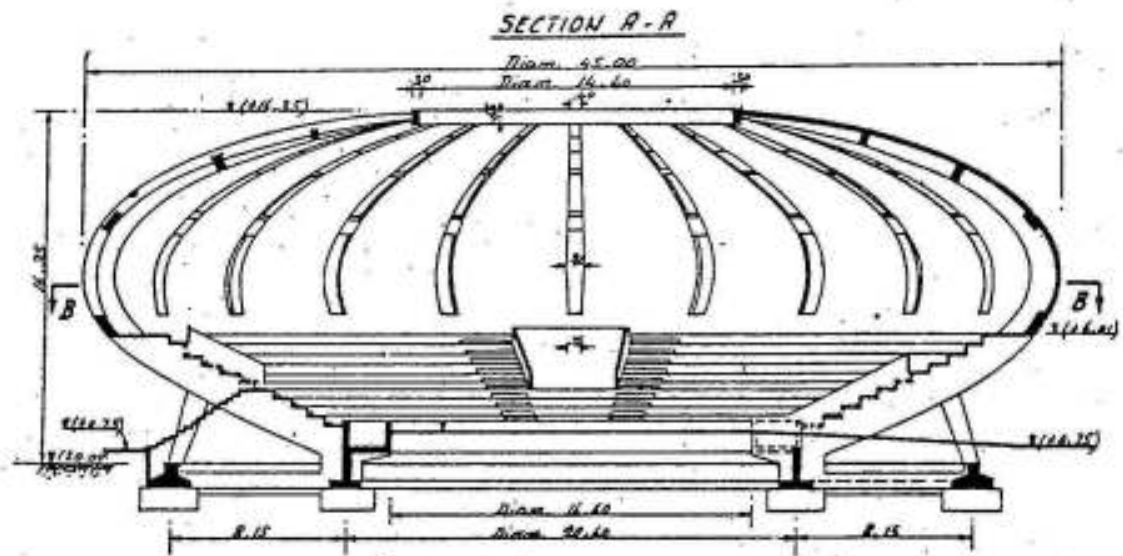


Fig. IV-68

4) Radial frames supporting the Planetarium at Cairo. Figure IV-71.

It was required to construct a floor for the Planetarium inside one of the main buildings in the exhibition land at Gezirah. It was further specified that the new structure must be completely separated from the original building and to arrange the supporting columns in such a way that the use of the ground area for exhibition purposes is possible in a convenient manner. The hall reserved for this purpose was circular, 30 ms diameter at ground level and 23.5 ms diameter at floor level.

In order to satisfy these requirements, it was decided to support the floor on 10 columns arranged radially along the rays from the center of the hall to the main intermediate columns of the existing build-



PLAN B-B

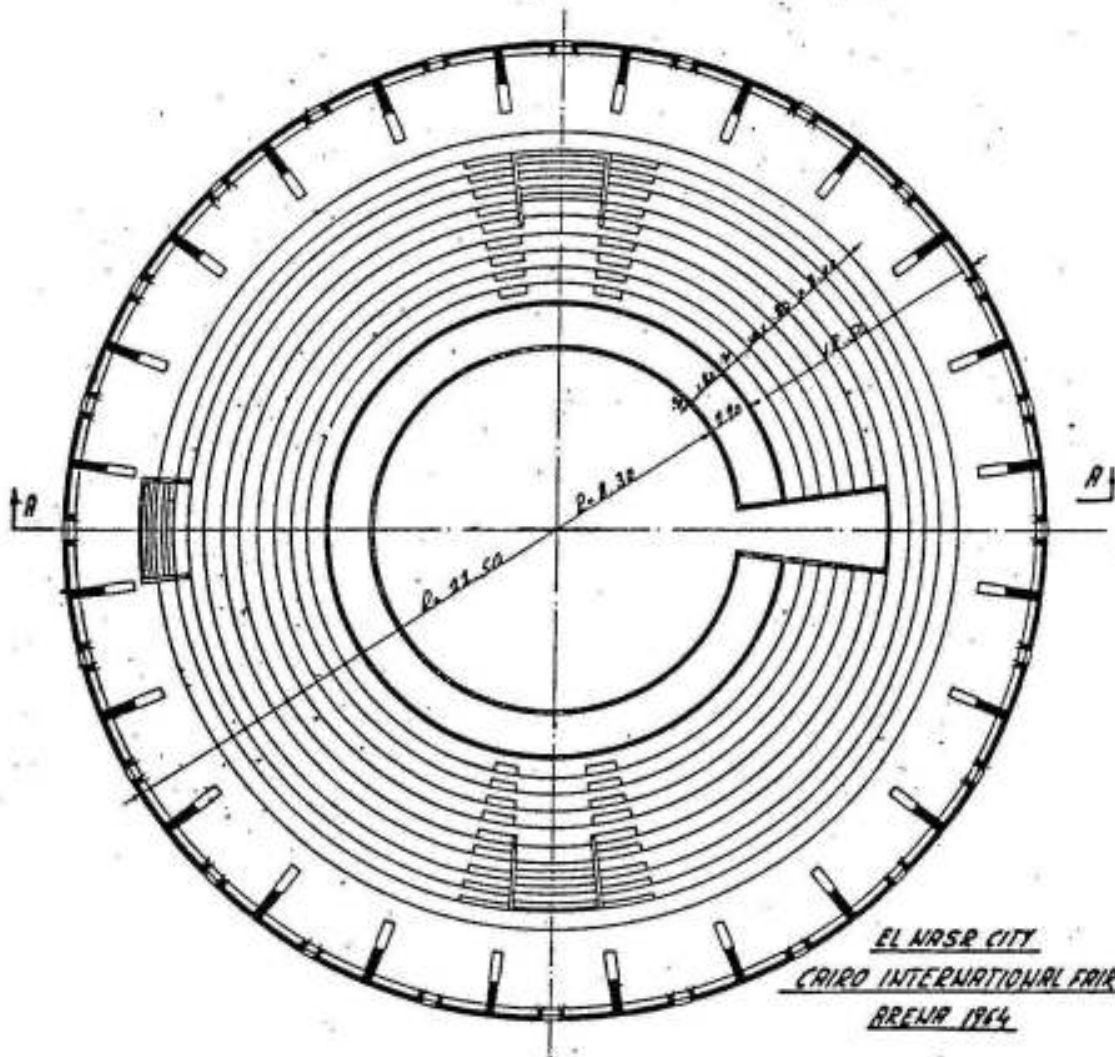


Fig. IV-69



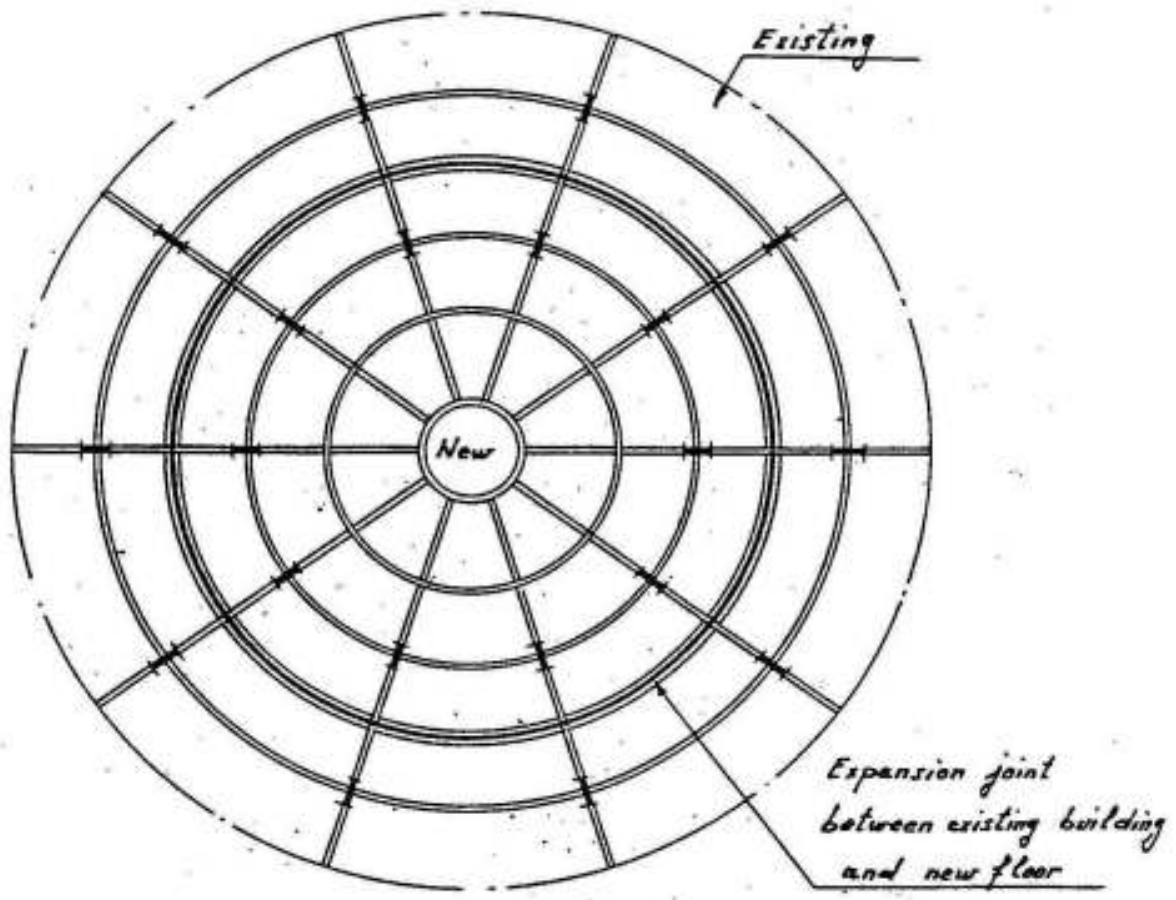
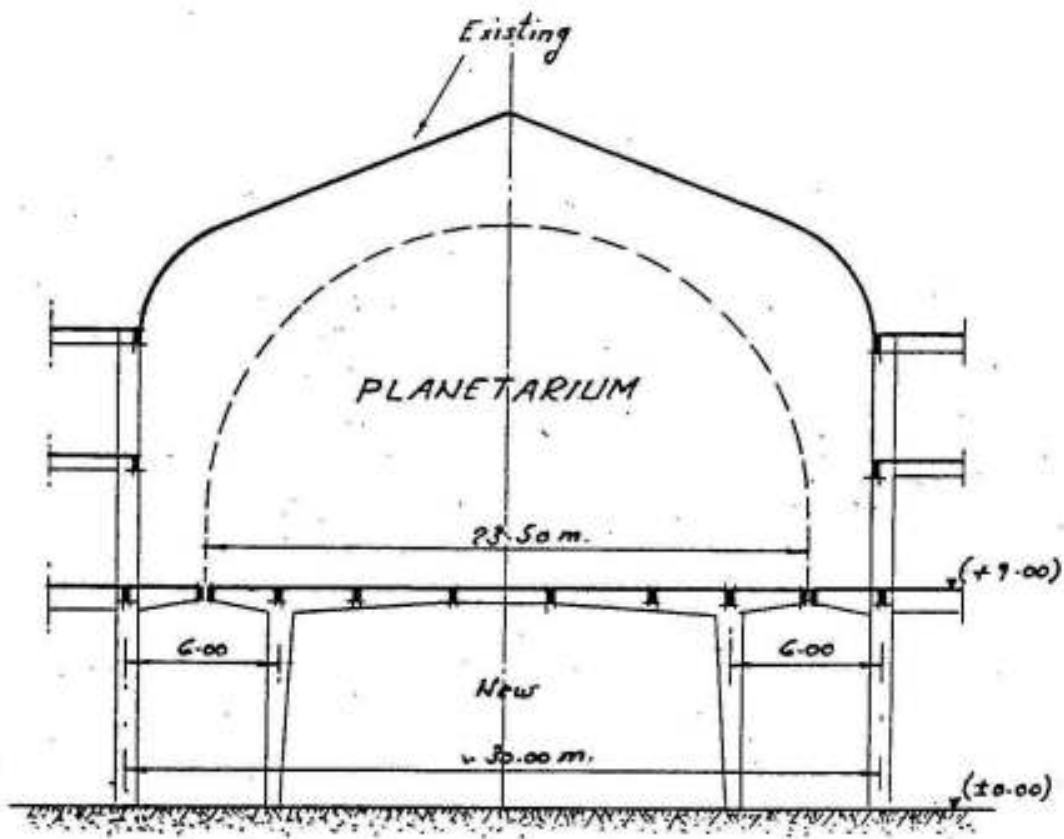


Fig. IV-71

ding and at 6 ms from them in order to have adequate space between the two rows of columns. Figure IV-71 shows the general layout of the new floor and its supporting circular beams and radial frames.

Due to the loading, the frame ab has the tendency to rotate around the lower hinge b pressing the inner circular ring beam at a ,

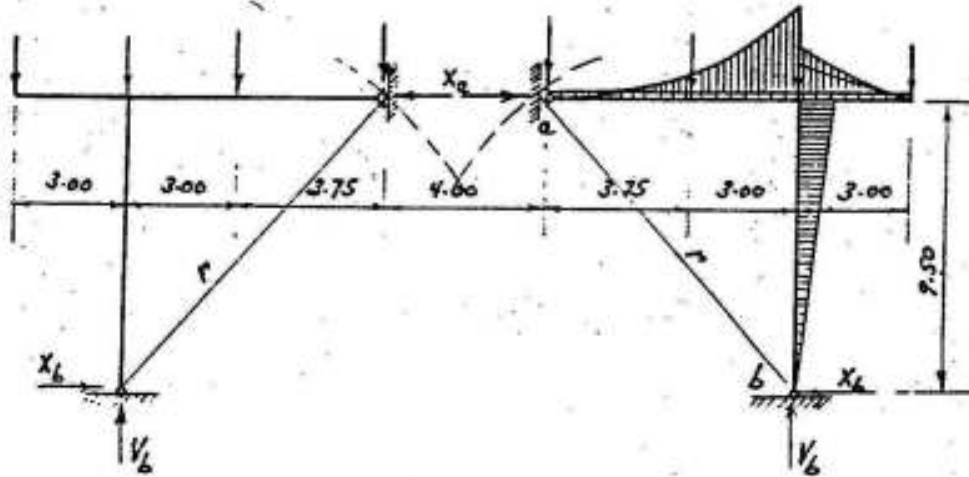


Fig. IV-72

so that each of the frames can be assumed as hinged at b and supported on the circular beam at a as shown in figure IV-72.

The concrete dimensions and details of reinforcements are shown in figure IV-73.

5) Continuous frames with ties as shown in figure IV-74.

The systems shown in figure IV-74 represent economic solutions for halls of moderate spans because the slabs and secondary beams are arranged in such a way that the axis of the polygonal girder coincides approximately on the line of pressure of the loads. If the spans are equal to or smaller than 10 ms, the effect of the elongation of the tie on the columns is small and may be neglected. In this case, the polygonal girder with its tie may be assumed as a shed giving for vertical loads on the girder, vertical reactions on the columns.

The internal forces can be determined for one single span both for vertical loads and wind pressure. However, adequate top reinforcement must be arranged and well anchored at the supports to resist the connecting moments that are liable to take place.





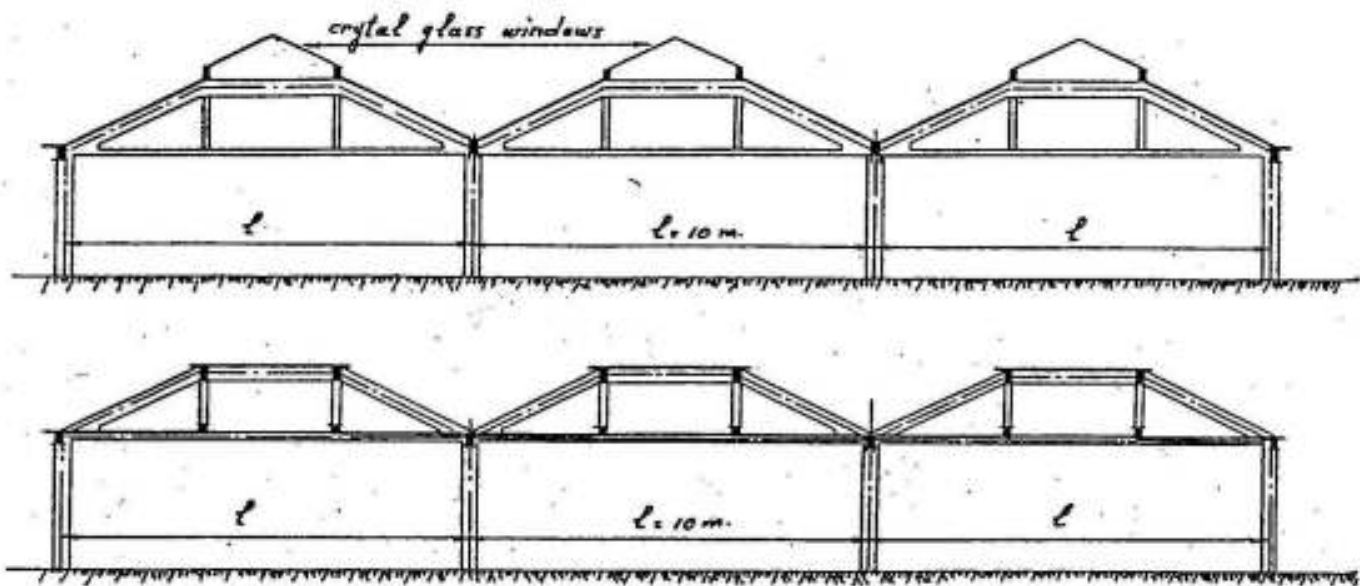


Fig. IV-74

For vertical roof loads, the girder may be treated as a two hinged frame with a tie, externally statically determinate and internally once statically indeterminate as shown in figure IV-75.

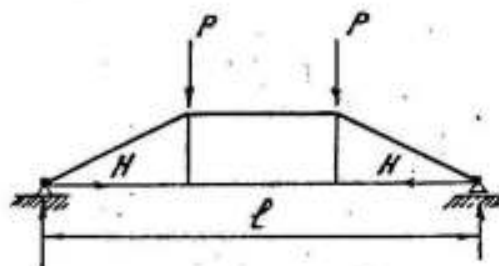


Fig. IV-75

The bending moments due to this case of loading are generally very small giving relatively small concrete dimensions and reinforcements.

For wind loads, the internal forces may be determined for one single polygonal frame without a tie as shown in figure IV-76.

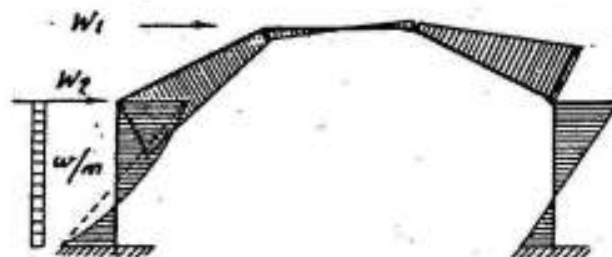


Fig. IV-76

The details of reinforcements can be done as shown in figure IV-77.

DETAILS OF REINFORCEMENTS  
OF  
A POLYGONAL SHED

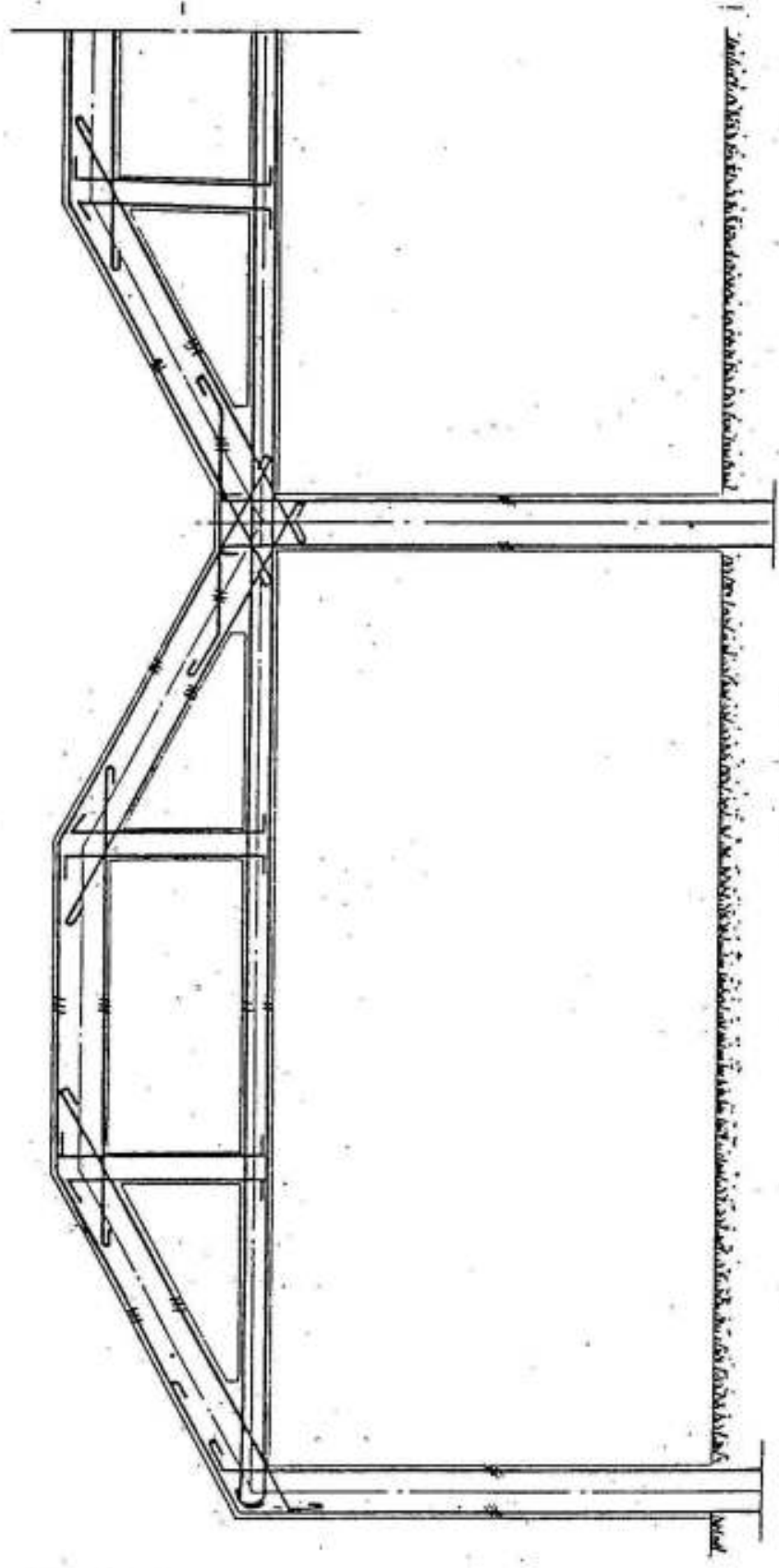


FIG. IV-77

## V- VIERENDEEL GIRDERS

If the depth of the main supporting girder is relatively big, a Vierendeel girder as shown in figure V-1 may in some cases be used.

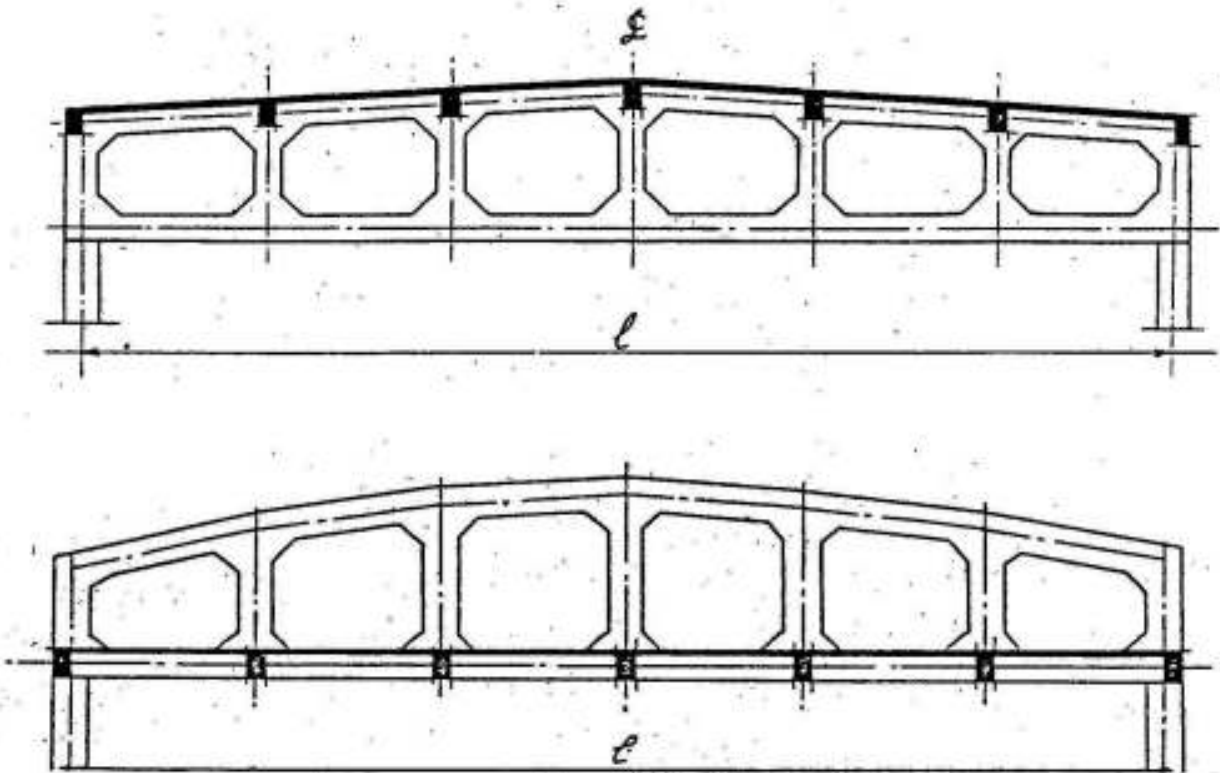
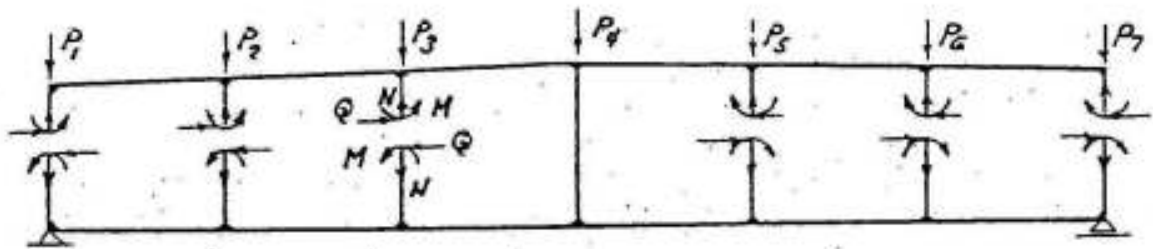


Fig. V-1

A Vierendeel girder is a high grade statically indeterminate structure composed of a top chord, a bottom chord and verticals only. Internally, it is  $3n$  times statically indeterminate;  $n$  being the number of the panels (fig V-2); whereas, externally, it may be statically determinate as in simply supported girders, or indeterminate as in continuous girders.

The exact solution of a Vierendeel girder is relatively complicated but essential if the members are thin compared to the height

of the girder. In reinforced concrete, the dimensions of the different members, chords and verticals are generally big and the following proposed approximate solution is simple and gives acceptable results for normal Vierendeel girders with parallel chords and verticals having equal stiffness. The method can however be applied if the top chord is polygonal, slightly curved or inclined. (Fig V-1).



*Statically determinate main system and statically indeterminate forces.*

*$n=6$ , hence system is 12 times internally statically indeterminate*

Fig. V-2

Let us consider a vierendeel girder subject to concentrated loads  $p_t$  and  $p_b$  acting at the joints of the top and bottom chords (fig V-3a). These loads cause the external bending moments  $M_I, M_{II}, \dots$  etc. at the joints (fig V-3b) and the shearing forces  $Q_1, Q_2, \dots$  etc in the panels  $a_1, a_2, \dots$  etc (fig V-3c).

The bending moments in the different members - being not directly loaded - are linear (fig V-3d) and can be determined from the external bending moments if the points of zero bending moments in the members are known.

In case of symmetrical vierendeel girders with equally stiff chords and verticals subject to symmetrical loads, the point of zero bending moments in any of the panels of the top and bottom chords and in the verticals may be assumed at the middle. If we imagine that hinges are introduced at the above mentioned points of zero bending moments, the girder will be internally statically determinate and the internal forces can be calculated as follows:

Assuming:

$I_t = I_b$  and  $I_1 = I_2 = \dots$  etc. are the moments of inertia of the top chord, the bottom chord and the verticals 1,2, ... etc.

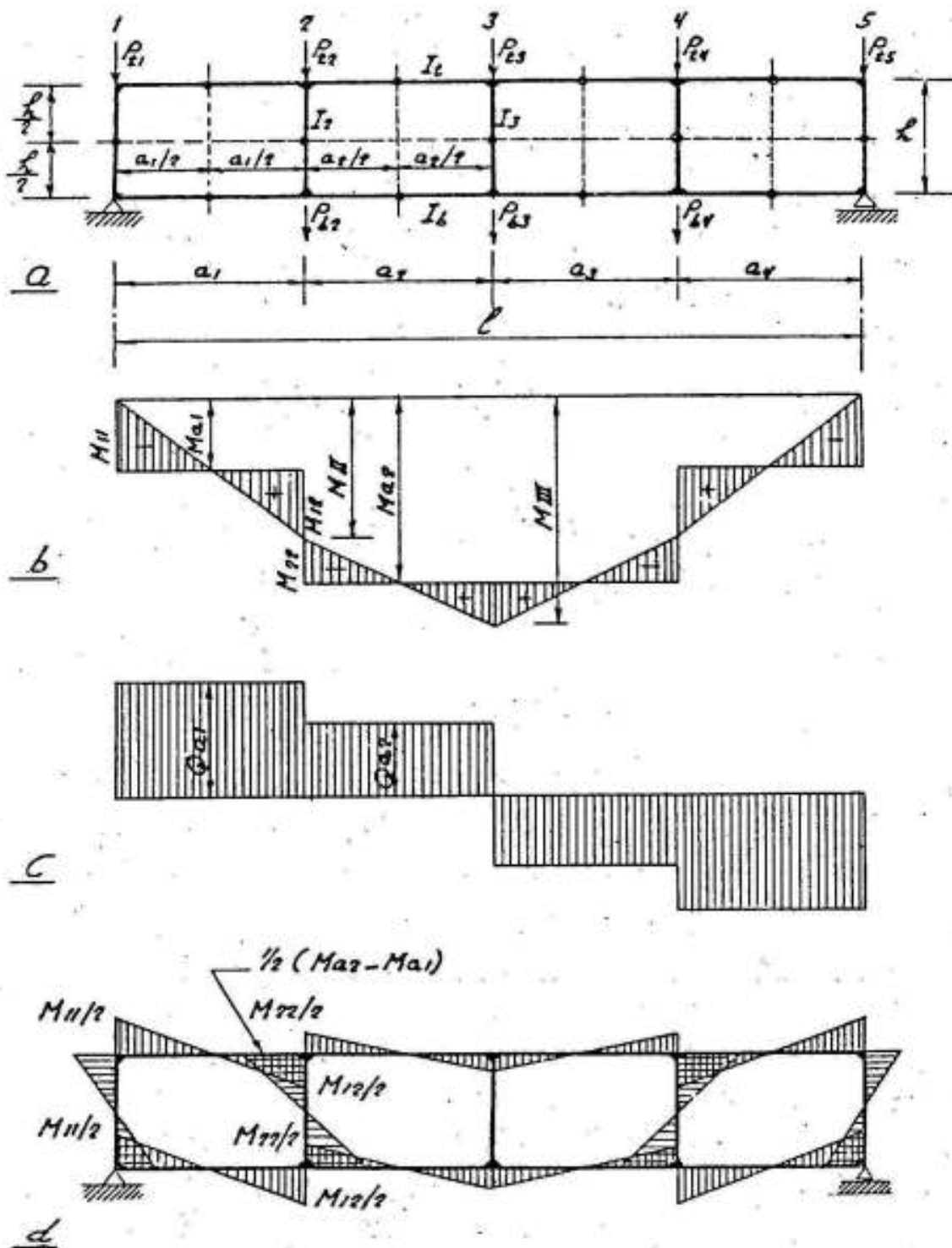


Fig. V-3

$N_t, N_b, N_1, N_2 \dots$  etc are the normal forces in chords and verticals  
 $Q_t, Q_b, Q_1, Q_2 \dots$  etc " " shearing forces " " " "  
 $M_t, M_b, M_1, M_2 \dots$  etc " " bending moments " " " "

Then: (fig V-4)

The normal forces in any of the panels say  $a_1$  are given by:

$$N_{b1} = -N_{t1} = M_{a1} / h$$

tension in the bottom chord and compression in the top chord . The shearing force  $Q_{a1}$  will be equally resisted by the two chords,

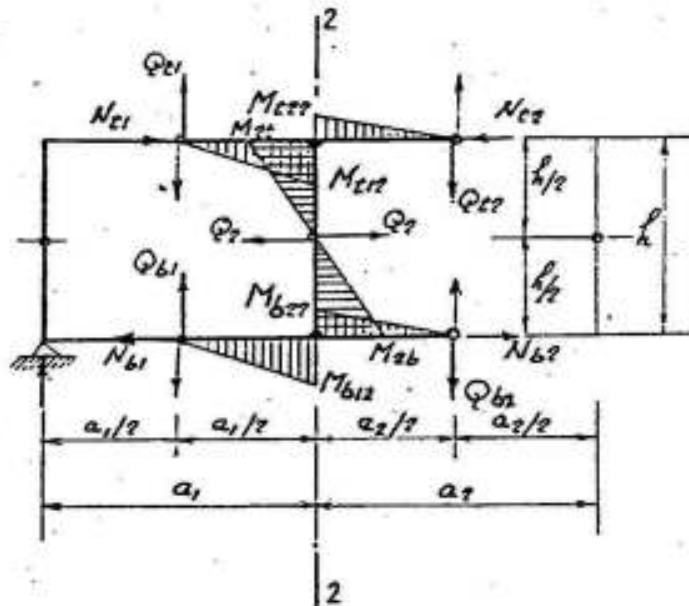


Fig. V-4

therefore

$$Q_{b1} = Q_{t1} = Q_{a1} / 2$$

It has to be noted here that  $Q_{b1} = Q_{t1}$  shown in figure express the vertical component of the resultant of the loads and reactions to the left of the vertical through the middle of  $a_1$  and hence their sense is upwards, whereas  $Q_{b2} = Q_{t2}$  give the vertical component of the resultant of the loads and reactions to the right of the vertical through the middle of  $a_2$  and hence their sense is downwards.

The bending moments to the left of vertical 2 are given by:

$$M_{b12} = Q_{b1} \cdot a_1 / 2$$

and

$$M_{t12} = Q_{t1} \cdot a_1 / 2$$

Therefore:

$$M_{b12} = M_{t12} = Q_{a1} \cdot a_1 / 4$$

Similarly

$$M_{b22} = M_{t22} = Q_{a2} \cdot a_2 / 4$$

It is recommended to draw the bending moment diagrams on the tension side as shown.

The normal force in vertical 2 can be calculated according to figure V-5 from the relation

$$\begin{aligned} N_2 &= Q_{t1} - Q_{t2} - P_{t2} \\ &= \frac{1}{2} ( Q_{a1} - Q_{a2} ) - P_{t2} \\ &= \frac{1}{2} ( P_{b2} + P_{t2} ) - P_{t2} \quad \text{i.e.} \end{aligned}$$

$$N_2 = \frac{1}{2} ( P_{b2} - P_{t2} )$$

The bending moments in the verticals can be determined from the equilibrium of the joints as shown in figure V-6; thus

$$M_{2t} = M_{t12} + M_{t22}$$

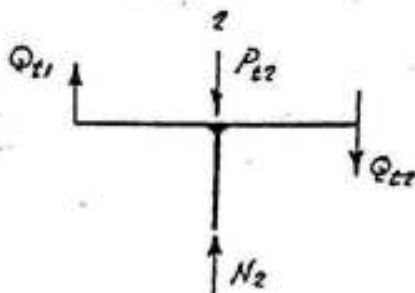


Fig. V-5

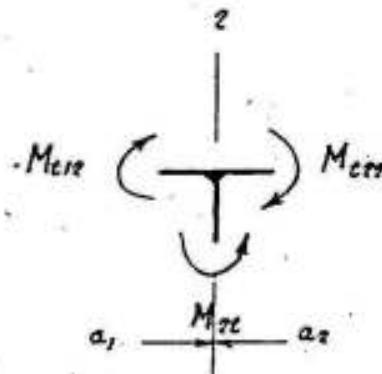


Fig. V-6

It has to be noted here that the known moments  $M_{t12}$  and  $M_{t22}$  are expressed in figure V-6 by arrows giving their sense ; i.e.  $M_{t12}$  is clockwise (positive) causing tension at the lower fiber and compression at the upper fiber to the left of joint 2, it will therefore be expressed by a clockwise arrow from the tension side to the compression



side. Whereas  $M_{t22}$  is also clockwise but causing tension at the upper fiber and compression at the lower fiber to the right of the same joint. The unknown moment  $M_{2t}$  at the upper joint of vertical 2 must keep the equilibrium of the two moments  $M_{t12}$  and  $M_{t22}$ , therefore its magnitude must be equal to their sum and its sense must be anti-clockwise i.e causing tension on the left side and compression on the right side of vertical 2.

The final bending moment diagrams drawn on the tension side are shown in figure V-4.

The shearing forces at the points of zero bending moments in the verticals can be determined by dividing the bending moment at any of the corresponding joints by  $h/2$ .

The shearing forces  $Q_2$  and the bending moments  $M_{2t}$  and  $M_{2b}$  acting on vertical 2 can also be determined as follows:

Referring to figure V-4, we find that:

$$Q_2 = N_{t1} - N_{t2} = N_{b1} - N_{b2} = - ( M_{a2} - M_{a1} ) / h$$

$$M_{2t} = - M_{2b} = - Q_2 h/2 = - \frac{1}{2} ( M_{a2} - M_{a1} )$$

The bending moments in the chords can be determined graphically by drawing vertical lines through the points of zero bending moments of the chords to meet the sides of the external bending moment diagram. Through the points of intersection draw horizontal lines as shown in figure V-3; the diagrams enclosed between these horizontals and the sides of the external bending moment diagram, hatched diagrams, give the bending moments to be resisted by the two chords. If the chords are of equal stiffness, then each chord will resist half the bending moment.

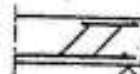
Having determined the bending moments in the chords, the bending moments in the verticals can be determined from the equilibrium of the joints shown in figure V-6.

The final bending moment diagram drawn on the tension side for the whole Vierendeel girder is shown in figure V-3d. Such an illustration is very convenient as it gives the tension side and respectively the position of the longitudinal reinforcement in every part of the girder. It has been further found that the diagonal tension in a beam is in the direction of the sides of the bending moments diagram

if it is drawn on the tension side. Hence, the direction of the diagonal tension corresponding to the bending moment shown in figure V-3d will be in the chords and verticals to the left in the left half



, and to the right in the right half



, see fig V-9.

If the moments of inertia of the chords or the verticals are not equal, the points of zero bending moments cannot be assumed at the middle of the chords or the verticals and can approximately be determined as follows:

Assume  $I_t$ ,  $I_b$ ,  $I_{v1}$ ,  $I_{v2}$  ... are the moments of inertia of the top chord, the bottom chord and the verticals 1,2 ... etc., and

$$\kappa_{gt} = \frac{a}{I_t} \cdot \frac{I_t}{a} = 1 \quad \text{is the relative rigidity of the top chord}$$

$$\kappa_{gb} = \frac{a}{I_b} \cdot \frac{I_t}{a} = \frac{I_t}{I_b} \quad \text{" " " " " " " " bottom chord}$$

$$\kappa_v = \frac{h}{I_v} \cdot \frac{I_t}{a} \quad \text{" " " " " " " " verticals}$$

If we consider the panel 2-3, length  $a_2$ , and assume that the point of zero bending moment in vertical 2 lies at a distance  $y_2$  from the top chord, and that the point of zero bending moment in the chords 2-3 lies at a distance  $x_2$  from vertical 2, fig. V-7, it is possible to prove that:

$$-\frac{M_{2t}}{M_{2b}} = \frac{y_2}{h-y_2} = \frac{3\kappa_v + \kappa_{gb}}{3\kappa_v + \kappa_{gt}} = C_t$$

and

$$-\frac{M_{t22}}{M_{t23}} = \frac{x_2}{a_2-x_2} = \frac{3\kappa_g + \kappa_{v3}}{3\kappa_g + \kappa_{v2}} = C_2$$

So that

$$y_2 = \frac{C_t}{C_t + 1} \cdot h = k_t \cdot h$$

and

$$x_2 = \frac{C_2}{C_2 + 1} \cdot a_2 = k_2 \cdot a_2$$

The external shearing force acting in panel  $a_2$  is given by  $Q_{a2}$  and is distributed between the top and bottom chords according to the ratios :

$$Q_{t2} = k_t \cdot Q_{a2}$$

and

$$Q_{b2} = (1 - k_t) Q_{a2}$$

Having known  $Q_t$  and  $Q_b$  in the different panels the other internal forces can be easily determined as shown before.

If the loads act directly on the top or bottom chords, the bending moments due to these direct loads are to be determined for each chord as a continuous beam supported on the verticals. Such bending moments are to be added to those due to the concentrated loads acting at the joints. FigV-8.

In this case,  $P_t$  and  $P_b$  are the sum of the direct loads on the joints plus the reactions of the top and bottom chords as continuous beams.

The corners of a Vierendeel girder are subject to high secondary stresses so that girders free from corner cracks can only be obtained by careful study of the reinforcements and very good execution. The use of haunches in the corners is in this respect, where possible, recommended.

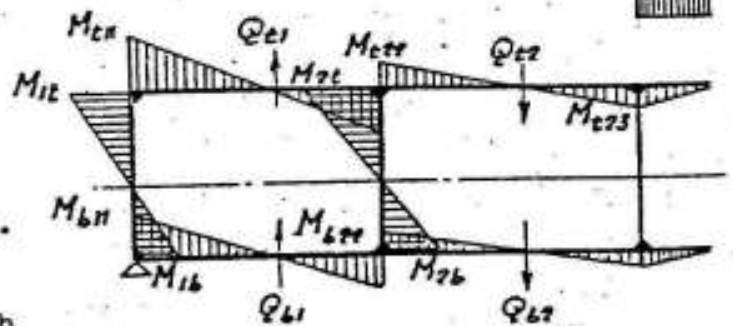
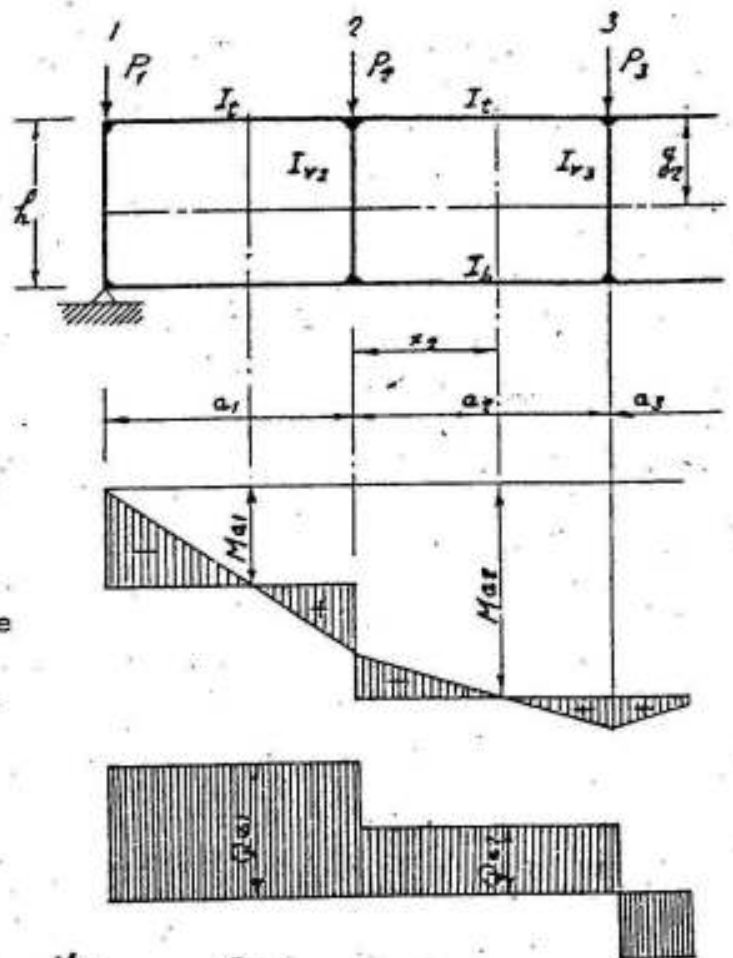


Fig. V-7

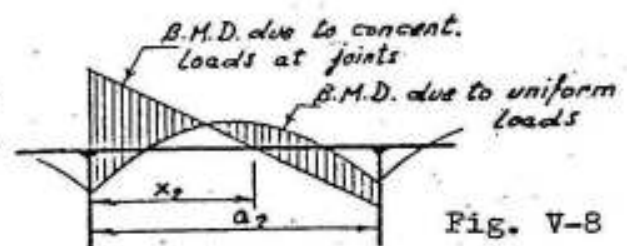


Fig. V-8

The bending moments of this system change their sign in every

panel so that a simple arrangement of the reinforcements can only be obtained by careful study. Its deflection is generally bigger than that of solid girders.

It is generally recommended to use this system when it gives the only convenient solution; especially because it is relatively expensive.

Example:

It is required to determine the internal forces in the Vierendeel girder shown in figure V-9.

As the moments of inertia of the top and bottom chords are equal ( $= I$ ) and the moments of inertia of the verticals are equal ( $= I_v$ ), then the points of zero bending moments can be assumed at the middle of every panel or vertical.

In order to determine the internal forces:

- 1) Draw the external bending moment and shearing force diagrams.
- 2) Draw vertical lines through the points of zero bending moment in the chords (middle points); extend them to meet the sides of the external B.M.D.
- 3) Through the points of intersection draw horizontal lines. The hatched diagrams between these horizontals and the sides of the external B.M.D. give the bending moments in the two chords. Each of the chords is subject to half these values.
- 4) The bending moments at the upper and lower joints of the verticals can be determined from the equilibrium of the joints.
- 5) The shearing forces in the chords and verticals can be determined by dividing the moment at the joint by half the length of the corresponding panel.
- 6) The normal forces in any of the chords can be determined by dividing the ordinates of the external B.M.D. at the middle of the chord by the height of the Vierendeel  $h = 4^m$ .

Figure V-10 shows the details of a Vierendeel girder designed by the author in 1968. It gave the only convenient solution for the control area of the main studio in the television building at Cairo. In spite of the change of the sign of the bending moment in every panel and post and the relatively high diagonal stresses, it was possible by a careful study of the reinforcement to get the shown relatively simple forms for the bars.

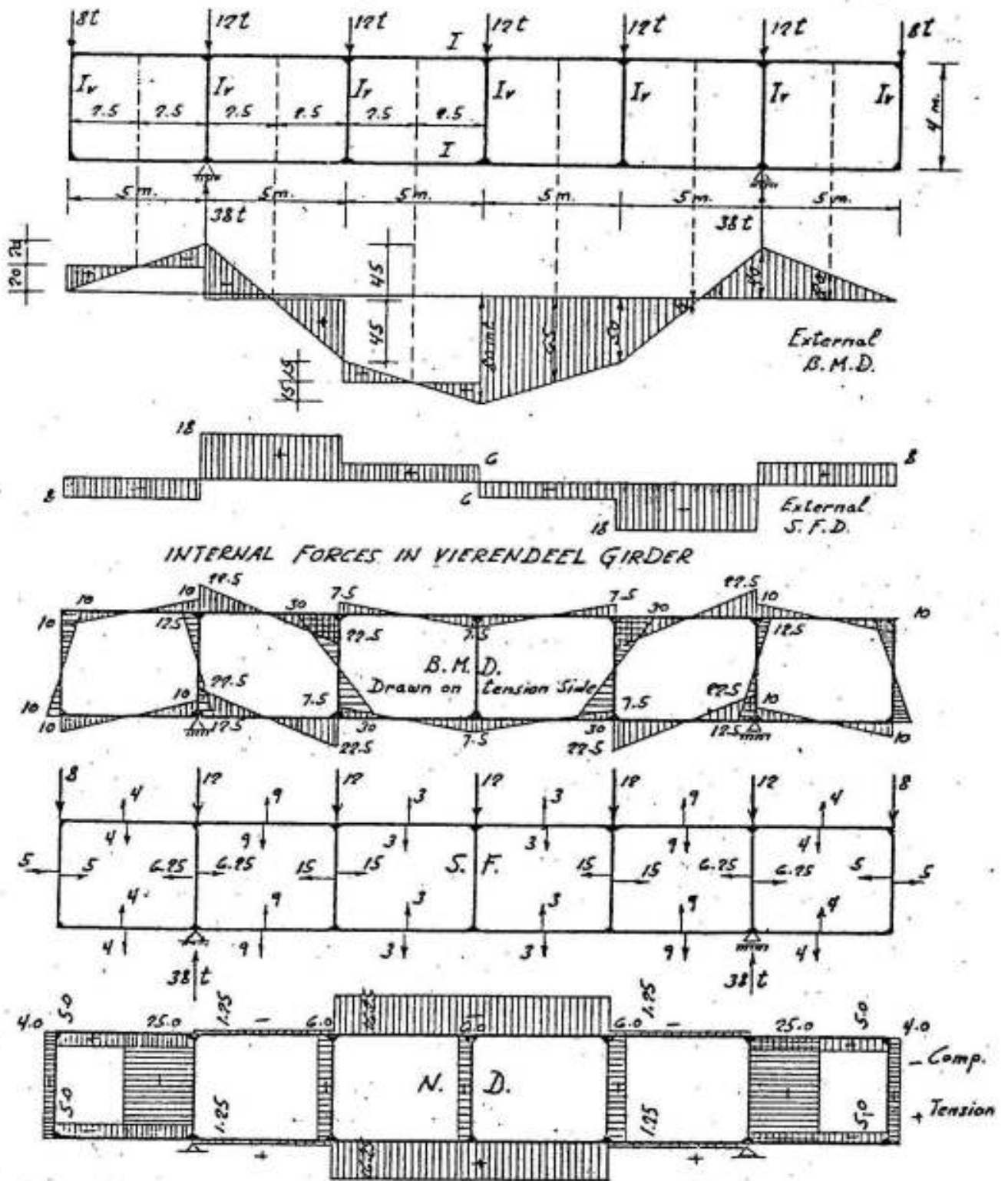
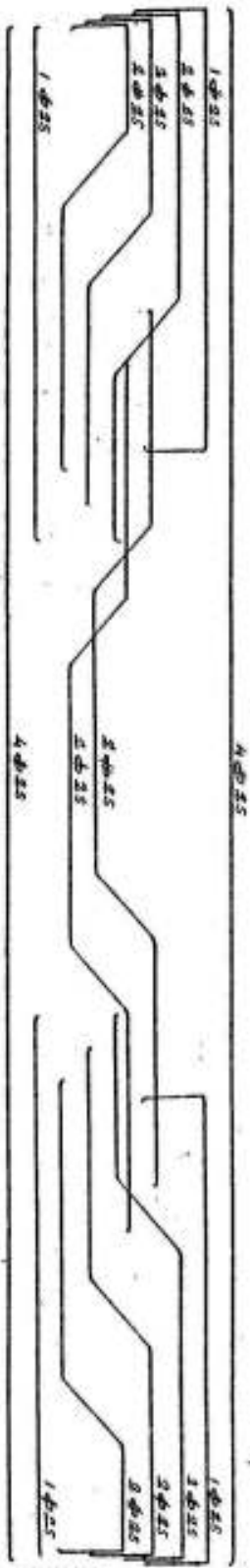
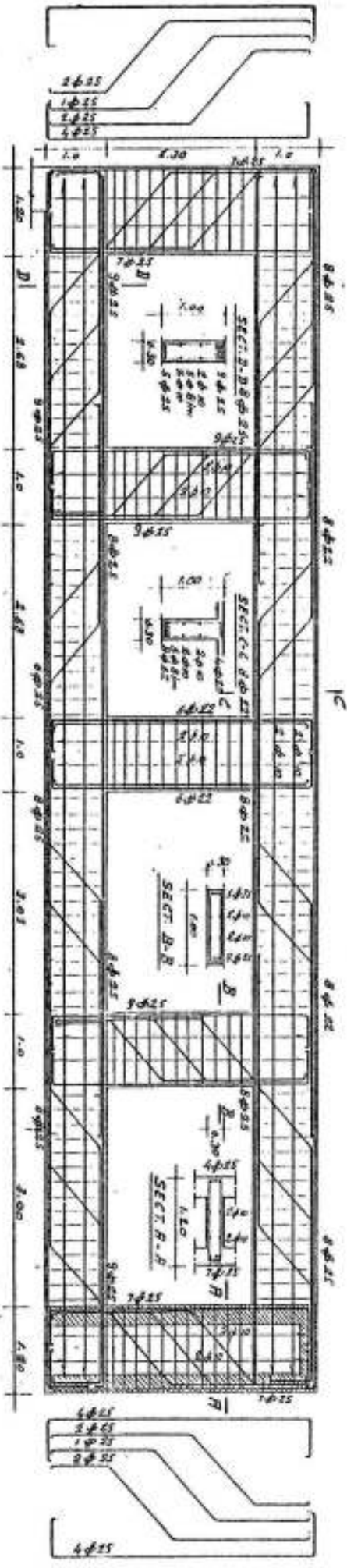
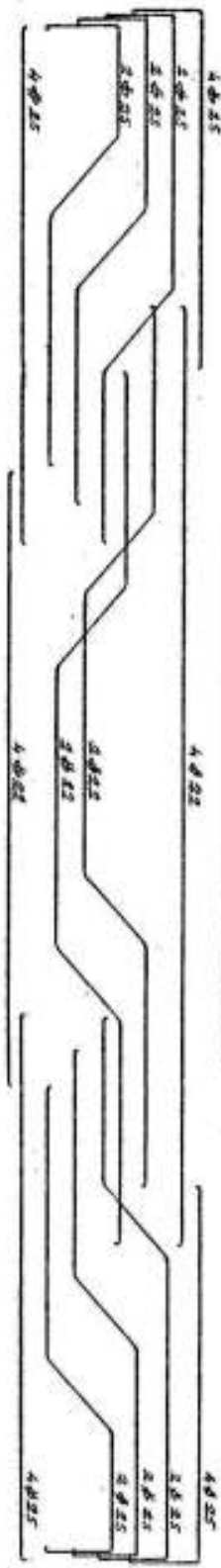


Fig. V-9

CHIRO T. V. MAIN STUDIO



VERENDEEL GIRDRE

P13. V-10

## VI- TRUSSES

Trusses in reinforced concrete are seldom used; their shape is generally chosen similar to those constructed in steel. (Fig.VI-1).

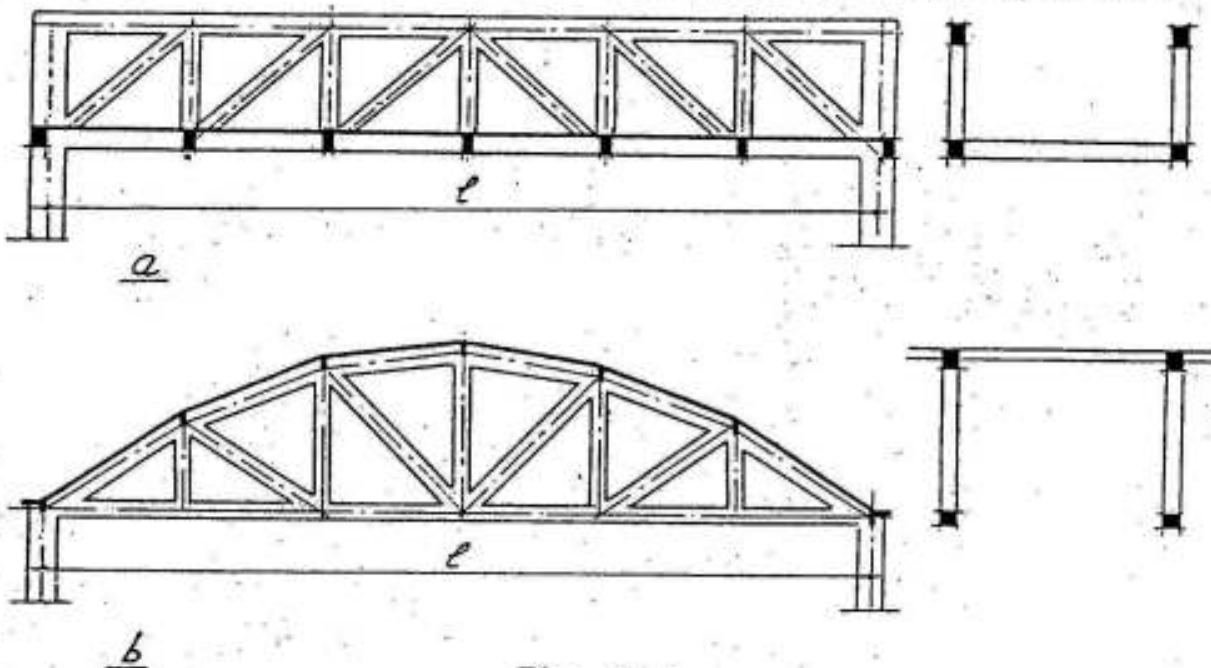


Fig. VI-1

Figure VI-1a shows a reinforced concrete truss bridge with parallel chords whereas figure VI-1b shows a reinforced concrete roof truss with polygonal top chord. In both trusses, the members are mainly subjected to axial forces and small bending moments due to the rigid joints. If, in case a, we dispense with the diagonals, we get a Vierendeel girder with parallel chords, in which case all members must be sufficiently stiff to resist the bending moments, shearing forces and thrusts acting on them as was shown in the previous article. If in case b, we cancel the diagonals, choose a stiff polygonal top chord and a slender bottom chord, the main girder may be treated as an arch (or polygonal girder) with a tie, a system which is generally well adapted for reinforced concrete structures as will be shown later.

In special cases of saw-tooth roofs in which the north is parallel

to the span of the hall, the truss may give a convenient solution which adapts very well to the case under consideration. (Fig VI-2).

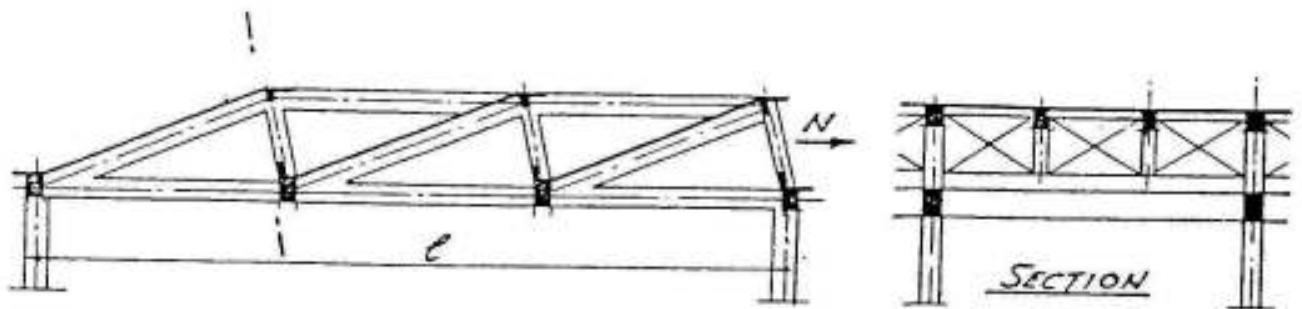


Fig. VI-2

It is possible to get a convenient distribution of the forces in the members if the compression diagonals of the truss are chosen such that they bisect the angle between the tension diagonals and the bottom chord as shown in figure VI-3, in which case the force in the tension diagonal is equal to the difference between the tension forces in the bottom chord at the connecting joint. Accordingly, the steel reinforcement in the tension diagonal will be equal to the difference

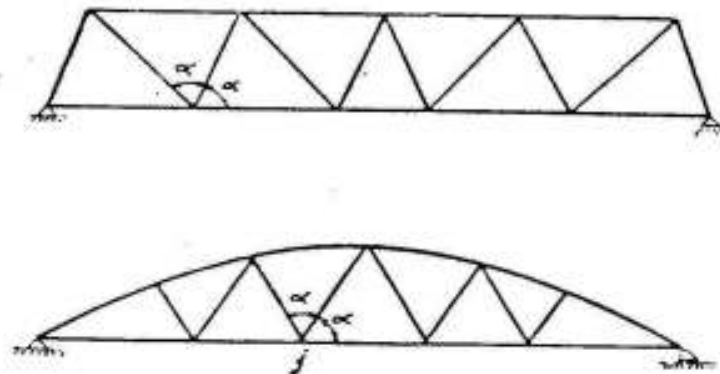


Fig. VI-3

between the reinforcements of the bottom chord at the joint as shown in figure VI-4 which gives the details of joint J.

The disadvantages of reinforced concrete trusses are:

- 1) Formwork of concrete and form of reinforcements are complicated and hence they are relatively expensive .
- 2) Safety against cracking is low.

In order to avoid cracking of the tension members, Finsterwalder proposes to concrete the compression members only first, after hardening and removal of shuttering, the truss can be artificially loaded



so as to stress the steel reinforcement in the tension members to high tensile stresses. With the truss loaded, the tension members are to be concreted and when hardened, the load can be removed.

The internal forces in the members of a truss are:

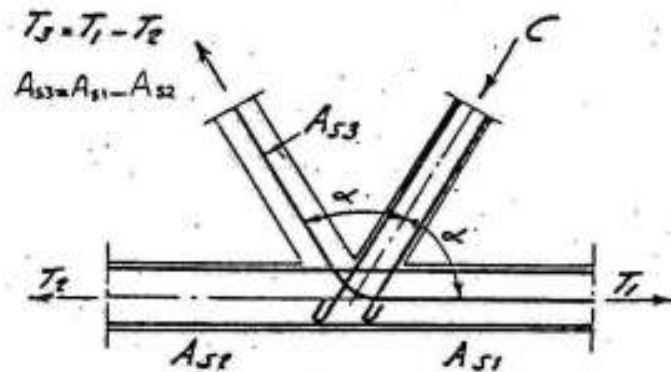


Fig. VI-4

- 1) The axial forces  $N$  due to the concentrated loads at the joints.
- 2) The bending moments and shearing forces due to the eventual direct loads on some members of the truss, and
- 3) The bending moments and shearing forces due to the rigidity of the joints.

The axial forces  $N$  due to the concentrated loads at the joints may be determined by any of the known methods of trusses with hinged joints.

The bending moments due to the direct load on any of the members can be determined by the moment distribution method in which the member under consideration is first assumed fixed at both ends and the fixed-end-moments due to the direct load on the member are determined, then the unbalanced moments in the joints are distributed in the usual way.

The shearing force  $Q$  acting on any member is given by:

$$Q = Q_0 + \frac{M_r - M_l}{l}$$

in which

$Q_0$  = the shearing force due to the direct load on the member assumed as a simple beam.

$M_r$  and  $M_l$  are the final connecting moments at the right and left ends

of the member

$l$  = the span of the member under consideration.

Based on the assumption of Mohr which states that the deformation of a pin joined truss is not so far from the deformation of the corresponding truss with rigid joints, the bending moments and the corresponding shearing forces due to the rigidity of the joints can approximately be determined as follows:\*

- a) Due to the loads on the truss, determine the axial forces  $N$  in the members assuming hinged joints.
- b) Draw the Williot-Mohr displacement diagram, then determine for the various members, the relative displacements of the ends  $\Delta$ , that are normal to the members.
- c) Assume that the members are fixed at their ends, and compute the fixed-end-moments  $\bar{M}$  due to  $\Delta$  from the relation:

$$\bar{M} = \pm \frac{6EI}{l^2} \cdot \Delta$$

The signs may be taken according to the known Grinter's notations in which the clockwise direction around the joint is assumed negative and the anti-clockwise is assumed positive as shown in figure VI-5.



Fig. VI-5

- d) Applying the moment distribution method, the unbalanced moments in the joints can be distributed in the normal way, leading to the final connecting moments in the different members of the truss.

#### Example 1

To illustrate the application of the method, the axial forces and bending moments in the members of the main trusses supporting the saw-tooth roof of the machine workshop in the forging plant at Helwan shown in figure VII-17 are given for the following data:

---

\* Refer to "plane Analysis of Indeterminate Structures" by Prof. Dr. A. Shaker. Published by the Arab Writer, Cairo.

span of truss = 18 ms                      height = 3 ms                      spacing = 6 ms

The inclined slabs are 9 cms thick. They are supported by the diagonals of the truss and inclined secondary beams arranged midway between the trusses, so that the slabs are one-way with a span of 3 ms.

In this manner, the diagonals of the truss are directly loaded from the slab by a direct uniform vertical load equal to 1.25 t/m'.

Due to the own weight of the roof elements and slab loads, each of the lower intermediate joints of the truss is subject to a concentrated load of 32 tons. The normal forces in the members of the truss  $N$  due to these concentrated loads are shown in figure VI-7a. The Williot-Mohr diagram giving the displacement of the joints is shown in figure VI-6. The bending moments due to the displacement of the joints, the direct loads on the diagonals and the final bending moments are shown in figures VI-7b, c and d.

It can be seen that the values of the bending moments in the members of such a truss are not big and it may be allowed to design its members for their axial forces plus a bending moment equal to:

$$M = \frac{t}{10} (N + 0.8 M_0) \quad \text{in which}$$

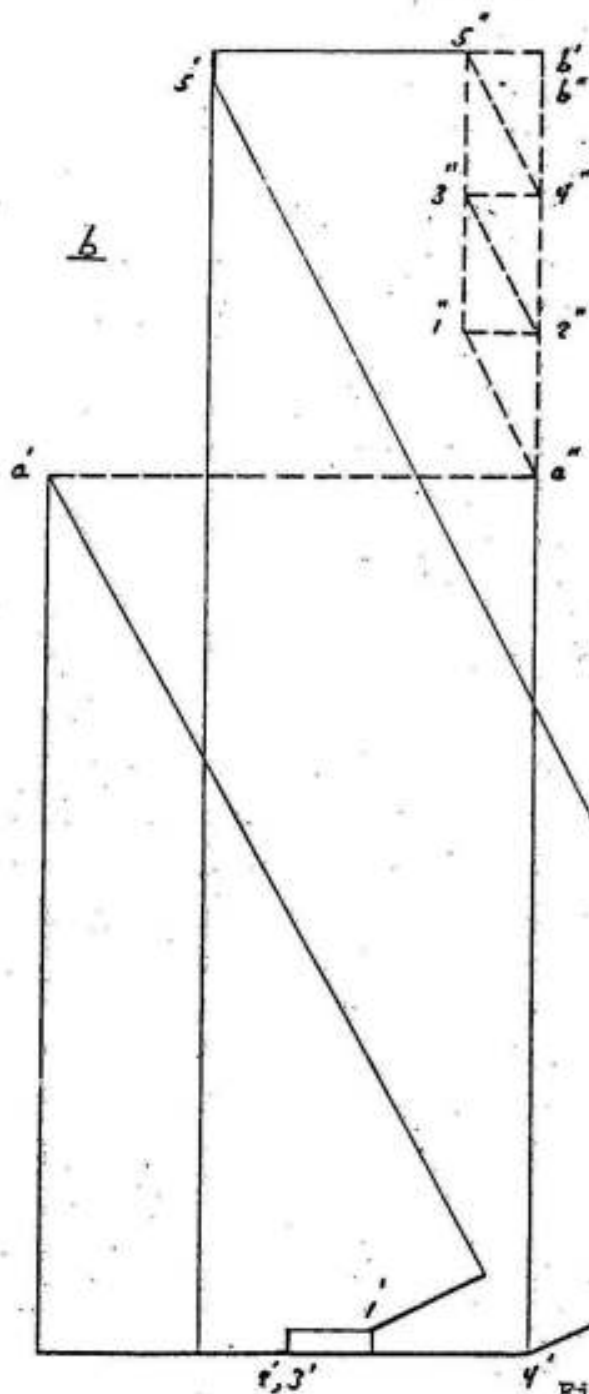
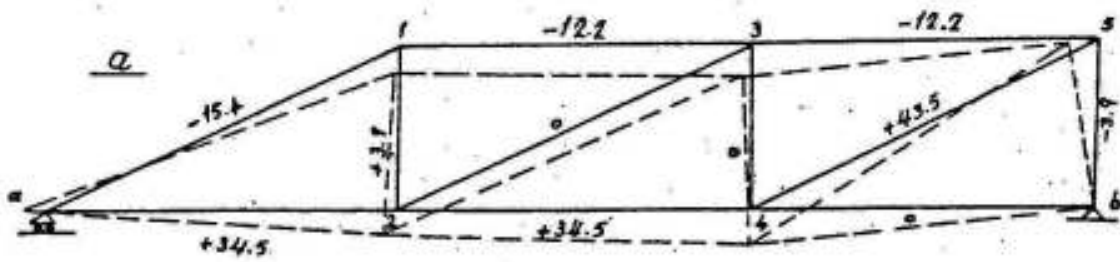
$t$  = the thickness of the member in the plane of the truss

$M_0$  = The biggest maximum bending moment in the diagonals considered as simple beams under their direct load.

Figure VI-8 shows the general layout and main dimensions of the workshop and figure VI-9 shows the details of the saw-tooth trusses used as main supporting elements of the roof of the structure.

In order to have a convenient shape for the members of the truss and a relatively low percentage of the steel reinforcement in the tension members, the top and bottom chords, the diagonals, and the verticals have been chosen with the same concrete dimensions for each of the three groups.

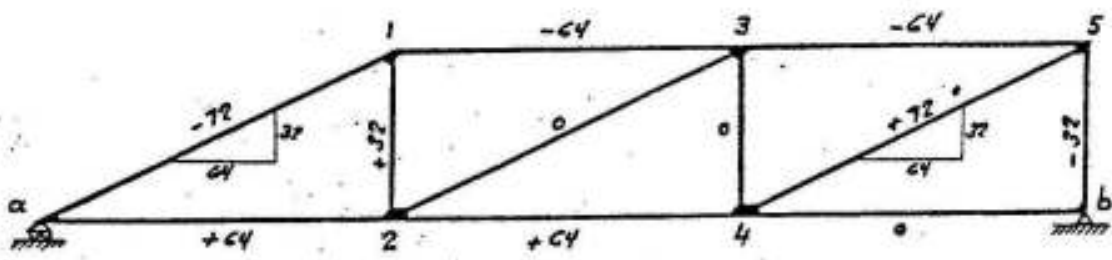
Due to the direct loads of the slabs on the diagonals and the rigid joints of the truss, the members are subject to bending moments  $M$  and shearing forces  $Q$ . These bending moments being small relative to the axial forces  $N$ , the members are reinforced with symmetrical straight bars only (i.e. no bent bars are used). This is explained in the following:



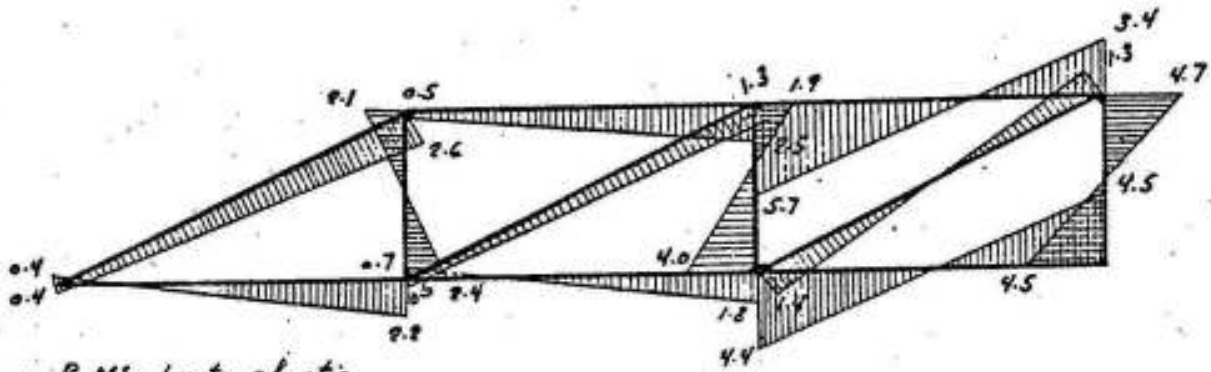
The values of  $S$  multiplied by  $10^2$  are written on each member with its sign. (+) means elongation

- Point (2) fixed point
- Member (2-4) fixed direction
- Scale 1cm = 0.1 cm.

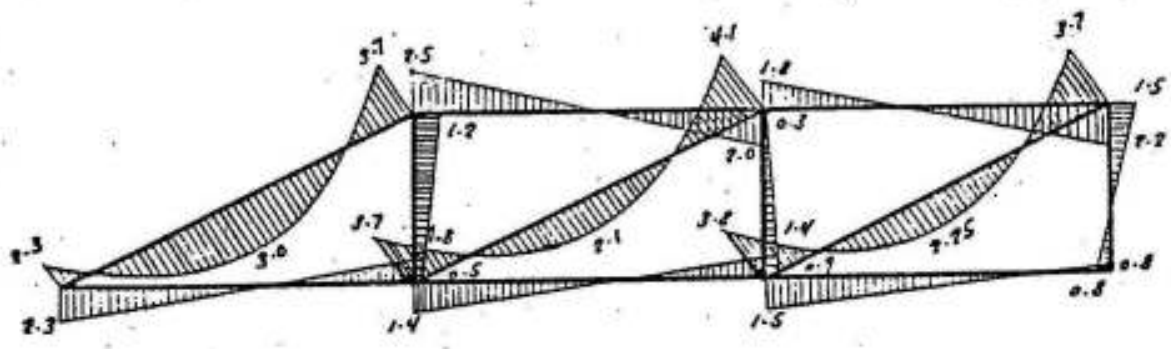
Fig. VI-6



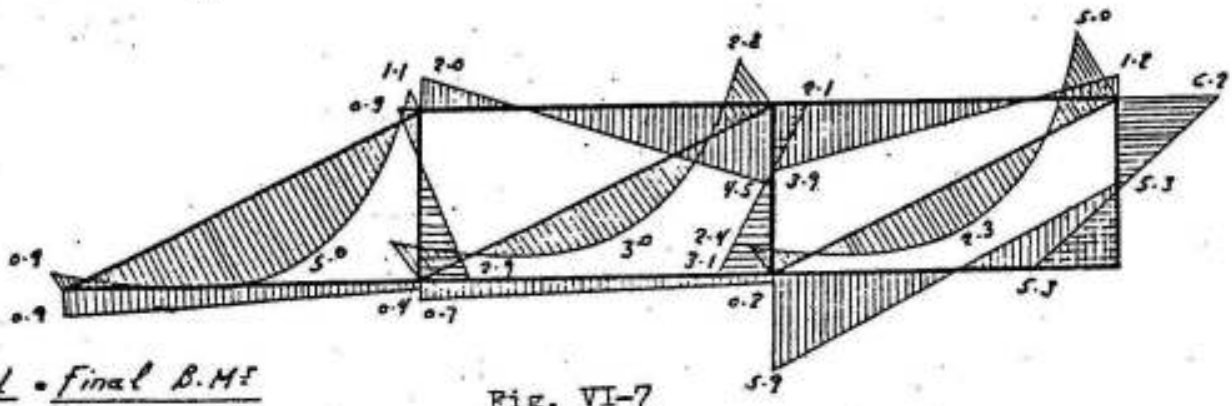
a • Axial forces



b • B.M. due to elastic deformations



c • B.M. due to direct loading



d • final B.M.

Fig. VI-7

If N is compressive and the normal stress  $\sigma$  due to M and N is high say  $50 \text{ kg/cm}^2$  while the corresponding shear stress  $\tau$  calculated from, the relation

$$\tau = Q S / I b \quad \text{where}$$

S = statical moment of area of the part of the section above the plane under consideration about the c.g. axis,

I = moment of inertia of section about c.g. axis, and

b = breadth of section under consideration,

is equal to say  $15 \text{ kg/cm}^2$ , then the principal diagonal tensile stress  $\sigma_1$  is given by:

$$\begin{aligned} \sigma_1 &= -\frac{\sigma}{2} + \sqrt{\frac{\sigma^2}{4} + \tau^2} = -\frac{50}{2} + \sqrt{\frac{2500}{4} + 225} = -25 + 29.2 \\ &= 4.2 \text{ kg/cm}^2 \end{aligned}$$

which is relatively low and does not need any diagonal reinforcement.

If N is tensile and the normal stress due to M and N is high, say  $80 \text{ kg/cm}^2$ , and the shear stress  $\tau$  is say  $12 \text{ kg/cm}^2$  then the principal tensile stress  $\sigma_1$  is:

$$\sigma_1 = \frac{80}{2} + \sqrt{\frac{6400}{4} + 144} = 40 + 42 = 82 \text{ kg/cm}^2$$

its inclination to the axis of the member is given by:

$$\tan 2\alpha = \frac{2\tau}{\sigma} = 2 \times 12/80 = 0.3$$

which means that

$$2\alpha \cong 20^\circ \quad \text{and} \quad \alpha \cong 10^\circ$$

i.e. the principal tensile stress is nearly parallel to the axis of member and again here no bents are required.

It has to be further noted that the tension bars are anchored in the direction forming an obtuse angle with the bar because if they are anchored so that an acute angle is created, undesirable high splitting tensile stresses  $\sigma_{sp}$  are developed. (Fig. VI-10)

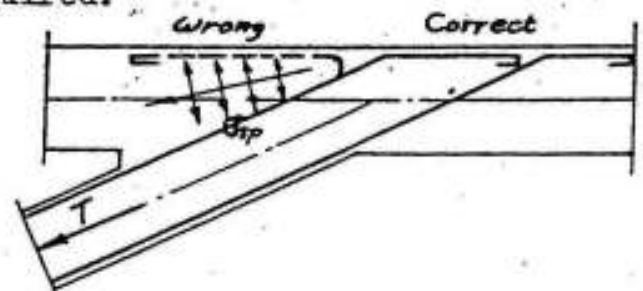
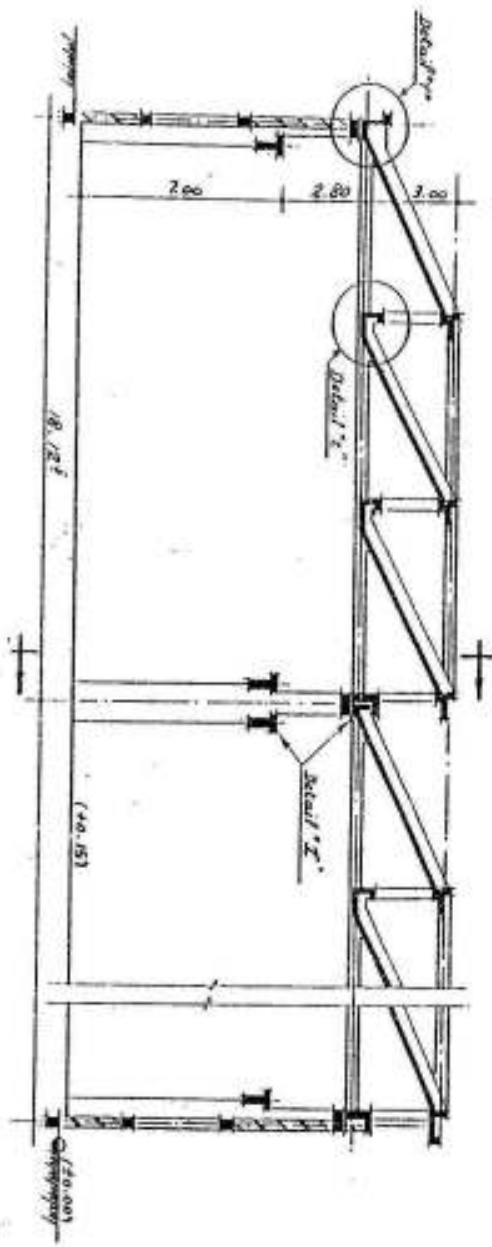
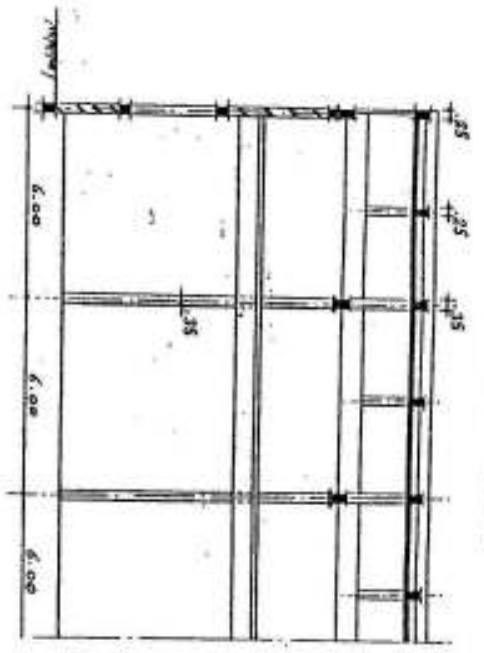


Fig. VI-10

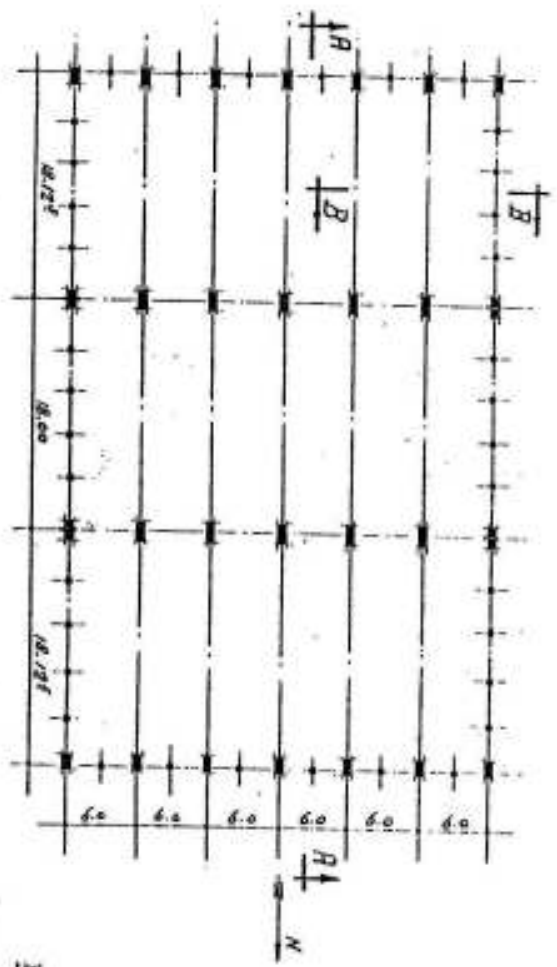
SECTION R-R



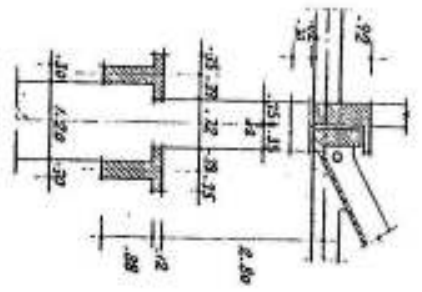
SECTION B-B



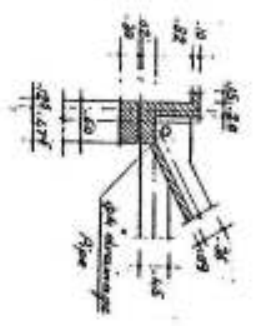
KEY PLAN



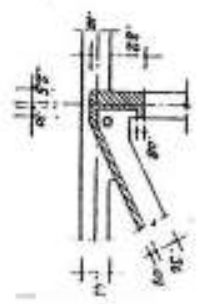
DETAIL "X"



DETAIL "Y"



DETAIL "Z"



EL-NRSR FORGING PLANT

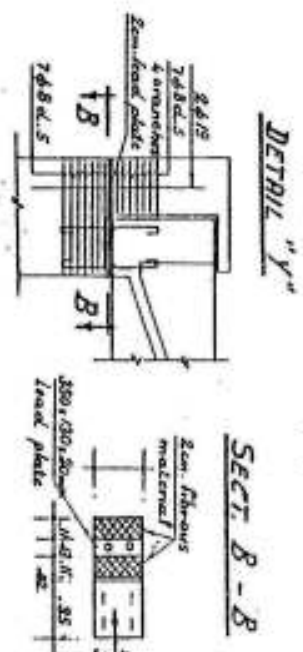
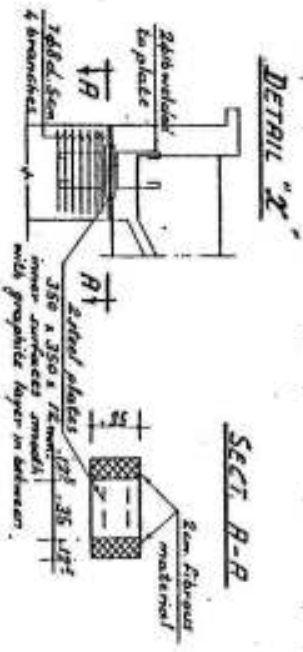
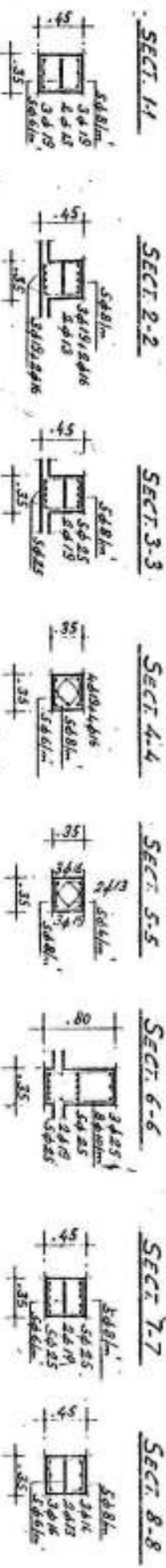
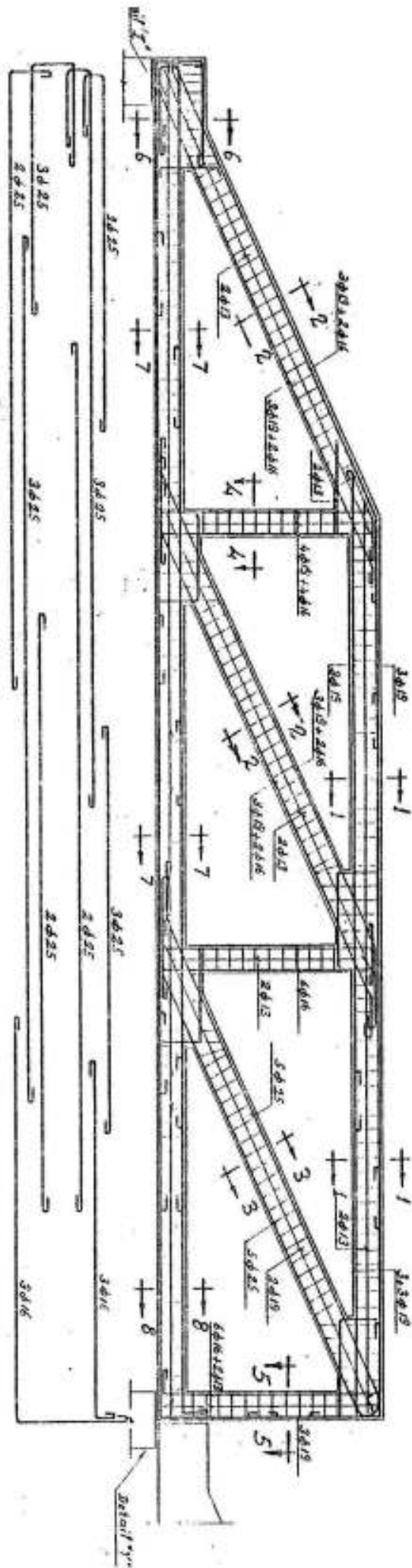
HELVAN

MACHINE WORKSHOP

1962

FIG. VI-3

REINFT. DETAILS OF MAIN TRUSS



P15. VI-9

EL-NRSR FORGING PLANT  
HELWAN  
MACHINE WORKSHOP  
1962



## Example 2

In the following example we show the use of a truss, rigidly connected to the columns, as the main supporting element of a heavily loaded girder of relatively big span.

Fig. VI-11a shows the general layout of the stage-roof of Heliopolis Cinema and Theater. It is about 42 ms long and 12.5 ms maximum width. The reinforced concrete roof slab, 12 cms thick, is supported on cross-girders of 12.5 ms maximum span and having cantilever arms of 7.0 ms maximum projection of the form shown in figure VI-11b; the distance between the center-lines of the cross-girders is 5 ms. The slab in the projecting part is arranged at the lower fiber of the cantilevers so that they act as T-beams. The cross-girders are supported at their outer edges on two columns creating a couple to fix the girders and reduce their bending moments; their details of reinforcement are shown in figure VI-11b.

This stage was originally constructed for the national theater of the U.A.R. The main supporting element was a frame, 31 ms clear span and 11.25 ms clear height as shown in figure VI-12. In order to reduce the bending moments due to the own weight of the girder of the frame, 3 openings 1.6 ms high and 10.20 ms total length were arranged at the middle third of the span. The effect of the possible concentration of the stresses in the upper outside corner of the frame due to the change of direction of the tensile forces has been reduced by bending the tension reinforcements around relatively big radii increasing gradually from row to row as shown in the details given in figure VI-12.

During construction and after executing foundations, it was decided to raise the level of the roof by 3.5 ms in order to have the possibility of hanging timber floor for operation and control purposes. Due to this change and because of the big loads on the main girder, it was decided to replace it by a truss rigidly connected to the columns in the form shown in figure VI-13 which gives full concrete dimensions and details of reinforcements.

In order to reduce the required area of reinforcing steel and to have a good distribution of the tension cracks high grade steel was chosen for the tension reinforcements of the cross-girders, the main frame and the truss.

To avoid splices, the main reinforcing bars have been supplied with their full required length although they were relatively big.











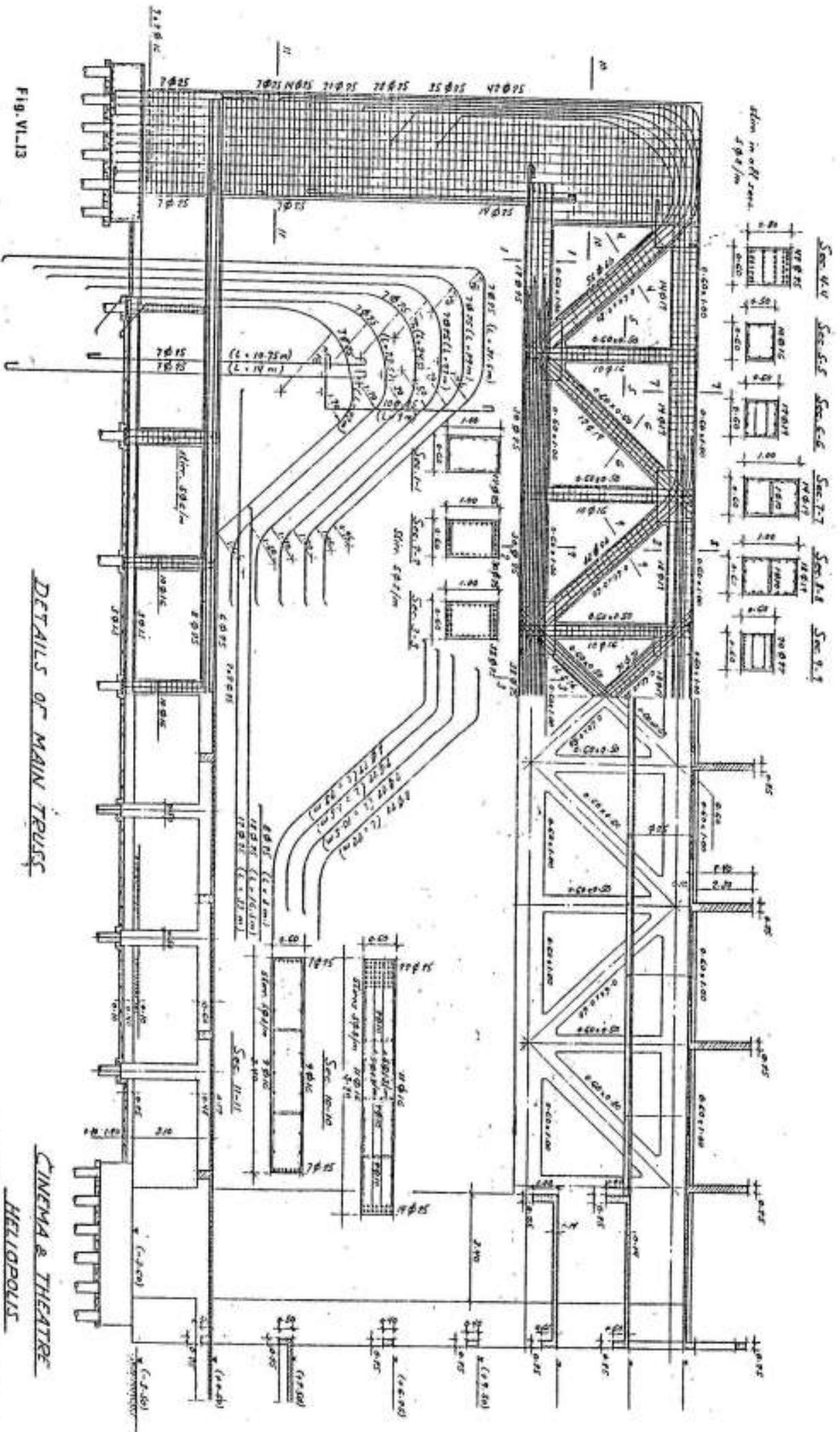


FIG. VI.13

DETAILS OF MAIN TRUSS

CINEMA & THEATRE

DETAILS OF ROOF OF STAGE-3

HELIOPOLIS

## VII - SAW - TOOTH ROOF STRUCTURES.

In big covered halls where a uniform distribution of natural light, that is not possible from windows in outside walls, is required, the saw tooth roofs in which the light from the windows is directly reflected by the roof inside the hall, gives a convenient solution, fig VII-1.

For industrial buildings, it is generally recommended not to allow

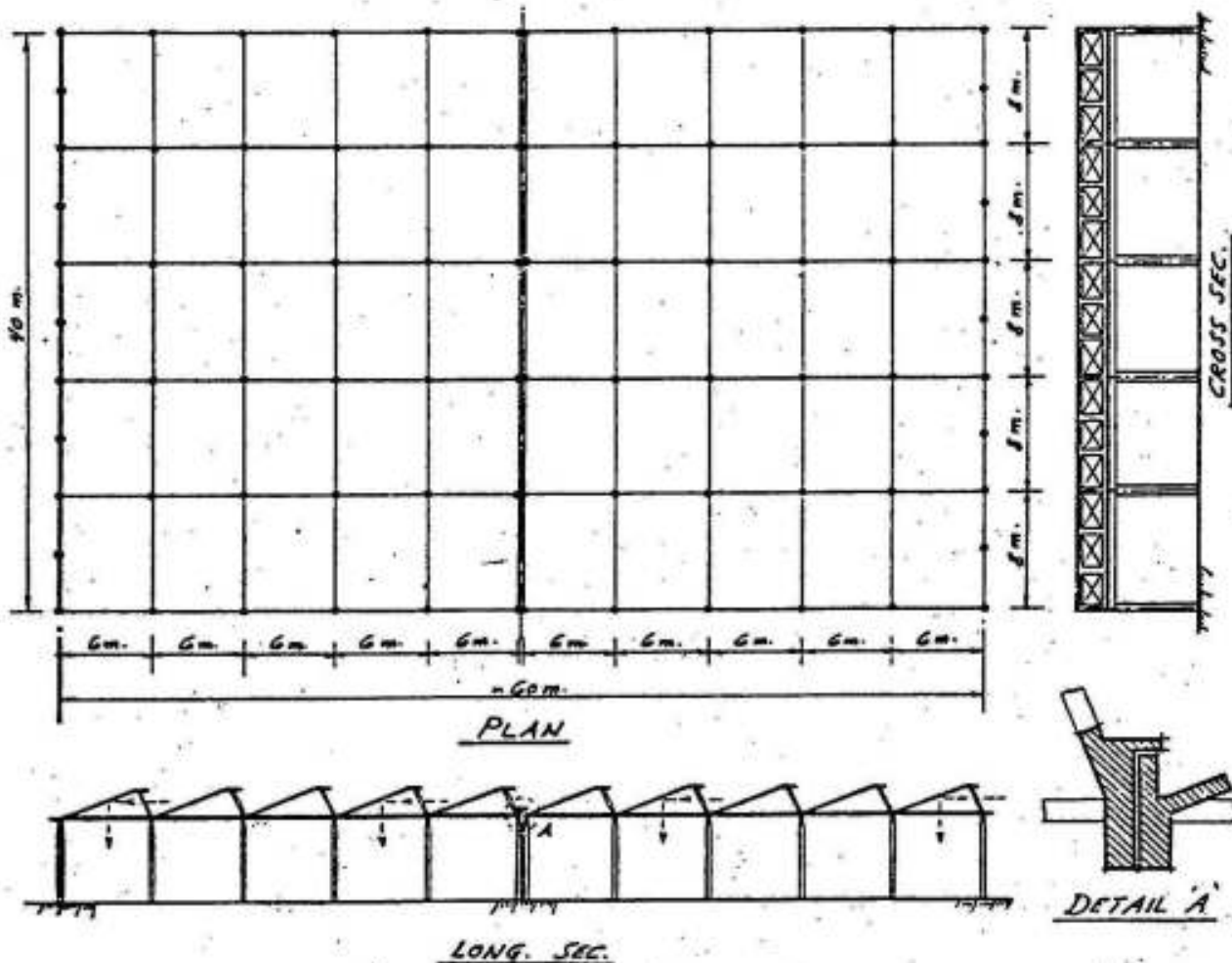


Fig. VII-1



any direct sunrays to fall inside the hall for which purpose, saw-tooth north light roofs, in which the windows are arranged to face the north, are used.

The convenient slope of the roof slab lies between  $20^\circ$  and  $30^\circ$  with the horizontal so that the concreting can be done without double shuttering. The windows are either vertical or inclined with a maximum angle of ca  $15^\circ$  with the vertical.

In order to have sufficient uniform light inside a hall, the area of the windows must be bigger than 20% of the horizontal area and the spacing between them to be maximum 10 ms. The steel sections required for the windows being proportional to their area, it is recommended to divide the windows by reinforced concrete posts at 2 to 3 ms between centers.

The saw-tooth slab type shown in figure VII-2 gives the simplest

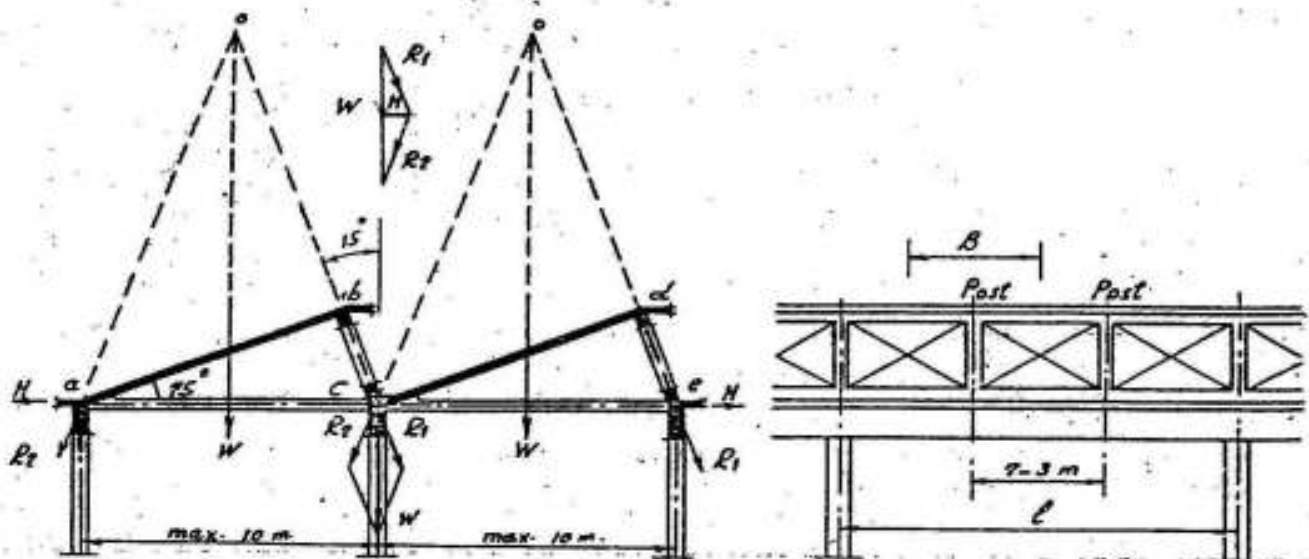


Fig. VII-2

form of this system. Its structural elements are:

The inclined slab supported at its top edge by the ridge beam and at its bottom edge by the Y-beam, the upper continuous ridge beam supported by the inclined posts which are again supported on the Y-beam and, the continuous Y-beam supported by the main columns. If the inclination of the posts is big, a tie is to be arranged to resist the horizontal thrust of the system.

As the rain water is accumulated at the lowest point of the slab, it is essential to choose the form of the Y-beam so that there is

sufficient space for the rain water and the necessary slopes of the gutter. (Fig VII-3):

The statical behavior of the system can be shown if we consider the equilibrium of a frame composed of a slab of breadth B hinged at a and supported at b on the post bc (Fig VII-2). Assuming that the slab thickness

$$t = 16 \text{ cms}$$

the post bc 20 x 16 cms

the distance between centers of posts

$$B = 800/3 = 266 \text{ cms}$$

the span of the slab  $l_s = 2.5$  length of post  $l_p$

then, the moment of inertia of the slab is

$$I_s = 266 \times 16^3 / 12 = 91130 \text{ cm}^4$$

and, the moment of inertia of the post is

$$I_p = 20 \times 16^3 / 12 = 6830 \text{ cm}^4$$

The relative stiffness  $\chi$  of slab to post is therefore given by:

$$\chi = \frac{I_s}{l_s} \cdot \frac{l_p}{I_p} = \frac{91130}{2.5 \times 6830} = 5.35$$

This means that the post is very slender relative to the slab and can be assumed as a pendulum that can resist axial forces only i.e. hinged at both ends b and c. Therefore any of the units of the saw-tooth may be assumed as three hinged.

Assuming further that the dead weight plus the superimposed loads on slab ab for a breadth B is W, then the reaction at b is equal to  $R_1$  acting in the direction of cb and the reaction at a is equal to  $R_2$  acting in the direction of ao where o is the point intersection of W and  $R_1$ .

Considering now two adjacent panels of the saw-tooth, we find that the reactions at the intermediate support are equal to  $R_1$  from panel abc and  $R_2$  from panel cde, their resultant is again vertical and equal to W. The horizontal components of  $R_2$  at a and  $R_1$  at e are the same and equal to H. If the posts are vertical then  $H = 0$  and if their

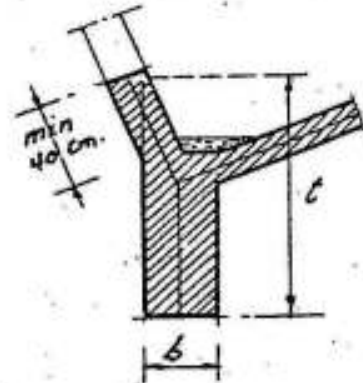


Fig. VII-3

inclination with the vertical is small ( $< 15^\circ$ ), then  $H$  is small and can be easily resisted by the outside columns. If the inclination of the posts is big,  $H$  is big and arranging a tie is recommended.

The previous investigation shows that the inclined slab may be considered as simply supported. The reaction at its top edge can be assumed in the direction of the supporting posts. (Fig VII-4).

The ridge beam is continuous over the posts. It carries in addition to its own weight, the reaction  $R_1$  of the slab acting along its axis.

The posts carry the reactions of the ridge beam; they can be assumed as axially loaded.

The intermediate Y-beam is continuous over the main columns; it carries, in addition to its own weight, the reactions of the slab,  $R_2$  at its lower edge as a uniform load and  $R_1$  as concentrated loads transmitted through the posts. If the intermediate posts in a span are two or more, the load on the beam may be assumed uniform and vertical. For resisting the field moments of the Y-beam, the section may be assumed as rectangular with breadth  $b$  and depth  $t$  (fig VII-3), whereas, for resisting the connecting moments, the breadth is  $b$  and the theoretical depth over the columns is equal to the distance from the center of the tension steel over the supports to the lower surface of the compression zone.

The outside beams are continuous over the outside columns, the load on the beam at  $a$  (fig VII-2) is uniform, inclined and equal to  $R_2$ , the loads on the beam at  $e$  are concentrated, equal to the loads on the posts and act in their direction. If the inclination of the post is big, it is recommended to arrange a horizontal beam as shown.

From the economic point of view, a one way solid slab as that shown in figure VII-2 may be recommended if its thickness is smaller than or equal to  $\sim 16$  cms which corresponds to a distance between the windows  $\ll 5$  ms. For bigger spans, a one way hollow-block or ribbed slab may be used. Cross ribs having the same cross-section and reinforcement as the main ribs must be arranged; for a slab span  $< 8$  ms, one cross rib

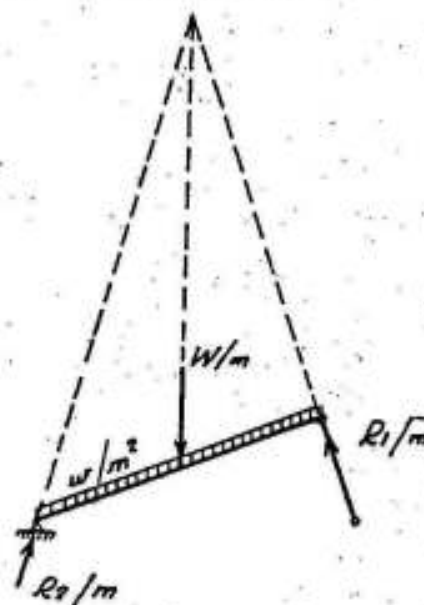
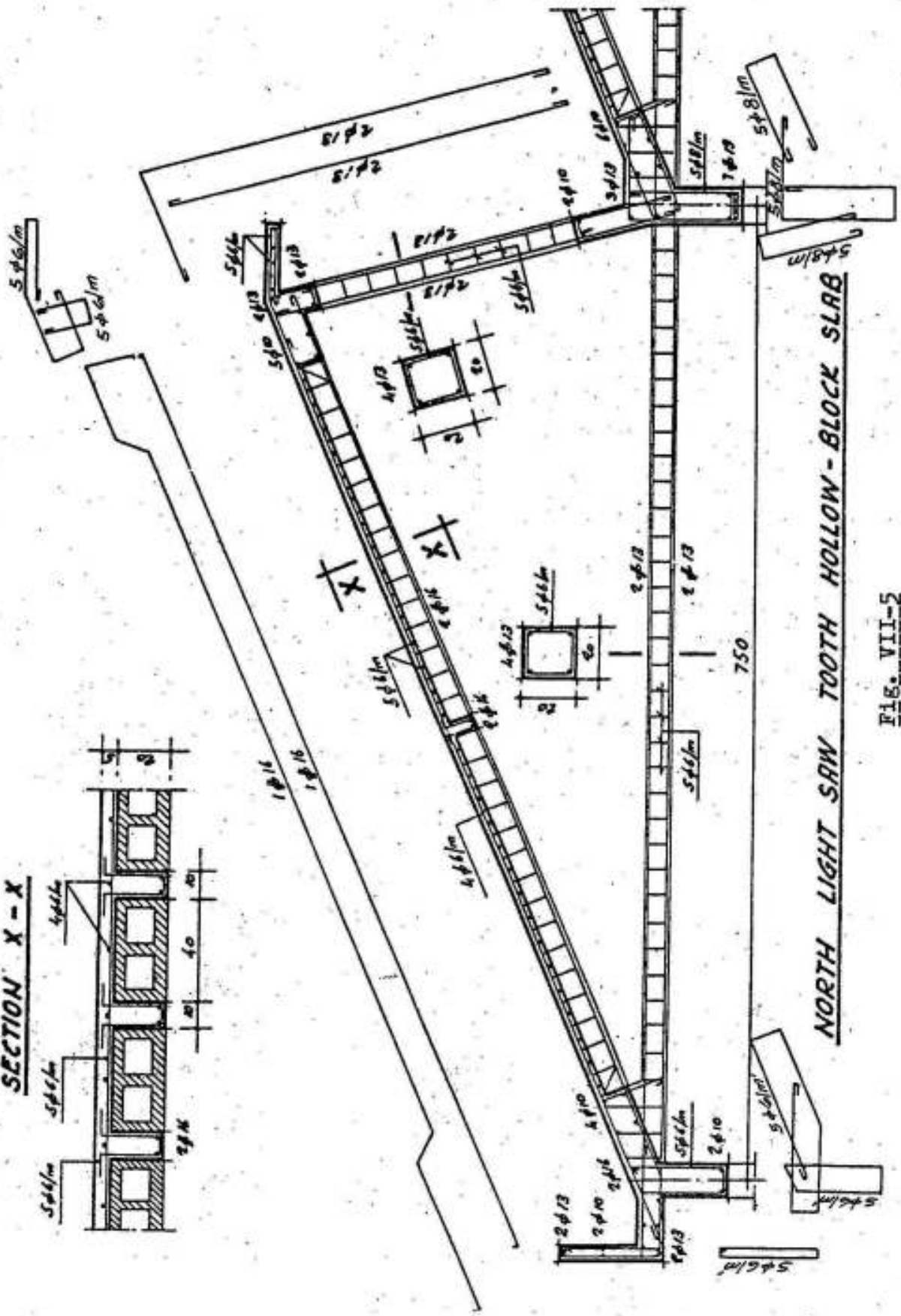
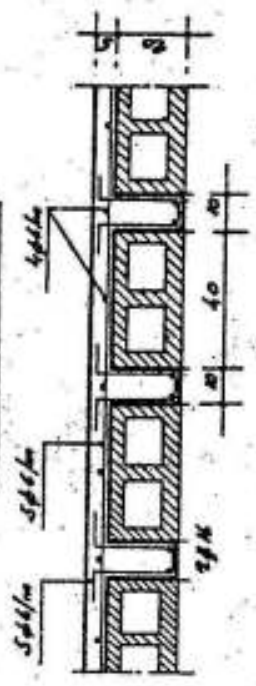


Fig. VII-4

**SECTION X - X**



**FIG. VII-2**

and for  $8 \text{ m} < l < 10 \text{ ms}$  two ribs. (Fig VII-5).

For big saw-tooth spans, it is possible to get very economic solutions by arranging secondary inclined beams @ 2-3 ms, supported at their upper edge over the posts and at their lower edge over the Y-beams, giving a one way slab whose main supporting direction is normal to the inclined direction (refer to fig III-15). In this manner, the thickness of the slab is 8 to 9 cms. For the mentioned structure, the span of the saw-tooth is 10 ms, the spacing between the secondary inclined beams is 2.5 ms which means that the slab is one way and continuous over the secondary beams. Its span is 2.5 ms and its total load normal to the roof is max.  $350 \text{ kg/m}^2$  giving a thickness of 8 cms.

The inclined secondary beams may be assumed simply supported. As the posts are vertical, then the reactions are also vertical and the max. bending moment is given by: (Fig VII-6).

$$M_{\text{max}} = wl'l/8$$

where

$w$  = total vertical load per meter beam

$l$  = horizontal span and  $l'$  = inclined span of beam.

In our case  $l = 10 \text{ ms}$  and the beam is  $20 \times 63 \text{ cms}$  only because it behaves as a T-beam.

The average thickness of the slab and secondary beams is therefore

$$8 + 20 \times 55/250 = 8 + 4.4 = 12.4 \text{ cms only}$$

In some cases, e.g. dusty and smoky halls, a plane roof is required; in such cases the beams may be inverted (refer to figs VII-17 & VII-21) ; but because the slab lies in the tension zone of the beam, the sections behave as rectangular and need bigger depths. In some cases it may be

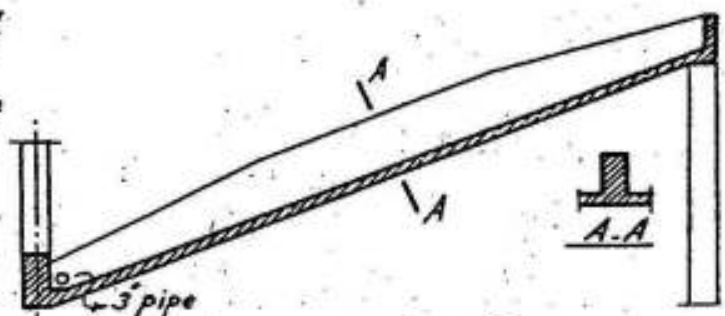


Fig. VII-7

convenient to choose a beam of variable depth as shown in figure VII-7.

In order to be able to drain the rain water, a steel pipe of 3" min. diameter must be concreted inside the web.

The main columns are to be calculated for the vertical reactions of the Y-beams plus the bending moments due to wind; these may approx. be assumed as shown in fig VII-8a, if the columns are of equal moment of inertia and the wind loads are assumed concentrated.

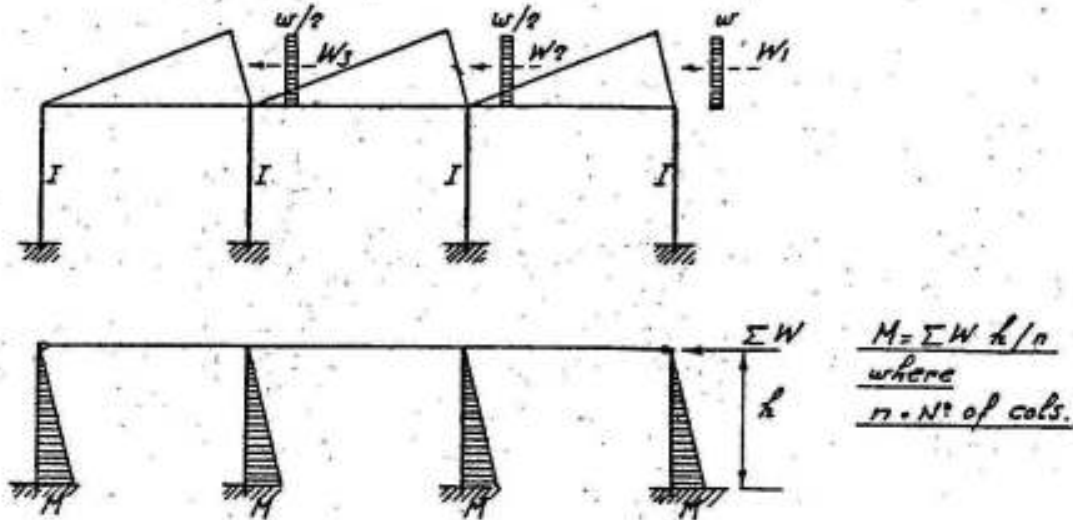


Fig. VII-8a

If the wind loads  $w$  are assumed uniformly distributed we get:

For two columns of equal moment of inertia: (Fig VII-8b).

$$X = -\frac{3}{16} wh$$

$$M = -\frac{5}{16} wh^2$$

$$M_1 = +\frac{3}{16} wh^2$$

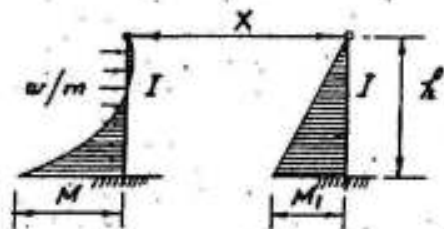


Fig. VII-8b

For three columns where the moments of inertia are not equal, we get: (Fig VII-8c).

$$X_1 = \frac{3}{8} wh \frac{1+k}{2+k} \quad \text{and}$$

$$X_2 = \frac{3}{8} wh \frac{1}{2+k} \quad \text{where } k = I_1/I$$

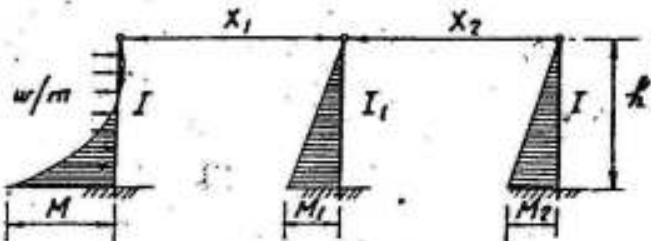


Fig. VII-8c

Therefore

$$M = \frac{wh^2}{8} \cdot \frac{5+k}{2+k}, \quad M_1 = \frac{3wh^2}{8} \cdot \frac{k}{2+k} \quad \text{and} \quad M_2 = \frac{3wh^2}{8} \cdot \frac{1}{2+k}$$

For four columns, we get : (Fig VII-8d)

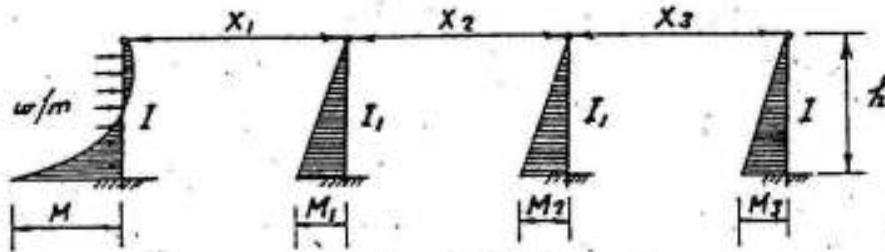


Fig. VII-8d

$$X_1 = \frac{3}{16} wh \frac{1 + 2k}{1 + k}$$

$$X_2 = \frac{3}{16} wh$$

$$X_3 = \frac{3}{16} wh \frac{1}{1 + k}$$

and

$$M = \frac{wh^2}{16} \frac{5 + 2k}{1 + k}$$

$$M_1 = \frac{wh^2}{16} \cdot \frac{3k}{1 + k}$$

$$M_2 = M_1$$

$$M_3 = \frac{3wh^2}{16} \cdot \frac{1}{1 + k}$$

It is however possible to get reasonable dimensions for the saw-tooth roof elements if triangular frames are arranged at convenient distances varying between 5 and 6 ms as shown in figure VII-9. This system is generally used for distances between windows varying between 7 and 10 ms.

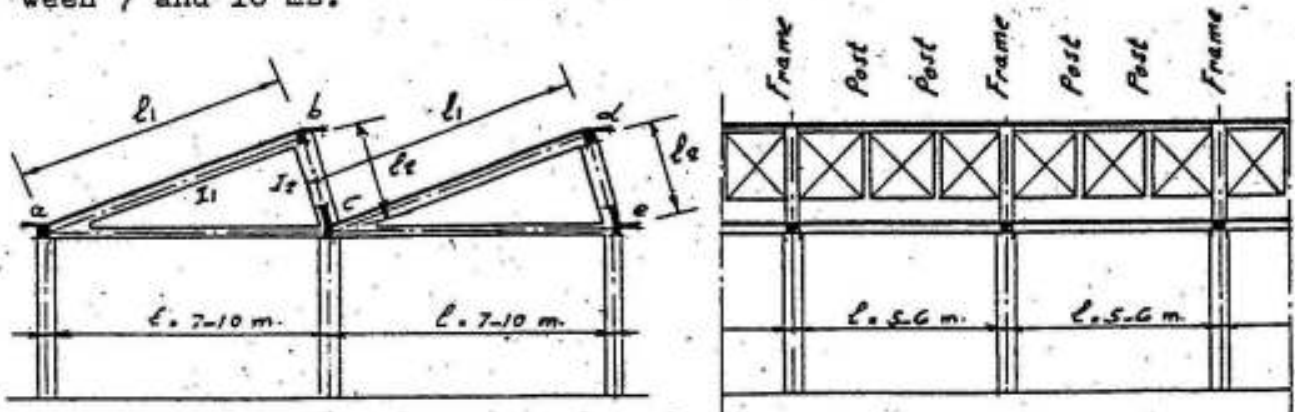


Fig. VII-9

In this case, the different elements of the saw-tooth roof are :

1) The slab:

It is generally two way; its rectangularity is to be determined for the side lengths  $l_1$  and  $l_2$  measured in the plane of the slab. The component of the load normal to the slab only causes the bending moments and shearing forces. (Fig VII-10).

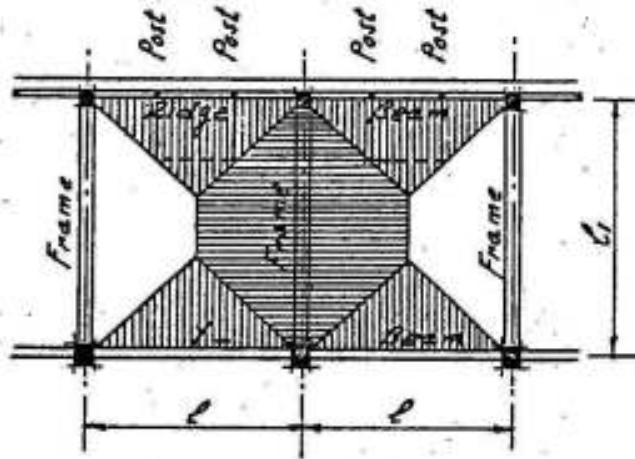


Fig. VII-10

2) The ridge beam:

It is continuous over the posts and frames, it carries, in addition to its own weight the triangular load shown acting in the direction of the axis of the beam. The equivalent uniform loads on the different spans are not equal.

3) The posts:

These are axially loaded, carry the reactions of the ridge beam and transmit them to the Y-beam.

4) The Y-beam:

It behaves as a continuous beam, of spans  $l$ , supported by the main columns. It carries, in addition to its own weight, the triangular load at the lower edge of the slab plus the concentrated loads from the intermediate posts. If these posts are two or more, the Y-beam may be calculated for an equivalent uniform vertical load in the usual way.

5) The triangular frame:

It carries the trapezoidal load from the slab plus its own weight, both may be replaced by an equivalent uniform load in the usual way. The internal forces can be determined by one of two methods:

First method: as a continuous beam

Neglecting the elastic deformation of the tie ac, then points a, c and e may be assumed fixed in position and consequently points b and d can also be considered as fixed in space. In this manner, the continuous frame can be considered as a continuous beam abcde of unequal spans  $l_1$  and  $l_2$ , unequal moments of inertia  $I_1$  and  $I_2$  and unequal loading  $w_1$  and  $w_2$ . The moment of inertia  $I_1$  is to be determined for



a T-section with breadth of flange  $B = 6t_s + b$  in which  $t_s$  is the thickness of the slab and  $b$  is the breadth of the web and  $I_2$  to be determined for the rectangular section of  $l_2$ . The load  $w_2$  on  $l_2$  may be neglected without making an appreciable error. (Fig VII-11).

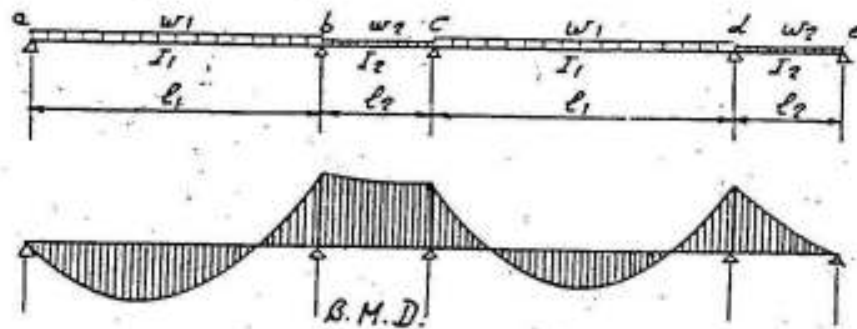


Fig. VII-11

Second method: as isolated triangular frames

If the continuity of the two triangular units at  $c$  is neglected, each unit may be calculated as a triangular frame with a tie in the usual way as follows: (Fig VII-12).



Fig. VII-12

The tensile force  $H$  in the tie is: 
$$H = - \frac{\delta_0}{\delta_1} = - \frac{\int \frac{M_0 M_1 ds}{EI}}{\int \frac{M_1^2 ds}{EI} + \frac{l}{A_t E_t}}$$

According to figure VII-11, the connecting moment at  $c$  may be estimated equal to  $M_b$ .

It is practically sufficient to determine the internal forces due to wind pressure for a single frame neglecting the tie. (Fig VII-13)

The details of reinforcements are shown in figure VII-14.

If north light is required in big span halls without intermediate supports, the choice of the system of the main supporting element depends on the dimensions of the hall and its disposition with respect to the north. For a hall with the span parallel to the north, frames at 4-6 ms between centers spanning the shorter dimension of the

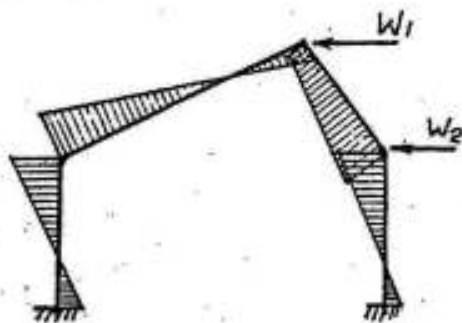


Fig. VII-13

hall supporting saw-tooth roofs arranged according to any of the forms shown in figure VII-15 may give a convenient solution.

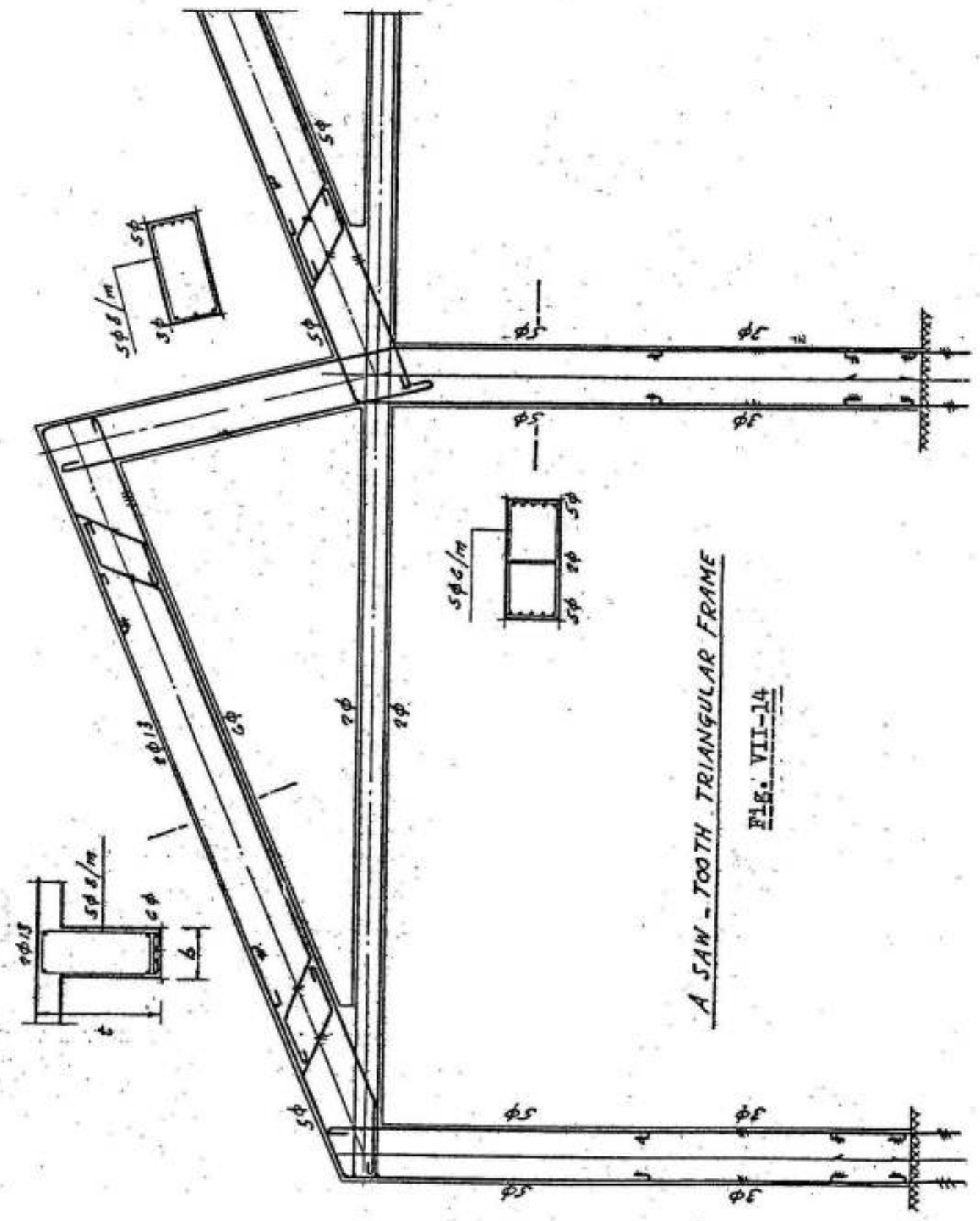
Figure VII-15b shows a saw-tooth roof arranged above the frames, it gives a big construction height which may be reduced if the saw-tooth slabs are arranged in between the frames as shown in fig. VII-15c. This new solution may need a bigger depth for the main girder giving sufficient space for the windows and the beams supporting the slab. The rain water can, in this case, be drained by inserting 3" steel pipes in the web of the main girder at the lower edge of the slab. One can dispense with the pipes if the saw-tooth slabs are arranged as shown in figure VII-15d in which the rain water passes free below the main girders and the lower beams are hung to the frame by steel reinforcements sufficient to resist the reaction of the beam.

The truss shown in figure VI-2 gives another typical solution for the hall shown in figure VII-15a. The construction height of trusses (ca  $1/6 - 1/7 l$ ) being relatively big, this solution can be well adapted for bigger spans.

We give in the following the details of two typical structures. The first structure is the main factory hall of the "Paints and Chemical Industries" at Matarieh. Figure VII-16 gives the general layout and the concrete dimensions of the main supporting frames of the factory hall, the details of reinforcements are shown in figure IV-13.

The machine workshop of the "Forging Plant" at Helwan (Fig. VI-8,9) gives the second typical solution for this type of structures.

If the north is parallel to the longer side of the hall, i.e., normal to the span, the following systems for the main supporting element may be used: (Figure VII-17).



A SAW - TOOTH TRIANGULAR FRAME

FIG. VII-14

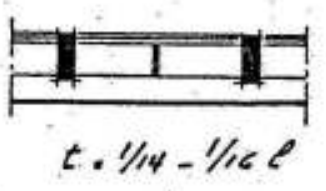
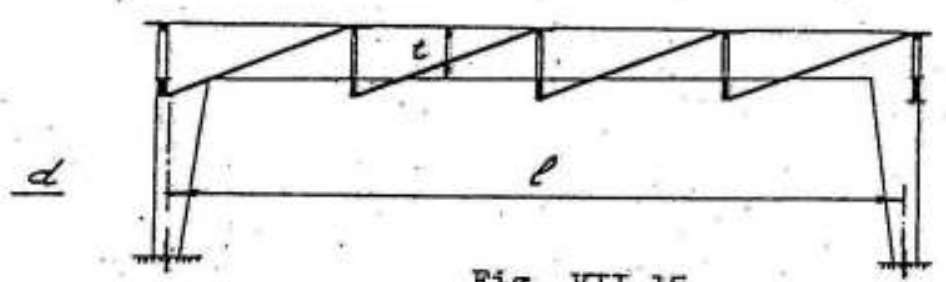
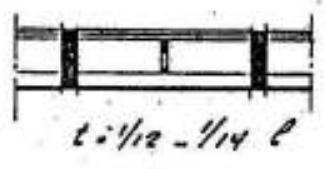
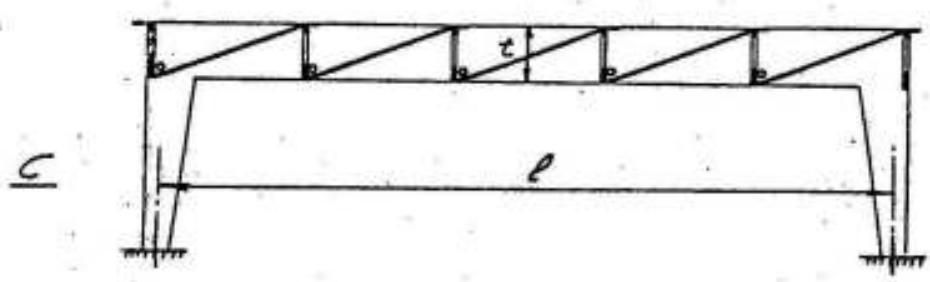
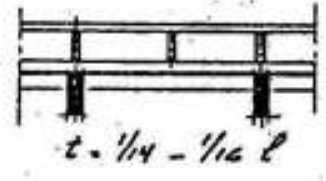
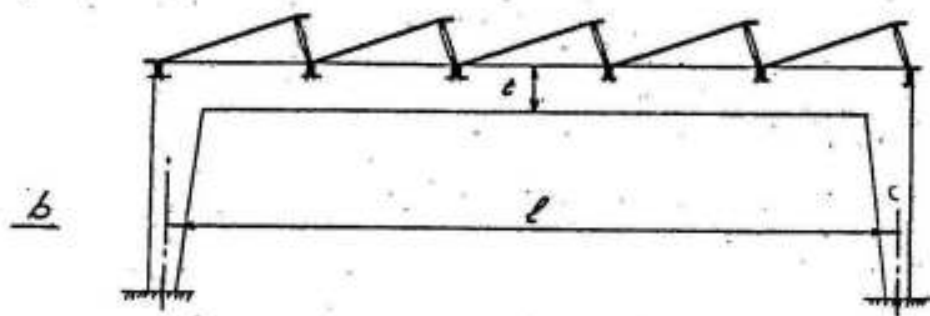
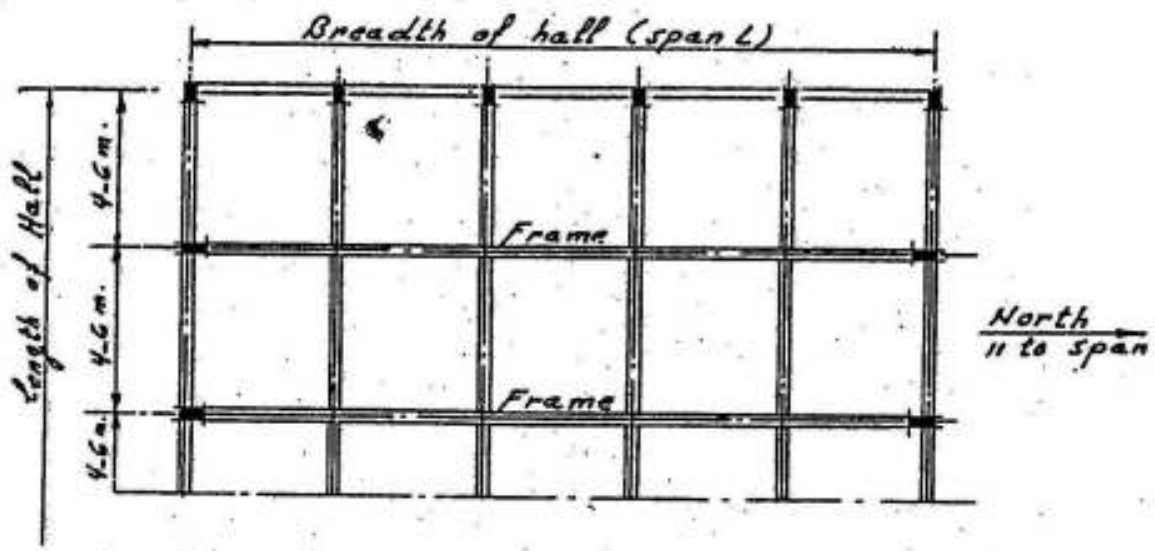
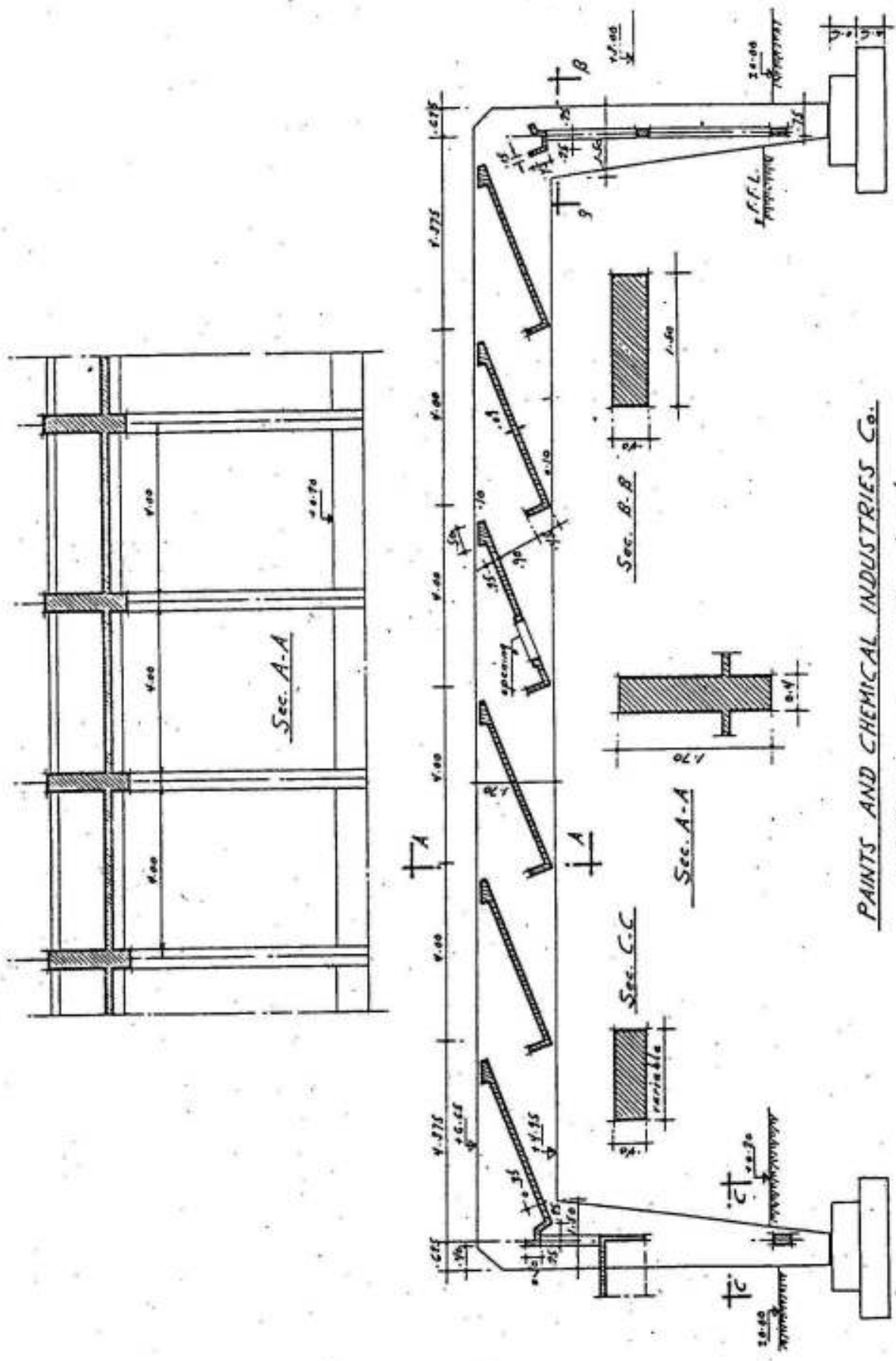


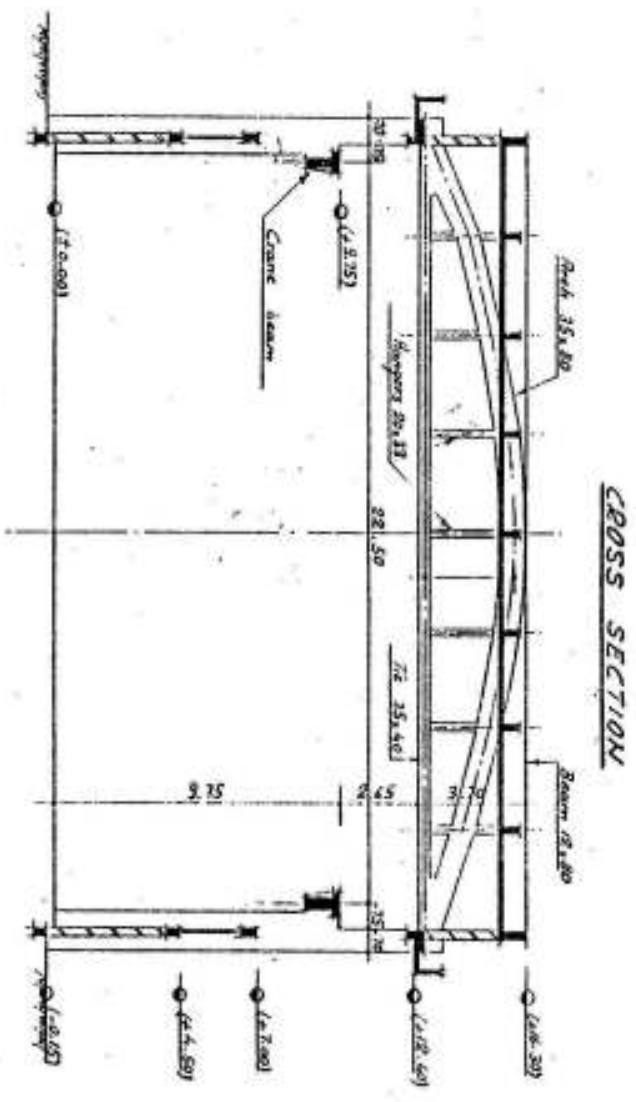
Fig. VII-15



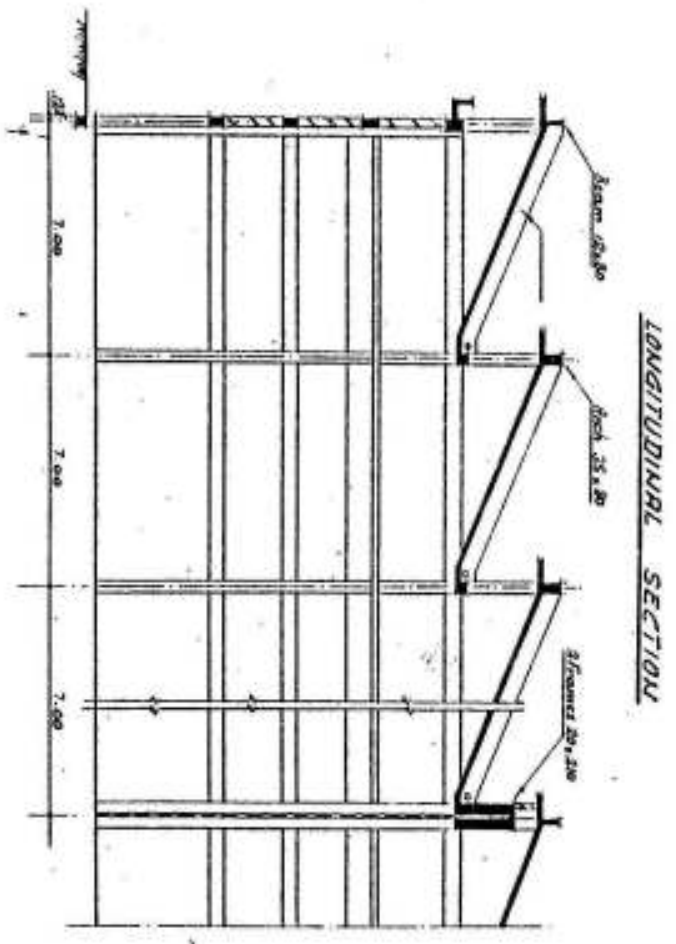
*PAINTS AND CHEMICAL INDUSTRIES Co.*

*Details of main supporting elements*

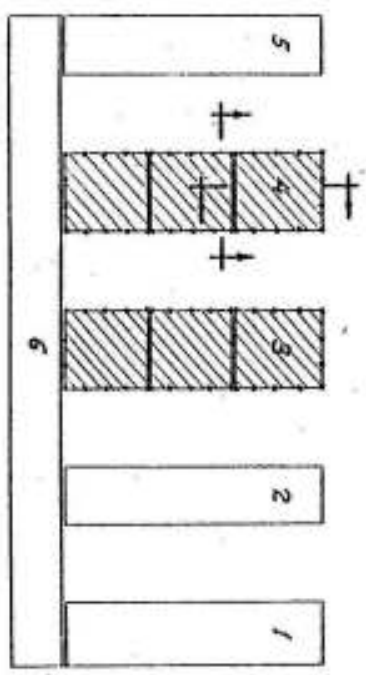
FIG. VII-16



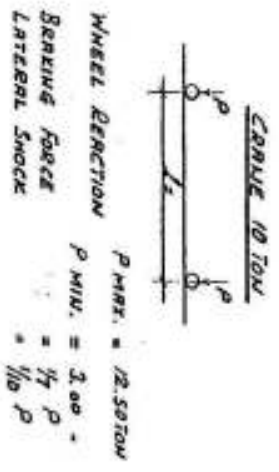
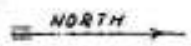
CROSS SECTION



LONGITUDINAL SECTION



KEY PLAN



$P_{MRT} = 12.5070N$   
 $P_{MIN.} = 3.00 \cdot P$   
 $= \frac{1}{4} P$   
 $= \frac{1}{10} P$

EL-NRSR FORGING PLANT

HELMAN

MRII WORKSHOP

1962

FIG. VII-18

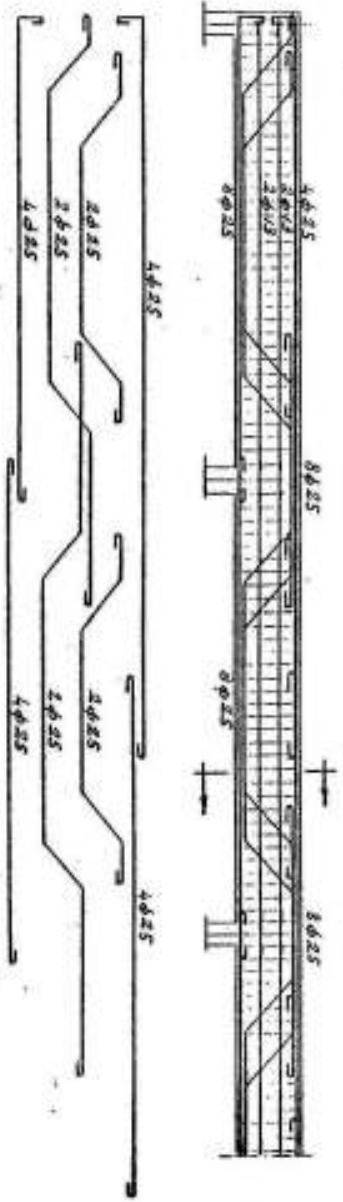
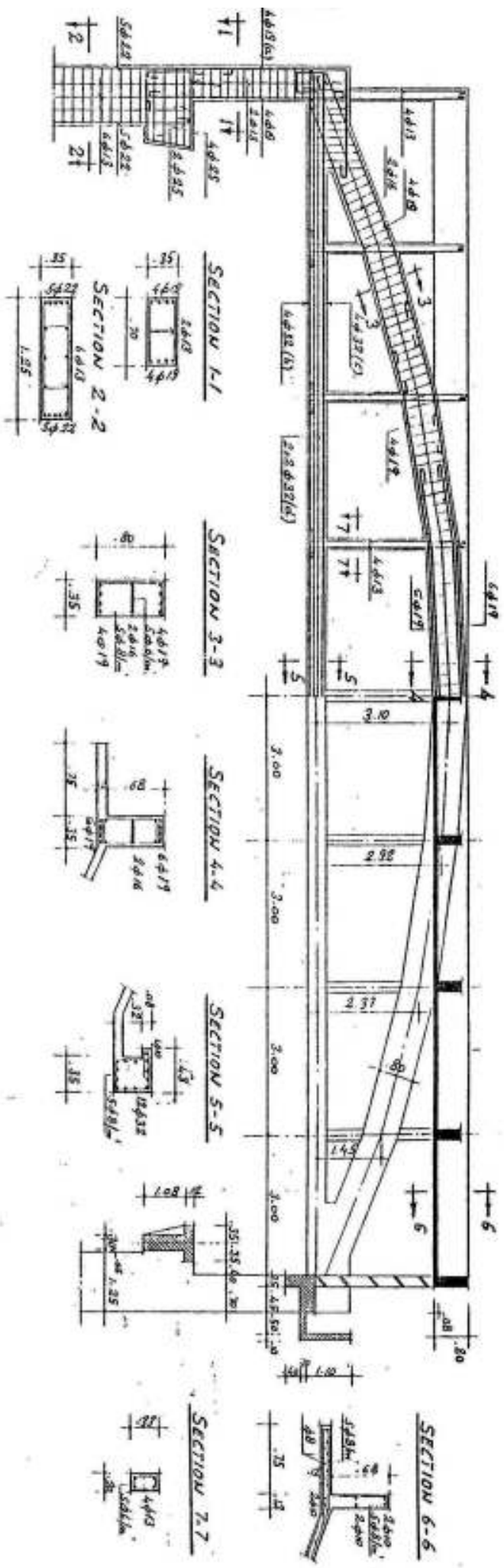


FIG. VII-19

EL NRSR FORGING PLANT

HELVIN

MAIN WORKSHOP

1962





- 1) Two-hinged frames (Figure VII-17b) spaced every 4-6 ms; the required depth for the main girders varies between  $l/14$  and  $l/16$ .
- 2) If the clear construction height necessary for the hall does not allow for the required depth of the main girder or for bigger spans where the use of a simple frame gives heavy cross-sections, a Vieren-deel girder (figure VII-17c), in which the saw-tooth roof is supported at its upper edge on the top chord and its lower edge on the bottom chord of the girder, may be used. The depth and spacing of the girder must be so chosen that they give a convenient slope for the saw-tooth slab.
- 3) The two-hinged arch with a tie shown in figure VII-17d gives another convenient system in which the saw-tooth roof is supported at its upper edge on a horizontal beam, parallel to the main girder and supported by it, arranged at the crown of the arch and at its lower edge on the tie hung to the arched girder by hangers spaced every 2.5-4 ms. It is recommended to arrange the hangers and the posts along the same line so that they form one element.

The main workshops of "El-Nasr Forging Plant" at Helwan give a typical example for this last solution. Figure VII-18 gives the general layout and main dimensions of the workshop and figure VII-19 shows the details of reinforcements of the parabolic arch used as main supporting element as well as the details of the crane girder carrying the rails of a  $10^t$  crane giving the wheel loads shown in figure VII-18.

This workshop is 24 ms wide, 84 ms long and 12.5 ms clear height. It is used for forging operations and includes a series of furnaces which necessitate sufficient uniform indirect light and good ventilation. Because the hall is dusty and smoky, a plane roof surface is specified. The hall is provided with a  $10^t$  crane; the clear height below the crane rail is 9.9 ms and is 2.5 ms above it. The workshop is divided into 3 blocks, 28 ms each, by two expansion joints.

To satisfy the specified requirements, a north-light saw-tooth roof with a plane bottom surface was chosen.

The span of the hall being relatively big, an arch with a tie as the main supporting element for the roof was preferred. To reduce the construction height of the structure and to get a reasonable distance between the arches, the minimum rise of  $l/8 = 3$  ms was chosen. To get a convenient slope for the saw-tooth roof, a minimum spacing of

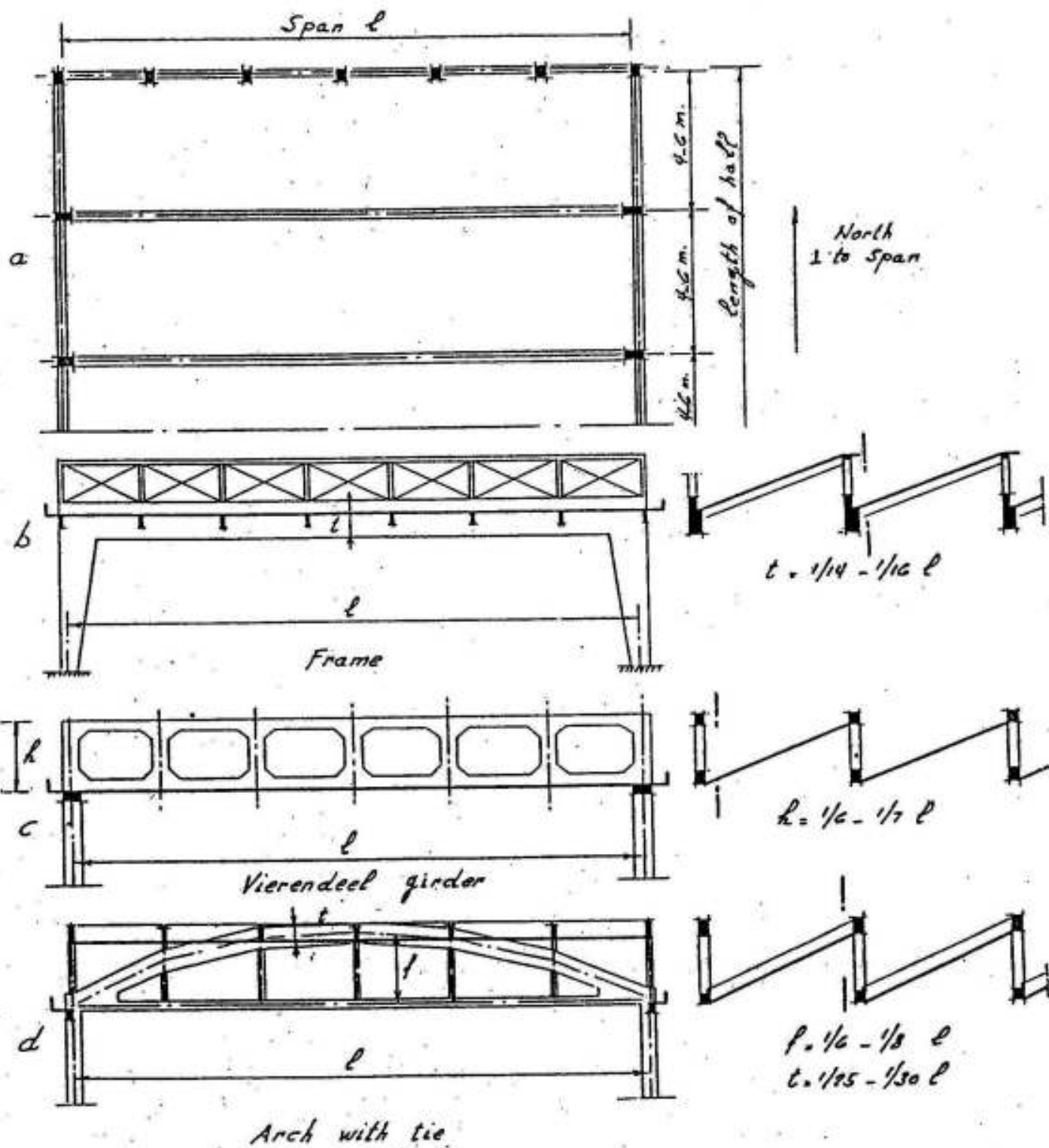


FIG. VII-17

7 ms between the arches was necessary. In order to reduce the thickness of the slab, inclined secondary beams @ 3 ms are arranged; the beams are inverted to give the specified plane bottom surface of the roof.

In this manner, the roof is composed of a one-way continuous slab 3 ms span and inclined simple beams, 7 ms horizontal span. The total vertical load being 350 kg /m<sup>2</sup> surface, a slab thickness of 8 cms and secondary beams 20 x 60 cms were sufficient.

The arch carries its own weight plus the loads from the roof which are transmitted to the arch and concentrated through the secondary beams and the supporting posts and ties. In order to simplify the construction of the main girder and to reduce the bending moments to a minimum, its axis was chosen polygonal with the corners coinciding on a parabola following the equation: (Figure VII-20)

$$y = 4 f \xi \xi$$

in which

$$\xi = x/l \quad \text{and} \quad \xi' = x'/l$$

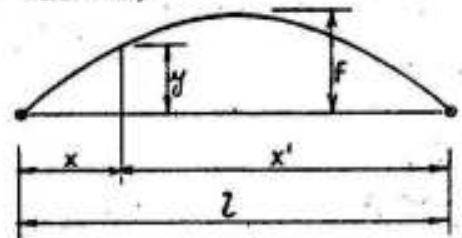


Fig. VII-20

Assuming the loads as uniformly distributed, then the internal forces in the arch can be estimated in the following manner:

Loads from slab	$0.350 \times 7 \times 1.15$	= 2.8 t/m'
Loads from secondary beams	$0.2 \times 0.52 \times 2.5 \times 7 \times 1.15/3$	= 0.7 t/m'
Own weight of the main girder		1.2 t/m'
Concrete for slopes of gutter+rain-water+windows ...		= 0.3 t/m'
		---
Total weight		= 5.0 t/m'

Due to the elongation of the tie and the elastic deformation of the arch girder due to the normal force, the horizontal thrust  $H$  may be estimated by 0.95 of that of the corresponding three-hinged arch  $H_0$ , i.e.,

$$\text{For a three-hinged arch} \quad H_0 = \frac{wl^2}{8f} = \frac{5 \times 24^2}{8 \times 3} = 120 \text{ t}$$

$$\text{For the two-hinged arch} \quad H = 0.95 H_0 = 0.95 \times 120 = 114 \text{ t}$$

$$\Delta H = H_0 - H = 6 \text{ t}$$

The maximum bending moment  $M$  is therefore

$$\text{max. } M = Hf = 6 \times 3 = 18 \text{ mt}$$

Accordingly, the arch girder can be estimated for a normal force  $N$  equal to 114 t and a bending moment  $M$  equal to 18 mt. A cross-section 35 x 80 cms ( $t = /30$ ) reinforced by 0.8 to 1.2 % normal mild steel was sufficient. The reinforcement is symmetrically arranged in the cross-section and the splices are staggered so that not more than two bars are spliced in any section.

The tie can be estimated for a normal tensile force of 114 t. Its tension bars are symmetrically arranged in a cross-section 35 x 40 cm without any splices. It is however recommended to use high grade or cold-twisted steel in the tie as it is of higher strength and has bigger bond with the concrete.

The arch was assumed externally statically determinate (giving vertical reactions only for vertical loads) due to the existence of the slender parts of the supporting columns.

It is clear that the systems shown in figures VII-15 & VII-17 may be of one or more spans. As an example, we show in figure VII-21 continuous frames spaced every 5 ms and supporting a saw-tooth roof with the north normal to the span.

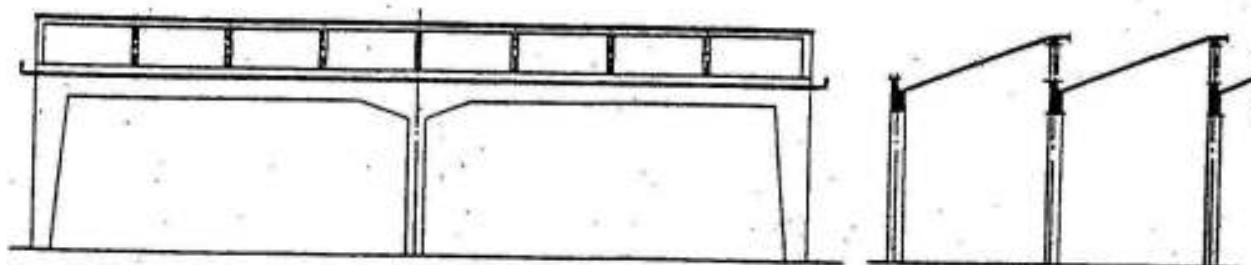
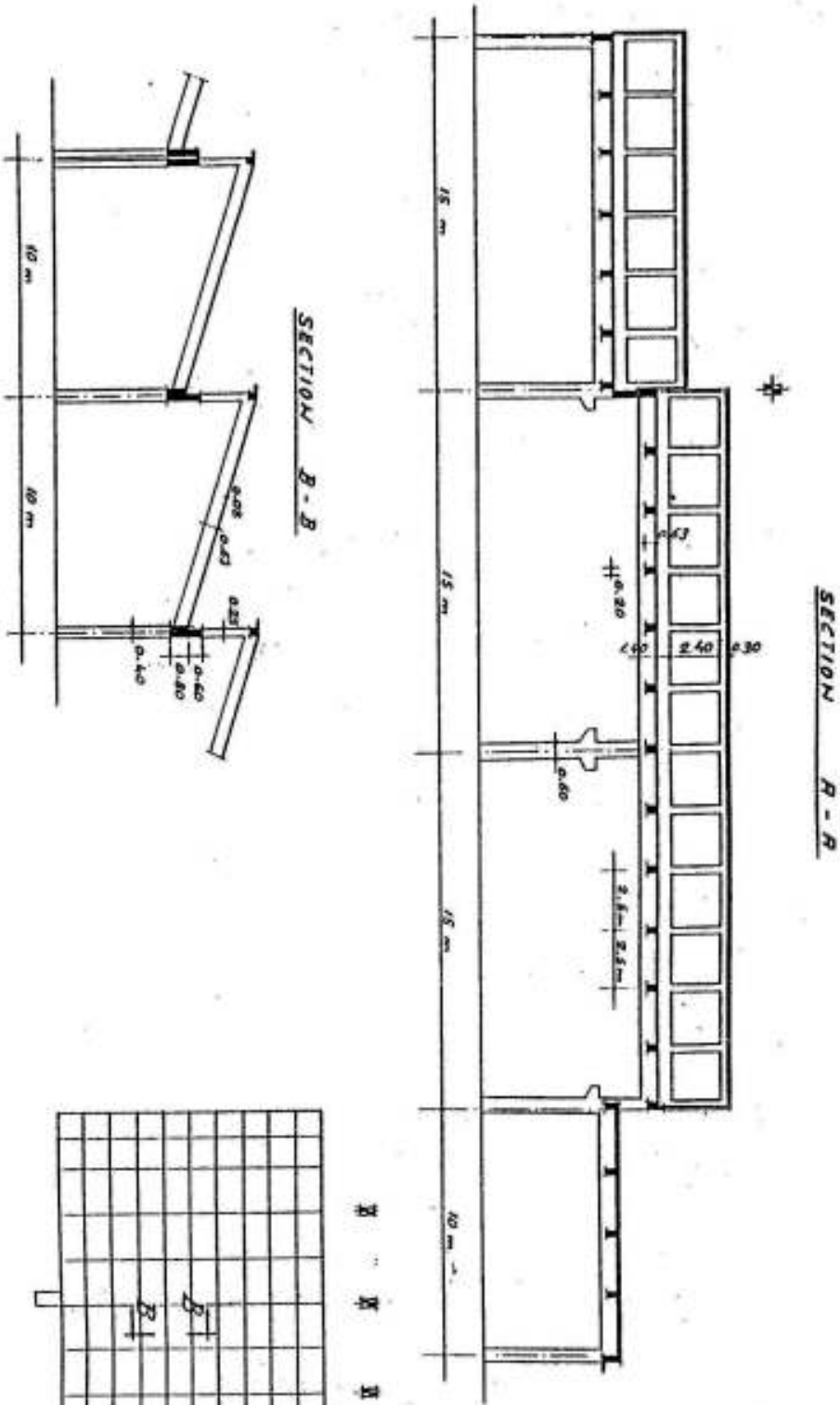


Fig. VII-21 A symmetrical continuous frame with intermediate pendulum

Because of symmetry in shape and loading, the intermediate columns will be, due to roof loads, subject to axial loads only; it is therefore recommended in such cases to choose a continuous frame with a slender pendulum support in the middle.

Factory 135 at Helwan, shown in figure VII-22 gives another typical solution. In this factory, the roof is saw-tooth 10 ms span supported on main girders (normal to the north) 15 ms span. The details of the different elements are shown in figure III-17.

Folded plates and shells have been recently extensively used as roof structures for halls in which indirect light is specified.



FRCTORY 135 HELWAN  
PL. VI-22

## VIII- ARCHED SLABS AND GIRDERS

In simple beams, commonly only one cross-section is subjected to the maximum design moment, and consequently, if the member is prismatic, only one cross-section of the beam is working at the maximum allowable stress at design load. Knowing that the mentioned maximum stresses act at the extreme fibers only and that all other fibers are understressed, one can directly observe that the simple beam is one of the least efficient of structural forms. This situation is somewhat improved by continuity because the maximum field and connecting moments are commonly smaller in magnitude than of a simple beam of the same span and the beam can be designed such that the extreme fiber stress is equal to the allowable values at sections of maximum positive and negative moments.

Arched girders of convenient form are mainly subject to high compressive forces and low bending moments and shearing forces so that nearly all sections of the arch are approximately subjected to the same average compressive stress which means a high efficiency in the use of reinforced concrete as a building material.

For these reasons, arched roofs give a convenient economic solution for long span roof structures without intermediate supports in cases where a plane roof surface is not necessary to meet the functional requirements of the structure; however plane roofs or floors can occasionally be supported on arched girders.

According to the conditions at the supports, arches generally used in reinforced concrete structures are of three main types:

- a) Three hinged arches supported at each end by a hinge resting on the abutment and provided with an intermediate hinge, generally placed at the crown.
- b) If the intermediate hinge in the previous system is not arranged, the arch is two hinged.
- c) If the arch is rigidly connected to the abuments in such a way

that no rotation and no vertical or horizontal displacements are allowed, then the arch is fixed.

The best form for the axis of an arch is that which coincides on the line of pressure of the loads; thus for uniform loads, parabolic arches are most convenient.

We give in the following, the theory and design of arches extensively used in reinforced concrete structures.

a) Three Hinged Arches

A three hinged arch is statically determinate; its horizontal thrust  $H$  can be determined from the condition that the bending moment at the intermediate hinge  $c$  is equal to zero. (Fig VIII-1)

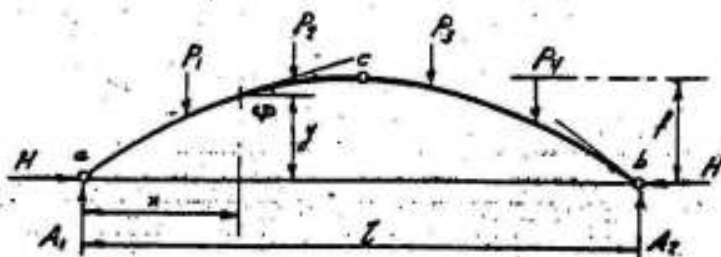


Fig. VIII-1

Assuming that  $M_c$  is the bending moment at the position of the intermediate hinge  $c$  of the arch  $ab$  assumed as a simple beam, then the horizontal thrust  $H$  can be calculated from the equation:

$$H = M_c / f$$

The bending moment  $M$ , shearing force  $Q$  and thrust  $N$  in any section  $x, y$  are given by:

$$M = M_0 - Hy$$

$$Q = Q_0 \cos\varphi - H \sin\varphi$$

$$N = H \cos\varphi + Q_0 \sin\varphi$$

in which

$M_0$  and  $Q_0$  are the bending moment and shearing force of  $ab$  assumed as a simple beam and

$\varphi$  = angle between the tangent to the section under consideration and the horizontal.

In flat arches one can approximately assume :

$$K = H \sec\varphi$$

### Parabolic Arches

As stated before, parabolic arches give the most convenient form for uniform loads.

The equation of the axis of the arch according to figure VIII-2 is given by:

$$y = \frac{4fx}{l^2} (l - x)$$

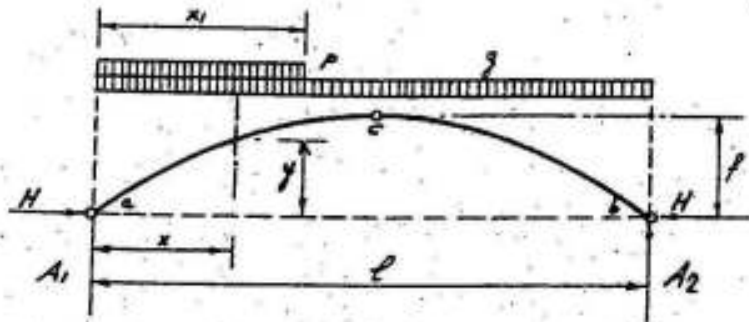


Fig. VIII-2

Due to a uniform load  $g$  over the whole span and a live load  $p$  acting on  $x_1 = 2l/5$  or  $l/2$  (fig VIII-2) the approximate value of the thrust at the quarter points is given by:

$$N = H \sqrt{1 + \left( \frac{2f}{l} \right)^2}$$

The vertical reactions  $A_1$  and  $A_2$ , the horizontal thrust  $H$  and the bending moments  $M$  at the quarter points are given in the following table:

Parabolic Arch

D.L. $g$ acting over the whole span $l$	L.L. $p$ acting on	
	$x_1 = 2l/5$	$x_1 = l/2$
Vert. reactions $A_1 = gl/2$	$8p_1 / 25$	$3p_1 / 8$
$A_2 = gl/2$	$2p_1 / 25$	$p_1 / 8$
Horiz. thrust $H = gl^2/8f$	$p_1^2 / 25f$	$p_1^2 / 16f$
B.M. at quarter pts $M = 0$	$\pm 3p_1^2 / 160$	$\pm p_1^2 / 64$

Flat arches subject to uniform loads may be constructed with a circular axis in which case we get the following internal forces:

Due to a uniform load  $g$  over the whole span and a live load  $p$



acting on half the span ( $x_1 = l/2$ ), the reactions are:

$$A_1 = (g/2 + 3p/8)l \quad ; \quad A_2 = (g/2 + p/8)l$$

$$H = (g + p/2)l^2 / 8f$$

The bending moments  $M$  and the approximate normal force  $N$  at the quarter points of the arch are given in the following table:

Circular Arch

Ratio $f/l$	Dead Load - $M_g$	Live Load On $\frac{1}{2}$ span		Approx. $N$ at $\frac{1}{4}$ points
		- $M_p$	+ $M_p$	
0.10	0.0009	0.0161	0.0152	1.0198
0.15	0.0019	0.0166	0.0146	1.0440
0.20	0.0038	0.0175	0.0136	1.0771
0.25	0.0061	0.0184	0.0124	1.1180
0.30	0.0088	0.0196	0.0108	1.1662
0.35	0.0122	0.0210	0.0088	1.2207
0.40	0.0162	0.0225	0.0063	1.2806
0.45	0.0189	0.0241	0.0034	1.3454
0.50	0.0259	0.0259	0.0000	1.4142
	$gl^2$	$pl^2$	$pl^2$	$H$

#### Example Of An Arched Roof Slab With Ties

A hall 18 ms wide is to be covered by a reinforced concrete circular slab with a tie as shown in figure VIII-3. At crown, the rise of the arch is 3.0 ms and its thickness  $t$  is 10 cms; at quarter points  $t = 12.5$  cms and at foot  $t = 14$  cms. The distance between the ties is 5 ms and the developed length of the arch is about 19 ms.

Because of the relatively big normal compressive force and small bending moments, such arched slabs are generally symmetrically reinforced with a minimum percentage of 0.8% of the average concrete section.

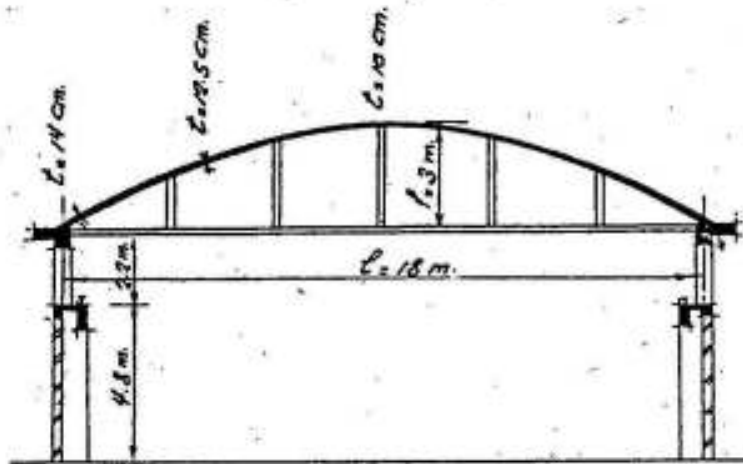


Fig. VIII-3

With the help of this choice and due to the slenderness of the concrete section, it is generally allowed to calculate such slab arched roofs as three hinged.

In order to simplify the calculations, the dead weight of the slab may be assumed as uniformly distributed. The live load is equivalent to 50 kg/m<sup>2</sup> horizontal and the wind load is assumed equivalent to another 50 kg/m<sup>2</sup> horizontal acting on half the span.

Accordingly, the main steps of the statical calculation can be done in the following manner:

1) Loads

Own weight of slab assumed uniformly distributed =		
	$0.125 \times 2500 \times \frac{19}{18}$	= 330 kg/m <sup>2</sup> horiz.
Roof cover		= 70 " "
		-----
Total dead load		g = 400 " "
Wind + live load		p = 100 " "

2) Maximum bending and axial force in circular arched slab

According to table given on page " 152 ", we get :

For  $f/l = 3/18 = 0.166$

$$M_{\max} \approx M_g + M_p = - (0.0025 g + 0.0169 p) l^2$$

$$= - (0.0025 \times 400 + 0.0169 \times 100) \times 18^2 = - 870 \text{ kgm}$$

$$N_{\max} \approx 1.055 H = 1.055 (g + p/2) l^2 / 8f$$

$$= 1.055 (400 + 50) 18^2 / 8 \times 3 = 6400 \text{ kgs}$$

### 3) Check of stresses

Thickness of arched slab at quarter points  $t = 12.5 \text{ cms}$

Assume section symmetrically reinforced and  $\mu = \mu' = 0.4\%$

i.e  $A_s = A'_s = \frac{0.4}{100} \times 12.5 \times 100 = 5 \text{ cm}^2$  chosen  $7\phi 10 \text{ mm/m}$

$M = 870 \text{ kgm}$  ;  $N = 6400 \text{ kgs}$

Eccentricity  $e = M/N = 870/6400 = 0.135 \text{ ms}$

Eccentricity to tension steel  $e_s = e + t/2 - 2 = 13.5 + 12.5/2 - 2 = 17.75 \text{ cm}$

$e_s/d = 17.75/10.5 = 1.67$

Moment about tension steel  $M_s = N \cdot e_s = 6400 \times 0.1775 = 1140 \text{ kgm}$

Max. compressive stress in concrete

$$\sigma_c = C_1 M_s / bd^2 = 5.1 \times 1140 \times 100 / 100 \times 12^2 = 40 \text{ kg/cm}^2$$

Max. tensile stress in steel

$$\sigma_s = C_2 M_s / bd^2 = 140 \times 1140 \times 100 / 100 \times 12^2 = 1100$$

The longitudinal reinforcement  $A'_s$  must be minimum 20% of main steel  
i.e

min.  $A'_s = 0.2 A_s = 0.2 \times 5 = 1.00 \text{ cm}^2/\text{m}$  chosen  $5\phi 6 \text{ mm/m}$

### 4) The tie

Max. horizontal thrust  $H_{\max} = (g + p) l^2 / 8f$

$$= 500 \times 18^2 / 8 \times 3 = 6750 \text{ kg/m}$$

Max. tension in tie  $T_{\max} = 5 \times 6750 = 33750 \text{ kgs}$

Using high grade steel with a max. allowable stress  $\sigma_s = 2000 \text{ kg/cm}^2$ , then the required area of steel is

$$A_s = T/\sigma_s = 33750/2000 = 16.875 \text{ cm}^2$$

chosen  $6 \phi 19 \text{ mm}$ .

5) Vertical and horizontal beams

Span = 5.0 ms

The maximum vertical reaction A of the arch will be resisted by a vertical beam, thus

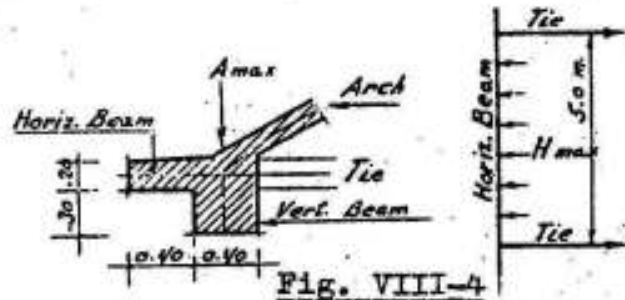
$$A_{\text{max}} = (G + p)l / 2 = 500 \times 18/2 = 4500 \text{ kg/m}' \quad \text{and}$$

the maximum horizontal thrust  $H_{\text{max}} = 6750 \text{ kg/m}'$  will be resisted by a horizontal beam. (Fig VIII-4).

Assuming that the

Vertical beam is 40x60 cms &  
the horiz. " " 20x80 cms

The load on the vertical beam is:



$$w = 4500 + (0.4 \times 0.3 + 0.2 \times 0.4) 2500 = 5000 \text{ kg/m}'$$

Its max. bending moment  $\approx 12000 \text{ kgm}$  and  
its max. tension steel  $6 \phi 19 \text{ mm}$

The load on the horizontal beam is  $H_{\text{max}} = 6750 \text{ kg/m}'$

its max. bending moment  $\approx 16000 \text{ kgm}$  and  
its max. tension steel  $6 \phi 19 \text{ mm}$

It is recommended in such beams to resist the diagonal tensile stresses by stirrups and to use straight bars for the longitudinal reinforcement of the beams.

6) Details of reinforcements as shown in fig. VIII-5

7) Wind pressure and crane loads

For resisting the wind pressure (and eventual crane loads) the system may be assumed as composed of two stiff columns fixed at their bottom end and connected together by a rigid tie i.e. a simple once statically indeterminate system. (Fig VIII-6). The main system can

ARCHED SLAB ROOF WITH TIES

Thickness at crown = 10.0 cm.  
 Thickness at quarter point = 19.5 cm.  
 Distance between centres of ties and columns = 5.0 m.

Reinforcements of ties:  $3\phi 19$   
 $3\phi 17$

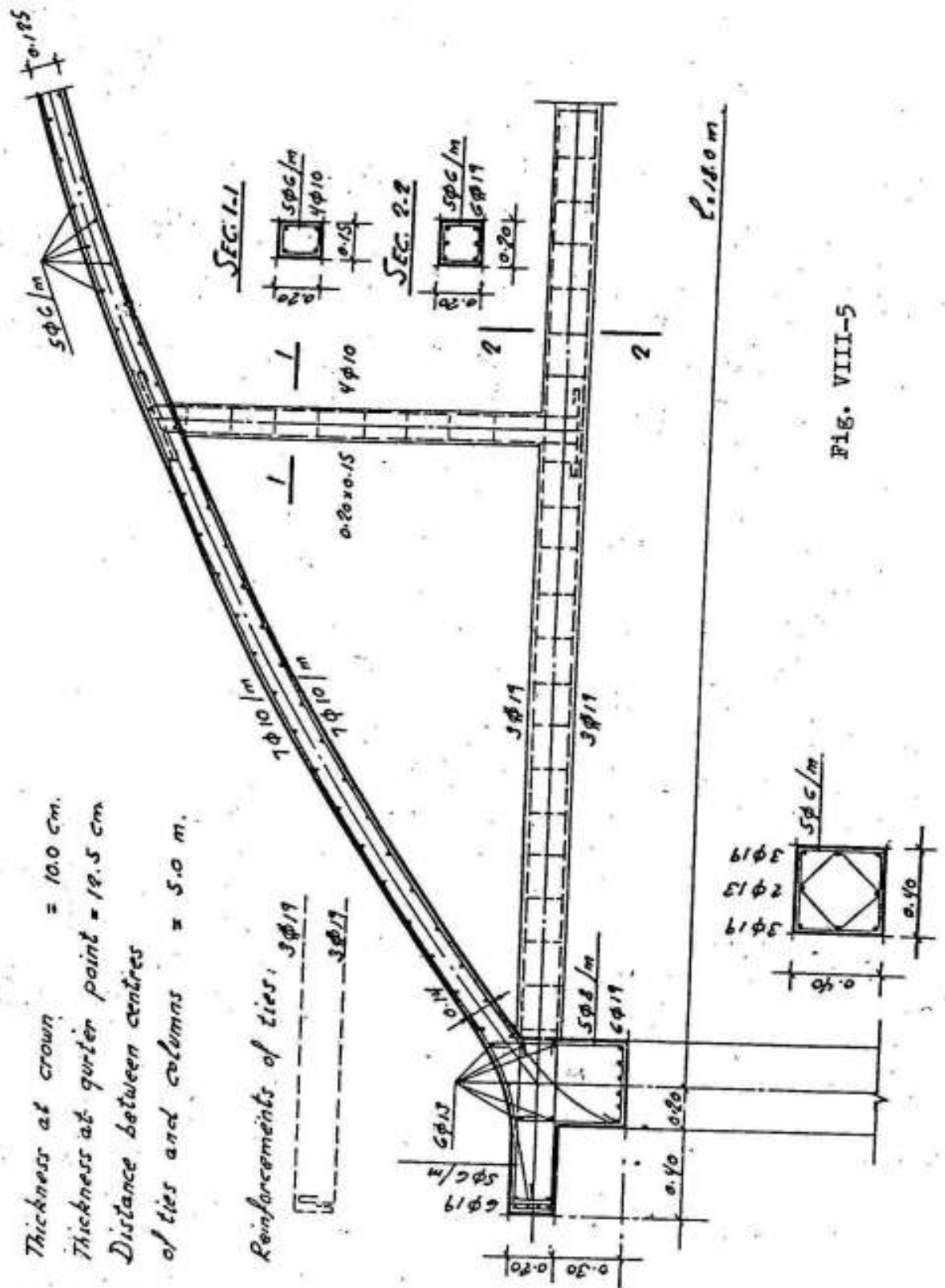
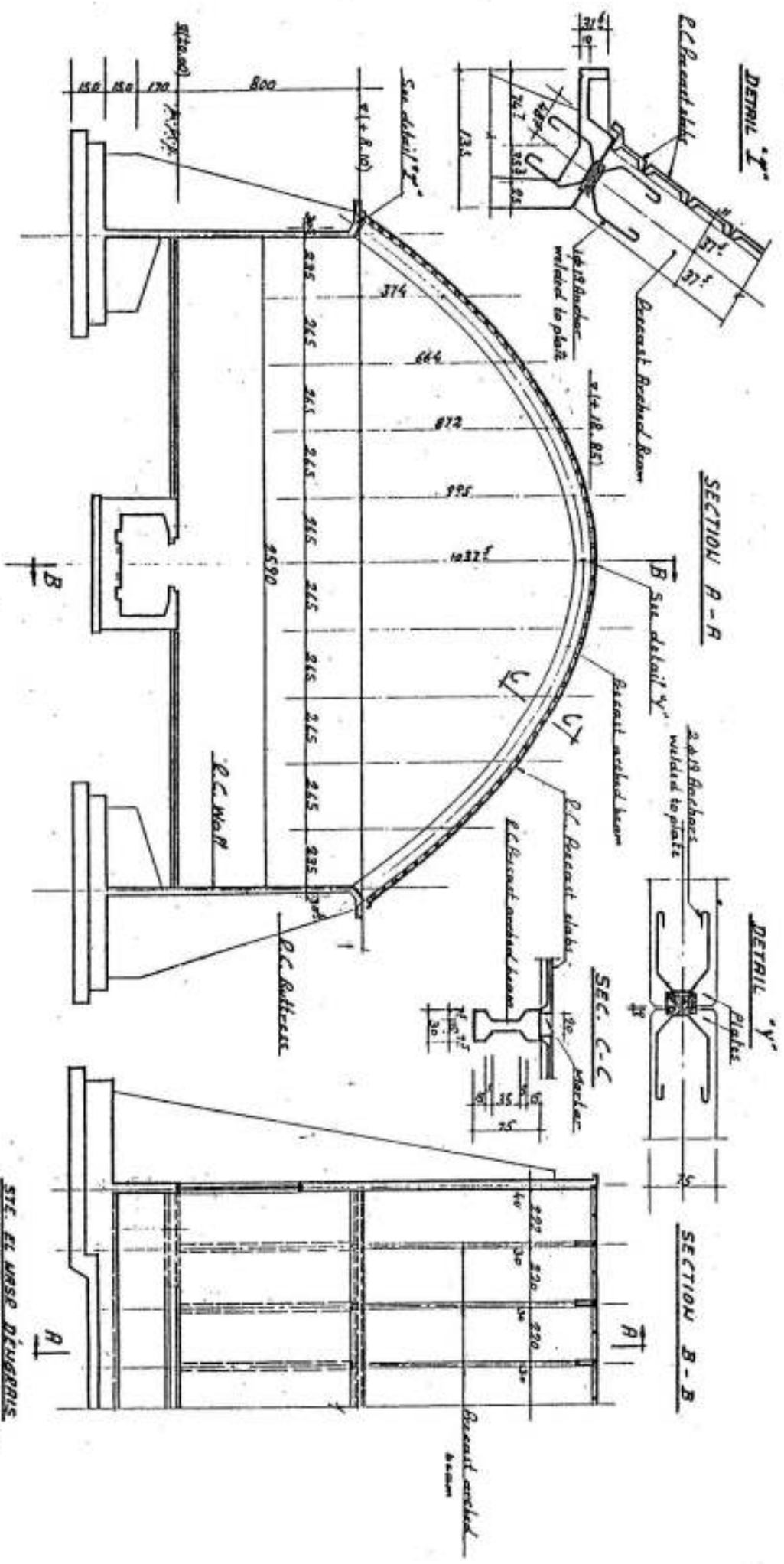


FIG. VIII-5



FILE VIII-7

STE. EL MASR D'EGYPTE  
 ET D'INDUSTRIES CHIMIQUES  
 SUEZ  
 AMMONIUM NITRATE LIMESTONE SILA

be obtained by cutting the tie, in which case, the statically indeterminate value is  $X$  and

$$X = - \int M_0 M_1 ds / \int M_1^2 ds$$

in which  $M_0$ ,  $M_1$  and  $ds$  are the notations normally used in the theory of virtual work.

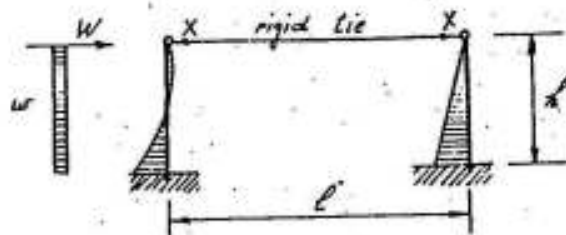


Fig. VIII-6

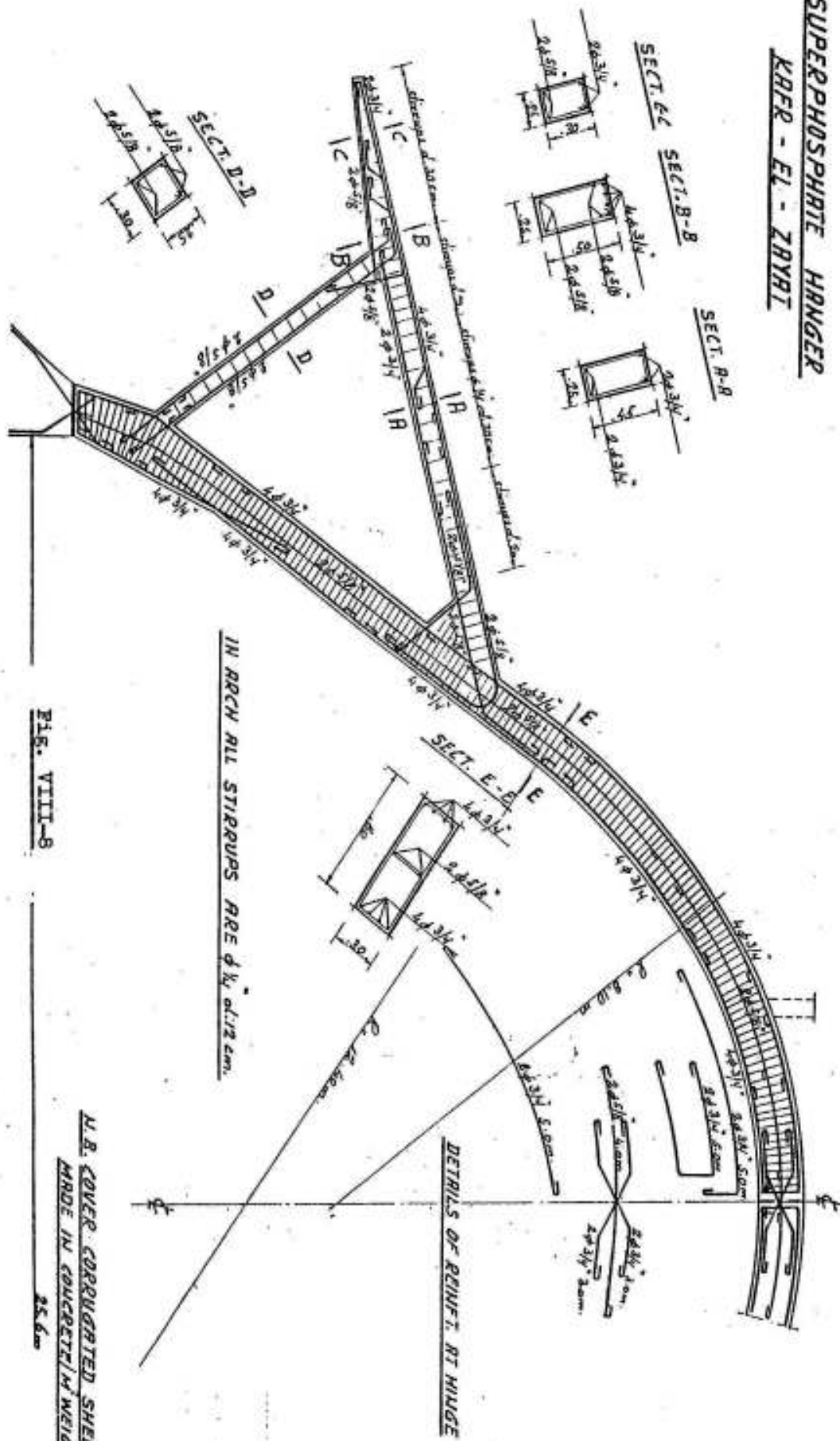
We give in the following some other examples showing the use of 3-hinged arches or arched frames in covering relatively big spans.

Fig. VIII-7 shows a project for prefabricated 3-hinged arched roof prepared to cover the ammonium nitrate limestone silo of El Nasr Fertilizer and Chemical industries at Suez. The span of the arch is 26.5 ms, its rise is 10.375 ms, the distance between the center lines is 2.2 ms, the roof cover is composed of precast reinforced concrete slabs (Fig. VIII-7a). In addition to the dead and live loads acting on the arch after construction, each half must be checked as a beam for the internal forces due to its own weight under transportation and lifting conditions before and during construction Fig. VIII-7b. The sections of the arch shown in this figure are chosen such that they give maximum resistance and minimum weight.

Fig. VIII-8 shows the 3-hinged superphosphate hangar at Kafr El-Zayat, its span is 26 ms and its rise is 13 ms. This big rise is chosen in order to have minimum air volume between the roof and the stored superphosphate because of the bad undesired effect of the air humidity on the fertilizer. The side cantilevering structure is used as a shed covering the railway lines serving the hangar. In order to reduce the loads on the arches, the roof cover is made of corrugated sheets weighing 20 kg/m<sup>2</sup> only.

Fig. VIII-9 shows the details of the main frames supporting the roof slab of the urea silo at Abu-Kir Fertilizers and Chemical Industries plant. This silo is ~50 ms span, 186 ms long and 20 ms high. The max. height of the stored urea is 14.3 ms. The soil at the site is extremely weak and for this reason, the floor slab carrying the urea and the roof structure are supported on cast in-situ, ~25 ms long piles. A three hinged structure with ties is found to be the most convenient for this case. The roof is chosen circular with inverted main frames @ 6 ms. The one-way roof slab is chosen at the bottom surface of the main frames to enable the use of mechanically moving forms and to have the frames acting as T. In this case, isolation of roof is essential.

**SUPERPHOSPHATE HANGER**  
**KAFR - EL - ZAYYI**



**IN ARCH ALL STIRRUPS ARE  $\phi 3/8$  IN.**

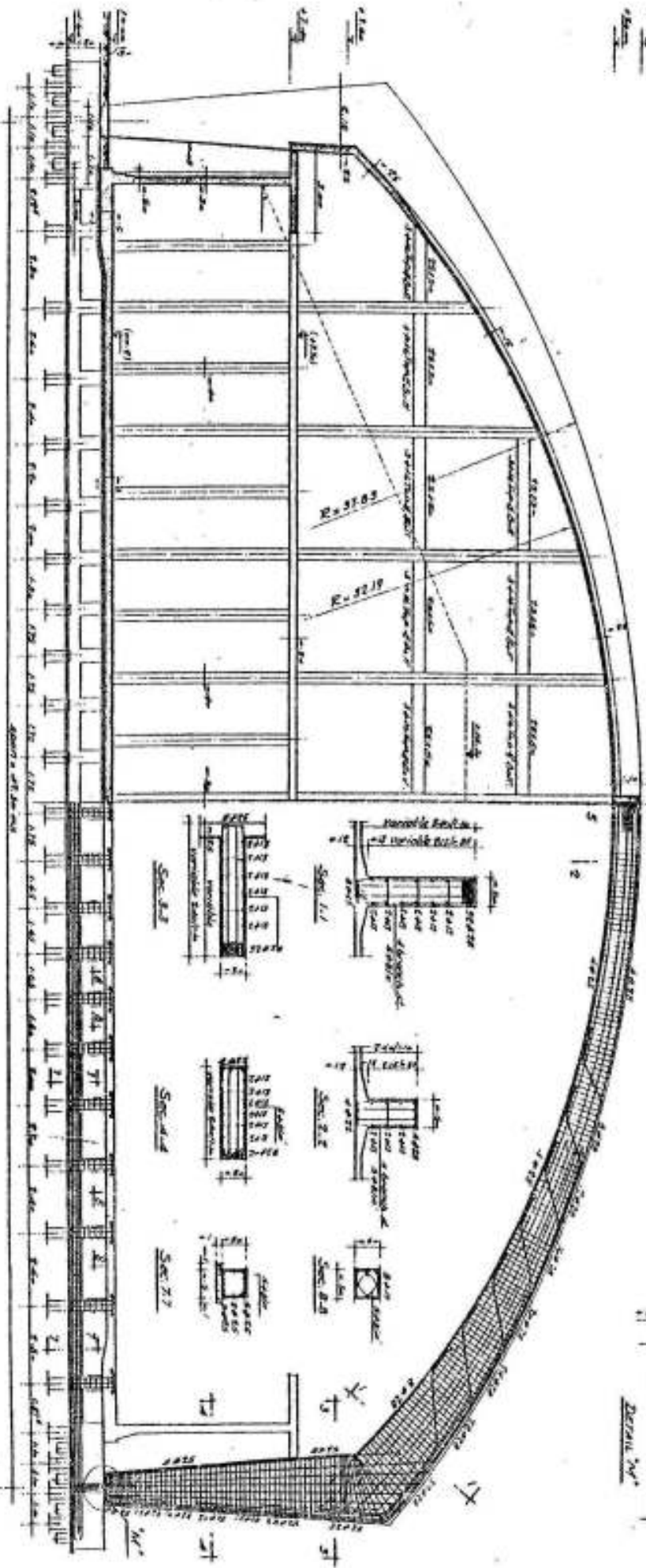
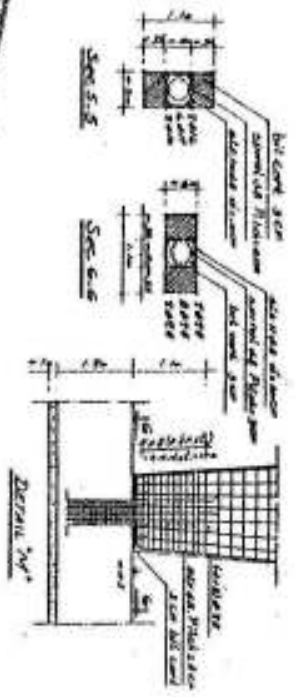
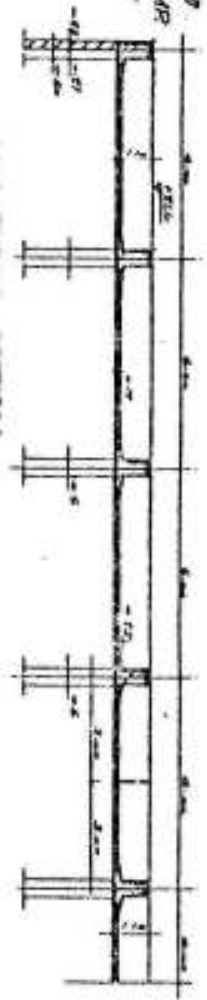
**FIG. VIII-8**

**N.B. COVER CORRUPTED SHEETS.**  
**MADE IN CONCRETE WITH WEIGHT 25 kg.**  
**25.6**



ABULKER FERTILIZERS AND  
 CHEMICAL INDUSTRIES CORP  
 BULK UREA STORAGE  
 1978

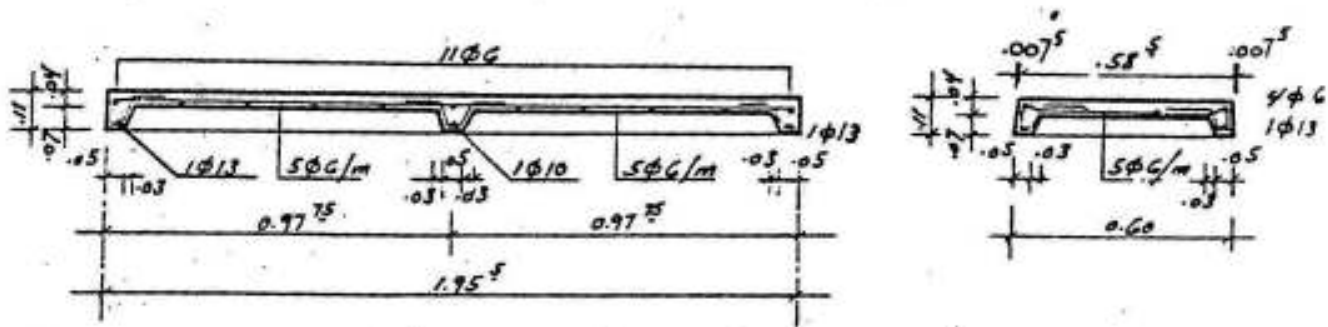
LONGITUDINAL SECTION



CONCRETE DIMENSIONS & END GABLE

DETAILS OF MAIN FRAME

Fig. VIII-9



a) REINFORCED CONCRETE PRECAST SLABS.

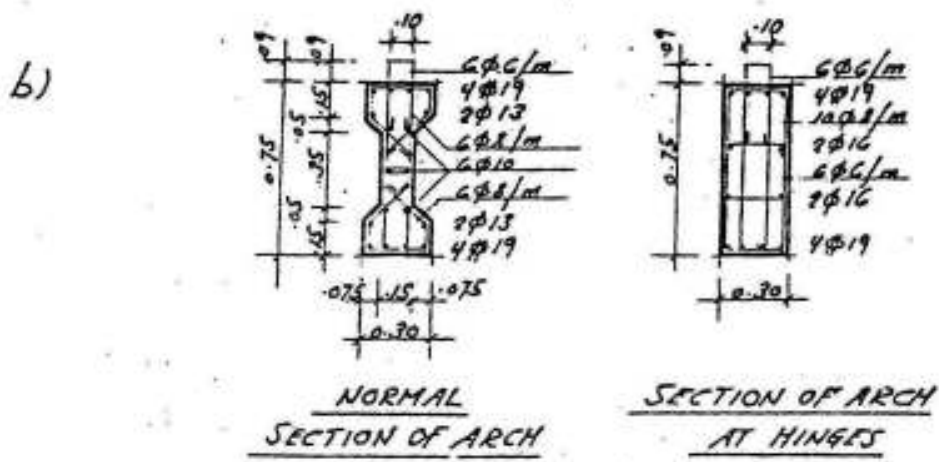
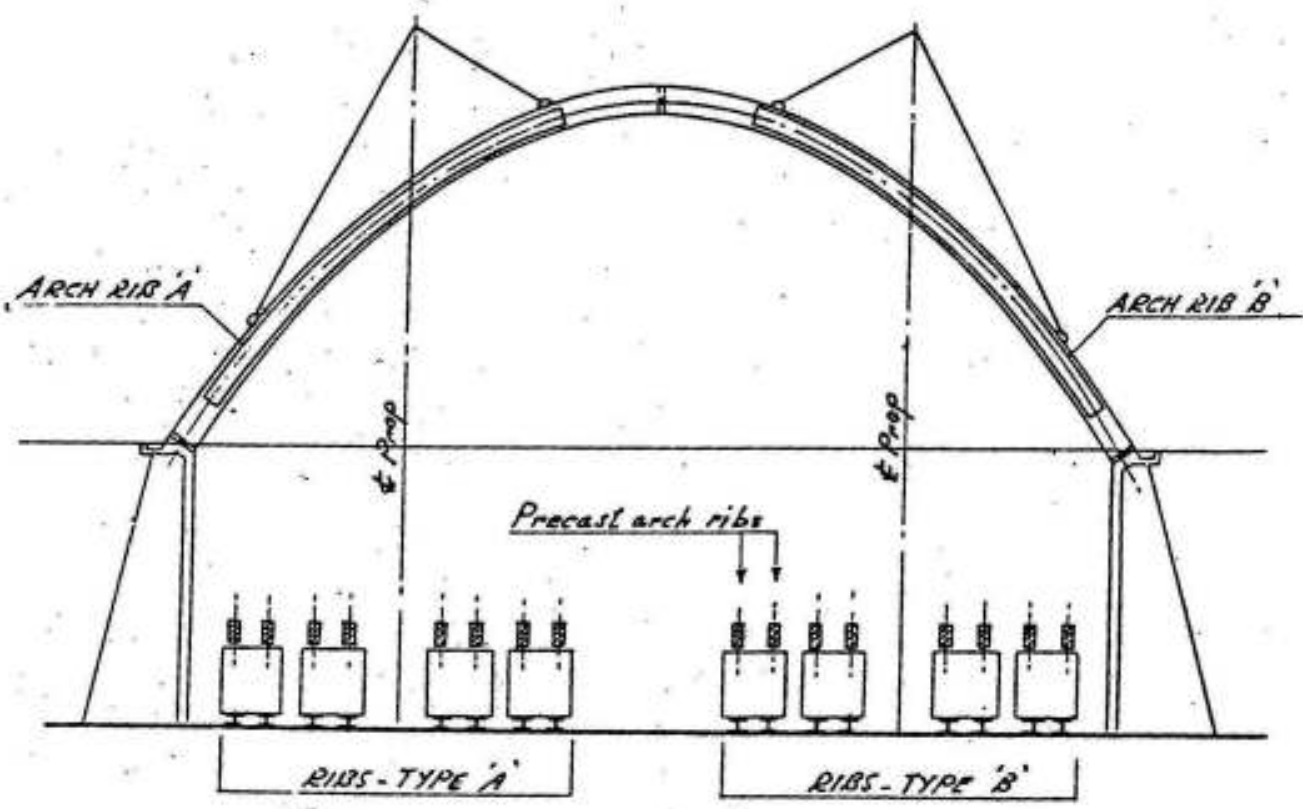
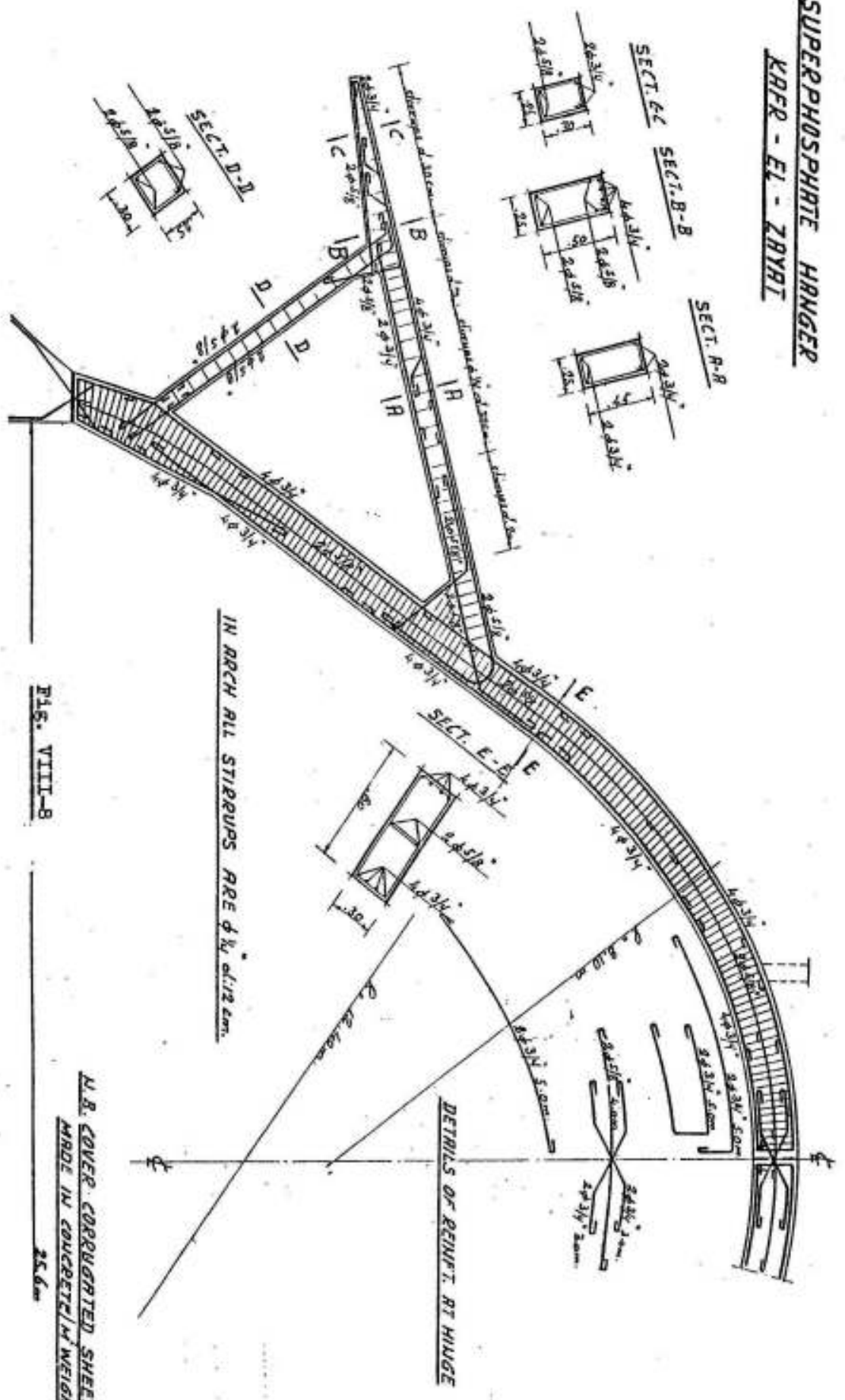


FIG. VIII-7

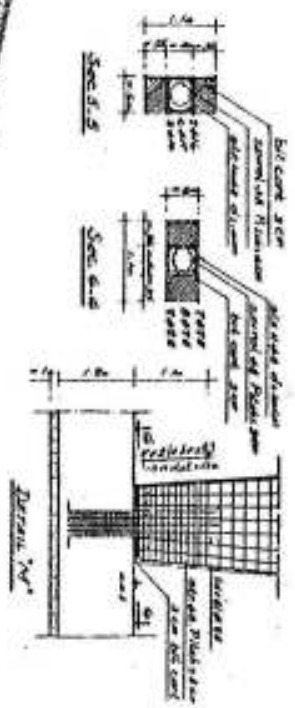
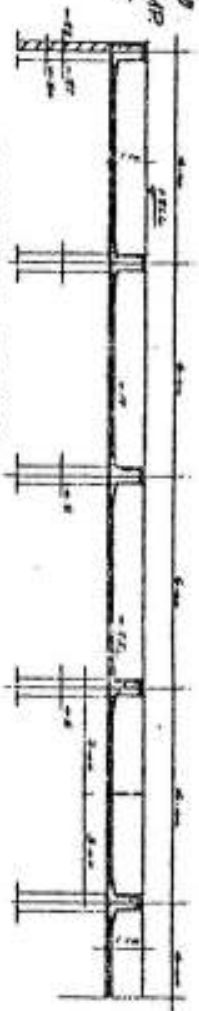
**SUPERPHOSPHATE HRNGER**  
**KRRR - E1 - ZBYRT**



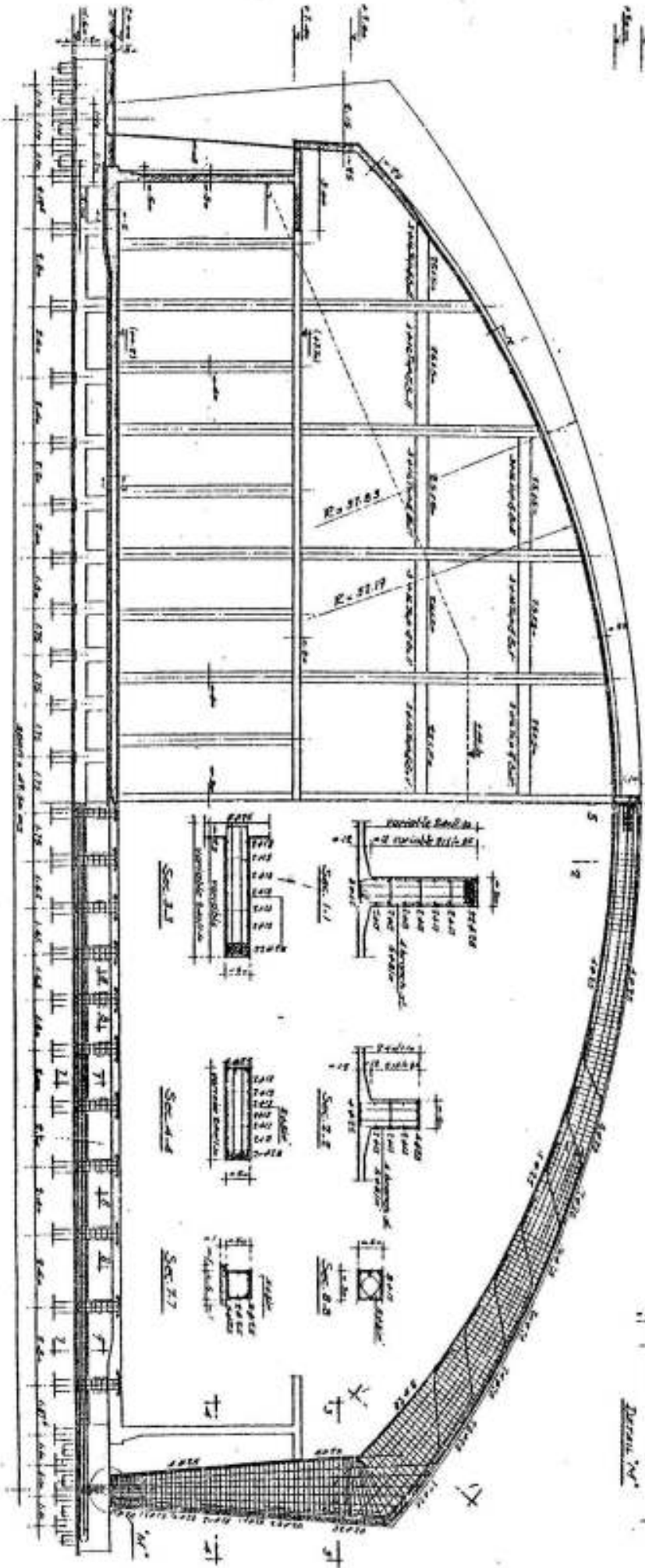
**PLS. VIII-8**

ABULKIR FERTILIZERS AND  
 CHEMICAL INDUSTRIES CAMP  
 BULK UREA STORAGE  
 1978

LONGITUDINAL SECTION



CONCRETE DIMENSIONS & END GABLE



DETAILS OF MAIN FRAME

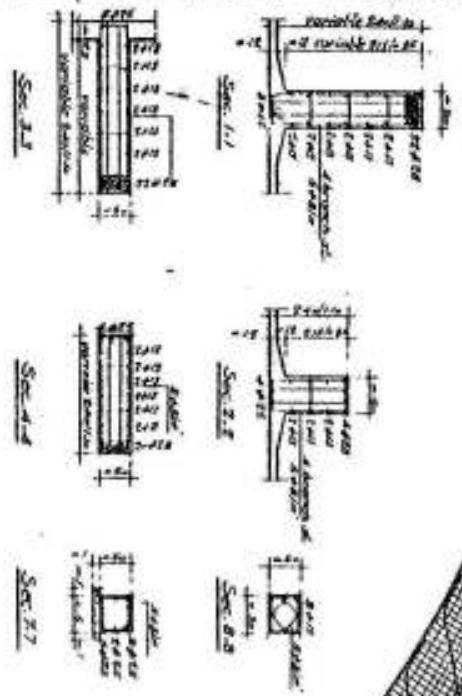


Fig. DIM-9

b) Two Hinged Arches

A two hinged arch is once statically indeterminate. Choosing the simple girder with a hinge at a and a roller at b as main system, then the equation of elasticity is : (Fig VIII-10).

$$\delta = 0 = \delta_0 + H\delta_1$$

and

$$H = - \frac{\delta_0}{\delta_1}$$

Due to  $H = 1$ , we have:

$$M_1 = -1 \cdot y$$

$$N_1 = 1 \cdot \cos \varphi$$

$$Q_1 = -1 \cdot \sin \varphi$$

According to theory of virtual work, we have:

$$\delta_0 = - \int \frac{M_0 y ds}{EI} + \int \frac{N_0 \cos \varphi ds}{EA} - \int \frac{Q_0 \sin \varphi ds}{GA'}$$

and

$$\delta_1 = \int \frac{y^2 ds}{EI} + \int \frac{\cos^2 \varphi ds}{EA} + \int \frac{\sin^2 \varphi ds}{GA'}$$

In these equations, we have:

1) The elastic deformation due to shear stresses is generally small compared to that due to normal stresses so that  $\int \frac{Q_0 \sin \varphi ds}{GA'}$  may

be neglected without making an appreciable error.

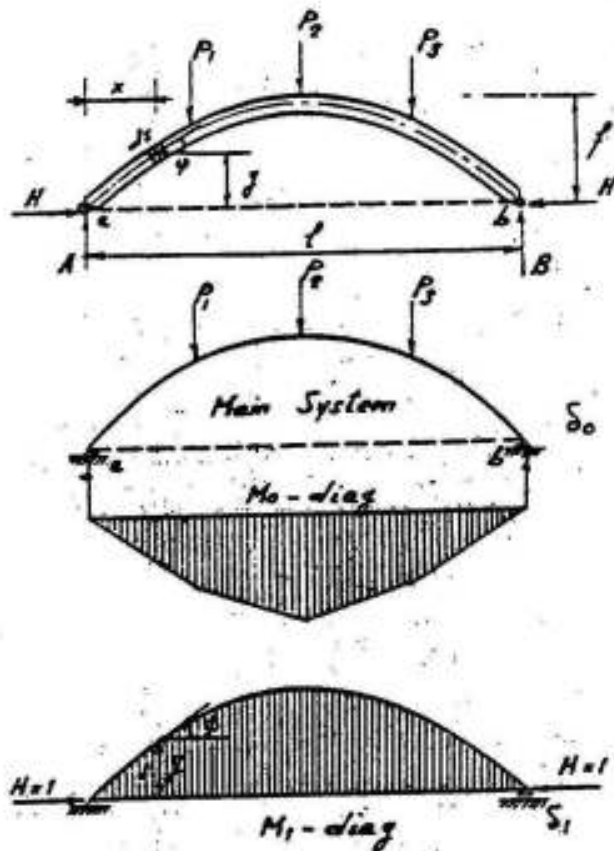


Fig. VIII-10

2) The normal force  $N_x$  in any section of a two hinged arch subject to vertical loads only can be calculated from the relation:

$$N_x \cos \varphi = H \quad \text{i.e.} \quad N_x = H / \cos \varphi$$

But  $N_x = N_0 + H \cos \varphi$

Therefore  $H / \cos \varphi = N_0 + H \cos \varphi$

or  $H = N_0 \cos \varphi + H \cos^2 \varphi$

For flat arches  $\cos^2 \varphi \approx 1$  and accordingly  $N_0 \cos \varphi \approx 0$

3) It is known that  $G = \frac{E}{2(1 + \nu)}$  in which

$\nu =$  Poissons ratio  $\approx 0.2$  for reinforced concrete

So that  $G \approx 0.4E$ , and

$A' = \frac{5}{6} A$  for rectangular sections ; hence

$$GA' \approx \frac{1}{3} EA$$

4) As  $\cos^2 \varphi = 1 - \sin^2 \varphi$ , we get

$$\int \frac{\cos^2 \varphi ds}{EA} + \int \frac{\sin^2 \varphi ds}{GA'} = \int (1 - \sin^2 \varphi) \frac{ds}{EA} + \int 3 \frac{\sin^2 \varphi ds}{EA}$$

$$= \int \frac{ds}{EA} + 2 \int \frac{\sin^2 \varphi ds}{EA} \approx \int \frac{ds}{EA}$$

The second term has been neglected because in flat arches  $\varphi$  is small and  $\sin^2 \varphi$  is a very small value.

Accordingly, in normal cases, it is sufficiently accurate to assume that:

$$\delta_0 = - \int \frac{M_0 y ds}{EI}$$

$$\delta_1 = \int \frac{y^2 ds}{EI} + \int \frac{ds}{EA}$$

and

$$H = \frac{\int \frac{M_o y ds}{I}}{\int \frac{y^2 ds}{I} + \int \frac{ds}{A}}$$

Due to an increase  $\Delta l$  of the span , we get

$$H_{\Delta l} = - \frac{E \cdot \Delta l}{\int \frac{y^2 ds}{I} + \int \frac{ds}{A}}$$

and due to a temperature increase of  $t^{\circ}$  , we get

$$H_t = \frac{E \alpha t l}{\int \frac{y^2 ds}{I} + \int \frac{ds}{A}}$$

### Symmetrical Parabolic Two Hinged Arches

The axis of a symmetrical parabolic arch is given by the equation:

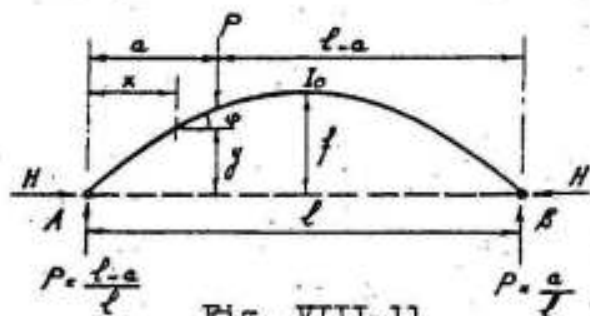
$$y = \frac{4f}{l^2} \cdot x \cdot (l - x)$$

If the moment of inertia  $I$  and the area  $A$  of any section are chosen such that

$$I \cos \varphi = I_o \quad \text{and} \quad A \cos \varphi = A_o$$

where  $I_o$  and  $A_o$  are the moment of inertia and the area of the cross-section at the crown, the integrals in the equations of  $H$  can be mathematically evaluated as follow : (Fig VIII-11).

For a concentrated load  $P$  acting at a distance "a" from the left support, we get:



$$\begin{aligned}
\int \frac{M_o \cdot y \cdot ds}{I} &= \int \frac{M_o \cdot y \cdot \cos \psi \cdot ds}{I \cdot \cos \psi} = \frac{1}{I_o} \int M_o \cdot y \cdot dx \\
&= \frac{1}{I_o} \int_0^a \frac{P(1-a)}{l} \cdot x \cdot \frac{4f}{l^2} \cdot x \cdot (1-x) \\
&+ \frac{1}{I_o} \int_a^l \frac{P \cdot a}{l} (1-x) \cdot \frac{4f}{l^2} \cdot x (1-x) \cdot dx \\
&= \frac{1}{I_o} \cdot \frac{f}{3l^2} \cdot P \cdot a (1-a) (l^2 + la - a^2)
\end{aligned}$$

Further

$$\int \frac{y^2 \cdot ds}{I} = \int_0^l \frac{y^2 \cdot \cos \psi \cdot ds}{I \cos \psi} = \frac{1}{I_o} \int_0^l \frac{16f^2}{l^4} \cdot x^2 (1-x)^2 \cdot dx = \frac{8f^2 \cdot l}{15 I_o}$$

and

$$\int \frac{ds}{A} = \int_0^l \frac{ds \cos \psi}{A \cos \psi} = \frac{1}{A_o} \int_0^l dx = \frac{l}{A_o}$$

So that, for a series of concentrated loads  $P$ , we get:

$$H = \frac{5 \sum_0^l P \cdot a (1-a) (l^2 + la - a^2)}{8f \cdot l^3 \left( 1 + \frac{15 I_o}{8A_o f^2} \right)}$$

in which

$\frac{15 I_o}{8A_o f^2} = \epsilon$  is a correction factor due to the elastic deformation of

the normal force; for a rectangular section of breadth  $b$  and depth  $t$  we have:

$$I_o = bt^3/12 \quad , \quad A_o = bt \quad \text{and} \quad \epsilon = 0.155 t^2/f^2$$



Therefore

$$H = \frac{5 \sum_0^l P \cdot a (1-a) (l^2 + la - a^2)}{8f^3 (1+\epsilon)}$$

This equation can be used for determining the ordinates of the influence line of H if P is assumed equal to 1 and acts at a series of distances a.

For an increase  $\Delta l$  of span l, we have:

$$H_{\Delta l} = \frac{-15 E \cdot I_o \cdot \Delta l}{8f^2 \cdot l (1+\epsilon)} \approx \frac{15 E \cdot I_o \cdot \Delta l}{8f^2 l}$$

whereas for a temperature increase of  $t^o$ , we get:

$$H_t = \frac{15 E \cdot I_o \cdot \alpha \cdot t}{8f^2 (1+\epsilon)} \approx \frac{15 E \cdot I_o \cdot \alpha \cdot t}{8f^2}$$

For a uniform load g acting over the whole span, we get:

$$H_g = \frac{g l^2}{8f (1+\epsilon)}$$

Assuming  $\frac{1}{1+\epsilon} = k$ , then

$$H_g = k \frac{g l^2}{8f}$$

For different values of t/f, the magnitude of  $\epsilon$  and k are accordingly as follows:

t/f	$\epsilon$	k
0.2	0.0062	0.994
0.3	0.014	0.986
0.4	0.025	0.976

Fig VIII-12 shows the general layout of a two hinged arch 55 ms span and 28.7 ms high used as the main supporting element of an airplane Hangar.

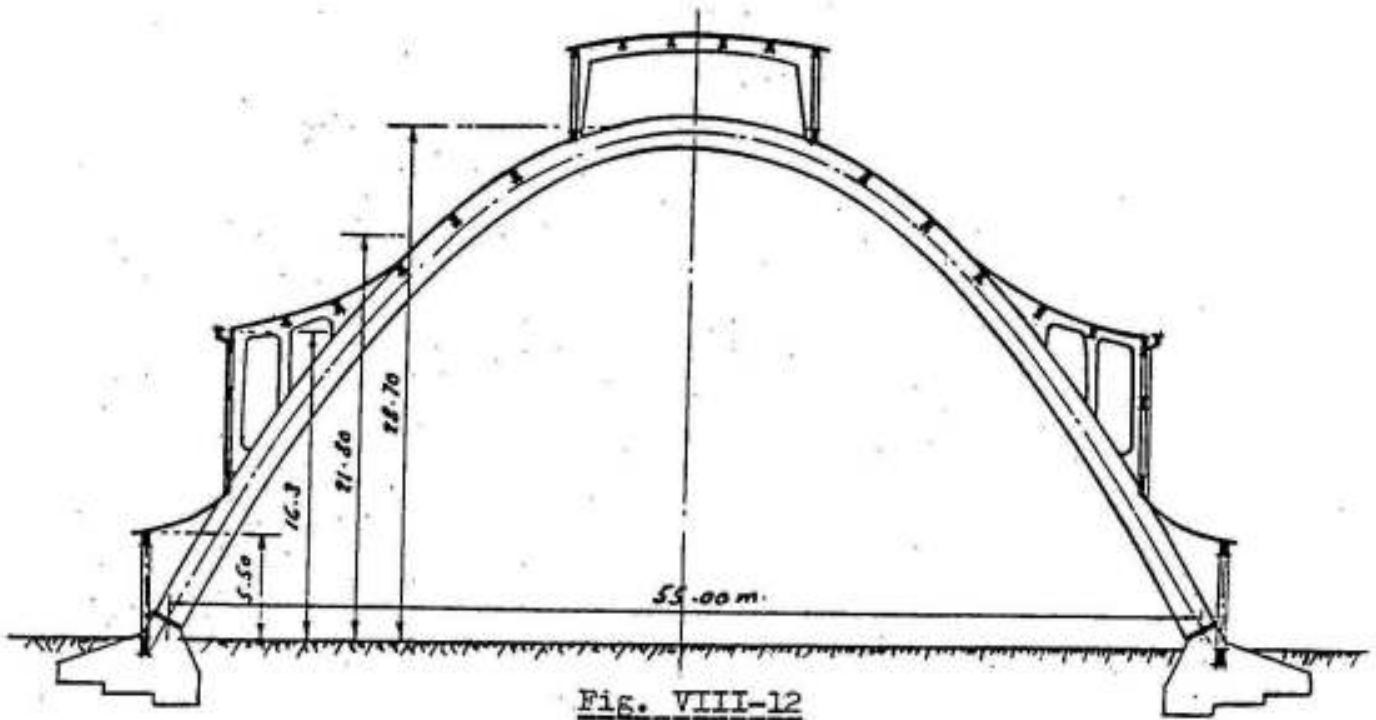


Fig. VIII-12

Fig VIII-13 shows the general layout, concrete dimensions and details of reinforcements of a two hinged arch used as the main supporting element for one of the halls in the Copper Factory at Alexandria. It has to be noticed here that the slabs are so arranged that the hall has sufficient light, and that the cantilever arms supporting the crane girders are smoothly connected to the arch in such a way that the bending moments transmitted to the arch are easily resisted. The reinforcements are arranged with staggered splices and such that not more than 20% of the reinforcement bars are spliced in any section.

c-Two Hinged Arch with a Tie

This system is externally statically determinate and internally once statically indeterminate. The main system is chosen by cutting the tie. The equation

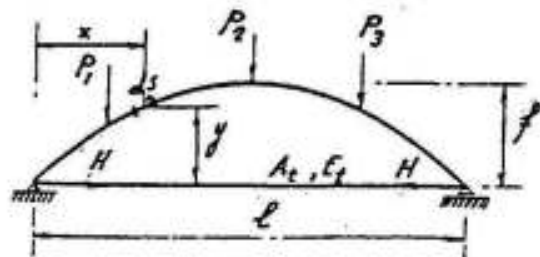
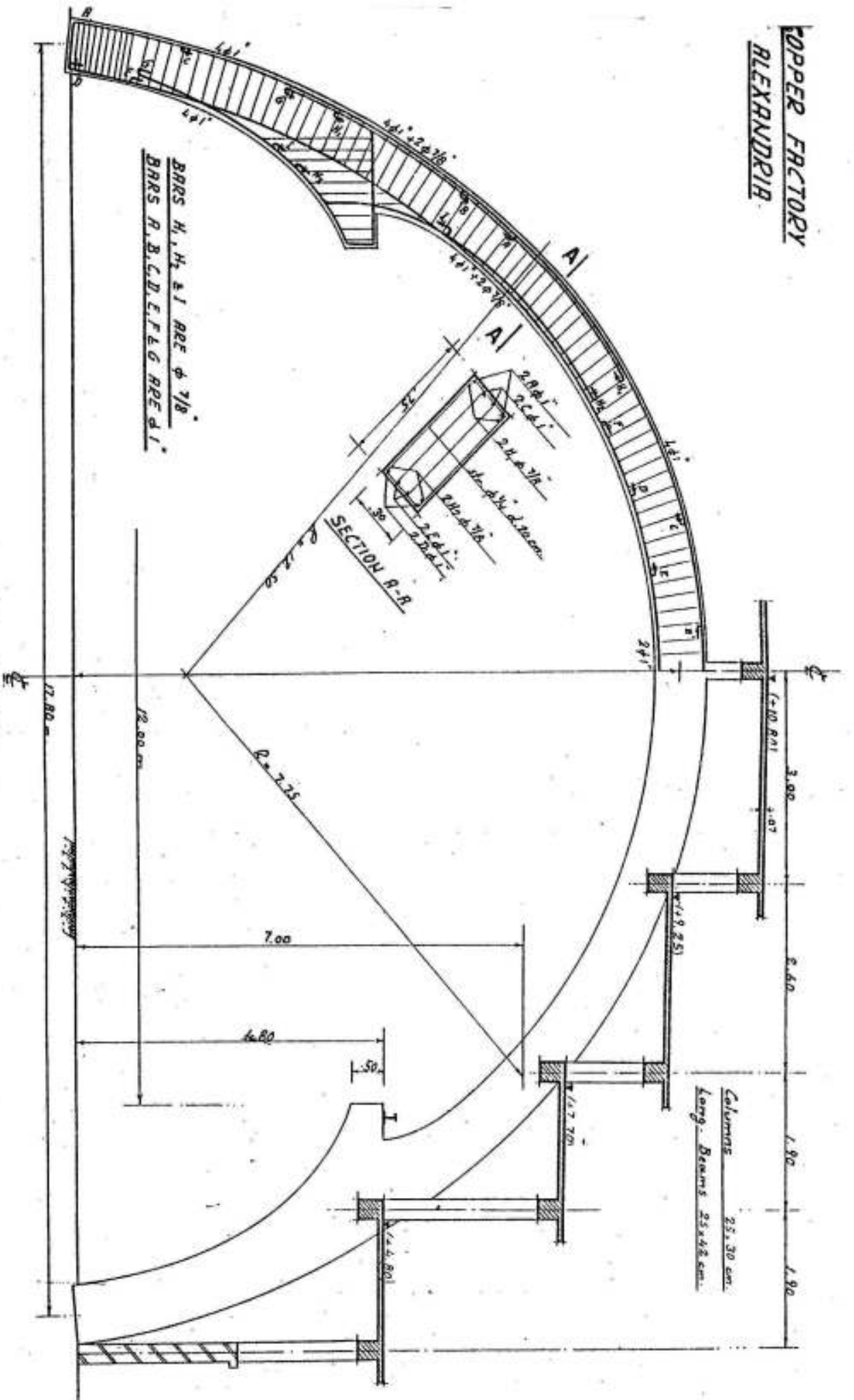


Fig. VIII-14

**COPPER FACTORY**  
**ALEXANDRIA**



**FIG. VIII-13**

of elasticity is given by: Fig VIII-14.

$$\delta = - \frac{Hl}{A_t E_t} = \delta_o + H\delta_1$$

so that  $H = - \frac{\delta_o}{\delta_1 + \frac{l}{A_t E_t}}$

Proceeding in the same way as in the previous case we get:

$$H = \frac{\int \frac{M_o y ds}{EI}}{\int \frac{M_1^2 ds}{EI} + \int \frac{ds}{EA} + \frac{l}{A_t E_t}}$$

For a symmetrical parabolic arch with  $I \cos \psi = I_o$  and  $A \cos \psi = A_o$  subject to a series of concentrated loads  $P$ , we get:

$$H = \frac{\frac{1}{6} \sum P \cdot a (1-a) (l^2 + la - a^2)}{8fl^3 (1 + \epsilon) + \frac{15I_o}{f} \cdot \frac{l^3}{A_t} \cdot \frac{E}{E_t}}$$

For a uniform load  $g$ , we get:

$$H = \frac{gl^2}{8f (1 + \epsilon + \frac{15 I_o E}{f^2 A_t E_t})}$$

Assuming that the section of the arch is rectangular with breadth  $b$  and depth  $t$  then  $I_o = \frac{bt^3}{12}$  and as  $\frac{E}{E_t} = \frac{1}{10}$  then,

$$\frac{15 I_o E}{f^2 A_t E_t} = \frac{bt^3}{80f^2 A_t} = \epsilon'$$

$\epsilon'$  is a factor expressing the effect of the elongation of the tie .  
Therefore

$$H = \frac{El^2}{8f(1 + \epsilon + \epsilon')}$$

Assuming  $\frac{1}{1 + \epsilon + \epsilon'} = k'$  , we can write

$$H = k' \frac{El^2}{8f}$$

For an arch with  $b = 30$  cms,  $t = 80$  cms,  $f = 3.00$  ms and 12  $\Phi$  25 mm in the tie ( $A_t = 60$  cm<sup>2</sup>) we get:

$$\epsilon = \frac{0.155 t^2}{f^2} = \frac{0.155 \times 80^2}{300^2} = 0.011$$

$$\epsilon' = \frac{bt^3}{80f^2 A_t} = \frac{30 \times 80^3}{80 \times 300^2 \times 60} = 0.0356$$

$$k' = \frac{1}{1 + \epsilon + \epsilon'} = \frac{1}{1.0466} = 0.956$$

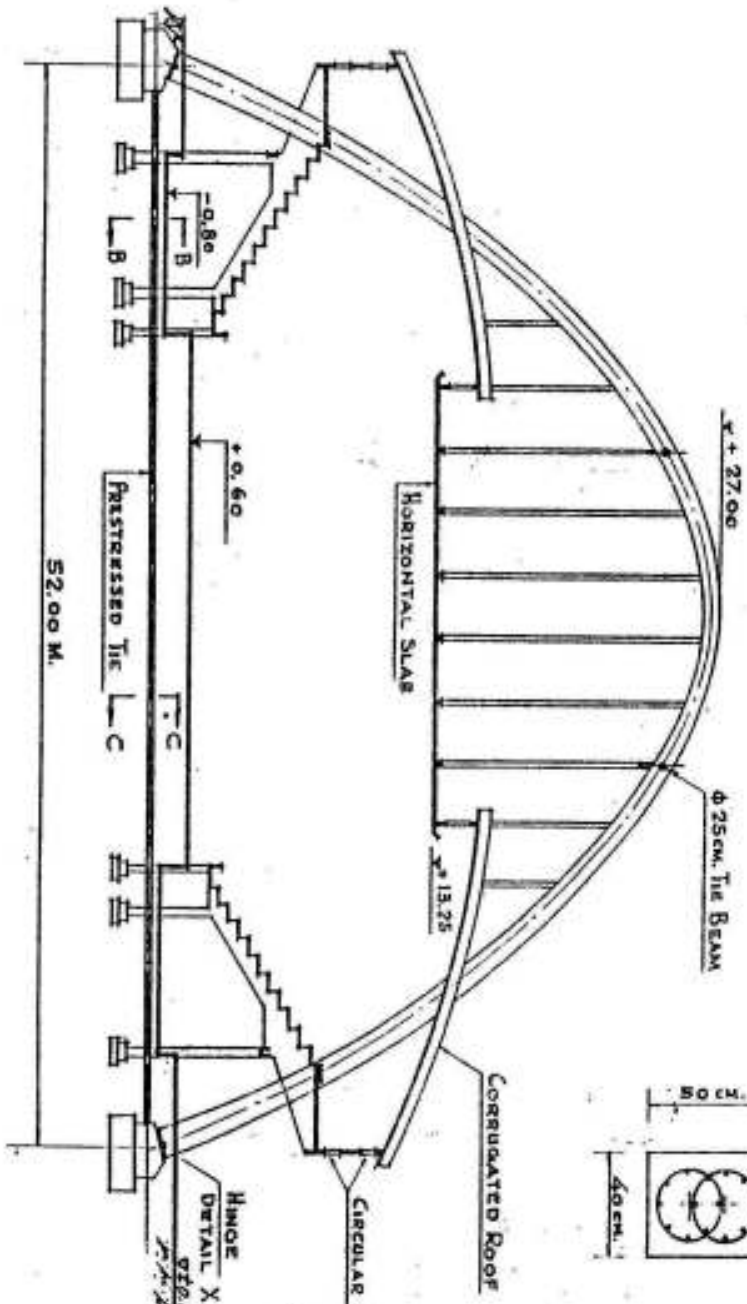
So that  $H = 0.956 \frac{El^2}{8f}$

This means that the horizontal thrust of a two-hinged arch with a tie is generally 4 to 5 % smaller than that of the corresponding three-hinged arch. The bending moment at the crown is therefore:

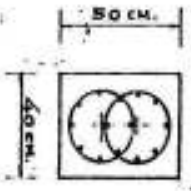
$$M = 0.04 \text{ to } 0.05 \frac{El^2}{8}$$

The parabolic arch shown in figure IV-3 gives a typical example for this system. The polygonal frame shown in the same figure gives another example in which the corners of the polygon coincide on the line of pressure of the loads. The slabs are arranged in the middle

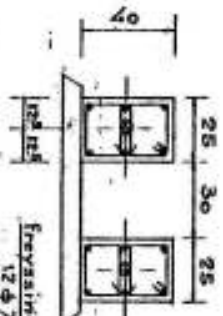
CROSS SECTION



SECTION A-A



SECTION B-B



SECTION C-C

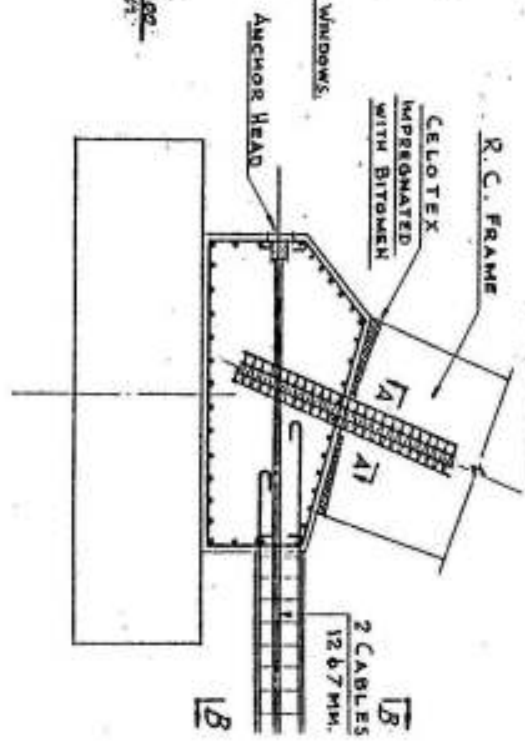
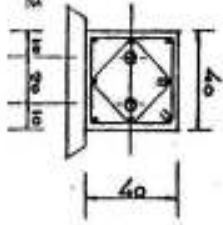


FIG. VIII-15

FACULTY OF POLICE  
COVERED GYMNASIUM 1964

third at the level of the arch and at the outside thirds at the level of the tie. Such an arrangement is well adapted to halls containing smoke or fumes. The cross ventilation between the upper windows do not allow the fumes to accumulate inside the hall.

Figures VII-21 and VII-22 give the general layout and details of reinforcements of the main workshops of "El Nasr Forging Plant" at Helwan in which arched girders with ties were used as the main supporting element for the saw-tooth roof.

Figure VIII-15 gives the general layout of the "Covered Gymnasium" at the Faculty of Police, El Nasr City Cairo. The roof is flat at the middle part of the hall and is composed of curved inverted shells on the two sides, all are hung to the arched girders as shown. The tie between the footings of the main arches is post-tensioned by two Freyssinet cables  $12 \phi 7$  mm each.

d) Two Hinged Arch with Polygonal Tie

Two hinged arches with parabolic ties as shown in figure VIII-16 may be used in roof structures as well as in bridges.

The statically indeterminate value is the horizontal component  $H$  of the forces in the tie.

The horizontal thrust  $H$  due to a series of concentrated loads  $P$  is given by:

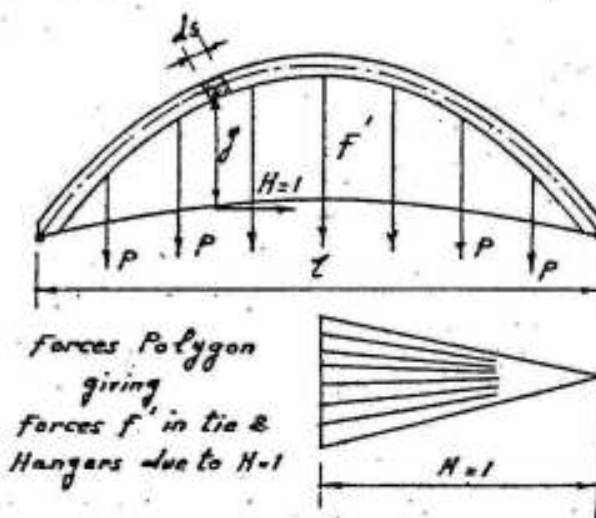


Fig. VIII-16

$$H = \frac{\sum_h \frac{F_o \cdot F' \cdot s}{E_h A_h} + \int \frac{M_o \cdot y \cdot ds}{EI}}{\sum_t \frac{F_t^2 \cdot s}{E_t A_t} + \sum_h \frac{F_h^2 \cdot s}{E_h A_h} + \int \frac{y^2 \cdot ds}{EI} + \int \frac{ds}{EA}}$$

in which

$\sum_h, \sum_t$  = sum of forces in hangers and tie respectively

$E_h, E_t$  = modulus of elasticity of hangers and tie respectively, generally =  $E_s$

- $A_h, A_t$  = effective area of cross-section of hangers and tie respectively, generally equal to the area of steel in the member.
- $F_o$  = forces in hangers due to loading  $P$  and are equal to  $P$  if the loads act at the level of the tie and are equal to zero if the loads act on the arch.
- $F'$  = forces in tie and hangers due to  $H = 1$  and can be determined from the force polygon shown in figure VIII-16.
- $s$  = length of any of the hangers or elements of the tie

e) Fixed Arches

A fixed arch is three times statically indeterminate. It can be treated in the same way as fixed frames. Choosing the simple cantilever as main system and applying the statically indeterminate values,  $H$ ,  $V$  and  $M$  in the elastic center  $O$ , we get: (Fig VIII-17).

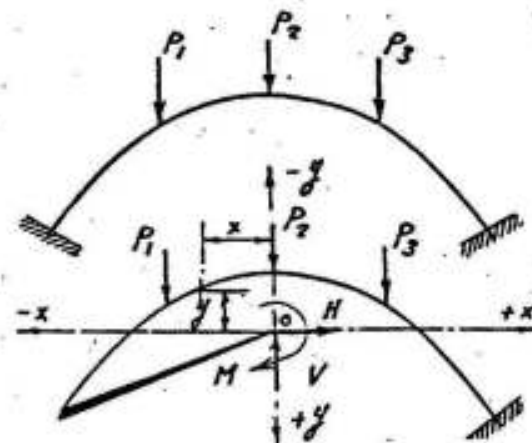


Fig. VIII-17

$$H = - \frac{\int \frac{M_o y ds}{I}}{\int \frac{y^2 ds}{I} + \int \frac{ds}{A}} \quad V = - \frac{\int \frac{M_o x ds}{I}}{\int \frac{x^2 ds}{I}} \quad M = - \frac{\int \frac{M_o ds}{I}}{\int \frac{ds}{I}}$$

The bending moment in any section can be determined by superposition; thus

$$M = M_o + H y + V x + M$$

Due to a change of temperature of  $t^o$ , we get only the reaction:

$$H_t = \frac{E \alpha t l}{\int \frac{y^2 ds}{I} + \int \frac{ds}{A}}$$

This force acts at the level of the  $x$  - axis as shown in figure VIII-18.

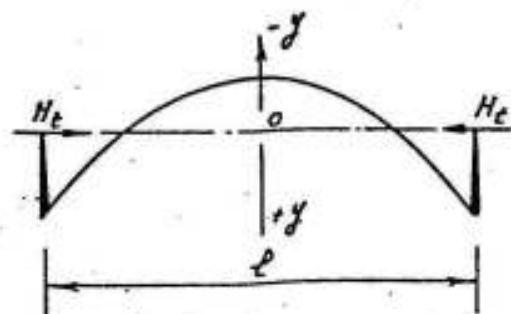


Fig. VIII-18



Fixed arches or frames are to be used only if they are constructed on firm soils and the foundations are chosen such that they do not allow any displacement or rotation of the supports. Such displacements as well as temperature changes and shrinkage cause relatively high internal stresses and hence must be considered in the design. It is recommended to take all possible means to reduce the shrinkage stresses. For this purpose, a key ca 30 cms wide is concreted only when most of the shrinkage of the arch has taken place (say after 3 weeks).

f) Continuous Arches

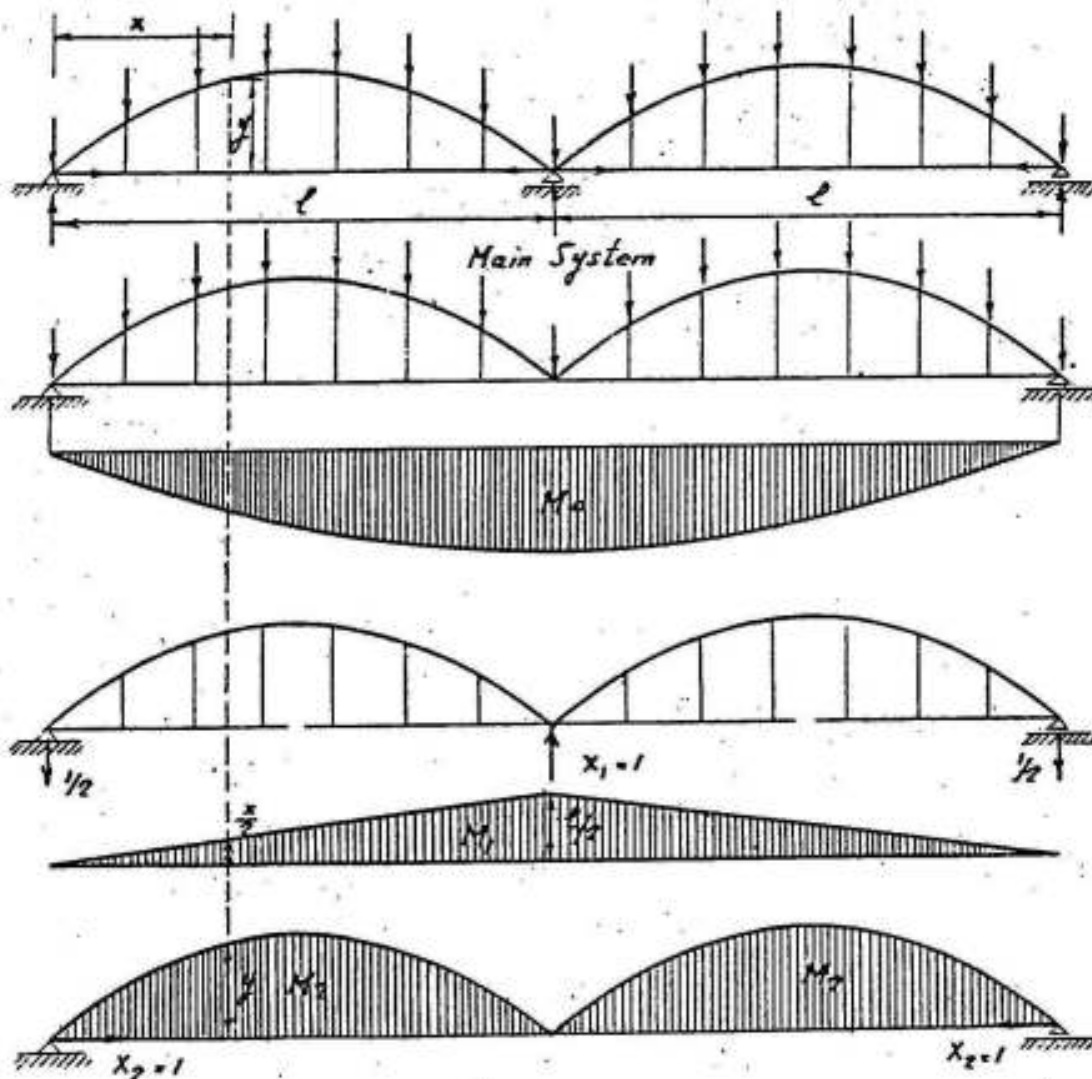


Fig. VIII-19

A symmetrical continuous arch with a tie symmetrically loaded as shown in figure VIII-19 is twice statically indeterminate. The main system may be chosen by removing the intermediate support and cutting the ties. The statically indeterminate values are  $X_1$  and  $X_2$ . The equations of elasticity are:

$$1) \delta_1 = 0 = \delta_{10} + X_1 \delta_{11} + X_2 \delta_{12}$$

$$2) \delta_2 = -\frac{2X_2 l}{A_t E_t} = \delta_{20} + X_1 \delta_{21} + X_2 \delta_{22}$$

Neglecting the elastic deformations due to the normal and shearing forces, we get:

$$1) E \delta_{10} = \int M_0 M_1 \frac{ds}{I} = 2 \int_0^l M_0 M_1 \frac{ds}{I} = 2 \int_0^l M_0 \left(-\frac{x}{2}\right) \frac{ds}{I} = - \int_0^l M_0 x \frac{ds}{I}$$

$$2) E \delta_{11} = \int M_1^2 \frac{ds}{I} = 2 \int_0^l \left(-\frac{x}{2}\right)^2 \frac{ds}{I} = \frac{1}{2} \int_0^l x^2 \frac{ds}{I}$$

$$3) E \delta_{12} = E \delta_{21} = 2 \int_0^l M_1 M_2 \frac{ds}{I} = 2 \int_0^l \left(-\frac{x}{2}\right)(-y) \frac{ds}{I} = \int_0^l xy \frac{ds}{I}$$

$$4) E \delta_{20} = \int M_0 M_2 \frac{ds}{I} = 2 \int_0^l M_0 (-y) \frac{ds}{I} = -2 \int_0^l M_0 y \frac{ds}{I}$$

$$5) E \delta_{22} = \int M_2^2 \frac{ds}{I} = 2 \int_0^l (-y)^2 \frac{ds}{I} = 2 \int_0^l y^2 \frac{ds}{I}$$

For a continuous parabolic arch with  $I \cos \varphi = I_0$  and subject to uniform load  $p/m'$ , we get:

$$y = 4 \frac{fx}{l^2} (l - x)$$

and

$$M_0 = p \frac{x}{2} (2l - x)$$

So that

$$\begin{aligned} E \delta_{10} &= - \int_0^l M_0 x \frac{ds}{I} = - \int_0^l M_0 x \frac{ds \cos \varphi}{I \cos \varphi} = - \frac{1}{I_0} \int_0^l M_0 x dx \\ &= - \frac{1}{I_0} \int_0^l p \frac{x^2}{2} (2l - x) dx = - \frac{5pl^4}{24I_0} \end{aligned}$$

$$E\delta_{11} = \frac{1}{2} \int_0^l x^2 \frac{ds}{I} = \frac{1}{2} \int_0^l x^2 \frac{ds \cos \psi}{I \cos \psi} = \frac{1}{2I_0} \int_0^l x^2 dx = \frac{l^3}{6I_0}$$

$$E\delta_{12} = \int_0^l xy \frac{ds}{I} = \int_0^l xy \frac{ds \cos \psi}{I \cos \psi} = \frac{1}{I_0} \int_0^l xy dx$$

$$= \frac{1}{I_0} \int_0^l 4f \frac{x^2}{l^2} (1-x) dx = \frac{fl^2}{3I_0}$$

$$E\delta_{20} = -2 \int_0^l M_{0y} \frac{ds}{I} = -2 \int_0^l M_{0y} \frac{ds \cos \psi}{I \cos \psi} = -\frac{2}{I_0} \int_0^l M_{0y} dx$$

$$= -\frac{2}{I_0} \int_0^l p \frac{x}{2} (2l-x) \cdot 4f \frac{x}{l^2} (1-x) dx$$

$$= -\frac{4pf}{I_0 l^2} \int_0^l (2l^2 x^2 - 3l x^3 + x^4) dx = -\frac{7pfl^3}{15 I_0}$$

$$E\delta_{22} = 2 \int_0^l y^2 \frac{ds}{I} = 2 \int_0^l y^2 \frac{ds \cos \psi}{I \cos \psi} = \frac{2}{I_0} \int_0^l y^2 dx$$

$$= \frac{2}{I_0} \int_0^l 16 \frac{f^2}{l^4} x^2 (1-x)^2 dx = \frac{32f^2}{I_0 l^4} \int_0^l x^2 (1-x)^2 dx = \frac{16f^2 l}{15 I_0}$$

Substituting these values in the equations of elasticity we get:

$$1) \quad 0 = -\frac{5pl^4}{24 I_0} + x_1 \cdot \frac{l^3}{6I_0} + x_2 \cdot \frac{fl^2}{3I_0}$$

$$2) \quad \frac{-2x_2 l E}{A_t E_t} = -\frac{7pfl^3}{15 I_0} + x_1 \cdot \frac{fl^2}{3I_0} + x_2 \cdot \frac{16f^2 l}{15 I_0}$$

These two equations give:

$$x_2 = \frac{pl^2}{8f \left( 1 + \frac{5E I_0}{f^2 A_t E_t} \right)}$$

Assuming  $\frac{5E I_o}{f^2 A_t E_t} = \mu$  and  $\frac{1}{1 + \mu} = k$ , then

$$X_2 = \frac{Pl^2}{8f(1 + \mu)} = k \frac{Pl^2}{8f} \quad \text{and}$$

$$X_1 = \frac{Pl}{4} \cdot \frac{4 + 5\mu}{1 + \mu} = \frac{(5 - k)}{4} Pl$$

Example:

Parabolic arch, continuous over two spans 24 ms each, rise 3.0 m  
 cross-section of arch at crown 30 x 80 cms, reinforcement of tie  
 12  $\phi$  25 mm ( $A_t = 60 \text{ cm}^2$ ),  $E = 210 \text{ t/cm}^2$ ,  $E_t = 2100 \text{ t/cm}^2$  and load  
 $p = 5 \text{ t/m}$ .

$$\mu = \frac{5 I_o}{f^2 A_t} \cdot \frac{E}{E_t} = \frac{5 \times 30 \times 80^3}{12 \times 300^2 \times 60} \cdot \frac{1}{10} = 0.12$$

$$k = \frac{1}{1 + \mu} = \frac{1}{1.12} \approx 0.9$$

$$X_2 = k \frac{Pl^2}{8f} = 0.9 \frac{5 \times 24^2}{8 \times 3} = 0.9 \times 120 = 108 \text{ ton}$$

$$X_1 = \frac{(5 - k)}{4} Pl = \frac{(5 - 0.9)}{4} 5 \times 24 = 1.025 \times 120 = 123 \text{ ton}$$

Reaction at outside supports:

$$A = B = \frac{1}{2} (5 \times 48 - 123) = \frac{117}{2} = 58.5 \text{ ton}$$

Maximum bending moment  $M_m$  at crown:

$$M_m = A \cdot \frac{l}{2} - \frac{Pl^2}{8} - X_2 f = \frac{58.5 \times 24}{2} - \frac{5 \times 24^2}{8} - 108 \times 3 = 18 \text{ mt}$$

Maximum bending moment  $M_s$  at intermediate support:

$$M_s = A \cdot l - \frac{Pl^2}{2} = 58.5 \times 24 - \frac{5 \times 24^2}{2} = -36 \text{ mt}$$

For preliminary calculations, one may assume here also that the maximum bending moment  $M_m$  at the crown and the maximum bending moment  $M_s$  at the support are given by:

$$M_m \approx 0.05 \frac{Pl^2}{8}$$

$$M_s \approx -0.10 \frac{Pl^2}{8}$$

Applying these two equations on our example, we find that:

$$M_m = 0.05 \times \frac{5 \times 24^2}{8} = 18 \text{ mt}$$

and

$$M_s = -0.10 \times \frac{5 \times 24^2}{8} = -36 \text{ mt}$$

Tables of Internal Forces in Two Hinged and Fixed Parabolic Arches:

with  $I \cos \psi = I_0$

The axis of a parabolic arch fig. VIII-20 is given by:

$$y = \frac{4fx}{l^2} \cdot (l - x) \quad \text{or}$$

$$y = 4f\xi\xi' \quad \text{where } \xi = \frac{x}{l} \text{ and } \xi' = \frac{l-x}{l}$$

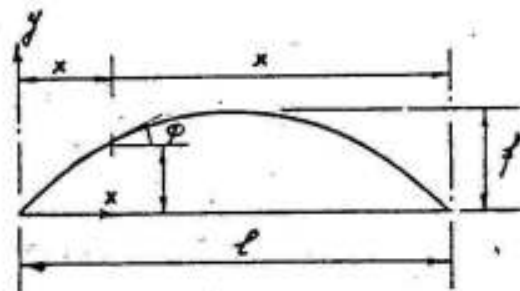


Fig. VIII-20

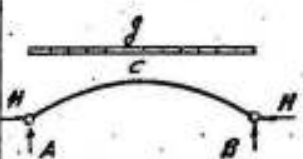
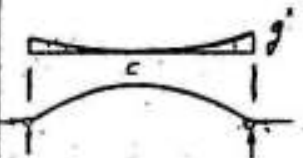
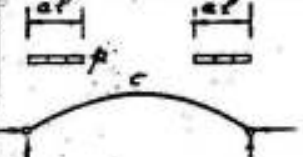
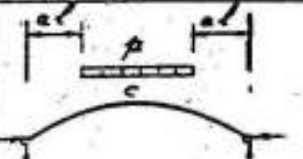
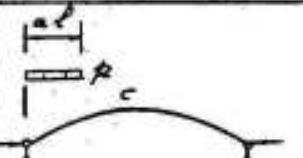
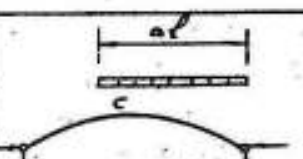
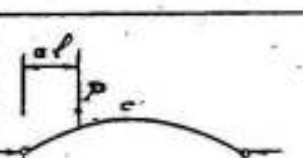
The length of the axis  $s$  for parabolic arches is approximately given by:

$$s = l \left( 1 + \frac{8}{3} \eta^2 \right) \quad \text{where } \eta = \frac{f}{l}$$

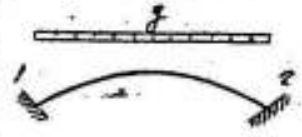
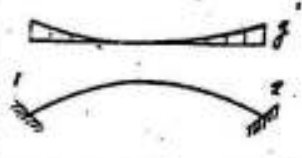
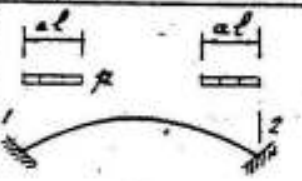
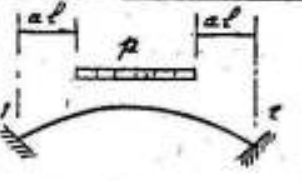

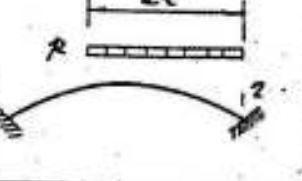
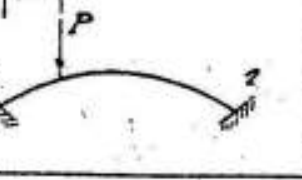
The following tables\* give the reactions and maximum moments in two hinged and fixed arches, they help much in the preliminary design.

\* "Design of Concrete Structures" by Winter, Urquhart, O'Rourke and Nilson, Published by McGraw-Hill Book Company. New York.

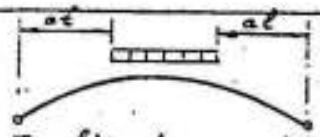
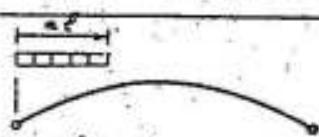
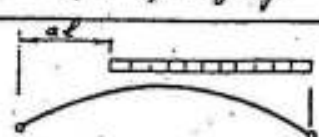


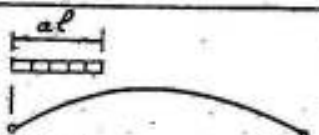
MOMENTS AND REACTIONS OF TWO HINGED PARABOLIC ARCHES

	$A = B = \frac{q l}{2}$ $M_c = 0$	$H = \frac{q l^2}{8 f}$ $M_{\frac{l}{4}} = 0$
	$A = B = \frac{q l}{6}$ $M_c = -\frac{q l^2}{336}$	$H = \frac{q l^2}{42 f}$ $M_{\frac{l}{4}} = \frac{q l^2}{252}$
	$A = B = p a l$ $M_c = \frac{p l^2}{8} a^2 (7a^3 - 5a^2 + 1)$	$H = \frac{p l^2}{8 f} a^2 (7a^3 - 5a^2 + 5)$
	$A = B = \frac{p l}{2} (1 - 2a)$ $M_c = \frac{p l^2}{8} a^2 (7a^3 - 5a^2 + 1)$	$H = \frac{p l^2}{8 f} (7a^5 - 5a^4 + 5a^2 - 1)$
	$A = \frac{p a l}{4} (1 - a) \quad B = \frac{p a^2 l}{2}$ <p>For <math>\frac{l}{4} \leq a l \leq \frac{l}{2}</math>:</p>	$H = \frac{p l^2}{16 f} a^2 (7a^3 - 5a^2 + 5)$ $M_{\frac{l}{4}} = \frac{p l^2}{64} (6a^5 - 15a^4 + 23a^2 - 16a + 2)$
	$A = \frac{p a^2 l}{2} \quad B = \frac{p a l}{2} (1 - a)$ <p>For <math>\frac{l}{2} \leq a l \leq \frac{3l}{4}</math>:</p>	$H = \frac{p l^2}{16 f} a^2 (7a^3 - 5a^2 + 5)$ $M_{\frac{l}{4}} = \frac{p l^2}{64} a^2 (6a^3 - 15a^2 + 7)$
	$A = P(1 - a) \quad B = P a$ $M_c = \frac{P l (1 - a)}{8} (-5a^3 + 10a^2 - 1)$	$H = \frac{5 P l}{8 f} a (a^3 - 7a^2 + 1)$
<p>Uniform temp. change of <math>t^\circ</math></p>	<p>Coeff. of linear expansion <math>\alpha</math></p> $M_c = \frac{-15 E I \alpha t}{8 f}$	$A = \frac{15 E I \alpha t}{8 f^2}$ $M_{\frac{l}{4}} = \frac{-45 E I \alpha t}{32 f}$

# MOMENTS AND REACTIONS OF FIXED PARABOLIC ARCHES

	$A = B = \frac{qL}{2}$ $M_1 = 0$	$H = \frac{qL^2}{8f}$ $M_2 = 0$
	$A = B = \frac{q'L}{6}$ $M_1 = -\frac{q'L^2}{210}$	$H = \frac{q'L^2}{56f}$ $M_2 = -\frac{q'L^2}{210}$
	$A = B = paL$ $M_1 = -\frac{pbL^2}{2} a^2 (1-a)(1-2a)$	$H = \frac{pbL^2}{4f} a^3 (6a^2 - 15a + 10)$ $M_2 = -\frac{pbL^2}{2} a^2 (1-a)(1-2a)$
	$A = B = \frac{pbL}{2} (1-2a)$ $M_1 = \frac{pbL^2}{2} a^2 (1-a)^2 (1-2a)$	$H = -\frac{pbL^2}{8f} (12a^5 - 30a^4 + 20a^3 - 1)$ $M_2 = \frac{pbL^2}{2} a^2 (1-a)^2 (1-2a)$
	$A = \frac{Pl}{2} a (a^3 - 2a^2 + 2)$ $M_1 = -\frac{Pl^2}{2} a^2 (1-a)^3$	$H = \frac{Pl^2}{8f} a^3 (6a^2 - 15a + 10)$ $M_2 = \frac{Pl^2}{2} a^3 (1-a)^2$
	$A = \frac{Pl}{2} (1+a)(1-a)^3$ $M_1 = \frac{Pl^2}{2} a^2 (1-a)^3$	$H = \frac{Pl^2}{8f} (1-a)^3 (6a^2 + 3a + 1)$ $M_2 = -\frac{Pl^2}{2} a^3 (1-a)^2$
	$A = P(1-a)^2 (1+2a)$ $M_1 = -\frac{Pl}{2} a (1-a)^2 (2-5a)$	$H = \frac{15}{4} \frac{Pl}{f} a^3 (1-a)^2$ $M_2 = \frac{Pl}{2} a^2 (1-a) (3-5a)$
Uniform temp. change of $t^\circ$	$A = 0$ $B = 0$ $M_1 = \frac{15EI\alpha t}{2f}$	$H = \frac{45EI\alpha t}{4f^2}$ $-M_2 = \frac{15EI\alpha t}{2f}$

Positions of loads and values of "a" which result with good accuracy in maximum moments at the crown, quarter point, or springing are given for both types of arches in the following table.

	Crown	left quarter point	left springing
Positive Moment	 Two hinged $a = 0.350$ Fixed $a = 0.375$	 Two hinged $a = 0.425$ fixed $a = 0.400$	 Fixed $a = 0.40$
Negative Moment	 Two hinged $a = 0.350$ Fixed $a = 0.375$	 Two hinged $a = 0.575$ Fixed $a = 0.400$	 Fixed $a = 0.460$



## IX - CONSTRUCTIONAL DETAILS

### IX-1 INSULATION AND ISOLATION OF ROOFS

In big span roof structures supporting mainly their own weight, it is recommended to choose the shape of the main supporting element giving the minimum dimensions. The spacing between the main girders and the secondary longitudinal beams should be so chosen as to give a thickness of slab varying between 8 and 10 cms. Such thin slabs are generally not water-tight and must be given a sufficient slope ( $\geq 1/100$ ) so that rain water can be directly drained and is not allowed to gather on the roof. An effective isolating material such as pluvex or asphaltoid in 2 or more layers may be used.

Insulation of these thin slabs by the use of 5-8 cms. celton, airocrete, thermocrete, no fine light concrete... etc. is also essential. Cement tiles may also be used as a covering material for horizontal and lightly inclined roofs. The details are shown in fig. IX-1

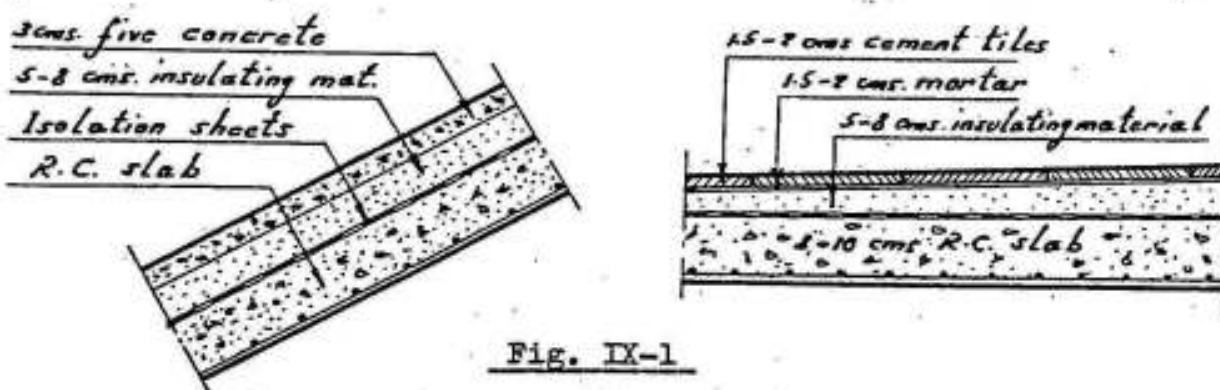



Fig. IX-1

### IX-2). SECONDARY BEAMS

Secondary beams are generally arranged normal to the main supporting frames or arches giving together a stable space structure and dividing the slab in convenient areas giving economic dimensions. The spacing lies generally between 2.5 and 5.0 ms, while the span varies between 4 and 8 ms. These are determined by economical and practical considerations. They will be affected by the use to which the structure is to be put, the size and shape of the structure and the load

which must be carried. A comparison of a number of trial designs and estimates should be made and the most satisfactory arrangement selected.

If the slope of the roof is smaller than 1 : 3 , the secondary beams are made vertical, for bigger slopes, the beams are made normal to the slab. The arrangement of intermediate, edge, wall and crane beams can be chosen according to figure IX-2

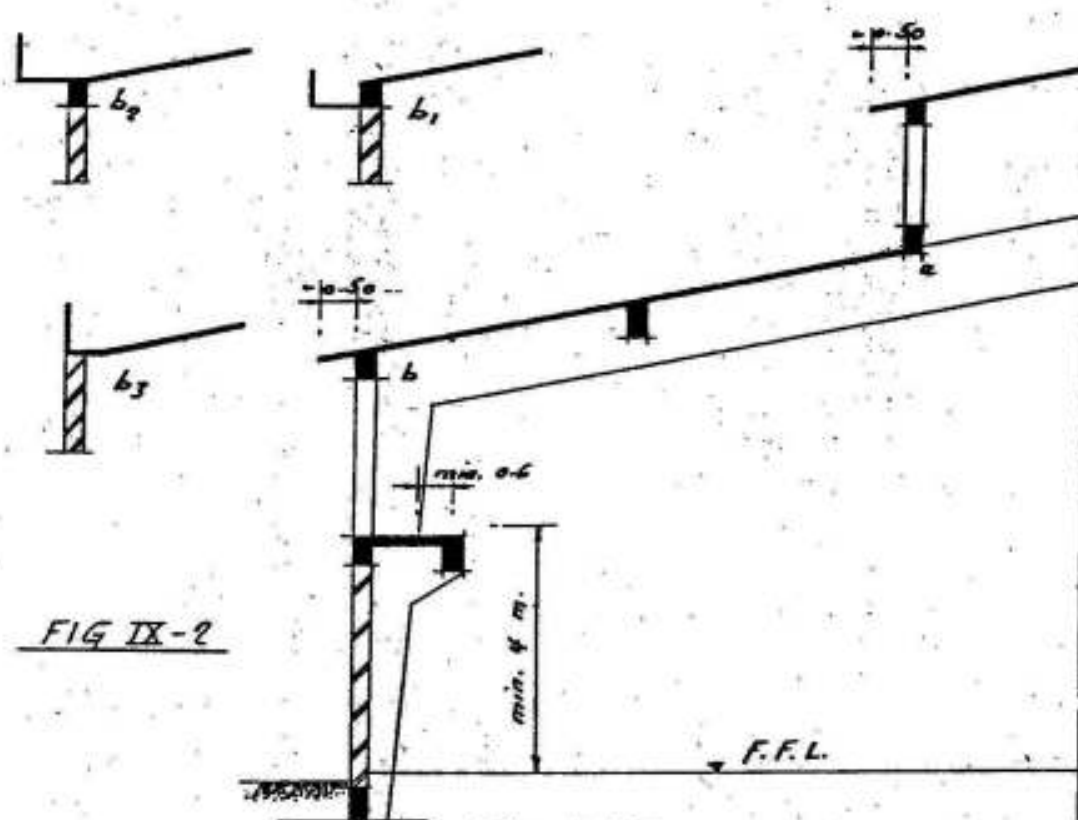


FIG IX-2

Fig. IX-2

The slabs in the structure shown project  $\sim 0.5$  ms. outside the windows so that the rain water does not seep on them. The rain water is either left to fall freely from the roof of the monitor to the roof of the hall and then to the free area outside the structure, or it is collected in a gutter as shown in  $b_1$ ,  $b_2$  or  $b_3$ . The beam at  $a$  is inverted in order to allow for a good fixation of the window crystal frame and to prevent seeping of the rain water at the lower edge of the window. It gives more stiffness if the wall beam and the crane girder ( if any ) are arranged in the same horizontal plane and connected with a slab which may be used as a foot-path at the windows and helps in resisting the horizontal component of the crane load.

IX-3) SHORT CANTILEVERS ( Fig. IX-3 )

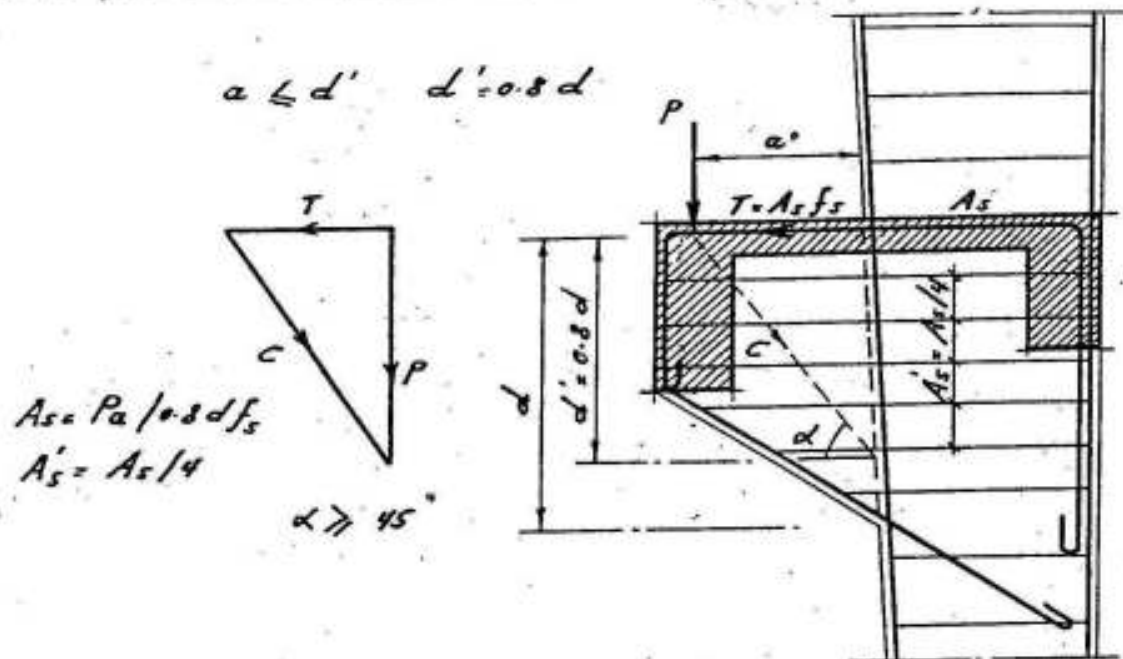


Fig. IX-3

Crane girders are generally supported by short cantilevers as shown in figure IX-3. If the projection  $a$  is smaller than  $d'$  ( $=0.8 d$ ) or equal to it so that  $\alpha \geq 45^\circ$ , the tension  $T$  can be determined by direct resolution of forces for the same reasoning given in ( X-5 ). Hence

$$T/P = a/d'$$

$$\text{but } T = A_s \sigma_s \quad \text{and } d' = 0.8 d$$

then

$$A_s = P a / 0.8 d \sigma_s$$

Horizontal stirrups having an area  $A'_s = A_s / 4$  to resist the possible tensile forces normal to the direction of the compression  $C$  are essential.

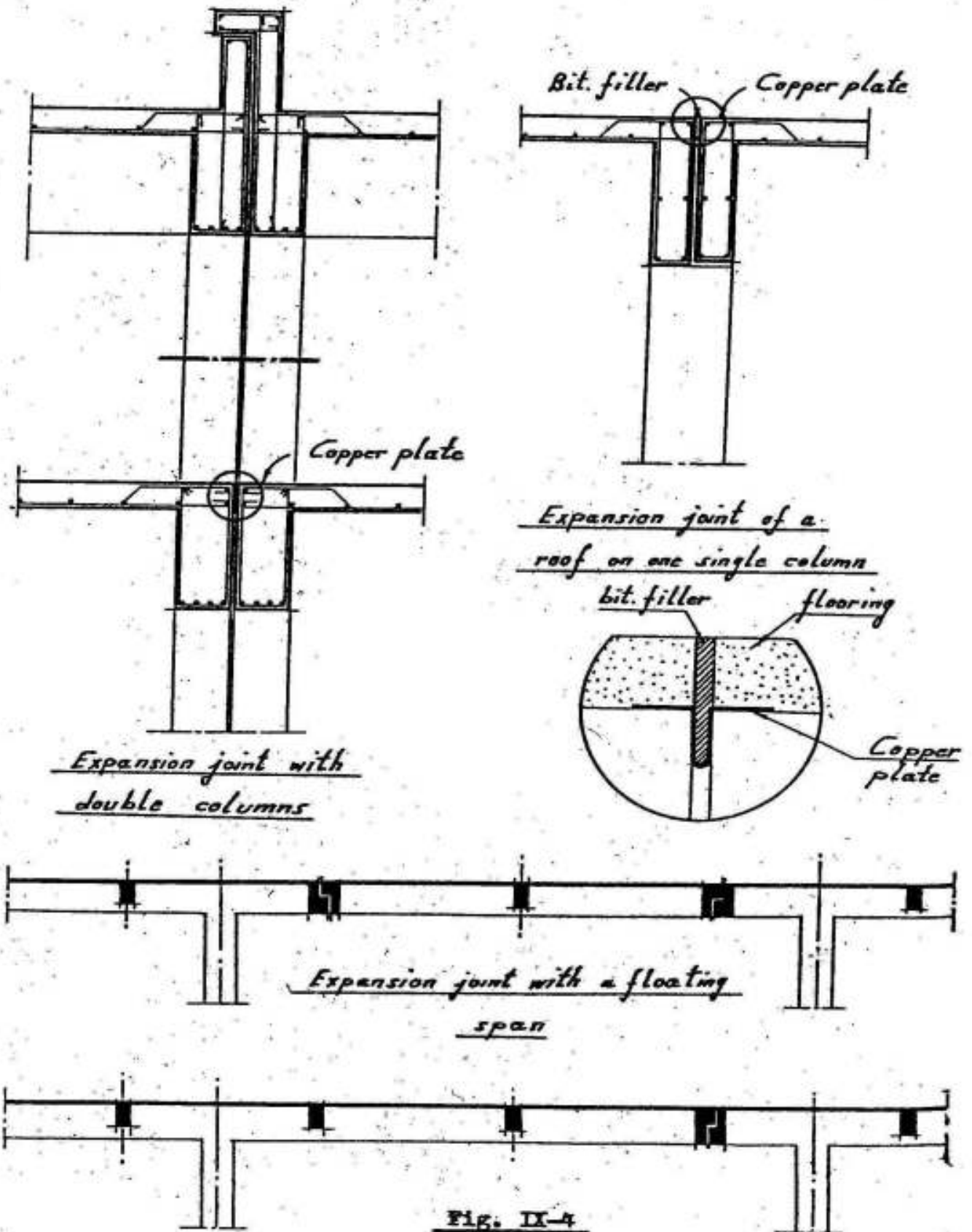
IX-4) EXPANSION JOINTS

Long structures are to be divided into blocks of maximum length or breadth equal to 40 ms. by expansion joints according to one of the systems shown in figure IX-4

IX-5) END GABLES

In order to resist the wind pressure acting on the end cross-walls of big span halls one has to arrange a series of columns, generally framing with the longitudinal beams of the roof at distances of 4-6 ms. To reduce the bending moments on such columns, horizontal beams

at convenient distances - 4.0 to 6.0 ms. are essential. As an example refer to section C-C of fig. IV-34



## X - HINGED AND FREE BEARINGS

A free bearing is arranged to give a reaction at the point of support in a specified direction without any restraint. It must therefore be free to rotate and slide normal to the specified direction of the reaction so that the reaction at a free bearing includes one unknown only.

A hinged bearing is free to rotate without any restraint so that the point of application of the reaction is known but its direction and magnitude are unknown i.e. a reaction at a hinged support includes two unknowns as shown in figure X-1

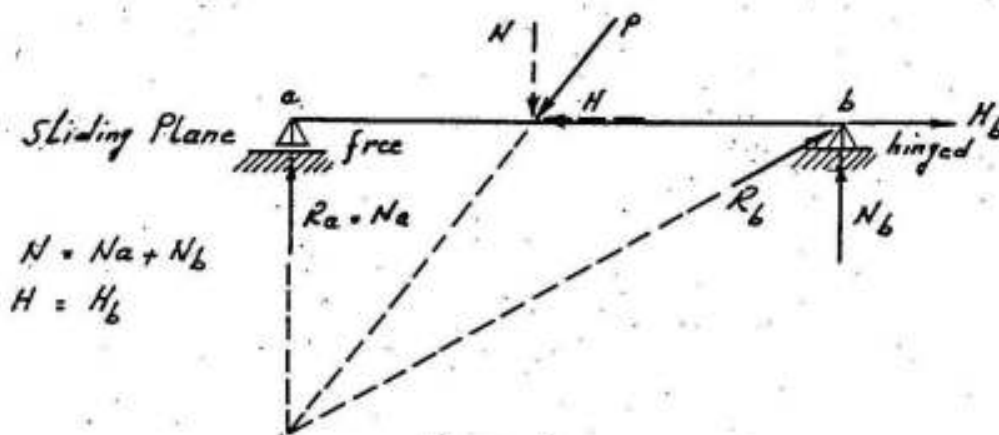


Fig. X-1

Such ideal free and hinged bearings cannot be constructed, since friction or other inevitable restraining factors cannot be avoided.

### A. HINGED BEARINGS

The main practical types of hinges used in concrete structures are :

#### X-1) STEEL HINGES

The steel hinges e.g. as shown in figure X-2 result in more perfect hinge action than the concrete hinges, but are considerably more expensive. Their use today, is restricted to bridges and unusually heavy concrete structures.

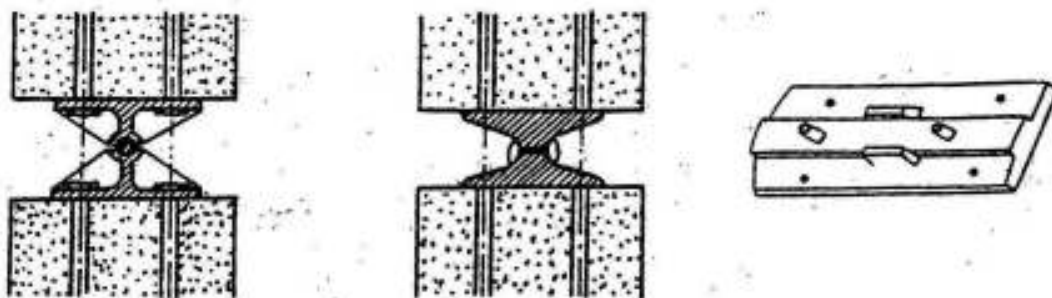


Fig. X-2

X-2) MESNAGER HINGES

In this type of hinge, the reaction  $R$  is transmitted through the crossing bars  $A_{s1}$  and  $A_{s2}$ . Their inclination with the free face of hinge lies between  $30^\circ$  and  $60^\circ$ . They are protected from rusting by 2.5 cms. oxidized asphalt, bituminous cork or bituminous felt arranged as shown in figure X-3.

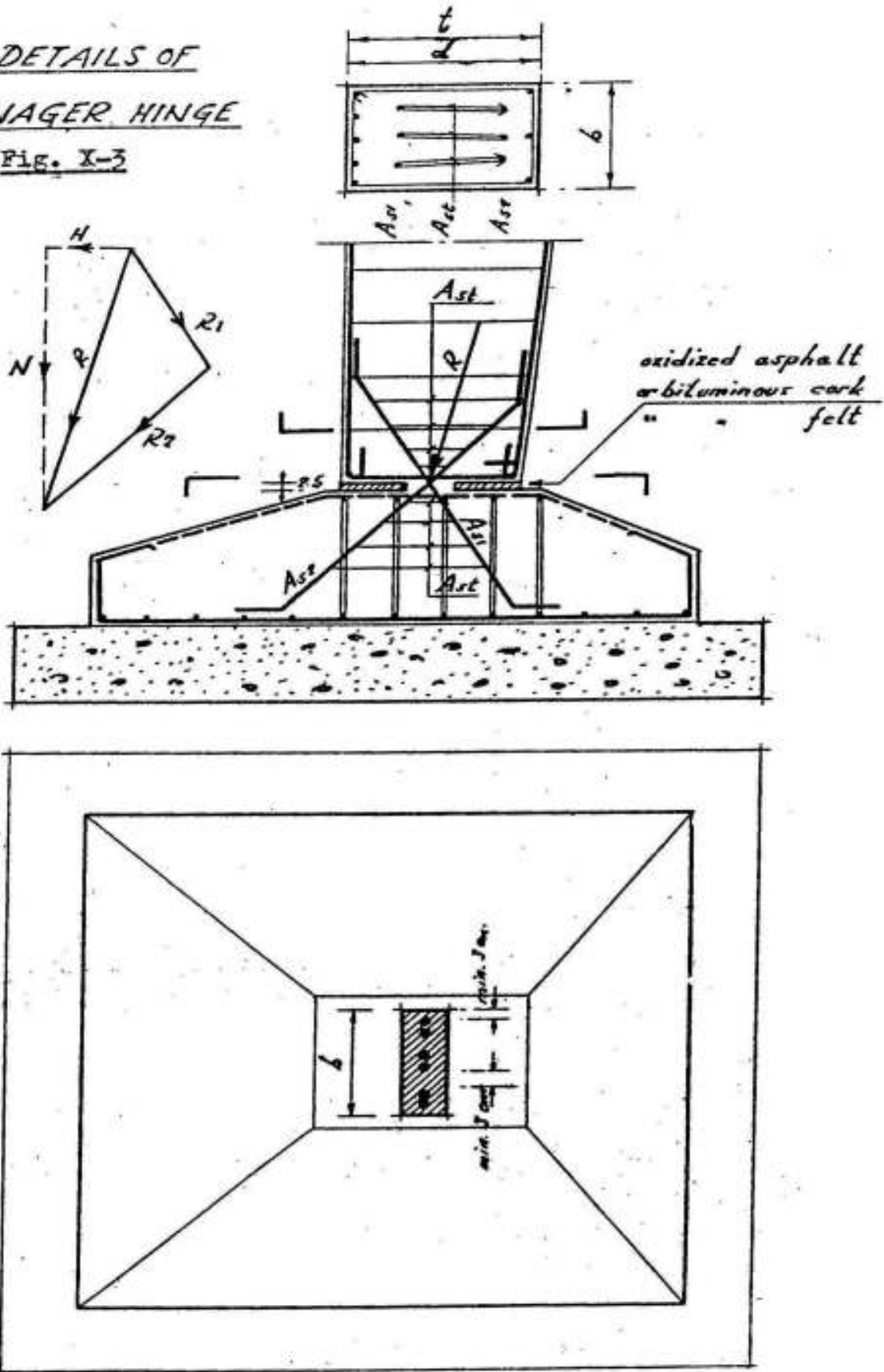
The crossing bars are in this manner subject to compressive stresses  $\sigma'_s$  which must not exceed  $0.3 \sigma_y$ . This low stress is assumed because any rotation actually occurring at the hinge bends the bars and induces corresponding flexural stresses. Such rotations actually do take place during the lifetime of the structure and are caused primarily by changes in live load and temperature. These flexural stresses superpose on the computed compression and correspondingly increase the value of the actual maximum stresses in the bars. Rather than to attempt computing these additional stresses, it is generally satisfactory to keep the compression stress  $\sigma'_s$  sufficiently low so that the bars will not be overstressed by superposed bending.

The crossing bars, transmitting their force to the concrete by bond along the embedded length, exert a bursting force which must be resisted by additional ties. Only the part of the lateral reinforcement within a distance  $a = 8 \phi$  ( $\phi$  being the diameter of crossing bars) from the face of the concrete is considered effective in resisting the bursting force. The tensile stress  $\sigma_{st}$  in the ties  $A_{st}$  can be computed according to figs. X-3 & X-4 from the relation.

$$\sigma_{st} = \frac{(N/2) \tan \theta + H a / Y_{CT}}{0.005 a b + A_{st}}$$

DETAILS OF  
A MESNAGER HINGE

FIG. X-3



where, in addition to previously defined quantities,  $A_{st}$  is the combined area of lateral ties located within  $a = 8\phi$  from the free face of the hinge and  $y_{CT} = 0.87 d$

Example :

A Mesnager hinge of the form shown in figure X-3 is subject to an inclined reaction  $R$  whose component normal to the free face of the hinge  $N = 25t$  and its component parallel to it  $H = 5t$ . The breadth  $b$  and depth  $t$  of the foot of the column are :  $b = 40$  cms. and  $t = 60$  cms. Determine the reinforcements required for the hinge using mild steel with  $\sigma_y = 2700$  kg/cm<sup>2</sup>.

Referring to figure X-3, assume :

$$R_1 = 14 \text{ ton} \quad \text{so that} \quad A_{s1} = R_1 / \sigma'_s = 14 / 0.8 = 18 \text{ cm}^2 \quad \underline{4\phi 25}$$

and

$$R_2 = 17.6 \text{ ton} \quad \text{so that} \quad A_{s2} = R_2 / \sigma'_s = 17.6 / 0.8 = 22 \text{ cm}^2 \quad \underline{4\phi 28}$$

The stress in the lateral ties required to transmit the forces in these crossing bars by bond along a length  $a = 8\phi = 8 \times 2.8 = 22.4$  cm. to the concrete is calculated in the following manner :

Assuming the ties are  $8\phi 6$  spaced at  $\sim 7.5$  cms., then we will have four rows of ties with  $4 \times 8 = 32$  branch and having a total area

$$A_{st} = 32 \times 0.24 = 7.68 \text{ cm}^2 \quad \text{and} \quad \tan \theta = 0.8$$

We have further  $d = 55$  cms and  $y_{CT} = 0.87 d = 48$  cms.

So that :

$$\sigma_{st} = \frac{12500 \times 0.8 + 5000 \times 22.4 / 48}{0.005 \times 22.4 \times 40 + 7.68} = 1015 \text{ kg/cm}^2 < 1400 \text{ Safe!}$$

This type of hinges can only be used for relatively small values of  $R$  ( $\sim 30$  tons) and is limited by the maximum amount of crossing bars that can be placed in the breadth of the foot of the column giving a clear distance of minimum 3 cms. between the couples of crossing bars as shown in figure X-3.

X-3) CONSIDERE HINGES fig. X-5

In this type of hinge, the normal component  $N$  of the reaction

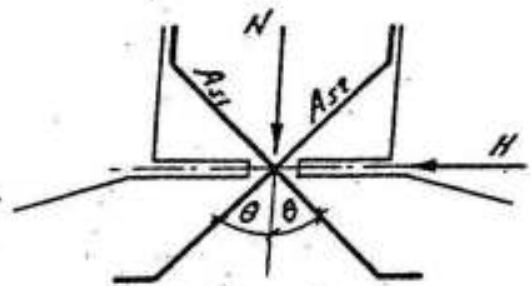


Fig. X-4



A CONSIDERE HINGE

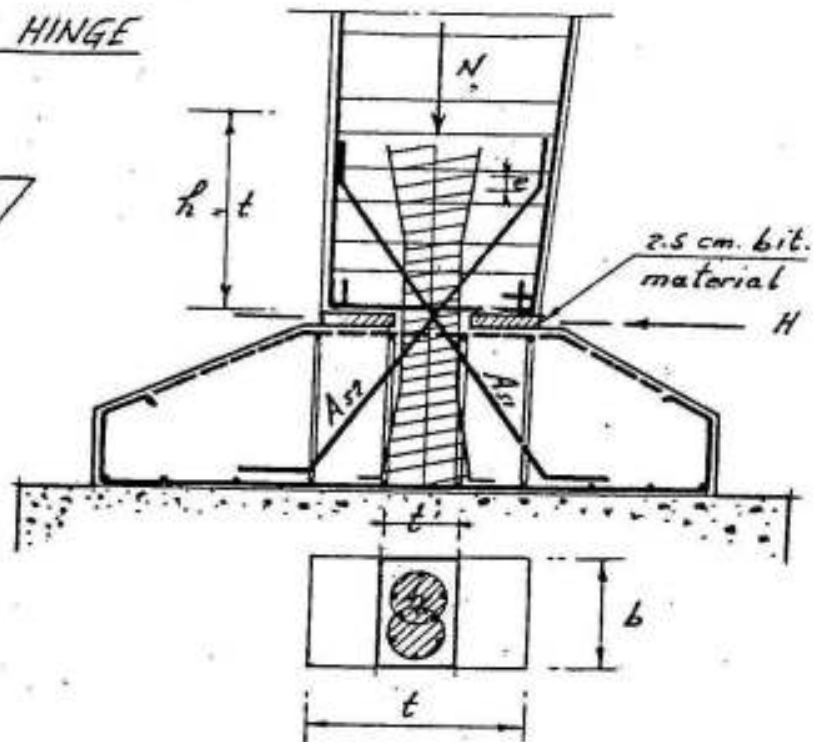
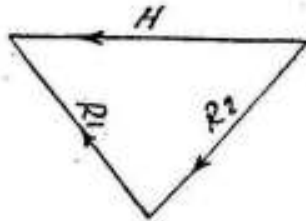


Fig. X-5

is transmitted to the foundation by the short spirally reinforced concrete column arranged at the middle of the foot of the main column where as the thrust  $H$  is resisted by the crossing bars  $A_{s1}$  and  $A_{s2}$ .

In order to have an acceptable hinge action,  $t'$  must be  $\leq t/3$ . The spirally reinforced short column may be calculated from the known relation of the elastic theory.

$$N = \sigma_b A_k + \sigma'_s A_s + 2.5 \cdot \sigma_s A'_s \leq 2 (\sigma_b A_c + \sigma'_s A_s)$$

in which

$A_k$  = the area of the core inside the spirals ( hatched area )

$A_c$  =  $b t'$

$A_s$  = area of cross-section of longitudinal reinforcements inside the spirals

$A'_s$  = imaginary longitudinal reinforcements having the same volume of the spirals with cross-sectional area  $A_{sp}$ , pitch  $e$  ( $\leq 8$  cms) and diameter  $D$  i.e.  $A'_s = A_{sp} \pi D/e$

$\sigma_b = \sigma_{co} \sqrt[3]{A/A'} \leq \sigma_{c28} / 2$  the bearing stress of partially loaded areas.

$\sigma_{co}$  = allowable compressive stress of the concrete used

$A = b t' =$  area of foot of column

$A' = A_k$  or  $A_c$  effective loaded area

$\sigma'_s =$  allowable compressive stress of longitudinal reinforcement

$\sigma_s =$  allowable tensile stress of spirals

$n = 15 =$  modular ratio

If the ultimate strength theory is applied the corresponding equation with the specified load and reduction factors can be used.

Due to the concentration of the stresses in the hinge horizontal splitting tensile forces are created at the foot of the column. The stirrups along the height  $h = t$  are generally increased to resist these splitting forces.

X-4) LEAD HINGES fig. X-6

In this type of hinges, the normal component  $N$  of the hinge is transmitted to the foundation by bearing through a 2 cms thick lead plate arranged at the middle of the column foot. The horizontal component  $H$  is resisted by the shear resistance of the connecting bars  $A_s$  which are protected from rusting by 2cms.thick bituminous cork, bituminous felt or oxidized asphalt arranged as shown in fig. X-6.

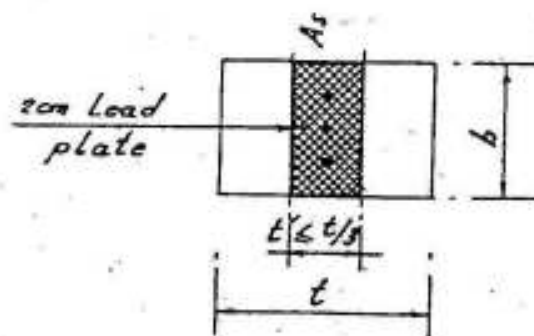
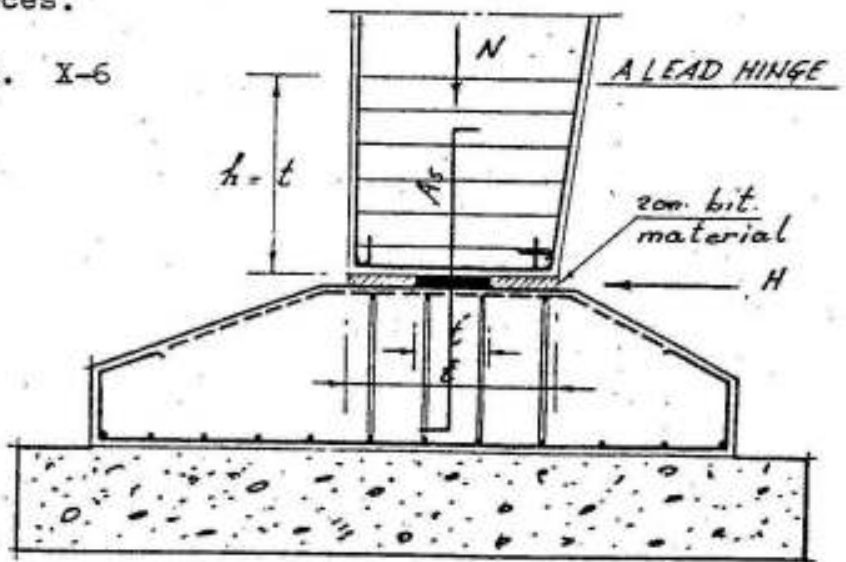


Fig. X-6

In order to have acceptable hinge action, the length of the lead plate  $t'$  must be

smaller than or equal to one third of the depth of the column at the position of the hinge measured in the direction of the required rotation.

The lead hinge can accordingly be calculated in the following manner :

$$N/bt' < \sigma_b = \sigma_{co} \sqrt[3]{A/A'} \leq \sigma_{c28}/2$$

$$A_s = H/\tau_s \text{ where } \tau_s = 0.8 \sigma_s = \text{allow. shear stress of steel.}$$

If it is required to reduce the amount of the connecting steel  $A_s$  to a minimum, the lead plate is to be arranged normal to the direction of the reaction due to dead loads as shown in figure X-7, in which case,  $A_s$  can be calculated to resist the thrust due to live loads only.

Due to the concentration of the stresses at the position of the hinge transverse tensile splitting forces are created; These can be explained as follows ( fig. X-8 ).

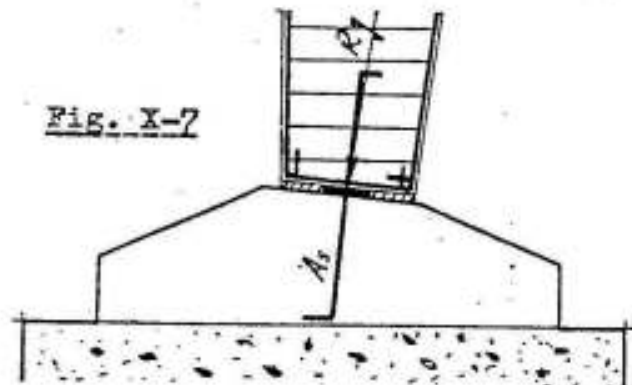


Fig. X-7

The transmission of the normal compressive stresses is assumed to take place from the breadth of the column  $t$  to the breadth of the lead plate  $t'$  in a height  $h$  approximately equal to the breadth  $t$

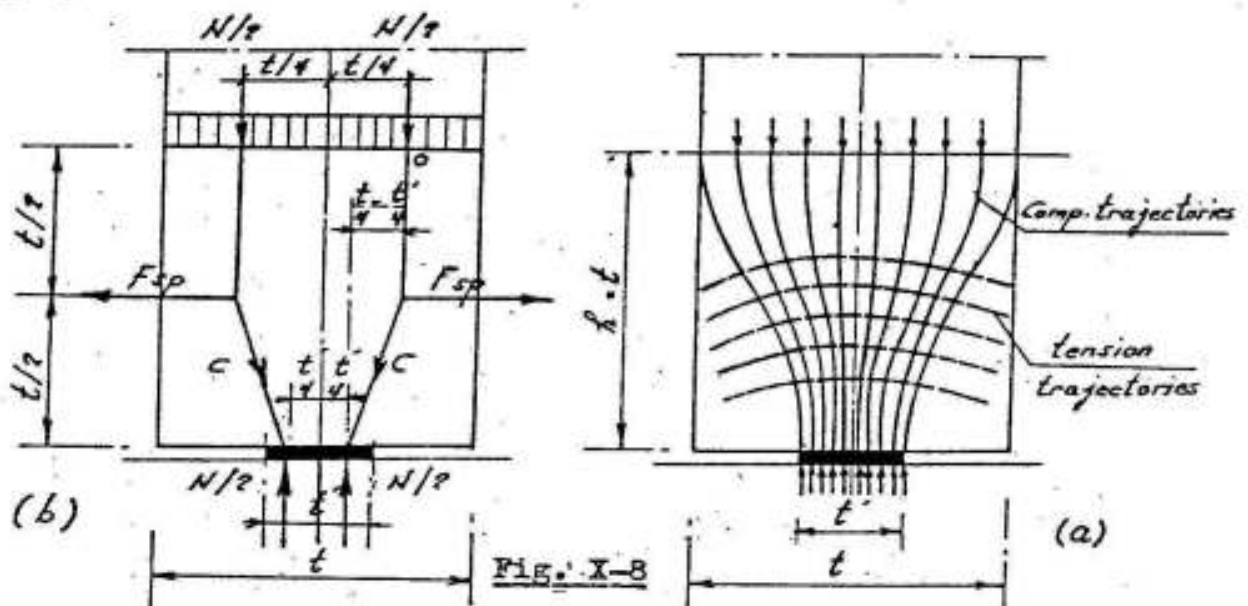


Fig. X-8

of the column so that the compression trajectories and the corresponding tension trajectories will be as shown in fig. X-8a .

Considering the equilibrium of any half of the concrete block, height  $h = t$ , at the hinge, we can see that the two forces  $N/2$  are equal and opposite but not colinear and equilibrium is only possible if a transverse force  $F_{sp}$  is assumed acting as shown in figure X-8b. Its magnitude can be determined, according to Moersch, if we take moments of the forces acting on say the right half about point O.

Hence :

$$\frac{N}{2} \left( \frac{t}{4} - \frac{t'}{4} \right) = F_{sp} \cdot \frac{t}{2}$$

So that

$$F_{sp} = N ( t - t' ) / 4t \approx N/4$$

$F_{sp}$  is tension and called the transverse splitting tensile force, it assumes its max. value of  $N/4$  for  $t' = 0$ . It must be resisted by horizontal stirrups of area  $A_{st} = F_{sp} / \sigma_B$  arranged at the foot of the column in a height  $h = t$ . Refer to figures X-5, 6 & 7 .

#### X-5) CONCRETE HINGES

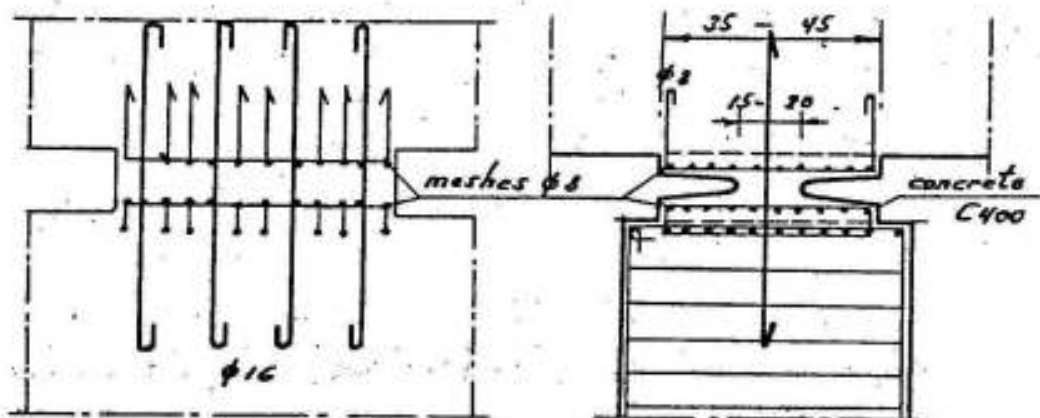


Fig. X-9

This type can only be used if the hinge is subjected to small angles of rotation. The vertical component of the reaction is transmitted to the supporting element by bearing on concrete with a stress  $\sigma_b = \sigma_{co} \sqrt[3]{A/A'} \leq \sigma_{c28} / 2 = 150$  to  $200 \text{ kg/cm}^2$ . The horizontal component of the reaction is taken by the shear resistance of the vertical connecting bars

It is recommended to arrange reinforcing meshes  $\phi 8$  mm. on both sides of the hinge as shown in figure X-9 . It is not allowed

to make a construction joint through the hinge and to make it of high grade concrete.

For this reason precast hinges ( or rockers ) as shown in figure X-10 may be used.

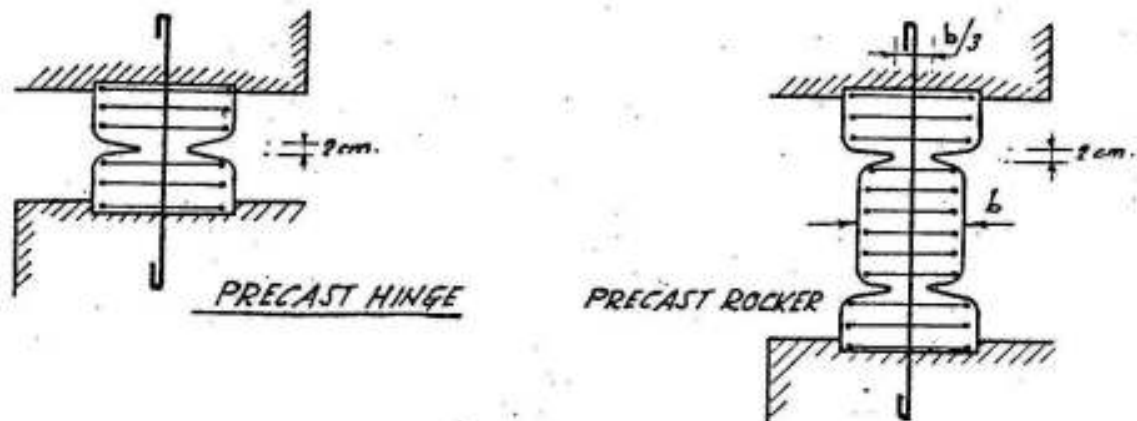


Fig. X-10

It is however essential to arrange sufficient cross-reinforcement to resist the possible splitting forces.

In all previous types, the minimum anchorage length of crossing or longitudinal bars must be  $\geq 30 \phi$  and  $\geq 50$  cms. on each side of the hinge.

#### B. FREE BEARING

The main types of free bearings used in concrete structures are :

##### X-6) STEEL BEARINGS

The different types of steel bearings may be used in concrete structures. Types of low cost and low construction height are recommended.

##### X-7) ROCKER BEARINGS ( Fig. X-11)

A rocker is a short reinforced concrete element between two hinges as shown in figure X-11. As the rocker is not laterally loaded, the reaction supported by a rocker will be in the direction of the line connecting the two hinges. Its height  $h$  depends on the required displacement and rotation. It supports the reaction by the combined action of the concrete, the longitudinal reinforcement and eventually the cross reinforcements which if placed in layers at a small spacing  $e < 8$  cms., they increase the resistance

of the rocker by an amount equal to  $2.5 n A'_s \sigma_s$  similar to that of spiral reinforcement ;  $A'_s$  is in this case equal to the volume of the cross reinforcements per unit height i.e. total length of cross reinforcements multiplied by their cross-section and divided by their pitch  $e$ .

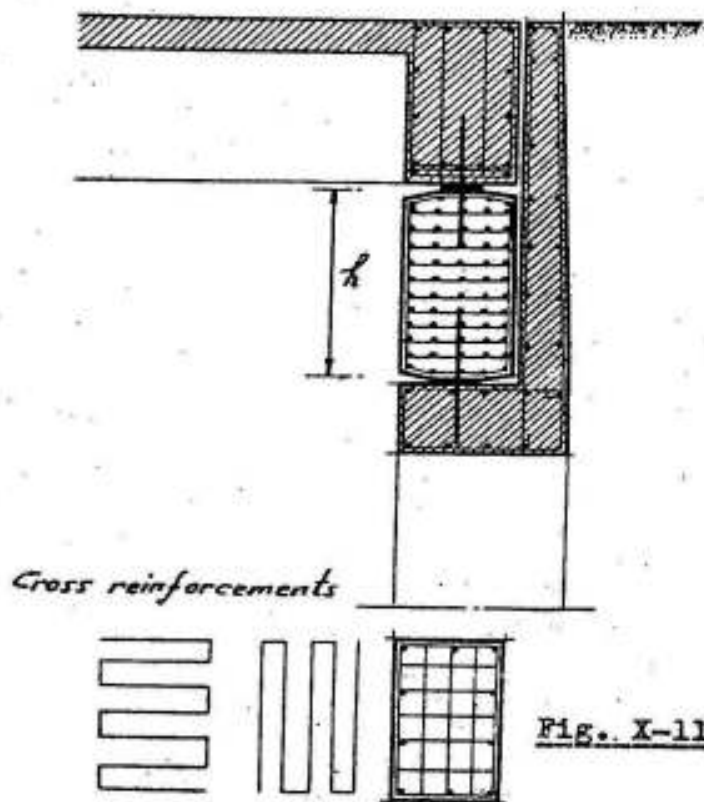


Fig. X-11

X-8) RUBBER BEARINGS ( Fig. X-12 )

A rubber bearing is composed of steel plates or wire meshes embedded in a special material - the neoprene - made of artificial synthetic rubber. It possesses very high resistance to climatic changes and chemical actions of acids or alkalis that are liable to exist in air or water. The steel in these bearings is completely protected against rusting. A neoprene bearing possesses the high resistance of steel and the elasticity of rubber. It can

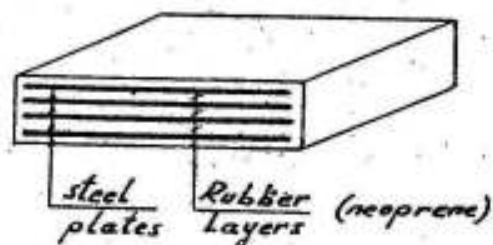


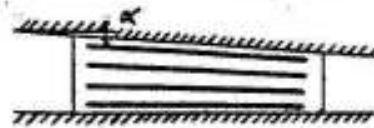
Fig. X-12

resist high vertical forces without appreciable vertical displacements. It allows for horizontal displacements  $\delta$  and rotations  $\alpha$  in two normal

directions as shown in figure X-13



Horiz. displ.  $\delta$



Rotation  $\alpha$

Fig. X-13

This kind of bearings is to be assumed as free allowing rotations and horizontal displacements in any direction.

The exact stress distribution in a neoprene bearings is very complicated but for practical designs, the following method may be used. One has to check.

- 1) The axial compressive stress

$$\max. \sigma = \max. N/A \leq \text{allow. } \sigma = 100 \text{ kg/cm}^2$$

- 2) Sliding angle

$$\tan \gamma = \delta / h. < \text{allow. } \tan \gamma$$

- 3) Horizontal force

$$H = G. A. \tan \gamma$$

- 4) Angle of friction between neoprene bearing and concrete

$$\max. \mu = \max. H / \min N \leq \text{allow. } \mu$$

- 5) Angle of rotation of every rubber layer

$$\beta < \text{allow. } \beta$$

in which

max. N and min. N are the maximum and minimum normal components of the reaction.

- A is the area of the bearing in plan
- $\delta$  the horizontal displacement of the point of support
- h. the net height of the bearing (sum of all rubber layers)
- h the height of the bearing
- n number of rubber layers
- G bulk modulus of rubber

The following two cases of loading must be recognised :

Case I - Permanent Loads

( dead loads, prestressing, creep, shrinkage, temperature)

Case II - Live Loads (acting for a short time)  
(tractive & wind forces)

The following values must not be exceeded.

Table 1

Case of loading	tan $\gamma$	allow. normal $\sigma$ in kg/cm <sup>2</sup>					allow. $\beta$ in minutes			G kg/cm <sup>2</sup>
		20	40	60	80	100	150x200	200x300	300x400	
I	0.7	0.50	0.45	0.40	0.35	0.30	10.0	7.5	5.0	13
II	0.3	0.30	0.26	0.22	0.18	0.15	4.0	3.0	2.0	20
I + II	0.9	0.50	0.45	0.40	0.35	0.30	14.0	10.5	7.0	

all values are related to the effective depth  $h_e$ .

The compressibility of the neoprene bearing due to vertical forces is very small and has no effect on the internal forces in statically indeterminate structures.

The standard dimensions are :

150 x 200 mm	for max. N = 30 t	with E = 3500 kg/cm <sup>2</sup>
200 x 300 mm	for max. N = 60 t	with E = 7000 kg/cm <sup>2</sup>
300 x 400 mm	for max. N = 120 t	with E = 14500 kg/cm <sup>2</sup>

Its height is chosen according to the statical requirements and should be  $\leq 1/5$  of its breadth. The rubber layers are 5mm. thick

Table II

No. of rubber layers	n=	2	3	4	5	6	7	8	9	10	11	12	
effective depth	$h_e =$	10	15	20	25	30	35	40	45	50	55	60	mm.
total depth	$h =$	14	21	28	35	42	49	56	63	70	77	84	"
for case of load I	$w =$	7.0	10.5	14.0	17.5	21.0	24.5	28.0	31.5	35.0	38.5	42.0	"
for bearing 150 x 200	max V=	30	30	30	30	30	-	-	-	-	-	-	t
for bearing 200 x 300	"	60	60	60	60	60	60	60	-	-	-	-	t
for bearing 300 x 400	"	-	-	-	-	120	120	120	120	120	120	120	t



Example :

Design the required neoprene bearings for the shown simple prestressed foot bridge. ( Fig. X-14)

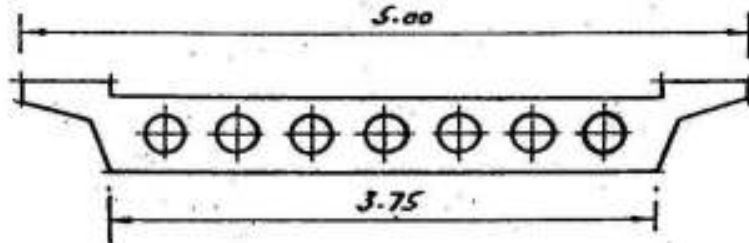


Fig. X-14

data :

Cross-section	$A = 2.8 \text{ m}^2$	$I_c = 0.08 \text{ m}^4$
Initial prestressing force		$F_o = 900 \text{ t}$
Span		$l = 20 \text{ ms}$
Temperature change		$\Delta t = \pm 20^\circ$
Creep strain $\epsilon_{cr} = 3$ times elastic strain		$\epsilon_c$
Shrinkage strain $0.20 \text{ mm/m}$		$\epsilon_{sh} = 0.2 \times 10^{-3}$
Modulus of elasticity of concrete		$E_c = 300\,000 \text{ kg/cm}^2$
Bulk modulus of bearing		$G = 13 \text{ kg/cm}^2$
Dead load		$g = 7.5 \text{ t/m}$
Live load		$p = 2.5 \text{ t/m}$
Average concrete stress $\sigma_c$ due to		$F_o + g$ is given by

$$\sigma_c = F_o / A = 900 / 2.8 = 320 \text{ t/m}^2 = 32 \text{ kg/cm}^2$$

The horizontal displacements of the bridge are :

Due to prestress	$\epsilon_o = \sigma_c / E_c = 32 / 300\,000 = 0.11 \times 10^{-3}$
Due to creep	$\epsilon_{cr} = 3 \times \epsilon_o = 3 \times 0.11 \times 10^{-3} = 0.33 \times 10^{-3}$
Due to shrinkage	$\epsilon_{sh} = 0.2 \text{ mm/m} = 0.20 \times 10^{-3}$
Due to temperature	$\epsilon_{-t} = 20 \times 10^{-5} = 0.20 \times 10^{-3}$
	$\text{total } \epsilon = 0.84 \times 10^{-3}$

Horizontal displacement of point of support

$$w = l \epsilon / 2 = 20\,000 \times 0.84 \times 10^{-3} / 2 = 8.4 \text{ mm.}$$

### Reactions

$$\text{max. } N = (g + p) l / 2 = (7.5 + 2.5) \times 20 / 2 = 100 \text{ t}$$

$$\text{min. } N = g l / 2 = 7.5 \times 20 / 2 = 75 \text{ t}$$

For each side of the bridge, we choose

2 neoprene bearings each 200 x 300 x 20 mm

$$\text{Bearing area } A = 2 \times 20 \times 30 = 1200 \text{ cm}^2$$

$$\text{Height of bearing } h_0 = 20 \text{ mm (4 rubber layers 5 mms. each)}$$

$$\text{Normal stress } \sigma_{\text{max}} = \text{max } N/A = 100\,000/1200 = 83 \text{ kg/cm}^2 < 100$$

$$\text{Displacement angle } \tan \gamma = w/h_0 = 8.4/20 = 0.42 < 0.7$$

$$\text{Max. horizontal force } H_{\text{max}} = G A \tan \gamma = 13 \times 1200 \times 0.42 = 6500 \text{ kg} = 6.5 \text{ t}$$

$$\text{Coeff. of friction } \mu_{\text{max}} = \text{max } H/\text{min } N = 65/75 = 0.087 < 0.40$$

Note = 0.40 is the allowed value for  $\sigma_{\text{min}} = \text{min } N/A = 75\,000/1200 = 62 \text{ kg/cm}^2$ )

Angle of rotation  $\beta$  per layer of rubber

$$= \frac{1}{4} \frac{pl^3}{24 E_c I_c} = \frac{1}{4} \frac{2.5 \times 20^3}{24 \times 300\,000 \times 0.80} = 0.86 \text{ } \circ\text{ } = 2.95 < 3.0$$

Neoprene bearings do not generally need any sort of fixation and are loosely placed on the bearing surface. They can be used both for steel and concrete structures. It is, however, of utmost importance that the bearing surface is smooth, clean, plane and dry.

For the construction of neoprene supports in concrete structures, they are to be encased in such a way that the shuttering can be easily removed. For supports of small height, cork plates are to be used. The surface of the neoprene support must be flush with the shuttering.

After the removal of the shuttering (or cork), the lateral surfaces of the support must be entirely free so as to guarantee a smooth functioning of the support (Fig. X-15).

For small bridges and buildings in which the reactions are generally small, neoprene supports without steel plates may be used. The max. normal stress is to be chosen smaller than  $25 \text{ kg/cm}^2$  and  $\tan \gamma \leq 0.5$ .

Neoprene strips can be conveniently used as supports for cylindrical tanks with sliding base where they transmit the load of the wall (and eventually the roof) to the floor and, allow for the

free movement of the wall and give a watertight joint.

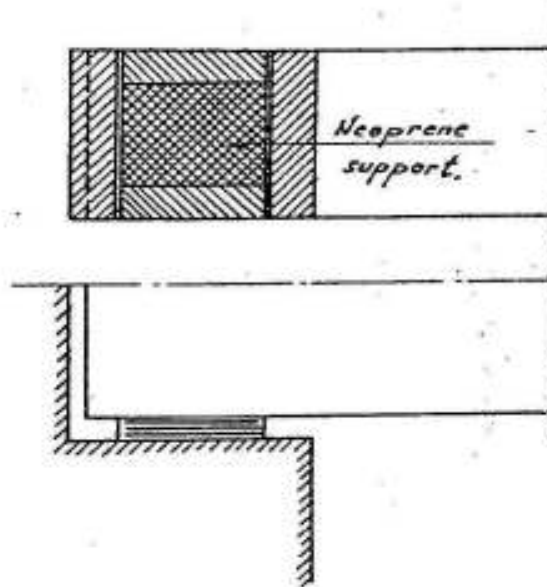


Fig. X-15

## XI - FOLDED PLATE STRUCTURES

### XI-1) DEFINITION AND TYPES

Folded or hipped-plate structures consist of an assembly of flat plate strips intersecting at fold lines and arranged such that they form a stable three-dimensional structure. Fig. XI-1.

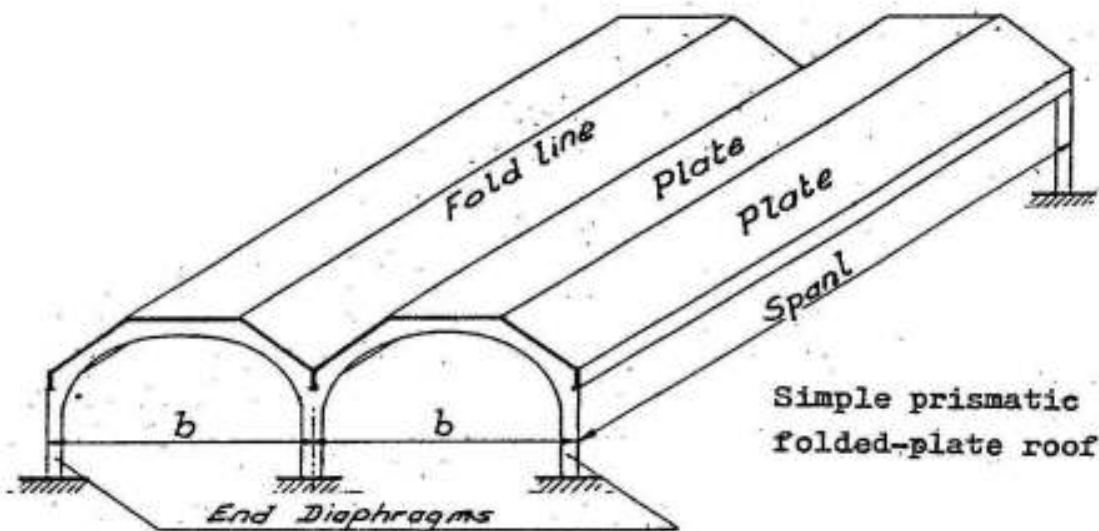


Fig. XI-1

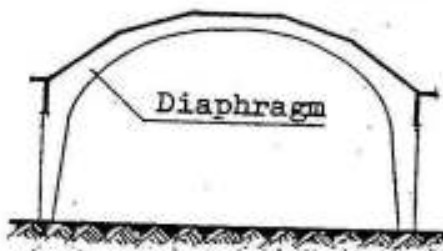
They may be prismatic, prismoidal, pyramidal, .... etc.; they find application as roofs, coal bunkers, cooling towers, bridges, stair-cases, etc. .... Fig. XI-2.

Prismatic structures must be stiffened by diaphragms in at least two cross-sections.

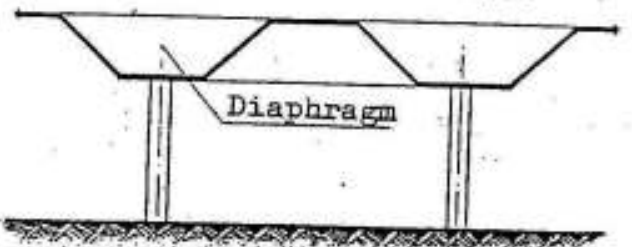
The plate elements of a folded structure being straight, they are subject to bending moments between the fold lines and hence, they consume a little more material than continuously curved cylindrical shells, but the extra cost on this account is much smaller than the saving in the forms.

Examples of prismatic folded-plates

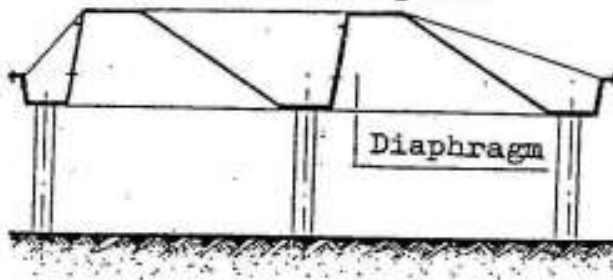
Wide folded-plate



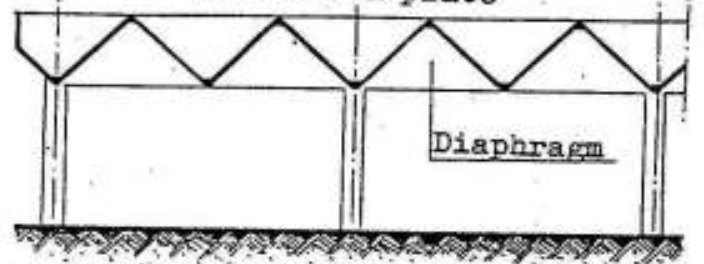
Continuous folded-pl.



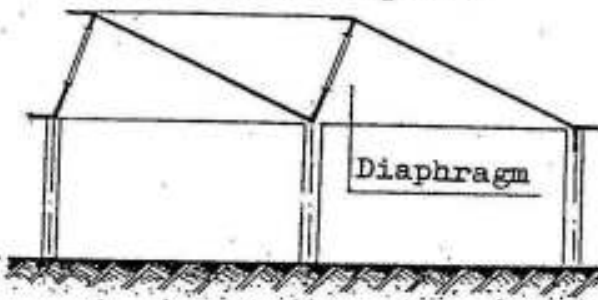
Saw-tooth folded plate



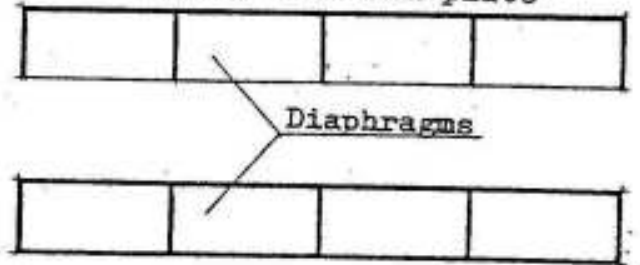
Vee folded plate



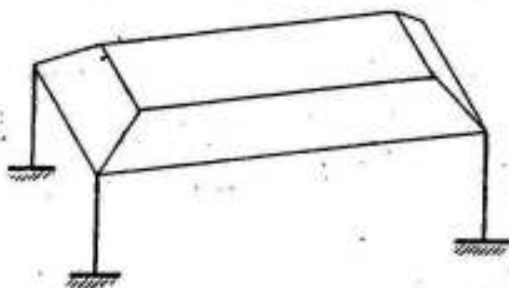
Saw-tooth folded plate



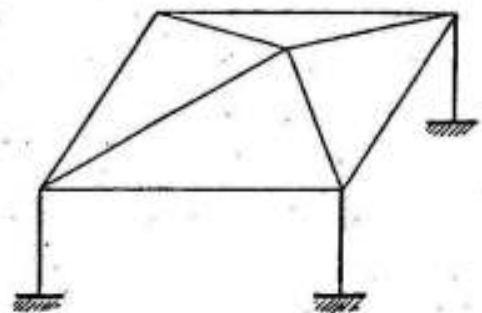
Multiple folded plate



Examples of non-prismatic folded-plates



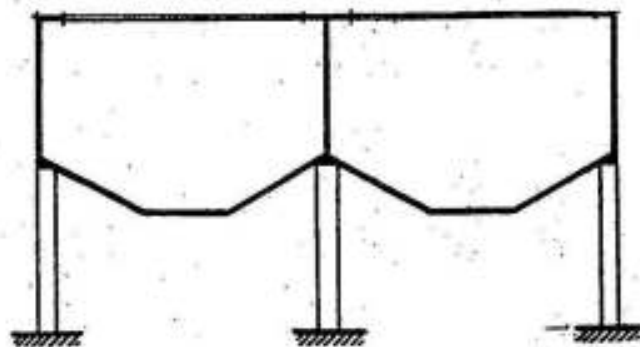
Prismoidal folded-plate



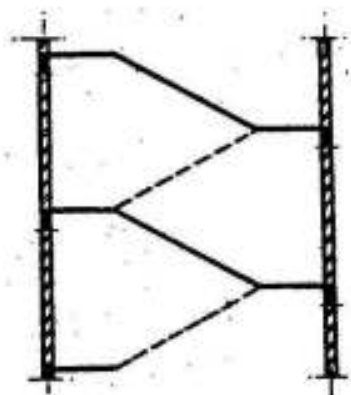
Pyramidal folded plate

Fig. XI-2

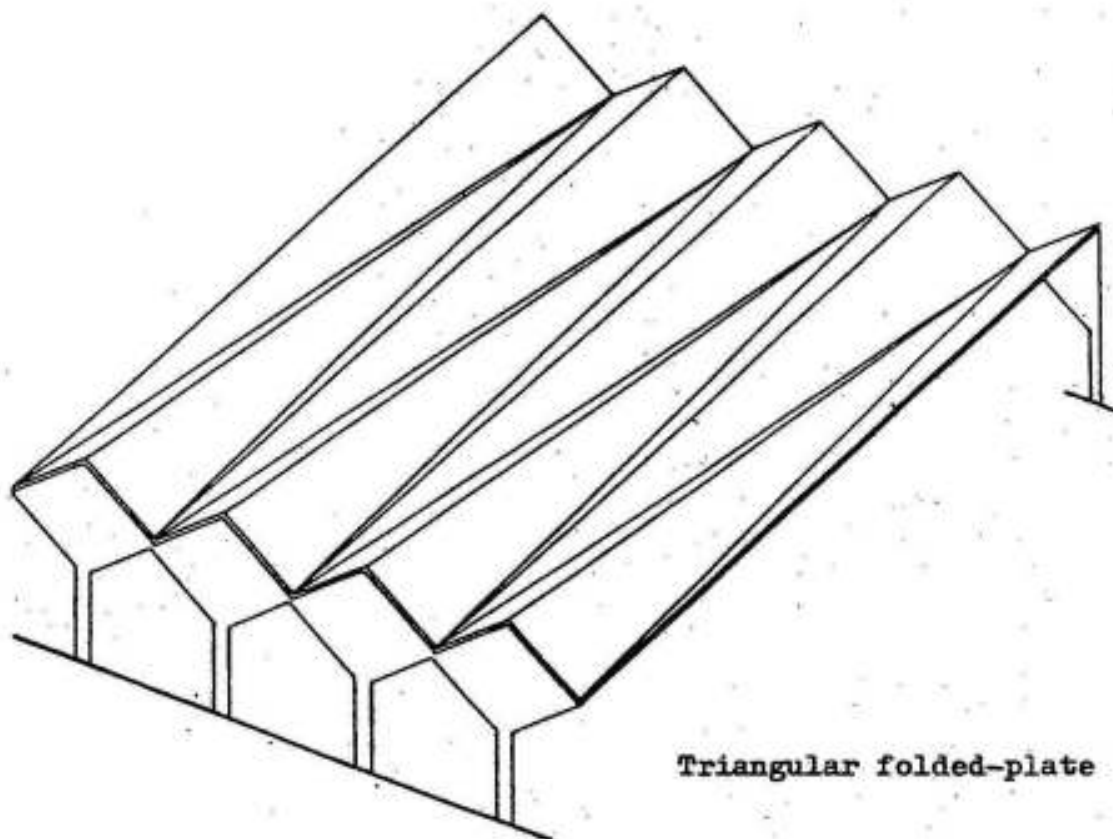
Examples of non-prismatic folded-plates (continued)



Bunker



Stair case



Triangular folded-plate

Fig. XI-2  
(continued)

XI -2) ASSUMPTIONS AND STRUCTURAL BEHAVIOR

Being primarily interested in folded plates as roofs, our study will be restricted to prismatic folded plates consisting of rectangular plates, each plate being of uniform thickness.

The following assumptions are usually made in the computations:

- i) The structure is monolithic and the joints are rigid.
- ii) The material is elastic, homogeneous and isotropic.
- iii) The length of each plate is more than twice its width.
- iv) In all plates, plane sections remain plane after deformation. (It is, however, to be carefully noted that a plane cross section of the entire structure does not necessarily remain plane after deformation).

XI-3) SLAB AND BEAM ACTION

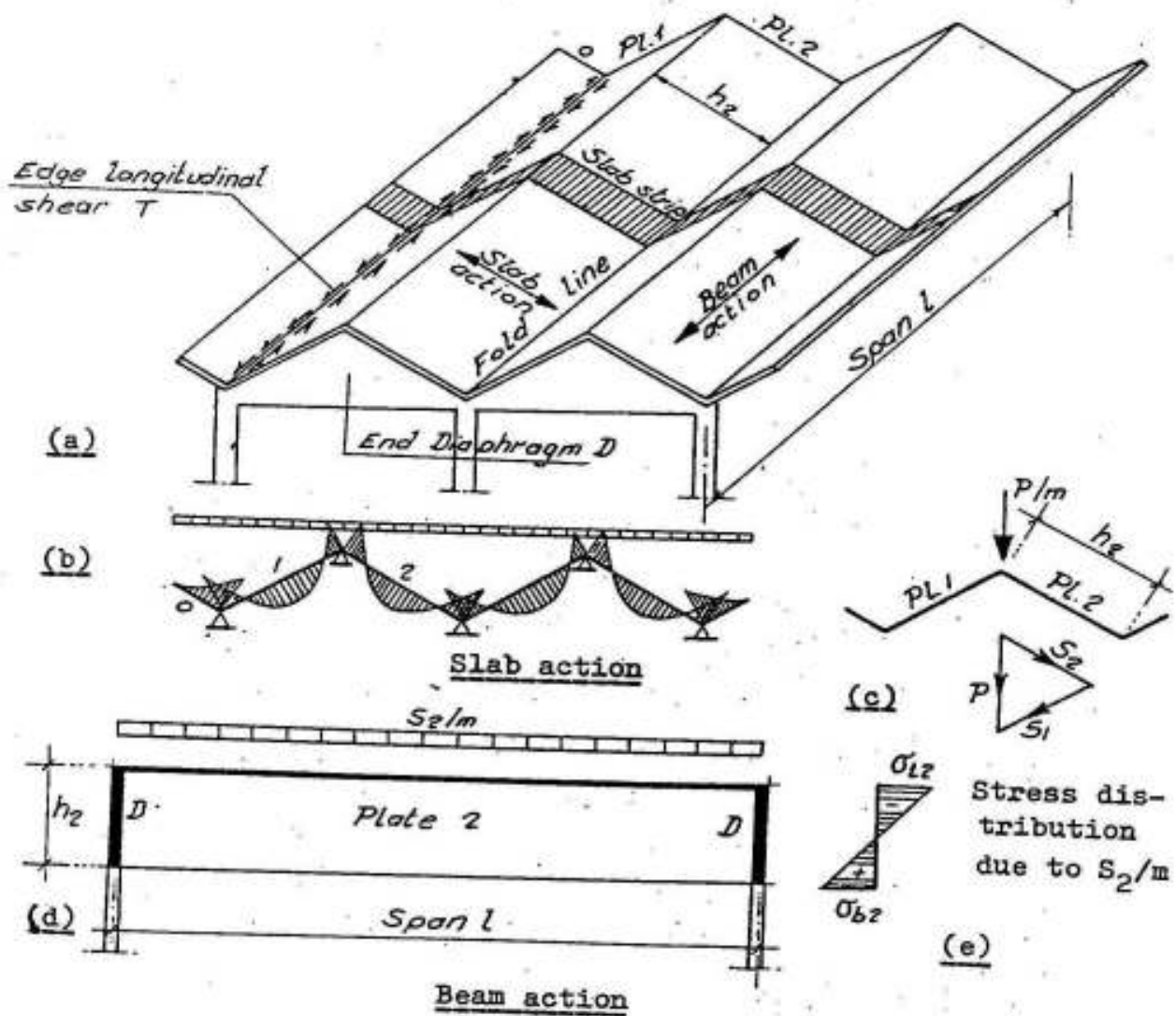


Fig. XI-3

### A) Slab Action

In prismatic folded plates, the length of each plate is more than twice its width (assumption iii) that the surface loads are carried by each plate as a one way slab supported on the fold lines. This is termed as slab action. A typical transverse strip is shown in Fig. XI-3 a. The corresponding bending moments as a one-way continuous slab are shown in Fig. XI-3 b.

### B) Beam Action

The reactions  $P/m$  from such slab strips are applied as line loads to the fold lines. The only direction in which each plate can apply a reactive force to resist this line load is parallel to its own surface. The resultant line load  $P/m$  (see Fig. XI-3 c) therefore resolves into components parallel to the two adjacent plates. The plates in turn carry this edge loading longitudinally between the end diaphragms 'D' by beam action as shown in Fig. XI-3 d.

#### a) Ridge and plate loads

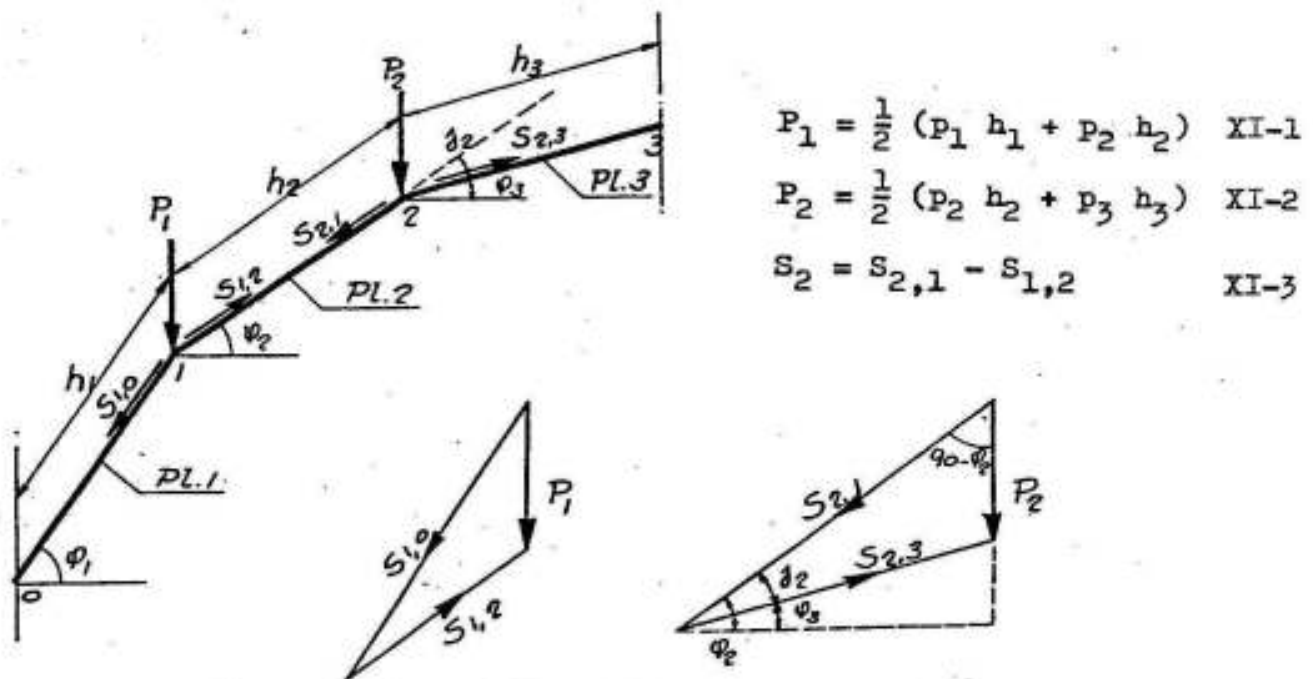


Fig. XI-4

Loads such as  $P_2$  applied at the ridge 2 are known as ridge loads. Considering a unit length of the folded plate, then  $P_2 = \frac{1}{2} (p_2 h_2 + p_3 h_3)$ .  $P_2$  may be resolved into plate loads  $S_{2,1}$  and  $S_{2,3}$  lying respectively in the planes of the second and third plates by means of a triangle of forces as shown in Fig. XI-4.

In the designation of plate loads such as  $S_{2,1}$  the first subscript



stands for the joint at which the load acts and the second subscript indicates the joint toward which the plate load is directed. Thus the plate load  $S_{2,1}$  is directed from joint 2 to joint 1 at ridge 2. The plate loads  $S$  may include the effect of the connecting moments in the cross direction. It is clear that the net plate load carried as a beam by e.g. the second plate is

$$S_{2,1} - S_{1,2} \quad \text{XI-3}$$

From the triangle of forces given in Fig. XI-4, it is easy to prove that:

$$S_{2,1} = \frac{P_2 \cos \phi_3}{\sin \phi_2} \quad \text{and} \quad S_{2,3} = \frac{P_2 \cos \phi_2}{\sin \phi_2} \quad \text{XI-4}$$

b) Free edge stresses and compatibility at the ridges

The distribution of the normal stresses in any section of a free plate subject to a bending moment  $M_0$  is given by:

$$\sigma_{b,t} = \pm M_0 / Z$$

where  $Z$  is the section modulus of a plate,  $Z = b h^2 / 6$  for rectangular sections of breadth  $b$  and height  $h$  as shown for plate 2 in Fig. XI-3 d and e.

If conditions are such that the free edge stresses are the same on both sides of all fold lines, then they are identical with the final stresses. This would be the case, for example, at the edges of an interior unit of a roof consisting of many identical units (e.g. intermediate joints of the Vee folded plate of Fig. XI-2). If, on the other hand, the initial plate analysis indicates a stress difference on either side of a fold line, an incompatibility is indicated which cannot actually exist, because the strains on either sides of a given fold line must be equal. This indicates the presence of longitudinal shears acting along the joint as shown in Fig. XI-3 a.

The stress due to an edge shear  $T$  can be calculated as follows:

Fig. XI-5

$$\sigma_{t,b} = T/A \pm M/Z \quad \text{where}$$

$$M = Th/2 \quad \text{and} \quad Z = bh^2/6, \quad \text{so that}$$

$$\sigma_{t,b} = \frac{T}{A} \pm \frac{T h}{2} \cdot \frac{6}{b h^2} = \frac{T}{A} \pm \frac{3 T}{A} \quad \text{or}$$

$$\sigma_t = + \frac{4 T}{A} \quad \text{and} \quad \sigma_b = - \frac{2 T}{A}$$

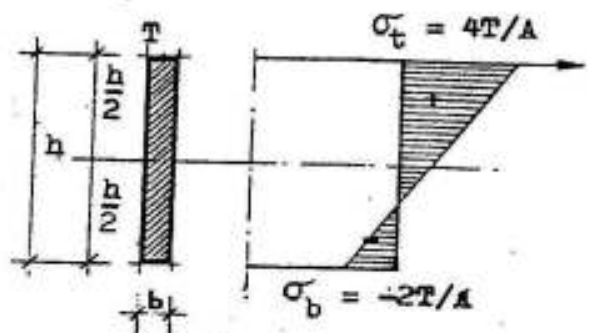


Fig. XI-5

XI-4) DETERMINATION OF EDGE SHEARS AND FINAL STRESSES

A) Theorem of Three Edge Shears

Stress at joint 2 in plate 2 is given by: Fig. XI-6.

$$\sigma_2 = -\frac{M_{o2}}{z_2} + \frac{4 T_2}{A_2} + \frac{2 T_1}{A_2}$$

Stress at joint 2 in plate 3 is given by:

$$\sigma_2 = +\frac{M_{o3}}{z_3} - \frac{4 T_2}{A_3} - \frac{2 T_3}{A_3}$$

But the fiber stress at joint 2 from plates 2 and 3 has to be the same as

the plates are monolithically connected; we may equate the two previous expressions to get:

$$\frac{T_1}{A_2} + 2 \left( \frac{T_2}{A_2} + \frac{T_2}{A_3} \right) + \frac{T_3}{A_3} = \frac{1}{2} \left( \frac{M_{o2}}{z_2} + \frac{M_{o3}}{z_3} \right) \quad \text{XI-5}$$

This relation is called the theorem of three edge shears similar to the known theorem of three moments.

Having determined the edge shears  $T$ , the final stresses can be computed by superposition.

B) Stress Distribution Method

The final stresses in a folded plate can be determined by the stress distribution method in the following manner: Fig. XI-7.

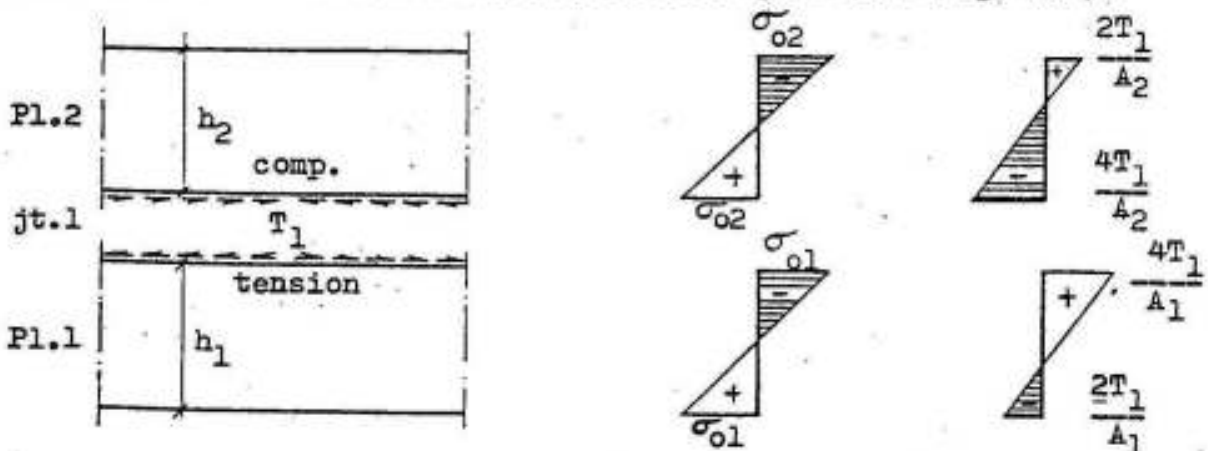


Fig. XI-7

Stresses in individual pl. for  $M_o$

Stresses in individual pl. for  $T_1$

The compatibility of strains at joint 1 necessitates that the stress  $\sigma$  at both sides of joint 1 be the same. Hence

$$\sigma_{o2} - \frac{4 T_1}{A_2} = \sigma_{o1} + \frac{4 T_1}{A_1} \quad \text{or} \quad \sigma_{o2} - \sigma_{o1} = 4 T_1 \left( \frac{1}{A_1} + \frac{1}{A_2} \right) \quad \text{i.e.}$$

$$\frac{4 T_1}{A_1} = (\sigma_{o2} - \sigma_{o1}) \frac{A_2}{A_1 + A_2} \quad \text{and} \quad -\frac{4 T_1}{A_2} = -(\sigma_{o2} - \sigma_{o1}) \frac{A_1}{A_1 + A_2} \quad \text{XI-6}$$

This means that the correction of the stress  $\sigma_{o1}$  due to  $T_1$ , which is  $4 T_1/A_1$ , is equal to the difference  $(\sigma_{o2} - \sigma_{o1})$  multiplied by the distribution factor  $A_2/(A_1+A_2)$  and the correction of the stress  $\sigma_{o2}$  due to  $T_1$ , which is  $-4T_1/A_2$  is equal to  $-(\sigma_{o2} - \sigma_{o1})$  multiplied by the distribution factor  $A_1/(A_1+A_2)$ .

These relations show that the difference of stresses in a joint can be distributed on the plates 1 and 2 meeting in joint 1 in the following ratio:

Distribution factor for plate 1 equals	$A_2 / (A_1 + A_2),$	and
" " " " 2 "	$A_1 / (A_1 + A_2),$	

It is clear that the carry-over-factor is  $- 1/2$ .

This method can be directly used instead of the three shears equation XI-5.

#### XI-5) SHEAR STRESSES IN FOLDED PLATES

The shear stresses due to slab action are generally very small and need not to be considered.

The main shear stresses are due to the beam action of the different plates; they are caused by the shearing forces of the plate loads  $S$  and the edge shears  $T$ .

Our study will be restricted to simple prismatic folded plates only.

Due to the force  $S/m$  acting on a plate of breadth  $b$ , depth  $h$  i.e. (area  $A = b h$ ) and span  $l$ , the maximum shearing force  $Q_{\max}$  at the dia-

phragms is given by:

$$Q_{\max} = S l / l$$

It causes parabolic shear stresses  $\tau_o$ , with a maximum value at the middle height of the section of the plate equal to: Fig. XI-8.

$$\tau_o \max = \frac{3}{2} \frac{Q_{\max}}{A} \quad \text{XI-7}$$

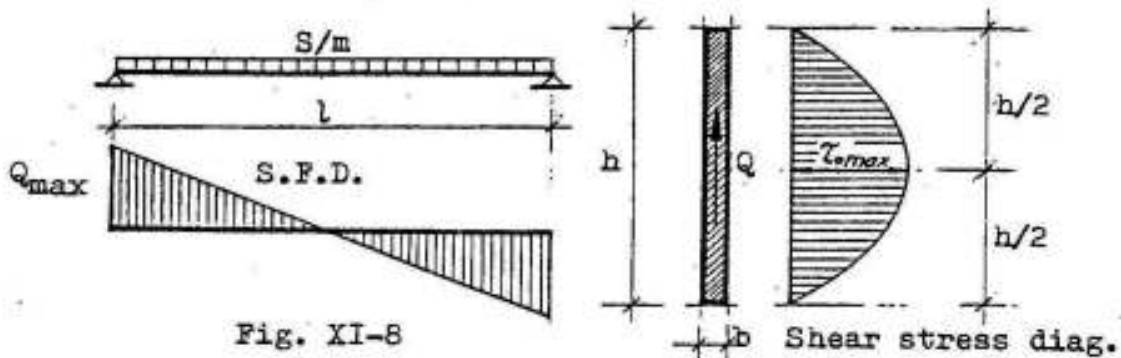


Fig. XI-8

When calculating the shear stresses  $\tau$  due to the edge shears  $T$ , one has to notice that the edge shear diagram at any fold line is similar to that of the bending moment due to  $S$ , i.e. parabolic with maximum value at midspan and zero at the supports in case of simple folded plates. It is therefore easy to prove that the edge shear  $T$  at a distance  $x$  from the support of a plate is given by:

$$T = T_{\max} \frac{4x}{l} \left(1 - \frac{x}{l}\right) \quad \text{XI-8}$$

where  $T_{\max}$  is the maximum edge shear at midspan ; it may be calculated from equation XI-5.

The shear stress distribution on a section at a distance  $x$  from the support due to an edge shear  $T$  at one of the edges of a plate is also parabolic as shown in Fig. XI-9. Its maximum value  $\tau$  at the edge

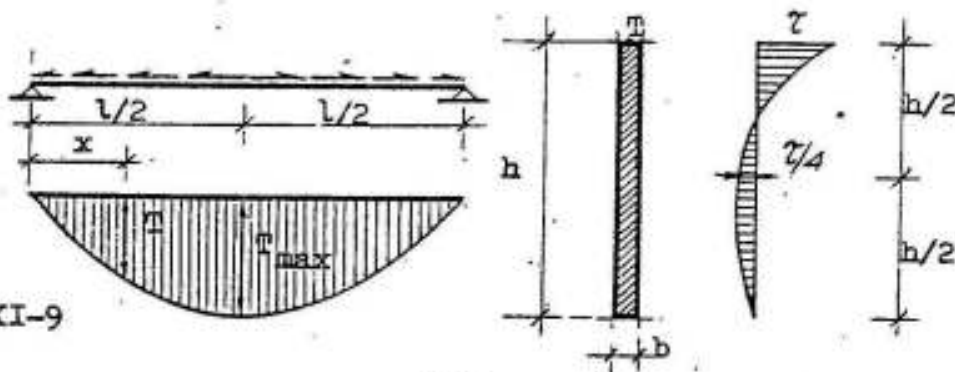


Fig. XI-9

where  $T$  is applied is given by:

$$\tau = \frac{4 T_{\max}}{b l} \left(1 - \frac{2x}{l}\right) \quad \text{XI-9}$$

The shear stress at midheight of plate is equal to  $\tau/4$ . Fig. XI-9.

If the plate is subject to two edge shears  $T_1$  and  $T_2$  at its top and bottom edges, the distribution of shear stresses will be as shown in Fig. XI-10.

At the end diaphragms of a plate ( $x = 0$ ), the shear stress due to an edge shear  $T$  is therefore:

$$\tau = \frac{4 T_{\max}}{b l} \quad \text{XI-10}$$

and the value at midheight of plate is

$$\frac{\tau}{4} = \frac{T_{\max}}{b l} \quad \text{XI-11}$$

In simple folded plates, the sense of the shear stresses due to edge shears is positive at the top and bottom edges of the plate and negative at midheight and hence, these last values are to be subtracted from  $\tau_{\max}$ .

The determination of the longitudinal and transverse reinforcements as well as the web reinforcements will be shown in the following examples.

#### XI-6) ILLUSTRATIVE EXAMPLES

1) It is required to cover an area  $32.8 \times 20.0$  ms by a folded plate roof. Columns are allowed in the outside perimeter only. Fig. XI-11.

The arrangement shown in Fig. XI-11 gives a convenient simple solution for the following reasons:

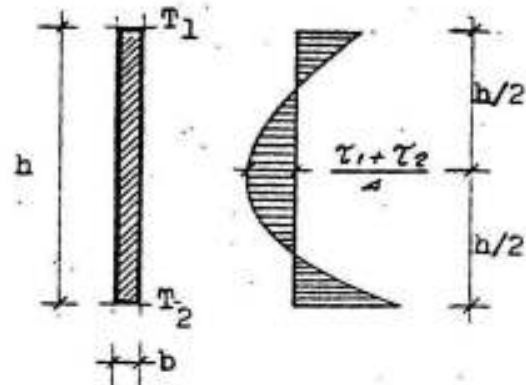


Fig. XI-10

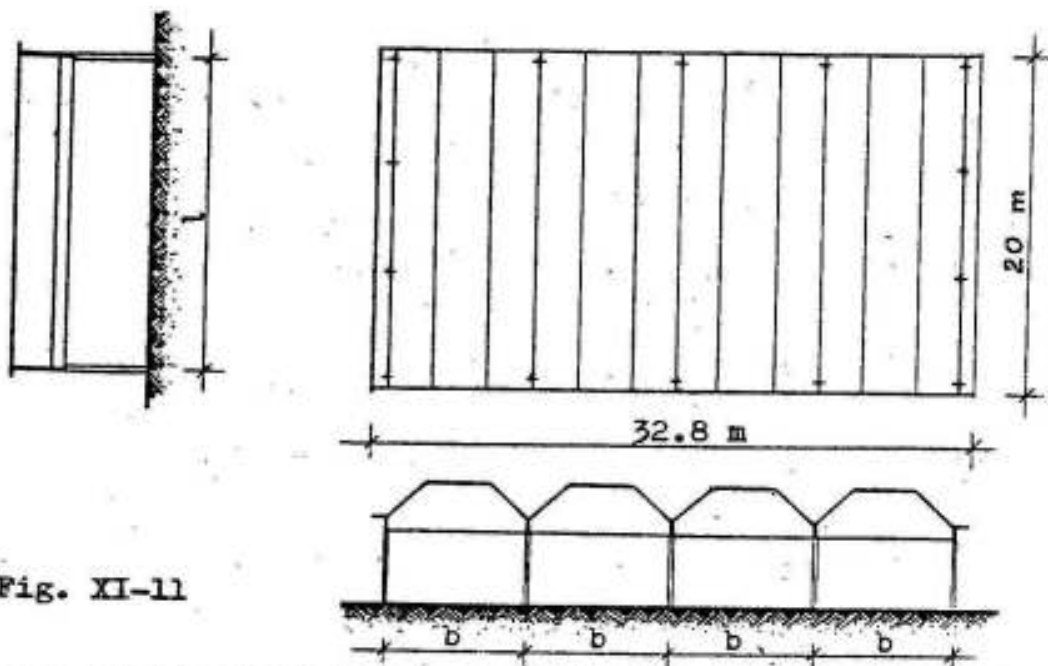


Fig. XI-11

- a) The span of the folded plate roof is chosen in the shorter direction.
- b) The span being relatively big, the system is chosen such that the compressive stresses can be easily resisted by the horizontal part of the folded roof and the big amount of the tension steel can be easily arranged in the edge beams.
- c) The height of the folded slab is chosen 1.8 ms and that of the edge beam is -theoretically- 0.70 ms so that the total height of 2.5 ms is @  $1/7.5$  the span  $l$  of 18.4 ms.
- d) All interior folded plates have the same length of 3.0 ms.

The chosen concrete dimensions are shown in details in Fig. XI-12.

Design of interior bay of roof in transverse direction (slab action)

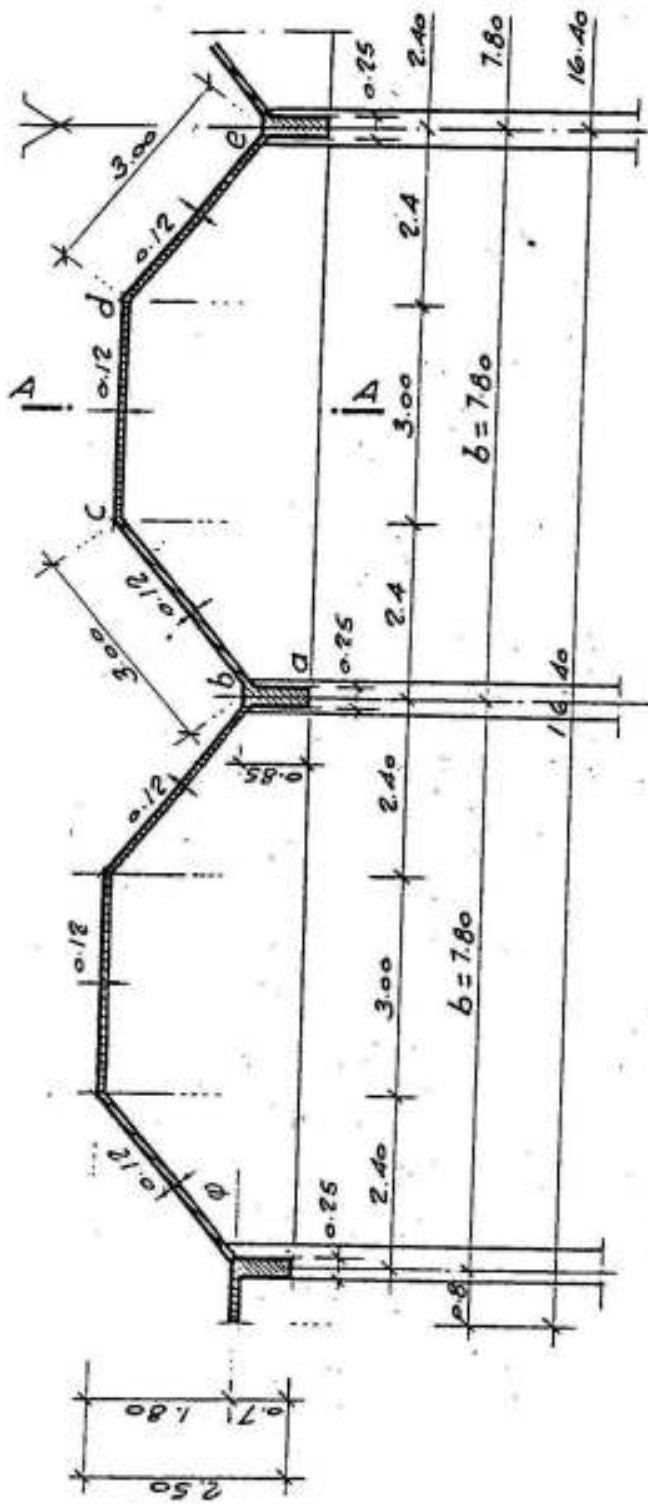
Assume slab thickness = 12 cms      Load/m<sup>2</sup> surface =  $0.12 \times 2500 = 300 \frac{\text{kg}}{\text{m}^2}$   
 " superimposed load (L.L, cover & plaster) / m<sup>2</sup> surface = 100

Total load on horizontal slab       $w = 400$

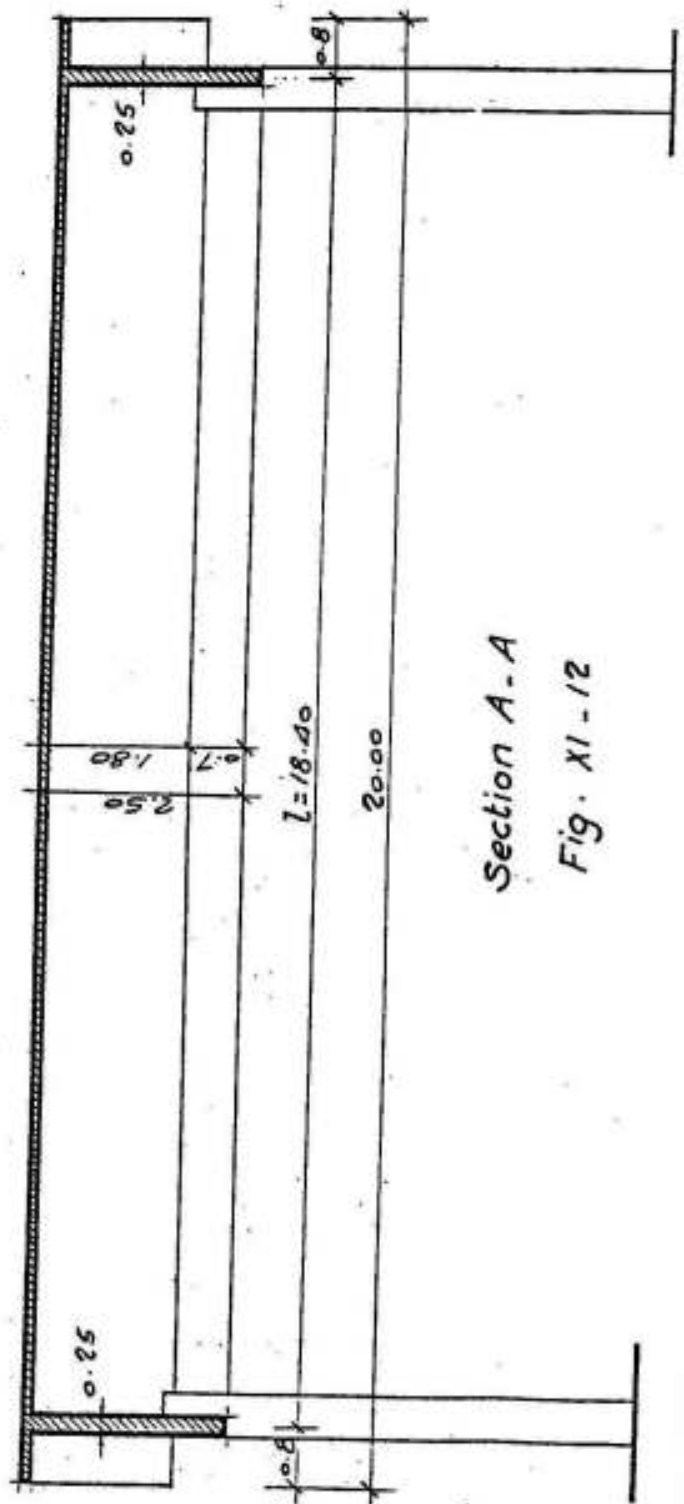
Total load, causing bending moments, on inclined slabs

$$w' = w \cos \phi = 320$$

The slab may be assumed as fixed at  $b$  and  $e$ , so that the bending mo-



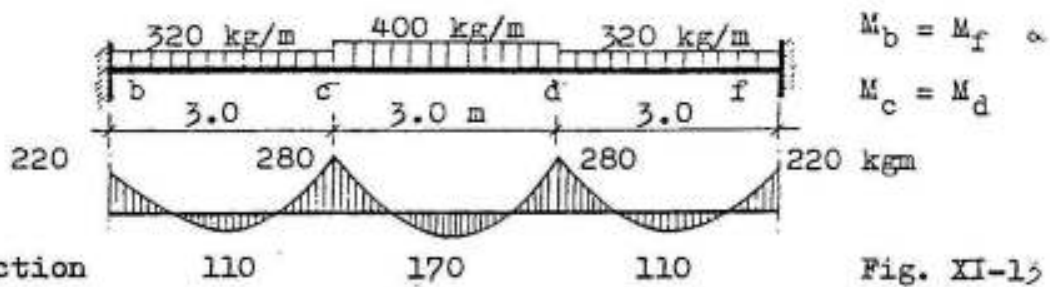
$\sin \phi = 0.6$      $\cos \phi = 0.8$      $\tan \phi = 0.75$



Section A-A

Fig. XI-12

ment in the transverse direction as follows: (Fig. XI-13)



$$2 M_b \times 3.0 + M_c \times 3.0 = -6 \times \frac{320 \times 3.0^3}{24} \quad \text{or} \quad 2 M_b + M_c = -720$$

$$M_b \times 3.0 + 2 M_c \times 6.0 + M_c \times 3.0 = -6 \left( \frac{320 \times 3.0^3}{24} + \frac{400 \times 3.0^3}{24} \right)$$

$$\text{or} \quad M_b + 5 M_c = -1620$$

giving  $M_b = -220 \text{ kgm}$  and  $M_c = -280 \text{ kgm}$

Hence, the bending moment diagram is as shown in Fig. XI-13. However, the field moment in panels b c and d f should not be smaller than:

$$M_+ = \frac{320 \times 3.0^2}{24} = 120 \text{ kgm}$$

The bending moments are very small for a slab thickness of 12 cms, hence, a minimum main steel of 6  $\phi$  8 mm/m may be used. The distributors are chosen 5  $\phi$  6 mm/m.

#### Design of interior bay of roof in longitudinal direction (beam action)

Since each of the 25 cms wide beams is common for two bays of the folded roof, the beams belonging to one bay are to be introduced with a breadth of 12.5 cms

#### Ridge loads per bay

$P_b$  = own weight of ridge beam +  $\frac{1}{2}$  load of plate b c + weight of slope concrete plus rain water in gutter, or

$$P_b = 0.125 \times 0.85 \times 2500 + 1.5 \times 400 + 135 = 265 + 600 + 135$$

$$= \underline{1000 \text{ kg/m}}$$

$$P_c = 3.0 \times 400 = \underline{1200 \text{ kg/m}}$$



Resolution of ridge-load (Fig. XI-14)

Load on plate 1 =  $P_b = 1000 \text{ kg/m}$   
 " " " 2 =  $S_{c,b} = 2000$  "  
 " " " 3 =  $S_{c,d} = S_{d,c} = 0$

because of symmetry:

$$S_{c,d} = S_{d,c}$$

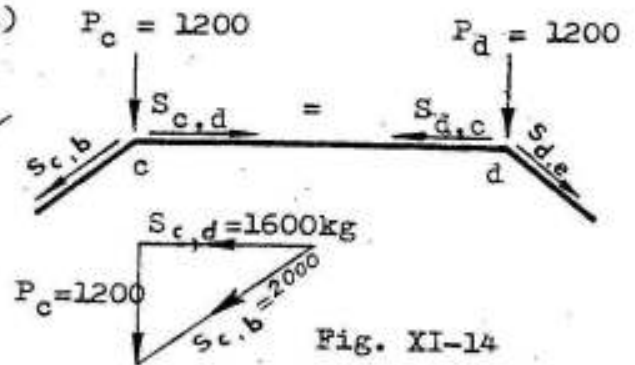


Fig. XI-14

Moments and properties of individual plates

Plate	b m	h m	A = b h m <sup>2</sup>	Z = $\frac{b h^2}{6}$ m <sup>3</sup>	S kg/m	M <sub>o</sub> = S $\frac{18.4^2}{8}$ kg m
1	0.125	0.85	A <sub>1</sub> = 0.106	Z <sub>1</sub> = 0.0151	1000	M <sub>o1</sub> = 42320
2	0.120	3.00	A <sub>2</sub> = 0.360	Z <sub>2</sub> = 0.180	2000	M <sub>o2</sub> = 84640
3	0.120	3.00	A <sub>3</sub> = 0.360	Z <sub>3</sub> = 0.180	0	M <sub>o3</sub> = 0

Edge shears

The application of equation XI-5 to joints b and c respectively gives:

$$\text{Joint b: } 0 + 2 \left( \frac{T_b}{A_1} + \frac{T_b}{A_2} \right) + \frac{T_c}{A_2} = \frac{1}{2} \left( \frac{M_{o1}}{Z_1} + \frac{M_{o2}}{Z_2} \right) \quad \text{or}$$

$$0 + 2 \left( \frac{T_b}{0.106} + \frac{T_b}{0.36} \right) + \frac{T_c}{0.36} = \frac{1}{2} \left( \frac{42320}{0.0151} + \frac{84640}{0.180} \right) \quad \text{or}$$

$$8.72 T_b + T_c = 589 \times 10^3 \quad \text{and}$$

$$\text{Joint c: } \frac{T_b}{A_2} + 2 \left( \frac{T_c}{A_2} + \frac{T_c}{A_3} \right) + \frac{T_d}{A_3} = \frac{1}{2} \left( \frac{M_{o2}}{Z_2} + 0 \right) \quad \text{but } T_d = -T_c$$

$$\text{then } \frac{T_b}{0.36} + 2 \left( \frac{T_c}{0.36} + \frac{T_c}{0.36} \right) - \frac{T_c}{0.36} = \frac{1}{2} \times \frac{84640}{0.180} \quad \text{or}$$

$$0.33 T_b + T_c = 28.213 \times 10^3$$

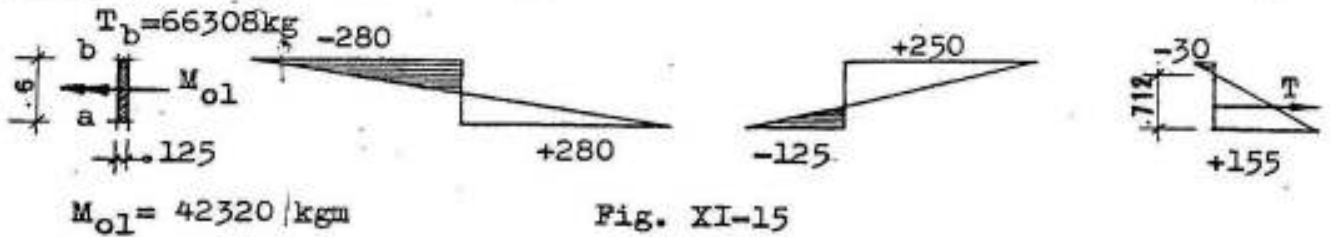
Therefore  $T_b = 66308 \text{ kgs}$  and  $T_c = 6113 \text{ kgs}$

The final normal stresses in the different plates will be determined

by superposition as follows:

Normal stresses in the different plates due to beam action

Plate 1: Fig. XI-15



Stresses due to:  $M_{o1} = 42320 \text{ kgm} : \sigma_b = \mp \frac{M_{o1}}{Z_1} = \mp \frac{4232000}{15100} = \mp 280 \text{ kg/cm}^2$

$T_b = 66308 \text{ kgs} : \sigma_b = + \frac{4T_b}{A_1} = + \frac{4 \times 66308}{1060} = + 250 \text{ ''}$

$\sigma_a = - \frac{2T_b}{A_1} = - \frac{2 \times 66308}{1060} = - 125 \text{ ''}$

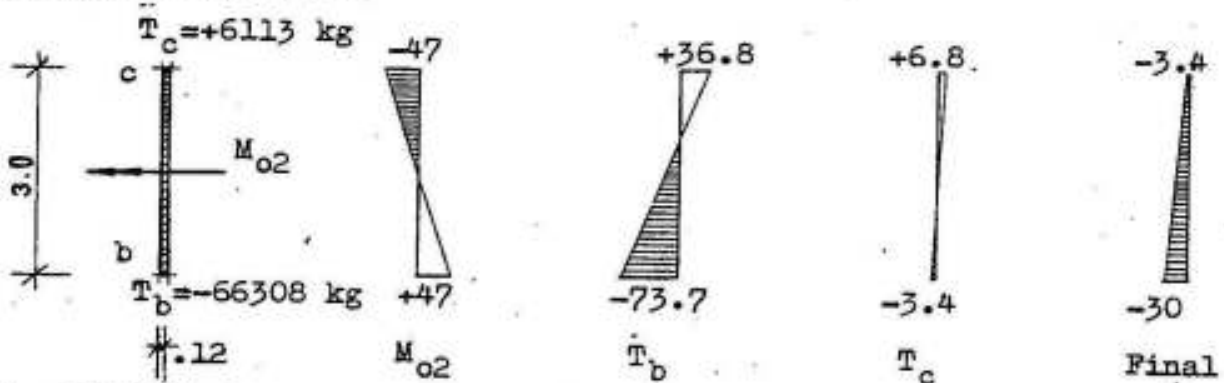
Final stresses:

$\sigma_a = + 280 - 125 = + 155 \text{ ''}$

$\sigma_b = - 280 + 250 = - 30 \text{ ''}$

Height of tension zone:  $= 0.85 \times \frac{155}{155 + 30} = 0.712 \text{ ms}$

Plate 2: Fig. XI-16



$M_{o2} = 84640 \text{ kgm}$

Stresses due to:  $M_{o2} = 84640 \text{ kgm} : \sigma_b = \pm \frac{M_{o2}}{Z_2} = \pm \frac{8464000}{180000} = \pm 47 \text{ kg/cm}^2$

$T_b = -66308 \text{ kgs} : \sigma_b = + \frac{4T_b}{A_2} = - \frac{4 \times 66308}{3600} = - 73.7 \text{ ''}$

$\sigma_c = - \frac{2T_b}{A_2} = + \frac{2 \times 66308}{3600} = + 36.3 \text{ ''}$

Plate 2 (contd)

Stresses due to:  $T_c = + 6113$  kgs :  $\sigma_c = + \frac{4T_c}{A_2} = + \frac{4 \times 6113}{3600} = + 6.8$  kg/

$$\sigma_b = - \frac{2T_c}{A_2} = - \frac{2 \times 6113}{3600} = - 3.4 \quad "$$

Final stresses:

$$\sigma_b = + 47 - 73.7 - 3.4 = \underline{- 30} \quad "$$

$$\sigma_c = - 47 + 36.8 + 6.8 = \underline{- 3.4} \quad "$$

Plate 3

Stresses due to:  $T_c = - 6113$  kgs :  $\sigma_c = - \frac{4T_c}{A_3} = - \frac{4 \times 6113}{3600} = - 6.8 \quad "$

$$T_d = - 6113 \text{ kgs} : \sigma_c = + \frac{2T_c}{A_3} = + \frac{2 \times 6113}{3600} = + 3.4 \quad "$$

Final stresses:

$$\sigma_c = \sigma_d = - 6.8 + 3.4 = \underline{- 3.4} \quad "$$

The final normal stress distribution in the folded plate is shown in Fig. XI-18.

The final stresses calculated above can be determined using the stress-distribution method in the following manner:

Areas  $A_1 = 1060 \text{ cm}^2$        $A_2 = 3600 \text{ cm}^2$        $A_3 = 3600 \text{ cm}^2$   
 D.F.  $D_1 = \frac{1060}{1060 + 3600} = 0.227$        $D_2 = \frac{3600}{3600 + 3600} = 0.50$

Plate	a	1	b	2	c	3
Dist. Factor		0.773	0.227	0.500	0.500	
Distribution	+280	-280	+47.0	-47.0	0	
		+252	-75.0	+23.5	-23.5	
Carry over Distribution	-126	0	-11.75	+37.5	+11.25	
		-9.10	+ 2.65	-13.13	+13.13	
Carry over Distribution	+4.6	0	+ 6.57	-1.33	- 6.56	
		+5.07	- 1.50	-2.62	+ 2.62	
Carry over Distribution	-2.54	0	+ 1.31	+0.57	- 1.31	
		+1.01	- 0.30	-1.03	+ 1.03	
Final stresses	+156	-31	-31	-3.4	-3.4	

The results are approximately the same as in the previous solution.

Determination of longitudinal tension steel

The longitudinal tension steel is chosen such that it resists all the tensile force  $T$  in the section. Accordingly, the tension in any intermediate edge beam 25 x 85 cms is given by: Fig. XI-17.

$$T = 155 \times \frac{712}{2} \times 25 = 138\,000 \text{ kgs}$$

Using high grade tension steel with  $f_y = 3600 \text{ kg/cm}^2$  and  $\sigma_s = 0.9 \times 2000$  i.e.  $\sigma_s = 1800 \text{ kg/cm}^2$ , we get:

$$A_s = \frac{138\,000}{1800} = 76.5 \text{ cm}^2 \quad 13\phi 28.$$

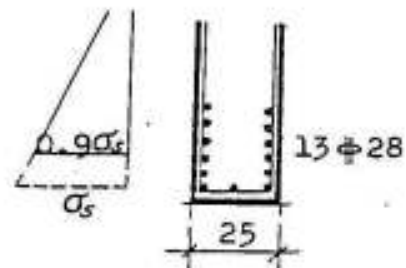


Fig. XI-17

Shear stresses in plate 1

Max. shearing force at diaphragms:  $Q_{\max} = \frac{P_b l}{2} = \frac{1000 \times 18.4}{2} = 9200 \text{ kgs}$

Shear stress at midheight of plate  $\tau_{\text{omax}} = \frac{3}{2} \frac{Q_{\max}}{A} = \frac{3}{2} \frac{9200}{1060} = 13 \text{ kg/cm}^2$

Shear stress at diaphragms due to  $T_b \text{ max} = 66308 \text{ kgs}$  is:

at top edge  $\tau = \frac{4T_{\text{max}}}{b l} = \frac{4 \times 66\,308}{12.5 \times 1840} = 11.6 \text{ ''}$

at mid-height  $\tau/4 = 11.6 / 4 = 2.9 \text{ ''}$

Total shear stress at mid-height =  $13 - 2.9 = 10.1 \text{ ''}$

In plate 2

Max. shearing force at diaphragms:  $Q_{\max} = \frac{S_{c,b} l}{2} = \frac{2000 \times 18.4}{2} = 18400 \text{ kgs}$

Shear stress at midheight of plate  $\tau_{\text{omax}} = \frac{3}{2} \frac{Q_{\max}}{A} = \frac{3}{2} \frac{18400}{3600} = 7.7 \text{ kg/cm}^2$

Shear stress at b due to  $T_b \text{ max} = 66308 \text{ kgs}$  is  $\frac{4 \times 66308}{12 \times 1840} = 12.0 \text{ ''}$

Shear stress at c due to  $T_c \text{ max} = 6113 \text{ kgs}$  is given by:

$$\tau_c = \frac{4 \times 6113}{12 \times 1840} = 1.10 \text{ kg/cm}^2$$

Shear stress at middle of b c =  $7.7 - \frac{12}{4} - \frac{1.1}{4} = \underline{4.42 \text{ kg/cm}^2}$

Accordingly, the shear stresses may be assumed as shown in Fig. XI-18 a. in which the maximum value of  $12 \text{ kg/cm}^2$  can be assumed constant in the tension zone of the section.

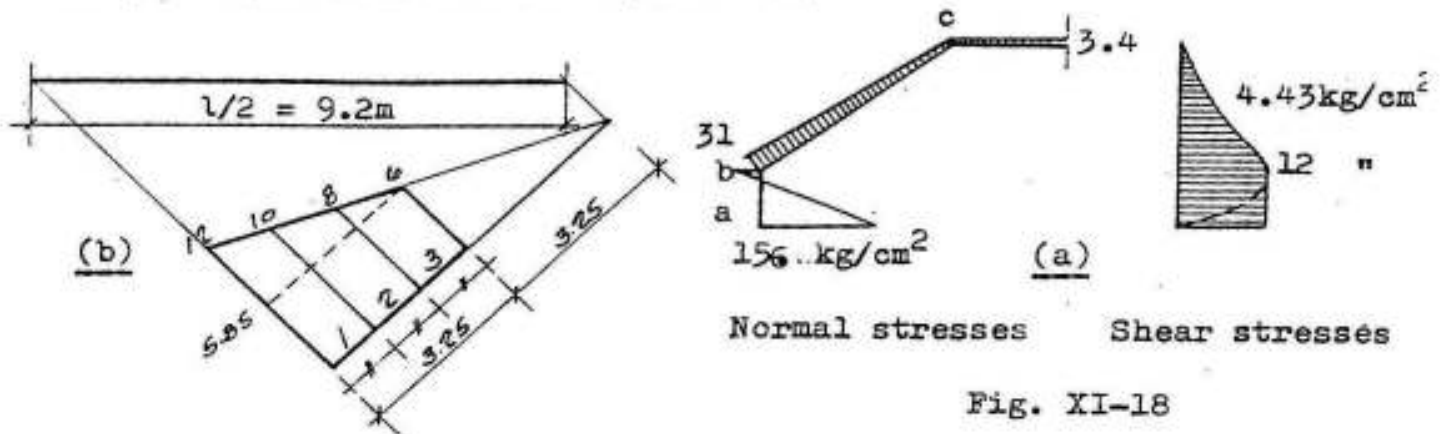


Fig. XI-18

The required diagonal web reinforcement can be calculated as in beams in the following manner: Fig. XI-18 b.

In zone 1 (1.08 m)  $A_{sb} = \frac{12 + 10}{2} \times 12 \times \frac{325}{3} \times \frac{1}{1400} = 10.2 \text{ cm}^2 \quad 8 \text{ } \phi \text{ } 13$

" " 2 "  $A_{sb} = \frac{10 + 8}{2} \times 12 \times \frac{325}{3} \times \frac{1}{1400} = 8.35 \text{ cm}^2$   
4  $\phi$  13 + 4  $\phi$  10

" " 3 "  $A_{sb} = \frac{8 + 6}{2} \times 12 \times \frac{325}{3} \times \frac{1}{1400} = 6.5 \text{ cm}^2 \quad 8 \text{ } \phi \text{ } 10$

It is however possible to resist a part of the diagonal tension at the diaphragms by the cross reinforcement  $6 \text{ } \phi \text{ } 8 \text{ mm/m}$  in which case it is advisable to have symmetrical reinforcement in top and bottom fibers of the slab as shown dotted in Fig. XI-19. In such a case, one proceeds as in beams by determining first the diagonal tension ( $\tau_{st}$ ) resisted by the cross reinforcements, where  $\tau_{st} = A_s \sigma_s / b s$ , and the rest of the diagonal tension diagram is to be resisted by bent bars.

Hence  $\tau_{st} = \frac{2 \times 0.5 \times 1400}{12 \times 20} = 5.85 \text{ kg/cm}^2$

and the area of bent bars in each zone is therefore:

In zone 1  $A_{sb} = \left( \frac{12+10}{2} - 5.85 \right) \times 12 \times \frac{325}{3} \times \frac{1}{1400} = 4.8 \text{ cm}^2 \quad 6 \text{ } \phi \text{ } 10$

Similarly, one needs in zone 2,  $6 \text{ } \phi \text{ } 8$ , and in zone 3,  $5 \text{ } \phi \text{ } 8 / 1.08 \text{ m}$ .

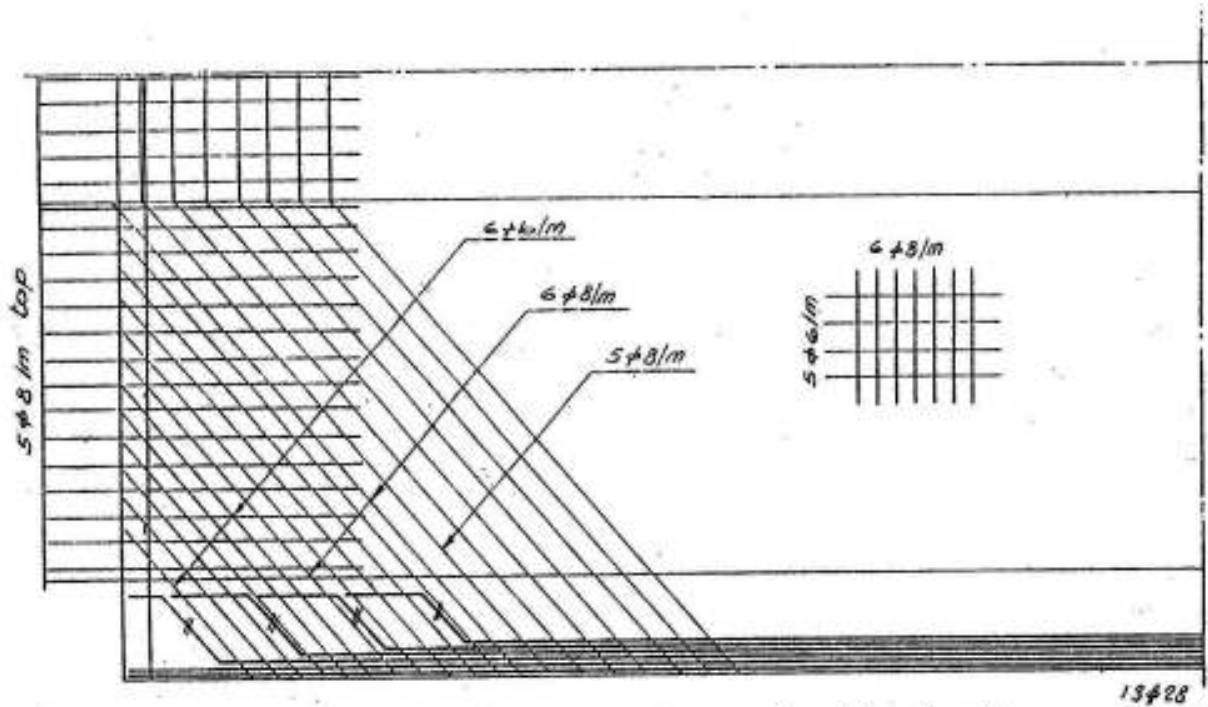
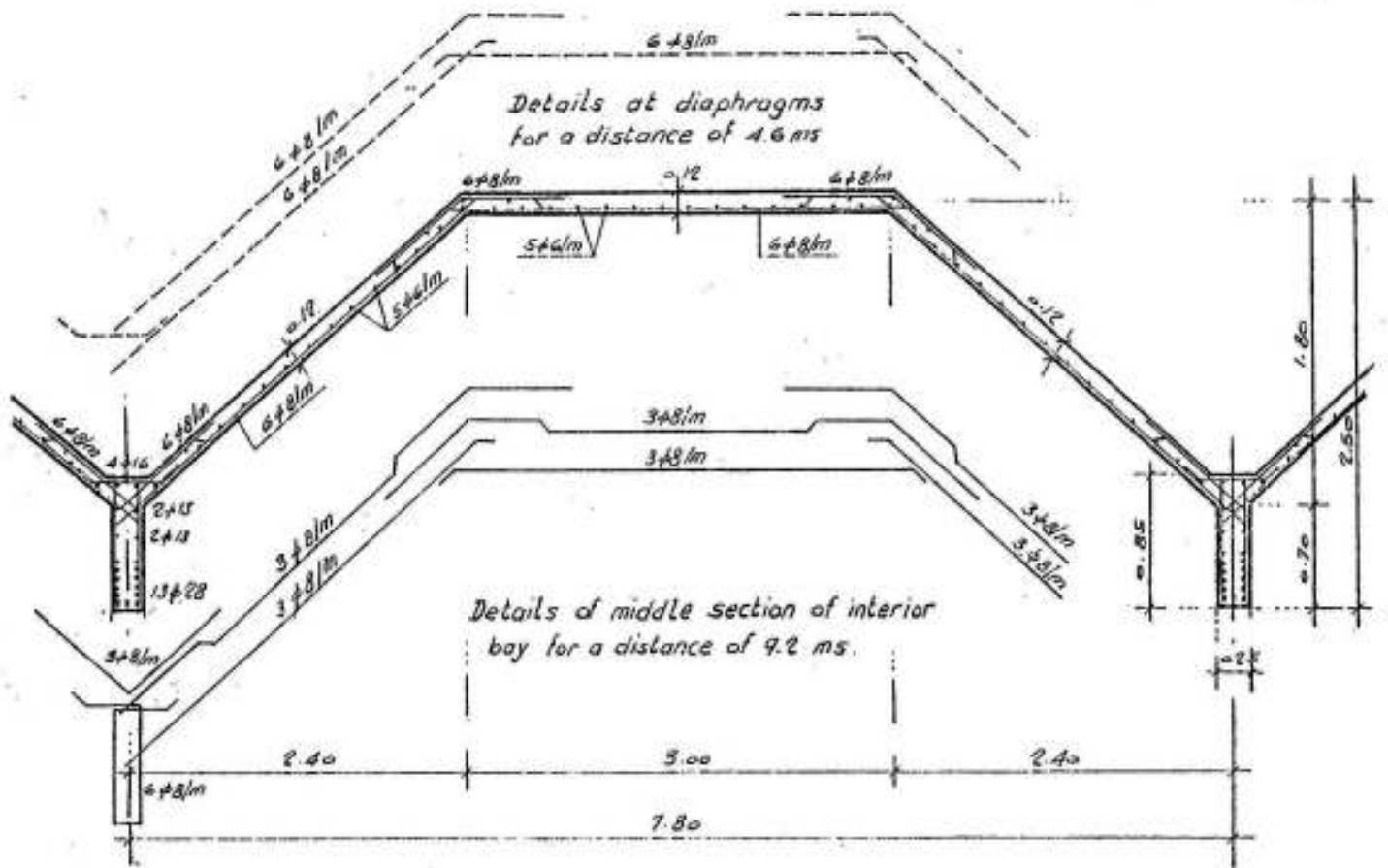


Fig. XI-19

The details of reinforcements are shown in Fig. XI-19.

2) It is required to design an interior panel of the simple saw-tooth folded plate roof (20.0 x 32.0 ms) shown in Fig. XI-20 for its own weight plus a superimposed load of  $100 \text{ kg/m}^2$  surface.

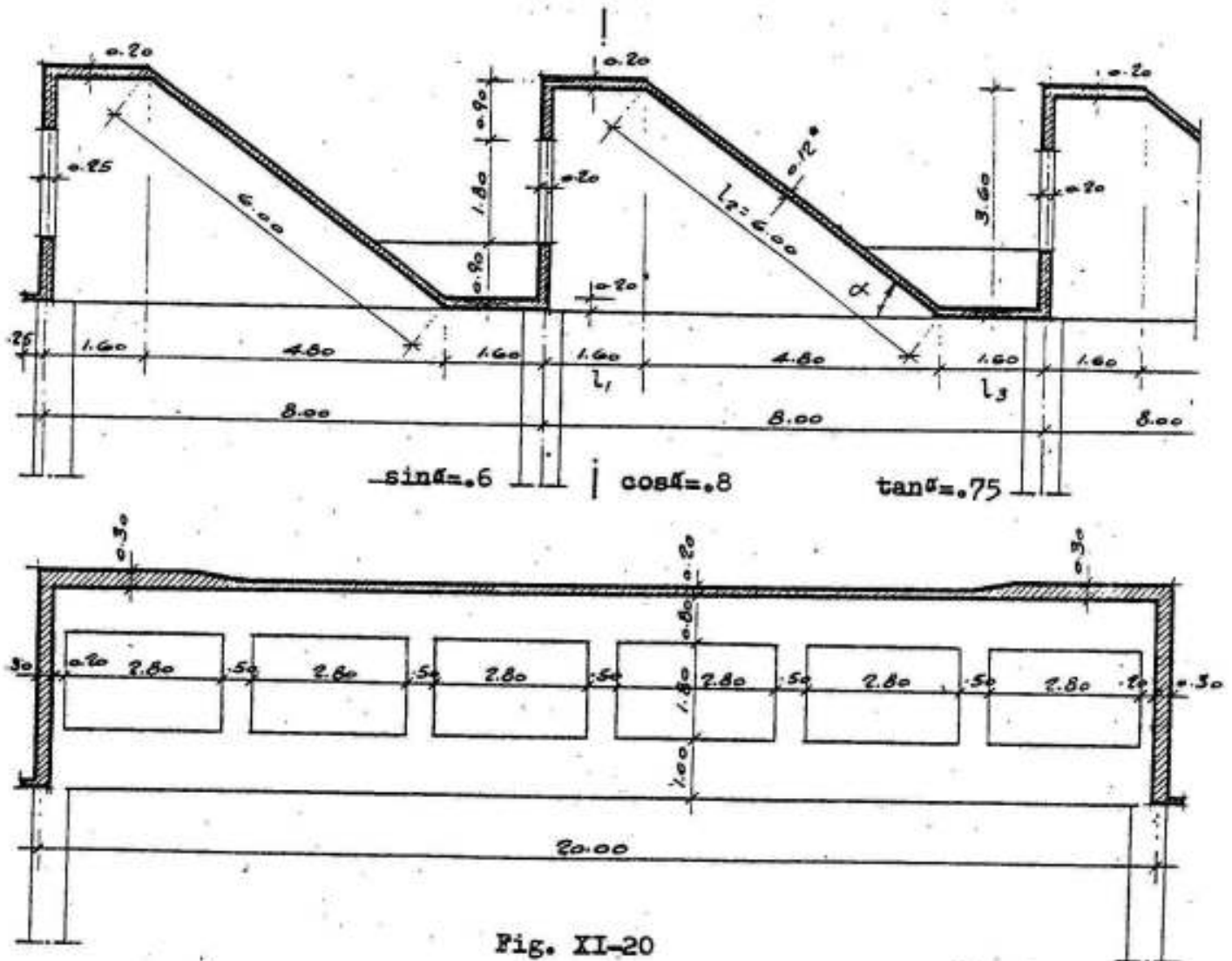


Fig. XI-20

Design of interior panel of roof in transverse direction (slab action)

The bending moments of the slab in the transverse direction shall be determined by the equation of three moments in which  $M_2 = M_3$  due to symmetry. Fig. XI-21

Further, the plates 2 and 4 are short relative to plate 3, then their elastic reactions at corners 2 and 3 due to loading of these

plates may be neglected. Hence

$$2 M_2 \left( \frac{l_2}{I_2} + \frac{l_3}{I_3} \right) + M_3 \frac{l_3}{I_3} = - 6 \frac{w' l_3^3}{24 I_3}$$

Multiplying both sides by  $\frac{I_2}{l_2}$  and assuming  $\lambda = \frac{I_2}{I_3} \cdot \frac{l_3}{l_2}$ , we get:

$$2 M_2 (1 + \lambda) + M_3 \lambda = - \frac{w' l_3^2}{4} \cdot \lambda \quad \text{but}$$

$$\lambda = \left( \frac{0.2}{0.12} \right)^3 \times \frac{6.0}{1.6} = 17.4$$

Assuming  $w' = 320 \text{ kg/m}^2$  (refer to example 1), then

$$2 M_2 (1 + 17.4) + 17.4 M_2 = - \frac{320 \times 6.0^2}{4} \times 17.4$$

Therefore  $M_2 = M_3 = - 920 \text{ kg m}$  and

$$M_m = \frac{w' l_3^2}{8} - 920 = \frac{320 \times 6.0^2}{8} - 920 = 1440 - 920 = 520 \text{ kgm}$$

By redistribution, one may assume  $M_m = - M_2 = - M_3 = 720 \text{ kgm}$ ; so that a thickness of plate 3 of 12 cms and main reinforcements  $7 \phi 10 \text{ mm/m}$  may be safely accepted. The distributors are chosen  $5 \phi 6 \text{ mm/m}$ .

Ridge loads P Fig. XI-21

Own weight of plate 1 (and 5) ..... =  $0.2 \times 0.9 \times 2500 = 450 \text{ kg/m}$   
 Load on plate 2 (and 4), 20 cms thick, + concrete cover + superimposed load ..... =  $0.2 \times 2500 + 200 + 100 = 800 \text{ kg/m}$   
 Load on plate 3, 12 cms thick, ..... =  $0.12 \times 2500 + 100 = 400 \text{ kg/m}$

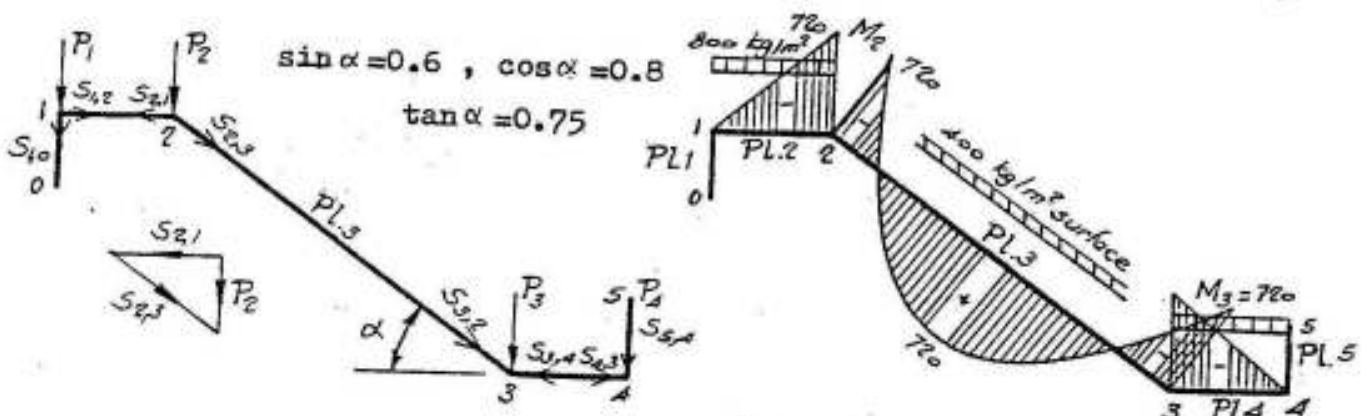


Fig. XI-21



Therefore:

$$P_1 = P_4 = \text{own wt of plate 1} + \frac{1}{2} \text{ load on plate 2} + \text{glazing} - \frac{M_2}{l_2}$$

$$= 450 + \frac{1}{2} \times 800 \times 1.6 + 100 - \frac{720}{1.6} = 740 \text{ kg/m'}$$

$$P_2 = P_3 = \text{half loads on plates 2 and 3} + \frac{M_2}{l_2} + \frac{M_3 - M_2}{l_3}$$

$$\frac{1}{2} (800 \times 1.6 + 400 \times 6.0) + \frac{720}{1.6} + 0 = 2290 \text{ kg/m'}$$

Resolution of ridge loads Fig. XI-21

$$S_{1,0} = S_{5,4} = P_1 = P_4 = 740 \text{ kg/m'}$$

$$S_{2,1} = S_{3,4} = P_2 / \tan \alpha = 2290 / 0.75 = 3053 \text{ kg/m'}$$

$$S_{2,3} = S_{3,2} = P_2 / \sin \alpha = 2290 / 0.60 = 3817 \text{ kg/m'}$$

$$\text{Total force on plate 3: } S = 2 \times 3817 = 7634 \text{ kg/m'}$$

Free moments and properties of individual plates

Plate	b m	h m	A = b h m <sup>2</sup>	Z = $\frac{b h^2}{6}$ m <sup>3</sup>	S kg/m	M <sub>o</sub> = S $\frac{20.0^2}{8}$ kgm
1	0.20	0.90	A <sub>1</sub> = 0.18	Z <sub>1</sub> = 0.0270	740	M <sub>o1</sub> = 37.00x10 <sup>3</sup>
2	0.20	1.60	A <sub>2</sub> = 0.32	Z <sub>2</sub> = 0.0853	3053	M <sub>o2</sub> = 152.65x10 <sup>3</sup>
3	0.12	6.00	A <sub>3</sub> = 0.72	Z <sub>3</sub> = 0.7200	7634	M <sub>o3</sub> = 381.70x10 <sup>3</sup>
4	0.20	1.60	A <sub>4</sub> = 0.32	Z <sub>4</sub> = 0.0853	3053	M <sub>o4</sub> = 152.65x10 <sup>3</sup>
5	0.20	0.90	A <sub>5</sub> = 0.18	Z <sub>5</sub> = 0.0270	740	M <sub>o5</sub> = 37.00x10 <sup>3</sup>

Edge shears

The application of equation XI-5 to joints 1 and 2 respectively gives:

$$\text{Joint 1: } 0 + 2 \left( \frac{T_1}{A_1} + \frac{T_1}{A_2} \right) + \frac{T_2}{A_2} = \frac{1}{2} \left( \frac{M_{o1}}{Z_1} + \frac{M_{o2}}{Z_2} \right) \quad \text{or}$$

$$0 + 2 \left( \frac{T_1}{0.18} + \frac{T_1}{0.32} \right) + \frac{T_2}{0.32} = \frac{1}{2} \left( \frac{37000}{0.027} + \frac{152650}{0.0853} \right) \quad \text{or}$$

$$17.36 T_1 + 3.125 T_2 = 1579968 \quad \text{and}$$

Joint 2:  $\frac{T_1}{A_2} + 2 \left( \frac{T_2}{A_2} + \frac{T_2}{A_3} \right) + \frac{T_3}{A_3} = \frac{1}{2} \left( \frac{M_{o2}}{Z_2} - \frac{M_{o3}}{Z_3} \right)$  but  $T_2 = T_3$

then  $\frac{T_1}{0.32} + 2 \left( \frac{T_2}{0.32} + \frac{T_2}{0.72} \right) + \frac{T_2}{0.72} = \frac{1}{2} \left( \frac{152650}{0.0853} - \frac{381700}{0.72} \right)$  or

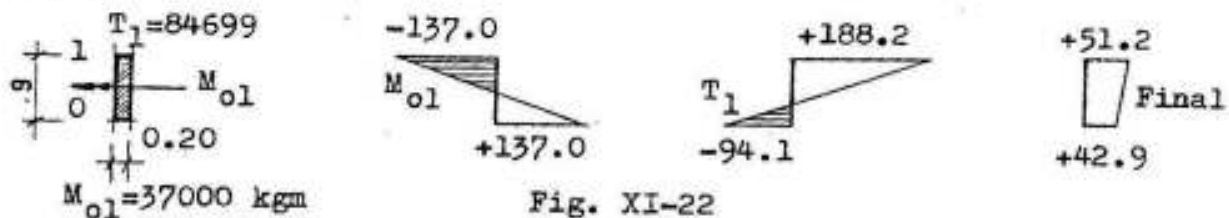
$$3.125 T_1 + 10.40 T_2 = 629713$$

Therefore  $T_1 = 84699$  kgs and  $T_2 = 35071$  kgs

The final normal stresses in the different plates will be determined by superposition as follows:

Normal stresses in the different plates due to beam action

Plate 1 : Fig. XI-22



Stresses due to  $M_{o1} = 37000$  kgm:  $\sigma_0 = \mp \frac{M_{o1}}{Z_1} = \mp \frac{3700000}{27000} = \mp 137$  kg/cm<sup>2</sup>

$T_1 = 84699$  kgs:  $\sigma_1 = + \frac{4 T_1}{A_1} = + \frac{4 \times 84699}{1800} = + 188.22$  "

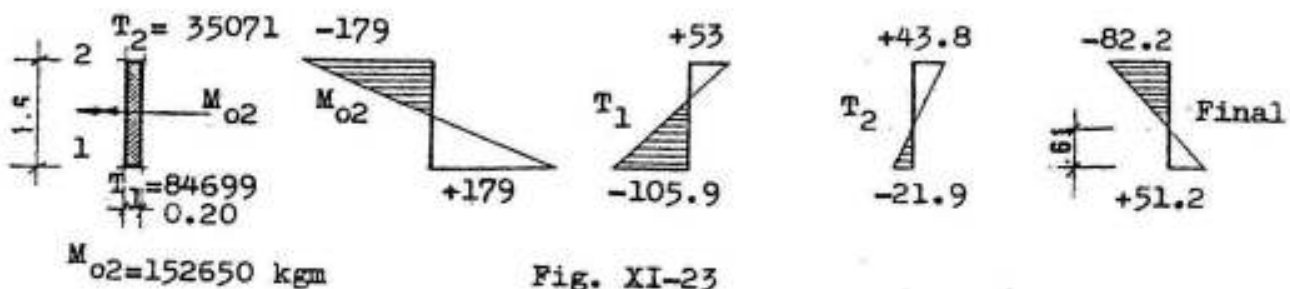
$\sigma_0 = - \frac{2 T_1}{A_1} = - \frac{2 \times 84699}{1800} = - 94.11$  "

Final stresses:

$\sigma_1 = - 137.00 + 188.22 = + 51.20$  "

$\sigma_0 = + 137.00 - 94.11 = + 42.90$  "

Plate 2: Fig. XI-23



Stresses due to  $M_{o2} = 152650 \text{ kgm}$ :  $\sigma_2 = \mp \frac{M_{o2}}{Z_2} = \mp \frac{15265000}{85300} = \mp 179 \text{ kg/cm}^2$

" " "  $T_1 = 84699 \text{ kgs}$ :  $\sigma_1 = - \frac{4T_1}{A_2} = - \frac{4 \times 84699}{3200} = - 105.9$  "

$\sigma_2 = + \frac{2T_1}{A_2} = + \frac{2 \times 84699}{3200} = + 53.0$  "

" " "  $T_2 = 35071 \text{ kgs}$ :  $\sigma_2 = + \frac{4T_2}{A_2} = + \frac{4 \times 35071}{3200} = + 43.8$  "

$\sigma_1 = - \frac{2T_2}{A_2} = - \frac{2 \times 35071}{3200} = - 21.9$  "

Final stresses:

$\sigma_1 = + 179 - 105.9 - 21.9 = + 51.2$  "

$\sigma_2 = - 179 + 53 + 43.8 = - 82.2$  "

Height of tension zone =  $1.6 \times \frac{51.20}{82.2 + 51.2} = 0.61 \text{ ms}$

Plate 3: Fig. XI-24

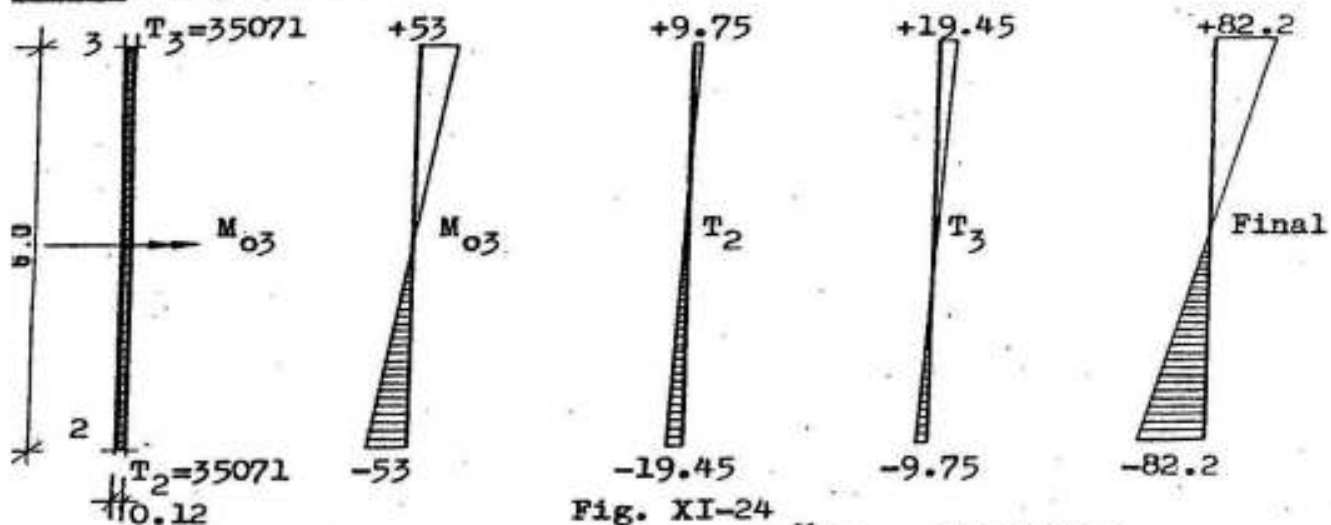


Fig. XI-24

Stresses due to  $M_{o3} = 381700 \text{ kgm}$ :  $\sigma_3 = \mp \frac{M_{o3}}{Z_3} = \mp \frac{38170000}{720000} = \mp 53 \text{ kg/cm}^2$

" " "  $T_2 = 35071 \text{ kgs}$ :  $\sigma_2 = - \frac{4T_2}{A_3} = - \frac{4 \times 35071}{7200} = - 19.45$  "

$\sigma_3 = + \frac{2T_2}{A_3} = + \frac{2 \times 35071}{7200} = + 9.75$  "

" " "  $T_3 = 35071 \text{ kgs}$ :  $\sigma_3 = + \frac{4T_3}{A_3} = + 19.45$ ,  $\sigma_2 = - \frac{2T_3}{A_3} = - 9.75$

Final stresses: .....  $\sigma_2 = -53 - 19.45 - 9.75 = \underline{-82.2 \text{ kg/cm}^2}$   
 $\sigma_3 = +53 + 19.45 + 9.75 = \underline{+82.2 \text{ "}}$

The final normal stresses calculated above can be determined using the stress-distribution method in the following manner:

Areas  $A_1 = 1800 \text{ cm}^2$   $A_2 = 3200 \text{ cm}^2$   $A_3 = 7200 \text{ cm}^2$ .

D.F.  $D_1 = \frac{1800}{1800 + 3200} = 0.36$   $D_2 = \frac{3200}{1800 + 3200} = 0.64$

$D_3 = \frac{3200}{3200 + 7200} = 0.308$   $D_4 = \frac{7200}{3200 + 7200} = 0.692$

Plate	1		2		3		4		5	
Dist. factor	.64	.36	.692	.308	.308	.692	.36	.64		
Stress	+137	-137	+179	-179	-53	+53	+179	-179	+137	-137
Distribution		+202.2	-113.8	+87.2	-38.8	+38.8	-87.2	+113.8	-202.2	
Carry-over	101.1	0	43.6	56.9	19.4	19.4	56.9	43.6	0	101.1
Distribution		-27.9	+15.7	-52.8	+23.5	-23.5	+52.8	-15.7	+27.9	
Carry-over	+14.0	0	26.4	7.9	11.8	11.8	7.9	26.4	0	14
Distribution		+16.9	-9.5	+13.6	-6	+6	-13.6	+9.5	-16.9	
Carry-over	8.5	0	6.8	4.8	3	3	4.8	6.8	0	8.5
Distribution		-4.4	+2.4	-5.4	+2.4	-2.4	+5.4	-2.4	+4.4	
Carry-over	+2.2	0	2.7	1.2	1.2	1.2	1.2	2.7	0	2.2
Distribution		+1.7	-1.0	+1.7	-0.7	+0.7	-1.7	+1.0	-1.7	
Carry-over	0.9	0	0.9	0.5	0.4	0.4	0.5	0.9	0	0.9
Distribution		-0.6	+0.3	-0.6	+0.3	-0.3	+0.6	-0.3	+0.6	
Carry-over	+0.3	0	0.3	0.2	0.2	0.2	0.2	0.3	0	0.3
Distribution		+0.1	-0.2	+0.3	-0.1	+0.1	-0.3	+0.2	-0.1	
Final	+43.0	+51.0	+51.0	82.1	82.1	82.1	82.1	-51.0	-51.0	-43.0

The results are approximately the same as in the previous solution.

The final normal-stress distribution in the folded plate is shown in Fig. XI-25.

### Longitudinal main reinforcements

The longitudinal tension reinforcements are chosen such that they resist all the tensile forces  $T$  in the section given by the area of the tension zones. Accordingly, the tension at joint 3 is given by : (refer to Fig. XI-25).

$$T = \frac{82.1 \times 300}{2} \times 12 + \frac{82.1 \times 99}{2} \times 20 = 229059 \text{ kgs}$$

Using high grade steel with  $f_y = 3600 \text{ kg/cm}^2$  and  $\sigma_s = 1800 \text{ kg/cm}^2$ , we get:

$$A_s = \frac{229059}{1800} = 127 \text{ cm}^2$$

The total tension at joint 1 is given by:

$$T = \left[ \frac{51 + 43}{2} \times 90 + \frac{51 \times 61}{2} \right] \times 20 = 115710 \text{ kgs}$$

$$A_s = \frac{115710}{1800} = 64.3 \text{ cm}^2$$

The chosen reinforcements are shown in Fig. XI-26.

### Shear stresses in the different plates

Plate 1  $Q_{\max} = \frac{P_1 \cdot l}{2} = \frac{740 \times 20}{2} = 7400 \text{ kgs}$

The shear stresses are calculated as follows:

Due to  $Q_{\max}$  at mid-height:  $\tau_{\text{omax}} = \frac{3}{2} \frac{Q_{\max}}{A} = \frac{3}{2} \frac{7400}{20 \times 90} = 6.17 \text{ kg/cm}^2$

Due to  $T_{\max} = 84699 \text{ kgs}$ :

at top edge  $\tau = 4 \frac{T_{\max}}{b \cdot l} = \frac{4 \times 84699}{20 \times 2000} = 8.47 \text{ "}$

at mid-height  $\frac{\tau}{4} = 8.47/4 = 2.12 \text{ "}$

Total shear at mid-height  $= \tau_{\text{omax}} - \frac{\tau}{4} = 6.17 - 2.12 = 4.05 \text{ "}$

Plate 2  $Q_{\max} = \frac{S_{2.1} \cdot l}{2} = \frac{3053 \times 20}{2} = 30530 \text{ kgs}$

The thickness of the horizontal plates 2 and 4 is increased to 30 cms at the diaphragms for a length of @ 3 ms; hence the shear stresses

in plates 2 and 4 are calculated as follows:

$$\text{Due to } Q_{\max} \text{ at mid-height: } \tau_{\text{omax}} = \frac{3}{2} \frac{Q_{\max}}{A} = \frac{3}{2} \frac{30530}{30 \times 160} = 9.54 \text{ kg/cm}^2$$

Due to  $T_1 \text{ max} = 84699 \text{ kgs}$ :

$$\text{at joint 1 } \tau_1 = \frac{4 \times 84699}{30 \times 2000} = 5.65 \text{ "}$$

Due to  $T_2 \text{ max} = 35071 \text{ kgs}$ :

$$\text{at joint 2 } \tau_2 = \frac{4 \times 35071}{30 \times 2000} = 2.34 \text{ "}$$

$$\text{Total shear at middle of plate 2} = 9.54 - \frac{5.65}{4} - \frac{2.34}{4} = 7.55 \text{ "}$$

$$\text{Plate 3 } Q_{\max} = \frac{S \cdot l}{2} = \frac{7634 \times 20}{2} = 76340 \text{ kgs}$$

The thickness of plate 3 is also increased to 20 cms for a length of @ 3 ms at the diaphragms; hence, the shear stresses are given by:

$$\text{Shear stress due to } Q_{\max} \quad \tau_{\text{o max}} = \frac{3}{2} \frac{76340}{20 \times 600} = 9.54 \text{ kgs/cm}^2$$

$\tau_2$  at top edge (jt 2) due to  $T_2 \text{ max} = 35071 \text{ kgs}$  is

$$\tau_2 = \frac{4 \times 35071}{20 \times 2000} = 3.51 \text{ "}$$

$\tau_3$  at bot. edge (jt 3) due to  $T_3 \text{ max} = 35071 \text{ kgs}$  is

$$\tau_3 = \frac{4 \times 35071}{20 \times 2000} = 3.51 \text{ "}$$

$$\text{Total shear at middle of plate 3} = 9.54 - 2 \times \frac{3.51}{4} = 7.79 \text{ "}$$

### Web reinforcements

Arranging 7  $\emptyset$  10 mm/m at the top and bottom fibers of the slab in the 3 ms of increased thickness at the diaphragms, the shear stresses resisted by these bars only (i.e. neglecting the resistance of the longitudinal reinforcements and the concrete) is given by:

$$\tau_{\text{st}} = \frac{n A_s \sigma_s}{b s} \quad \text{where } s \text{ is the spacing of the cross bars (14.3cm)}$$

$$\text{Hence, for plate 2: } \tau_{\text{st}} = \frac{2 \times 0.79 \times 1400}{30 \times 14.3} = 5.16 \text{ kg/cm}^2$$

$$\text{and " " 3: } \tau_{\text{st}} = \frac{2 \times 0.79 \times 1400}{20 \times 14.3} = 7.73 \text{ "}$$

Assuming that the concrete can resist a part  $\tau_c$  of the shear stresses ( $@ 0.25 \sqrt{f_{op}} \approx 3.0 \text{ kg/cm}^2$ ), one can dispense with any bent bars in the folded plates of the structure.

Fig. XI-25 shows the normal and shear stresses in the folded plate.

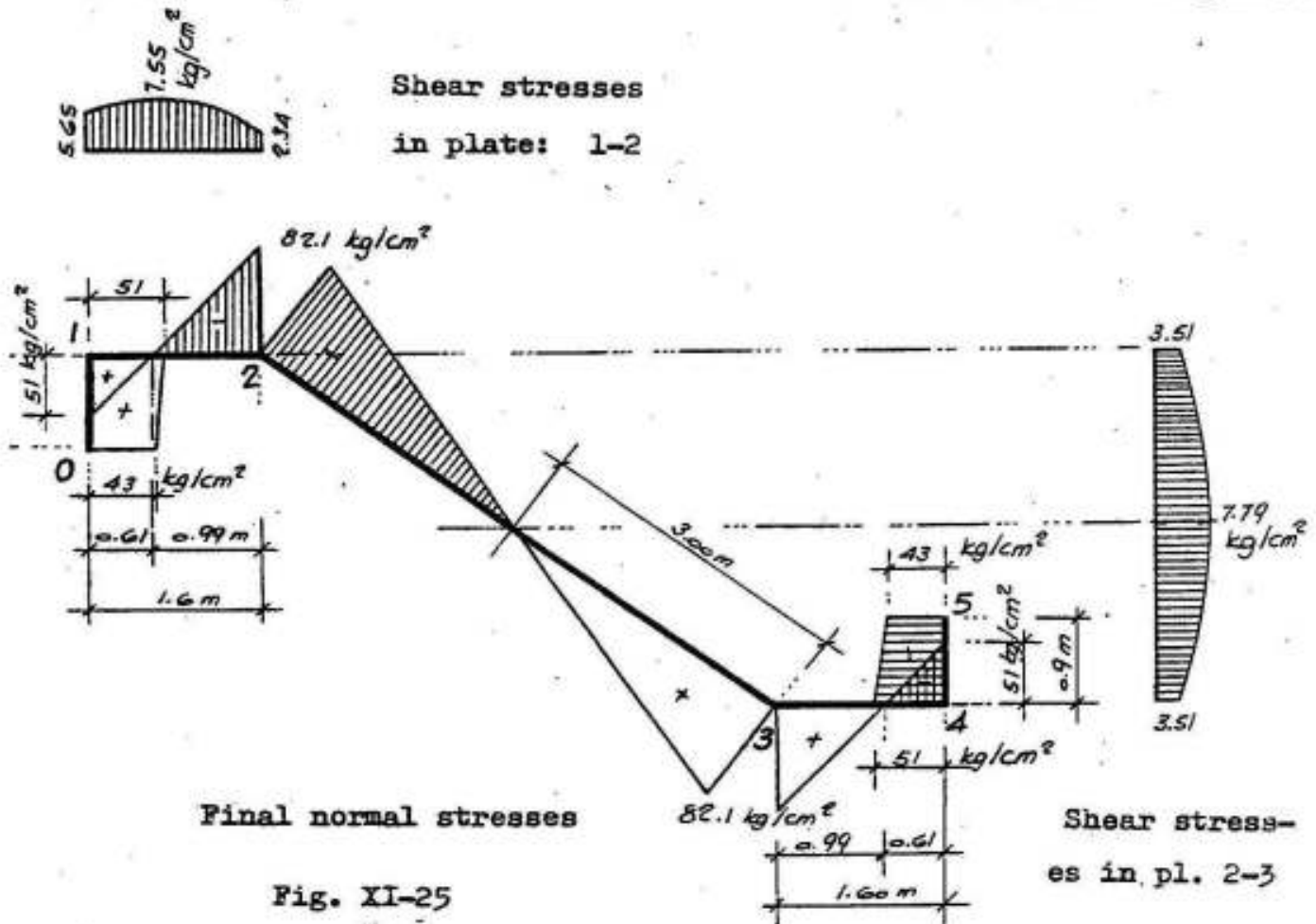


Fig. XI-25

The details of reinforcements in the cross section of one intermediate panel, both at middle of span and at supports, is shown in Fig. XI-26.

The shown solution is only approximate, because the displacements of the joints are neglected while they do affect the internal stresses. For the effect of these displacements one may refer to text books on the subject.

\* 'Design and Construction of Concrete Shell Roofs'. By Ramaswamy. Published by Mc Graw-Hill Book Company. New York and London.





## XI-7 DESIGN OF DIAPHRAGMS

The stresses arising in the diaphragms supporting folded-plates of symmetrical shape and symmetrically loaded, such as the folded-plate structure shown in Fig. XI-27, may be calculated in the following manner:

The ridge loads  $P_1$  and  $P_2$  acting on the nodes of the folded-plate, Fig. XI-27 a, cause plate forces  $S_1$  and  $S_2 / m$  and these exert shearing forces  $Q_1$  and  $Q_2$  on the end diaphragms. The shearing forces  $Q$  can be assumed to have a parabolic distribution, Fig. XI-27 b. The shearing force  $Q_2$  can be resolved into the components  $V_2$  and  $H_2$  which are the forces that effectively act upon the end diaphragm (the force  $Q_1$  is transmitted directly to the support). As is apparent from Fig. XI-27 c, the two symmetrical components  $V_2$  produce bending stresses in the end diaphragm; these can be determined by well known methods. The horizontal components  $H_2$  produce tension in the portion of the diaphragm situated between the two sloping plates of the structure. These tensile stresses can, likewise, be assumed to have a parabolic distribution, Fig. XI-27 c.

As presented in Fig. XI-27 d, the end diaphragms may be designed as two hinged frames (or the like), which are loaded by the shearing forces shown in (b) or their components shown in (c). On account of its far greater flexibility in comparison with a solid diaphragm, the frame is more conducive to the development of deformations of the st-

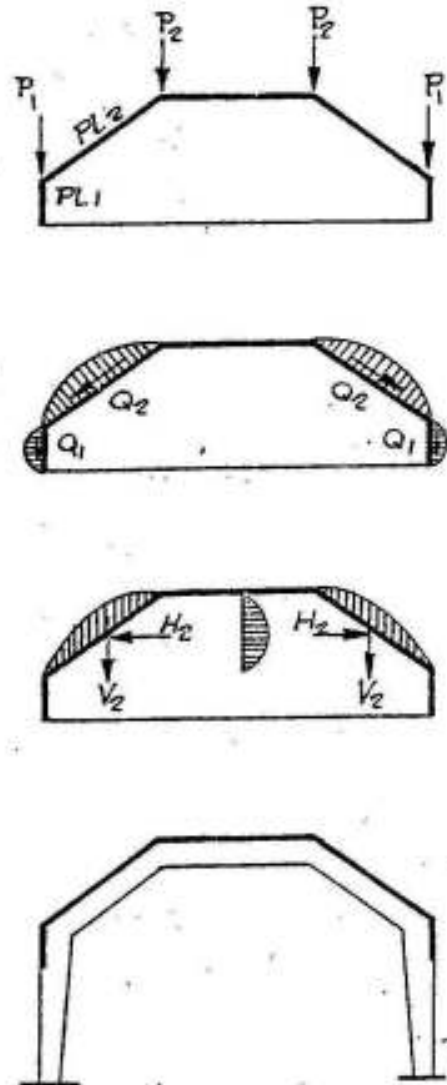


Fig. XI-27

ructure at the nodes.

### Example

It is required to design an intermediate diaphragm for a two-span folded-plate roof (Fig. XI-28). Assume the cross-section and dimensions are the same as those of the intermediate panel shown in Fig. XI-12. The spans are  $2 \times 18.4$  ms. The loads are the same as those of example 1 shown in Fig. XI-11.

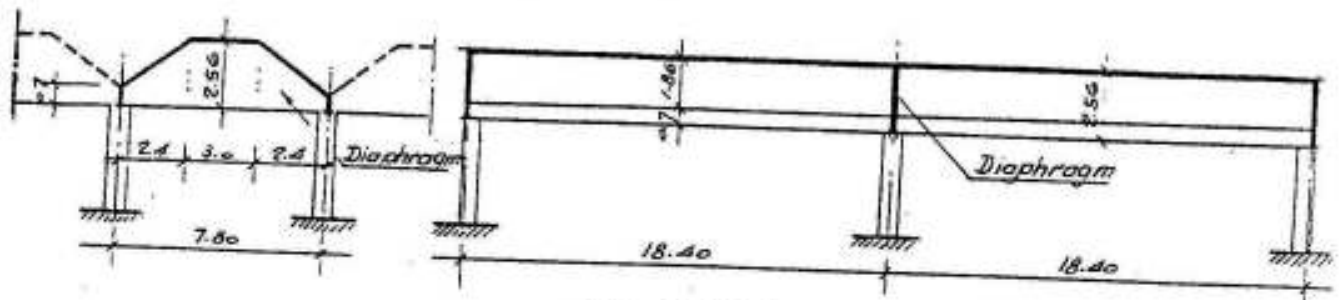


Fig. XI-28

The diaphragm shall be assumed as if it were simply supported at both ends although it is continuous with the side panels, because the depth of 0.7 ms at the supports is small relative to the depth of 2.56 ms at the middle of the spans. The bending moment that shall take place at the intermediate supports can be resisted by an adequate arrangement of reinforcements as shown in Fig. XI-31.

### Dimensions of diaphragm

Span:  $l = 7.8$  ms      Breadth:  $b = 0.30$  ms

Depths:  $t_{\min} = 0.70$  ms       $t_{\max} = 2.56$  ms

### Loads (Fig. XI-29)

The own weight is composed of three parts, namely:

Over the whole span       $w_1 = 0.3 \times 0.7 \times 2.5 = 0.525$  t/m

Triangular load over outside 2.4 ms with

$\max w_2 = 0.3 (2.56 - 0.7) \times 2.5 = 1.40$  t/m

Uniform load over middle 3.0 ms

$w_3 = 1.40$  t/m

Having computed the loads, the internal forces can be determined as follows:

External and internal forces (Fig. XI-29)

Total shearing force  $Q_{\text{omax.}}$  of inclined plate: (refer to example)

$$Q_{\text{omax.}} = 2 \times 18.40 = 36.80 \text{ t}$$

Its vertical component .....  $V = 0.6 \times 36.8 = 22.80 \text{ t}$

Its horizontal component .....  $H = 0.8 \times 36.8 = 29.44 \text{ t}$

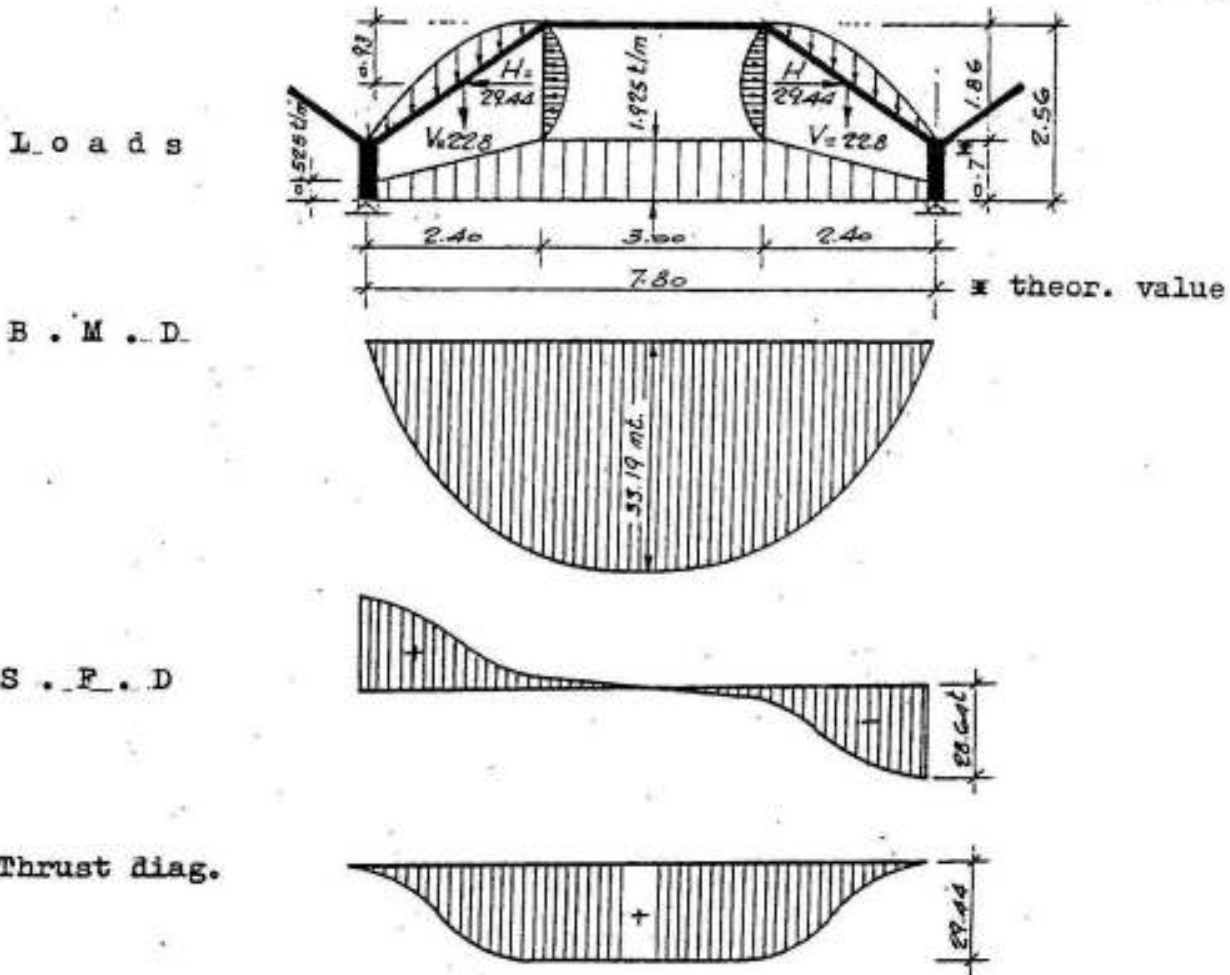


Fig. XI-29

$$\text{Reaction } R = \frac{0.525 \times 7.80}{2} + \frac{1.4 \times 2.4}{2} + 1.4 \times 1.5 + 22.80 = 28.64 \text{ t}$$

$$\text{Moment } M_{\text{max}} = 28.64 \times \frac{7.8}{2} - \frac{0.525 \times 3.9^2}{2} - \frac{1.4 \times 2.4}{2} \times 2.3 - \frac{1.4 \times 1.5^2}{2} - 22.8 \times 2.7 = 33.19 \text{ t}$$

$$Q_{\text{max}} = R = 28.64 \text{ t}$$

$$T = H = 29.44 \text{ t}$$

The bending moment, shearing force and thrust diag<sup>s</sup>. are in Fig. XI-29.

Reinforcements (Fig. XI-30)

$b = 30$  cms and  $d = 251$  cms; using normal mild steel, then  $\sigma_s = 1400$  kg/cm<sup>2</sup>. Eccentricity  $e$  of thrust  $T$  is given by:  $e = M/T = 33.19/29.44 = 1.13$  ms, i.e. the resultant  $T$  lies between the top and bottom reinforcements of the diaphragm. In this case,  $A_s$  and  $A_s'$  are inversely proportional to  $x'$  and  $x$ ,

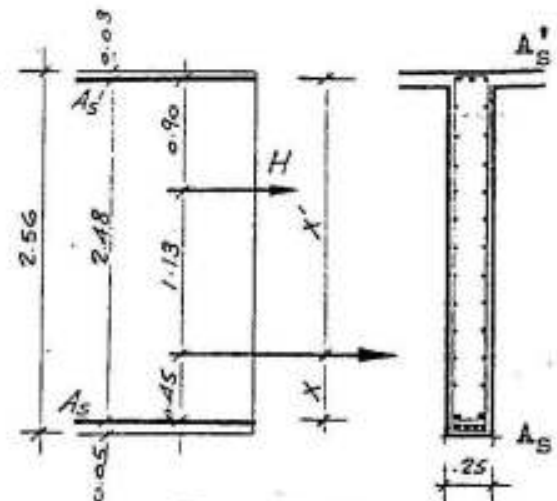


Fig. XI-30

where

$$x' = 90 + 113 = 203 \text{ cms} \quad \text{and} \quad x = 248 - 203 = 45 \text{ cms}$$

then

$$A_s = \frac{29.44}{1.4} \times \frac{203}{248} = 17.21 \text{ cm}^2 \quad 6 \text{ } \phi \text{ } 19$$

$$A_s' = \frac{29.44}{1.4} \times \frac{45}{248} = 3.82 \text{ cm}^2 \quad 3 \text{ } \phi \text{ } 16$$

Shear and principal stresses

Shear stress  $\tau = \frac{28640}{0.87 \times 30 \times 80} = 13.7 \text{ kg/cm}^2$

Average normal stress  $\sigma = \frac{29440}{30 \times 256} = 38.5 \text{ " tension.}$

Assuming that the inclination of the principal tensile stress with the horizontal is  $\alpha$ , then

$$\tan 2\alpha = \frac{2\tau}{\sigma} = \frac{2 \times 13.7}{38.5} = 0.71$$

or

$$\alpha = 17.8^\circ$$

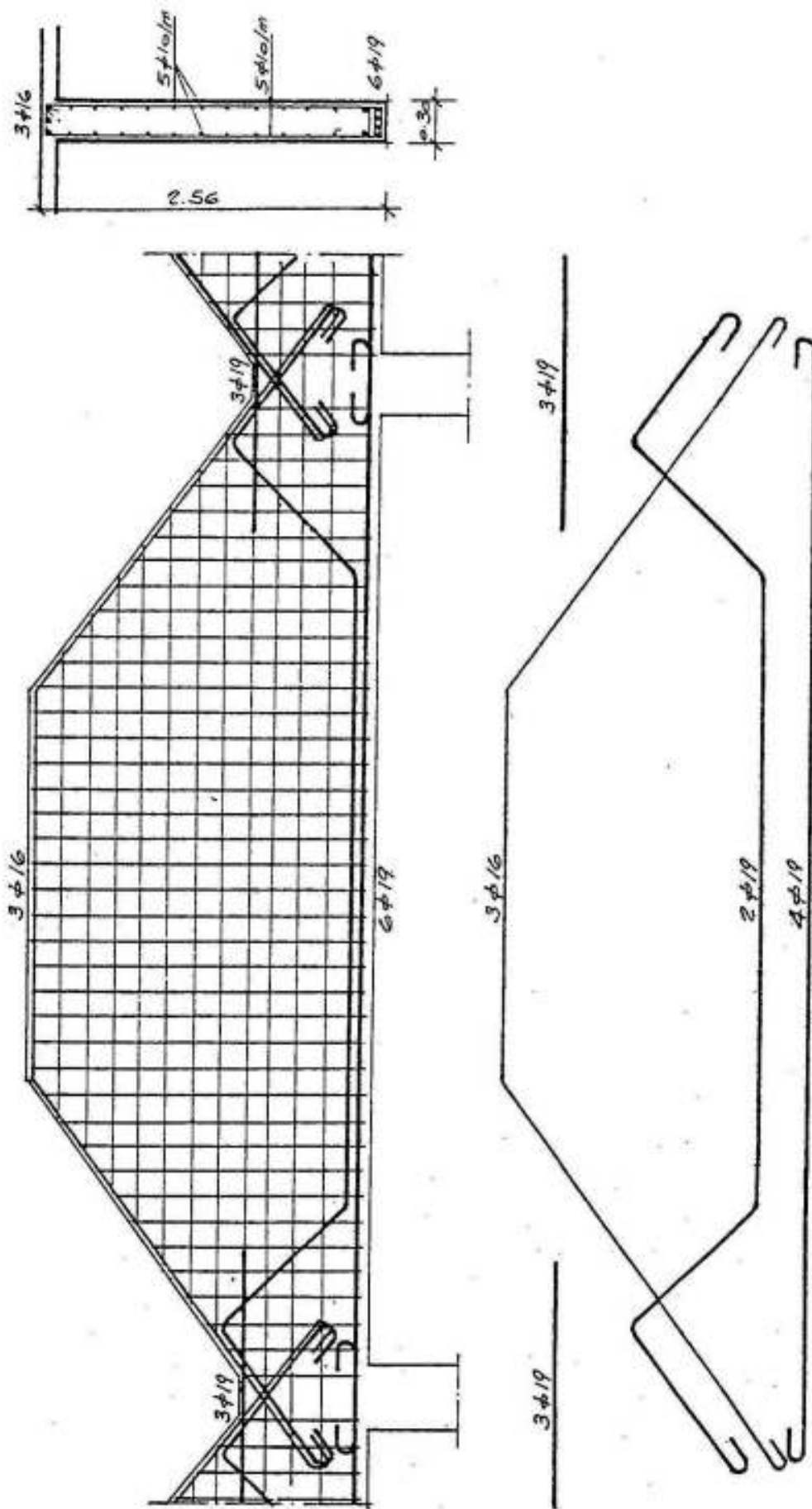
i.e. no bent bars are required; in spite of that, 3  $\phi$  19 will be bent and skin vertical and horizontal reinforcements 5  $\phi$  10 mm/m ( $> 0.05$  % of concrete section) are arranged.

The details of reinforcements of the diaphragm are shown in Fig. XI-31.

---

\* distance between top reinforcement and position of H.

*Details of Diaphragm*



*Fig. XI - 31*

### XI-8 MULTIPLE FOLDED-PLATE STRUCTURES

If more than two plates of a folded structure intersect at one or more junctions, then it is called a multiple folded plate structure. (Fig. XI-32).

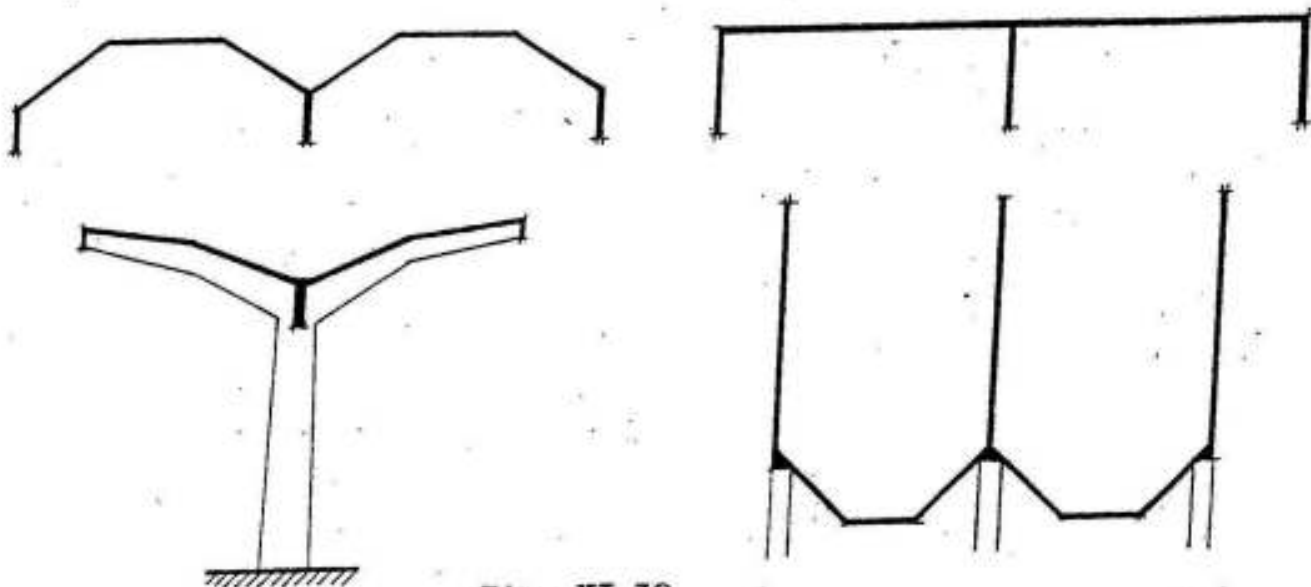


Fig. XI-32

In a junction  $b$ , where three plates intersect, there now occur two different shear forces  $T_{b1}$  and  $T_{b3}$  as against only one such force at each junction of a simple folded plate structure. Hence, the equation of three shears will be extended to an equation of four shears.

From the condition of equal stresses at the junction of intersection, (Fig. XI-33) we get:

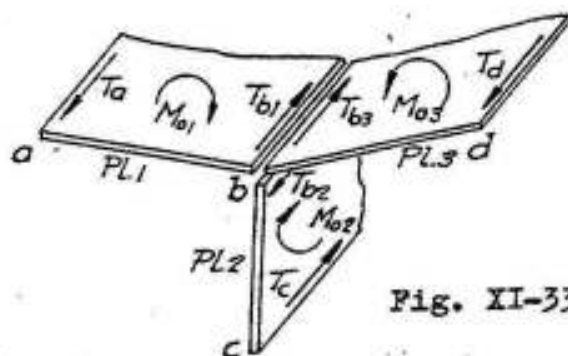


Fig. XI-33

$$\begin{aligned} \sigma_{b1} = \sigma_{b2} \quad \text{or} \quad \frac{T_a}{A_1} + \frac{2 T_{b1}}{A_1} + \frac{2 T_{b2}}{A_2} + \frac{T_c}{A_2} &= \frac{1}{2} \left( \frac{M_{o1}}{Z_1} + \frac{M_{o2}}{Z_2} \right) \\ \sigma_{b2} = \sigma_{b3} \quad \text{or} \quad \frac{T_c}{A_2} + \frac{2 T_{b2}}{A_2} + \frac{2 T_{b3}}{A_3} + \frac{T_d}{A_3} &= \frac{1}{2} \left( \frac{M_{o2}}{Z_2} + \frac{M_{o3}}{Z_3} \right) \end{aligned} \quad \left. \begin{array}{l} \text{and} \\ \text{XI-12} \end{array} \right\}$$

These two equations thus determine the shears  $T_{b1}$ ,  $T_{b2}$  and  $T_{b3}$  that occur at the junction  $b$ .

To obtain the right hand side of equation XI-12 in the form of the

equation of three shears, the sense of  $M_{o3}$  was changed in relation to that of  $M_{o2}$ .

In case  $T_c = 0$ , we have  $T_{b2} = T_{b1} + T_{b3}$  ..... XI-13  
and equations XI-12 can be given in the form:

$$\left. \begin{aligned} \frac{T_a}{A_1} + 2 T_{b1} \left( \frac{1}{A_1} + \frac{1}{A_2} \right) + 2 \frac{T_{b3}}{A_2} &= \frac{1}{2} \left( \frac{M_{o1}}{Z_1} + \frac{M_{o2}}{Z_2} \right) \\ \frac{T_d}{A_3} + 2 T_{b3} \left( \frac{1}{A_3} + \frac{1}{A_2} \right) + 2 \frac{T_{b1}}{A_2} &= \frac{1}{2} \left( \frac{M_{o3}}{Z_3} + \frac{M_{o2}}{Z_2} \right) \end{aligned} \right\} \dots \text{XI-14}$$

In case of symmetry,  $T_{b1} = T_{b3}$  ,  $T_{b2} = 2 T_{b1} = 2 T_{b3}$  XI-15

The application of these equations is shown in the following simple example. (Fig. XI-34).

Illustrative example

It is required to design the shed shown in Fig. XI-34 for a vert. superimposed dead load of  $100 \text{ kg/m}^2$  and a live load of  $200 \text{ kg/m}^2$ . The shed has a span of 12.0 ms between the columns and two overhanging cantilevers, 3.0 ms each, on both sides. The slab may be assumed 10 cms thick and reinforced by  $6 \text{ } \phi \text{ } 8 \text{ mm/m}$  in the transverse direction of the shed.

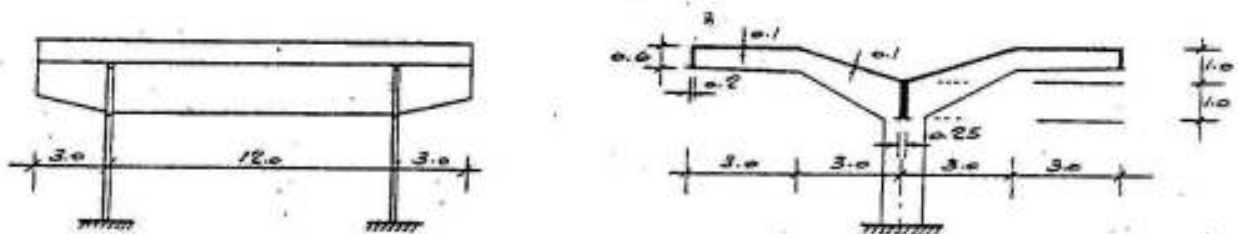


Fig. XI-34

The internal stresses in the folded plate shall be determined for the following two cases:

- A) Symmetrical case of loading with dead, superimposed, and live loads on b d g.
- B) Unsymmetrical case of loading with dead and superimposed load on b d g and live load on b d only.

A) Symmetrical case of loading

In this case, it is sufficient to study one half of the folded-plate only (i.e. part a b c d e) with half the beam d e (i.e. 12.5 x 100 cms) and half the load  $P_d$ .

Ridge and plate loads (Fig. XI-35)

$$P_b = 0.2 \times 0.6 \times 2500 + 1.5 \times 550 = 1125 \text{ kg/m'}$$

$$P_c = 3.0 \times 550 = 1650 \text{ "}$$

$$P_d = 0.25 \times 1.0 \times 2500 + 3.0 \times 550 = 2275 \text{ "}$$

Load on pl. 1,  $S_{ba} = P_b = 1125 \text{ kg/m'}$

Loads on plate 2,  $S_{bc} = 0$  and

$$S_{cb} = 3 P_c = 3 \times 1650 = 4950 \text{ kg/m'}$$

Loads on plate 3,  $S_{dc} = 0$  and

$$S_{cd} = \sqrt{10} P_c = \sqrt{10} \times 1650 = 5220 \text{ kg/m'}$$

Loads on  $\frac{1}{2}$  plate 4,  $S_{de} = \frac{1}{2} P_d$

$$= \frac{2275}{2} \text{ kg/m'}$$

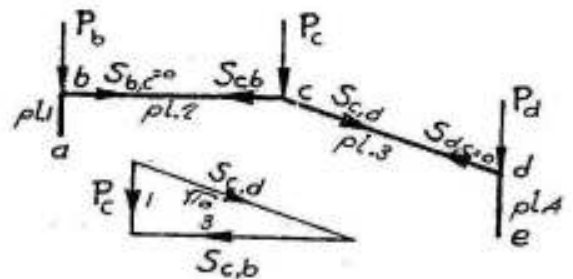


Fig. XI-35

Bending moments in longitudinal direction (Fig. XI-36)

The bending moments in the longitudinal direction due to a load  $S$  is as shown in Fig. XI-36.

$$M_o \text{ -ve} = S \cdot 3^2 / 2 = 4.5 S$$

$$\text{max. } M_o \text{ +ve} = S \frac{12^2}{8} - 4.5 S = 13.5 S$$

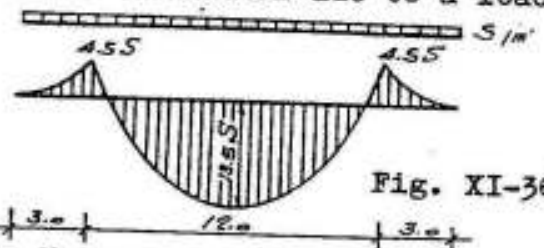


Fig. XI-36

Properties of individual plates, Moments  $M_o$  and stresses  $\sigma_o$

Plate	b cm	h cm	A=bh cm <sup>2</sup>	Z=bh <sup>2</sup> /6 cm <sup>3</sup>	S/m' kgs	$M_o = 13.5S \cdot 10^3$ kgcm	$\sigma_o = \pm M_o/Z$ kg/cm <sup>2</sup>
1	20	60	1200	$0.12 \times 10^5$	1125	$15.19 \times 10^5$	$\sigma_{oa} = +126.60$ $\sigma_{ob} = -126.60$
2	10	300	3000	$1.50 \times 10^5$	4950	$66.83 \times 10^5$	$\sigma_{oc} = +44.60$ $\sigma_{oc} = -44.60$
3	10	315	3150	$1.65 \times 10^5$	5220	$70.47 \times 10^5$	$\sigma_{od} = -42.70$ $\sigma_{od} = +42.70$
$\frac{1}{2}$ 4	12.5	100	1250	$.208 \times 10^5$	$\frac{2275}{2}$	$15.33 \times 10^5$	$\sigma_{oe} = -73.60$ $\sigma_{oe} = +73.60$



### Edge shears

Applying equations XI-14 on the different joints, we get:

$$\begin{aligned} \text{Joint b: } \quad 0 + 2 T_b \left( \frac{1}{A_1} + \frac{1}{A_2} \right) + \frac{T_c}{A_2} &= \frac{1}{2} \left( \frac{M_{o1}}{Z_1} + \frac{M_{o2}}{Z_2} \right) \\ 0 + 2 T_b \left( \frac{1}{1200} + \frac{1}{3000} \right) + \frac{T_c}{3150} &= \frac{1}{2} ( 126.6 + 44.6 ) \\ \text{or} \quad \quad \quad 7 T_b + T_c &= 256.8 \times 10^3 \quad (a) \end{aligned}$$

$$\begin{aligned} \text{Joint c: } \quad \frac{T_b}{A_2} + 2 T_c \left( \frac{1}{A_2} + \frac{1}{A_3} \right) + \frac{T_{d3}}{A_3} &= \frac{1}{2} \left( \frac{M_{o2}}{Z_2} + \frac{M_{o3}}{Z_3} \right) \\ \frac{T_b}{3000} + 2 T_c \left( \frac{1}{3000} + \frac{1}{3150} \right) + \frac{T_{d3}}{3150} &= \frac{1}{2} ( 44.6 - 42.7 ) \\ \text{or} \quad 0.330 T_b + 1.3 T_c + 0.317 T_{d3} &= 0.925 \times 10^3 \quad (b) \end{aligned}$$

Joint d: Because of symmetry,  $T_{d3}$  acting at joint d of plate 3 is equal to  $T_{d4}$  acting at joint d of half plate 4, so that the equation of three shears in its normal form can be applied. Hence

$$\begin{aligned} \frac{T_c}{A_3} + 2 T_{d3} \left( \frac{1}{A_3} + \frac{1}{A_4} \right) + 0 &= \frac{1}{2} \left( \frac{M_{o3}}{Z_3} + \frac{M_{o4}}{Z_4} \right) \\ \frac{T_c}{3150} + 2 T_{d3} \left( \frac{1}{3150} + \frac{1}{1250} \right) + 0 &= \frac{1}{2} ( -42.7 - 73.6 ) \end{aligned}$$

$$\text{or} \quad 0.317 T_c + 2.235 T_{d3} = - 58.15 \times 10^3 \quad (c)$$

Solving the three equations a, b and c, the values of  $T_a$ ,  $T_b$  and  $T_c$  can be determined. Accordingly:

$$\underline{T_b = 37.01 \times 10^3}, \quad \underline{T_c = - 2.47 \times 10^3} \quad \text{and} \quad \underline{T_{d3} = - 25.67 \times 10^3}$$

The stresses in the different plates due to  $M_o$  and  $T$  are shown in Fig. XI-37, whereas the final stresses in the middle section of the folded-plate due to this symmetrical case of loading is shown in Fig. XI-38.

The longitudinal bending moments at the diaphragms of the folded-plate are  $- 4.5/13.5 = - 1/3$  those at the middle section (refer to Fig. XI-36), hence, the final stresses at the diaphragms shall have the same ratio both in magnitude and sense and are as shown in Fig. XI-39.

Symmetrical loading: Stresses in the different plates (in kg/cm<sup>2</sup>)

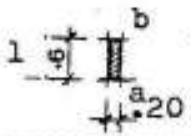
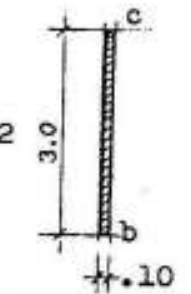
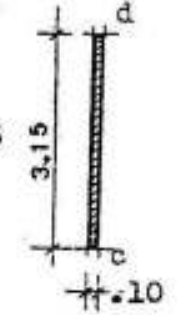
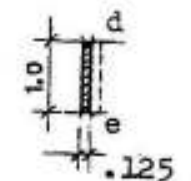
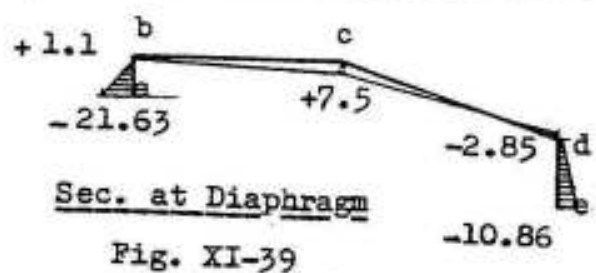
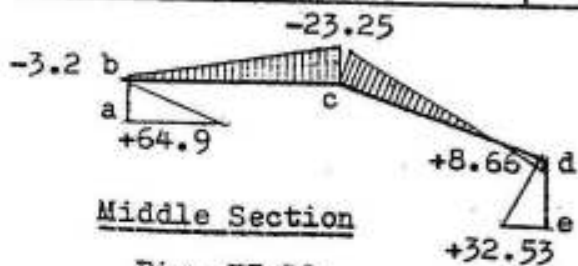
Plate No.	$M_o$ kg cm	T kgs		Final stresses kg/cm <sup>2</sup>
1 	$M_{o1} = 15.19 \times 10^5$ -126.6 +126.6	$T_a = 0$ 0 0	$T_b = +37.01 \times 10^3$ +123.4 -61.7	$\sigma_{M_{o1}} + \sigma_{T_a} + \sigma_{T_b}$ -3.2 +64.9
2 	$M_{o2} = 66.83 \times 10^5$ -44.6 +44.6	$T_b = -37.01 \times 10^3$ +24.67 -49.35	$T_c = -2.47 \times 10^3$ -3.29 +1.65	$\sigma_{M_{o2}} + \sigma_{T_b} + \sigma_{T_c}$ -23.22 -3.1
3 	$M_{o3} = 70.47 \times 10^5$ +42.7 -42.7	$T_c = +2.47 \times 10^3$ -1.57 +3.14	$T_d = 25.67 \times 10^3$ -32.6 +16.30	$\sigma_{M_{o3}} + \sigma_{T_c} + \sigma_{T_d}$ +8.53 -23.26
4 	$M_{o4} = 52.98 \times 10^5$ -73.6 +73.6	$T_d = +25.67 \times 10^3$ +82.4 -41.67	$T_e = 0$ 0 0	$\sigma_{M_{o4}} + \sigma_{T_d} + \sigma_{T_e}$ +8.8 +32.53

Fig. XI-37



B) Unsymmetrical case of loading (Fig. XI-40)

Live loads of  $200 \text{ kg/m}^2$  are assumed acting on b c d only.

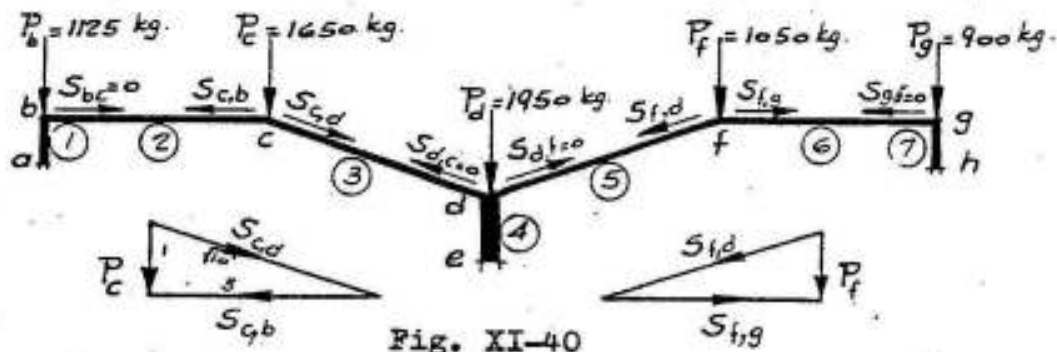


Fig. XI-40

Ridge and plate loads

$P_b = 1125 \text{ kg/m'}$ ,  $P_c = 1650 \text{ kg/m'}$ . (Refer to case A)

$P_d = 0.25 \times 1.0 \times 2500 + 1.5 \times 350 = 1950 \text{ kg/m'}$

$P_f = 3.0 \times 350 = 1050 \text{ kg/m'}$ ,  $P_g = 0.20 \times 0.60 \times 2500 + 1.5 \times 350 = 900 \text{ kg/m'}$

Resolution of ridge loads

Loads on plate 1	$S_{b,a} = P_b = 1125 \text{ kg/m'}$
" " " 2	$S_{b,c} = 0$ , $S_{c,b} = 3 P_c = 3 \times 1650 = 4950 \text{ kg/m'}$
" " " 3	$S_{c,d} = 10 P_c = 5220 \text{ kg/m'}$ , $S_{d,c} = 0$
" " " 4	$S_{d,e} = 1975 \text{ kg/m'}$
" " " 5	$S_{d,f} = 0$ , $S_{f,d} = 10 P_f = 3320 \text{ kg/m'}$
" " " 6	$S_{f,g} = 3 P_f = 3 \times 1050 = 3150 \text{ kg/m'}$ , $S_{g,f} = 0$
" " " 7	$S_{g,h} = P_g = 900 \text{ kg/m'}$ .

Properties of individual plates, Moments  $M_o$  and Stresses

The properties, moments and stresses of plates 1, 2 and 3 are the same as in the previous case.

Plate	b cm	h cm	A=bh cm <sup>2</sup>	Z=bh <sup>2</sup> /6 cm <sup>3</sup>	S/m' kgs	$M_o = 13.5S \cdot 10^3$ kg cm	$\sigma_o = \pm M_o/2$ kg/cm <sup>2</sup>
4	25	100	2500	.417 x 10 <sup>7</sup>	1975	26.66 x 10 <sup>7</sup>	$\sigma_{oe}^{od} = -63.9$ $\sigma_{oe}^{od} = +63.9$
5	10	315	3150	1.65 x 10 <sup>7</sup>	3320	44.82 x 10 <sup>7</sup>	$\sigma_{of}^{od} = +27.16$ $\sigma_{of}^{od} = -27.16$
6	10	300	3000	1.50 x 10 <sup>7</sup>	3150	42.50 x 10 <sup>7</sup>	$\sigma_{og}^{oi} = -28.33$ $\sigma_{og}^{oi} = +28.33$
7	20	60	1200	0.12 x 10 <sup>7</sup>	900	12.15 x 10 <sup>7</sup>	$\sigma_{oh}^{og} = -104.17$ $\sigma_{oh}^{og} = +104.17$

### Edge shears

The equations of edge shears applied to joints b and c will be the same as in previous case. Hence:

$$\text{Joint b: } 7 T_b + T_c = 256.8 \times 10^3 \quad (a)$$

$$\text{Joint c: } 0.330 T_b + 1.3 T_c + 0.317 T_{d3} = 0.925 \times 10^3 \quad (b)$$

$$\text{Joint } d_3: \frac{T_c}{A_3} + 2 T_{d3} \left( \frac{1}{A_3} + \frac{1}{A_4} \right) + 2 \frac{T_{d5}}{A_4} = \frac{1}{2} \left( \frac{M_{o3}}{Z_3} + \frac{M_{o4}}{Z_4} \right)$$

$$\frac{T_c}{3150} + 2 T_{d3} \left( \frac{1}{3150} + \frac{1}{2500} \right) + 2 \frac{T_{d5}}{2500} = \frac{1}{2} (-42.7 - 63.9)$$

$$\text{or } 0.315 T_c + 1.43 T_{d3} + 0.80 T_{d5} = 53.3 \times 10^3 \quad (c)$$

$$\text{Joint } d_5: \frac{2 T_{d3}}{A_4} + 2 T_{d5} \left( \frac{1}{A_4} + \frac{1}{A_5} \right) + \frac{T_f}{A_5} = \frac{1}{2} \left( \frac{M_{o4}}{Z_4} + \frac{M_{o5}}{Z_5} \right)$$

$$\frac{2 T_{d3}}{2500} + 2 T_{d5} \left( \frac{1}{2500} + \frac{1}{3150} \right) + \frac{T_f}{3150} = \frac{1}{2} (-63.9 - 27.16)$$

$$\text{or } 0.80 T_{d3} + 1.43 T_{d5} + 0.313 T_f = -45.53 \times 10^3 \quad (d)$$

$$\text{Joint f: } \frac{T_{d5}}{A_5} + 2 T_f \left( \frac{1}{A_5} + \frac{1}{A_6} \right) + \frac{T_g}{A_6} = \frac{1}{2} \left( \frac{M_{o5}}{Z_5} + \frac{M_{o6}}{Z_6} \right)$$

$$\frac{T_{d5}}{3150} + 2 T_f \left( \frac{1}{3150} + \frac{1}{3000} \right) + \frac{T_g}{3000} = \frac{1}{2} (-22.16 + 28.33)$$

$$\text{or } 0.313 T_{d5} + 1.30 T_f + 0.333 T_g = +0.585 \times 10^3 \quad (e)$$

$$\text{Joint g: } \frac{T_f}{A_6} + 2 T_g \left( \frac{1}{A_6} + \frac{1}{A_7} \right) + 0 = \frac{1}{2} \left( \frac{M_{o6}}{Z_6} + \frac{M_{o7}}{Z_7} \right)$$

$$\frac{T_f}{3000} + 2 T_g \left( \frac{1}{3000} + \frac{1}{1200} \right) + 0 = \frac{1}{2} (28.33 + 104.17)$$

$$\text{or } 0.330 T_f + 2.33 T_g + 0 = -66.25 \times 10^3 \quad (f)$$

The solution of these six equations gives the required edge shears.

$$T_b = + 36.93 \times 10^3 \text{ kgs} \quad T_c = - 1.74 \times 10^3 \text{ kgs}$$

$$T_{d3} = - 28.36 \times 10^3 \text{ kgs} \quad T_{d5} = - 15.25 \times 10^3 \text{ kgs}$$

$$T_f = - 3.243 \times 10^3 \text{ kgs} \quad T_g = + 28.86 \times 10^3 \text{ kgs}$$

The stresses in the different plates are shown in Fig. XI-41.

Unsymmetrical loading: Stresses in the different plates (in kg/cm<sup>2</sup>)

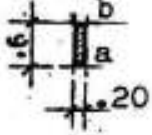
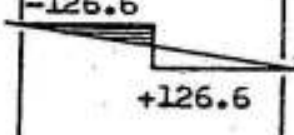
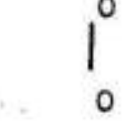
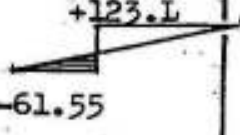
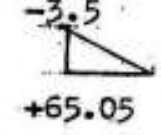
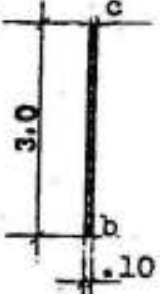
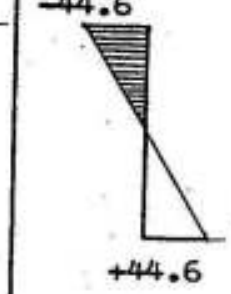
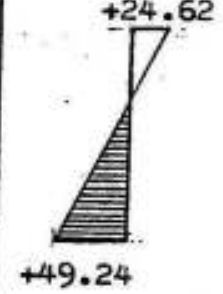


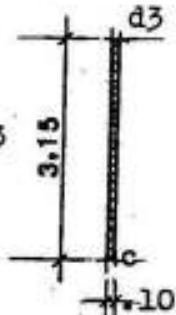
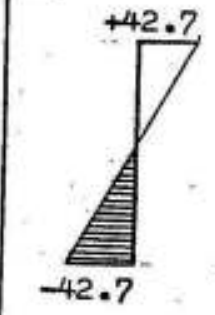



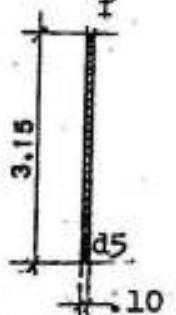




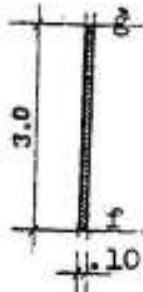




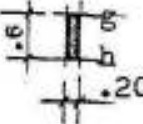
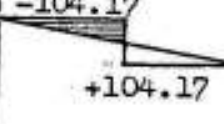
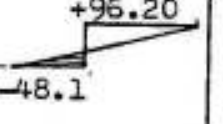
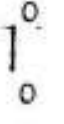
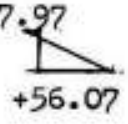
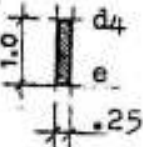
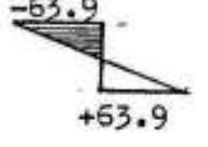
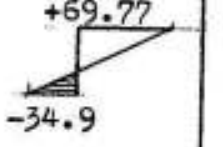

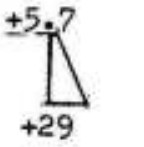
Plate No.	$M_o$ kg cm	$T$ kgs		Final stresses kg/cm <sup>2</sup>
1 	$M_{o1} = 15.19 \times 10^5$ -126.6 +126.6 	$T_a = 0$ 0 0 	$T_b = 36.93 \times 10^3$ +123.1 -61.55 	$\sigma_{M_{o1}} + \sigma_{T_a} + \sigma_{T_b}$ -3.5 +65.05 
2 	$M_{o2} = 66.83 \times 10^5$ -44.6 +44.6 	$T_b = -36.93 \times 10^3$ +24.62 +49.24 	$T_c = -1.74 \times 10^3$ -2.32 +1.16 	$\sigma_{M_{o2}} + \sigma_{T_b} + \sigma_{T_c}$ -22.3 -3.5 
3 	$M_{o3} = 70.47 \times 10^5$ +42.7 -42.7 	$T_c = +1.74 \times 10^3$ -1.1 +2.2 	$T_{d3} = -28.36 \times 10^3$ -36 +18 	$\sigma_{M_{o3}} + \sigma_{T_c} + \sigma_{T_{d3}}$ +5.6 -22.5 
5 	$M_{o5} = 44.82 \times 10^5$ -27.16 +27.16 	$T_{d5} = -15.25 \times 10^3$ +9.68 -19.36 	$T_f = +3.24 \times 10^3$ +4.1 -2.06 	$\sigma_{M_{o5}} + \sigma_{T_{d5}} + \sigma_{T_f}$ -13.38 +5.74 

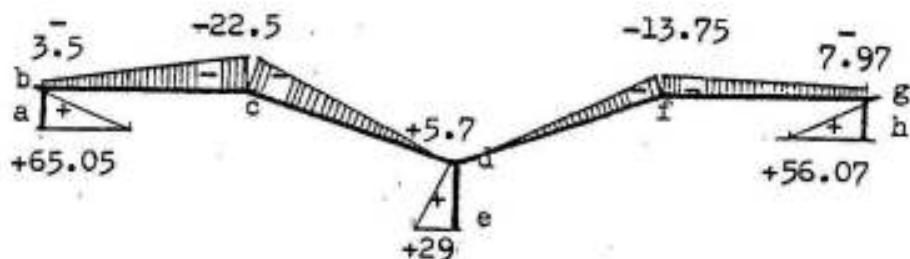
Fig. XI-41

Unsymmetrical loading: Stresses (in kg/cm<sup>2</sup>) continued.

Plate No.	M <sub>o</sub> kg cm	T kgs	Final stresses kg/cm <sup>2</sup>	
6 	M <sub>o6</sub> = 42.5 x 10 <sup>5</sup> 	T <sub>f</sub> = -3.243 x 10 <sup>3</sup> +2.16 -4.32 	T <sub>g</sub> = -28.36 x 10 <sup>3</sup> -37.8 +18.9 	σ <sub>M<sub>o6</sub></sub> + σ <sub>T<sub>f</sub></sub> + σ <sub>T<sub>g</sub></sub> -7.31 -13.75 
7 	M <sub>o7</sub> = 12.15 x 10 <sup>5</sup> -104.17 +104.17 	T <sub>g</sub> = +28.36 x 10 <sup>3</sup> +96.20 -48.1 	T <sub>h</sub> = 0 0 0 	σ <sub>M<sub>o7</sub></sub> + σ <sub>T<sub>g</sub></sub> -7.97 +56.07 
4 	M <sub>o4</sub> = 26.66 x 10 <sup>5</sup> -63.9 +63.9 	T <sub>d4</sub> = 43.61 x 10 <sup>3</sup> +69.77 -34.9 	T <sub>e</sub> = 0 0 0 	σ <sub>M<sub>o4</sub></sub> + σ <sub>T<sub>d4</sub></sub> +5.7 +29 

Note: T<sub>d4</sub> = T<sub>d3</sub> + T<sub>d5</sub> = - (-28.36 - 15.25) = + 43.61 t

Fig. XI-41 (contd)



Stresses in middle section of folded-plate for case of unsymmetrical loading

Fig. XI-42

### Longitudinal main reinforcement

It is clear from figures XI-38 and XI-42 that the main tension takes place at the middle of the vertical plates a b, d e and g h. It is bigger in the case of symmetrical loading.

Assuming that the longitudinal tension reinforcements resist all the tension forces T in the section (area of tension zone), then:

For plates a b and g h, we get:

$$\text{Height of tension zone} = \frac{60 \times 64.9}{64.9 + 3.2} = 57.2 \text{ cms} \quad \text{and}$$

$$\text{Total tension } T \dots\dots = \frac{57.2 \times 64.9}{2} \times 20 = 37123 \text{ kgs}$$

Choosing high grade steel with an average  $\sigma_s = 1800 \text{ kg/cm}^2$  for the main reinforcement, we get:

$$\text{Total tension steel } A_s = 37123 / 1800 = 20.62 \text{ cm}^2 \quad \text{chosen } 7 \# 19$$

For plate d e, we have

$$\text{Total tension } T \dots\dots = \frac{32.57 + 8.54}{2} \times 100 \times 25 = 51400 \text{ kgs}$$

$$\text{Total tension steel } A_s = 51400 / 1800 = 28.50 \text{ cm}^2 \quad \text{chosen } 8 \# 22$$

At the diaphragms, the tension takes place in the upper plates, with a maximum value at joints c and f. Hence

$$\text{Max. tension } T/m \dots\dots = 7.5 \times 100 \times 10 = 7500 \text{ kgs}$$

Using normal mild steel with allowable stress  $\sigma_s = 1400 \text{ kg/cm}^2$ , we get:

$$\text{Total steel per m } A_s = 7500 / 1400 = 5.30 \text{ cm}^2 \quad \text{chosen } 6 \# 8/m$$

top and bottom.

The details of reinforcements are shown in Fig. XI-46.

### Shear stresses and web reinforcements

Plates 1 and 7 (a b and g h)

$$\text{Max. shearing force at diaphragms: } Q_{\max} = \frac{P_b l}{2} = \frac{1125 \times 12}{2} = 6750 \text{ kgs}$$

$$\text{Shear stress at midheight of pl}^s. \tau_{\text{omax}} = \frac{3}{2} \frac{Q_{\max}}{A} = \frac{3}{2} \frac{6750}{1200} = 8.44 \text{ kg/cm}^2$$

Shear stress at diaphragms due to  $T_b \text{ max} = 37010$  kgs is:

at top edge.....  $\tau = \frac{4 T_{\text{max}}}{b l} = \frac{4 \times 37010}{20 \times 1200} = 8.44 \text{ kg/cm}^2$

at mid-height .....  $\tau/4 = 8.44 / 4 = 1.54$  "

Total shear at mid-height ..... =  $8.44 - 1.54 = 6.90$  "

Plates 2 and 6 (b c and f g)

Max. shearing force at diaphragms:  $Q_{\text{max}} = \frac{S_{c,b} l}{2} = \frac{4950 \times 12}{2} = 29700$  kgs

Shear stress at midheight of plate  $\tau_{o \text{ max}} = \frac{3}{2} \frac{Q_{\text{max}}}{A} = \frac{3}{2} \frac{29700}{3000} = 14.85 \text{ kg/cm}^2$

The shear stress being high, it may be advisable to increase the thick- of these plates to 16 cms gradually towards the diaphragms over a len- gth of 3.0 ms; in which case  $\tau_{o \text{ max}}$  will be reduced to  $\tau'_{o \text{ max}}$ , where

$$\tau'_{o \text{ max}} = \frac{3}{2} \frac{29700}{16 \times 300} = 9.2 \text{ kg/cm}^2$$

Shear stress at b (and g) due to  $T_b \text{ max} = 37010$  kgs is:

$$\tau_b = \frac{4 \times 37010}{16 \times 1200} = 7.71 \text{ kg/cm}^2$$

Shear stress at c (and f) due to  $T_c \text{ max} = 2470$  kgs is:

$$\tau_c = \frac{4 \times 2470}{16 \times 1200} = 0.51 \text{ kg/cm}^2$$

Shear at middle of b c (and f g) =  $9.2 - \frac{7.71}{4} - \frac{0.51}{4} = 7.14 \text{ kg/cm}^2$

Plates 3 and 5 (c d and d f)

The thickness of these plates is also increased gradually to 16 cms over 3.0 ms at the diaphragms. Hence:

$$Q_o \text{ max} = \frac{5220 \times 12}{2} = 31320 \text{ kgs}$$

$$\tau_o \text{ max} = \frac{3}{2} \frac{31320}{16 \times 315} = 9.32 \text{ kg/cm}^2$$

Shear stresses at c due to  $T_c \text{ max} = 2470$  kgs and at d due to



$T_d = 25670$  kgs are respectively:

$$\tau_c = \frac{4 \times 2470}{16 \times 1200} = 0.51 \text{ kg/cm}^2$$

and

$$\tau_d = \frac{4 \times 25670}{16 \times 1200} = 5.35 \text{ "}$$

$$\text{Shear at middle of c d (and d f)} = 9.32 - \frac{0.51}{4} - \frac{5.35}{4} = 7.86 \text{ kg/cm}^2$$

Plate 4 (d e)

$$Q_o \text{ max} = \frac{2275 \times 12}{2} = 13650 \text{ kgs}$$

$$\tau_o \text{ max} = \frac{3}{2} \frac{13650}{25 \times 100} = 8.2 \text{ kg/cm}^2$$

Due to  $T_d = 25670$  kgs

$$\tau_d = \frac{4 \times 25670}{25 \times 1200} = 3.42 \text{ kg/cm}^2$$

$$\text{Shear at middle of d e} = 8.20 - \frac{3.42}{4} = 7.35 \text{ kg/cm}^2$$

The distribution of the shear stresses on the different plates is shown in Fig. XI-43.

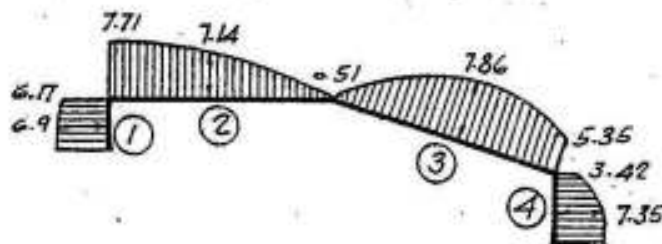


Fig. XI-43

### Diagonal tension reinforcements

If 6  $\phi$  10 mm/m are arranged at top and bottom fibers of plates 2, 3, 5 and 6 in the 3.0 ms of increased thickness at the diaphragms, the diagonal tensile stresses that can be resisted by these bars only (i.e. neglecting the longitudinal reinforcements), are given by:

$$\tau = \frac{n A_s \sigma_s}{b s} = \frac{2 \times 0.79 \times 1400}{16 \times 16.67} = 8.27 \text{ kg/cm}^2$$

This value being bigger than the shear stresses in the mentioned plates, no bent bars are required. Further, if the allowable diagonal tensile stress is 6 kg/cm<sup>2</sup>, then the required area of steel to be bent in the vert. plates shall also be small and may be chosen by designer.

Design of diaphragm

The main dimensions of the diaphragms in longitudinal and cross-section are shown in Fig. XI-44.

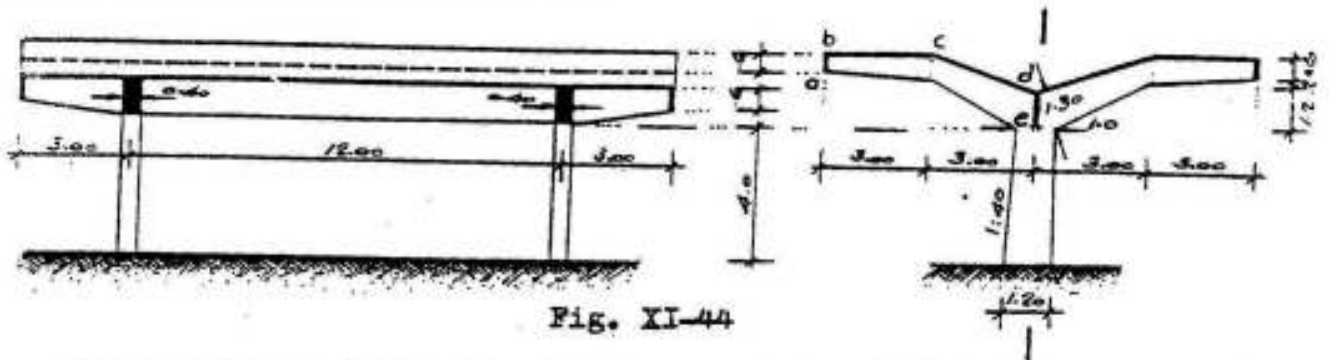


Fig. XI-44

To be able to design the diaphragms, one must determine the maximum internal forces (bending moments, shearing forces and thrust). The bending moments and shearing forces shown in Figs. XI-45 b and c can be determined from the vertical ridge loads directly. The thrust diagram Fig. XI-45 e) is to be determined from the parabolic shearing force distribution on the diaphragms. (Fig. XI-45 d)

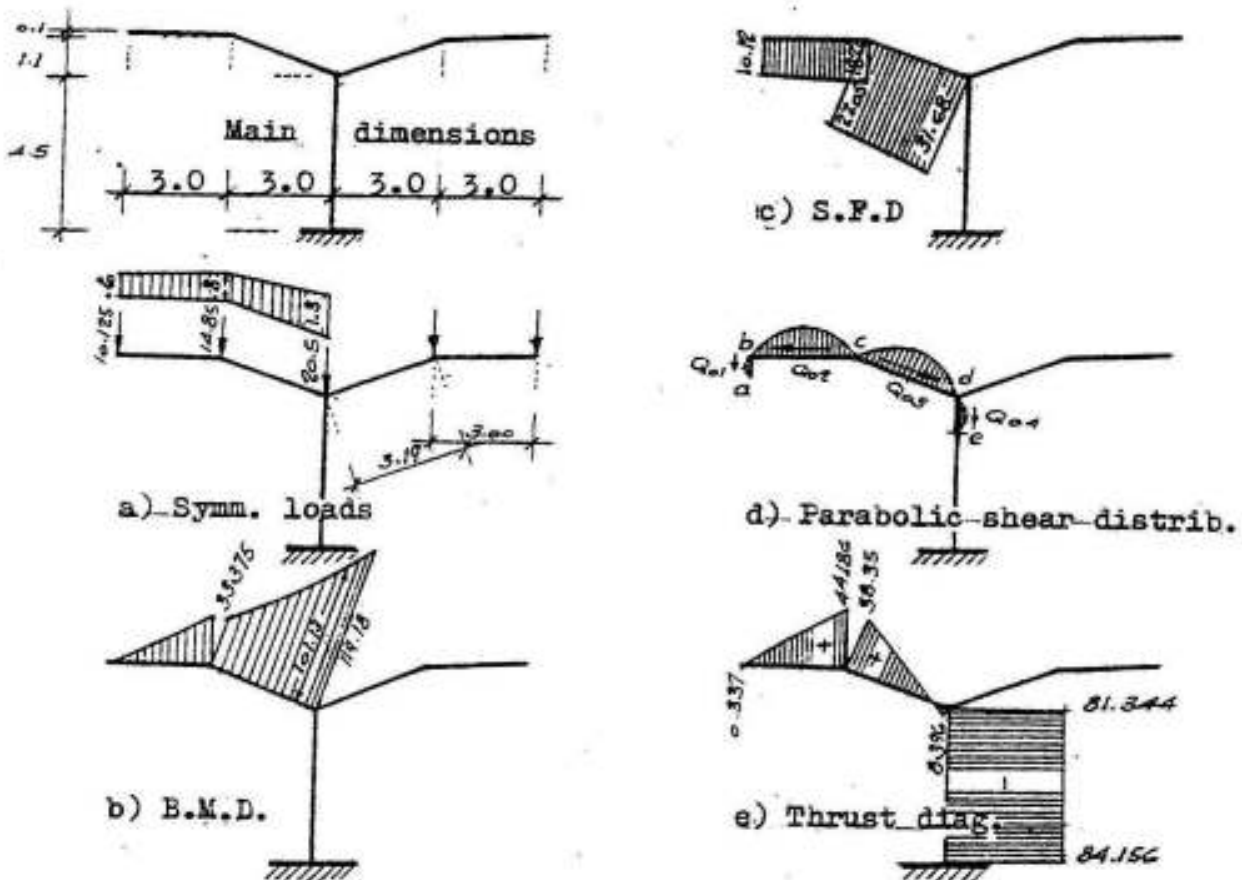


Fig. XI-45

### Loads

Assume breadth of diaphragm = 40 cms, depths at b, c and d = 60, 80 & 130 cms respectively, i.e. weight/m depth =  $0.4 \times 2.5 = 1.0$  ton. Thus  
Own weight: at b = 0.6 t/m, at c = 0.8 t/m and at d = 1.3 t/m.

Ridge loads:

$$P_b = 1.125 \times 9 = 10.125, P_c = 1.650 \times 9 = 14.85, P_d = 2.275 \times 9 = 20.5^t$$

### Maximum shearing forces of different plates

Plate 1 (a b) .....	$Q_{01} = 1.125 \times 9 = 10.125$	t	} distributed parabolically on plates 1-4 Fig. XI-45 d.
Plate 2 (b c) .....	$Q_{02} = 4.950 \times 9 = 44.550$	t	
Plate 3 (c d) .....	$Q_{03} = 5.220 \times 9 = 46.980$	t	
Plate 4 (d e) .....	$Q_{04} = 2.275 \times 9 = 20.475$	t	

### Thrust (along center-line of diaphragm)

At point b  $N_b = -10.125 \times 0.0333 = -0.337$  t  
 At middle of b c  $= 0.337 + \frac{44.55}{2} \times 0.9994 = 22.60$  t  
 At point c (left)  $N_c = -0.337 + 44.55 \times 0.9994 = +44.186$  t  
 " " (right)  $N'_c = -10.125 \times 0.344 + 44.55 \times 0.939 = 38.35$  t  
 " " d  $N_d = -10.125 \times 0.344 + 44.55 \times 0.939 - 46.98 \times 0.995 = -8.396$  t

The corresponding bending moment, shearing force and thrust are shown in Fig. XI-45.

### Design of different sections

The sections shall be designed by the U.S.D-method assuming an average load factor of 1.6, concrete with  $f_{cp} = 165 \text{ kg/cm}^2$  and high grade steel 36/50.

#### Section I-I at c 40 x 80 cms

$$M = 10.125 \times 3 + 0.6 \times \frac{3^2}{2} + 0.2 \times \frac{3^2}{6} = 33.375 \text{ mt} \quad M_u = 1.6 M = 53.4 \text{ mt}$$

$$N = +44.186 \text{ t (tension)}, \quad N_u = 44.186 \times 1.6 = 70.698 \text{ t}$$

$$e = \frac{M_u}{N_u} = \frac{53.4}{70.698} = 0.755 \text{ ms} \quad e_s = 0.755 - \frac{0.8}{2} + 0.05 = 0.405 \text{ ms}$$

$$M_{su} = N_u \cdot e_s \quad \text{or} \quad M_{su} = 70.698 \times 0.405 = 28.53 \text{ mt}$$

$$As \quad d = c \sqrt{\frac{M_{su}}{f_{cp} b}} \quad \text{then} \quad 75 = c \sqrt{\frac{28.63 \times 10^5}{165 \times 40}} \quad \text{giving } c = 3.6$$

The value of  $c$  being bigger than 2, then the failure is ductile and no compression reinforcement is required. Table 4-8 gives  $\eta = 0.85$ .

$$A_s = \frac{M_{su}}{f_y \eta d} + \frac{N_u}{\Omega f_y} = \frac{28.63 \times 10^5}{3600 \times 0.85 \times 75} + \frac{70.698 \times 10^3}{0.9 \times 3600}$$

$$= 12.47 + 21.82 = 34.29 \text{ cm}^2 \quad \text{chosen } 7 \# 25$$

Section II-II at d 40 x 130 cms

$$M = 10.125 \times 6 + 0.6 \times 3 \times 4.5 + \frac{0.2 \times 3}{2} \times 4 + 14.85 \times 3 + 0.8 \times 3.19 \times \frac{3}{2} + 0.5 \times \frac{3.19}{2}$$

$$\times \frac{3}{3} = 119.182 \text{ mt} \quad \text{at center line of column.}$$

Bending moment at face of column is given by:

$$M = 10.125 \times 5.35 + 0.6 \times 3 \times 4.15 + \frac{0.2 \times 3}{2} \times 3.35 + 14.85 \times 2.35 + 0.8 \times 3.19 \times \frac{2.35}{2}$$

$$+ 0.5 \times \frac{3.19}{2} \times \frac{2.35}{3} = 101.13 \text{ mt} \quad (\text{design value for section II-II}).$$

$$M_u = 101 \times 1.6 = 161.6 \text{ mt}, \quad N = -8.4 \text{ t}, \quad N_u = -8.4 \times 1.6 = -13.44 \text{ t}$$

$$e = \frac{161.6}{13.44} = 12.03 \text{ ms}, \quad e_s = 12.03 + \frac{1.3}{2} - 0.07 = 12.61 \text{ m.} \quad \text{So that}$$

$$M_{su} = N_u \cdot e_s \quad \text{or} \quad M_{su} = 13.44 \times 12.61 = 169.4 \text{ mt}$$

$$123 = c \sqrt{\frac{169.4 \times 10^5}{165 \times 40}} \quad \text{giving } c = 2.43 > 2 \quad \text{and} \quad \eta = 0.875$$

$$A_s = \frac{169.4 \times 10^5}{3600 \times 0.785 \times 123} - \frac{13.44 \times 10^3}{0.9 \times 3600} = 48.65 - 4.15 = 44.5 \text{ cm}^2$$

chosen 9 # 25.

Section III-III at top of column 40 x 100 cms

Bending moment at d on loaded side = 119.18 mt (refer to sec. II-II)

Bending moment at d on unloaded side d h is given by:

$$M = 8.1 \times 6 + 0.6 \times \frac{3}{2} \times 4.5 + 0.2 \times \frac{3}{2} \times 4 + 9.45 \times 3 + 0.8 \times 3.19 \times \frac{3}{2}$$

$$+ 0.5 \times \frac{3.19}{2} \times \frac{3}{3} = 86.83 \text{ mt}$$

$$\text{Bending moment on column} = 119.18 - 86.83 = 32.35 \text{ mt}$$

Corresponding normal force:  $N = 70.974 \text{ t}$

Assuming an accidental eccentricity  $= t/10 = 0.1 \text{ m}$  then

$M_{\text{total}} = 32.35 + 0.1 \times 70.974 = 39.45 \text{ mt}$  therefore

$M_u = 1.6 \times 39.45 = 63.12 \text{ mt}$  and  $N_u = 1.6 \times 70.974 = 113.56 \text{ t}$

$e = \frac{63.12}{113.56} = 0.556 \text{ ms}$ ,  $e_s = 0.556 + \frac{1.0}{2} = 0.05 = 1.005 \text{ ms}$  so that

$M_{su} = N_u e_s$  or  $M_{su} = 113.56 \times 1.006 = 114.24 \text{ mt}$  and

$95 = c \sqrt{\frac{114.24 \times 10^5}{165 \times 40}}$  giving  $c = 2.28 > 2$  and  $\eta = 0.76$  so that

$A_s = \frac{114.24 \times 10^5}{0.76 \times 3600 \times 95} - \frac{113.56 \times 10^3}{0.9 \times 3600} = 43.95 - 35.05 = 8.9 \text{ cm}^2$

Choosing  $A_s = A'_s = 0.5\%$ , then  $A_s = A'_s = \frac{0.5}{100} \times 40 \times 100 = 20 \text{ cm}^2$  or  
4 # 25 on each face.

#### Shear stresses and diagonal tension

$Q_b = 10.12 \text{ t}$   $\tau_b = \frac{10120}{0.87 \times 40 \times 55} = 5.28 \text{ kg/cm}^2$

$Q_c = 27.02 \text{ t}$   $M_c = 33.37 \text{ mt}$   $\tan \alpha = \frac{0.5}{3.19} = 0.158$

Reduced  $Q_c = Q_c - \frac{M_c \tan \alpha}{0.87 d} = 27.02 - \frac{33.37 \times 0.158}{0.87 \times 0.75} = 19 \text{ t}$

Neglecting the effect of  $N$ ,  $\tau_c = \frac{19000}{0.87 \times 40 \times 75} = 7.25 \text{ kg/cm}^2$

$Q_d = 31.68 \text{ t}$   $M_d = 119.18 \text{ mt}$   $\tan \alpha = 0.158$

Reduced  $Q_d = 31.68 - \frac{119.18 \times 0.158}{0.87 \times 1.23} = 14.18 \text{ t}$  so that

$\tau_d = \frac{14180}{0.87 \times 40 \times 123} = 3.3 \text{ kg/cm}^2$

The given study shows that the shear stresses in the diaphragms are relatively low; in spite of that bent bars are arranged as shown in Fig. XI-46 which gives the details of reinforcements in both the diaphragms and the folded-plate nearby.



## XII. THIN SHELL STRUCTURES

### XII-1 - INTRODUCTION

The roofing of large unobstructed areas, with a minimum amount of material is a goal that has claimed the attention of engineers and architects for years. Of the various types of roof construction, the concrete shell by its strength, beauty, simplicity and economy of construction, offers the best possibility of attaining this desirable end.

The famous big monumental domes that have been constructed in the last centuries (16th. to 19th.) depended in their strength on the big masses of the building materials that were used, as can be seen in the following three examples :

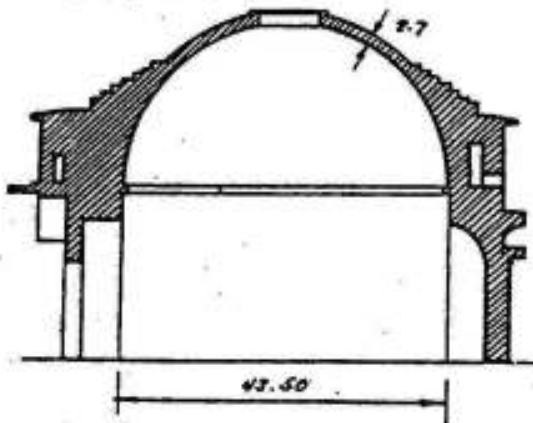


Fig. XII-1 Pantheon of Rome

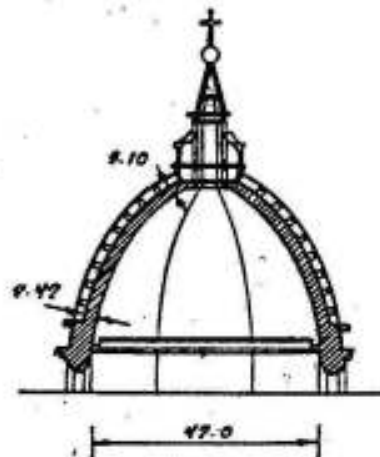


Fig. XII-2 Cathedral of Florence

- 1) The pantheon of Rome shown in figure XII-1 with a span of 43.5 ms and a minimum dome thickness of 2.70 ms.
- 2) The Cathedral of Florence with a span of 42 ms. for the inner dome and a thickness varying between 2.1 ms. at the crown and 2.42 ms. at the foot-ring as shown in figure XII-2.
- 3) The double-walled dome of Saint-Peters Cathedral in Rome, having a span of 42.0 ms. The two slabs of the dome are joined together at their shoulders giving a total thickness of 2.8 ms; the inner shell is 1.6 ms. thick while the outer one is 1.2 ms. only as shown in figure XII-3.

Due to the continual efforts of engineers and scientists and the available technical tools, it has been possible to analyse the deformations and internal forces in different forms of shells and, as a result, it has been found that it is possible to construct very thin

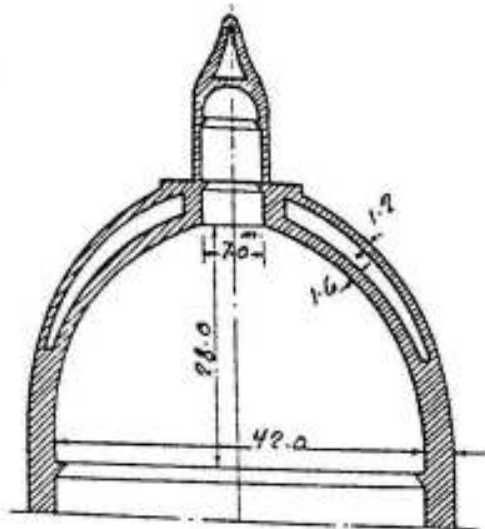


Fig. XII-3 Saint-Peters Cathedral

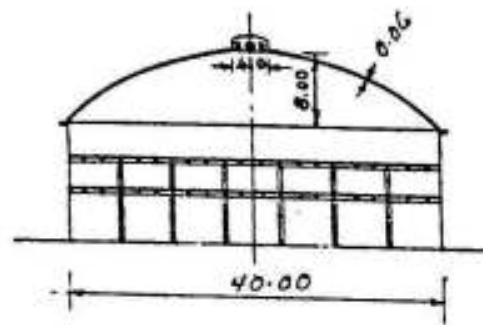


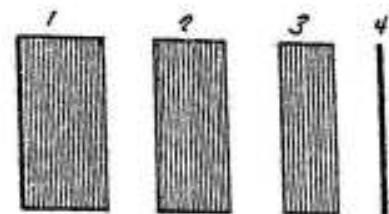
Fig. XII-4 Scott Factory at Jena

shells covering relatively big spans and having very big strength by giving them convenient structural forms.

The 6cms. shell used as a roof for the 40 ms. span Scott factory in Jena, shown in figure XII-4, gives an example of the tremendous saving in the building materials that can be achieved by the use of modern shells.

The relative roof thickness of the old and new domes shown in figures XII-1 to XII-4 is illustrated in figure XII-5 by proportionally thick rectangles.

Many different shell-forms of single and double curvature proved to be of very high resistance, economic, easy to construct and architecturally very impressive. Samples of such existing shell structures are shown in the following figures: XII-23 and 24 for surfaces of revolution; XII-73, 74, 81, 82 and 87 for cylindrical shells and XII-



*Relative roof thickness of structures 1 to 4*

Fig. XII-5

106, 110, 114 & 115 for double curved shells.

It has however been possible to construct reinforced concrete shells having a ratio of thickness to span almost equal to that provided by nature in its protective covering of an egg.



Except for some simple forms, subjected to few simple symmetrical cases of loading, an exact analysis of concrete shells is a difficult, if not impossible, task because the design must take in consideration not only all the variables in loading and physical make-up of the structure but also the physical properties of the materials used and their composite action under load.

However, a qualitative understanding of the fundamental nature of the behavior of some forms of shells can be gained without detailed mathematical analysis and in many cases suggests a reasonable safe method of solution.

Such solutions are generally accepted because of the remarkable reserve strength of shell construction, which makes it practically impossible for a shell structure to collapse.

## XII-2 LOADING

Dead weight : We shall now discuss the different loading conditions that are of importance in the design of dome structures. We are principally concerned with the load components in the direction of the meridian, in the direction of the rings and in the direction normal to the shell surface. The most important load is the dead load  $g$  composed of the weight of the structure and the roofing. Using the notations :

$g$  = dead weight per unit area of surface

$p_\psi$  = component of  $g$  in direction of the tangent to the meridian

$p_\theta$  = " " " " " " " " " " ring

$p_r$  = " " " normal to the surface of the shell

we get : ( Fig. XII-6 )

$$p_\psi = g \sin \psi$$

$$p_\theta = 0$$

$$p_r = g \cos \psi$$

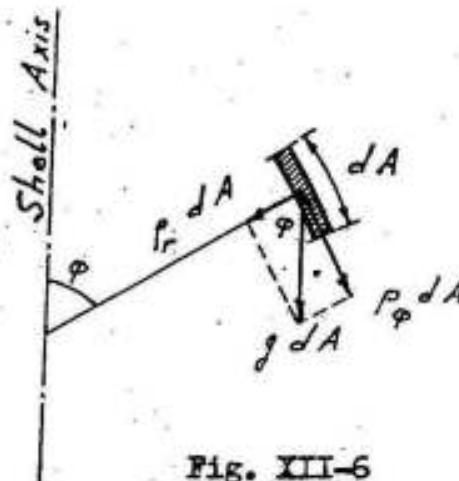


Fig. XII-6

### Live load

The live load  $p$  ( e.g. the snow load ) is generally assu-

med per  $m^2$  horizontal. Referring to figure XII-7

we get :

$$p_{\theta} = p \sin \varphi \cos \varphi$$

$$p_{\theta} = 0$$

$$p_r = p \cos^2 \varphi$$

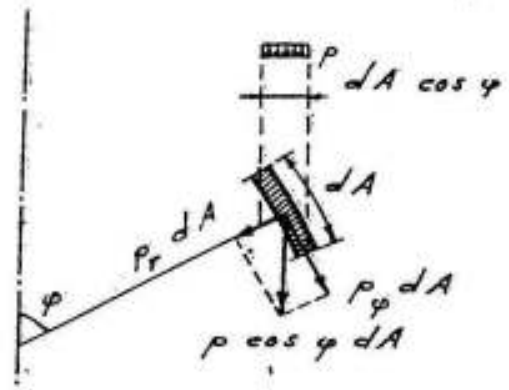


FIG. XII-7

### Wind load

The wind load of shells is composed of pressure on the wind side and suction on the leeward side. Only the load component acting normal to the shell surface is of importance, since the other components are due to friction and are almost equal to zero. In order to calculate the wind pressure, one can use the following hypothesis, which has the merit of great simplicity : ( Fig. XII-8 )

$p_{\varphi} = 0$  ,  $p_{\theta} = 0$  ,  $p_r = w \sin \varphi \cos \theta$   
 in which  $w =$  the wind load /  $m^2$  surface at  $\theta = 0$  ,  $\varphi = \pi / 2$  .

This distribution can be used for cylindrical and spherical shells the introduction of more exact laws will unduly complicate the calculations . One may assume :

$$w = 0.26 q$$

for the sphere

and

$$w = 0.45 q$$

for the cylinder

where

$$q = \text{the specified wind pressure}$$

For all other shells of revolution values will have to be assigned according to their shape between these two limits.

### XII-3 SURFACES OF REVOLUTION

Roofs and floors of circular big span areas may be flat and

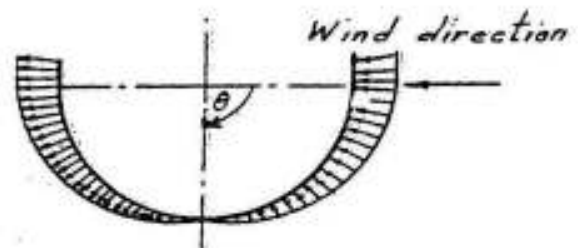


FIG. XII-8

supported on any convenient system of girders as shown in figure XII-9a or radial frames as shown in figure XII-9b.

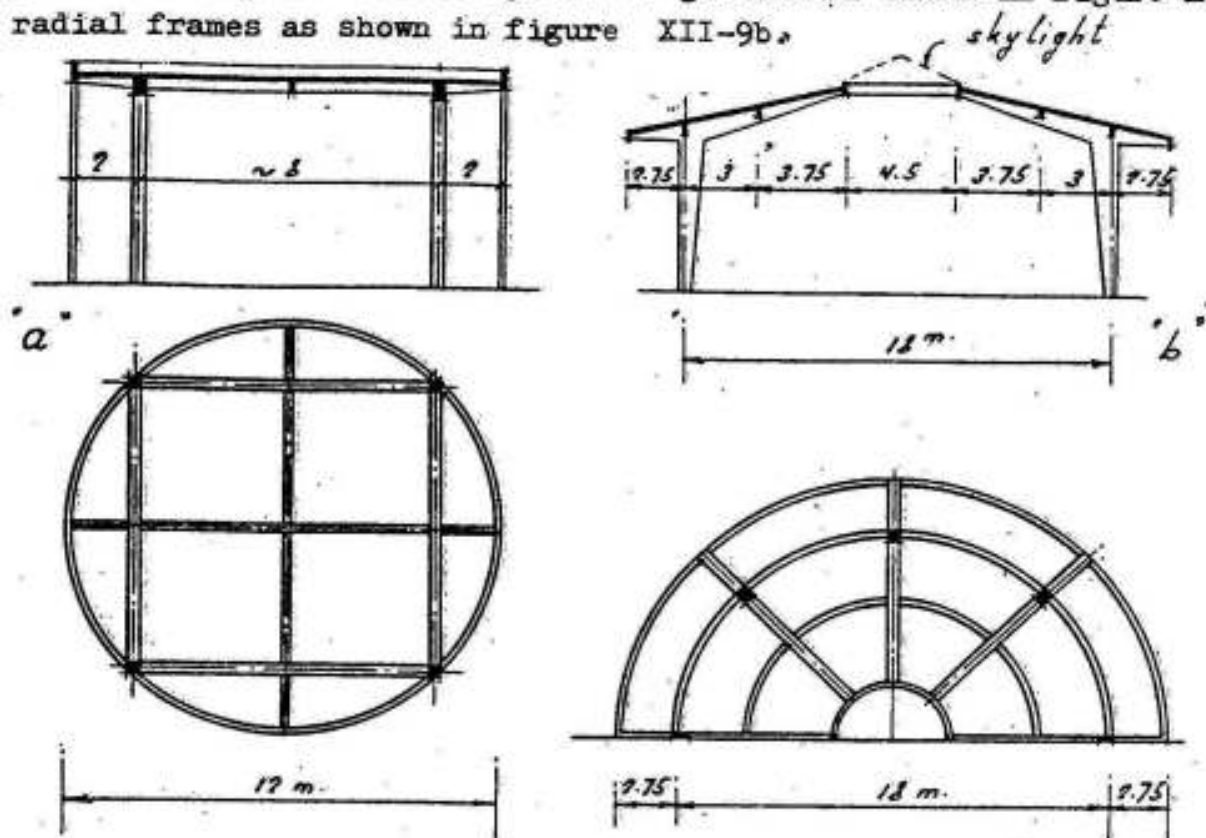


FIG. XII-9

In many cases, the choice of a reinforced concrete surface of revolution e.g. a cone or a dome ( Fig. XII-4) results in an ultimate saving in materials and cost even when the greater cost of the shuttering is taken into consideration.

In the following, we give the general principles involved in the design of simple popular forms of surfaces of revolution according to the membrane theory.

1 - Membrane Theory of Surfaces of Revolution

In this theory, it is assumed that the thickness of the shell is so small that it may be considered as a membrane which can resist meridian and ring forces only i.e. the bending moments due to the fixation at the supports, unsymmetrical loading and similar effects are neglected.

a) Analytical Method ( Refer to figure XII-10 )

It will be assumed that :

$r$  = radius, normal to axis of rotation, of any circular ring at a horizontal plane  $z$   $z$

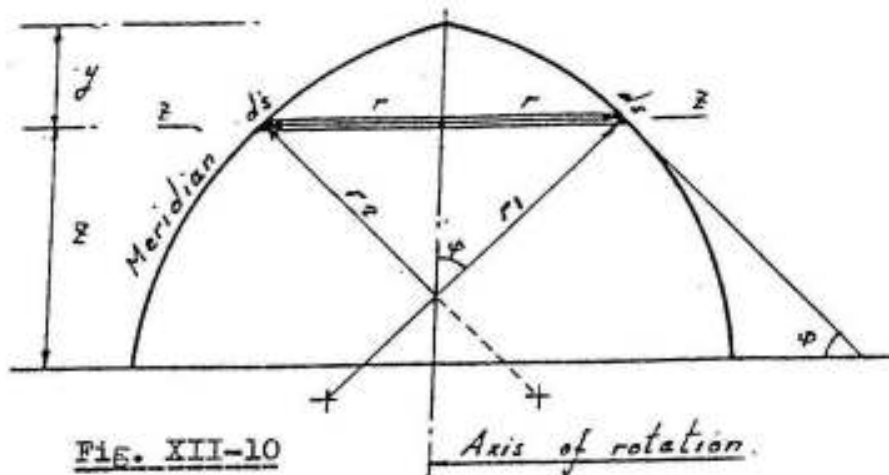


FIG. XII-10

Axis of rotation.

- $r_1$  = radius of curvature of meridian
- $r_2$  = cross radius of curvature along the normal to axis of rotation
- $N_\varphi$  = resultant meridian force per unit length of circumference  
 =  $\sigma_\varphi t$  where  $\sigma_\varphi$  = meridian stress and  $t$  = thickness of shell
- $N_\theta$  = resultant ring force per unit length of meridian
- $\sigma_\theta$  =  $\sigma_\theta t$  where  $\sigma_\theta$  = ring stress
- $H$  = horizontal thrust of shell per unit length of circumference
- $W_\varphi$  = sum of vertical forces above  $z z$  ( expressed through the angle  $\varphi$  )

In order to have equilibrium at any horizontal section  $z z$ , the vertical component of the meridian forces  $N_\varphi$  must be equal to the vertical load above  $z z$  per meter run circumference. Hence, we get : ( fig. XII-11 )

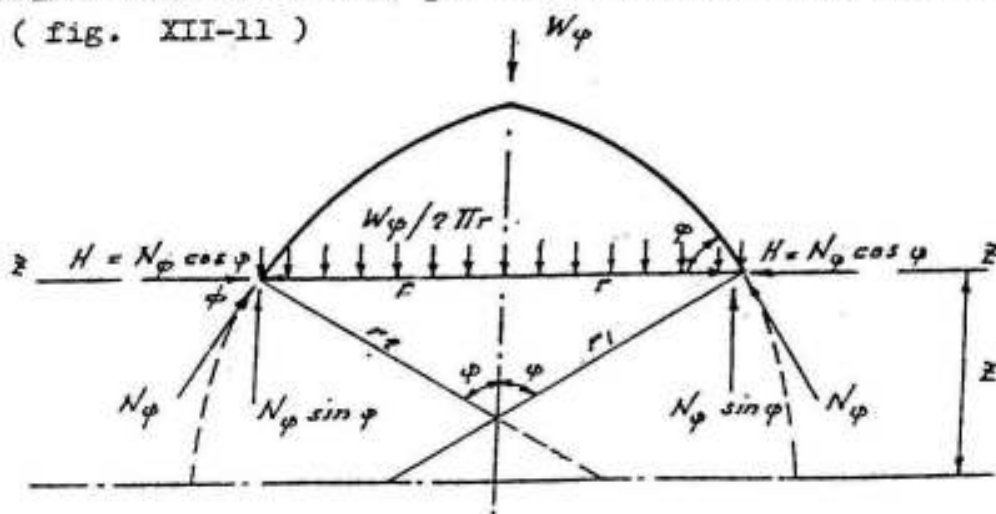


Fig. XII-11

$$W_\varphi / 2 \pi r = N_\varphi \sin \varphi$$

$$N_\varphi = W_\varphi / 2 \pi r \sin \varphi \quad \text{or} \quad (a)$$

But  $r = r_2 \sin \varphi$ , so that  $N_\varphi$  can also be given in the form :

$$N_\varphi = \frac{W_\varphi}{2\pi r_2 \sin^2 \varphi} \quad (a')$$

The horizontal thrust  $H$  per unit length of circumference is :

$$H = \frac{W_\varphi}{2\pi r} \cdot \tan \varphi = N_\varphi \cos \varphi$$

considering the equilibrium of the element  $ds$  under the forces shown in figure XII-12, we find that :

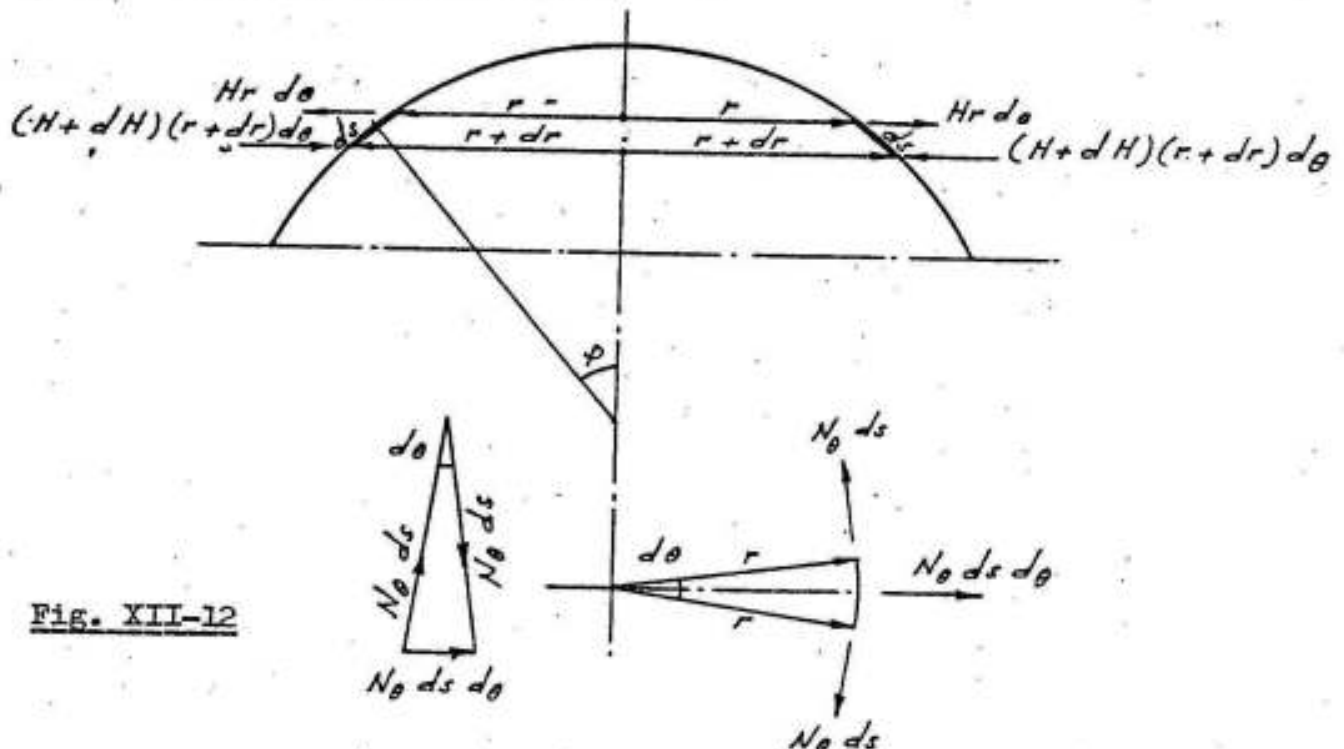


Fig. XII-12

$$N_\theta ds ds = (H + dH)(r + dr) ds - Hr ds$$

Reducing by  $ds$  and neglecting  $dH dr$  being a small value of the second degree, we get :

$$N_\theta ds = Hr + dH r + H dr - Hr \quad \text{or} \quad N_\theta ds = d(Hr) \quad \text{i.e.}$$

$$N_\theta = d(Hr) / ds \quad (b)$$

If the dome were simply supported, the maximum ring force at the lowest strip would be : ( Fig. XII-13 ).

$$\text{max. } N_\theta = H r_{\text{max.}}$$

This force must be resisted by tension ring reinforcement given by

$$A_s = \frac{\text{max. } N_\theta}{\sigma_s}$$

The relation between the external forces and the internal stresses can be determined if we consider the equilibrium of all the forces acting on an element  $ds_1 ds_2$ , in a radial direction normal to the surface of the shell (fig. XII-14) as follows :

Assume radial component of external forces on the element :

$$p_r ds_1 ds_2$$

Radial component of the meridian force  $N_\varphi ds_2$  due to change of its direction by an angle  $d\varphi$  is :

$$N_\varphi ds_2 d\varphi$$

Horizontal component of ring force  $N_\theta ds_1$  due to change of its direction by an angle  $d\theta$  is :

$$N_\theta ds_1 d\theta$$

Its radial component is

$$N_\theta ds_1 d\theta \sin\varphi$$

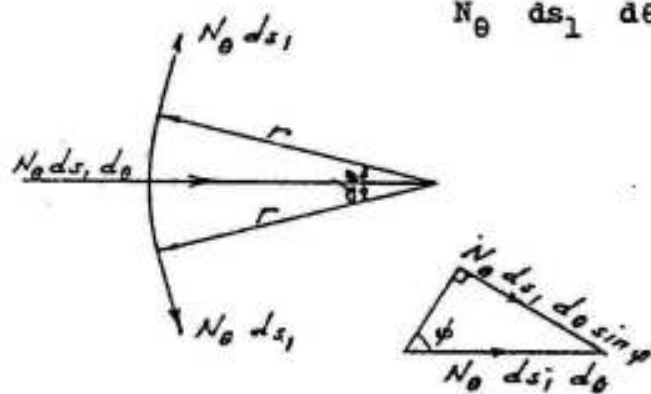


Fig. XII-14

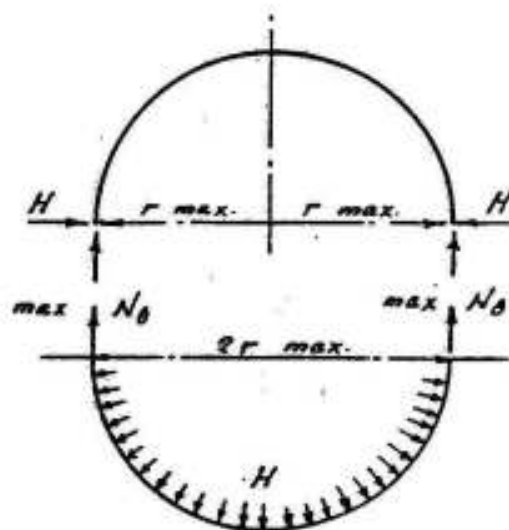
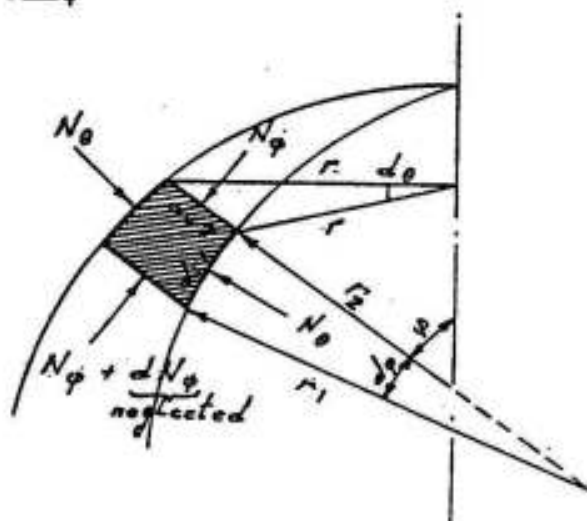


Fig. XII-13



The equilibrium between these forces is given by the relation

$$N_\varphi ds_2 d\varphi + N_\theta ds_1 d\theta \sin\varphi = p_r ds_1 ds_2$$

$$\text{But } ds_1 = r_1 d\varphi, \quad ds_2 = r d\theta = r_2 \sin\varphi d\theta$$

Therefore, we get :

$$N_\varphi r_2 \sin\varphi d\theta d\varphi + N_\theta r_1 d\varphi d\theta \sin\varphi = p_r r_1 d\varphi r_2 \sin\varphi d\theta \quad \text{or}$$

$$N_\varphi r_2 + N_\theta r_1 = p_r r_1 r_2 \quad \text{i.e.}$$

$$\frac{N_\varphi}{r_1} + \frac{N_\theta}{r_2} = p_r \quad (c)$$

For a spherical surface  $r_1 = r_2 = a$  and

$$N_\varphi + N_\theta = p_r a \quad (c')$$

For a conical surface  $r_1 = \infty$  and

$$N_\theta = p_r r_2 \quad (c'')$$

Accordingly, the meridian force can be determined from equation (a) while the ring force from equations b or c.

#### b) Graphical Method

The meridian and ring forces in surfaces of revolution whose meridian does not follow a simple mathematical equation can be determined using the following graphical method (fig. XII-15) which is based on equations a and b.

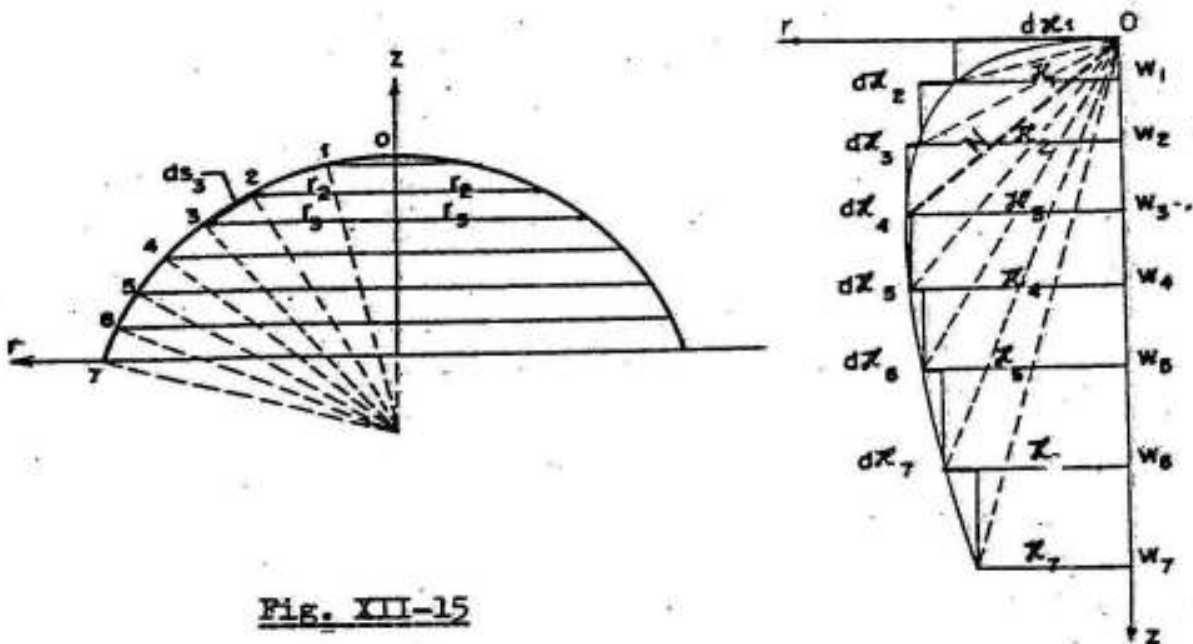


Fig. XII-15

Assume  $w_1, w_2, w_3 \dots$  etc. are the loads on the zones 0-1, 0-2, 0-3 ... etc. and that they consist of the dead weight  $g$  plus the live load  $p$ . If the surface area of any strip is  $dA$  so that e.g.  $dA_4 = ds_4 \cdot 2\pi \cdot \frac{r_3 + r_4}{2}$ , then  $dW_3 = dA_3 (g + p)$  and  $W_1 = dW_1$ ,  $W_2 = W_1 + dW_2$ ,  $W_3 = W_2 + dW_3 \dots$  etc.

If we draw through  $O$  parallels to the tangents of the meridian curve at 1, 2, 3 ... etc., the curve passing through the points of intersection of these parallels with the horizontals through  $W$  gives the values of the total horizontal thrust  $\mathcal{H}$ , where  $\mathcal{H} = 2\pi rH$ , in the different sections of the shell.

This curve can be directly used for determining the meridian and ring forces in the following manner:

The meridian forces can be determined according to equation a from the relation:

$$N_\varphi = \frac{W}{2\pi r \sin\varphi} = \frac{N}{2\pi r}$$

and the ring forces, according to equation b, from the relation:

$$N_\theta = \frac{d(Hr)}{ds} = \frac{1}{2\pi} \cdot \frac{\Delta \mathcal{H}}{\Delta s}$$

It has to be noted that  $N_\varphi$  is always compression while  $N_\theta$  is compression so long as  $\mathcal{H}$  increases (i.e.  $\Delta \mathcal{H}$  is outside the curve) and tension when  $\mathcal{H}$  decreases (i.e.  $\Delta \mathcal{H}$  is inside the curve).

In domes with vertical tangent at their foot, the horizontal thrust there is equal to zero and vertical reactions only are created at the supports so that no tension ring is required.

## 2 - Application to Popular Reinforced Concrete Surfaces of Revolution

### a) Spherical Shells

The relation between  $a$ ,  $r$  and  $y$  is given by: (Fig. XII-16).

$$a = \frac{r^2 + y^2}{2y}$$

The surface area of a spherical shell is:

$$A = 2\pi a y$$

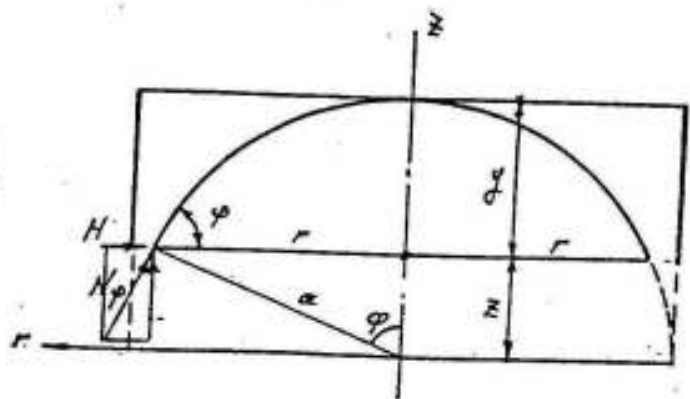


Fig. XII-16



i.e. it is equal to the surface area of a cylinder having the same radius  $a$  and height  $y$ .

Internal forces and Reactions due to Dead Load  $g/m^2$  Surface

The dead weight of a shell height  $y$ , and included in a central angle  $\varphi$  is given by :

$$W_{\varphi} = g A = g \cdot 2 \pi a y$$

but

$$r = a \sin \varphi \quad \text{and}$$

$$y = a (1 - \cos \varphi)$$

then

$$W_{\varphi} = g \cdot 2 \pi a^2 (1 - \cos \varphi)$$

The horizontal thrust  $H$  is given by :

$$H = \frac{W_{\varphi}}{2 \pi r \tan \varphi} = g a \frac{\cos \varphi}{1 + \cos \varphi} = g a \frac{z}{a + z}$$

The meridian force  $N_{\varphi}$  can be calculated from the relation ,

$$N_{\varphi} = \frac{H}{\cos \varphi} = g \frac{a}{1 + \cos \varphi} = g \frac{a^2}{a + z}$$

at crown  $\varphi = 0$  ,

$$\cos \varphi = 1$$

and

$$z = a, \text{ then}$$

$$N_{\varphi} = H = g \frac{a}{2}$$

compression

at the foot of half spherical shells,

where

$$\varphi = 90^{\circ} , \cos \varphi = 0$$

and

$$z = 0, \text{ we get}$$

$$N_{\varphi} = g a \text{ (comp.)}$$

and

$$H = 0$$

The ring force  $N_{\theta}$  is given by :

$$N_{\theta} = \frac{d(Hr)}{ds} = g a \left( \cos \varphi - \frac{1}{1 + \cos \varphi} \right) = g \left( z - \frac{a^2}{a + z} \right)$$

at crown  $\varphi = 0$  ,

$$\cos \varphi = 1$$

and

$$z = a, \text{ then}$$

$$N_{\theta} = H = g \frac{a}{2}$$

compression

at foot of half spherical shells, we have

$$N_{\theta} = -g a$$

tension

$$N_{\theta} = 0 \quad \text{at } \varphi = 51^{\circ} 49'$$

and

$$z = 0.618a$$

$$\text{or} \quad \text{at } y = 0.382 a \quad \text{and} \quad r = 0.787a$$

Introducing  $\varphi = 51^{\circ} 49'$  or  $z = 0.618a$  in the equation of  $H$ , we get the magnitude of the maximum horizontal thrust; thus

$$H_{\max} = 0.382 g a$$

i.e. the maximum total horizontal thrust  $\mathcal{H}_{\max} = 2 \pi r H_{\max}$  is therefore given by

$$\mathcal{H}_{\max} = 2 \pi \times 0.787 a \times 0.382 g a = 0.3 (2 \pi a^2 g)$$

i.e. the maximum total horizontal thrust of a spherical shell is equal to 0.3 the total dead weights on half the sphere.

The meridian and ring forces of spherical shells subject to dead

loads  $g/m^2$  surface can accordingly be expressed in the form shown in figure XII-17).

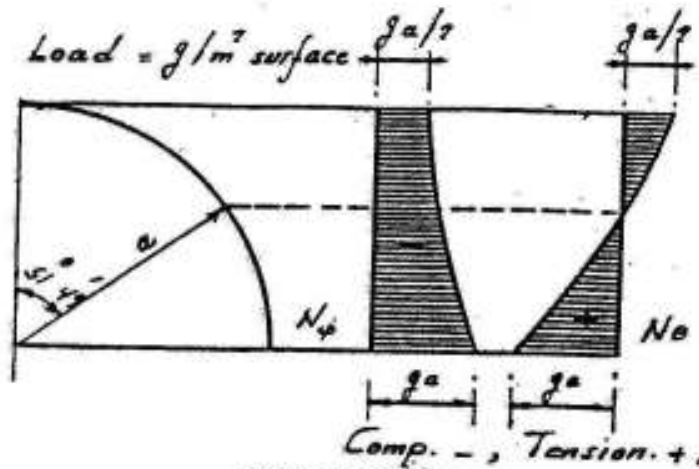


Fig. XII-17

Internal Forces and Reactions due to Live Load  $p/m^2$  Horizontal

Total load 
$$W_\psi = p \pi r^2 = p \pi \cdot a^2 \cdot \sin^2 \psi$$

The horizontal thrust 
$$H = \frac{W_\psi}{2 \pi r \tan \psi} = p a \frac{\cos \psi}{2} = p z/2$$

The meridian force 
$$N_\psi = \frac{H}{\cos \psi} = p a/2 = \text{constant}$$

i.e. the meridian forces due to  $p$  are constant in the shell. This striking result can also be proved in the following manner :

The general equation a gives 
$$W_\psi = N_\psi \cdot 2 \pi r \sin \psi$$

But 
$$W_\psi = p \pi r^2 \quad \text{and} \quad r = a \sin \psi$$

So that

$$N_\psi = \frac{p \pi r^2}{2 \pi r \sin \psi} = p a/2 = \text{constant}$$

The ring force 
$$N_\theta = \frac{d(H r)}{ds} \quad \text{or}$$

$$N_\theta = \frac{p a \cos 2\psi}{2} = \frac{p}{2 a} (2 z^2 - a^2)$$

at crown  $z = a$  and 
$$N_\psi = N_\theta = p a/2 \text{ compression}$$

at foot of half spherical shells = 
$$z = 0$$

and 
$$N_\theta = - p a/2 \text{ tension}$$

The ring force  $N_\theta = 0$  where 
$$2 z^2 = a^2 \quad \text{or} \quad z = 0.707 a$$

This result corresponds to  $\psi = 45^\circ$  i.e.  $r = z = 0.707 a$

Introducing this value in the equation of  $H$ , we get the magnitude of

$H_{\max}$ , thus :

$$H_{\max} = pz/2 = 0.3535 p a$$

and the maximum total horizontal thrust  $\mathcal{H}_{\max} = 2 \pi r H_{\max}$  is therefore given by :

$$\mathcal{H}_{\max} = 2 \pi \times 0.707 a \times 0.3535 p a.$$

Or

$$\mathcal{H}_{\max} = 0.5 \pi a^2 p$$

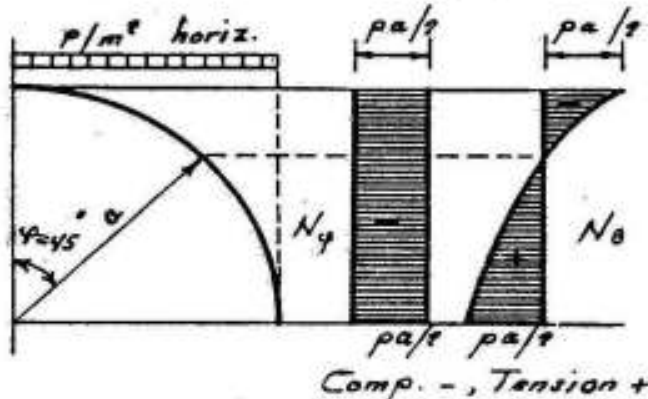


Fig. XII-18

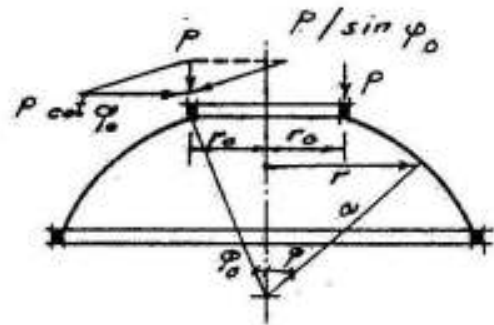


Fig. XII-19

which means that the maximum total horizontal thrust of a spherical shell is equal to half the total live loads on half the sphere.

The meridian and ring forces can accordingly be illustrated as shown in figure XII-18

### Lantern Load

Most domes are not closed at the vertex but have a skylight, or a ventilation opening, covered by a superstructure, the lantern. Assume its weight is  $P t/m'$  acting on the upper edge of the shell as a vertical line load. Since the shell can resist only tangential forces, this edge also needs a stiffening that resists the other component -  $P \cot \phi_0$  - and gets a compressive force from it (Fig. XII-19). The internal forces are for this case given by :

$$N_{\phi} = - W_{\phi} / 2 \pi r \sin \phi \quad \text{in which}$$

$$W_{\phi} = 2 \pi r_0 P = 2 \pi a \sin \phi_0 P \quad \text{and} \quad r = a \sin \phi$$

So that

$$N_{\phi} = - 2 \pi a \sin \phi_0 P / 2 \pi a \sin^2 \phi = - P \sin \phi_0 / \sin^2 \phi \quad \text{compression}$$

$N_{\theta}$  can be directly calculated from equation  $c'$ , thus

$$N_{\phi} + N_{\theta} = P_r a = 0 \quad \text{or} \quad N_{\theta} = - N_{\phi} \text{ i.e.}$$

$$N_{\theta} = + P \sin \phi_0 / \sin^2 \phi$$

b) Conical Shells

The surface area of a conical shell fig. XII-20; is given by :

$$A = 2 \pi r s/2 \quad \text{but}$$

$$r = y \cot \varphi \quad \text{and} \quad s = y / \sin \varphi$$

then

$$A = \pi y^2 \cos \varphi / \sin^2 \varphi$$

The meridian force  $N_s$  is given according to equation a by :

$$N_s = \frac{W_\varphi}{2 \pi r \sin \varphi} = \frac{W_\varphi}{2 \pi y \cos \varphi}$$

The ring force  $N_\theta$  is given according to equation c" by :

$$N_\theta = p_r r_2 \quad \text{in which} \quad r_2 = r \frac{s}{y} = y \frac{\cos \varphi}{\sin^2 \varphi} \quad \text{or}$$

$$N_\theta = p_r y \frac{\cos \varphi}{\sin^2 \varphi}$$

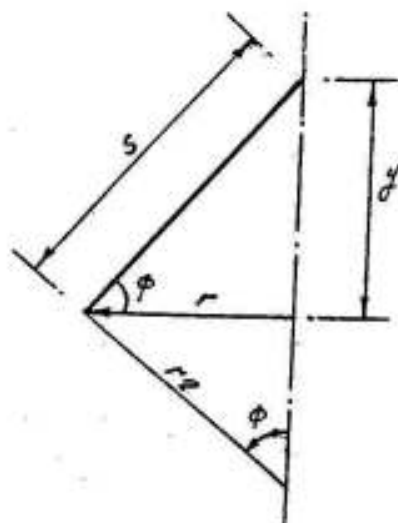


Fig. XII-20

Internal Forces due to Dead Load  $g/m^2$  Surface

The dead weight of a cone, height  $y$ , and included in a central angle  $\varphi$  is given by :

$$W_\varphi = g A = g \pi y^2 \cos \varphi / \sin^2 \varphi$$

The meridian force  $N_s$  is therefore given by :

$$N_s = \frac{W_\varphi}{2 \pi y \cos \varphi} = \frac{g \pi y^2 \cos \varphi / \sin^2 \varphi}{2 \pi y \cos \varphi} \quad \text{or}$$

$$N_s = \frac{g y}{2 \sin^2 \varphi} \quad \text{compression}$$

The ring force  $N_\theta$  can be determined from the given general equation if we replace  $p_r$  by  $g \cos \varphi$ ; hence

$$N_\theta = g \cos \varphi y \frac{\cos \varphi}{\sin^2 \varphi} = g y \cot^2 \varphi \quad \text{or}$$

$$N_\theta = g r^2 / y \quad \text{always compression}$$

Internal Forces due to Live Load  $p/m^2$  Horizontal

The live load  $p/m^2$  horizontal corresponds to  $p \cos \varphi$  per meter square surface, so that we can determine  $N_s$  and  $N_\theta$  if we replace  $g$  by  $p \cos \varphi$  in the previous equations, so that :

$$N_s = \frac{p y}{2} \frac{\cos \phi}{\sin^2 \phi} \quad \text{and}$$

$$N_\theta = p y \frac{\cos^3 \phi}{\sin^2 \phi}$$

### 3 - Tables of Membrane Forces in Popular Shells of Revolution

Alf Pfluger gives in his book "Elementary Statics of Shells" the membrane forces in some popular forms of shells under the effect of different cases of loading. We give in the following tables a choice of these cases :

### 4 - Edge Forces and Transition Curves

It has been shown that the upper zones of domes are subject to compressive ring forces, while the lower zones are subject to tensile ring forces. In case the dome, or cone, does not end with a vertical tangent, the horizontal thrust H must be resisted by a tension ring (Fig. XII-21a).

On the other hand, the meridian forces in domes and conical roofs due to vertical dead and live loads are always compressive giving relatively low stresses.

In conical shells and flat spherical domes, bending moments will be developed due to the big difference between the high tensile stresses in the foot ring and the compressive stresses or low tensile stresses in the adjacent zones of the shell.<sup>¶</sup> The bigger the difference in the strains between the ring and the adjacent zone, the higher will be the bending moments. The shape and magnitude of the bending moments at

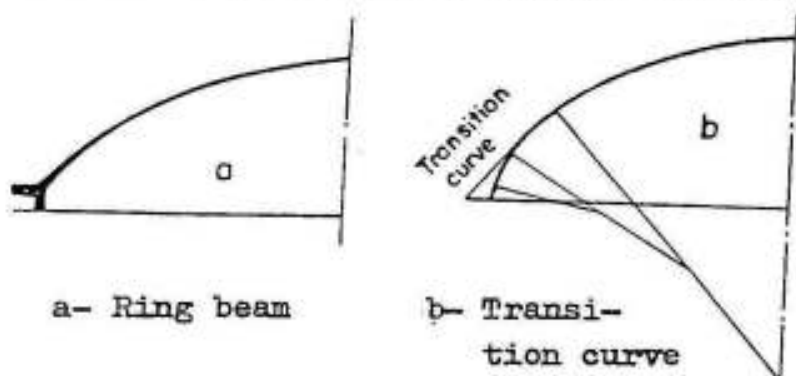


Fig. XII-21

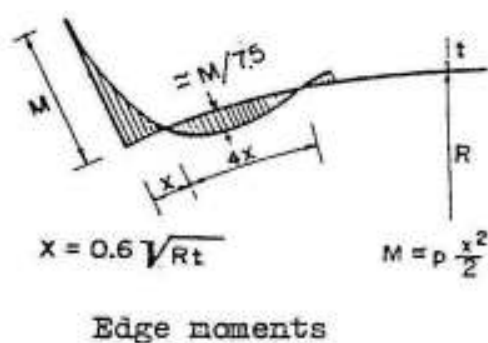


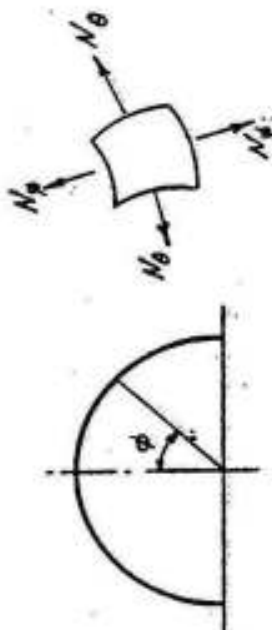
Fig. XII-22

¶ Refer to text books on shells such as :

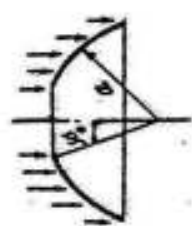
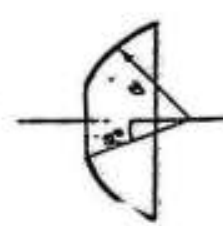
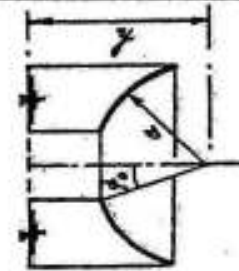
Flügge "Stresses in shells" published by Springer - Verlag. New-York  
 Ramaswamy " Design and Construction of Concrete Shell Roofs " Publi-  
 shed by Mc Graw-Hill book company.

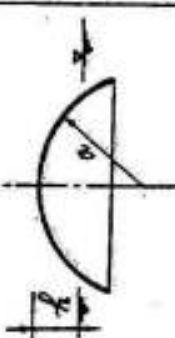
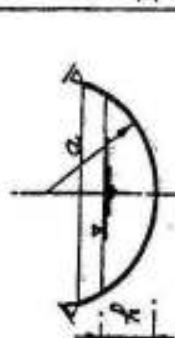
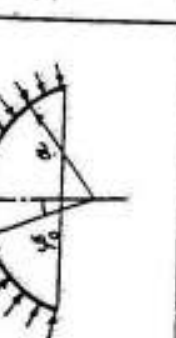
Markus : "Theorie und Berechnung Rotationssymmetrischer Bauwerke" Pu-  
 blished by Werner- Verlag- Düsseldorf.

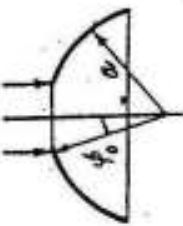
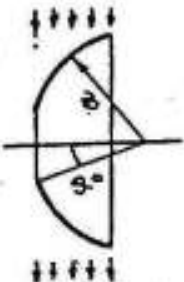
Spherical Shell



$N_\phi$  = Meridian force / m  
 $N_\theta$  = Ring force / m  
 T = Unit central shear

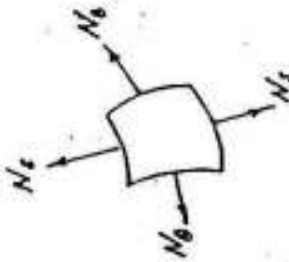
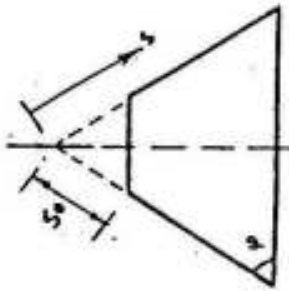
System	Loading	$N_\theta$	$N_\phi$
 <p>Dead Load  <math>g/m^2</math> surface  <math>P_r = g \cos \phi</math></p>	$-g a \frac{\cos \phi_0 - \cos \phi}{\sin^2 \phi}$ <p>For <math>\phi_0 = 0</math> (no vertex opening)</p> $-g a \frac{1}{1 + \cos \phi}$	$g a \left( \frac{\cos \phi_0 - \cos \phi}{\sin^2 \phi} - \cos \phi \right)$ $g a \left( \frac{1}{1 + \cos \phi} - \cos \phi \right)$	$g a \left( \frac{\cos \phi_0 - \cos \phi}{\sin^2 \phi} - \cos \phi \right)$ $g a \left( \frac{1}{1 + \cos \phi} - \cos \phi \right)$
 <p>Live load  <math>p/m^2</math> horizontal  <math>P_r = p \cos^2 \phi</math></p>	$-p \frac{a}{2} \left( 1 - \frac{\sin^2 \phi_0}{\sin^2 \phi} \right)$ <p>For <math>\phi_0 = 0</math> (no vertex opening)</p> $-p \frac{a}{2}$	$p \frac{a}{2} \left( 1 - \frac{\sin^2 \phi_0}{\sin^2 \phi} - 2 \cos^2 \phi \right)$ $-p \frac{a}{2} \cos 2 \phi$	$p \frac{a}{2} \left( 1 - \frac{\sin^2 \phi_0}{\sin^2 \phi} - 2 \cos^2 \phi \right)$ $-p \frac{a}{2} \cos 2 \phi$
 <p>Liquid pressure  <math>P_r = \gamma (h - a \cos \phi)</math>  <math>\gamma = wt/m^3</math> liquid</p>	$-\gamma a^2 \left[ \frac{h}{2a} \left( 1 - \frac{\sin^2 \phi_0}{\sin^2 \phi} \right) - \frac{1}{3} \frac{\cos^3 \phi_0 - \cos^3 \phi}{\sin \phi} \right]$ <p>For <math>\phi_0 = 0</math> (no vertex opening)</p> $-\gamma a^2 \left[ \frac{h}{2a} - \frac{1}{3} \left( 1 + \frac{\cos^2 \phi}{\cos \phi} \right) \right]$	$-\gamma a \left[ \frac{h}{2} \left( 1 + \frac{\sin^2 \phi_0}{\sin^2 \phi} \right) + \frac{a}{3} \left( \frac{\cos^3 \phi_0 - \cos^3 \phi}{\sin^2 \phi} - 3 \cos \phi \right) \right]$ $-\gamma a^2 \left[ \frac{h}{2a} - \cos \phi + \frac{1}{3} \left( 1 + \frac{\cos^2 \phi}{\cos \phi} \right) \right]$	$-\gamma a \left[ \frac{h}{2} \left( 1 + \frac{\sin^2 \phi_0}{\sin^2 \phi} \right) + \frac{a}{3} \left( \frac{\cos^3 \phi_0 - \cos^3 \phi}{\sin^2 \phi} - 3 \cos \phi \right) \right]$ $-\gamma a^2 \left[ \frac{h}{2a} - \cos \phi + \frac{1}{3} \left( 1 + \frac{\cos^2 \phi}{\cos \phi} \right) \right]$

System	Loading	$N_\phi$	$M_\phi$
	Liquid pressure $P_r = \gamma(a - a \cos \phi - h)$	$-\gamma \frac{a^2}{6} \left\{ \frac{h}{a} \left[ \frac{1}{\sin^2 \phi} - \frac{h(3-h)}{a} \right] + 1 - \frac{2 \cos^2 \phi}{1 + \cos \phi} \right\}$	Points above the liquid level $0$ Points below the liquid level $-\gamma a^2 \left( 1 - \cos \phi - \frac{h}{a} \right) - N_\phi$
	liquid pressure $P_r = \gamma(a - a \cos \phi - h)$	$\gamma \frac{h^2}{6} \left( 3 - \frac{h}{a} \right) \frac{1}{\sin \phi}$ $\gamma \frac{a^2}{6} \left[ 3 \frac{h}{a} - 1 + \frac{2 \cos^2 \phi}{1 + \cos \phi} \right]$	Points above the liquid level $-\gamma \frac{h^2}{6} \left( 3 - \frac{h}{a} \right) \frac{1}{\sin^2 \phi}$ Points below the liquid level $\gamma a^2 \left[ \frac{h}{a} - 1 + \cos \phi \right] - N_\phi$
	Normal pressure $P_r = p$	$-p \frac{a}{2} \left( 1 - \frac{\sin^2 \phi_0}{\sin^2 \phi} \right)$ $-p \frac{a}{2}$	$-p \frac{a}{2} \left( 1 + \frac{\sin^2 \phi_0}{\sin^2 \phi} \right)$ $-p \frac{a}{2}$ For $\phi_0 = 0$ ( no vertex opening )

System	Loading	$N_{\phi}$	$N_{\phi_0}$
	Edge load p/m Vertex load P	$- P \frac{\sin \phi_0}{\sin^2 \phi}$ <p>For <math>\phi_0 = 0</math> (no vertex opening, single load P at the vertex)</p> $- \frac{P}{2 \pi a \sin^2 \phi}$	$P \frac{\sin \phi_0}{\sin^2 \phi}$ $\frac{P}{2 \pi a \sin^2 \phi}$
	Wind load w $P_r = w \sin \phi \cos \theta$	$- w \frac{a}{3} \frac{\cos \theta \cos \phi}{\sin^3 \phi} x$ $x \left[ 3 (\cos \phi_0 - \cos \phi) - (\cos^3 \phi_0 - \cos^3 \phi) \right]$ <p>The unit central shear <math>T = N_{\phi\theta}</math> is given by :</p> $T = w \frac{a}{3} \frac{\sin \theta}{\sin^3 \phi} x \left[ 3 (\cos \phi_0 - \cos \phi) - \cos^3 \phi_0 - \cos^3 \phi \right]$ <p>For <math>\phi_0 = 0</math> (no vertex opening)</p> $- w \frac{a}{3} \frac{\cos \theta \cos \phi}{\sin^3 \phi} x$ $x (2 - 3 \cos \phi + \cos^3 \phi)$ $T = w \frac{a}{3} \frac{\sin \theta}{\sin^3 \phi} x (2 - 3 \cos \phi + \cos^3 \phi)$	$w \frac{a}{3} \frac{\cos \theta}{\sin^3 \phi} x$ $x \left[ \cos \phi (3 \cos \phi_0 - \cos^3 \phi_0) - 3 \sin^2 \phi - 2 \cos^4 \phi \right]$ $w \frac{a}{3} \frac{\cos \theta}{\sin^3 \phi} x$ $x \left[ \cos \phi (3 \cos \phi_0 - \cos^3 \phi_0) - 3 \sin^2 \phi - 2 \cos^4 \phi \right]$



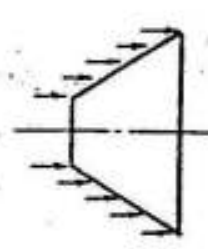
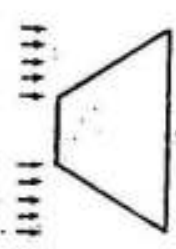
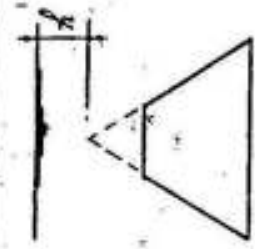
Conical Shell



$N_s$  = Meridian force / m

$N_\theta$  = Ring force / m

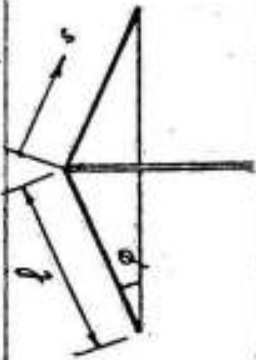
$T$  = Unit central shear

System	Loading	$N_s$	$N_\theta$
 Dead load $g / m^2$ surface $P_r = g \cos \psi$	$-g \frac{s^2 - s_0^2}{2s} \frac{1}{\sin \psi}$ <p>For <math>s_0 = 0</math> (complete cone)</p> $-g \frac{s}{2 \sin \psi}$	$-gs \frac{\cos^2 \psi}{\sin \psi}$	
 Live load $p / m^2$ horizontal $P_r = p \cos^2 \psi$	$-p \frac{s^2 - s_0^2}{2s} \cot \psi$ <p>For <math>s_0 = 0</math> (complete cone)</p> $-p \frac{g}{2} \cot \psi$	$-ps \frac{\cos^3 \psi}{\sin \psi}$	
 Liquid pressure $P_r = \gamma (h + s \sin \psi)$ $\gamma = wt/m^3$ liquid	$-\frac{\gamma}{g} \left( h \frac{s^2 - s_0^2}{2} \cot \psi + \frac{s^3 - s_0^3}{3} \cos \psi \right)$ <p>For <math>s_0 = 0</math> (complete cone)</p> $-\gamma s \left( \frac{h}{2} \cot \psi + \frac{s}{3} \cos \psi \right)$	$-\gamma s (h \cot \psi + s \cos \psi)$	

System	Loading	$N_s$	$N_\theta$
	Liquid pressure $P_r = \gamma (s \sin\phi - h)$	Points above the liquid level 0 Points below the liquid level $-\frac{\gamma}{6s} \left[ \frac{\cos\phi}{\sin^2\phi} h^3 + s^2 (2s \cos\phi - 3h \cot\phi) \right]$	0 $-\gamma s (s \cos\phi - h \cot\phi)$
	Liquid pressure $P_r = \gamma (h - s \sin\phi)$	Points above the liquid level $\frac{\gamma h^3}{6s} \frac{\cos\phi}{\sin^2\phi}$ Points below the liquid level $\gamma \frac{s}{2} (3h \cot\phi - 2s \cos\phi)$	0 $\gamma s (h \cot\phi - s \cos\phi)$
	Normal pressure $P_r = p$	$-p \frac{s^2 - s_0^2}{2s} \cot\phi$ For $s_0 = 0$ (complete cone) $-p \frac{s}{2} \cot\phi$	$-ps \cot\phi$ $-ps \cot\phi$
	Edge load p/m Axial load P	$-p \frac{s_0}{s} \frac{1}{\sin\phi}$ $-P \frac{1}{2\pi s \sin\phi \cos\phi}$ For $s_0 = 0$ (end axial single load)	—
	Wind load $w / m^2$ $P_r = w \sin\phi \cos\theta$	$-w \frac{s}{2} \left[ \cos\phi - \frac{1}{3\cos\phi} - \frac{s_0^2}{s^2} \right] \times$ $\times \left[ \cos\phi - \frac{1}{\cos\phi} - \left(\frac{s_0}{s}\right)^2 \frac{2}{3\cos\phi} \right] \cos\theta$ $-w \frac{s}{2} \left( \cos\phi - \frac{1}{3\cos\phi} \right) \cos\theta$ For $s_0 = 0$ (complete cone)	$\frac{T}{N_\theta}$ $-\frac{ws \cos\phi \cos\theta}{s^3 - s_0^3}$ $-\frac{w}{3s^2} \frac{2}{3} \sin\theta$ $-\frac{ws \cos\phi \cos\theta}{s^3 - s_0^3}$ $-\frac{ws \cos\phi \cos\theta}{s^3 - s_0^3}$

Conical Shell

Supported at Vertex  
and with Free Edge



System	Loading	$N_s$	$N_\theta$	T
	Dead load $g / m^2$ surface $P_r = g \cos \psi$	$g \frac{l^2 - s^2}{2s} \frac{1}{\sin \psi}$	$- g s \frac{\cos^2 \psi}{\sin \psi}$	0
	Live load $p / m^2$ horizontal $P_r = p \cos^2 \psi$	$p \frac{l^2 - s^2}{2s} \cot \psi$	$- p s \frac{\cos^3 \psi}{\sin \psi}$	0
	Normal load $P_r = p$	"	$p s \cot \psi$	0
	Wind load $w / m^2$ $P_r = w \sin \psi \cos \theta$	$w \left[ \frac{l^3 - s^3}{3s^2} \frac{2}{2s} \frac{-s^2 \sin^2 \psi}{\cos \psi} \right]$	$- w s \cos \psi \cos \theta$	$w \frac{l^3 - s^3}{3s^2} \sin \theta$

the foot-ring can be estimated according to the values given in Fig. XII-22.

As the bending moments are due to the sudden change from high tensile stresses in the foot-ring to low tensile stresses or even compressive stresses in the shell, they can be avoided if the shape of the meridian is changed in a convenient manner. This change can be done by a transition curve (Fig. XII-21b) which, when well chosen gives a relief to the stresses at the foot-ring. It is recommended to make the change of the stresses gradual from foot-ring to shell.

In order to decrease the stresses due to the forces at the foot ring, it is recommended to increase the thickness of the shell in the region of the transition curve.

#### 5 - Examples:

Figure XII-23 shows a project of a covered circular gymnasium, 50 ms diameter. The upper part of the roof is covered by a flat dome 30 ms diameter, 3.4 ms high, and 10 cms thick. It is provided with a central lantern 1.5 ms diameter and supported at its lower edge on 96 posts 1.0 m center to center. The dome is bounded by two circular rings, one compression ring at the upper edge below the lantern, and the other tension ring at the lower edge over the posts. The upper dome is supported by a truncated cone, 4.5 ms high, 10 cms thick and having a diameter of 30 ms at its upper edge and of 50 ms at its lower edge. This cone is again provided with two ring beams, one at the upper edge to resist the compression forces created from the loads of the upper dome, and one at the lower edge to resist the tensile forces created from the horizontal thrust of the cone. The lower ring beam is again here supported on 72 vertical posts 2.0 ms center to center.

The three main parts of the roof, the lantern, the upper dome, and the lower cone, are supported on the posts shown in order to give the required architectural effect, to support the windows necessary for lighting and to allow for the free lateral movement of their lower edge.

The meridian and ring forces in both upper dome and lower cone are compressive and relatively low so that a thickness of 10 cms is ample. The thickness of the shell roof is gradually increased to 15 cms over a length of 1.20 ms in order to resist the edge moments due to the local shear.

PROJECT  
OF  
A COVERED CIRCULAR MALL  
(I)

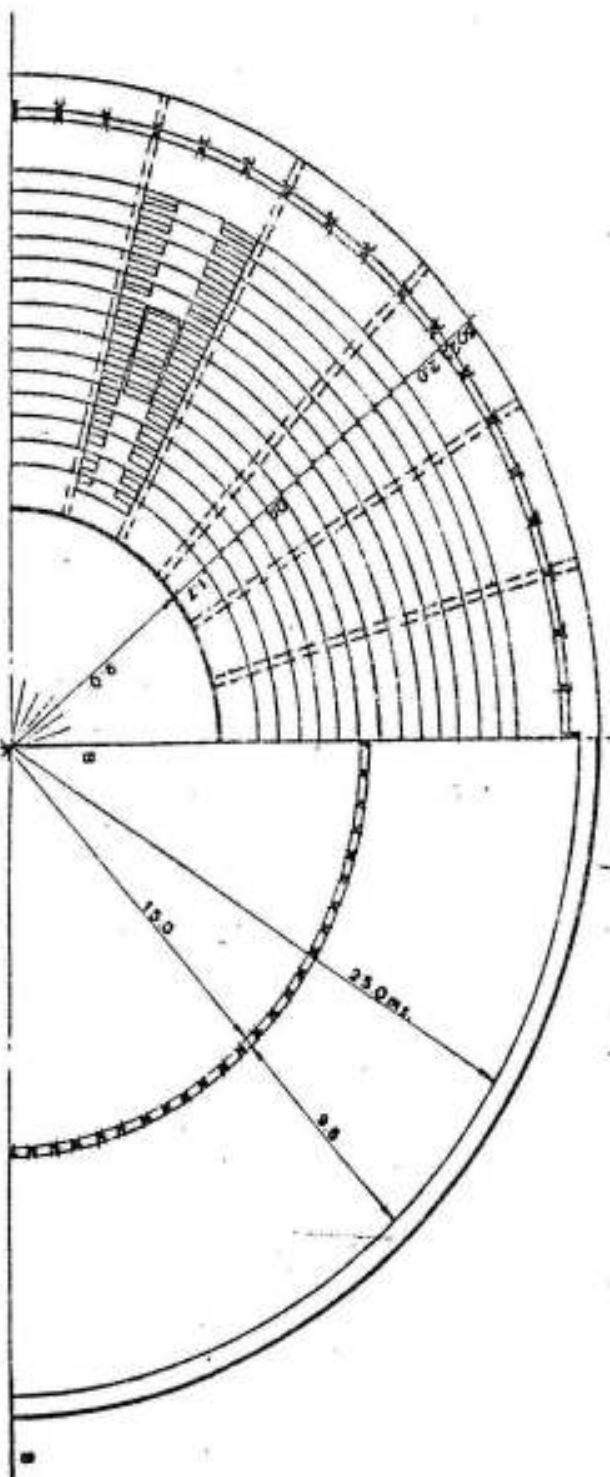
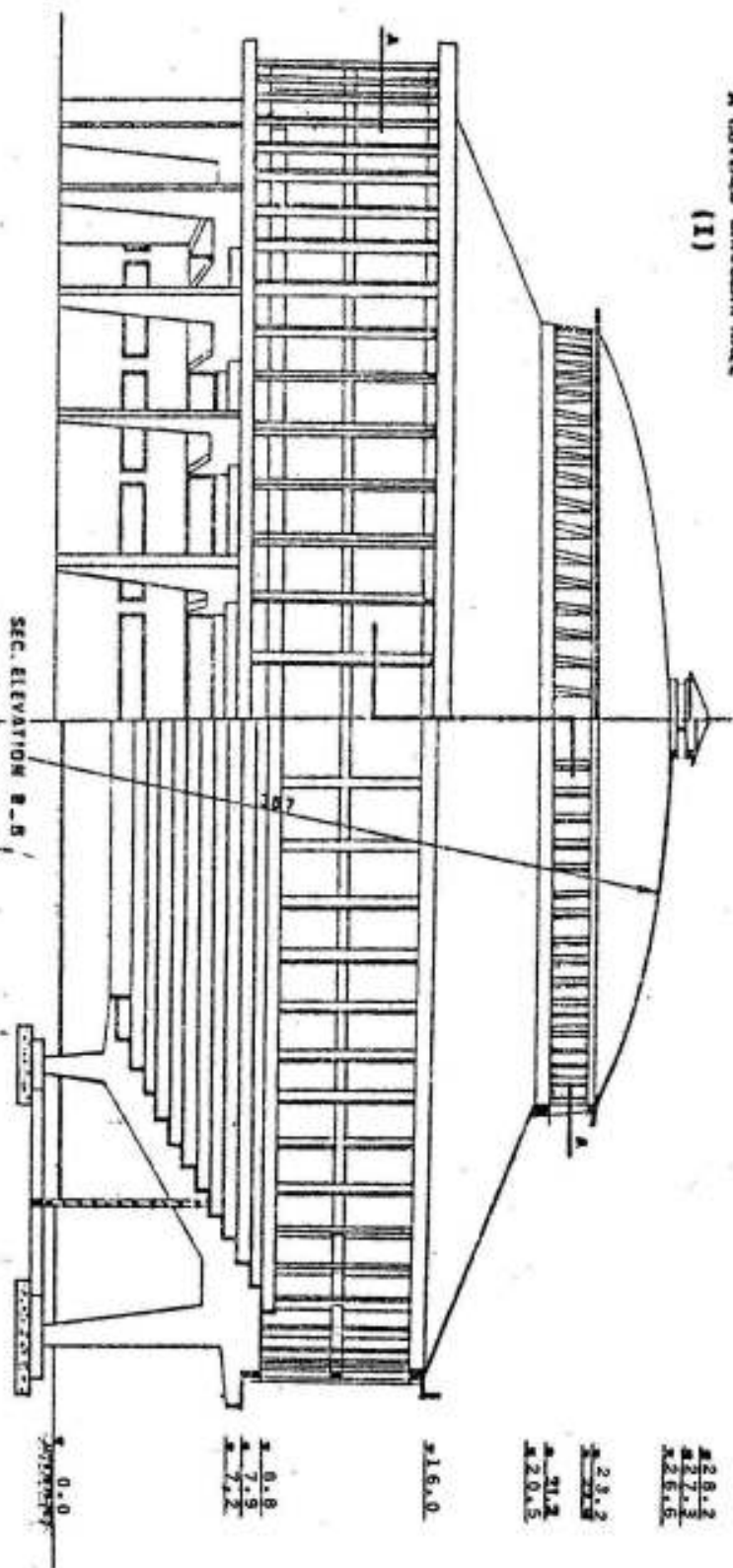


Fig. XII-23

HALF SEC. PLAN A-A





The shell is reinforced by one mesh  $5 \Phi 8$  mm in each direction except at the edges where two meshes are essential.

The reinforcements required in the foot-rings of the upper dome and the lower cone are high because both dome and cone are relatively flat.

Figure XII-24a gives an alternative solution for the same project in which the upper truncated cone of the roof with its lantern are supported on the free edge of the upper cantilever of the main stands. The details of the cone and the main frames of the stand are shown in Fig. XII-24b.

#### 6 - Circular beams

Circular beams loaded and supported normal to their plane (fig. XII-25) are dealt with in detail in textbooks on theory of elasticity<sup>x</sup>. We give in the following the fundamental equations required to determine the internal forces in a circular beam over  $n$  supports and subjected to a uniform load  $p/m$ .

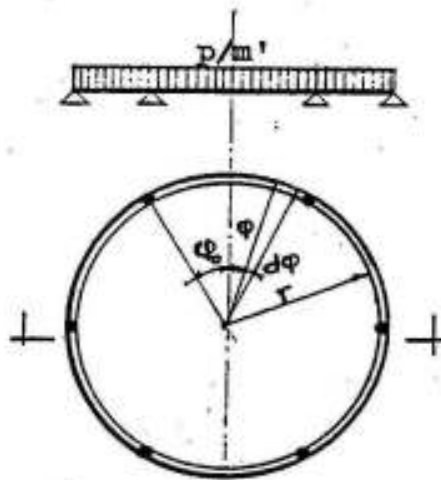


Fig. XII-25

The equations of equilibrium governing the relation between the load  $p$ , the shearing force  $Q$ , the bending moment  $M$  and the torsional moment  $M_t$  acting on an element  $ds$  enclosing a central angle  $d\phi$  of a circular beam having a radius  $r$  are as follows:

---

Refer for example to:

Kurt Beyer " Statik in Stahlbetonbau " , published by : Springer-Verlag , Berlin.



$$\frac{dQ}{ds} = -p \quad \text{but } ds = r d\psi \quad \text{so that}$$

$$\frac{dQ}{d\psi} = -p r \dots \dots \dots \quad (a) \quad \text{further}$$

$$\frac{dM}{ds} + \frac{dM_t}{dr} - Q = 0 \quad \text{as } r = \text{const. then } \frac{dM_t}{dr} = \frac{M_t}{r} \quad \&$$

$$\frac{dM}{ds} + \frac{M_t}{r} - Q = 0 \quad \text{substituting } ds = r d\psi \quad \text{we get}$$

$$\frac{dM}{d\psi} + M_t = Q r \quad (b)$$

The component of the moment  $M$  along  $ds$  in the radial direction must be equal to the difference of the torsional moments along the same element, thus

$$dM_t = M d\psi = \frac{M ds}{r} \quad \text{or}$$

$$\frac{dM_t}{d\psi} = M \quad (c)$$

which means that the torsional moment is maximum at point of zero bending moments.

Differentiating equation (b) with respect to  $\psi$ , we get

$$\frac{d^2 M}{d\psi^2} + \frac{dM_t}{d\psi} = \frac{dQ r}{d\psi} = r^2 \frac{dQ}{ds} \quad \text{or}$$

$$\frac{d^2 M}{d\psi^2} + M = -p r^2 \quad (d)$$

The solution of this differential equation is given by :

$$M = A \sin \psi + B \cos \psi - p r^2 \quad (e)$$

The integration constants  $A$  and  $B$  can be determined from the conditions at the supports.

The torsional moment  $M_t$  can be determined according to equation (c) from the relation

$$M_t = \int M d\psi \quad (f)$$

The internal forces are in this manner statically indeterminate. In many cases, they can be determined from the conditions of equilibrium alone because the statically indeterminate values are either known or equal to zero.

We give in the following the internal forces for some cases of circular beams.

a) Circular Beam Subject to Uniform Load  $p$  and Supported Symmetrically on  $n$  Supports.

The solution of equation (e) is given in the following relations:

$$2\psi_0 = \frac{2\pi}{n} \quad \text{and} \quad \psi_0 = \frac{\pi}{n}$$

$$\text{Reaction} \quad R = \frac{2\pi r p}{n}$$

Max. shearing force to the right or left of any support :

$$Q_{\max} = \pm \frac{\pi r p}{n}$$

The bending moment  $M$ , the torsional moment  $M_t$  and the shearing force  $Q$  in any section at an angle  $\psi$  from the center line between two successive supports, are given by :

$$M = r^2 p \left( \frac{\pi \cos \psi}{n \sin \psi_0} - 1 \right)$$

$$M_t = -r^2 p \left( \frac{\pi \sin \psi}{n \sin \psi_0} - \psi \right)$$

$$Q = -r p \psi$$

We give in the following table, the reactions, the maximum shearing forces, bending moments and torsional moments in a circular beam of radius  $r$  supported symmetrically on  $n$  supports and subject to a total, uniformly distributed, load  $P$ .

$$P = 2\pi r p$$

Number of Cols.	Load on each Column	Max. Shearing Force	Max. Bending Moment		Max. Torsional Moment	Angle bet. axis of Col. & Sec. of max. $M_t$
			at C.L. of span	over C.L. of columns		
$n$	$V$	$Q_{\max}$	$M (+)$	$M (-)$	$M_t$	Degree
4	$P/4$	$P/8$	$.0176 P r$	$.0053 P r$	$.0053 P r$	$19^\circ 21'$
6	$P/6$	$P/12$	$.0075 P r$	$.0148 P r$	$.0015 P r$	$12^\circ 44'$
8	$P/8$	$P/16$	$.0042 P r$	$.0083 P r$	$.0006 P r$	$9^\circ 33'$
12	$P/12$	$P/24$	$.0019 P r$	$.0037 P r$	$.0002 P r$	$6^\circ 21'$

b) Cantilever Circular Beam Symmetrically Loaded. Fig. XII-2

Due to symmetry, the shearing force  $Q$  and the torsional moment  $M_t$

at c are equal to zero, thus :

$$Q_c = 0 \quad \text{and} \quad M_{tc} = 0$$

For a single concentrated load

P acting at c

Reactions :

$$R_A = - \frac{P f}{2 l} \quad \text{and} \quad R_B = \frac{P}{2} \left( 1 + \frac{f}{l} \right)$$

Bending moment at c

$$M_c = \frac{P b}{2} \left( 1 - \frac{d f}{b l} \right)$$

For two equal concentrated loads

P acting at e and e'

$$R_A = - \frac{P n}{l} \quad \text{and} \quad R_B = P \left( 1 + \frac{n}{l} \right)$$

$$M_c = P b \left( 1 - \frac{m}{b} - \frac{n d}{b l} \right)$$

For a uniform load p/m on circular part B B'

$$R_A = - p r \psi_0 \frac{s}{l} \quad \text{and} \quad R_B = p r \psi_0 \left( 1 + \frac{s}{l} \right)$$

$$M_c = p b r \left[ \psi_0 \left( 1 - \frac{s d}{l b} \right) - \frac{f}{b} \right]$$

in which  $s$  = distance of center of gravity of arch from B B'

$$\text{and } s = \left( \sin \psi_0 - \psi_0 \cos \psi_0 \right) \frac{r}{\psi_0}$$

c) Totally Fixed Cantilever Circular Beam Symmetrically Loaded

Fig. XII-27

Due to symmetry  $Q_c = 0$  and  $M_{tc} = 0$

This beam is once statically indeterminate, the statically indeterminate value  $M_c$  can be determined as follows :

$$M_c = - \frac{\alpha_0}{\alpha_1} \quad \text{in which}$$

$$\alpha_0 = 2 r \int_0^{\psi_0} (M_0 \cos \psi - M_{t0} \sin \psi) d\psi$$

and

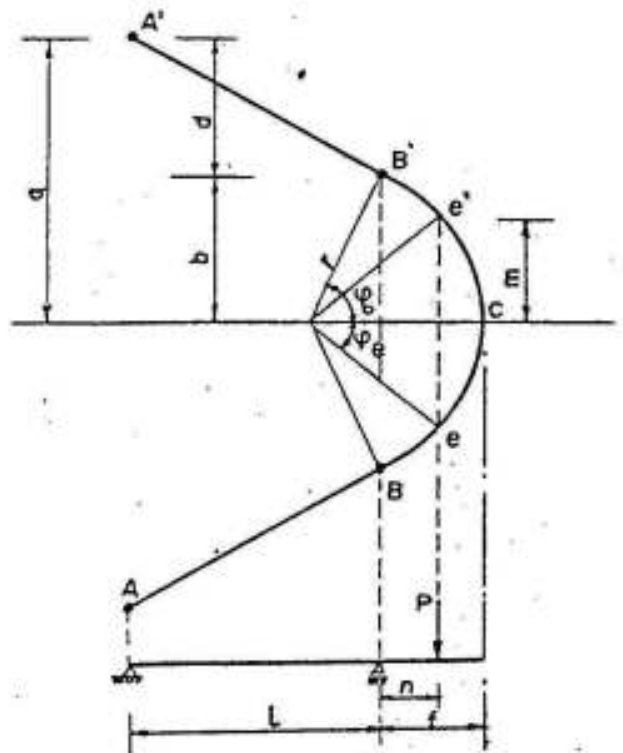


Fig. XII-26

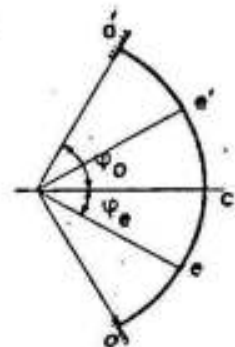


Fig. XII-27

$$\alpha_1 = 2 r \int_0^{\psi_0} (\cos^2 \psi + \kappa \sin^2 \psi) d\psi =$$

$$\frac{r}{2} \left[ 2(\kappa + 1) \psi_0 - (\kappa - 1) \sin 2\psi_0 \right]$$

for half a circle  $\psi_0 = \frac{\pi}{2}$  and  $\alpha_1 = \frac{r\pi}{2} (\kappa + 1)$  in which

$$\kappa = \frac{E}{G} \cdot \frac{I}{I'}$$
 and

$E$  = modulus of elasticity

$$G = \text{modulus of rigidity} = \frac{E}{2 \left(1 + \frac{1}{m}\right)}$$

$$\frac{1}{m} = \text{poisson ratio} = \frac{1}{6} \div \frac{1}{5} \text{ i.e.}$$

$$\frac{E}{G} = 2.4$$

$$I_y = \text{moment of inertia about } y - y = \frac{t b^3}{12}$$

(fig. XII-28).

$I'$  = torsion modulus

$$\text{For a rectangular section with } \frac{t}{b} = n > 1 \quad I' = n \psi b^4$$

In the following table, the values of  $\psi$  are given as a factor of  $n = \frac{t}{b}$

n	1	1.5	2	3	4	6	8	10	$\infty$
$\psi$	0.140	0.196	0.229	0.263	0.281	0.298	0.307	0.312	0.333

Therefore  $\kappa = 2.4 \frac{t b^3}{12} \cdot \frac{b}{t \psi b^4} = \frac{1}{5 \psi}$  and can be extracted from the following table :

n	1	1.5	2	3	4	6	8	10	$\infty$
$\kappa$	1.425	1.020	0.875	0.760	0.711	0.670	0.651	0.640	0.600

For a single concentrated load  $P$  at  $c$  we get :

$$M_c = - P r \cdot \frac{2 \frac{\kappa}{\kappa - 1} (\cos \psi_0 - 1) + \sin^2 \psi_0}{2 \frac{\kappa + 1}{\kappa - 1} \psi_0 - \sin 2\psi_0}$$

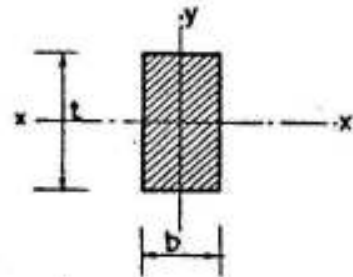


Fig. XII-28

$$M_a = -\frac{P}{2} r \sin \varphi_0 - M_c \cos \varphi_0$$

$$M_t = \frac{P}{2} r (1 - \cos \varphi_0) - M_c \sin \varphi_0$$

For a uniform load p/m'

$$M_c = + p r^2 \frac{\frac{\kappa+1}{\kappa-1} (4 \sin \varphi_0 - 2 \varphi_0) - \frac{4\kappa}{\kappa-1} \varphi_0 \cos \varphi_0 + \sin 2\varphi_0}{2 \frac{\kappa+1}{\kappa-1} \varphi_0 - \sin 2\varphi_0}$$

$$M_a = - p r^2 (1 - \cos \varphi_0) + M_c \cos \varphi_0$$

$$M_t = p r^2 (\varphi_0 - \sin \varphi_0) - M_c \sin \varphi_0$$

If the beam is a fixed cantilever half circle, we get :

For a single concentrated load P at c :

$$M_c = \frac{P r}{\pi} \quad M_a = -\frac{P r}{2} \quad M_{ta} = \frac{P r}{\pi} \left( \frac{\pi}{2} - 1 \right)$$

For two equal concentrated loads P at e and e'

$$M_c = \frac{2 P r}{\pi} \left[ \cos \varphi_e - \left( \frac{\pi}{2} - \varphi_e \right) \sin \varphi_e \right]$$

$$M_a = - P r \sin \left( \frac{\pi}{2} - \varphi_e \right)$$

$$M_{ta} = \frac{2 P r}{\pi} \left( \frac{\pi}{2} - \cos \varphi_e - \varphi_e \sin \varphi_e \right)$$

For a uniform load p/m'

$$M_c = p \frac{r^2}{\pi} (4 - \pi) = 0.274 p r^2$$

$$M_a = - p r^2$$

$$M_{ta} = p r^2 \left( \frac{\pi}{2} - \frac{4}{\pi} \right) = 0.3 p r^2$$

## XII-4 CYLINDRICAL SHELLS

### 1- Introduction

A cylindrical shell is generated by moving a straight line "generator" along a curve "profile or basic curve" while maintaining it parallel to its original direction.

Cylindrical shells of horizontal axis are used in engineering practice either as tube-like closed structures (Fig. XII-29a), as barrel-like open structures (Fig. XII-29b) or of the saw-tooth form (Fig. XII-30). They may be "long" if their span (distance between

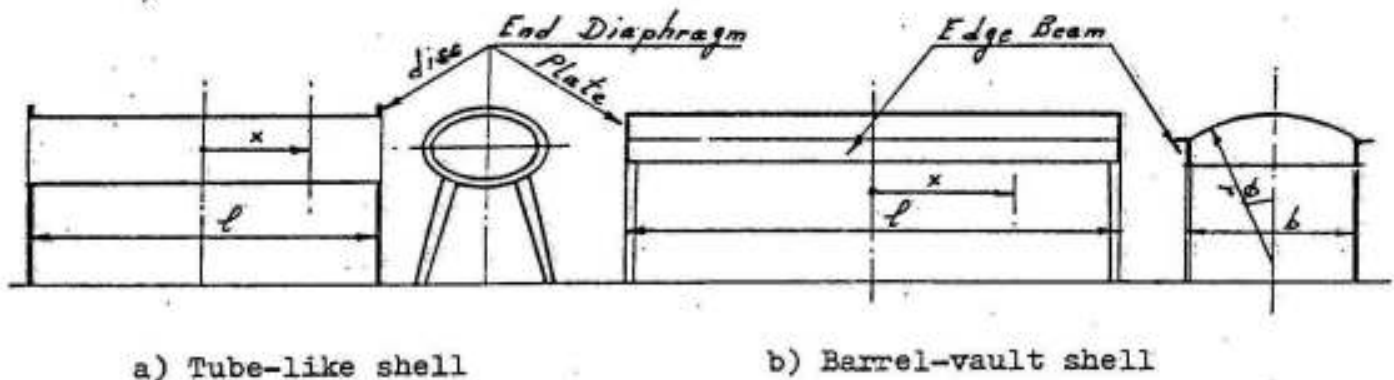


Fig. XII-29

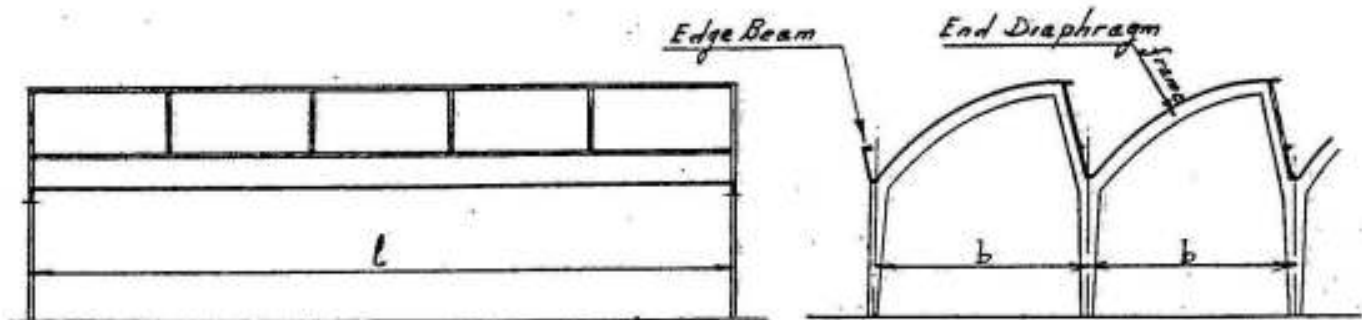


Fig. XII-30 Saw-tooth shell

diaphragms) is big relative to its breadth  $b$  (distance between edge beams), Fig. XII-29 and 30, or short if their span  $l$  is small relative to their breadth  $b$  (Fig. XII-31).

In the plane of the supports, normal to the generators, such shells must be provided with end diaphragms in the form of discs, plates, arches, trusses, or frames to resist the central shear of the shell.

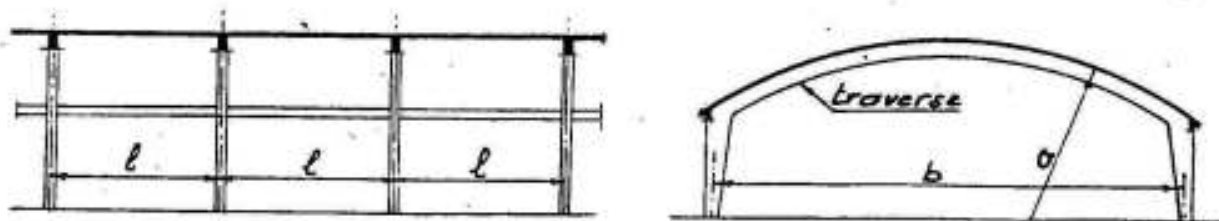


Fig. XII-31 a short shell

## 2- The Membrane Theory

The membrane theory may be used for determining the internal forces in cylindrical shells. In the analysis according to this theory, moments, torsion, and transverse shear forces are neglected while considering the equilibrium with normal forces and shear forces in the plane of the shell only.

In cylindrical shells, generators and profiles suggest themselves as a natural net of coordinate lines. We choose an arbitrary profile as the datum line and from this measure the coordinate  $x$  along the generators, positive in one direction and negative in the other; The second coordinate must vary from generator to generator. In analogy to the angle  $\Phi$  used on surfaces of revolution, we introduce here the angle  $\phi$  which a tangent to the profile makes with a horizontal plane (Fig. XII-32).

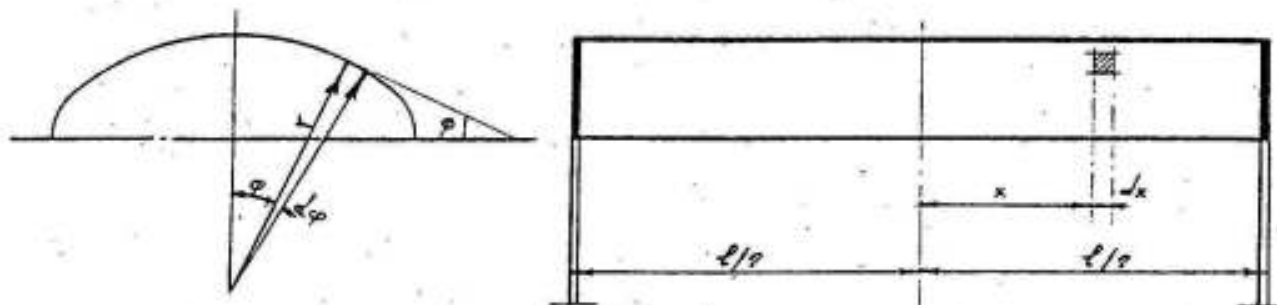
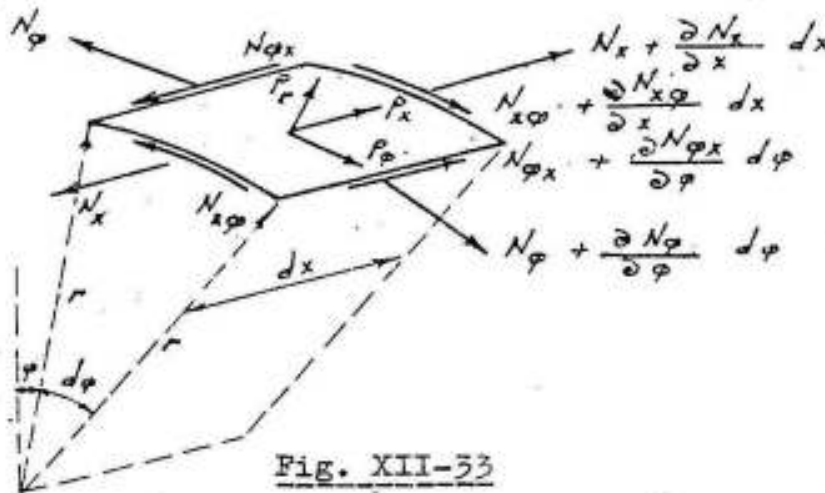


Fig. XII-32

We consider now the conditions of equilibrium of a cylindrical shell. For this purpose, we cut from it an element bounded by two adjacent generators  $\Phi$  and  $\Phi + d\Phi$  and by two adjacent profiles  $x$  and  $x+dx$  (Fig. XII-32). The membrane forces which act on the four edges must all lie in tangential planes to the middle surface and may be resolved into normal and shear components as shown.

The internal forces per unit length of section are  $N_x$ ,  $N_\varphi$  (normal forces) and  $N_{x\varphi} = N_{\varphi x}$  (shearing forces). The load per unit area of shell element has the components  $p_x$ ,  $p_\varphi$  in the directions of increasing  $x$  and  $\varphi$ , respectively, and a radial (normal) component  $p_r$  positive upward.



The stress resultants  $N_x$ ,  $N_\varphi$ ,  $N_{x\varphi}$  can be determined from three conditions of equilibrium. These conditions may easily be read from figure XII-33. For the equilibrium normal to the middle surface we have, besides the external forces  $p_r \cdot dx \cdot r d\varphi$ , only the resultant of the two forces  $N_\varphi \cdot dx$ , pointing inwards. Thus:

$$N_\varphi \cdot dx \cdot d\varphi - p_r \cdot dx \cdot r d\varphi = 0 \quad (1)$$

For the forces parallel to a tangent to the profile, we have

$$\frac{\partial N_\varphi}{\partial \varphi} d\varphi \cdot dx + \frac{\partial N_{x\varphi}}{\partial x} \cdot dx \cdot r d\varphi + p_\varphi \cdot dx \cdot r d\varphi = 0 \quad (2)$$

The equilibrium in the  $x$ -direction yields the equation

$$\frac{\partial N_x}{\partial x} \cdot dx \cdot r d\varphi + \frac{\partial N_{\varphi x}}{\partial \varphi} d\varphi \cdot dx + p_x \cdot dx \cdot r d\varphi = 0 \quad (3)$$

Dividing by the two differentials, we get the following differential equations for the membrane forces in the shell;

$$N_\varphi = p_r \cdot r \quad (4)$$

$$\frac{\partial N_{x\varphi}}{\partial x} = -p_\varphi - \frac{1}{r} \cdot \frac{\partial N_\varphi}{\partial \varphi} \quad (5)$$

$$\frac{\partial N_x}{\partial x} = -p_x - \frac{1}{r} \cdot \frac{\partial N_{x\varphi}}{\partial \varphi} \quad (6)$$

In order to calculate  $N_\varphi$ ,  $N_{x\varphi} = N_{\varphi x}$ ,  $N_x$ , we proceed as follows:



1) First, we determine  $N_\varphi$  according to equation 4. This "hoop force" depends only on the local intensity of the normal load  $p_r$  and cannot be influenced by the boundary conditions. This is not of great importance for shells whose profiles are closed curves and which have two profiles as boundaries, e.g., the shell shown in figure XII-29a. But for shells as that shown in figure XII-29b, the impossibility of prescribing arbitrary values of  $N$  at the straight edges leads to the crucial point in the membrane theory of cylindrical shells.

2) For the determination of the shearing forces  $N_{x\varphi} = N_{\varphi x}$ , we integrate equation 5 with respect to  $x$  and get an integration constant  $C_1$ .

3) In order to determine the normal force  $N_x$ , we integrate equation 6 with respect to  $x$  and get a new integration function  $C_2$ .

The integration functions  $C_1$  and  $C_2$  do not permit any boundary conditions; so that the problem of cylindrical shells can only be solved under some special supporting conditions as shown in the following special cases:

#### Special Cases

In the special case  $p_x = 0$  the internal forces can be given in the form :

$$1) \quad N_\varphi = p_r r \quad (4)$$

$$2) \quad N_{x\varphi} = N_{\varphi x} = - \left( p_\varphi + \frac{1}{r} \frac{dN_\varphi}{d\varphi} \right) x + C_1(\varphi)$$

The value  $p_\varphi + \frac{1}{r} \frac{dN_\varphi}{d\varphi}$  is a function of  $\varphi$  and if we call it  $F(\varphi)$  we shall have

$$N_{x\varphi} = N_{\varphi x} = - x F(\varphi) + C_1(\varphi) \quad (7)$$

$$3) \quad N_x = \frac{x^2}{2r} \frac{dF(\varphi)}{d\varphi} - \frac{x}{r} \frac{dC_1(\varphi)}{d\varphi} + C_2(\varphi) \quad (8)$$

In the following, we are going to limit our discussion to shells stiffened at both ends by diaphragms which can resist forces acting in their plane only, and symmetrically loaded with respect to the middle cross-section. In such cases, we have :

$$\begin{array}{llll} \text{at } x = 0 & N_{x\varphi} = 0 & \text{and} & C_1(\varphi) = 0 \\ \text{at } x = \frac{l}{2} & N_x = 0 & \text{and} & C_2(\varphi) = \frac{-1}{8} \frac{2}{r} \frac{dF(\varphi)}{d\varphi} \end{array}$$

Introducing these values in the previous equations 4, 7 & 8, we get finally :

$$N_\varphi = p_r r$$

$$N_{x\varphi} = N_{\varphi x} = -xP(\varphi) \quad (9)$$

$$N_x = -\frac{1}{8r} (l^2 - 4x^2) \frac{dF(\varphi)}{d\varphi}$$

It is clear from these formulae that the shearing force  $N_{x\varphi}$  and the longitudinal normal force  $N_x$  vary in the direction of the generators according to the same pattern as in the case of a simple beam of span  $l$  loaded by a uniformly distributed load as shown in fig. XII-34.

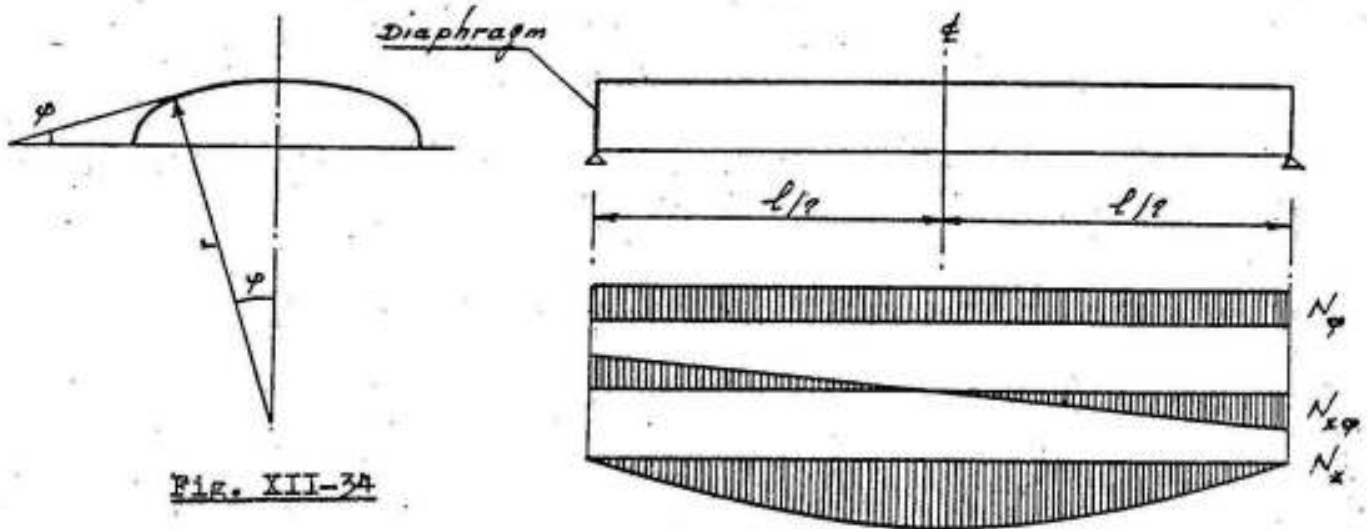


Fig. XII-34

Of course, the distribution of the forces  $N_{x\varphi}$  and  $N_x$  over the cross section cannot be derived from the beam formulas but is governed by equation 1 for the equilibrium of the shell element.

Another case of boundary conditions is represented by fig. XII-35.

Here one end,  $x = l$ , of the shell is completely built in, i.e., the support at this side can resist not only shearing forces  $N_{x\varphi}$  but also normal forces  $N_x$ . The other end,  $x = 0$ , may then be left without any support at all, and we have the boundary conditions:  
 $N_x = 0$ ,  $N_{x\varphi} = 0$  and  $N_x = 0$   
 Equations 7 and 8 show that in this case  $C_1(\varphi)$  and  $C_2(\varphi)$  must be zero, and hence we have

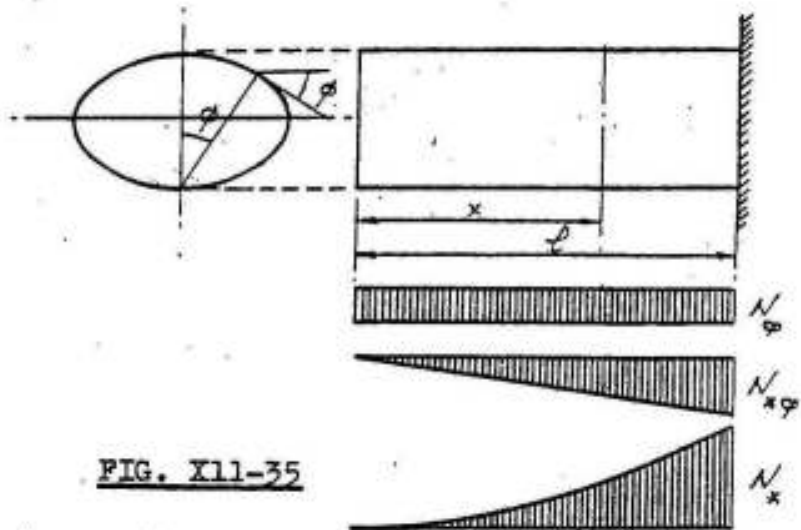


FIG. XII-35

$$N_{x\varphi} = -x F(\varphi) \quad N_x = \frac{x^2}{2r} \frac{dF(\varphi)}{d\varphi} \quad (10)$$

This shell is supported like a cantilever beam, and, again the span wise distribution of  $N_{x\varphi}$  and  $N_x$  are those of the shear and the bending moment of the beam analogue.

The three-dimensional support of such a cantilever shell will scarcely be accomplished by a solid wall, as shown in figure XII-35, but rather by an adjoining span of the same shell (fig. XII-36).

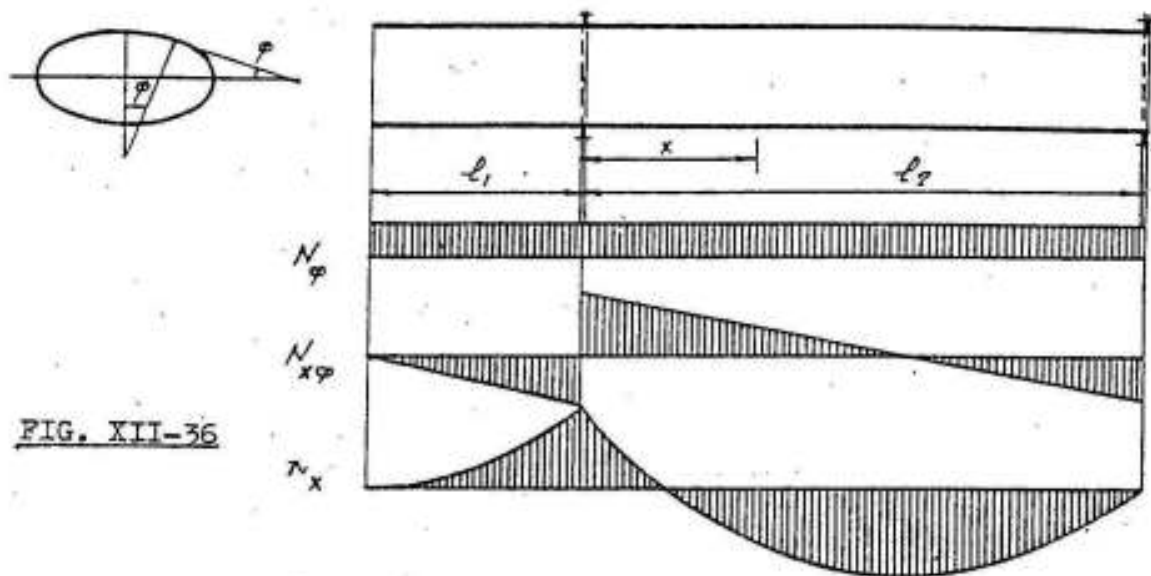


FIG. XII-36

In such a structure, we have again two diaphragms of the usual type which resist only shearing forces but do not accept forces  $N_x$  from the shell. The forces  $N_x$  coming from the cantilever section must therefore be transmitted across the diaphragm to the adjoining bay of the shell which therefore has the boundary conditions

$$x = 0 \quad N_x = \frac{l_1^2}{2r} \frac{dF(\varphi)}{d\varphi}$$

$$x = l_2 \quad N_x = 0$$

When we determine  $C_1(\varphi)$  and  $C_2(\varphi)$  from these conditions, we get:

$$\left. \begin{aligned} N_{x\varphi} &= \left( \frac{l_1^2 + l_2^2}{2l_2} - x \right) \cdot F(\varphi) \\ N_x &= \frac{1}{2r} \left( x^2 - x \frac{l_1^2 + l_2^2}{l_2} + \frac{l_1^2}{2} \right) \frac{dF(\varphi)}{d\varphi} \end{aligned} \right\} (11)$$

Again here  $N_{x\varphi}$  and  $N_x$  have the same distribution as the shearing force and the bending moment of a beam with overhanging cantilever. This coincidence will also be found if another cantilever shell is added at the other end of the main span, but the analogy cannot be extended to statically indeterminate cases as, for example, that of a two span continuous cylindrical shell between three diaphragms. Here the result will be influenced by the deformation of the shell which is different from that of a simple beam.

In all the preceding cases,  $N_\varphi$  is found from equation 1 which is not affected by the choice of the boundary conditions.

### The Circular Cylindrical Shell

#### A.) Tube-Like Shells

It will be assumed here that the radius of the middle surface is equal to "a" i.e.  $r = a$  and that the circular edges of the shell are stiffened by diaphragms capable of resisting forces in their plane only. The loads are symmetrical with respect to the middle axis.

The internal forces can be calculated according to equations 9 from the relations.

$$\left. \begin{aligned} N_\varphi &= P_r a \\ N_{x\varphi} = N_{\varphi x} &= -x F(\varphi) \\ N_x &= \frac{1}{8a} (1^2 - 4x^2) \frac{dF(\varphi)}{d\varphi} \end{aligned} \right\} \quad (12)$$

#### Examples

##### 1.) Circular Cylindrical Shell Loaded by its own Weight

Assuming that the dead weight per square meter surface =  $g$ , then the surface load components are :

$$\underline{P_\varphi = g \sin \varphi} \quad \text{and} \quad \underline{P_r = -g \cos \varphi}$$

The first of equations 12 is therefore given by

$$\underline{N_\varphi = -g a \cos \varphi} \quad (13a)$$

The function  $F(\varphi)$  and its derivative are :

$$F(\varphi) = P_\varphi + \frac{1}{r} \frac{dN_\varphi}{d\varphi} = g \sin \varphi + \frac{1}{a} \cdot g a \sin \varphi = 2 g \sin \varphi \quad \text{and}$$

$\frac{dR(\varphi)}{d\varphi} = 2 g \cos \varphi$   
 accordingly we get

$$\underline{N_{x\varphi} = N_{\varphi x} = -2 g x \sin \varphi} \quad (13b)$$

$$\underline{N_x = \frac{E}{4a} (l^2 - 4x^2) \cos \varphi} \quad (13c)$$

The distribution of the stresses on the cross section is shown in figure XII-37. One has to notice that  $N_x$  is linear as is generally assumed in elementary statics. However, this statement cannot be generalized for other shells and for other cases of loading.

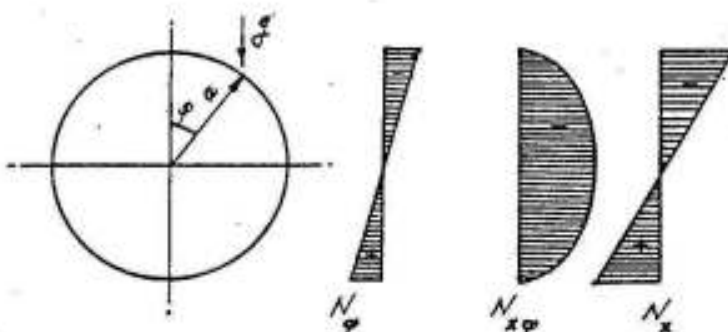


FIG. XII-37

### 2.) Circular Cylinder Filled with Liquid

For a pipe filled with liquid of specific weight  $\gamma$ , the external forces (the water pressure) are :

$$p_x = p_\varphi = 0, \quad \underline{p_r = p_0 - \gamma a x \cos \varphi}$$

Here  $p_0$  is the pressure at the level of the axis of the pipe and may be anything  $\geq \gamma a$ , but not less.

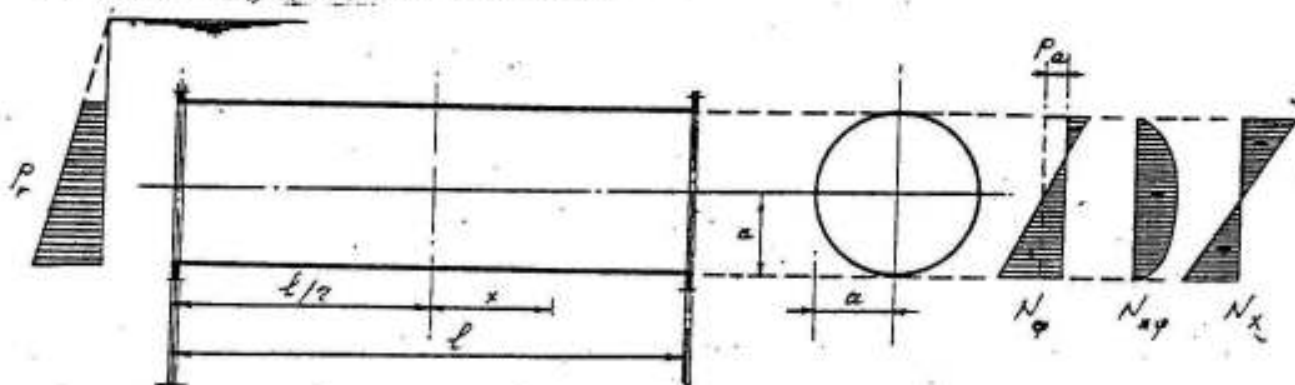


FIG. XII-38

If we choose the boundary conditions of figure (XII-34) we find at once from equations 12 the stress resultants : (Fig. XII-38).

$$\left. \begin{aligned} \underline{N_\varphi = p_0 a - \gamma a^2 \cos \varphi} \\ \underline{N_{x\varphi} = N_{\varphi x} = -\gamma a x \sin \varphi} \\ \underline{N_x = -\frac{1}{8} \gamma (l^2 - 4x^2) \cos \varphi} \end{aligned} \right\} \quad (14)$$

The average pressure  $p_0$  produces only hoop stresses. The load term with  $\gamma$  represents the weight of the liquid and produces a kind of overall bending of the pipe, which acts as a beam carrying this weight between the supports. We have already seen that therefore the shear  $N_{x\phi}$  and the normal force  $N_x$  have the same span wise distribution as the shear and the bending moment of a beam. The distribution of  $N_x$  over the profile is incidentally the same linear distribution as that of bending stresses in common beam theory. This result is a peculiarity of the circular cylinder and, even there, is restricted to certain simple loads.

## B.) Barrel Vaults

### 1) Semicircular Simple Barrel Vault Loaded by its own Weight

As an introduction to the theory of barrel vaults, we are going to discuss the stress distribution of the internal forces, given by equations 13, in the circular cylindrical shell subjected to its own weight treated in example 1 and shown in figure XII-37.

The most remarkable feature of this force system is that on the generators at midheight,  $\phi = \pm \pi/2$  we have  $N_\phi = 0$ . If we cut away the lower half of the shell, the upper half need not be supported at the straight edges and may carry its weight freely between the diaphragms, just as the tubular shells do. Such barrel vaults have been used as roof structures.

However, the straight edges of a barrel vault are not completely free of external forces. There is a shear  $N_{x\phi} = \pm 2gx$ , and a structural element must be provided to which it can be transmitted. This so called "edge beam" is a straight member, and if properly placed, it is stressed only in tension (fig. XII-39). Its axial tensile force  $T$  is of course variable along the span. It can easily be found by integrating the shear  $N_{x\phi}$ , beginning at the end  $x = \frac{l}{2}$  where  $T = 0$ . For the edge  $\phi = + \pi/2$  the integration gives:

$$T = \int_{-l/2}^x N_{x\phi} dx = -2g \int_{-l/2}^x x \sin \phi dx = -2g \int_{-l/2}^x x dx = \frac{1}{4} g (l^2 - 4x^2)$$

and at the other end, we get a similar result.

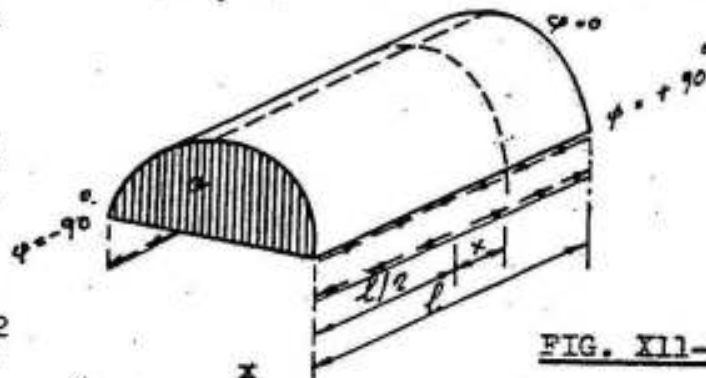


FIG. XII-39

The statical necessity of this force may be understood from a look at the  $N_x$  diagram in fig. XII-40 which shows the stress resultants of a barrel vault with semicircular profile.

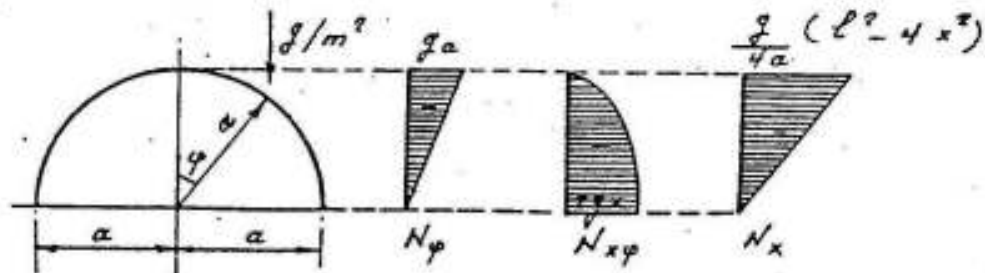


FIG. XII-40

The section has only longitudinal compressive forces  $N_x$ , and if we cut the shell apart in a plane  $x = \text{constant}$ , the horizontal equilibrium of each half requires that tensile forces of the same amount also appear. Now the integral of the forces  $N_x$  in the cross-section

$$+ \int_{-\pi/2}^{+\pi/2} N_x a d\varphi = - \frac{1}{4} g (l^2 - 4x^2) + \int_{-\pi/2}^{+\pi/2} \cos\varphi d\varphi = - \frac{1}{2} g (l^2 - 4x^2)$$

This is exactly the same compressive force as the two tensile forces  $T$  in the edge beams so that they maintain the horizontal equilibrium.

The resultant of the compressive forces lies somewhere in the semi-circular profile and higher than the tensile force  $2T$  and both combine to form a couple equal to the external moment. When we consider the barrel vault as a beam of span  $l$ . Since the load of the "beam" per unit length is  $\pi a g$ , its bending moment is

$$M = \pi a g (l^2 - 4x^2)/8$$

The moment of the stress resultants  $N_x$  and  $T$  in the cross-section can be determined by taking moments about the lower horizontal diameter which is at the same time the line of action of the tension  $T$ . Hence

$$+ \int_{-\pi/2}^{+\pi/2} N_x \cdot a \cos\varphi \cdot a d\varphi = + \int_{-\pi/2}^{+\pi/2} \frac{g}{4a} (l^2 - 4x^2) \cos^2\varphi \cdot a^2 d\varphi = \pi a g (l^2 - 4x^2)/8$$

which is exactly equal to  $M$ . In the same way check that the vertical resultant of the shearing forces  $N_{x\varphi}$  in the cross-section is equal to the transverse shearing force  $-\pi a g x$  of the beam analogue.

This comparison between the barrel vault and its beam analogue gives a good general idea of the stress system in the shell and yields

a useful check for the computations. It cannot disclose details of the membrane stress distribution, since they depend essentially on the shape of the shell.

2.) Semicircular Simple Barrel Vault Loaded by a Vertical Live Load

$$p \text{ t / m}^2 \text{ horizontal}$$

The load components are in this case given by :

$$P_{\varphi} = p \sin\varphi \cos\varphi \quad P_r = - p \cos^2\varphi$$

Substituting these values in equations 12, we get : (fig.XII-41)

$$N_{\varphi} = - p a \cos^2\varphi$$

$$N_{x\varphi} = N_{\varphi x} = - \frac{3}{2} p x \sin 2\varphi$$

$$N_x = - \frac{3 p}{8 a} (l^2 - 4 x^2) \cos 2\varphi$$

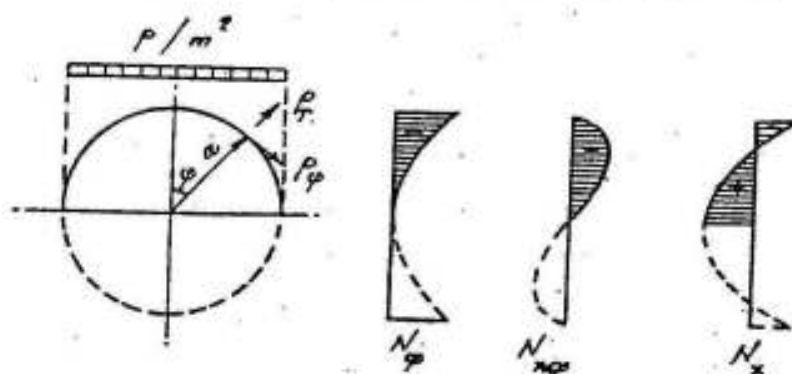


FIG. XII-41

It is interesting to observe that at the shell edges where  $\varphi = \pm \pi/2$ , both  $N_{\varphi}$  and  $N_{x\varphi} = N_{\varphi x}$  equal zero. Consequently, in this loading case, the shell need no support at its longitudinal edges.

In order to make a shell suitable for the construction of free-spanning barrel vaults, the force  $N_{\varphi}$  must be zero at the straight edges. This is always possible for shell profiles subject to vertical loads and terminating with vertical tangents. Accordingly, the semi-circular, elliptical, cycloidal and similar profiles are considered as convenient forms for freespreading barrel vaults.

As an example, we give in the following, the stress resultants in a cycloidal barrel shell loaded by dead and superimposed loads acting per square meter surface.



The Cycloidal Barrel Shell.

The equation of the cycloid ( fig. XII-42 ) is given by the formulae

$y = a ( 2\psi + \sin 2\psi )$ ,  $z = a(1 + \cos 2\psi)$   
The radius of curvature is there-  
fore :

$$r = 4 a \cos \psi$$

Thus :

In case of own weight ( fig. XII-43 )

$$P_\psi = g \sin \psi \quad P_x = - g \cos \psi$$

$$N_\psi = - 4 g a \cos^2 \psi$$

$$N_{x\psi} = N_{\psi x} = - 3 g x \sin \psi$$

$$N_x = - \frac{3 g}{32 a} ( l^2 - 4 x^2 )$$

$$= \text{constant}$$



FIG. XII-43

Here the force  $N_x$  is constant over the whole profile. This may sometimes be desirable since it indicates that all material is efficiently used. But in most cases we should rather like to have a tensile force  $N_x$  along the edge to avoid large differences between the length wise strain in the shell and in its edge member.

The Wiedemann's Barrel Shell

It is however possible to improve the properties of the cycloidal shell by using the Wiedemann's profile which is given by the equation.

$$r = a_0 + a_1 \cos \psi$$

This curve can be originated by rolling a circle on the outside of a cycloid as shown in figure XII-44 . The Wiedemann's curve is the locus of the center point of the circle. We find the ordinates  $y$  and  $z$  in the plane of a profile by simple integration of the projections of the line element  $r d\psi$  : thus

$$y = \int_0^\psi r \cos \psi d\psi = a_0 \sin \psi + \frac{1}{4} a_1 ( 2\psi + \sin 2\psi )$$

$$z = - \int_{\pi/2}^{\psi} r \sin \psi d\psi = a_0 \cos \psi + \frac{1}{4} a_1 (1 + \cos 2\psi)$$

These relations show that the curve lie somewhere between the circle ( $a_1 = 0$ ), and a cycloid ( $a_0 = 0$ ). But this does not mean that the stresses lie halfway between the two cases. The stress resultants are accordingly :

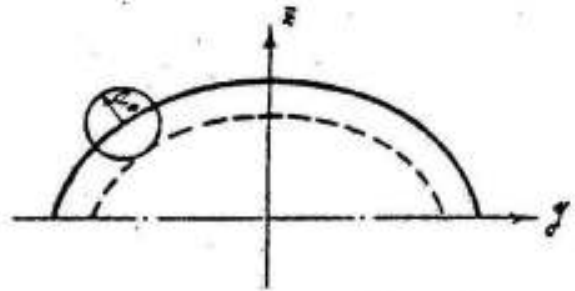


FIG. XII-44

For the own weight  $g/m^2$  surface

$$p_{\psi} = g \sin \psi \qquad p_r = -g \cos \psi$$

$$N_{\psi} = -g (a_0 + a_1 \cos \psi) \cos \psi$$

$$N_{x\psi} = N_{\psi x} = -g x \sin \psi \frac{2 a_0 + 3 a_1 \cos \psi}{a_0 + a_1 \cos \psi}$$

$$N_x = -\frac{g}{8} (1^2 - 4 x^2) \frac{(2 a_0 + 3 a_1 \cos \psi)(a_0 + a_1 \cos \psi) \cos \psi - a_0 a_1 \sin^2 \psi}{(a_0 + a_1 \cos \psi)^2}$$

at the lower edge where  $\psi = \pm \pi/2$

$$N_{\psi} = 0, \quad N_{x\psi} = N_{\psi x} = -2 g x \quad \text{and} \quad N_x = + \frac{g a_1}{8 a_0^2} (1^2 - 4 x^2)$$

For a live load  $p/m^2$  horizontal

$$p_{\psi} = p \sin \psi \cos \psi \qquad p_r = -p \cos^2 \psi$$

$$N_{\psi} = -p (a_0 + a_1 \cos \psi) \cos^2 \psi$$

$$N_{x\psi} = N_{\psi x} = -p x \sin \psi \cos \psi \frac{3 a_0 + 4 a_1 \cos \psi}{a_0 + a_1 \cos \psi}$$

$$N_x = -\frac{p}{8} (1^2 - 4 x^2) \frac{(3 a_0^2 + 4 a_1^2 \cos^2 \psi) \cos 2\psi - a_0 a_1 \cos \psi (8 - 15 \cos^2 \psi)}{(a_0 + a_1 \cos \psi)^2}$$

at the lower edge, where  $\psi = \pm \pi/2$

$$N_{\psi} = 0, \quad N_{x\psi} = N_{\psi x} = 0 \quad \text{and} \quad N_x = + \frac{3 p}{8 a_0} (1^2 - 4 x^2)$$

This means that at the edges  $\psi = \pm \pi/2$ , tensile  $N_x$  forces of

reasonable values are developed both for dead weight and vertical live loads. Since tensile forces are also acting on the upper edge of the straight edge beams, we have the possibility to eliminate or to decrease the difference of elongations by proper choice of the dimensions of the shell.

### 3- The Beam Theory

We have seen in figures XII-34, 35 & 36, that the shearing force  $N_{x\phi}$  and the longitudinal force  $N_x$  vary in the direction of the generators according to the same pattern as in the case of a simple beam of span  $l$  loaded by a uniformly distributed load. We will discuss now whether it is possible to consider the shell as a beam.

It has been found that the analysis of a shell as a three dimensional problem in a strict sense, is very complicated; but its structural behavior can be best understood by comparing its action to that of an ordinary beam, whose cross-section is a thin curved slab spanning between the transverse stiffeners<sup>\*</sup> -the diaphragms-.

The application of load on the shell induces longitudinal fiber stresses similar to those induced in any homogenous beam under load, and if the span  $l$  is large compared to the transverse chord width  $b$ , the variation of the fiber stresses across any section is the same as that created in a beam, that is, it is linear from top to bottom.

As the ratio of  $b$  to  $l$  increases the variation of the longitudinal force per unit width,  $N_x$ , changes from straight line to curvilinear. The extent of this change is shown in figure XII-45, in which the ordinate represents vertical distance measured from the bottom of a cylindrical shell in terms  $z'/f$  and the abscissa indicates magnitude of  $N_x$  - forces. For convenience, the curves are drawn for various values of  $a/l$ , the ratio of shell radius to span length, rather than the previously discussed ratio of  $b$  to  $l$ . Although the two ratios are independent,  $a/l$  is a more suitable parameter since it includes the effect of shell rise as well as chord width. When  $a/l$  is less than 0.2, the variation is almost linear, while for larger values of  $a/l$  the force at the lower edge is greater than that given by ordinary beam theory.

---

\* Refer to H. Lundgren "Cylindrical Shells" . Published by the Danish Technical Press. The institution of Danish Civil Engineers.

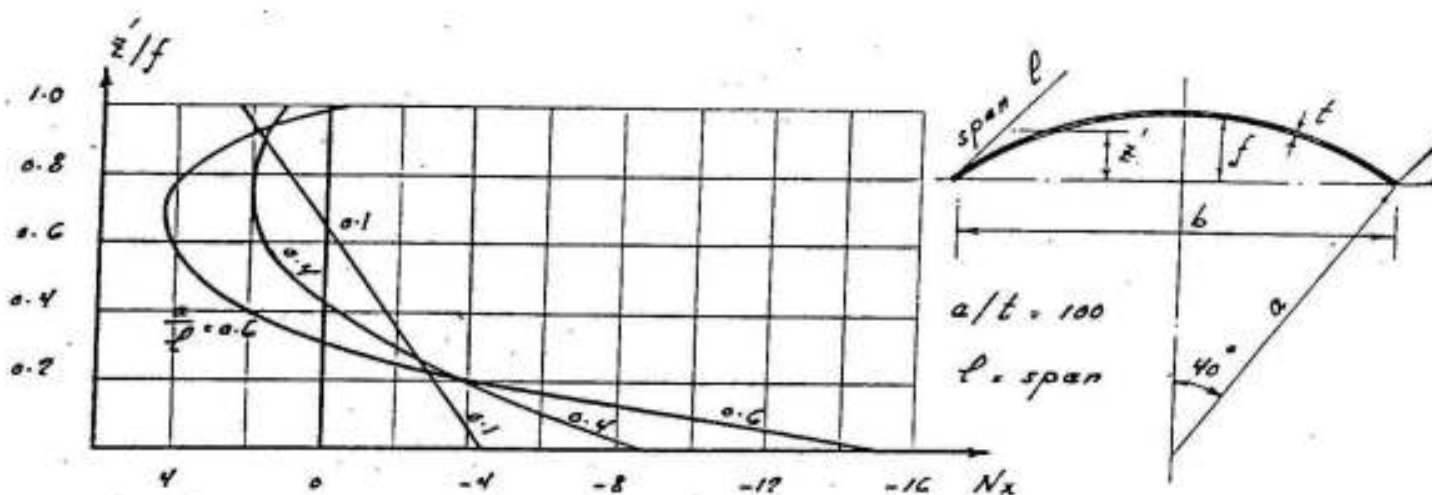


FIG. XII-45

Although the magnitude of the tensile stresses at the lower edge of the shell is sometimes quite sensitive to variations of  $a/l$ , the total tensile area under these curves does not vary to the same degree. For example, the ratio of bottom fiber stresses for values of  $a/l$  of 0.6 and 0.1 is 3.2 while the ratio of tensile areas below the neutral axis for these cases is only 1.4. Since the reinforcement required depends essentially on the total tensile area rather than the maximum fiber stress, the design of a shell is not so sensitive a problem. Moreover, the curves are prepared for a single shell unrestrained at the lower edges. When these edges are restrained by adjoining shells or edge beams, longitudinal stresses conform more closely to the straight line variation. Studies indicate that the beam method is applicable to the following classes of shells provided they are uniformly loaded :

- 1) Single shells without edge beams if  $a/l < 0.2$ .
- 2) Long single shells with not too deep edge beams if  $a/l < 0.3$ .
- 3) Interior shells of a group of multiple shells with feather edge beams if  $a/l < 0.6$ .
- 4) Interior shells of a multiple group of shells with edge beams if  $a/l < 0.4$ .

However, close agreement with the results of the analytical theory have been obtained for ratios of  $a/l \approx 0.9$ .

The basic assumptions used in the beam theory are :

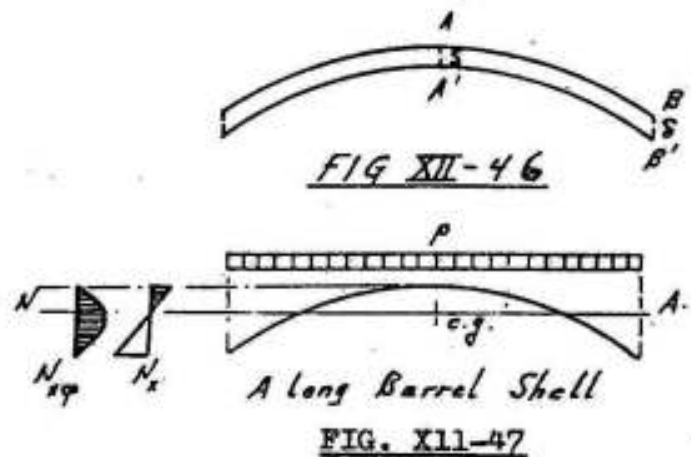
- 1) Plane sections before deformation remain plane after deformation.
- 2) Form of cross section is not changed i.e. points A and B shown in figure XII-46 deflect the same amount.

Accordingly :

- 1) Distribution of  $N_x$  is similar to  $\sigma$
- 2) Distribution of  $N_{x\phi}$  is similar to  $\tau$

as shown in figure XII-47

The analysis of the normal and shearing forces in a long barrel shell is similar to that of a beam, span  $l$ , and having a curved cross section as shown in following simple example.



### Analysis of Beam Action of Symmetrical Circular Cylindrical Shells

#### 1. Properties of Shell section

- a) Shell without edge beams : Fig. XII-48

The area of cross section of a symmetrical circular shell of radius  $a$  and subtending a central angle  $2\phi_0$  is given by :

$$A = 2 a \phi_0 t$$

The position of the c.g. of the section can be determined from the relation :

$$z_0 = a \sin \phi_0 / \phi_0$$

So that

$$\eta = a \left( 1 - \frac{\sin \phi_0}{\phi_0} \right)$$

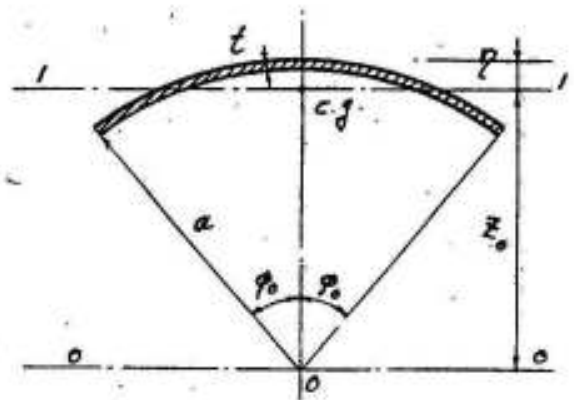


FIG. XII-48

The moment of inertia of the section about axis O-O passing through the center O is :

$$I_{O-O} = t a^3 \left( \phi_0 + \frac{1}{2} \sin 2 \phi_0 \right)$$

Hence, the moment of inertia of the section about axis l-l passing through the c.g. is therefore

$$I_{l-l} = t a^3 \left( \phi_0 + \frac{1}{2} \sin 2 \phi_0 - \frac{2 \sin^2 \phi_0}{\phi_0} \right)$$

The statical moment of the section above or below the neutral axis(c.g.)

axis can be calculated from the relation :

$$S_{1-1} = \frac{4}{3} t \eta \sqrt{2 \eta a} \left( 1 + \frac{\eta}{20 a} \right)$$

b) Shell with edge beams. ( Fig. XII-49 )

The area of cross-section of the shell is given by :

$$A = 2 ( a \varphi_0 t + b_0 d )$$

The statical moment of the section of the shell about axis o-o is :

$$S_{o-o} = 2 ( t a^2 \sin \varphi_0 + b_0 d \bar{z}_b )$$

where

$$\bar{z}_b = a \cos \varphi_0 - \frac{d}{2}$$

FIG. XII-49

The position of the c.g. can be determined from the relation :

$$z_o = S_{o-o} / A \quad \text{i.e.} \quad \eta = a - z_o$$

The angle  $\varphi$  is therefore given by :  $\cos \varphi = z_o / a$  and the statical moment  $S_{1-1}$  about axis passing through the c.g. will be the same as in previous case.

The moments of inertia about axes o-o and 1-1 are given by

$$I_{o-o} = a^3 t ( \varphi_0 + 1/2 \sin 2 \varphi_0 ) + \left( \frac{b_0 d^3}{6} + 2 b_0 d \bar{z}_b^2 \right)$$

$$I_{1-1} = I_{o-o} - A z_o^2$$

## 2. Internal Forces in the Shell

### Load

Total load per meter run shell is given by :

$$\begin{aligned} \bar{p} &= 2 a \varphi_0 p && \text{for a circular shell without edge beams,} \\ &= 2 ( a \varphi_0 p + p_b ) && \text{" " " " with " " } \end{aligned}$$

in which

$p$  = total vertical load, including own weight, per square meter shell

$p_b$  = load of edge beam per meter.

The dead weight of the shell slab may practically always be

considered uniformly distributed even in cases where light stiffening ribs are provided.

Since the greater part of the shell has only light reinforcement the weight per cubic meter slab may be assumed = 2.40 t .

On the other hand, for long shells, the edge beams are so heavily reinforced that in computing the weight due regard has to be given to the reinforcement.

As regards the live loads, one may follow the following rules:

1) For ordinary long shells where the exact distribution of load is less important, an average live load of  $65 \text{ kg/m}^2$  is assumed for the entire shell surface, provided that the maximum slope does not differ much from  $40^\circ$  .

2) For other shells, where the decrease of the load by increasing inclination is of importance, a load of  $\sim 100 \sin^2 \psi \text{ kg/m}^2$  of shell surface may be assumed.

3) For parallel shells, the valleys between the individual shells are to be considered half filled with snow having a unit weight of  $150 \text{ kg/m}^3$  or an equivalent weight of rain water.

4) For the composite shell structure of the ordinary long type, the additional load from one valley, due to snow, rain water or gutter plain concrete, may be assumed as a line load on the edge beam. Thereby, the snow - or rain water - load on the edge beam will be :

$25 b \left( f + \frac{1.5}{\sqrt{f}} - 2.5 \right) \text{ kg/m}$  where  $b$  = width of shell and  $f$  = rise in meters.

When using this formula a uniformly distributed snow or live load of  $65 \text{ kg/m}^2$  is to be applied to the entire shell surface.

5) The wind load on a cylindrical roof with an inclination of less than  $40^\circ$  may be assumed as a uniformly distributed suction of  $\sim 100 \text{ kg/m}^2$  . It reduces the stresses due to dead and snow or live loads.

#### Stresses and Stress Resultants

For a symmetrically loaded symmetrical section as that shown in fig. XII-50, a long shell may be considered as a beam subject to bending in the vertical plane

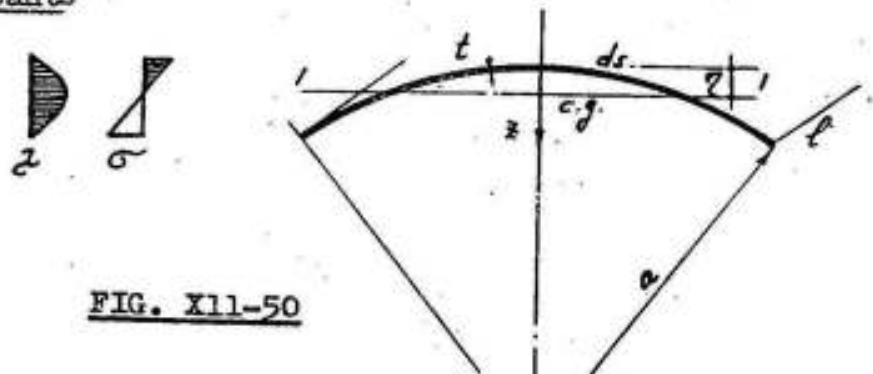


FIG. XII-50

only; hence, the normal stress  $\sigma$  in the longitudinal direction is given by :

$$\sigma = M z / I_{1-1}$$

The maximum compressive stress,  $\sigma_{c \max}$ , at the upper fiber must be smaller than the allowable buckling stress  $\sigma_{\text{buckl.}}$ . Hence

$$\sigma_{c \max} = M \eta / I_{1-1} < \text{allow. } \sigma_{\text{buckl.}} \quad \text{where}$$

$$\text{allow. } \sigma_{\text{buckl.}} = \frac{\sigma_{cb}}{1 + \frac{5 \sigma_{c28}}{E} \cdot \frac{a}{t}} \cdot \frac{1}{s} \quad s = \text{factor of safety}$$

$\sigma_{cb}$  = The bending compressive strength of concrete =  $\frac{4}{3} \sigma_{c28}$

$\sigma_{c28}$  = The cube compressive strength of concrete

E = Modulus of elasticity of concrete  $\approx 200\,000 \text{ kg/cm}^2$  for normal cases

s = Factor of safety = 4 in buckling problems

Assuming  $\sigma_{c28} = 200 \text{ kg/cm}^2$ , we should have :

$$\sigma_{c \max} < 65 / \left( 1 + \frac{a}{200 t} \right)$$

Thus, for normal cases, the maximum allowed concrete compressive stress  $\sigma_{c \max}$  can be extracted from the curve shown in figure XII-51.

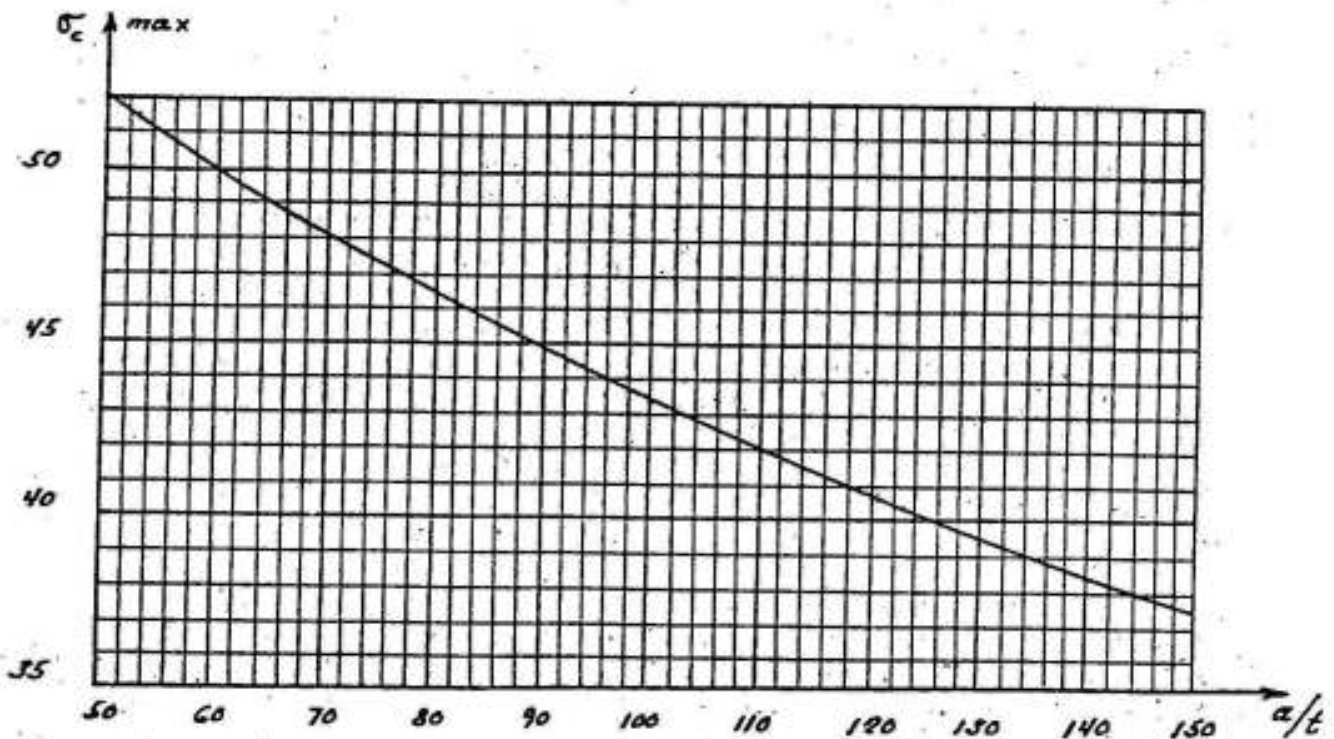


FIG. XII-51



The longitudinal stress resultant  $N_x$  is therefore given by :

$$N_x = M z t / I_{1-1}$$

The total tension  $T$  below the neutral axis being equal to the total compression  $C$  above the same axis, we get

$$C = T = \int_{z=0}^{z=\eta} N_x da = \frac{M}{I_{1-1}} \int_{z=0}^{z=\eta} t \cdot z ds = \frac{M S_{1-1}}{I_{1-1}}$$

Therefore, the total tension  $T$  in the section is given by :

$$T = M S_{1-1} / I_{1-1}$$

Knowing further that  $I_{1-1} / S_{1-1} = y_{CT}$  = the lever arm between the center of tension and the center of compression, then

$$T = M / y_{C-T}$$

In reinforced concrete shells (Fig.XII-52), the concrete in tension is generally neglected and all the tensile stresses are resisted by tension steel so that the real  $y_{CT}$  may be assumed equal to the distance between the center of the tension reinforcement and the center of compression which is generally bigger than  $I_{1-1} / S_{1-1}$ .

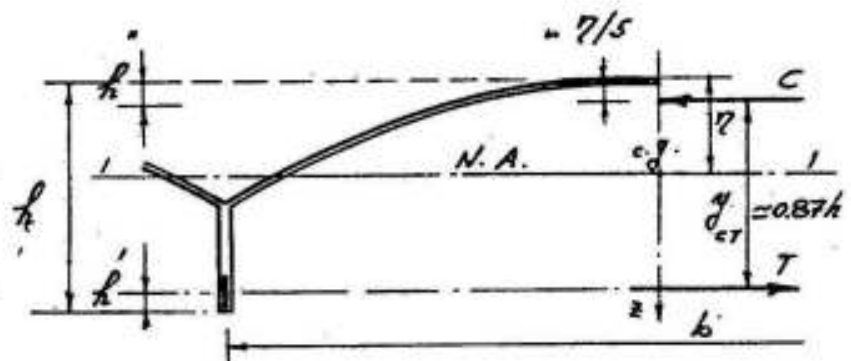


FIG. XII-52

For normal dimensions of symmetrical circular cylindrical shells where  $b = 8 - 12$  ms and  $t = 16 - 25$  ms,  $h$  may be chosen equal to  $t/10$ . In a preliminary estimate  $h'$  may be assumed 10-20 cms. and  $h' = 7/5$  may be assumed 15-25 cms., so that  $y_{CT}$  can be assumed equal to  $h = t/10$  minus 25 to 40 cms.  $y_{CT}$  may however be assumed equal to  $0.87 h$ .

The required tension steel in the shell can therefore be given by:

$$A_s = T / \sigma_s$$

This reinforcement is generally arranged in a narrow edge beam as shown in figure XII-53 ; the free space between the bars is equal

to their diameter so that if the tension reinforcement is for example  $13 \phi 25$  mm. then  $h' = 6 \phi = 15 \text{ cm}$ . The maximum stress in the tension steel  $\sigma_s \text{ max.}$  takes place in the lowest row, the average stress  $\sigma_s$  at the center of gravity of the tension steel is generally smaller. If no exact calculation is done  $\sigma_s$  may be assumed equal to 0.9 the maximum allowed values.

Assuming that  $N_{x\phi}$  denotes the total internal shearing force per unit length of the section then

$$N_{x\phi} = \tau \cdot t = Q S / I_{1-1}$$

in which  $Q$  and  $I$  are the shearing force and the shearing stress respectively,  $S$  is the statical moment of the section above any plane about the c.g. axis. Its distribution is, as stated before, parabolic and attains its maximum values at the diaphragms where  $Q$  is maximum.

So that :

$$\text{max. } N_{x\phi} = Q_{\text{max}} S / I_{1-1}$$

The maximum ordinate of the shear diagram lies at the axis passing through the center of gravity of the section, hence'

$$\text{max. max. } N_{x\phi} = Q_{\text{max}} S_{1-1} / I_{1-1} = Q_{\text{max}} / J_{CT}$$

As in ordinary beams this shearing force  $N_x$  will cause a diagonal tension  $T_x$ , resisted by both sides of the shell, and of equal magnitude, so that each side resists a diagonal force of the magnitude:

$$T_{x\phi} = \frac{1}{2} Q / J_{CT}$$

All shear stresses  $\tau$  bigger than the allowed values (6-8 kg/cm<sup>2</sup>) must be resisted either by stirrups or diagonal bars inclined 45° with the axis. The latter are preferred in cases when  $\tau$  is bigger than 10 kg/cm<sup>2</sup>.

The shear stress  $I$  is given by :

$$\tau = T_{x\phi} / A$$

where  $A$  is the area of 1 m strip of the shell = 100 x t cm<sup>2</sup>

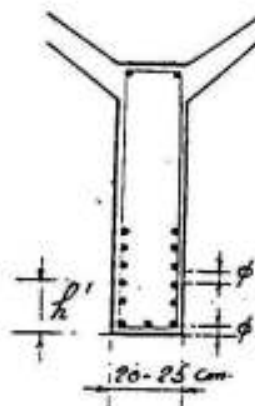


FIG. X11-53

Example

It is required to analyse the beam action and to determine the longitudinal and diagonal reinforcements for the intermediate long cylindrical shell roof with edge beams shown in figure XII-54.

The shell is simply supported on two edge diaphragms 25 ms apart.

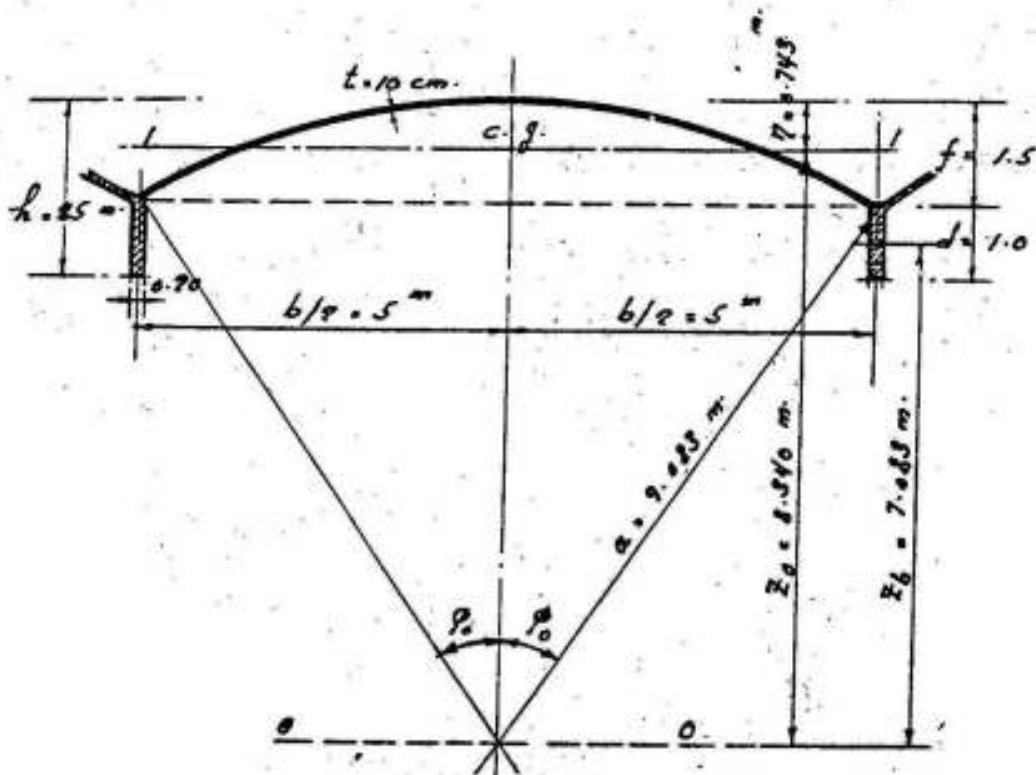


FIG. XII-54

Data :

Span  $l = 25$  m, width  $b = 10$  m, total rise  $h = 2.5$  m, rise of arc  $f = 1.5$  m  
 Depth of edge beam  $d = 1.00$  m, breadth  $b_0 = 0.10$  m. Thickness of shell  
 $= 0.10$  m.

Radius  $a$  can be calculated from the relation :

$$a^2 = 5^2 + (a - 1.5)^2 \quad \text{or} \quad a = 9.083 \text{ ms.}$$

Loads

Own weight of 10 cms. shell-slab	$0.1 \times 2400 = 240$	$\text{kg/m}^2$
Weight of 3 cms fine concrete	$0.03 \times 2200 = 66$	"
Weight of plaster + isolation	$= 34$	"
Live load	$= 60$	"
	<u>total p = 400</u>	"

\* Since each of the 20 cm wide edge beams is common for two shells, the beams belonging to one shell are to be introduced with a breadth  $b_0$  of 10 cms.

$$\begin{aligned} \text{Own weight of edge beam} &= 0.2 \times 0.9 \times 2500 = 450 \text{ kg/m'} \\ \text{Concrete slopes + rain water} &= 300 \text{ "} \end{aligned}$$

$$\begin{aligned} \sin \varphi_0 &= b/2a = 10/2 \times 9.083 = 0.5505 & \text{total } p_D &= 750 \text{ kg/m'} \\ \varphi_0 &= 33^\circ 24' = 33.4^\circ \end{aligned}$$

$$\text{i.e. } \varphi_0 = \frac{33.4}{180} \times 3.1416 = 0.583 \text{ radians}$$

$$\begin{aligned} \text{Total load } \bar{p} &= 2 \varphi_0 \cdot a p + p_D \\ &= 2 \times 0.583 \times 9.083 \times 400 + 750 = 5000 \text{ kg/m'} \end{aligned}$$

### Bending Moments and Shearing Forces

Maximum external bending moment at mid-span:

$$\text{max. } M = 5 \times 25^2 / 8 = 390 \text{ m t}$$

Maximum shearing force at diaphragms:

$$\text{max. } Q = 5 \times 25 / 2 = 62.5 \text{ tons}$$

### Determination of Center of Gravity, Statical Moment and Moment of Inertia of Section of Shell.

Referring to figure XII-49, we get:

$$A = 2 (a \varphi_0 t + b_0 d) = 2 (9.083 \times 0.583 \times 0.1 + 0.1 \times 1) = 1.259 \text{ m}^2$$

$$\bar{z}_b = a \cos \varphi_0 - \frac{d}{2} = 9.083 \times 0.835 - 0.50 = 7.583 - 0.5 = 7.083 \text{ ms}$$

$$\begin{aligned} S_{O-O} &= 2 (t a^2 \sin \varphi_0 + b_0 d \bar{z}_b) = 2 (0.1 \times 9.083^2 \times 0.5505 + 0.1 \times 1.0 \times \\ & \quad \times 7.083) = 10.500 \text{ m}^3 \\ z_0 &= S_{O-O} / A = 10.500 / 1.259 = 8.340 \text{ m} \end{aligned}$$

Therefore, the distance of the c.g.-axis (N.A.) from the top fiber is given by:

$$\eta = a - z_0 = 9.083 - 8.340 = \underline{0.743 \text{ m}}$$

$$\begin{aligned} I_{O-O} &= a^3 t \left( \varphi_0 + \frac{1}{2} \sin 2 \varphi_0 \right) + \left( \frac{1}{6} b_0 d^3 + 2 b_0 d \bar{z}_b^2 \right) \\ &= 9.083^3 \times 0.1 (0.583 + 0.5 \times 0.919) + \left( \frac{1}{6} \times 0.1 \times 1.0^3 + 2 \times 0.1 \times 1.0 \times 7.083^2 \right) \\ &= 88.180 \text{ m}^4 \end{aligned}$$

The moment of inertia of the section about the c.g. axis is:

$$I_{1-1} = I_{O-O} - A z_0^2 = 88.180 - 1.259 \times 8.340^2 = \underline{0.61 \text{ m}^4}$$

The statical moment of the cross-sectional area above or below the c.g. axis is given by:

$$S_{1-1} = \frac{4}{3} t \eta \sqrt{2 \eta a} \left( 1 + \frac{\eta}{20 a} \right)$$

$$= \frac{4}{3} \times 0.1 \times 0.743 \sqrt{2 \times 0.743 \times 9.083} \left( 1 + \frac{0.743}{20 \times 9.083} \right) = 0.365 \text{ m}^3$$

The theoretical lever arm is therefore :

$$\text{Theoretical } y_{OT} = I_{1-1} / S_{1-1} = 0.610 / 0.365 = 1.670 \text{ ms}$$

### Normal stresses and longitudinal reinforcements

Maximum concrete stress at top fiber:

$$\text{max. } \sigma_c = \text{max. } M \eta / I_{1-1} = 390 \times 0.743 / 0.61 = 475 \text{ t/m}^2 = 47.5 \text{ kg/cm}^2$$

For  $a/t = 9.083/0.1 = 90.83$ , the maximum allowed compressive stress in concrete according to relations given in Fig. XII-51 is:

$$\text{max. allowed } \sigma_c = 45 \text{ kg/cm}^2 \text{ only!}$$

The existing value of  $47.5 \text{ kg/cm}^2$  may be accepted; it means that the factor of safety 's' against buckling is 3.86 which is sufficient.

The center of compression is assumed at  $h'' = \eta/5$  from the upper fiber. Thus  $h'' = \eta/5 = 0.743/5 \approx 15 \text{ cms.}$  Whereas, the center of tension is assumed at the center of gravity of the tension steel which lies at a distance  $h' = 20 \text{ cms.}$  from the lower fiber of the edge beam. The actual lever arm is therefore given by:

$$\text{Actual } y_{OT} = h - (h' + h'') = 2.5 - (0.2 + 0.15) = 2.5 - 0.35 = 2.15 \text{ ms}$$

$$\text{Assuming } y_{OT} = 0.87 h, \text{ we get } y_{OT} = 0.87 \times 2.5 = 2.175 \text{ ms}$$

The two values are approximately the same and are about 1.3 times the theoretical value given before. Hence:

The maximum total tension in the section at midspan is:

$$\text{max. } T = \text{max. } M / \text{act. } y_{OT} = 390 / 2.15 = 180 \text{ tons}$$

Using high grade steel with an allowable average stress  $\sigma_s = 0.9 \times 2 = 1.8 \text{ ton/cm}^2$ , then the required tension reinforcement at mid-span is:

$$\text{max. } A_s = \text{max. } T / \sigma_s = 180 / 1.8 = 100 \text{ cm}^2 \text{ chosen } 20 \phi 25 \text{ mm}$$

### Shear stresses and diagonal reinforcements

The maximum total internal shearing force per unit length of section is given by:

$$\text{max. } N_{x\phi} = \text{max. } \tau t = \text{max. } Q / y_{OT} = 62.5 / 2.15 = 29 \text{ t/m}$$

The maximum diagonal tension resisted by each side of the shell is therefore:

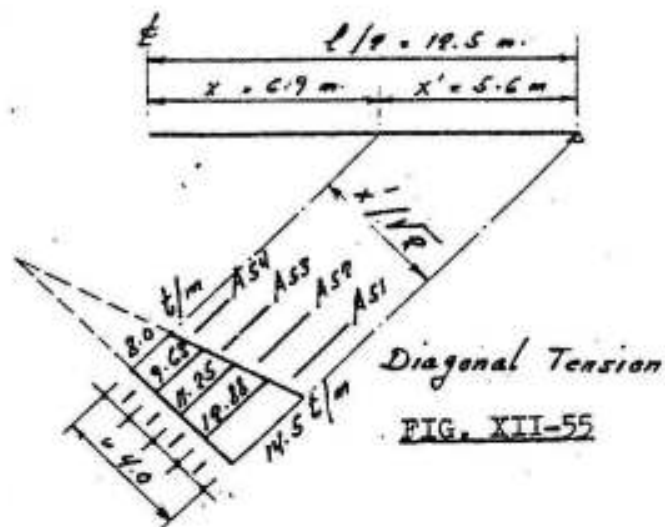
$$\text{max. } T_{x\phi} = 1/2 \text{ max. } N_{x\phi} = 29 / 2 = 14.5 \text{ t/m}$$

Hence the maximum shear stress is :

$$\text{max. } \tau = \text{max. } T_{x\phi} / A = 14500/100 \times 10 = \underline{14.5 \text{ kg/cm}^2}$$

All shear stresses bigger than the allowed value of 8 kg/cm<sup>2</sup> ( giving 8 t/m diagonal tension ) will be resisted by diagonal reinforcements in the manner shown in figure XII-55.

The shear stress is equal to zero at mid-span, it will be equal to 8 kg/cm<sup>2</sup> at a distance  $x$  from the center line where  $x = 8 \times 12.5/14.5 = 6.9$  m. Dividing the distance  $x' = l/2 - x = 12.5 - 6.9 = 5.6$  ms. into four equal strips, then the area of the diagonal tension reinforcement required in each strip is given by :



$$A_{s1} = \frac{14.5 + 12.88}{2} \times \frac{1.0}{\sigma_s} = \frac{13.69 \times 1}{1.4} = 9.75 \text{ cm}^2 \quad 8 \phi 13$$

$$A_{s2} = \frac{12.88 + 11.25}{2} \times \frac{1.0}{1.4} = 8.60 \text{ cm}^2 \quad 7 \phi 13$$

$$A_{s3} = \frac{11.25 + 9.63}{2} \times \frac{1.0}{1.4} = 7.45 \text{ cm}^2 \quad 6 \phi 13$$

$$A_{s4} = \frac{9.63 + 8}{2} \times \frac{1.0}{1.4} = 6.30 \text{ cm}^2 \quad 5 \phi 13$$

The lengths  $x$  and  $x'$  are to be measured at the neutral plane.

#### Analysis of Arch Action of Symmetrical Circular Cylindrical Shells

The characteristic feature of shell action is the transmission of loads primarily by direct stresses, with relatively small bending stresses. This unique property of cylindrical shells stems from the behavior of the shell in the transverse direction. To form a clear picture of the manner in which the shell operates and to contrast it with the behaviour of a plate, typical strips cut from a plate and a shell are shown in figure XII-56.

Considering the strip of fig. a as a free body, it is evident that shearing forces and bending moments are required in order to maintain the external load in equilibrium. On the other hand in the

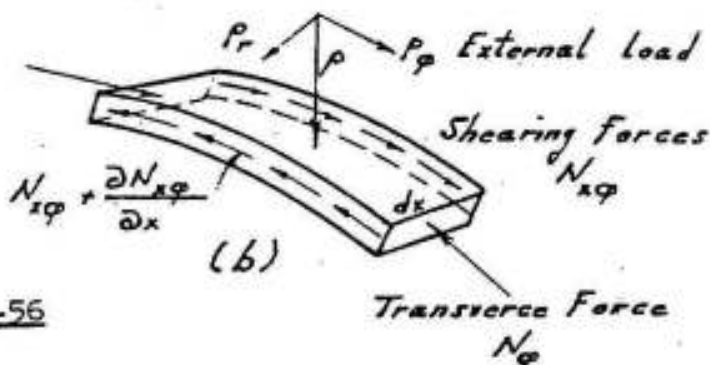
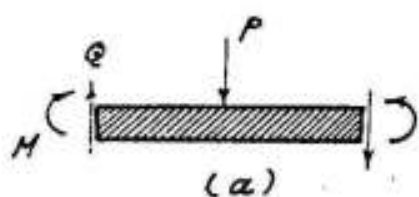


FIG. XII-56

strip of fig. b the radial component  $p_r$  of the external load  $p$  is resisted by transverse force  $N_\phi$  causing normal stresses on the radial sections, whereas the tangential component  $p_\phi$  is resisted by shearing forces on the transverse sections. The presence of these shearing forces distinguishes shell action from arch action. Because of them the shell, regardless of its shape, can support any type of loading by direct stresses, whereas the arch can carry, by direct stresses, only one type of loading.

In order to determine the transverse bending moments  $M_\phi$ , we consider a free body in the form of an elementary arch included between two adjacent cross-sections of the shell which are  $dx$  apart. The equilibrium of the arch is maintained by two sets of forces, namely the load  $p$  acting on the element and the forces  $\partial N_{x\phi} / \partial x$  (Fig. XII-57) the latter is known as the specific shear. The specific shear at any point, acting in the direction of the tangent to the shell arch, may be resolved into horizontal and vertical components. It is clear that the sum of the vertical components of the specific shear would balance the load on the shell arch; the horizontal components of the specific shear which are symmetrically disposed about the crown balance themselves.

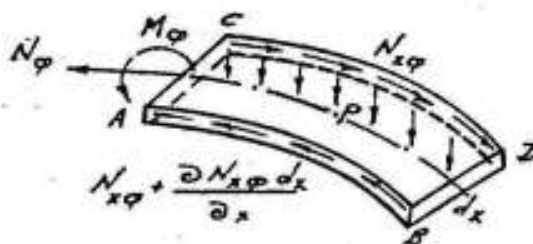


FIG. XII-57

We consider first a single shell with or without edge beams. It is clear that the elementary shell arch cut out from such a shell will not develop any restraining forces or moments at its ends. Hence, we have a statically determinate arch.

Next, we consider the elementary arch cut out from an interior shell of a symmetrically loaded group of multiple shells. As the shell

arch is restrained at the ends, it would behave as a fixed arch. If the loading on the shell arch is symmetrically distributed across the cross-section, one would expect the degree of indeterminacy to be three. But the degree of indeterminacy involved is only two, as no vertical reactions develop at the ends, the vertical loading on the shell being fully balanced by the sum of the vertical components of the specific shears. The elementary shell arch fixed at the ends and acted upon by the load and the specific shear may be analysed by any method applicable to fixed arches to determine the transverse moments  $M_\psi$ .

#### Applications

##### 1) Single circular shell without edge beams :

Denoting the angular distance from the crown to an arbitrary point by  $\psi$  and half the central angle of the shell by  $\psi_0$ , and assuming the unit load  $p$  to be uniformly distributed over the surface, Lundgren, in his book on cylindrical shells, gives the following relation :

$$M_\psi = - \frac{p a^2}{16 \psi_0^4} (\psi_0^2 - \psi^2)^2 (3 \psi_0^2 - \psi^2)$$

The moment is negative along the whole width of the shell and has the form shown in figure XII-58.

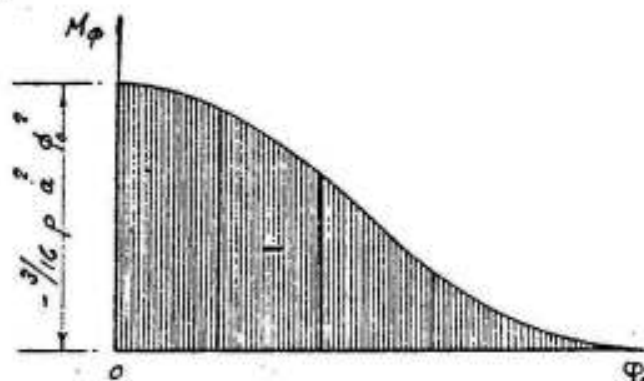


FIG. XII-58

Transverse Moments  
in a Circular Shell  
without Edge Beams

The maximum moment at the crown is therefore :

$$M_0 = - 3/16 p a^2 \psi_0^2$$

For a vertical concentrated load  $P$ , acting on the middle of a stiffening rib, the moment in the rib, for  $\psi > 0$ , is given by :

$$M_\psi = \frac{P a}{32 \psi_0^5} (\psi_0 - \psi)^4 (5 \psi_0^2 + 4 \psi_0 \psi + \psi^2)$$



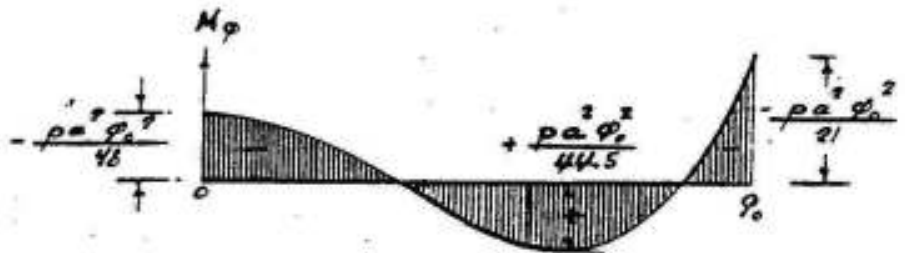
2) Circular inner shells without edge beams

The transverse bending moment of an inner circular shell, according to Lundgren, is given by :

$$M_{\varphi} = - \frac{p a^2}{336 \varphi_0^4} ( 7 \varphi_0^6 - 75 \varphi_0^4 \varphi^2 + 105 \varphi_0^2 \varphi^4 - 21 \varphi^6 )$$

The moment is negative at the springing and at the crown but positive at the quarter point (Fig. XII-59). Numerically, the statically indet-

Fig. XII-59  
Transverse moments  
in an inner shell  
without edge beams



eterminate negative moment at the springing is the greatest and equal to

$$M_{\varphi_0} = - p \cdot a^2 \cdot \varphi_0^2 / 21$$

i.e., only  $\frac{1}{9}$  maximum moment in a single shell. The moment at the crown is :

$$M_0 = - p \cdot a^2 \cdot \varphi_0^2 / 48$$

A value that is only  $\frac{1}{9}$  of maximum moment in a single shell.

The maximum positive bending moment takes place at an angle  $\varphi$  from the crown that can be determined from the relation :

$$dM_{\varphi} / d\varphi = 0$$

which gives

$$\varphi = 0.638 \varphi_0$$

Introducing this value in the general equation of  $M_{\varphi}$ , we get

$$\max M_{\varphi} = p \cdot a^2 \cdot \varphi_0^2 / 44.5$$

The normal force in long shells with  $a < 10 m$  may be estimated from the following relation :

$$N_{\varphi} = k \cdot p \cdot a$$

The values of  $k$  are shown in Fig. XII-60.

The bending moments and normal forces in the critical sections of an inner long cylindrical shell subject to uniform load  $p$  can accordingly be summarized as follows :

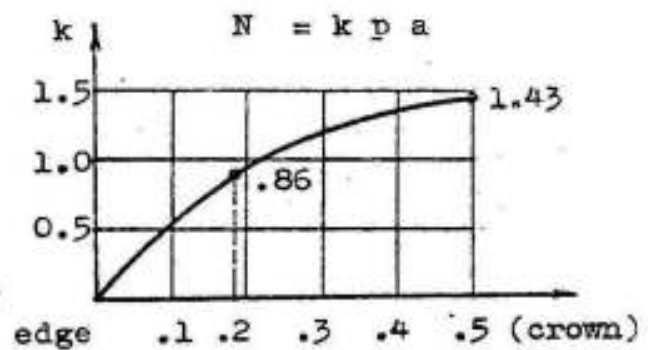


Fig. XII-60

Section	Springing	max $M_{\phi}$	Crown
$\phi$	$\phi = \phi_0$	$\phi = 0.638 \phi_0$	$\phi = 0$
Bending moment $M_{\phi}$	$- p a^2 \phi_0^2 / 21$	$+ p a^2 \phi_0^2 / 44.5$	$- p a^2 \phi_0^2 / 48$
Normal force $N_{\phi}$	---	$0.86 p a$	$1.43 p a$

The transverse bending moments in circular symmetrical inner shells with edge beams may be assumed of the same values shown in Fig. XII-59. Accordingly, the transverse bending moments and normal forces of the example given in Fig. XII-54 are :

Section	Springing	max $M_{\phi}$	Crown
$\phi$	$\phi = \phi_0$	$\phi = 0.638 \phi_0$	$\phi = 0$
$M_{\phi} = \frac{p a^2 \phi_0^2}{k}$	$- \frac{11220}{21} = -530$	$+ \frac{11220}{44.5} = 250$	$- \frac{11220}{48} = -235$
$N_{\phi} = k p a$	---	$0.86 \times 3633 = 3124$	$1.43 \times 3633 = 5200$

in which

$$p a^2 \phi_0^2 = 400 \times 9.083^2 \times 0.583^2 = 11220 \text{ kg.m.} \quad \text{and}$$

$$p a = 400 \times 9.083 = 3633 \text{ kg}$$

It is clear that the transverse bending moments are relatively low so that a shell thickness of 10 cms reinforced by two meshes  $6 \phi 8 \text{ mm/m}$  and  $5 \phi 6 \text{ mm/m}$  circular and longitudinal bars respectively is generally ample. It is however recommended to increase the thickness of the shell gradually from 10 cms to ~15 cms at the springing and at the diaphragms along a distance equal to 1/10 length of arch.

If the span of the shell is small ( $< \sim 15ms$ ), a slab thickness of 8 cms, increased to 12 cms at the springing and diaphragms, is generally sufficient. Such shells are reinforced by one mesh,  $6 \phi 8$  mm/m circular and  $5 \phi 6$  longitudinal, except at the edges where we need two meshes.

At the end diaphragms, local bending moments are induced in the longitudinal direction of the form shown in Fig. XII-61. The maximum ordinate can be estimated by :



Fig. XII-61

$$\max M_x = - p \cdot x_1^2 / 2$$

in which

$$x_1 = 0.76 \sqrt{a t}$$

$a$  = radius and  $t$  = thickness of shell ,  $p$  = total load /  $m^2$

The determination of the transverse bending moments at different points of a simple circular shell without edge beams can be treated in the following manner :

a slice of the shell one meter long , is considered as an arch which is in equilibrium under the action of the loads  $p$  and the specific shear  $\partial N_{x\phi} / \partial x$  (Fig. XII-62).

In a statically determinate shell subject to uniform load  $p$  per square meter,  $\partial N_{x\phi} / \partial x$  must be constant along any generator in direction  $x$  because  $N_x$  varies linearly in this direction (refer to Figs. XII-34, 35 and 36) ; so that in a simple shell, we have :

$$N_{x\phi} = \frac{\partial N_x}{\partial x} \cdot \frac{l}{2}$$

It has further been shown that

$$\max N_{x\phi} = \frac{\max Q}{y_{CT}} = \frac{\bar{p}}{2 y_{CT}}$$

in which

$\bar{p}$  = the total load on the shell per meter run . So that

$$\max \frac{\partial N_x}{\partial x} = \frac{\bar{p}}{y_{CT}}$$

Its distribution along the section of the shell is similar to that of

$N_{x\varphi}$ , i.e., with zero ordinates at crown and foot of arc and maximum at the c. g. axis. It may be assumed triangular with a maximum ordinate equal to  $\frac{4}{3} \frac{\bar{p}}{y_{CT}}$  as shown in Fig. XII-63.

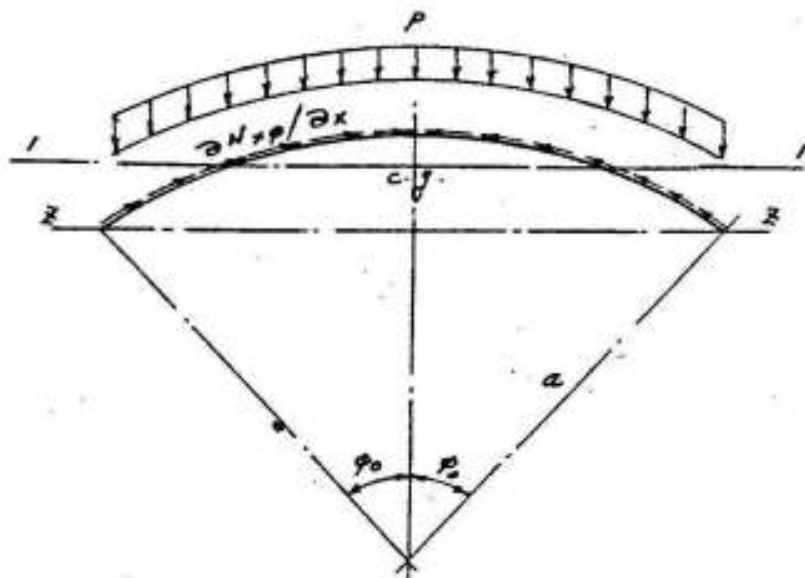


Fig. XII-62

Length of arc  $s = 2 a \varphi_0$

$$\max \frac{\partial N_{x\varphi}}{\partial x} = \frac{\bar{p}}{y_{CT}}$$

$$\frac{\bar{p}}{y_{CT}} = \max \frac{\partial N_{x\varphi}}{\partial x}$$

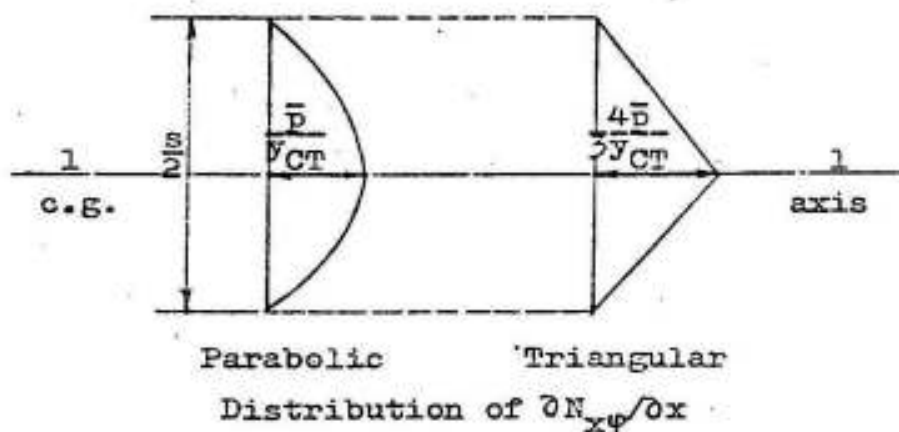


Fig. XII-63

All the statical values required for the design can be determined by the strip method as follows :

- 1) Determine the arc length from the relation  $s = 2 a \varphi_0$ , where  $\varphi_0$  is measured in radians .
- 2) Divide half the arc into a convenient number of strips, each of length  $\Delta s$  (normally 2 to 3 meters). Determine the coordinate  $z'$  from

a horizontal axis z-z and y from the middle vertical axis both for the middle and the edges of each strip so that  $\Delta z$  and  $\Delta y$  are known (Fig. XII-64).

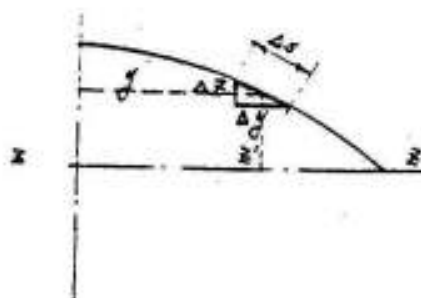


FIG. XII-64

3) The c.g. axis can be determined by dividing the statical moment of the elemental areas about any axis (e.g. z-z) by their total area. The statical moments  $S$ ,  $S_{1-1}$  and the moment of inertia  $I_{1-1}$  can then be easily determined

4) Determine the shear forces  $N_{x\varphi}$  and the specific shear  $\partial N_{x\varphi} / \partial x$  from the given relations; either the real parabolic distribution or the equivalent triangular distribution (fig. XII-63) may be used.

5) The statically determinate transverse moments for  $p$  and  $\partial N_{x\varphi} / \partial x$  at the middle of the different increments may be determined directly assuming the specific shear in every increment parallel to the tangent at its c.g. in which case if we assume that the specific shear on an element (e.g. 2-3) is  $\mathcal{S}$ , then its moment at points 3, 4 and 5 are  $\mathcal{S} n_3$ ,  $\mathcal{S} n_4$  and  $\mathcal{S} n_5$  where  $n_3$ ,  $n_4$  and  $n_5$  are the normals from points 3, 4 and 5 on the line of action of  $\mathcal{S}$ . (Fig. XII-65)

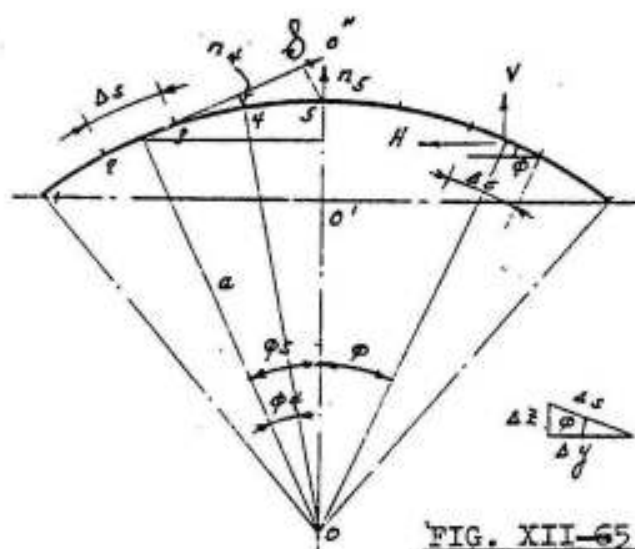


FIG. XII-65

In order to determine  $n_5$ , we have

$$\cos \varphi_5 = a / \overline{O - O''} \quad ,$$

hence  $\overline{O - O''} = a / \cos \varphi_5$  and

$$\cos \varphi_5 = n_5 / \overline{O'' - 5} =$$

$$= n_5 / \overline{O - O''} - a$$

therefore

$$n_5 = (\overline{O - O''} - a) \cos \varphi_5 = \left( \frac{a}{\cos \varphi_5} - a \right) \cos \varphi_5 \quad \text{or}$$

$$\text{Similarly} \quad \begin{aligned} n_5 &= a (1 - \cos \varphi_5) \\ n_4 &= a (1 - \cos \varphi_4) \\ n_3 &= a (1 - \cos \varphi_3) \quad \dots \text{ etc.} \end{aligned} \quad \text{and}$$

The transverse moments due to specific shear can also be determined by resolving  $\mathcal{S}$  to its vertical and horizontal components and multiplying them by their distances from the different points on the arc. It has to be noted that:

The vertical component  $V$  of the specific shear  $\mathcal{S}$  acting on the element  $\Delta s$ , is:

$$V = \mathcal{S} \sin \varphi = \frac{\partial N_x}{\partial x} \cdot \Delta s \cdot \frac{z}{s} = \frac{\partial N_x}{\partial x} \cdot \Delta z$$

The horizontal component  $H$  of the specific shear acting on the element  $\Delta s$ , is:

$$H = \mathcal{S} \cos \varphi = \frac{\partial N_x}{\partial x} \cdot \Delta s \cdot \frac{y}{s} = \frac{\partial N_x}{\partial x} \cdot \Delta y$$

The transverse bending moment is negative although as shown in Fig. XII-66a.

Transverse Bending Moments in a Simple Circular Shell with Edge Beams

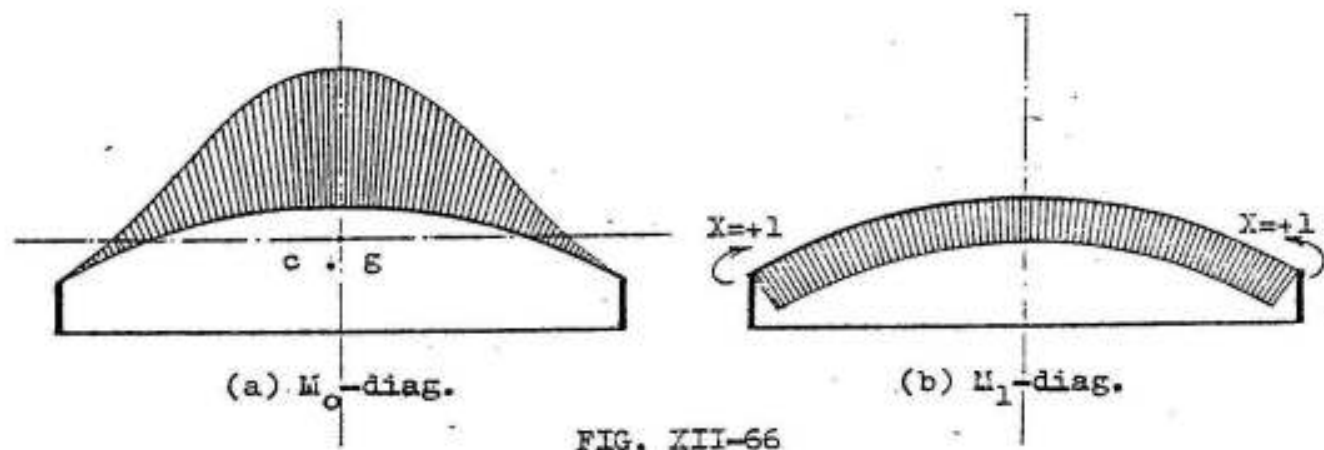


FIG. XII-66

A single shell with edge beams may be assumed, for symmetrical loading, as once statically indeterminate. The statically indeterminate value is the connecting moment  $X$  between the shell slab and the edge beam. (Fig. XII-66). If the edge beams are sufficiently deep and the necessary constructional provisions are taken to prevent them from rotation, we may assume that the angle of rotation at the springing is equal to zero and the statically indeterminate moment  $X$  can be determined from the equation of elasticity:

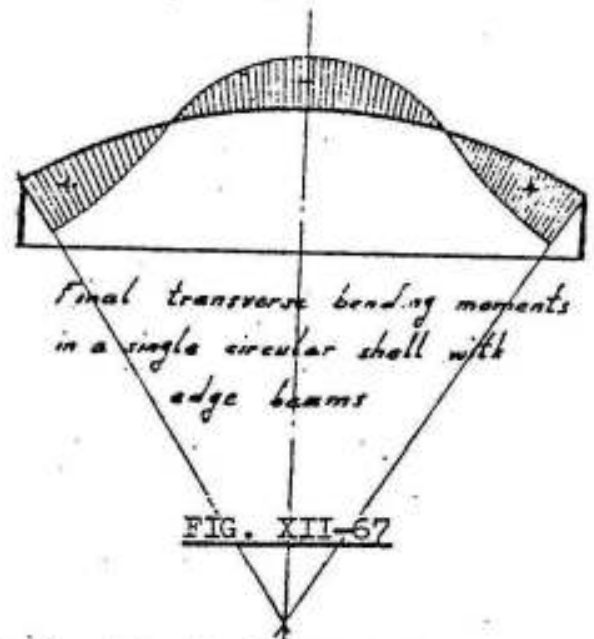
$$0 = \delta_0 + X \delta_1$$

So that

$$X = - \delta_0 / \delta_1 = - \sum \frac{M_0 M_1}{EI} \Delta s / \sum \frac{M_1^2}{EI} \Delta s$$

The  $M_0$ - diagram can be determined as shown in the previous case ( Fig. XII-66 a ), the  $M_1$  diagram is rectangular ( Fig. XII-66b) and the final transverse moments are therefore determined from the relation : ( Fig. XII-67 )

$$M = M_0 + X M_1$$



Transverse Bending Moments in an Inner Circular Shell with Edge Beams

This case is twice statically indeterminate, the unknowns are the connecting moments  $X_1$  and the horizontal thrust  $X_2$  at the joint between the shell slab and the edge beams. The equations of elasticity are :

$$\delta_{10} + X_1 \delta_{11} + X_2 \delta_{12} = 0$$

$$\delta_{20} + X_1 \delta_{21} + X_2 \delta_{22} = 0$$

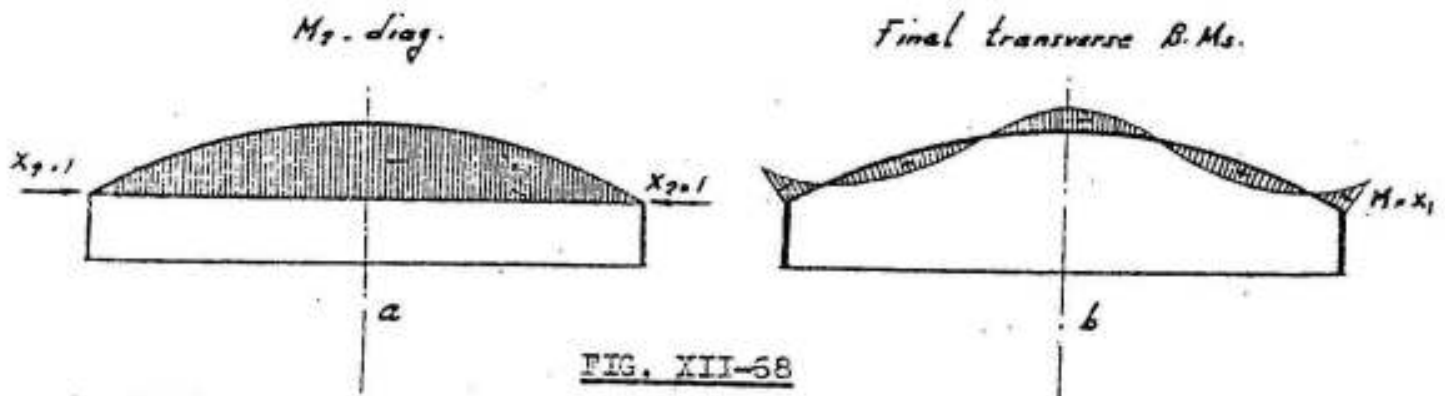


FIG. XII-68

in which

$$\delta_{10} = \sum M_0 M_1 \Delta s / EI, \quad \delta_{11} = \sum M_1^2 \Delta s / EI \text{ are the same as in previous case.}$$

$$\delta_{20} = \sum M_0 M_2 \Delta s / EI, \quad \delta_{22} = \sum M_2^2 \Delta s / EI \text{ and } \delta_{12} = \sum M_1 M_2 \Delta s / EI$$

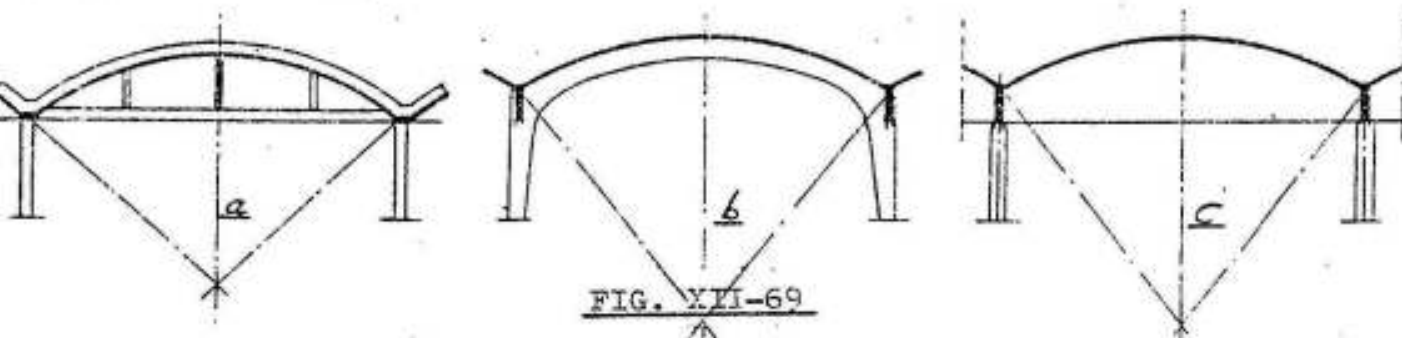
The  $M_0$  and the  $M_1$  - diagrams are the same as those of the previous case ( fig. XII-66 a and b ). The  $M_2$ - diagram is shown in fig.XII-68a. Generally  $X_1$  and  $X_2$  are negative which means that the bending moment at the springing is negative and that  $X_2$  acts outwards reducing the statically determinate axial forces. The final transverse moments are given by

$$M = M_0 + X_1 M_1 + X_2 M_2$$

The axial force in the shell is equal to the resultant of the specific shear and the components of the load  $p$  and  $X_2$  parallel to the axis of the shell.

External Loads and Internal Forces Acting on End Diaphragms.

The end diaphragm of a shell may be an arch with a tie, a frame with curved girder , a vertical plate , a truss ... etc. as shown in figure XII-69 a, b and c ).



The loads of the shell slab are transmitted to the diaphragms through the direct shearing forces  $N_{x\varphi}$  acting along the axis of the shell at the end cross-section.

Their magnitude can be determined from the relation :

$$N_{x\varphi} = Q_{\max} \cdot S / I_{1-1}$$

Their distribution is parabolic with a maximum ordinate ( $N_{x\varphi}$  max.) at the neutral axis of the shell given by :

$$N_{x\varphi} \text{ max} = Q_{\max} \cdot / J_{CT}$$

They may also be assumed triangular with a maximum ordinate equal to

$$N_{x\varphi} \text{ max} = 4 Q_{\max} / 3 J_{CT}$$



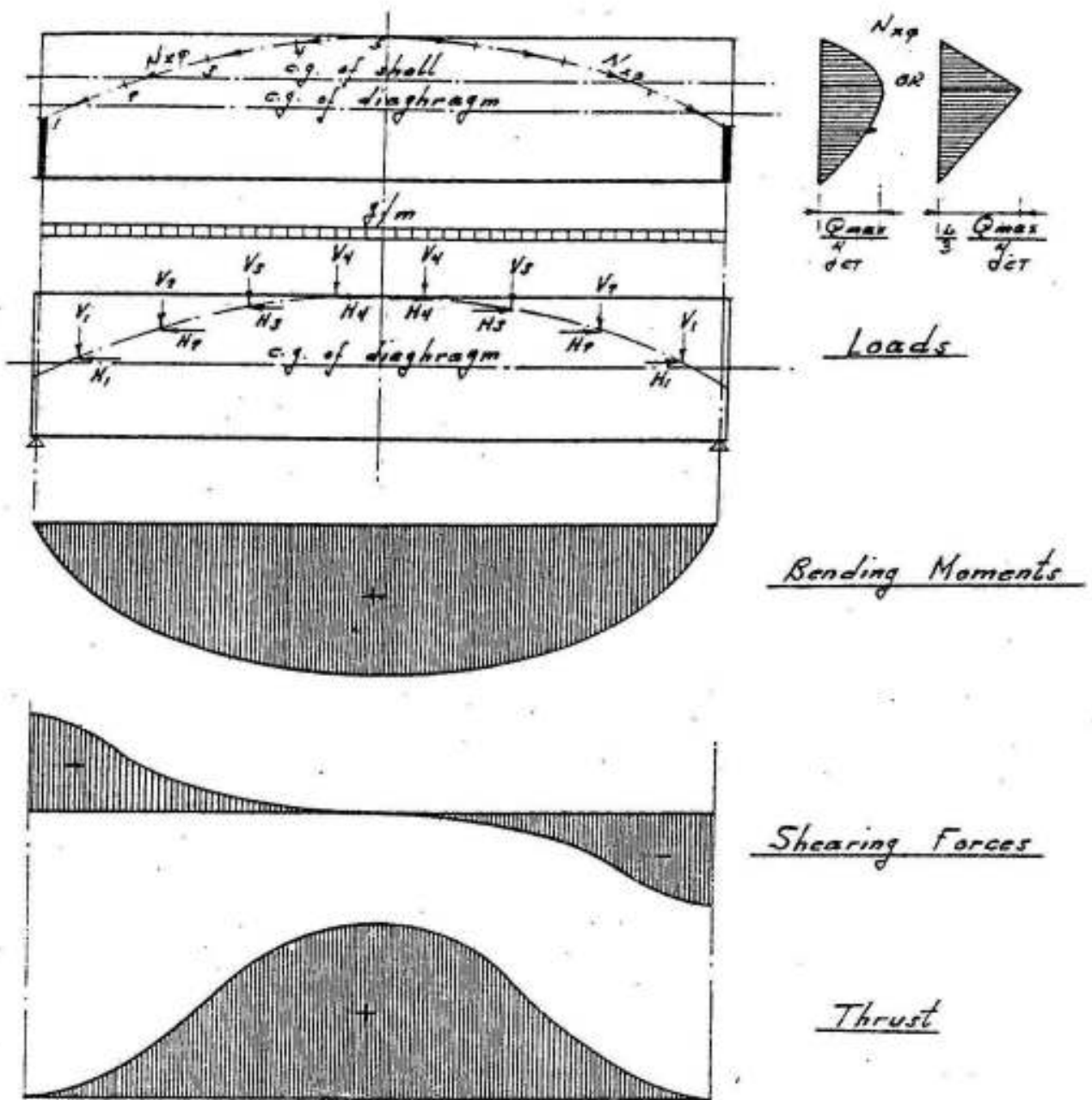


Fig. XII-70 External load and internal forces acting on end diaphragm

which is more convenient for the numerical calculations. Fig. XII-70 shows a simple diaphragm in which the forces  $N_{x\phi}$  acting on the different elements  $\Delta s$  of the shell are resolved to their vertical and horizontal components  $V$  and  $H$  where

$$V = N_{x\phi} \cdot \Delta s \sin\phi = N_{x\phi} \cdot \Delta s \cdot \frac{\Delta z}{\Delta s} = N_{x\phi} \Delta z \quad \text{and}$$

$$H = N_{x\varphi} \cdot \Delta s \cos\varphi = N_{x\varphi} \cdot \Delta s \cdot \frac{\Delta y}{\Delta s} = N_{x\varphi} \cdot \Delta y$$

in which  $\Delta z$  and  $\Delta y$  have the same meaning shown in figure XII-65  
As a check for the calculations  $\sum V$  must be equal to  $Q_{\max}$ .

Having determined  $V$  and  $H$ , the corresponding bending moment shearing force and thrust with respect to the axis of the diaphragm can be easily determined.

Prof. Dr. A. Shaker<sup>✶</sup> in an " Introduction to Three Dimensional Analysis of Structures " has given three examples showing the numerical analysis of the internal forces in long shell roofs by the beam method namely :

- 1) Single long cylindrical shell roof without edge beams.
- 2) " " " " " with vertical edge beams.
- 3) Intermediate long cylindrical shell roof with vertical edge beams.

Constructional Details.

For normal barrel vaults the maximum practical span  $l$  is 25 ms. It can be increased to 50 ms. if prestressing is used.

Figure XII-71 shows cylindrical parallel barrel vaults with and without edge valley beams.

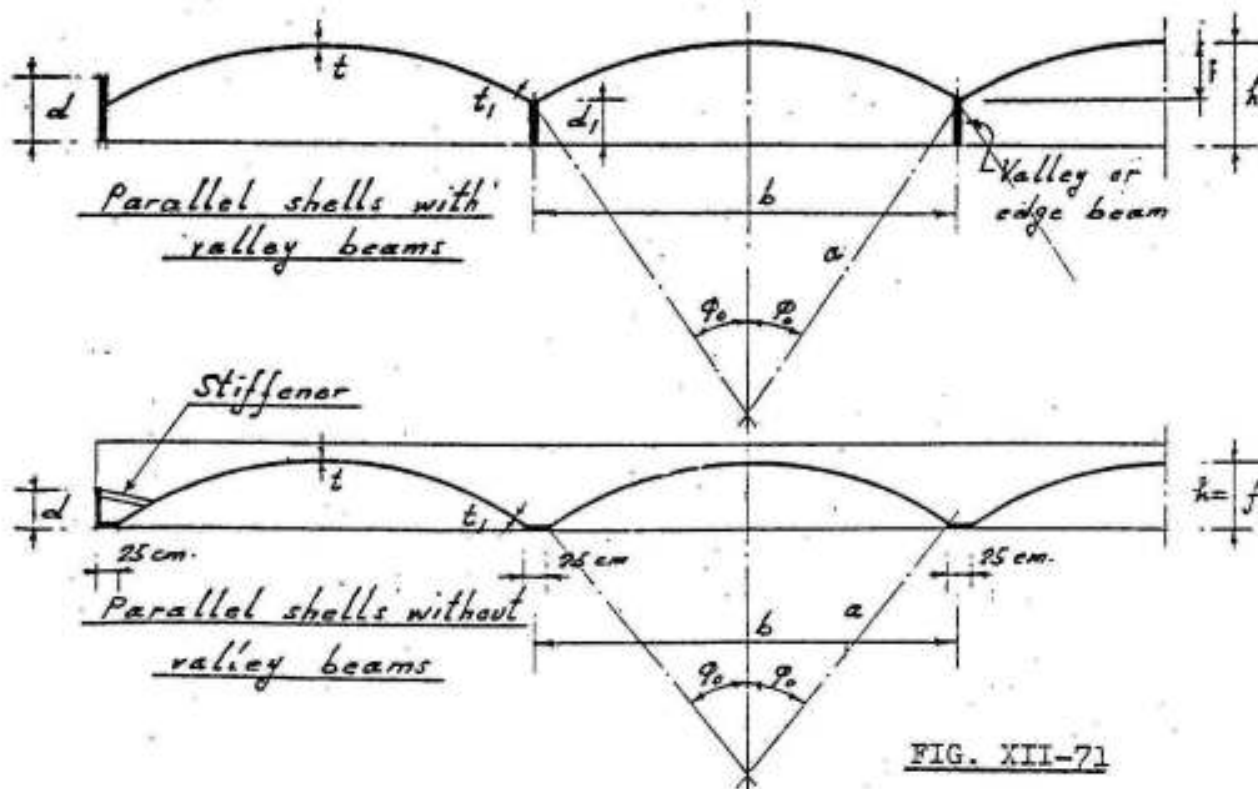


FIG. XII-71

✶ Professor of Theory of Structures at the Faculty of engineering Ain Shams University.

The following gives guide lines for the convenient proportions of cylindrical barrel vaults.

$$l/b \approx 2 \quad \text{and} \quad h/l \approx 1/10$$

These proportions give the optimum value for economy consistent with strength and deflection requirements.  $l/b$  may however be increased to 3 or even more and  $h/l$  may be decreased to  $1/12$ .

$d/l$  may be chosen  $1/15$ . If edge beams are not supported by intermediate columns, stiffeners with a cross-section varying between  $15 \times 15$  cm. and  $20 \times 20$  cms. at the third points of the spans are usually required to prevent lateral instability of the compression zone of the edge beam.

If the edge beams are supported by intermediate columns and  $d \geq 50$  cms, then stiffeners need not be used.

For cast in situ shells the thickness  $t$  should not be less than 8 cms to be increased to 10 cms for  $16m < l < 25$  ms. and 12 cms for bigger spans.

The thickness  $t_1$  at the springing may be chosen equal to  $l/120$  usually between 12 and 20 cms. It is a common practice to increase the thickness by  $\sim 4$  cms for a distance of  $l/10$  from each end.

The angle  $\varphi_0$  should always be kept less than  $45^\circ$ , otherwise double shuttering will be needed near the springing. If the above proportions are used,  $\varphi_0$  will automatically be less than  $45^\circ$ .

Sachnowski in his text book " Stahlbetonkonstruktionen " recommends the following proportions. ( fig. XII-72).

$$b < 20 \text{ ms.} \quad h \gg l/10 \quad \text{and} \quad \gg b/c$$

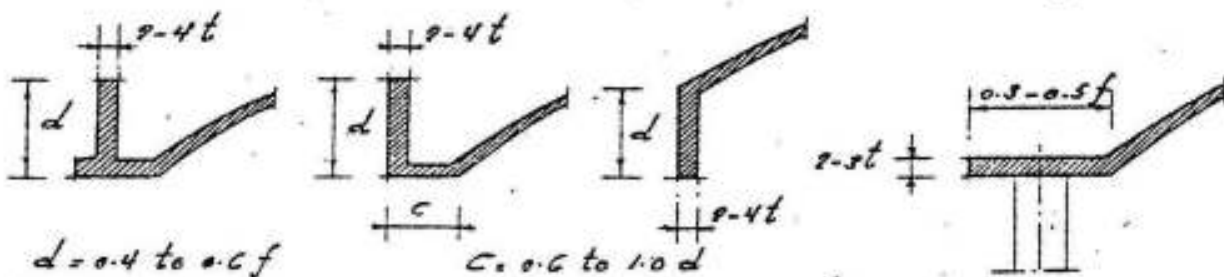
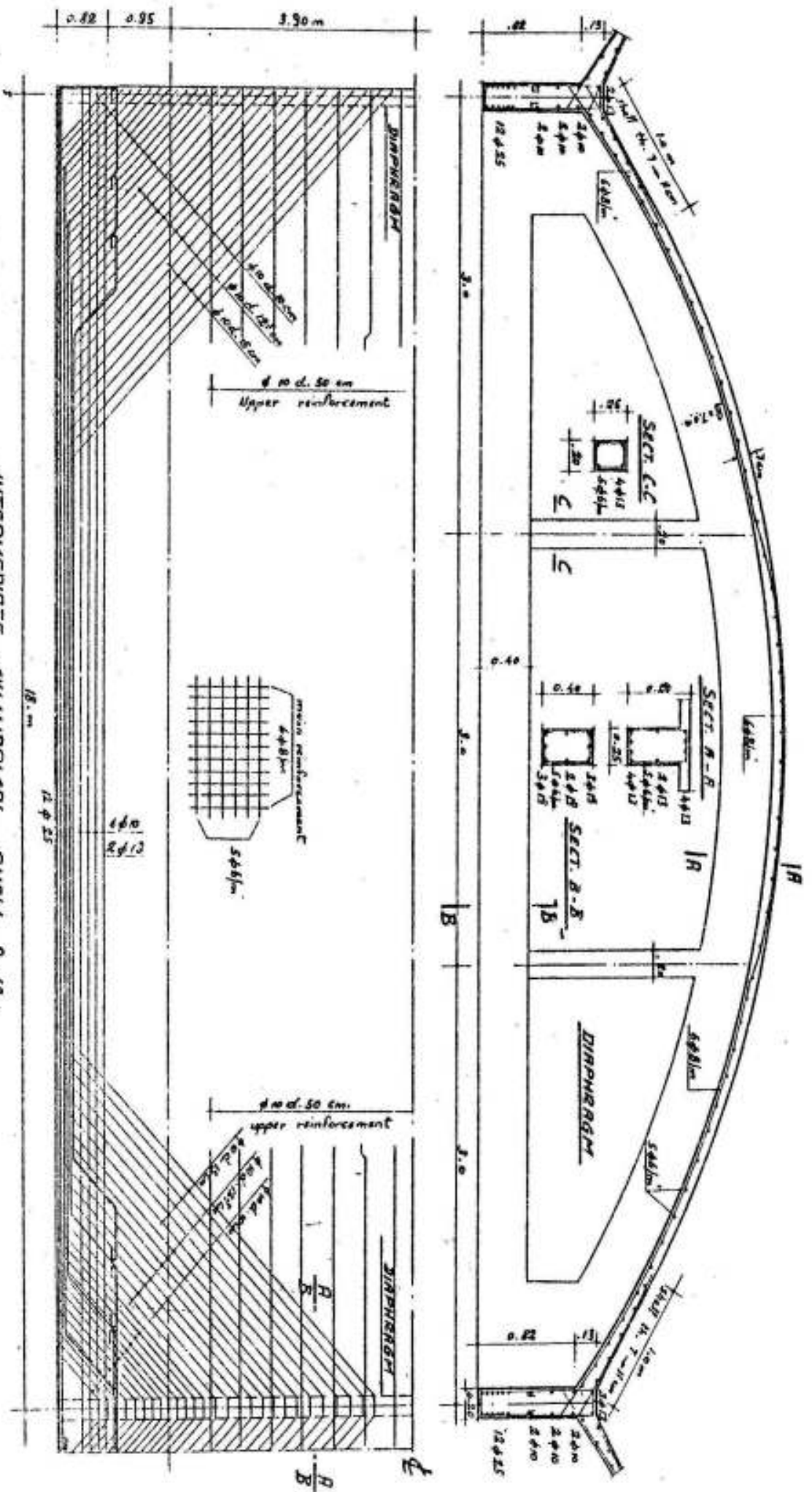


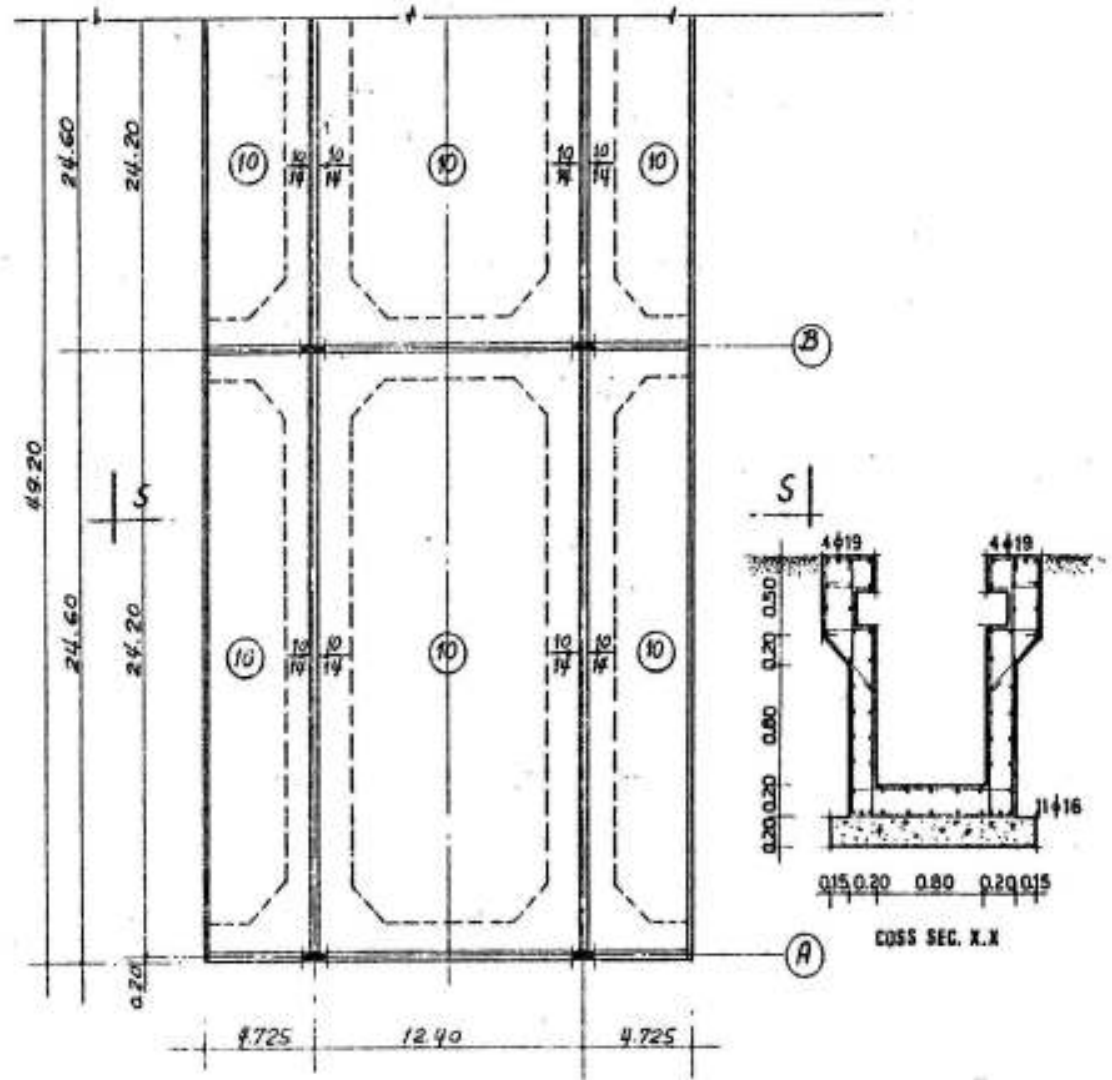
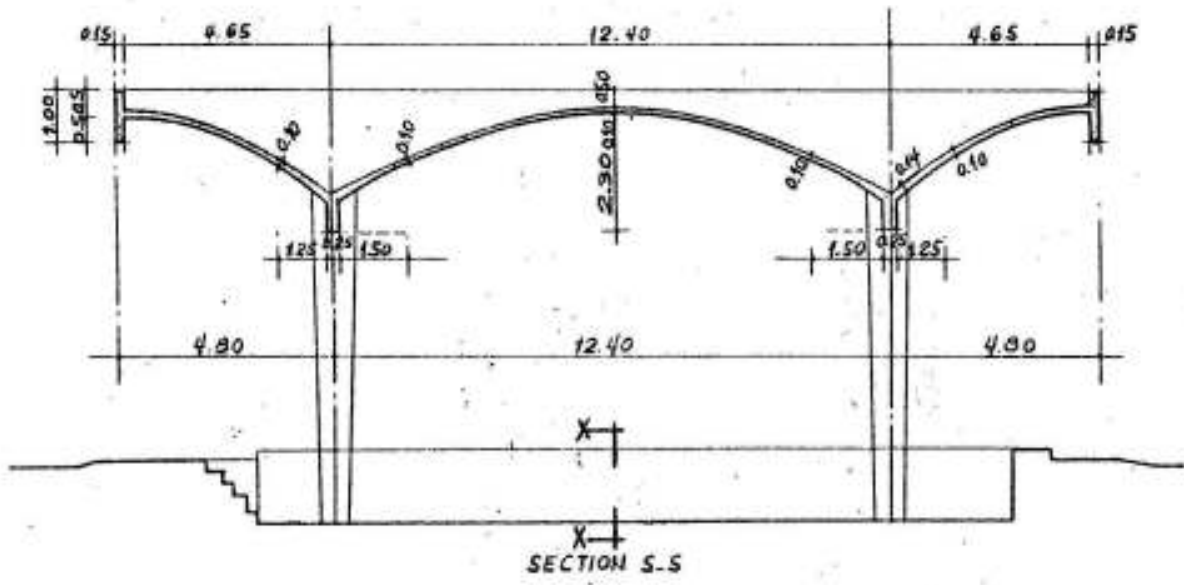
FIG. XII-72

Fig. XII-73 shows the details of reinforcements of an intermediate shell 9 meters wide and 18 ms span. The shell is 7 cms. thick, increased to 13 cms. over a length of 1.00 m at the springing and end diaphragms. It is reinforced with one mesh  $6\phi 8$  mm/m circular and  $5\phi 6$  mm/m longitudinal except at the edges where we have two meshes. The



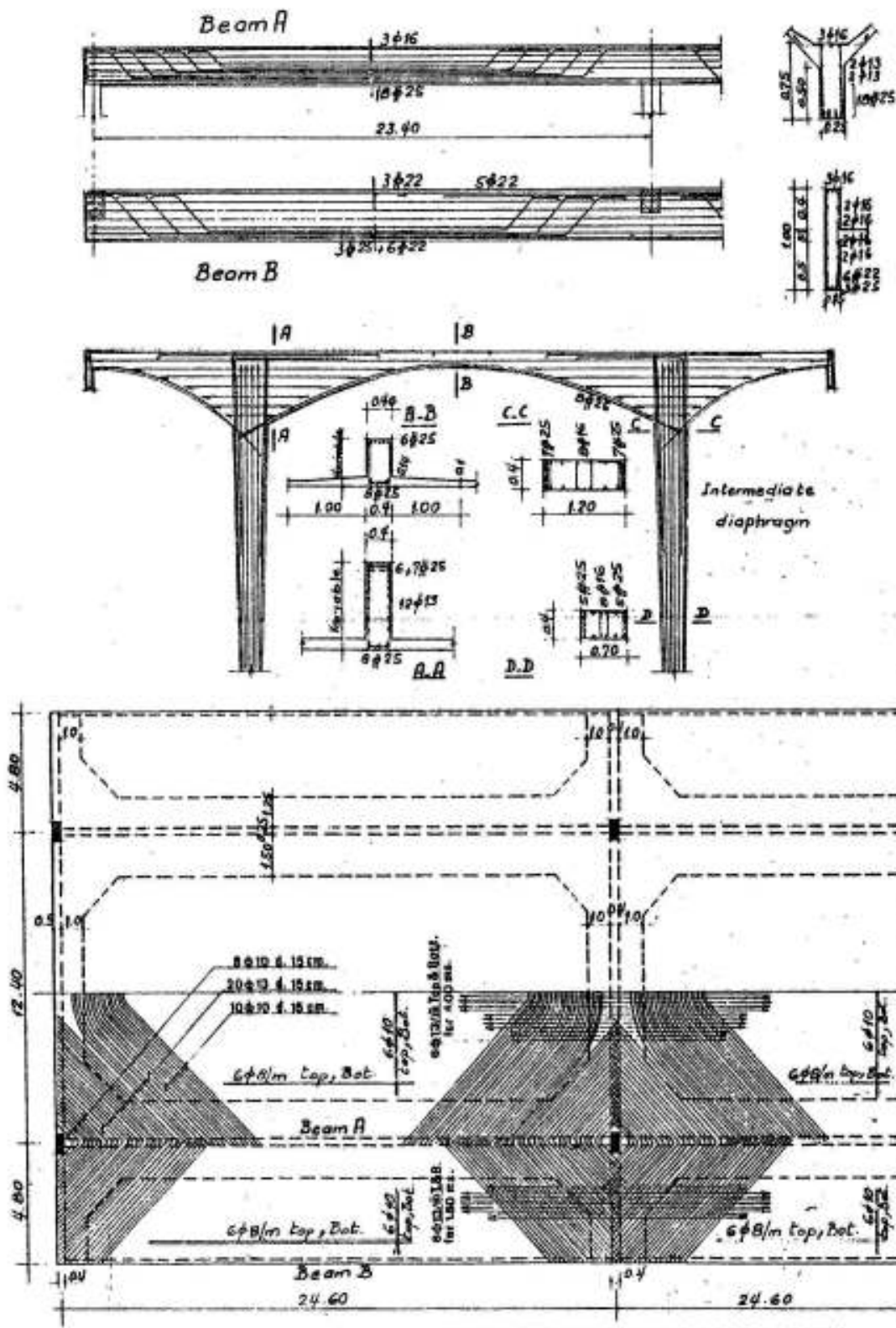
INTERMEDIATE CYLINDRICAL SHELL 3 x 18 m.

Pls. XII-73



PUBLIC TRANSPORTATION ORGANIZATION  
 GESR-EL-SUEZ GARAGE  
 INSPECTION SHED

Fig XII.74.9



PUBLIC TRANSPORTATION ORGANIZATION  
 GESR EL-SUEZ GARAGE  
 INSPECTION SHED

Fig. XII.74-3

diagonal reinforcement at the corners is arranged at the middle of the shell slab; they must be well anchored with the bent bars of the valley edge beams which are reinforced by 12  $\phi$  25 normal mild steel. It is however recommended to replace these longitudinal reinforcements by equivalent deformed high grade or cold twisted steel for bigger strength and higher bond.

Figures XII-74 a and b show the general layout, main dimensions and details of reinforcements of the inspection shed constructed at Gisar-El-Suez garage area. They show one of the wide possible applications of circular cylindrical shells. The shed in this structure, covering an area of 22 x 49 ms, is supported on six columns only. Its thickness is 10 cms increased to 14 cms on a small distance at the edge beams and end diaphragms. The shell, in its cross-section, is composed of a circular part 12.4 ms wide and two overhanging circular cantilevers 4.8 ms each. It has four edge beams: two outside ones 15 x 100 cms each and two intermediate ones 25 x 75 cms each at the joint between the cantilever arms and the central part. In the longitudinal direction, the shell is continuous over two spans 24.6 ms each. It is supported on three diaphragms: one intermediate and two edge ones. The reinforcement of the shell is composed of two meshes: each 6  $\phi$  10 mm/m circular and 6  $\phi$  8 mm/m longitudinal. The longitudinal reinforcement in the intermediate edge beams is 18  $\phi$  25 mm and in the outside edge beams is 3  $\phi$  25 + 6  $\phi$  22 mm. The longitudinal reinforcement resisting the connecting moment between the two spans of the shell over the intermediate diaphragm is 25  $\phi$  13 mm top and bottom. The diagonal reinforcement shown in plan is arranged to resist the principal diagonal tensile stresses in the shell.

The diaphragms are two hinged frames with overhanging cantilevers. Their main girders are inverted in order to have a plane bottom surface for the roof. Due to the severe variation of the moment of inertia of the diaphragm-girder, it has been possible to make its middle section 60 cms deep only.

The soil at the site of the garage is composed of clayey layers that are much affected by water to depths varying between 10 and 12 meters, underlaid by medium sand. The foundations for the main columns are single isolated footings composed of rectangular reinforced concrete footings 50 to 60 cms thick resting on rounded plain concrete deep ones reaching the sand and having a depth varying between 7 and 9 meters. Their top surface is 3 ms from ground level.

The cross-section x-x of the underground path necessary for in-

spection is 1.70 ms deep and 0.80 ms wide; it has been designed as a reinforced concrete U-section on elastic foundation subject to the rolling wheel load of the busses. Its walls and floor are chosen 20 cms thick and its main longitudinal reinforcement is 11  $\phi$  16 mm at the bottom of the floor slab and 8  $\phi$  19 mm at the top of the walls as shown in Fig. XII-74a.

#### 4- Cross-Supported Cylindrical Shells

If the cross-section of a shell is simply supported at the edges  $e$  and  $e'$ , there is only one statically indeterminate value, consisting of two vertical reactions  $X$ , from the longitudinal walls. (Figure XII - 75 a)  $X$  is to be so determined that the total vertical displacement at the springing is zero. For solving the problem, we choose as main system the free arc  $e e'$  without supports at the edges  $e$  and  $e'$ . The equation of elasticity is therefore

$$\delta = 0 = \delta_o + \delta_X$$

where

$\delta_o$  = vertical displacement of the middle section of the main system due to loads; and

$\delta_X$  = vertical displacement of the same section due to the statically indeterminate edge loads  $X$ .

Both values are to be calculated taking the beam and the arch action in consideration in the following manner :

$\delta_o = \delta_{bo} + \delta_{ao}$  = vertical displacement due bending moments in longitudinal direction (beam action) plus vertical displacement due to bending moments in cross direction (arch action).

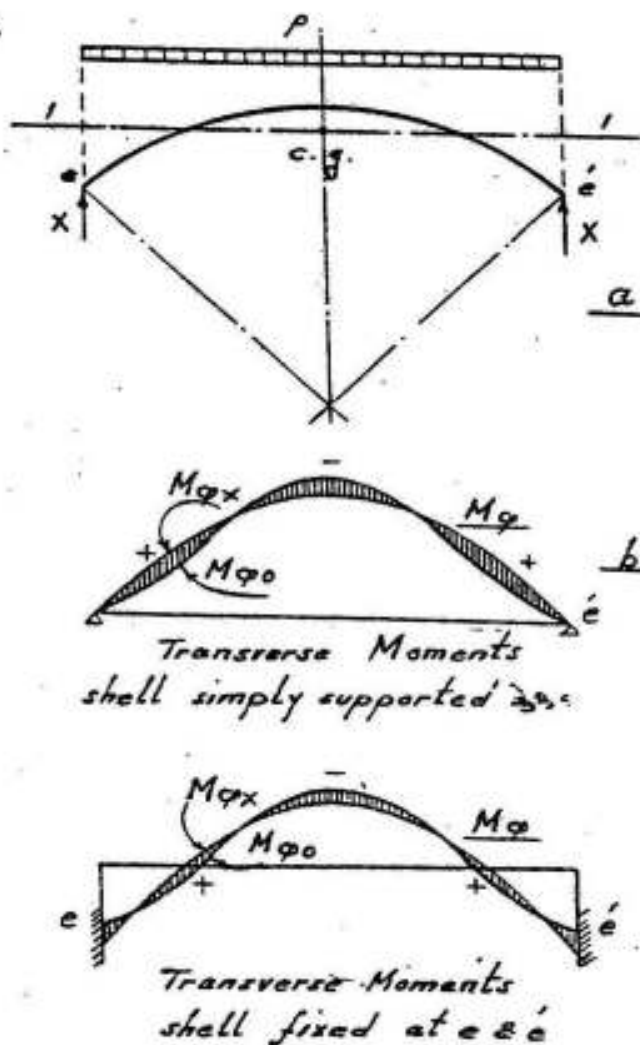


FIG. XII-75



For a shell simply supported between the diaphragms subjected to a uniform load  $\bar{p}$ , we have

$$\delta_{bo} = 5 \bar{p} t^4 / 384 E I_{1-1}$$

where,  $\bar{p}$  is the total load on the arc per meter run in the longitudinal direction, and  $I_{1-1}$  is the moment of inertia of the cross-section of the shell about the c.g. axis. The displacement  $\delta_{ao}$  can be computed according to the theorem of virtual work from the relation:

$$\delta_{ao} = \int \frac{M_{\phi 0} M_{\phi 1}}{E I_{\phi}} ds$$

where  $I_{\phi} = t^3 / 12$ ,  $M_{\phi 0}$  is the transverse bending moment due to the loads  $p$  and the specific shear  $\partial N_{x\phi} / \partial x$  shown in figure XII-75b-heavy curve - and is to be determined according to methods given in the previous article.  $M_{\phi 1}$  is the transverse bending moment due to  $X=1$ . It is however convenient to determine the transverse bending moment for  $X = -\bar{p} / 2$  because for this load, the corresponding specific shear and transverse moments are the same as for the uniform load  $\bar{p}$  but with opposite sign. (Fig. XII-75b, thin curve). In this manner, we have :

$$\delta_{ao} = \frac{2}{\bar{p}} \cdot \int \frac{M_{\phi 0} M_{\phi X}}{E I_{\phi}} ds$$

Analogously, for a load  $X = -\bar{p} / 2$ , the total edge vertical displacement can be given in the form :

$$\delta_X = \delta_{bX} + \delta_{aX}$$

where

$$\delta_{bX} = \delta_{bo}$$

and

$$\delta_{aX} = \frac{2}{\bar{p}} \cdot \int \frac{M_{\phi X}^2}{E I} ds$$

the value of  $X$  required to bring the edge back to the original level can now be computed from the relation :

$$X = \frac{2}{\bar{p}} : \frac{\delta_o}{\delta_X} = \frac{2}{\bar{p}} \cdot \frac{\delta_{bo} + \delta_{ao}}{\delta_{bX} + \delta_{aX}}$$

The variation of the final transverse moment is shown in figure XII-75 b ; it is negative in the neighbourhood of the crown and positive near the quarter points. Numerically the positive moments are

bigger.

Whether the shell is a little longer or shorter is not of much importance to X, because the beam deformations are small compared to the arch deformations.

If the cross-section is restrained at the springings, it is twice statically indeterminate. The two redundants are the vertical reactions and the restraining moments. Since the two restraining moments equilibrate each other, they have no influence on the beam action of the shell. The transverse moments for this case are shown in figure XII-75 c. In shells of ordinary lengths, the resulting moments are negative at the springing and in the neighbourhood of the crown, but positive near the quarter points. Numerically, the moments at the springings are the largest. However, the thickness of the shell may be increased here if necessary.

Shells restrained at the edges transfer a greater part of the load in the transverse direction than do shells with a simply supported cross-section especially in shells of considerable lengths.

Lundgren in his text-book on cylindrical shells, gives the following data for cross-supported circular shells.

a) Simply Supported Cross-Section

$$M_{\varphi} = - \frac{p a^2}{4 \psi_0} ( 0.0234 \psi_0^6 - 0.2138 \psi_0^4 \psi^2 + 0.2379 \psi_0^2 \psi^4 - 0.0476 \psi^6 )$$

The maximum moment is obtained for  $\varphi = 0.73 \psi_0$  and is given by :

$$\underline{\text{max. } M_{\varphi} = 0.03 p a^2 \psi_0^2}$$

The reaction from the longitudinal walls is :

$$\underline{X = 0.239 p a \psi_0}$$

i.e. ~ 24% of the load is transmitted to the transverse direction. In these relations, it was assumed that the beam deformation  $\delta_b$  is negligible compared with the arch deformation  $\delta_a$  at the edge of the main system. The ratio  $\delta_b / \delta_a$  can however be given in the form :

$$\delta_b / \delta_a = 10.7 l^4 I_{\varphi} / t a^6 \psi_0^8$$

and the beam deflection will increase X with factors  $(\delta_a + \delta_b) / \delta_a$  the consequent increase of the moment is somewhat larger. As an example, a 10% increase of X will increase the maximum moment by ~ 20%.

It has been stated before that transverse bending moments in single shells without edge beams (fig. XII-58) are relatively high and negative althrough with a maximum value at the crown of :

$$M_0 = - 0.187 p a^2 \psi_0^2$$

Whereas in cross supported single shells, the transverse bending moments ( fig. XII-75 a) are negative at the crown and with a value of

$$M_0 = - 0.023 p a^2 \psi_0^2$$

and positive in the outer parts of the arc; the maximum values lie at  $\psi = 0.73 \psi_0$  and are equal to

$$\text{max. } M_{\psi} + = 0.03 p a^2 \psi_0^2$$

i.e. smaller than 1/6 of  $M_0$  in cross-unsupported shells.

Moreover, the bending moments and the corresponding concrete compressive stresses and tension steel as well as the shearing forces and the corresponding shear stresses and diagonal steel are reduced by  $\sim 24 \%$ .

Lundgren in his text-book on cylindrical shells has given an example on a simple cross-supported shell. We show in the following a summary of the data, the design and a discussion to the final results. ( Fig. XII-76 ).

#### 1) Data

a shell, 30 ms. long and 14 ms. wide is simply supported in both directions. The slope at the springings will be  $\psi_0 = 37.5^\circ = 0.654$  radij is. The thickness of the shell is 8 cms. the sectional area of one edge beam including reinforcement may be put equal to  $A_b = 0.30 \text{ m}^2$ . The total dead and live load is  $p = 220 \text{ dead} + 65 \text{ live} = 285 \text{ kg/ m}^2$ .

Rise  $f = a ( 1 - \cos 37.5^\circ ) = 11.5 ( 1 - 0.793 ) = 2.37 \text{ ms}$   
 Distance of c.g. from top of arc  $\eta = 1.32 \text{ ms}$   
 Statical moment  $S$  and moment of inertia  $I$  about c.g. axis

$$S_{1-1} = 0.788 \text{ m}^3$$

$$I_{1-1} = 1.595 \text{ m}^4$$

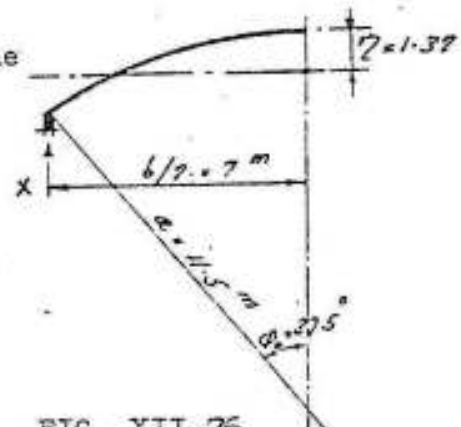


FIG. XII-76

Theoretical lever arm

$$y_{CT} = 1.595 / 0.788 = 2.02 \text{ ms.}$$

Actual lever arm

$$\text{act. } y_{CT} = h - \left( \frac{\eta}{5} + h' \right)$$

Assuming  $h = 2.5 \text{ ms}$

and  $h' = 10 \text{ cms}$ , we get

$$\text{actual } y_{CT} = 2.5 - \left( \frac{1.32}{5} + 0.1 \right) = 2.15 \text{ ms.}$$

Total load  $\bar{p} = 2 p a \varphi_0 = 2 \times 0.285 \times 11.5 \times 0.654 = 4.32 \text{ t/m shell}$

### Internal Forces

#### a) Shell Free at Edges

$$\text{max. } M = \bar{p} l^2 / 8 = 4.32 \times 30^2 / 8 = 485 \text{ m t}$$

$$\text{max. } Q = \bar{p} l / 2 = 4.32 \times 30 / 2 = 64.8 \text{ t}$$

$$\text{max. } \sigma_c = M \eta / I_{hl} = 485 \times 1.32 / 1.595 = 400 \text{ t/m}^2 = 40 \text{ kg/cm}^2$$

$$\text{For } a/t = 11.5/.08 = 144 \quad \text{max. allow. } \sigma_c = 38 \text{ kg/cm}^2$$

$$\text{max. } T = M/y_{CT} = 485 / 2.15 = 225 \text{ ton}$$

$$\text{max. } A_s = T/2 \sigma_s = 225 / 2 \times 1.8 = 62.5 \text{ cm}^2 \text{ high grade steel/edge}$$

$$\text{max. } N_{x\varphi} = Q/y_{CT} = 64.5 / 2.15 = 30 \text{ t/m on both sides}$$

$$\text{max. } T_{x\varphi} = \text{max. } N_{x\varphi} / 2 = 30/2 = 15 \text{ t/m on each side}$$

$$\text{max. } \tau = \text{max. } T_{x\varphi} / A = 15000/100 \times 8 = 18.7 \text{ kg/cm}^2$$

max. transverse bending moment at crown

$$M_0 = - 0.187 p a^2 \varphi_0^2 = - 0.187 \times 285 \times 11.5^2 \times 0.654^2 = - 3000 \text{ kgm}$$

Lundgren has computed the cross bending moment by the strip method and the maximum value at the crown was found to be equal to  $- 2028 \text{ kgm}$ . The difference is due to the existance of the edge beam. However, a shell 8 cms. thick cannot sustain such big moments by any means.

#### b) Shell Supported at Longitudinal Edges

The statically indeterminate vertical reaction can be estimated from the relation :

$$X = 0.239 p a \varphi_0 = 0.239 \times 285 \times 11.5 \times 0.654 = 510 \text{ kg/m}$$

The max. positive transverse bending moment can be estimated by

$$\text{max. } M_{\phi} + = 0.03 p a^2 \varphi_0^2 = 0.03 \times 285 \times 11.5^2 \times 0.654^2 = 480 \text{ kgm.}$$

If these values are determined by the strip method, they are found to be  $X = 436 \text{ kg/m}$  and  $\text{max. } M_{\phi} + = 321 \text{ kgm.}$

These differences show clearly the sensitivity of the calculations. But it is clear that the cross supports have reduced the transverse moments to less than 1/6 of  $M_0$  created in free shells that a thickness of 8 - 10 cms. is possible .

Accordingly, the total load transmitted in the longitudinal direction is given by :

$$\begin{aligned} \bar{p} &= 4320 - 2 X = 4320 - 2 \times 436 = 3442 \text{ kg/m}^2 && \text{and} \\ \text{max. } M &= \bar{p} l^2 / 8 = 3.442 \times 30^2 / 8 = 387 \text{ mt} \\ \text{max. } Q &= \bar{p} l / 2 = 3.442 \times 30 / 2 = 52 \text{ t} \\ \sigma_c \text{ max.} &= M \eta / I_{1-1} = 387 \times 1.32 / 1.595 = 320 \text{ t/m}^2 = 32 < 38 \text{ kg/cm}^2 \\ \text{max. } T &= M / Y_{CT} = 387 / 2.15 = 180 \text{ t i.e. 90 ton each side} \\ \text{max. } A_s &= T / 2\sigma_s = 180 / 2 \times 1.8 = 50 \text{ cm}^2 \text{ high grade steel/edge} \\ \text{max. } N_{x\phi} &= Q / Y_{CT} = 52 / 2.15 = 24.2 \text{ t/m} \\ \text{max. } T_{x\phi} &= \text{max } N_{x\phi} / 2 = 24.2 / 2 = 12.1 \text{ t/m on each side} \\ \text{max. } \tau &= \text{max } T_{x\phi} / A = 12100 / 100 \times 8 = 15.1 \text{ kg/cm}^2 \end{aligned}$$

#### B) Restrained Cross-Section

$$M_{\phi} = - \frac{p a^2}{\varphi_0^4} (0.0134 \varphi_0^6 - 0.1519 \varphi_0^4 \varphi^2 + 0.2173 \varphi_0^2 \varphi^4 - 0.0435 \varphi^6)$$

Numerically, the largest moment occurs at the springing, where

$$\text{min. } M_{\phi} = - 0.0353 p a^2 \varphi_0^2$$

The reactions from the longitudinal walls are :

$$X = 0.305 p a \varphi_0$$

i.e. 30% of the total load is transmitted to the transverse direction. The beam deflection gives a correction which is considerably greater than for a simply supported cross-section. First, the factor 10.7 in the formula of  $\delta_b / \delta_a$  must be replaced by 42.2 . Secondly, an increment to  $X$  of 10% will increase the transverse moment at the springing by 36 % .

## 5-Saw - Tooth Shells

Northlight cylindrical shell roofs as shown in figure XII - 77 provide ample and uniform daylighting and large column - free spaces for factory buildings located anywhere in the Northern Hemisphere. They are especially suitable for factories inside which precision operations are to be carried out. The distribution of the light in halls

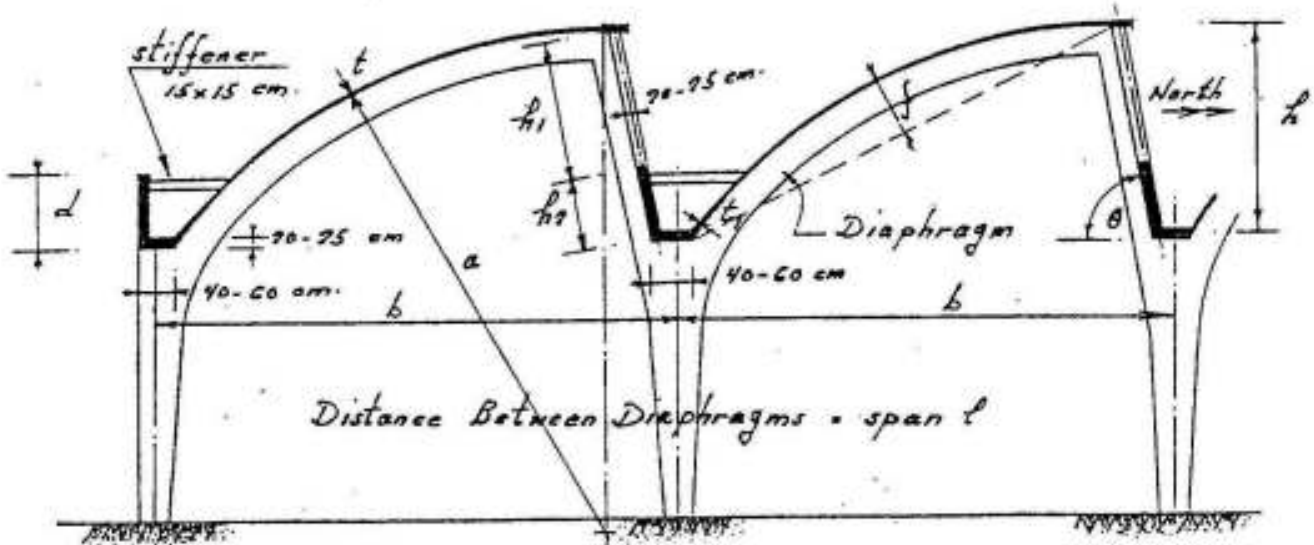


FIG. XII-77

covered by saw-tooth shells is much better than in halls covered by plain saw-tooth roofs as the luminance is uniform, shadow free and of much higher value.

The span of northlight shells, if not prestressed, is limited to about 30 ms. The more usual spans lie in the range of 12 to 25 ms. With prestressing, spans up to 40 ms are possible. Where large unobstructed column - free spaces are desired, the spacing of columns at right angles to the span may be made as large as 25 ms. by supporting a number of shells on a single diaphragm as shown in figure XII-78

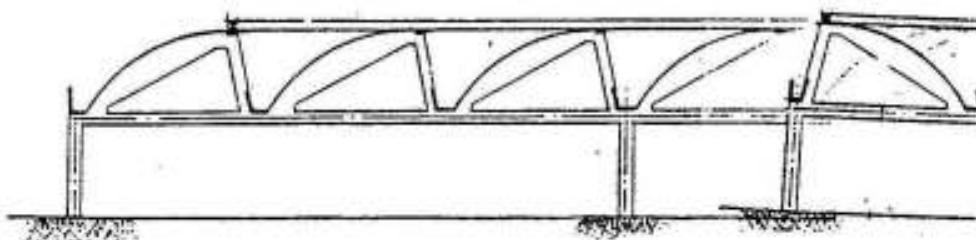


FIG. XII-78

The following guiding rules may be used for the proportioning of a saw-tooth shell :

The radius  $a$  is to be less than  $12 \text{ ms}$ . The width  $b$  to span  $l$  may be between  $1 : 2$  and  $1 : 4$ . The ratio of  $1 : 2$  leads to economic structures. The height  $h$  shall not be smaller than  $l/6$ ; the rise  $f$  of the circular segment shall as a rule be greater than  $l/18$ ; the height  $h_2$  of the gutter beam shall not generally be less than  $l/18$ . The angle  $\theta$  lies usually between  $60^\circ$  and  $90^\circ$ . The thickness of the shell  $t$  for cast in situ. roofs should not be less than  $8 \text{ cms}$ ,  $10 \text{ cms}$  for spans exceeding  $15 \text{ ms}$  and  $12 \text{ cms}$  for spans bigger than  $20 \text{ ms}$ . The thickness  $t_1$  at the springing is usually  $12 \text{ cms}$  ( for  $t = 8 \text{ cms}$  ) and  $20 \text{ cms}$  ( for  $t = 12 \text{ cms}$  ). If  $d$  or  $h_2$  are chosen smaller than  $l/15$ , stiffeners  $15 \times 15 \text{ cms}$  at the third points of the span are required to prevent lateral instability of the compression zone of the dege beam.

#### Determination of Internal Forces

The analysis of a saw-tooth shell is more time consuming than that of a symmetrical cylindrical shell because it is unsymmetrical. However, if the shell is long, i.e.,  $l/a \geq 3$ , the beam method, described in the previous article, with small modifications, gives satisfactory results. Instead of using the  $M_z/I$  formula, we have now to use the formulas relating to unsymmetrical bending because the shell beam cross-section is asymmetric. Otherwise the procedure remains the same as before. This method has the advantage that it avoids the use of higher mathematics, but it is exactly equivalent to the Lundgren beam method.

We give in the following the main steps required for determining the internal forces : ( Fig. XII-79 )

#### 1) Determination of the Properties of the Section

The total area of the section of the shell  $A$  is equal to the area of the edge beams, in which the reinforcements may be replaced by an equivalent concrete area, plus the area of the arc equal to  $2 a \varphi_0 t$ .

In order to determine the center of gravity, the statical moment and the moment of inertia of the section, choose an origin  $O$ , the mid-point of the arc; the axes  $Oz$  and  $Oy$  are chosen along the normal and tangent to the shell arc at  $\bar{O}$ .

---

\* Ramaswamy. " Design and Construction of concrete shell roofs " .  
Published by Mc Graw-Hill Book Company. New York and London.

Divide the shell to a convenient number of strips of length  $\Delta s_1, \Delta s_2, \Delta s_3 \dots$  etc, determine the area of each strip  $\Delta A$  and the co-ordinates  $z$  and  $y$  of its center of gravity. The co-ordinates  $z_G$  and  $y_G$  of the centroid  $G$  can be calculated from the relations

$$z_G = \frac{\sum z \Delta A}{A} \quad \text{and} \quad y_G = \frac{\sum y \Delta A}{A}$$

When the position of the centroid is thus determined, the moments and product of inertia about the axes  $Gz_1$  and  $Gy_1$ , passing through the centroid and parallel to  $\bar{O}z$  and  $\bar{O}y$  respectively, are next calculated. That is :

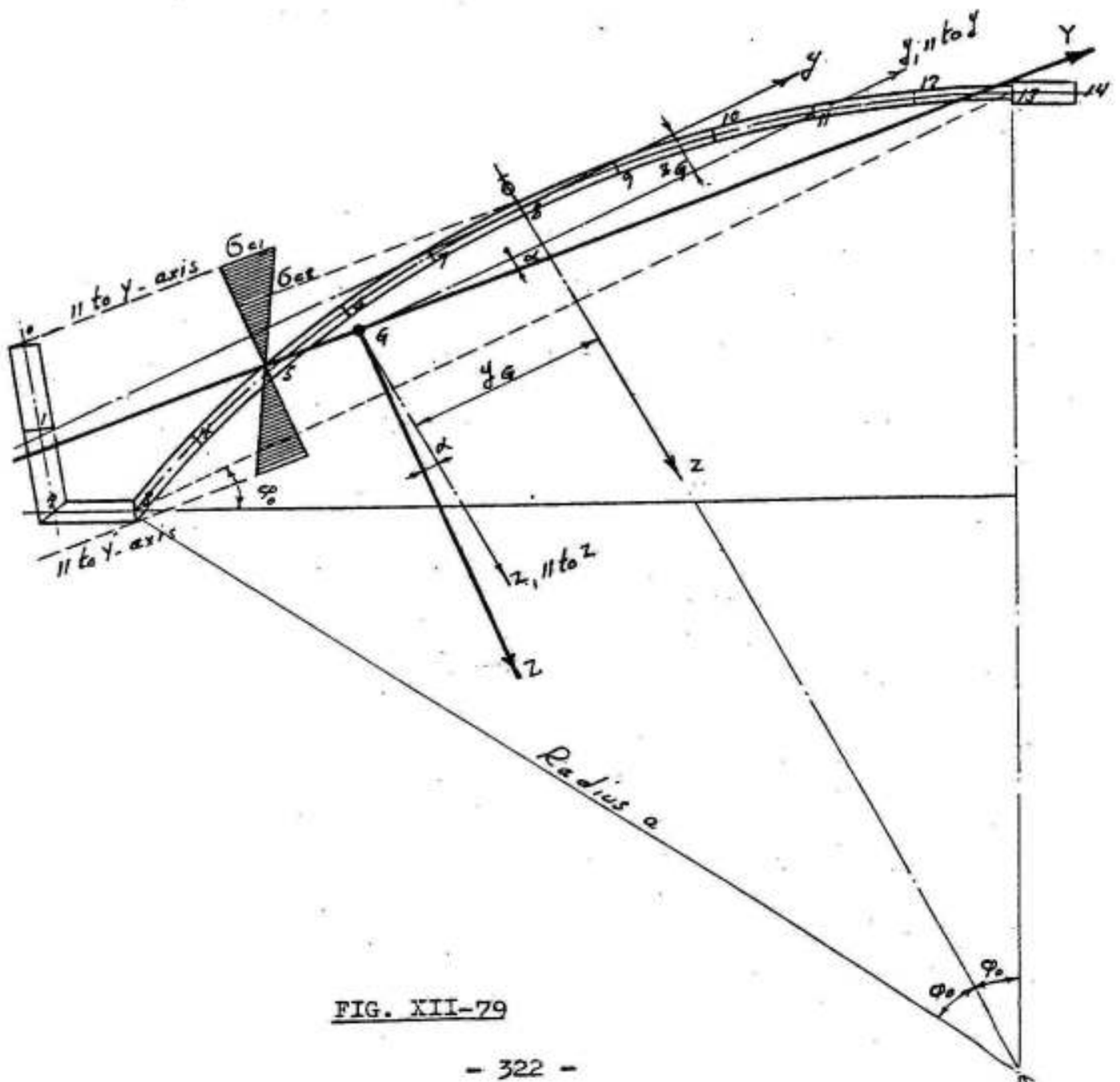


FIG. XII-79



$$I_{z_1 z_1} = \sum \Delta A y^2 - A y_G^2$$

$$I_{y_1 y_1} = \sum \Delta A z^2 - A z_G^2$$

$$I_{y_1 z_1} = \sum \Delta A y z - A y_G z_G$$

From these values, the orientation of the principal axes of inertia G Z and G Y can be fixed from the known relation :

$$\tan 2\alpha = 2 I_{y_1 z_1} / ( I_{z_1 z_1} - I_{y_1 y_1} )$$

( The angle  $\alpha$  is to be taken in the clockwise direction from G  $z_1$  )

The principal moments of inertia are therefore given by :

$$I_{ZZ} = I_{z_1 z_1} \cos^2 \alpha + I_{y_1 y_1} \sin^2 \alpha - I_{y_1 z_1} \sin 2\alpha$$

$$I_{YY} = I_{y_1 y_1} \cos^2 \alpha + I_{z_1 z_1} \sin^2 \alpha + I_{y_1 z_1} \sin 2\alpha$$

## 2) Bending Moments, Longitudinal Stresses $\sigma_x$ and Longitudinal Forces $N_x$

The co-ordinates of the points with reference to the principal axes G Z and G Y are next calculated using the formulas.

$$Z = ( z - z_G ) \cos \alpha - ( y + y_G ) \sin \alpha$$

$$Y = ( z - z_G ) \sin \alpha + ( y + y_G ) \cos \alpha$$

The load  $p$  is resolved into its components  $p_Z$  and  $p_Y$  along the two principal axes.  $p_Z$  causes bending about Y Y axis and  $p_Y$  about the Z Z axis. The moments caused by  $p_Z$  and  $p_Y$  are denoted by  $M_Z$  and  $M_Y$ , respectively.

The longitudinal stress  $\sigma_x = N_x / t$  at any point in the shell is then given by the formula

$$\sigma_x = N_x / t = \frac{M_Z}{I_{YY}} \cdot Z + \frac{M_Y}{I_{ZZ}} \cdot Y$$

where

$$M_Z = \frac{p_Z l^2}{8} \quad \text{and} \quad M_Y = \frac{p_Y l^2}{8}$$

in which

$$p_Z = p \cos (\varphi_0 - \alpha) \quad \text{and} \quad p_Y = p \sin (\varphi_0 - \alpha)$$

$p$  being the vertical load per square meter surface.

Assuming  $M_Z / I_{YY} = (F_Z)$  and  $M_Y / I_{ZZ} = (F_Y)$ , we can write:

$$\sigma_x = N_x/t = (F_Z) Z + (F_Y) Y$$

This expression gives the values of  $\sigma_x$  and  $N_x$  at all points of the shell; they are equal to zero at the neutral axis. Hence, the equation of the neutral axis is given by:

$$0 = (F_Z) Z + (F_Y) Y$$

Assuming further  $(F_Z) / (F_Y) = (F)$

the equation of the neutral axis can be written in the form:

$$\underline{(F) \cdot Z + Y = 0}$$

The longitudinal force  $N_x$  on each elemental area is determined by multiplying the stress  $\sigma_x$  at the center of the element by its area  $\Delta A$ .

In order to have sufficient safety against buckling, the maximum normal stress in the shell  $\sigma_{c2}$  must be smaller than  $\sigma_c$  max. shown in figure XII-51, while the stiffeners shown in figure XII-77 prevent the lateral buckling of the edge beam.

The correctness of the statical calculation can be verified if the following two conditions are satisfied:

a) The sum of the normal forces acting on the section = 0, or

$$\sum N_x \Delta s = 0$$

b) The internal resisting moment is equal to the bending moment due to loading, i.e.,

$$\sum N_x \Delta s y = M$$

The check is made at the midspan section, and the moments are taken about the  $Oy$ -axis which is equal to  $p \cos \varphi_0 \cdot l^2 / 8$ .

### 3) Shear Stresses

In case of saw-tooth shells, the direction of the shearing force  $Q$  does not coincide with the principal axes  $Z$  and  $Y$  of the section, hence

$$\tau = \frac{Q_Z S_Y}{I_Y t} + \frac{Q_Y S_Z}{I_Z t}$$

in which

$$Q_Z = Q \cos (\varphi_0 - \alpha)$$

$$Q_Y = Q \sin (\varphi_0 - \alpha)$$

are the components of the shearing force along the principal Z and Y axes.

However, Ramaswamy in his previously mentioned text book on shell structures computes the shear stress using the principle that in a beam subjected to uniform loading, the difference between the specific shears at any two points is equal to the longitudinal force between those two points divided by the bending moment factor, which is  $l^2 / 8$  for a simply supported beam. The proof of this statement is as follows :

It has been shown that

$$\int N_x ds = M S / I_{1-1} \qquad N_{x\varphi} = Q S / I_{1-1}$$

and for the section at the diaphragm, we have

$$\max. N_{x\varphi} = Q_{\max} S / I_{1-1}$$

So that

$$N_{x\varphi} / Q = \max. N_{x\varphi} / Q_{\max} = S / I_{1-1}$$

But for a simple beam subject to uniformly distributed load  $\bar{p}$ , we have :

$$Q_{\max} = \bar{p} l / 2 \qquad \text{so that}$$

$$\frac{N_{x\varphi}}{Q} = \max. N_{x\varphi} / \bar{p} l / 2 = S / I_{1-1}$$

at middle section, we have further  $M = \bar{p} l^2 / 8$  so that

$$\int N_x ds = \bar{p} \frac{l^2}{8} \cdot \frac{S}{I_{1-1}} = \bar{p} \frac{l^2}{8} \cdot \frac{\max N_{x\varphi}}{\bar{p} l / 2} = \frac{l^2}{8} \cdot \frac{\max N_{x\varphi}}{l / 2}$$

It has also been stated before that in a simple beam subject to uniform loads, the relation between the specific shear at the middle and the max. shear at the diaphragm is given by :

$$\frac{\partial N_{x\varphi}}{\partial x} = \max. N_{x\varphi} / l / 2, \qquad \text{so that}$$

$$\frac{\int N_x ds}{l^2 / 8} = \frac{\partial N_{x\varphi}}{\partial x} \quad \text{hence}$$

The difference between specific shears at points A and B = longit. force  $N_x$  on AB / ( $l^2/8$ ). The specific shears  $\partial N_{x\varphi} / \partial x$  at the c.g. of the strips are obtained by adding the differences of the specific shears already obtained. The shear resultant  $N_{x\varphi}$  is equal to the specific shear multiplied by  $l/2$ .

#### 4) Arch Calculation

In order to determine the cross bending moments  $M_\varphi$  and axial forces  $N_\varphi$ , a slice of the shell, of unit length, is regarded as an arch subjected to the action of the external loads  $p$  and the specific shears  $\partial N_{x\varphi} / \partial x$ . Calculate first their components  $q_z$  and  $q_y$  in the directions of the axes  $\bar{O}_z$  and  $\bar{O}_y$  according to the relations :

$$q_z = p_z + \frac{\partial N_{x\varphi}}{\partial x} \Delta z,$$

$$q_y = p_y + \frac{\partial N_{x\varphi}}{\partial x} \Delta y$$

Next, add these loads starting from point 0 and ending with point 14 to get  $N_z$  and  $N_y$  according to the relations :

$$N_z = \sum q_z \quad \text{and} \quad N_y = \sum q_y$$

Now starting from point 0 (and assuming that the shell is not connected to the adjacent shells), the increments of the bending moments from point to point of the cross-section are calculated as :

$$\Delta M_{\varphi 0} = N_y \Delta z - N_z \Delta y$$

in which  $\Delta z$  and  $\Delta y$  are the projected lengths of the elements. The summation of these increments gives the transverse bending moments  $M_{\varphi 0}$  at all the points of the cross-section.

This procedure does not include the force in the window posts and hence the bending moments at point 14 will not be zero. The cross bending moments can however be corrected due to this force in the following manner :

The correcting moment  $M_{\varphi 1}$  must satisfy the following conditions

- 1)  $M_{\varphi 1} = 0$  at points 0 and 14.
- 2)  $M_{\varphi 1}$  at point 8 ( $y = 0, z = 0$ ) = component of force in window

posts perpendicular to the line joining 8 and 14 multiplied by the perpendicular distance between the two points.

$M_{\phi_1}$  is however a linear function of  $y$  and  $z$  and may be represented as

$$M_{\phi_1} = A z + B y + C$$

The constants  $A$ ,  $B$  and  $C$  can be determined from the three conditions given under 1 and 2.

The final transverse moments are thus given by:

$$M_{\phi} = M_{\phi_0} + M_1$$

According to the above mentioned principles, Ramaswamy, in his text book on shell structures has given the numerical analysis of a saw-tooth shell as that shown in Fig. XII-79. The internal forces in the shell were as shown in Fig. XII-80.

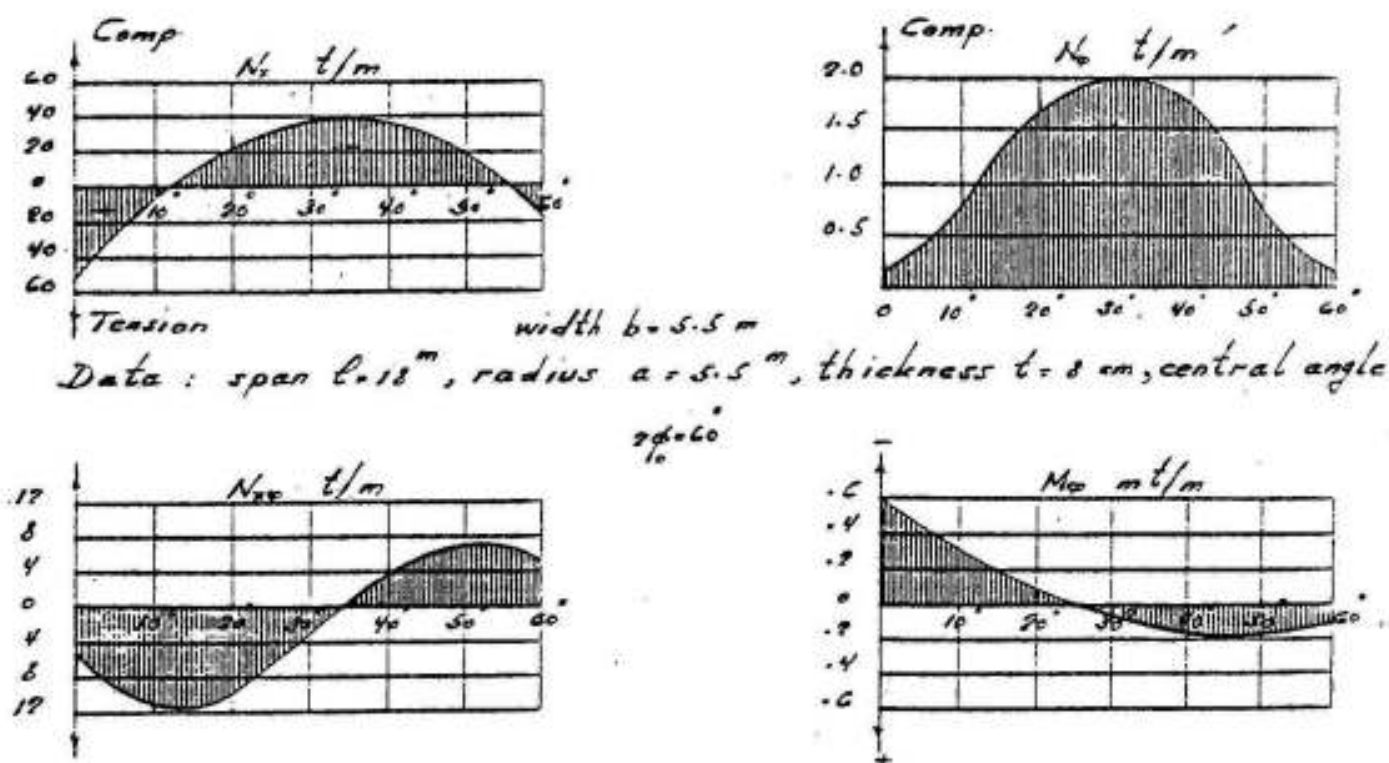
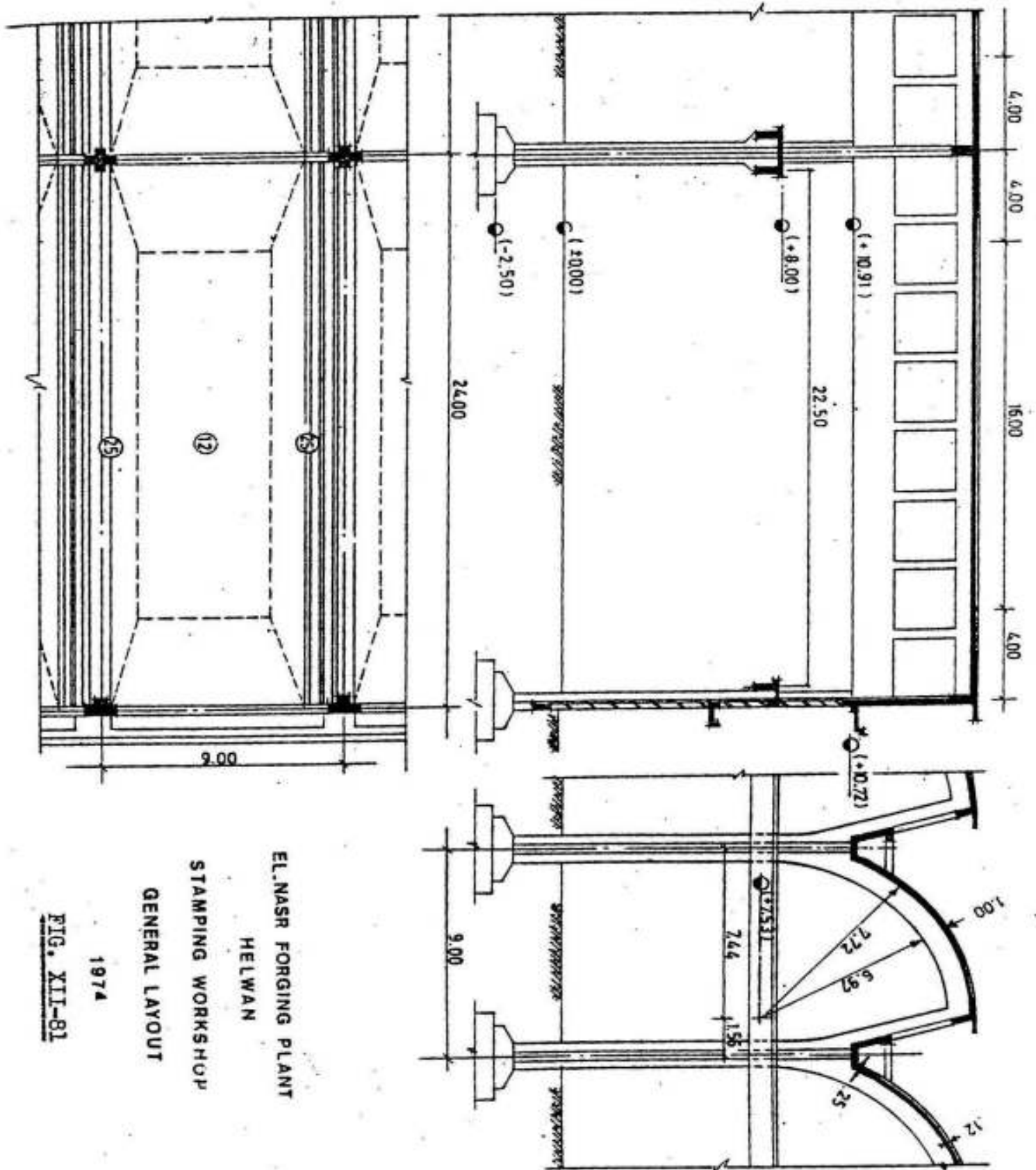


Fig. XII-80

Fig. XII-81 shows the general layout and main dimensions of a part of a saw-tooth shell covering one of the main halls of "El Nasr Forging Plant" at Helwan 48 ms wide and 144 ms long. The north is parallel to the longer side of the hall and the saw-tooth form of the shell is chosen such that the windows are facing the north. The distance between the windows (breadth  $b$  of saw-tooth shell) is 9 ms. The bigger length of the hall, 144 ms, is divided into 5 blocks: one block



EL. NASR FORGING PLANT  
 HELWAN  
 STAMPING WORKSHOP  
 GENERAL LAYOUT

1974

FIG. XII-81

EL. NASR FORGING PLANT  
 HELWAN  
 STAMPING WORKSHOP  
 DETAILS OF SHELL  
 1974

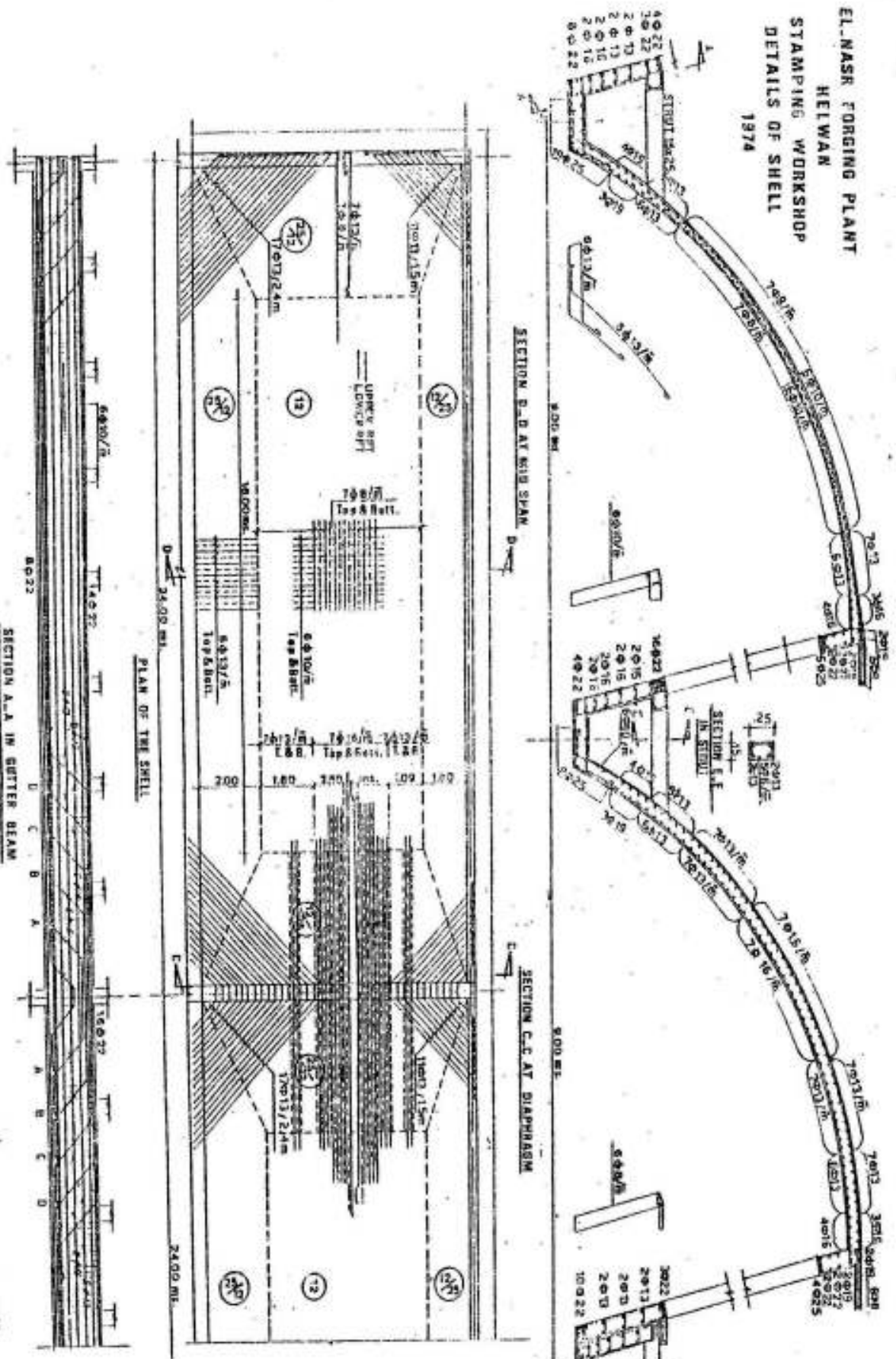
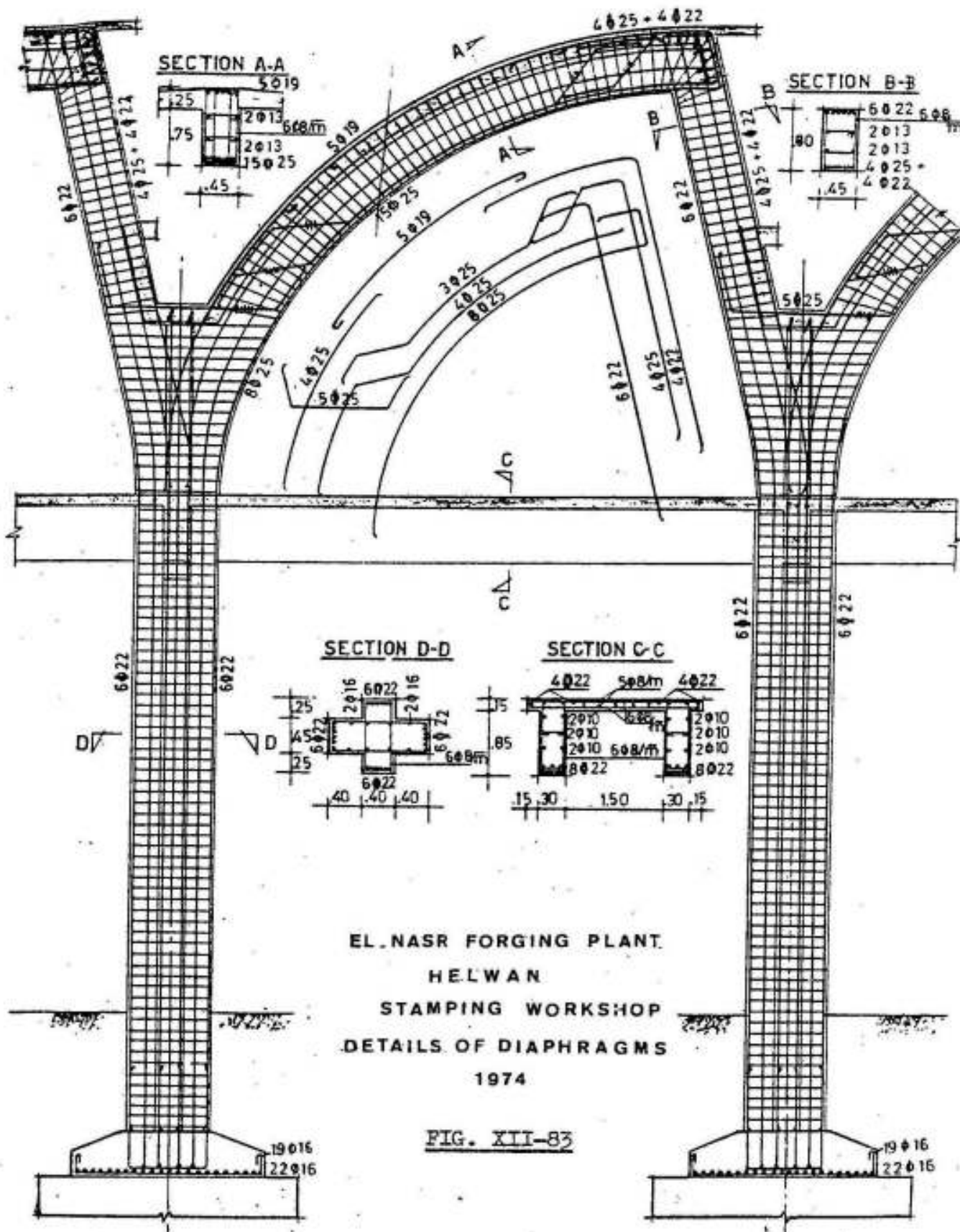


Fig. XII-82





been computed by the membrane theory, it is therefore necessary, afterwards, to consider a case where the edge carries the loads  $-N_\phi$  and  $-N_{\phi x}$ .

The load  $-N_{\phi x}$  does not give any essential perturbation (small). More important than the edge load from  $N_{\phi x}$  is the load originating from  $N_\phi = p r$ . For vertical loads  $p$  this force is  $N_\phi = -p r \cos \phi_0$  at the edge. This means that the shell is under the influence of a tangential line load at the edge of  $P = p r \cos \phi_0$ . (Fig. XII-84). This load is transferred to the traverses by the lowermost part of the shell which acts as a slightly curved deep beam with span  $l$  and width  $t$ .

Since the membrane shear forces are small, the stress distribution in a short shell may be imagined in such a way that the shell carries the load as a vault, and at the springings the normal forces in the vault are taken by the edge zones, which transfer their load to the traverses.

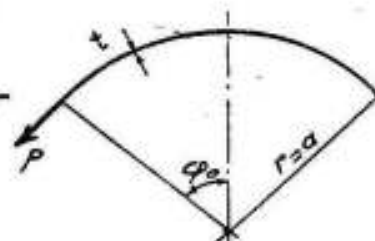


Fig. XII-84

According to the theory of deep beams<sup>‡</sup>, we

have:

For a simple deep beam of span  $l$  subject to a uniform load  $P$

$$\text{max. } T = 0.2 P l \quad (1)$$

Assuming  $y_{CT} = 0.5 l$ , we get for continuous beams:

At middle of outer spans and over intermediate supports

$$\text{max. } T = 0.2 P l \quad (2)$$

and at middle of inner spans

$$\text{max. } T = 0.13 P l \quad (3)$$

where max.  $T$  is the tension in the critical sections of the deep beam.

#### Central shear

Since the tensile force in the deep beam varies approx. parabolically between the traverses, the maximum central shear at the traverses may be set equal to:

$$\text{max. } N_x = 4 T/l \quad (4)$$

#### Transverse bending moments

According to Lundgren, the transverse bending moments may be taken

<sup>‡</sup> Refer to "Theory and Design of Reinforced Concrete Tanks" by M. Hilal. Published by J. Marcou & Co. Cairo.

as a function of the two dimensionless parameters  $\rho$  and  $\chi$  which may be found from the relations:

$$\rho^2 = 5.85 \frac{a}{l} \sqrt{\frac{a}{t}} \quad (5) \quad \text{and} \quad \chi = 1.688 \cdot \frac{\sqrt{t a}}{l} \quad (6)$$

For the transverse bending moment, the shell is assumed simply supported over the traverses because, so far, the analytical method is not practicable in other cases. This is a very important limitation since, in general, short shells are actually continuous over several spans.

For a shell simply supported at the springings, the transverse bending moments are negative, with a maximum value of

$$\max. M_{\varphi} = - \frac{1.4}{(1 + 3\chi)^2} \cdot \frac{P a}{\rho^2} \quad (7)$$

The corresponding normal force is given by:

$$N_{\varphi} = - \frac{0.84}{(1 + 1.4\chi)^2} \cdot P \quad (8)$$

It has to be noted that a free edge at the springing is seldom encountered in practice, but even if the edge is strengthened by a light edge beam, the formulae 7 and 8 for  $M_{\varphi}$  and  $N_{\varphi}$  may very well be applied.

If the support can take a restraining moment, it is reasonable to base the design on the following case:

For a shell fixed at the springings, the maximum negative fixing moment at the edge is given by:

$$\max. M_{\varphi} = - 0.50 (1 + 0.15\chi) \frac{P a}{\rho^2} \quad (9)$$

The corresponding normal force is P.

#### Example

Fig. XII-85 represents the cross section of a circular short shell with a radius  $a = 27.4$  ms and a width  $b = 35$  ms. The rise  $f = 6.32$  ms and the corresponding angle at the springing  $\varphi_0 = 39.7^\circ = 0.693$  radians. The length of the shell  $l = 10$  ms and its thickness  $t = 10$  cms.

Assuming that every second span is covered by a skylight, the shell may be considered as simply supported at

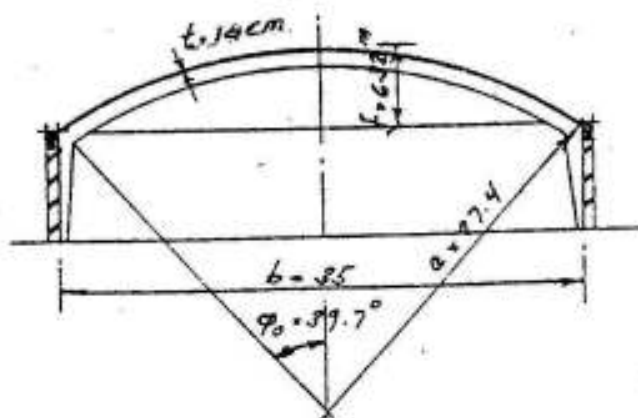


Fig. XII-85

at the traverses. At the springings, the shell is provided with edge beams which rest on vertical columns or walls. An investigation has shown that if the edge beams are of the order say 25 x 50 cms, their torsional rigidity is sufficient to secure complete clamping of the shell. Therefore the condition for applying formula 9 is fairly satisfied.

The internal forces in the shell be calculated for a total vertical load equal to  $p$ , where  $p = 350 \text{ kg/m}^2$  surface.

The shell is first calculated by the membrane theory. Hence:

Maximum transverse comp. at crown:  $N_{\phi_0} = -p a = -350 \times 27.4 = -9590 \text{ kg/m}$

Corresponding conc. comp. stress:  $\sigma_c = \frac{N}{A_c} = \frac{9590}{100 \times 10} = 9.59 \text{ kg/cm}^2$

Maximum allowed buckling stress:  $\sigma_c = 65 / (1 + \frac{2740}{200 \times 10}) = 27.4 \text{ kg/cm}^2$

Max. shear at the springing:  $N_{x\phi} = p l \sin \phi_0 = 350 \times 10 \times 0.639 = 2236 \text{ kg/m}$

Corresponding shear stress  $\tau = N_{x\phi} / A = 2236 / 100 \times 10 = 2.24 \text{ kg/cm}^2$

Membrane tensile force at middle of span ( $x = 0$ ):

$$T_0 = \int_{-l/2}^{l/2} N_{x\phi} dx = \int_0^{l/2} p x \sin \phi_0 dx = p \left( \frac{l^2}{4} - x^2 \right) \sin \phi_0 \quad \text{or}$$

$$T_0 = 350 \times \frac{10^2}{4} \times 0.639 = 5590 \text{ kgs}$$

Perturbational load at edge  $P = -N_{\phi_0} = p a \cos \phi_0$  but

$$\cos \phi_0 = \frac{a - f}{a} = \frac{27.4 - 6.32}{27.4} = 0.769 \quad \text{therefore}$$

$$P = 350 \times 27.4 \times 0.769 = 7374 \text{ kg/m!}$$

Tension due to  $P$  (equ. 2)  $T_p = 0.2 P l = 0.2 \times 7374 \times 10 = 14740 \text{ kgs}$

Total tensile force  $T = T_0 + T_p = 5590 + 14740 = 20330 \text{ kgs}$

Required reinforcement  $A_s = \frac{T}{\sigma_s} = \frac{20330}{1400} = 14.5 \text{ cm}^2$  chosen 5  $\phi$  19 mm

Max. shear at traverses according to equation 4 is given by:

$$\text{max. } N_{x\phi} = \frac{4}{l} T = \frac{4}{10} \times 20.33 = 8.13 \text{ t/m}$$

If this shear is to be resisted by transverse reinforcements (stirrups)

exclusively an area of  $A_s = \frac{6 \cdot 13}{1.5} = 6.25 \text{ cm}^2/\text{m}$  i.e.  $9 \text{ } \phi 10 \text{ mm/m}$  is sufficient. However, a part of the shear may be resisted by bent up bars from the longitudinal reinforcement. The design corresponds to that of an ordinary reinforced concrete deep beam with an arm of internal resistance  $\gamma_{CT} = 0.5 \text{ l} = 5.0 \text{ ms}$ .

The maximum transverse bending moment at the springings is, according to equ. 9, given by:

$$\text{max. } M_{\phi} = - 0.50 (1 + 0.15 \chi) \frac{P a}{\rho^2}$$

in which

$$\chi = \frac{1.688 \sqrt{a t}}{l} = \frac{1.688 \sqrt{27.4 \times 0.1}}{10} = 0.28$$

and

$$\rho^2 = 5.85 \frac{a}{l} \sqrt{\frac{a}{t}} = 5.85 \times \frac{27.4}{10} \sqrt{\frac{27.4}{0.10}} = 265 \quad \text{so that}$$

$$\text{max. } M_{\phi} = - 0.5 (1 + 0.15 \times 0.28) \times \frac{7374 \times 27.4}{265} = - 400 \text{ kgm}$$

The corresponding normal force is  $N_{\phi} = P = 7374 \text{ kgs}$  (compression).

The section of the shell at the springing is to be designed for these internal forces.

It is however advisable to increase the thickness of the shell gradually to 14 cms at the springing on a length  $x$  where

$$x = 0.76 \sqrt{a t} = 0.76 \sqrt{27.4 \times 0.10} = 1.25 \text{ ms}$$

A thickness of 14 cms and top reinforcement of minimum  $6 \text{ } \phi 8 \text{ mm/m}$  at the springing are supposed to be ample for the acting forces.

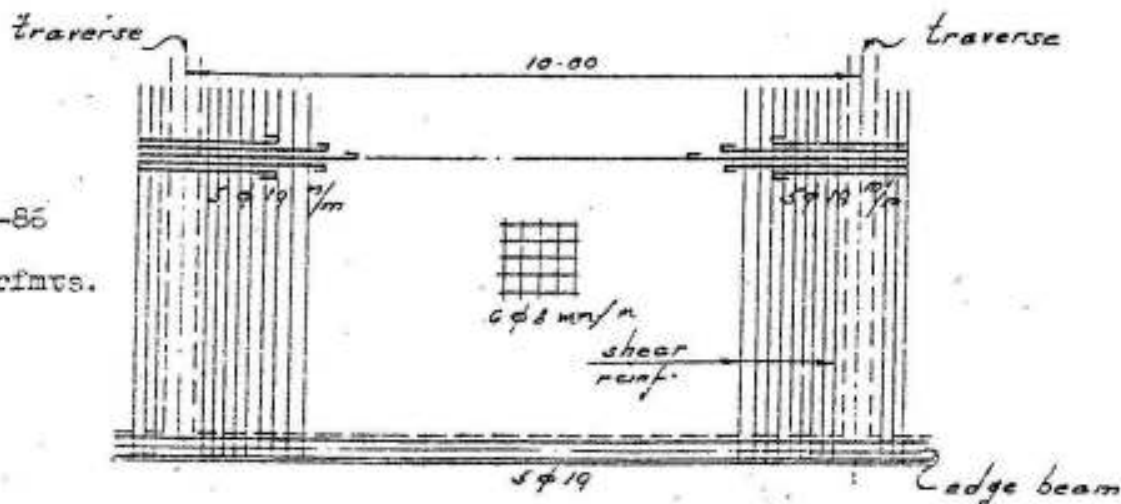
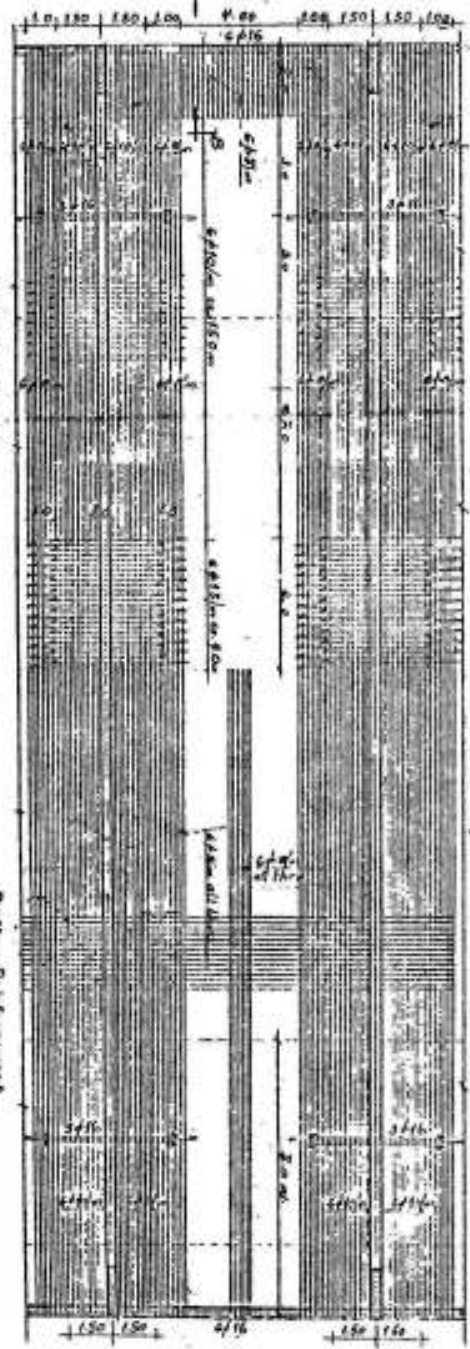
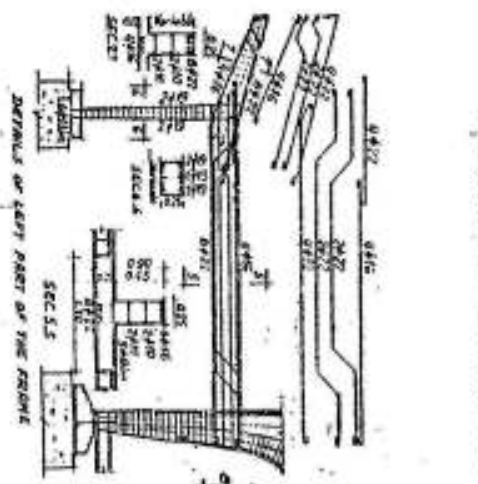
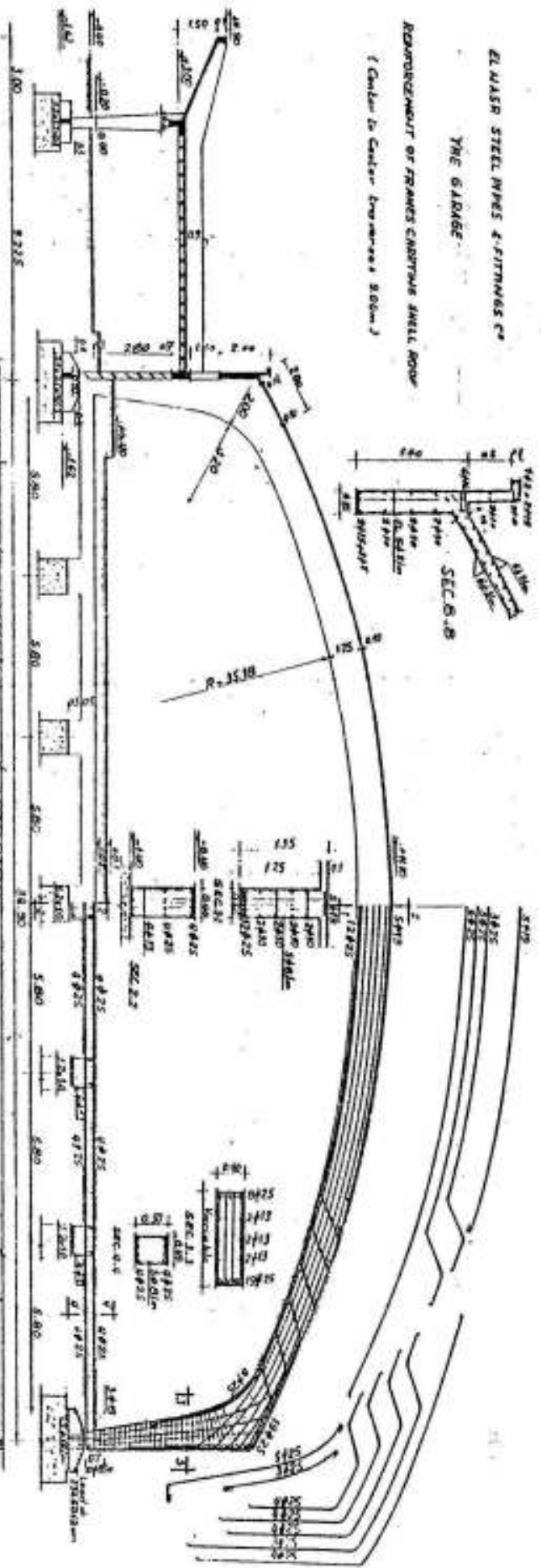


Fig. XII-86  
Details of rfmvs.

ELIASH STEEL PIPES & FITTINGS CO.  
THE GARAGE

REINFORCEMENT OF FRAMES CONCRETE SHELL ROOF  
(Center to Center Trusses 20m.)



PLAN OF SHORT SHELL

Fig. XII-87 shows the general layout, main dimensions and details of reinforcements of the main supporting elements of a part of the garage of "El Nasr Steel Pipes and Fittings Co." at Helwan. The main garage covers an area  $38 \times 90$  ms without intermediate supports. Attached to it, there is a shed for cars having a span of 9 ms and a cantilever arm of 3 ms. In the longitudinal direction, the hall is divided into three blocks:  $3 \times 9 \text{ m} + 4 \times 9 \text{ m} + 3 \times 9 \text{ m} = 90 \text{ ms}$ .

As a cover for the garage, a short shell 10 cms thick, increased to 14 cms over a length of 2 ms at the springing, is used. Its radius is 36.5 ms, its width is 38 ms and is supported in the longitudinal direction on arched frame traverses with ties every 9 ms. The traverses are 0.4 ms wide and 1.35 ms deep, increased to 2 ms at the corners and decreased to 0.7 ms at the lower hinges. The side shed is covered by a 25 cms two-way hollow block slab  $9 \times 9$  ms. It is supported on longitudinal beams and inverted cross beams, 9 ms span with 3 ms overhanging cantilevers.

The shell is reinforced at its bottom surface by a mesh  $6 \text{ } \phi \text{ } 8 \text{ mm/m}$  except for the first 8 ms from the springing where the circular reinforcement only, is increased to  $6 \text{ } \phi \text{ } 10 \text{ mm/m}$  in a distance of 1.5 ms at each side of the traverses. Top reinforcement for the shell is needed over the traverses and normal to them for a distance of 2.5 ms at each side. It is also needed at the straight edges and normal to them, for a distance of 2 ms from the springing. The top longit. reinforcement over the traverses is  $6 \text{ } \phi \text{ } 13 \text{ mm/m}$  for the middle 8 ms and then reduced to  $6 \text{ } \phi \text{ } 10 \text{ mm/m}$  on both sides. The top circular reinforcement is  $6 \text{ } \phi \text{ } 8 \text{ mm/m}$  except for the first 8 ms from the springing where it is increased to  $6 \text{ } \phi \text{ } 10 \text{ mm/m}$  in a distance of 1.5 ms at each side of the traverses. The top reinforcement at the springing is one mesh  $6 \text{ } \phi \text{ } 8 \text{ mm/m}$  in the space between the top reinforcements resisting the connecting moments at the traverses. The details of the intermediate traverses and their ties are also shown in Fig. XII-87.

XII- 5 MEMBRANE THEORY OF SHELLS OF GENERAL SHAPE

1- Basic Idea

The purpose of the following is to develop a a general membrane theory for shells of arbitrary shape and then to show its application to some simple cases of shells of double curvature and especially those which do not fall in one of the special groups considered before.

The basic idea of the solution, developed by Pucher, is to examine the entire system of external and internal forces acting on the shell in the plan projection. It will be shown that the determination of the internal forces in many cases can be done by a surprisingly simple way.

We choose for this purpose an orthogonal co-ordinate system  $x, y, z$  in which the  $z$ -axis is vertical. If we cut the shell surface under consideration by two pairs of vertical planes  $x, x+dx$  and  $y, y+dy$  they meet the shell surface in curves which in general are not normal to each other (Fig. XII-88). The elemental rectangular area in plan projection  $dA = dx dy$  will correspond to a rhombus on the shell surface of area  $\gamma dA$ ; in which

$$\gamma = \sqrt{1 + (\partial z/\partial x)^2 + (\partial z/\partial y)^2} \quad (1)$$

This equation can naturally be used only if  $\partial z/\partial x \neq \infty$  &  $\partial z/\partial y \neq \infty$

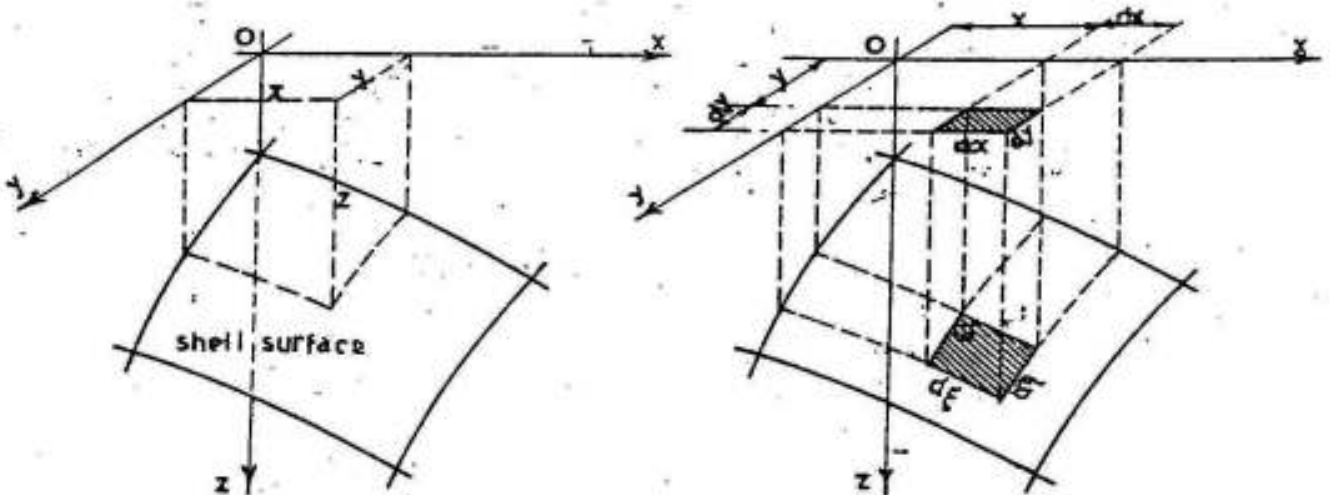


FIG. XII-88

assuming that the components of the load on the shell surface are  $P_x$ ,  $P_y$ ,  $P_z$ , and that their corresponding values on the horizontal projection are  $\epsilon_x$ ,  $\epsilon_y$ ,  $\epsilon_z$ , then we have :

$$\frac{\epsilon_x}{\lambda} = P_x \quad \frac{\epsilon_y}{\lambda} = P_y \quad \frac{\epsilon_z}{\lambda} = P_z \quad (2)$$

It will be assumed further that the real normal and shearing forces on the sides of the elemental area of the shell are  $N_x$ ,  $N_{xy}$ ,  $N_{yx}$ ,  $N_y$  and the corresponding reduced values on the plan projection  $n_x$ ,  $n_{xy}$ ,  $n_{yx}$ ,  $n_y$  as shown in figure XII-89.

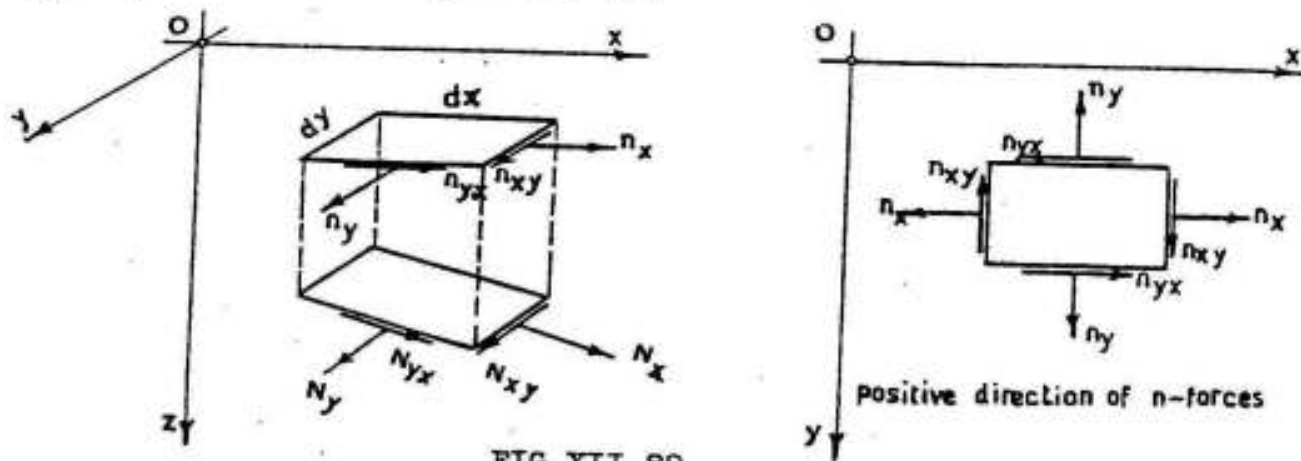


FIG. XII-89

The relation between the real and reduced forces can be expressed in the following manner : ( Fig XII-90 )

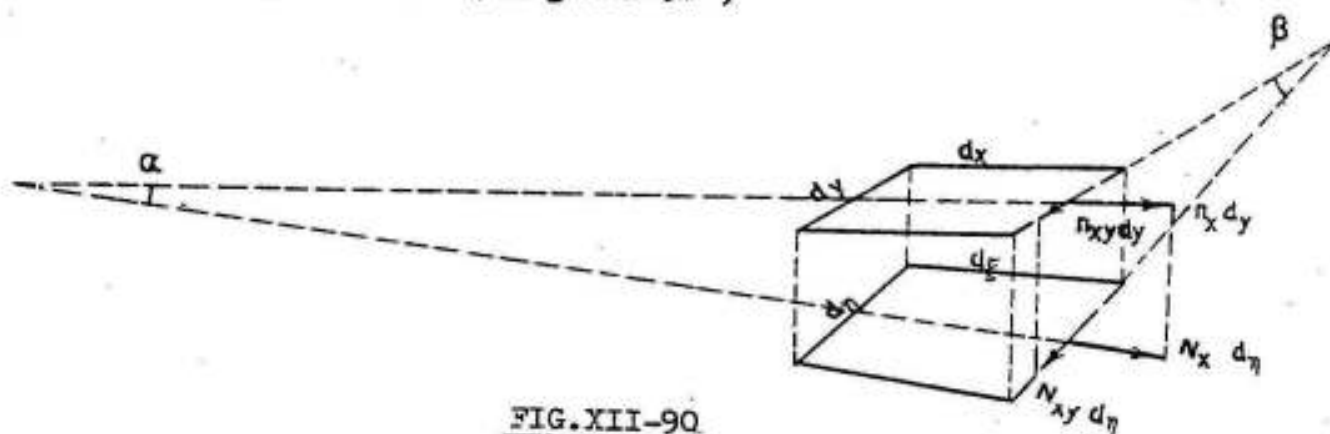


FIG. XII-90

$$n_x dy = N_x d\eta \cdot \cos \alpha,$$

$$n_{xy} dy = N_{xy} d\eta \cdot \cos \beta.$$

so that



$$N_x = \frac{n_x}{\cos \alpha} \frac{dy}{dn} = \frac{n_x}{\cos \alpha} \cos \beta,$$

$$N_{xy} = \frac{n_{xy}}{\cos \beta} \frac{dy}{dn} = \frac{n_{xy}}{\cos \beta} \cos \beta = n_{xy}$$

Similar equations can be extracted for the relations between  $n_y$ ,  $n_{yx}$  and  $N_y$ ,  $N_{yx}$ . Hence

$$\left. \begin{aligned} \frac{N_x}{n_x} &= \frac{\cos \beta}{\cos \alpha}, & \frac{N_{xy}}{n_{xy}} &= 1 \\ \frac{N_y}{n_y} &= \frac{\cos \alpha}{\cos \beta}, & \frac{N_{yx}}{n_{yx}} &= 1 \\ \text{but } N_{xy} &= N_{yx} \text{ then } & \frac{n_{xy}}{n_{yx}} &= 1 \end{aligned} \right\} (3)$$

This means that the reduced shearing forces are also equal. The values of  $\cos \alpha$  and  $\cos \beta$  are given by the following relations :

$$\tan \alpha = \frac{\partial z}{\partial x} \quad \text{and} \quad \tan \beta = \frac{\partial z}{\partial y} \quad (4)$$

Hence,  $\alpha$  and  $\beta$  and the cos-values required for calculating  $N_x$  and  $N_y$  can be easily determined.

These equations can naturally only be used if

$$\partial z / \partial x \neq \infty, \quad \partial z / \partial y \neq \infty$$

The previous relations give the reduced internal forces in a point in the two normal directions  $x$  and  $y$ . The forces acting at the same point in any two other normal directions  $u$  and  $v$  making an angle  $\alpha$  with  $x$  and  $y$  can be determined in the same way known in plane structures, thus: ( Fig XII-91)

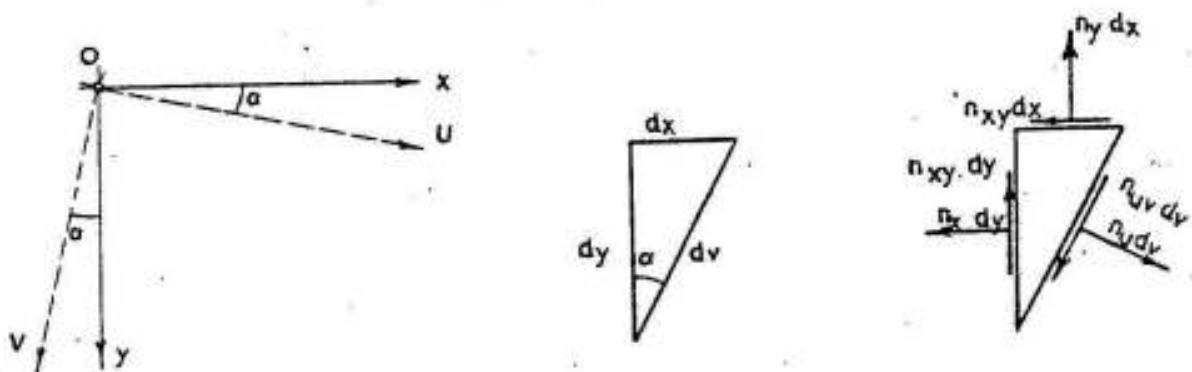


FIG. XII-91

$$\begin{aligned}
 n_u &= n_x \cos^2 \alpha + n_y \sin^2 \alpha + 2 n_{xy} \cos \alpha \sin \alpha \\
 n_v &= n_x \sin^2 \alpha + n_y \cos^2 \alpha - 2 n_{xy} \cos \alpha \sin \alpha \\
 n_{uv} &= n_{vu} = (n_y - n_x) \cos \alpha \sin \alpha + n_{xy} (\cos^2 \alpha - \sin^2 \alpha)
 \end{aligned}$$

The magnitude and directions of the principal reduced ( or actual ) forces can therefore be calculated by the known relations :

$$n_1 = \frac{n_x + n_y}{2} \pm \sqrt{\left(\frac{n_x - n_y}{2}\right)^2 + n_{xy}^2} \quad (5)$$

and

$$\tan 2\alpha = \frac{2 n_{xy}}{n_x - n_y} \quad (6)$$

## 2- Conditions of Equilibrium

We give in the following the conditions of equilibrium of the reduced forces  $n_x$ ,  $n_y$  and  $n_{xy} = n_{yx}$  acting on the sides  $dx$  and  $dy$  of the plan projection of an element of a shell due to the reduced load components  $\epsilon_x$ ,  $\epsilon_y$  and  $\epsilon_z$ .

### 2- 1 Condition of Equilibrium in the $\bar{x}$ - Direction

The reduced forces and loads acting in the  $x$ - direction are shown in figure XII-92. One has to notice that :

$$dn_x = \frac{\partial n_x}{\partial x} dx \quad \text{and} \quad dn_{xy} = \frac{\partial n_{xy}}{\partial y} dy$$

The condition of equilibrium in the  $x$   $y$  direction is given by :

$$dn_x dy + dn_{xy} dx + \epsilon_x dx dy = 0$$

Substituting for  $dn_x$  and  $dn_{xy}$ , we get

$$\begin{aligned}
 \frac{\partial n_x}{\partial x} dx dy + \frac{\partial n_{xy}}{\partial y} dy dx + \epsilon_x dx dy &= 0 \quad \text{or} \\
 \frac{\partial n_x}{\partial x} + \frac{\partial n_{xy}}{\partial y} + \epsilon_x &= 0 \quad (7)
 \end{aligned}$$

### 2- 2 Condition of Equilibrium in the $\bar{y}$ - Direction

The condition of equilibrium in the  $y$  - direction can similarly be expressed by the relation : (Fig. XII-93)

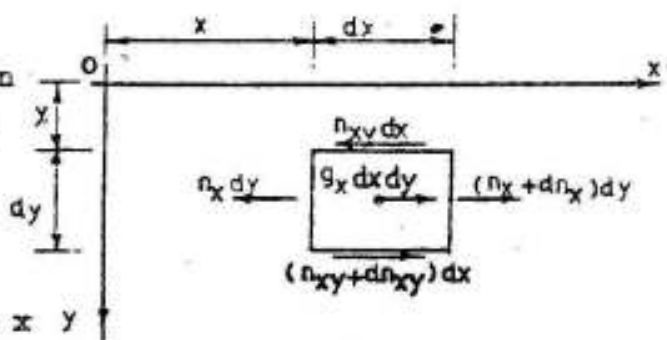


FIG. XII-92

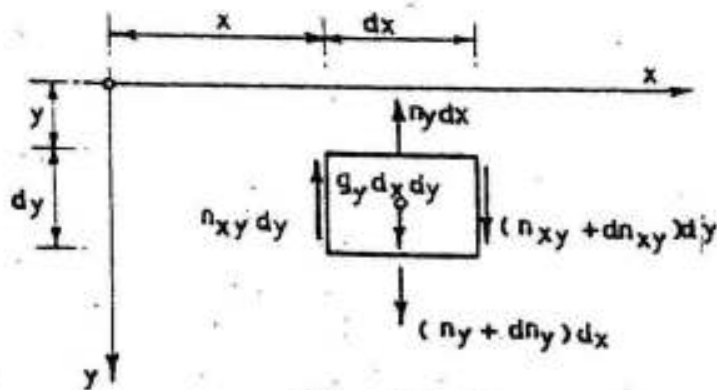


FIG. XII-93

$$\frac{\partial n_y}{\partial y} + \frac{\partial n_{xy}}{\partial x} + \epsilon_y = 0 \quad (8)$$

2-3 Condition of Equilibrium in the z - Direction

When writing the condition of equilibrium in the z-direction, the vertical components of the real forces are to be considered in the following manner : ( Fig XII-94)

The vertical component of  $N_x$  along the edge CD is given by

$$n_x \frac{\partial z}{\partial x}$$

whereas that of  $N_{xy}$  along the same edge is

$$n_{xy} \frac{\partial z}{\partial y}$$

so that the total vertical component along CD is given by

$$V_1 = n_x \frac{\partial z}{\partial x} + n_{xy} \frac{\partial z}{\partial y}$$

Similarly , along the edge BC ,we have

$$V_2 = n_y \frac{\partial z}{\partial y} + n_{yx} \frac{\partial z}{\partial x}$$

Therefore , the condition of equilibrium in the z - direction can be given in the form :

$$dV_1 dy + dV_2 dx + \epsilon_z dx dy = 0$$

in which

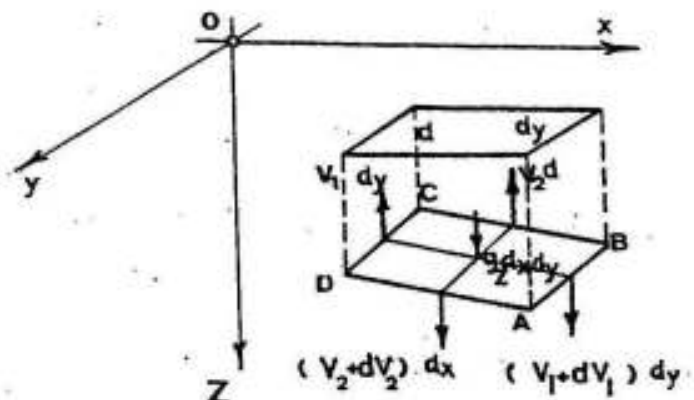


FIG. XII-94

$$dV_1 = \frac{\partial V_1}{\partial x} dx \quad \text{and} \quad dV_2 = \frac{\partial V_2}{\partial y} dy$$

So that

$$\frac{\partial V_1}{\partial x} + \frac{\partial V_2}{\partial y} + \epsilon_z = 0$$

Introducing the values of  $V_1$  and  $V_2$ , we get :

$$\frac{\partial}{\partial x} \left( n_x \frac{\partial z}{\partial x} + n_{xy} \frac{\partial z}{\partial y} \right) + \frac{\partial}{\partial y} \left( n_y \frac{\partial z}{\partial y} + n_{yx} \frac{\partial z}{\partial x} \right) + \epsilon_z = 0$$

Solving this equation, we get

$$n_x \frac{\partial^2 z}{\partial x^2} + \frac{\partial n_x}{\partial x} \frac{\partial z}{\partial x} + n_{xy} \frac{\partial^2 z}{\partial x \partial y} + \frac{\partial n_{xy}}{\partial x} \frac{\partial z}{\partial y} + n_y \frac{\partial^2 z}{\partial y^2} + \frac{\partial n_y}{\partial y} \frac{\partial z}{\partial y} \\ + n_{yx} \frac{\partial^2 z}{\partial x \partial y} + \frac{\partial n_{yx}}{\partial y} \frac{\partial z}{\partial x} + \epsilon_z = 0$$

This equation can also be given in the form :

$$n_x \frac{\partial^2 z}{\partial x^2} + (n_{xy} + n_{yx}) \frac{\partial^2 z}{\partial x \partial y} + n_y \frac{\partial^2 z}{\partial y^2} + \left( \frac{\partial n_x}{\partial x} + \frac{\partial n_{yx}}{\partial y} \right) \frac{\partial z}{\partial x} \\ + \left( \frac{\partial n_y}{\partial y} + \frac{\partial n_{xy}}{\partial x} \right) \frac{\partial z}{\partial y} + \epsilon_z = 0$$

But we have :  $n_{xy} = n_{yx}$  and

$$\frac{\partial n_x}{\partial x} + \frac{\partial n_{yx}}{\partial y} = -\epsilon_x \quad , \quad \frac{\partial n_y}{\partial y} + \frac{\partial n_{xy}}{\partial x} = -\epsilon_y$$

so that the equilibrium equation in the  $z$  - direction can be given in the form:

$$n_x \frac{\partial^2 z}{\partial x^2} + 2 n_{xy} \frac{\partial^2 z}{\partial x \partial y} + n_y \frac{\partial^2 z}{\partial y^2} + \dot{\epsilon}_z = 0 \quad (9)$$

in which

$$\dot{\epsilon}_z = \epsilon_z - \epsilon_x \frac{\partial z}{\partial x} - \epsilon_y \frac{\partial z}{\partial y} \quad (10)$$

For shells subject to vertical loads only

$$\epsilon_x = 0 \quad , \quad \epsilon_y = 0 \quad \text{and} \quad \dot{\epsilon}_z = \epsilon_z \quad (11)$$

### 3- The Pucher Stress Differential Equation

In order to simplify the problem, we will limit the following studies to shells subjected to vertical loads only. In this special case, the three conditions of equilibrium can be expressed by the relations :

$$\left. \begin{aligned} \frac{\partial n_x}{\partial x} + \frac{\partial n_{yx}}{\partial y} &= 0 \\ \frac{\partial n_y}{\partial y} + \frac{\partial n_{xy}}{\partial x} &= 0 \\ n_x \frac{\partial^2 z}{\partial x^2} + 2 n_{xy} \frac{\partial^2 z}{\partial x \partial y} + n_y \frac{\partial^2 z}{\partial y^2} + \epsilon_z &= 0 \end{aligned} \right\} \quad (12)$$

The determination of the reduced internal forces in shells by the use of these three simultaneous differential equations is generally complicated.

In order to simplify the problem Pucher has introduced a stress function  $F$  such that :

$$\left. \begin{aligned} n_x &= \frac{\partial^2 F}{\partial y^2} \\ n_{xy} = n_{yx} &= - \frac{\partial^2 F}{\partial x \partial y} \\ n_y &= \frac{\partial^2 F}{\partial x^2} \end{aligned} \right\} \quad (13)$$

With these relations, the first two conditions of equilibrium will be satisfied and it is sufficient to satisfy the third condition which can be put in the form :

$$\frac{\partial^2 z}{\partial x^2} \cdot \frac{\partial^2 F}{\partial y^2} - 2 \frac{\partial^2 z}{\partial x \partial y} \cdot \frac{\partial^2 F}{\partial x \partial y} + \frac{\partial^2 z}{\partial y^2} \cdot \frac{\partial^2 F}{\partial x^2} + \epsilon_z = 0 \quad (14)$$

giving 'Pucher differential equation' for shells subjected to vertical loads only.

With respect to the orthogonal axes  $x, y, z$ , the stress function  $F$  represents a stress surface independent of the origin  $O$  and the position of the horizontal plane  $x y$ .

When dealing with shell problems, the edge conditions of the shell define the shape of the stress surface at the edges and hence they must be taken in consideration as will be shown in the following illustrative examples.

#### 4- Illustrative Examples

##### 4- 1 Paraboloid Shell of Revolution with an Equilateral Triangular Plan

Shells supported on three points and bounded by three arches at the edges as shown in figure XII-95-a may give an architecturally striking solution for the roof covering of relatively big span halls.

It will be assumed that the edge arches can resist loads in their planes only and have no resistance to lateral forces so that the force components normal to them must be equal to zero. In order to satisfy this condition, we should have:

$$F_{\text{edge}} = 0 \quad (15)$$

A paraboloid of revolution as shown in figure XII-91-b has the equation

$$z = \frac{h}{4a^2} (x^2 + y^2) \quad (16)$$

Our study will be limited to shells subjected to uniformly

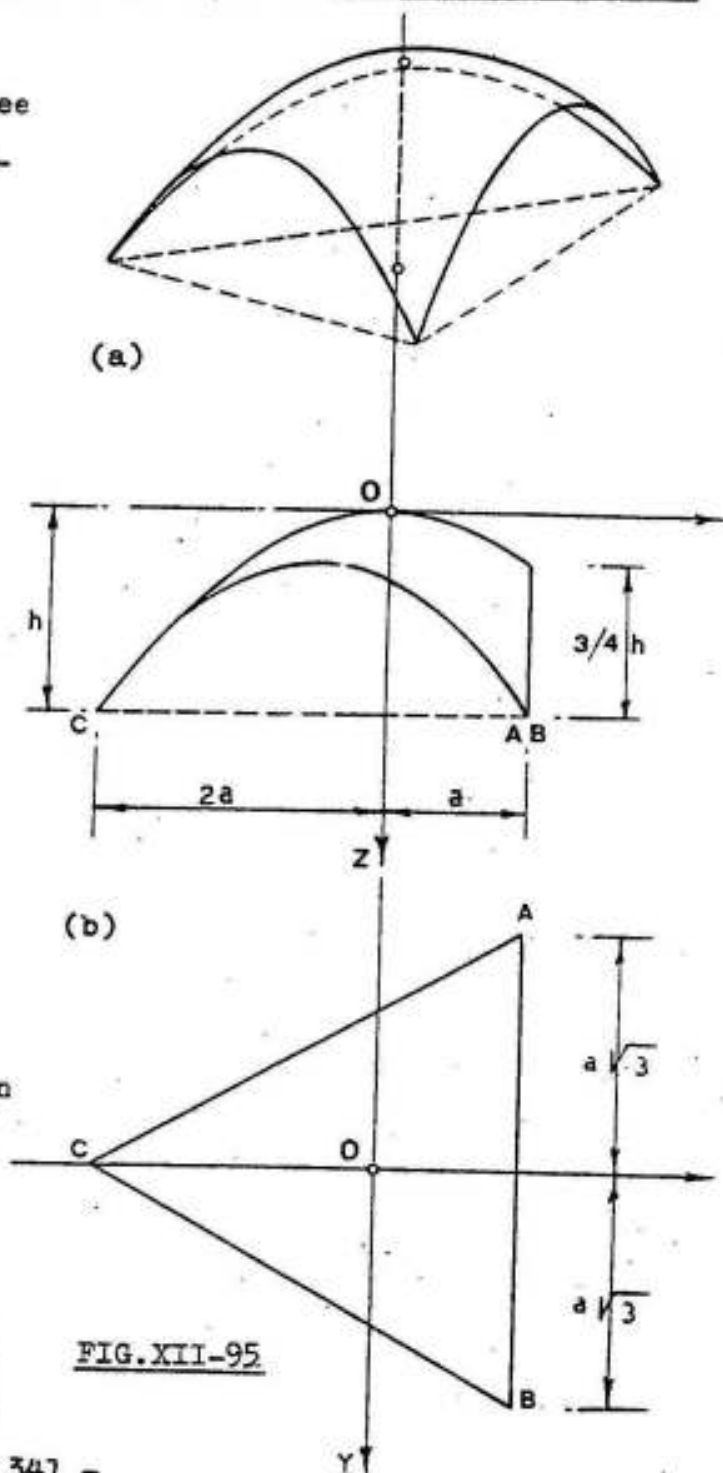


FIG. XII-95

distributed load  $g$ . In this case we have:

$$\frac{\partial^2 z}{\partial x^2} = h / 2 a^2 \quad , \quad \frac{\partial^2 z}{\partial x \partial y} = 0 \quad , \quad \frac{\partial^2 z}{\partial y^2} = h / 2 a^2$$

so that Pucher differential equation can be given in the form:

$$\frac{\partial^2 F}{\partial x^2} + \frac{\partial^2 F}{\partial y^2} = - \frac{2 a^2}{h} g \quad (17)$$

In order to satisfy the edge condition stated before, we have further :

$$F_{\text{edge}} = 0$$

A function equal to zero along the three sides of the ground plan can be constructed as follows:

a) Write the equations of the three sides of the triangular plan of the shell such that the right hand side of each equation is equal to zero . Thus

$$a - x = 0 \quad , \quad y - \frac{2a}{\sqrt{3}} - \frac{x}{\sqrt{3}} = 0 \quad \text{and} \quad y + \frac{2a}{\sqrt{3}} + \frac{x}{\sqrt{3}} = 0$$

b) The stress function  $F$  will be equal to a constant  $C$  multiplied by the left hand side of the equations of the sides . Hence

$$\begin{aligned} F &= C \left( a - x \right) \left( y - \frac{2a}{\sqrt{3}} - \frac{x}{\sqrt{3}} \right) \left( y + \frac{2a}{\sqrt{3}} + \frac{x}{\sqrt{3}} \right) \\ &= C \left( a x^2 + a y^2 + \frac{x^3}{3} - x y^2 - 4 \frac{a^3}{3} \right) \end{aligned}$$

c) It is possible to prove that this function satisfies Pucher differential equation if

$$C = - a g / 2 h$$

So that the stress function\*  $F$  is given by :

$$F = - \frac{ag}{2h} \left( a x^2 + a y^2 + \frac{x^3}{3} - x y^2 - 4 \frac{a^3}{3} \right) \quad (18)$$

and the reduced internal forces\* by :

\* Refer to Csonka "Membranschalen" Bauingenieur - Praxis. No 16

Published by Wilhelm Ernst & Sohn . Berlin. München.

$$\left. \begin{aligned}
 n_x &= \frac{\partial^2 P}{\partial y^2} = -\frac{a g}{h} (a - x) \\
 n_{xy} &= \frac{\partial^2 P}{\partial x \partial y} = -\frac{a g}{h} y \\
 n_y &= \frac{\partial^2 P}{\partial x^2} = -\frac{a g}{h} (a + x)
 \end{aligned} \right\} (19)$$

The internal forces  $N_x$ ,  $N_{xy} = N_{yx}$  and  $N_y$  acting on the shell can be calculated using equations 3 and 4 as follows :

According to equation 4, we have :

$$\cos \alpha = 1 / \sqrt{1 + (\partial z / \partial x)^2} \quad \text{and} \quad \cos \beta = 1 / \sqrt{1 + (\partial z / \partial y)^2}$$

$$\text{but } \partial z / \partial x = h x / 2 a^2 \quad \text{and} \quad (\partial z / \partial x)^2 = h^2 x^2 / 4 a^4$$

so that

$$\cos \alpha = 1 / \sqrt{1 + (h^2 x^2 / 4 a^4)}, \quad \text{similarly } \cos \beta = 1 / \sqrt{1 + (h^2 y^2 / 4 a^4)}$$

and

$$\cos \beta / \cos \alpha = \frac{\sqrt{1 + (h^2 x^2 / 4 a^4)}}{\sqrt{1 + (h^2 y^2 / 4 a^4)}} = \sqrt{\frac{4 a^4 + h^2 x^2}{4 a^4 + h^2 y^2}}$$

$$\text{similarly} \quad \cos \alpha / \cos \beta = \sqrt{\frac{4 a^4 + h^2 y^2}{4 a^4 + h^2 x^2}}$$

according to equation 3, we have

$$\left. \begin{aligned}
 N_x &= n_x \frac{\cos \beta}{\cos \alpha} = -\frac{a g}{h} (a - x) \sqrt{\frac{4 a^4 + h^2 x^2}{4 a^4 + h^2 y^2}} \\
 N_y &= n_y \frac{\cos \alpha}{\cos \beta} = -\frac{a g}{h} (a + x) \sqrt{\frac{4 a^4 + h^2 y^2}{4 a^4 + h^2 x^2}} \\
 N_{xy} &= N_{yx} = n_{xy} = n_{yx} = -\frac{a g}{h} y
 \end{aligned} \right\} (20)$$

#### Example

To illustrate the application of these equations, the internal forces in a triangular shell subject to uniformly distributed load  $g$



will be determined for the special case :

$$a = h$$

In this case , we have

$$\left. \begin{aligned} N_x &= -g(a-x) \sqrt{\frac{4a^2+x^2}{4a^2+y^2}} \\ N_y &= -g(a+x) \sqrt{\frac{4a^2+y^2}{4a^2+x^2}} \\ N_{xy} &= N_{yx} = -gy \end{aligned} \right\} \quad (21)$$

The evaluation of these values gives :

1- Along A-B :

$$x = a$$

$$N_x = 0, \quad N_y = -2ga \sqrt{\frac{4a^2+y^2}{5a^2}} = -2g \sqrt{\frac{4a^2+y^2}{5}}, \quad \text{thus}$$

$$\text{For } y = 0 \quad \pm \frac{a}{2}\sqrt{3} \quad \pm a\sqrt{3}$$

$$N_y = -1.79ga \quad -1.95ga \quad -2.36ga \quad \text{and}$$

$$N_{xy} = -gy \quad (\text{linear relation}), \quad \text{hence}$$

$$\text{For } y = 0, \quad N_{xy} = 0 \quad \text{and for } y = \pm a\sqrt{3}, \quad N_{xy} = \mp 1.735ga$$

2- Along the x-axis

$$y = 0$$

$$N_x = -g(a-x) \sqrt{\frac{4a^2+x^2}{4a^2}} \quad \text{hence}$$

$$\text{For } x = 0 \quad +a \quad -a \quad -2a$$

$$N_x = -ga \quad 0 \quad -2.24ga \quad -4.25ga$$

$$N_y = -g(a+x) \sqrt{\frac{4a^2}{4a^2+x^2}} \quad \text{hence}$$

$$\text{For } x = 0 \quad +a \quad -a \quad -2a$$

$$N_y = -ga \quad -1.79ga \quad 0 \quad +0.71ga$$

We have further

$$N_{xy} = 0 \quad \text{due to symmetry !}$$

3- Along n-n

$$y = \frac{a}{2}\sqrt{3}$$

$$N_x = -g(a-x) \sqrt{\frac{4a^2 + x^2}{4.75a^2}} \quad \text{hence}$$

For	$x =$	$0$	$+ a/2$	$a$	$- a/2$	
	$N_x =$	$-0.92ga$	$-0.47ga$	$0$	$-1.42ga$	

$$N_y = -g(a+x) \sqrt{\frac{4.75a^2}{4a^2 + x^2}} \quad \text{hence}$$

For	$x =$	$0$	$+a/2$	$a$	$- a/2$	
	$N_y =$	$-1.09ga$	$-1.59ga$	$-1.95ga$	$-0.53ga$	

$$N_{xy} = -g \frac{a}{2} \sqrt{3} = -0.867 g a = \text{constant} .$$

The calculated internal forces are shown in figure XII-96.

It is clear from the given diagrams that the shell is subject to compressive stresses over its whole surface with maximum values at the corners along the bisectors of the angles . The maximum compressive force is given by :

$$\text{max. } N_x = -4.25 g a$$

Due to symmetry , the compressive force at point O is the same in all directions

$$N_{xO} = N_{yO} = -g a$$

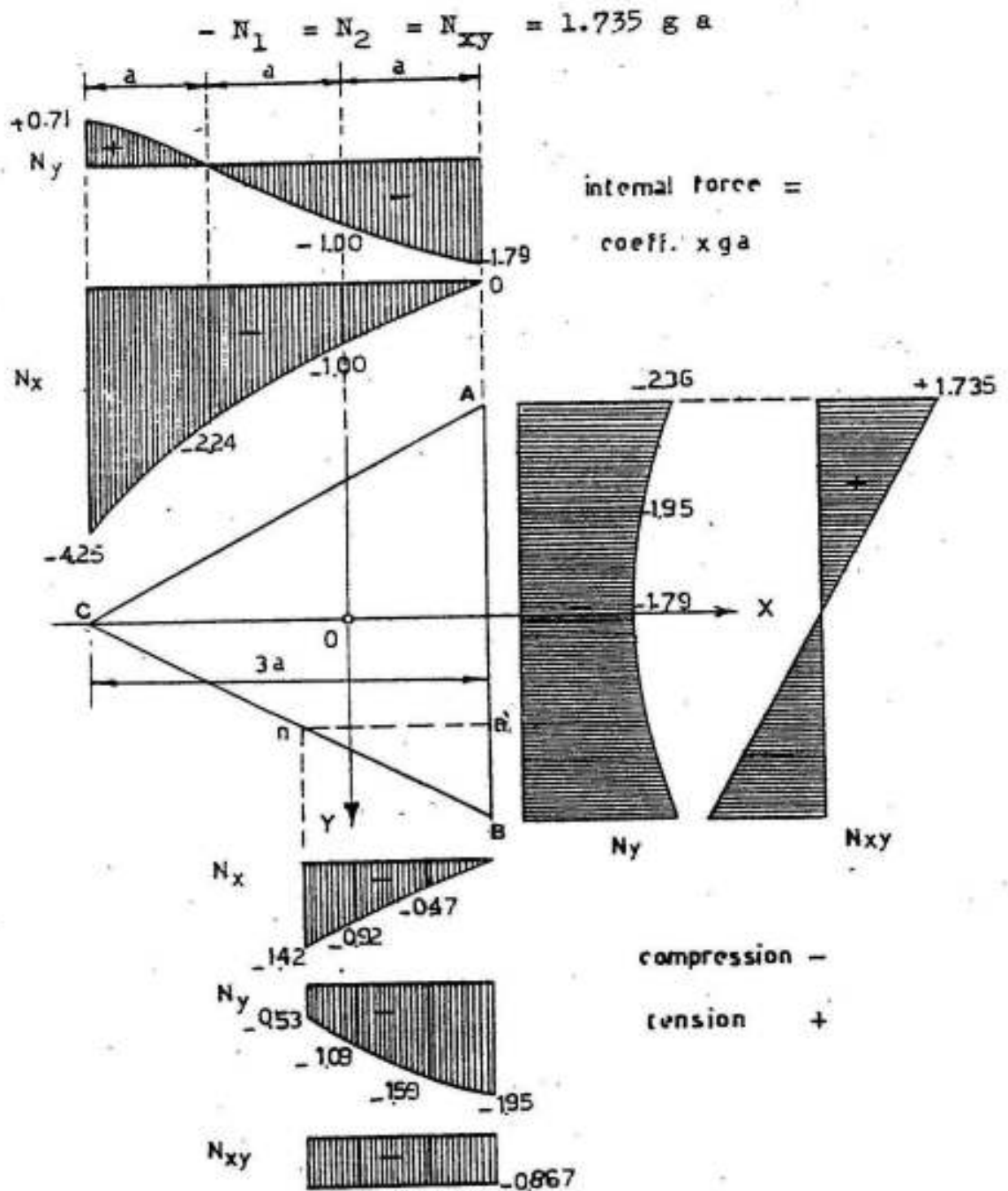
Tensile stresses exist at the corners normal to the bisectors of the angles. The maximum tensile force is .

$$\text{max. } N_y = +0.71 g a$$

The biggest shear stresses exist at the edges , zero at the middle - due to symmetry - and maximum at the corners. The maximum value is

$$\text{max. } N_{xy} = \pm 1.735ga$$

At the corners , a rhomboidal element with edges parallel to those of the the shell is in a state of pure shear. Hence the principal compressive and tensile stresses along the bisectors and normal to them are equal to the shear stresses , thus



Stress Resultants in a Triangular Shell for  $a = h$ .

FIG. XII-96

Accordingly, the stresses in a 10 cms thick shell with  $3a = 30$  ms and  $h = 10$  ms subject to a uniform vertical load  $g = 400 \text{ kg / m}^2$  horizontal are given by :

Maximum compressive stress at the corners :

$$\max. \sigma_x = \max. N_x / A_c = - 4.25 \times 400 \times 10 / 100 \times 10 = -17.0 \text{ kg/cm}^2$$

Compressive stress at crown

$$\sigma_c = - 1.00 \times 400 \times 10 / 100 \times 10 = - 4.0 \text{ "}$$

Principal tensile stress at corners normal to bisectors

$$\sigma_1 = +1.735 \times 400 \times 10 / 100 \times 10 = +6.94 \text{ "}$$

Although the stresses are low , it is recomended to increase the thickness of the shell gradually to 15 cms at the corners in a length of ca. 0.5 a measured along the bisectors of the angles. Accordingly , the compressive stress  $\sigma_c$  and the tensile stress  $\sigma_1$  at the corners will be reduced to  $10 / 15 = 2 / 3$  the given values. hence

$$\max. \sigma_x = - 17 \times 2/3 = - 11.3 \text{ kg/cm}^2$$

$$\max \sigma_1 = +6.94 \times 2/3 = + 4.63 \text{ "}$$

The reinforcement is generally one mesh  $5\phi 8 / m$  in each direction except at the corners and the edges where it is recommended to use two meshes as shown in figure XII-97.

The supporting arches are subject to the shearing forces of the shell acting parallel to the edge . These fprces are zero at the crown and increase linearly to their maximum value at the springing. The sum of vertical components of these forces acting on any of the arches must be equal to  $1/3$  total vertical loads acting on the snell.

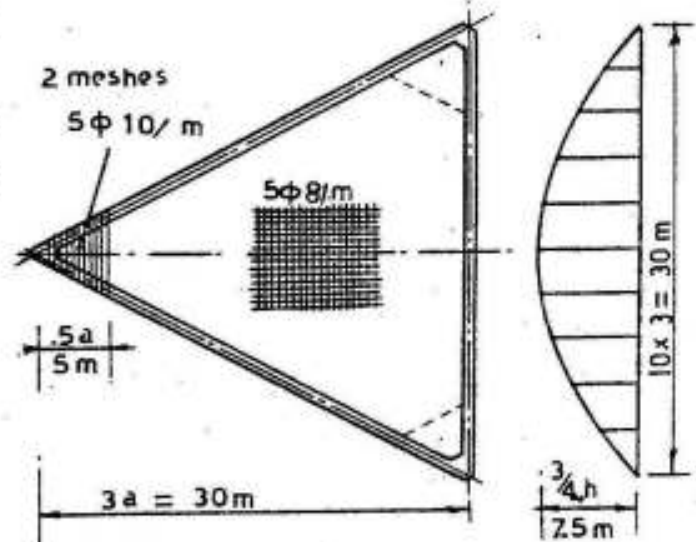


FIG.XII-97

#### 4- 2 Membrane Shells with Rectangular Ground Plan

For roof constructions, shells which permit covering rectangular big free areas ( fig XII-98 a ) are of much interest. They are

generally supported by four vertical arches that can resist vertical forces and are incapable to resist horizontal forces.

The equation of the middle surface of a paraboloid shell of revolution using an orthogonal system of coordinates  $O(x, y, z)$  shown on figure XII-98-b is given by

$$z = \frac{h}{2a^2} (x^2 + y^2) \quad (22)$$

Its second derivatives are:

$$\frac{\partial^2 z}{\partial x^2} = h / a^2$$

$$\frac{\partial^2 z}{\partial x \partial y} = 0$$

$$\frac{\partial^2 z}{\partial y^2} = h / a^2$$

Limiting our study to the case of uniformly distributed load  $g/m^2$  horizontal, the Pucher differential equation can be given in the form :

$$\frac{h}{a^2} \left( \frac{\partial^2 F}{\partial x^2} + \frac{\partial^2 F}{\partial y^2} \right) + g = 0 \quad (23)$$

As the edge arches are unable to resist lateral forces, the stress function  $F$  has to satisfy the boundary condition:

$$F_{\text{edge}} = 0 \quad (24)$$

The following relation<sup>(\*)</sup> gives

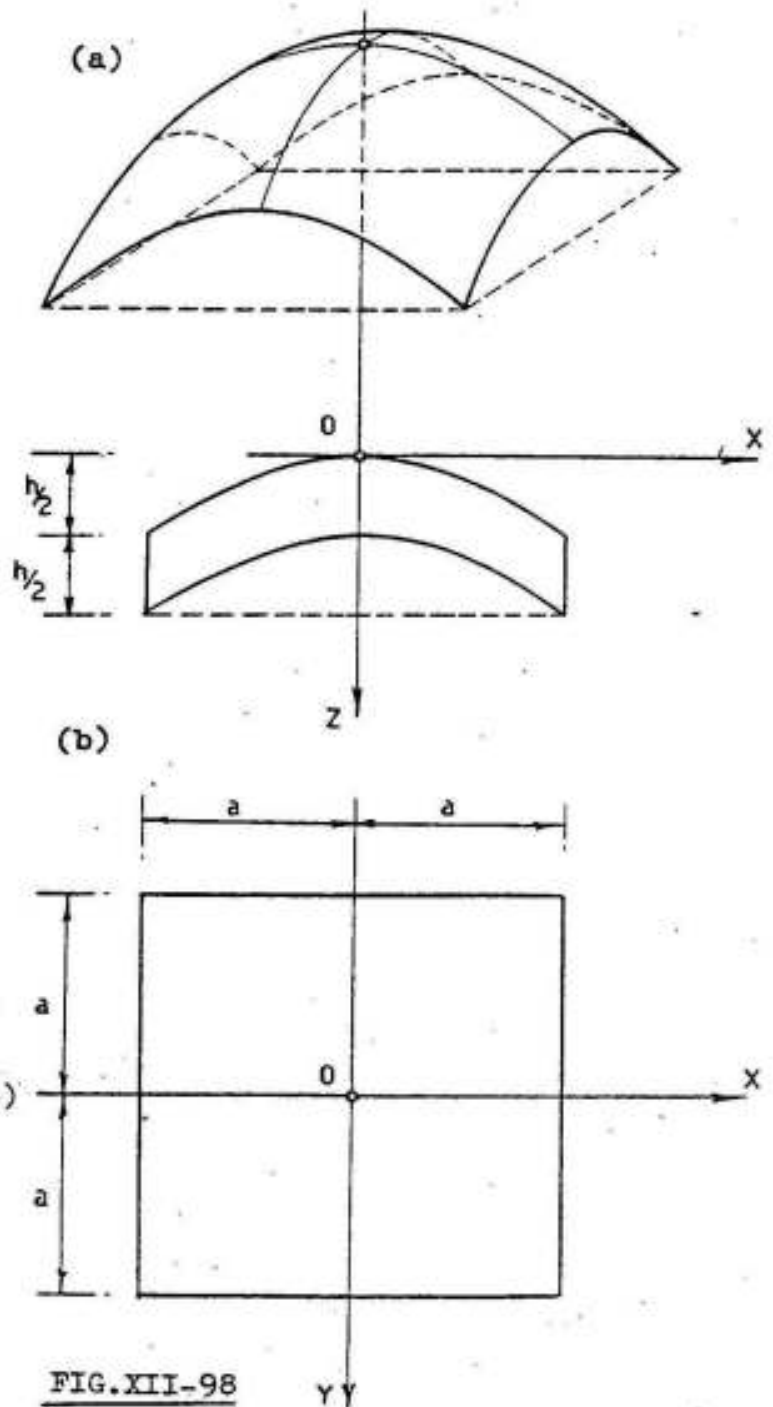


FIG. XII-98

\* Refer to Csonks "Membranschalen". Bauingenieur - Praxis. No 16

Published by Wilhem Ernst & Sohn . Berlin. München.

an approximate expression for the stress function satisfying equations (23) and (24)

$$F = \frac{a^4}{24 h} \varepsilon \left( 1 - \frac{x^2}{a^2} \right) \left( 1 - \frac{y^2}{a^2} \right) \left( 7 + \frac{x^2+y^2}{a^2} + \frac{x^2 y^2}{a^4} + 4 \frac{x^4 y^4}{a^8} \right) \quad (25)$$

The reduced internal forces are accordingly given by :

$$n_x = \frac{a^2 \varepsilon}{2 h} \left( -1 + \frac{x^2}{a^2} - \frac{y^2}{a^2} + \frac{5x^4 y^2}{a^6} - \frac{4 x^6 y^2}{a^8} - \frac{10x^4 y^4}{a^8} + \frac{10x^6 y^4}{a^{10}} \right)$$

$$n_{xy} = \frac{a^2 \varepsilon}{2h} \left( -\frac{2xy}{a^2} - \frac{20 x^3 y^3}{3 a^6} + \frac{8 x^3 y^5}{a^8} + \frac{8 x^5 y^3}{a^8} - \frac{12 x^5 y^5}{a^{10}} \right) \quad (26)$$

$$n_y = \frac{a^2 \varepsilon}{2 h} \left( -1 + \frac{x^2}{a^2} + \frac{y^2}{a^2} + \frac{5 x^2 y^4}{a^6} - \frac{4 x^2 y^6}{a^8} - \frac{10 x^4 y^4}{a^8} + \frac{10 x^4 y^6}{a^{10}} \right)$$

However, Jurashev, Sigalov and Baikov in their text book "Design of Reinforced Concrete Structures"(\*) have given the internal forces in a shallow convex shell of constant curvature. The shell is rectangular in plan and supported at the edges on four diaphragms absolutely rigid in their own plane and absolutely flexible normal to that plane. (Fig. XII-99). This determines the edge conditions of the shell, namely :

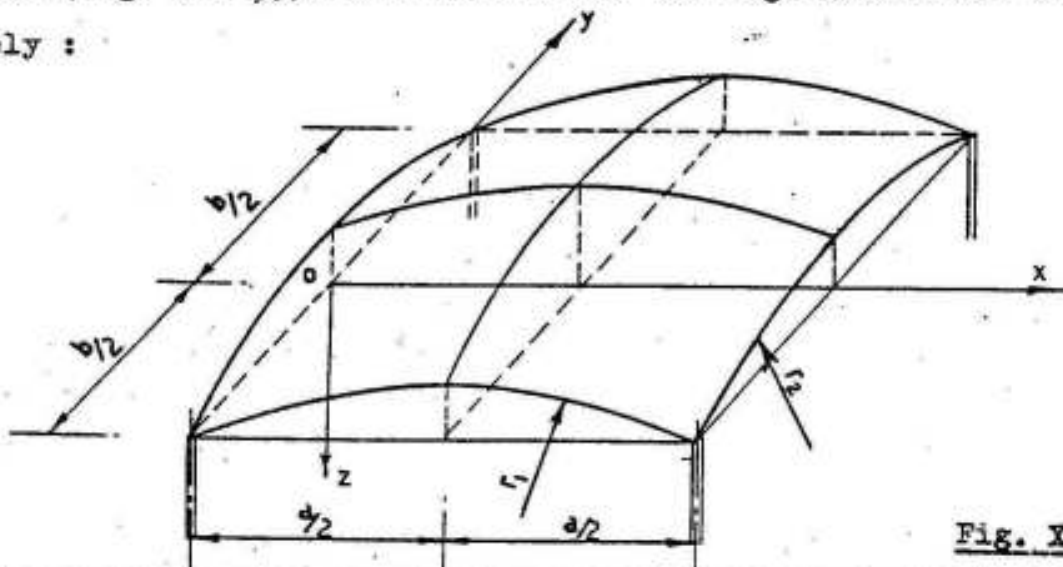


Fig. XII-99

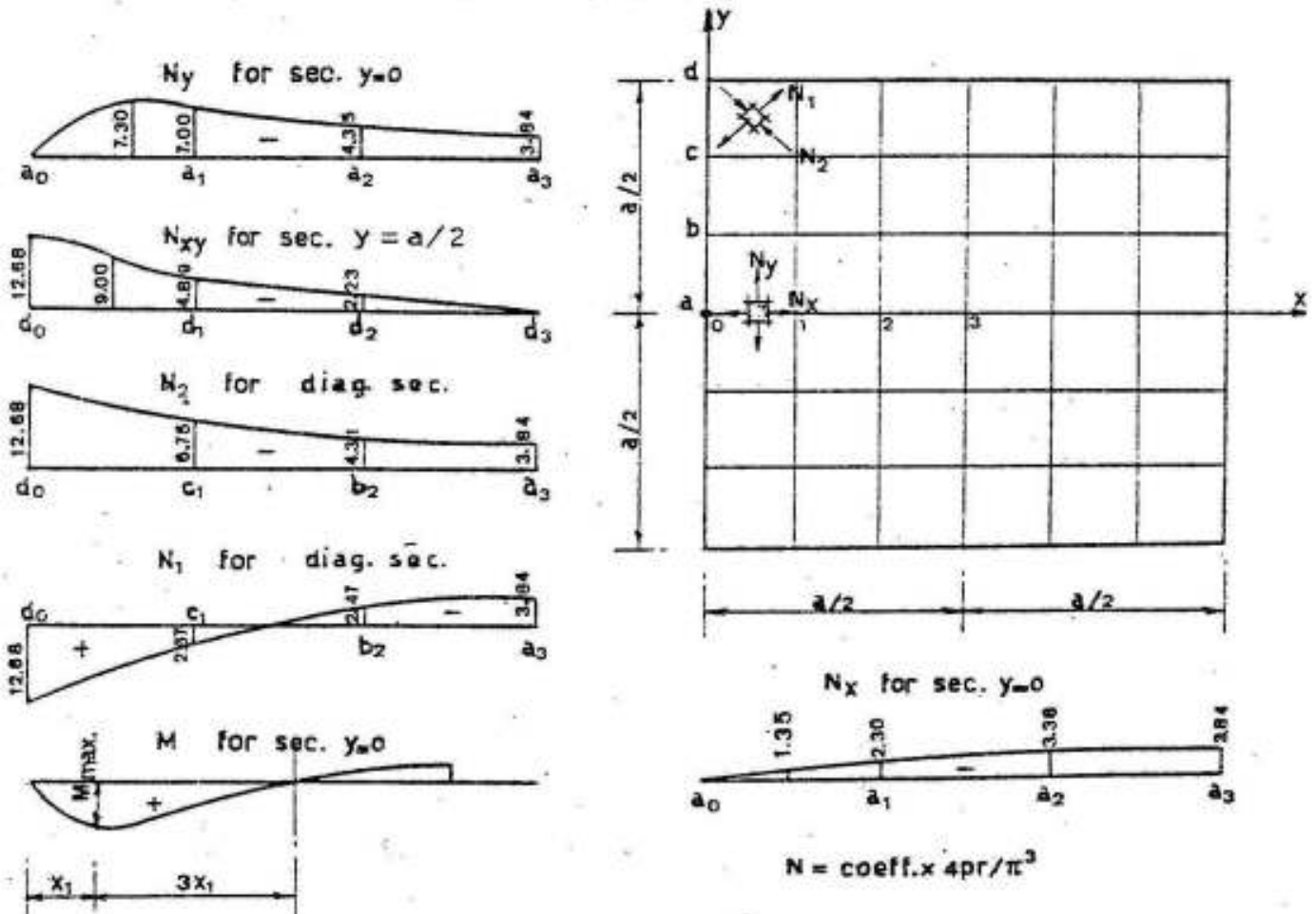
\*) Mir Publishers - Moscow

when  $x = 0$  and  $x = a$   $N_x = 0$

"  $y = \pm b / 2$   $N_y = 0$

The shell is subject to compressive normal forces  $N_x$ ,  $N_y$  and shear forces  $N_{xy}$ . At the corners, principal diagonal compressive and tensile forces  $N_2$  and  $N_1$  are created.

With  $a = b$  and  $r_1 = r_2 = r$ , the coefficients of the forces can be determined according to figure XII-100. The forces are obtained for the various points of the shell by multiplying the corresponding coefficients by a constant equal to  $4 p r / \pi^3$ .



Internal Forces in Shallow Convex Shells with Square Plan

FIG. XII-100

In the zones adjacent to the supports, bending moments are created. Their numerical values are not large, but however must be considered in the design. Their magnitude can be determined from the relations :

$$M = 0.3 p r t e^{-\psi} \sin \psi \quad (27)$$

where  $e$  is the base of natural logarithms,  $\psi = x / s$  and  $t =$  thickness of the shell.

The maximum bending moment is

$$\text{max. } M = 0.094 r t p \quad (28)$$

and acts in a section at a distance  $x_1$  from the edge, where

$$x_1 = 0.6 \sqrt{r t} \quad (29)$$

The diaphragms resist the shearing forces transmitted by the shell, they act parallel to its edge.

Example :

The numerical evaluation of the given method is shown in the following example.

It is required to determine the internal forces acting in a square shallow roof shell with  $l = 2 a = 2 b = 40$  ms; its rise  $h$  at the center is 6 ms, radius  $r = 68.2$  ms and shell thickness  $t = 10$ cms if it is subject to a uniformly load  $g = 500$  kg/m<sup>2</sup> horizontal.

All the required forces can be determined from the data given in figure XII-100. The constant factor for determining the forces is

$$4 p r / \pi^3 = 4 \times 0.5 \times 68.2 / \pi^3 = 4.35 \text{ t/m}$$

The maximum compressive force at the middle of the shell, :

$$N_x = N_y = - 3.84 \times 4.35 = -16.7 \text{ t/m}$$

The maximum compressive force at the zone adjacent to the edge:

$$N_y = - 7.30 \times 4.35 = -31.8 \text{ t/m}$$

The maximum principal compressive and principal tensile forces, and the shear forces at the corners of the shell, are

$$- N_2 = N_1 = N_{xy} = 12.68 \times 4.35 = 55.2 \text{ t/m}$$



The maximum bending moment

$$\text{max. } M = .094 r t p = .094 \times 68.2 \times 0.1 \times 500 = 300 \text{ kgm/m}$$

acting at a distance

$$x_1 = 0.6 \sqrt{r t} = 0.6 \sqrt{68.2 \times 0.1} = 1.57 \text{ m}$$

The compressive force  $N_x$  in this section can be determined by linear interpolation. Thus

$$N_x = -1.35 \times 4.35 \times 1.57 \times 12 / 40 = -2.95 \text{ t/m}$$

Due to the high principal compressive and tensile stresses at the corners, it is recommended to increase the thickness of the shell gradually from 10 to 16 cms along a length of about 0.15 l measured along the diagonal.

Accordingly, the maximum compressive stresses are:

$$\text{At crown } \sigma_c = -16700 / 100 \times 10 = -16.7 \text{ kg/cm}^2$$

$$\text{At edges } \sigma_c = -31800 / 100 \times 10 = -31.8 \text{ "}$$

$$\text{At corners } \sigma_c = -55200 / 100 \times 16 = -34.8 \text{ "}$$

In spite of that, the shell is reinforced over the greater part of its surface by one mesh  $5 \Phi 8\text{mm/m}$ .

The diagonal tension reinforcement on both sides at the corners can be calculated as follows: (Fig XII-101)

$$A_{s1} = \frac{55 + 44}{2 \sigma_s} = \frac{49.5}{1.4} = 35 \text{ cm}^2 / \text{m}$$

$$A_{s2} = \frac{44 + 34}{2 \sigma_s} = \frac{39}{1.4} = 28 \text{ "}$$

$$A_{s3} = \frac{34 + 26}{2 \sigma_s} = \frac{30}{1.4} = 22 \text{ "}$$

$$A_{s4} = \frac{26 + 20}{2 \sigma_s} = \frac{23}{1.4} = 16 \text{ "}$$

$$A_{s5} = \frac{20 + 11.6}{2 \sigma_s} = \frac{15.8}{1.4} = 11.2 \text{ "}$$

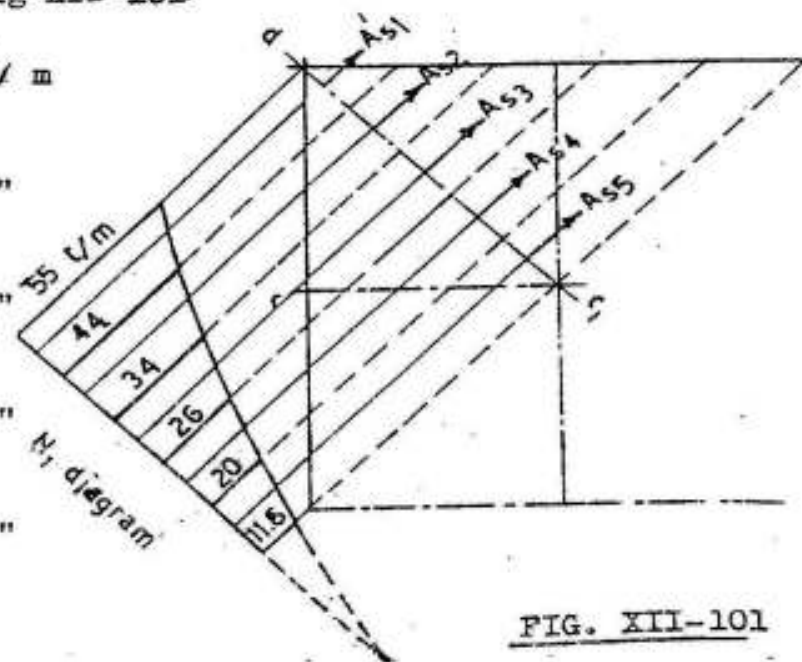


FIG. XII-101

In order to resist the bending moments at the edges of the shell additional reinforcements may be required normal to the edges.

The edge diaphragms have to support their own weight plus the shear of the shell  $\approx N_{xy}$ .

The arrangement of the reinforcement is shown in figure XII-102.

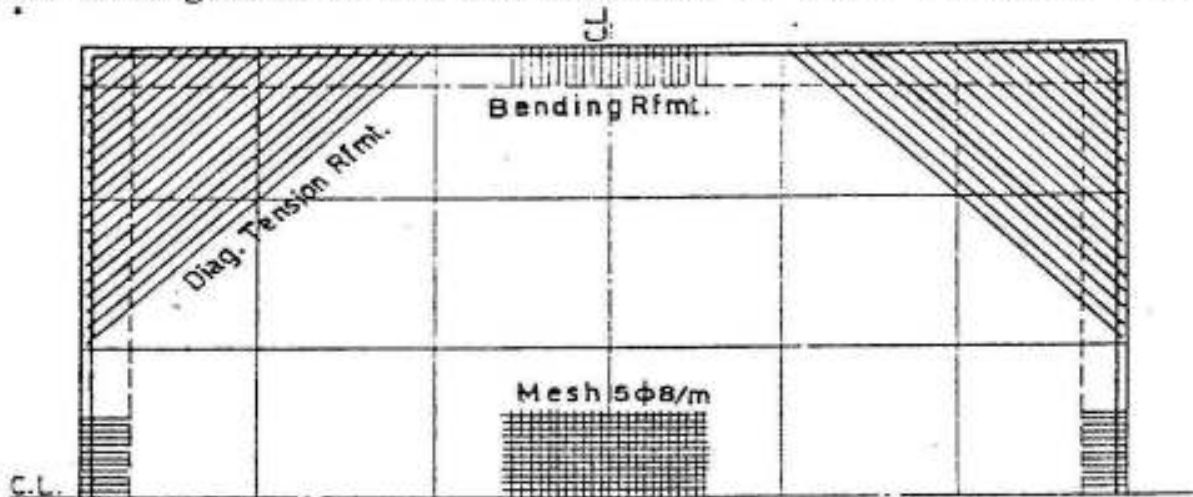


FIG. XII-102

For an elliptic paraboloid on rectangular plan with sides  $2a$  and  $2b$  and rise  $h_1$  and  $h_2$  as shown in figure XII-103 the equation of the surface is given by

$$z = \frac{h_1}{a^2} x^2 + \frac{h_2}{b^2} y^2 \quad (30)$$

The total central rise  $h$  of the shell is

$$h = h_1 + h_2$$

The derivatives of the equation are

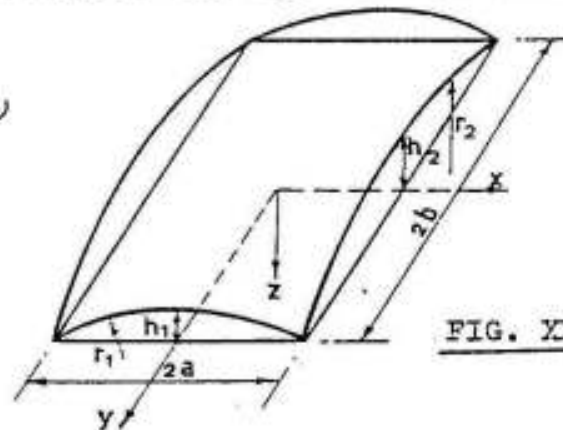


FIG. XII-103

$$\left. \begin{aligned} \frac{\partial z}{\partial x} &= 2h_1 x/a^2 & \frac{\partial z}{\partial y} &= 2h_2 y/b^2 \\ \frac{\partial^2 z}{\partial x^2} &= 2h_1/a^2 & \frac{\partial^2 z}{\partial x \partial y} &= 0 & \frac{\partial^2 z}{\partial y^2} &= 2h_2/b^2 \end{aligned} \right\} (31)$$

If  $r_1$  and  $r_2$  are the radii of the generating parabolas then

$$1/r_1 \approx \frac{\partial^2 z}{\partial x^2} = 2h_1/a^2 \quad \text{and} \quad 1/r_2 \approx \frac{\partial^2 z}{\partial y^2} = 2h_2/b^2 \quad (32)$$

Accordingly, the Pucher differential equation for a reduced vertical

load  $g$  is given by :

$$\frac{2h_1}{a^2} \frac{\partial^2 F}{\partial y^2} + \frac{2h_2}{b^2} \frac{\partial^2 F}{\partial x^2} = -g \quad (33)$$

If the two generating parabolas are identical, the surface is called a rotational paraboloid and is characterized by the relation

$$h_1/a^2 = h_2/b^2 \quad (34)$$

so that

$$1/r_1 = 1/r_2 = 1/r \quad (35)$$

$$\text{and } \frac{\partial^2 z}{\partial x^2} = \frac{\partial^2 z}{\partial y^2} = 1/r, \quad \frac{\partial^2 z}{\partial x \partial y} = 0 \quad (36)$$

The equation of the surface may therefore be given in the form :

$$z = \frac{1}{2r} (x^2 + y^2) \quad (37)$$

Hence

$$\frac{\partial z}{\partial x} = x/r \quad \text{and} \quad \frac{\partial z}{\partial y} = y/r \quad (38)$$

The Pucher differential equation can therefore be given in the form:

$$\frac{\partial^2 F}{\partial x^2} + \frac{\partial^2 F}{\partial y^2} = -gr \quad (39)$$

For the solution of this equation, Ramaswamy proposes to construct a polynomial stress function. For a vertical uniform load  $p/m^2$  surface, it takes the form :

$$F = (x^2 - a^2) (y^2 - b^2) (Ax^2 + By^2 + C) \quad (40)$$

which automatically satisfies the desired boundary conditions :

$$n_x = 0 \quad \text{at} \quad x = \pm a \quad (41)$$

$$\text{and} \quad n_y = 0 \quad \text{at} \quad y = \pm b$$

Thus

$$\left. \begin{aligned} \frac{\partial^2 F}{\partial y^2} = n_x &= 2 \left[ Ax^4 + 6Bx^2y^2 + (C - Aa^2 - Bb^2)x^2 \right. \\ &\quad \left. - 6Ba^2y^2 + a^2(Bb^2 - C) \right] \quad (a) \\ \frac{\partial^2 F}{\partial x^2} = n_y &= 2 \left[ By^4 + 6Ax^2y^2 + (C - Aa^2 - Bb^2)y^2 \right. \\ &\quad \left. - 6Ab^2x^2 + b^2(Aa^2 - C) \right] \quad (b) \end{aligned} \right\} (42)$$

$$-\partial^2 F / \partial x \partial y = n_{xy} = -8 (Ax^3y + Bxy^3) + 4xy (Aa^2 + Bb^2 - C) \quad (42c)$$

When the load acting is a vertical uniform load  $p$  per square meter surface then the Pucher differential equation assumes the form :

$$\partial^2 F / \partial x^2 + \partial^2 F / \partial y^2 = -gr = -pr\lambda \quad (43)$$

Substituting for  $\lambda$  the value given in equation 1 and expanding the right-hand side by the binomial theorem and limiting ourselves to the first two terms, then

$$\partial^2 F / \partial x^2 + \partial^2 F / \partial y^2 = -pr \left[ 1 + \frac{1}{2r^2} (x^2 + y^2) \right] \quad (44)$$

Substituting further for the derivatives of  $F$  from 42 a and 42b and equating the coefficients of like terms on the left- and right-hand sides of the equation, we arrive at the following three simultaneous equations in the three unknowns A, B and C :

$$\left. \begin{aligned} 2(C - Aa^2 - Bb^2 - 6Ab^2) &= -p/2r \\ 2(C - Aa^2 - Bb^2 - 6Ba^2) &= -p/2r \\ 2a^2(Bb^2 - C) + 2b^2(Aa^2 - C) &= -pr \end{aligned} \right\} \quad (45)$$

From the first two equations of the set, we find that

$$Ab^2 = Ba^2 \quad (45a)$$

Making use of this relation, B may be eliminated to give the two following simultaneous equations

$$C - Aa^2 - \frac{Ab^4}{a^2} - 6Ab^2 = -p/4r \quad (45b)$$

$$b^2A - C = -pr / 2 (a^2 + b^2) \quad (45c)$$

Knowing A, B and C, the reduced stresses are easily found. The method gives satisfactory accuracy if the shell is not too deep.

Example :

In order to show the application of the given relations the membrane analysis of a paraboloid of revolution will be illustrated for

the following data : ( Fig. XII-104 )

$$2a = 30 \text{ m}, \quad 2b = 40 \text{ m}$$

$$\text{Rise at crown } h = h_1 + h_2 = 5 \text{ ms}$$

$$\text{Thickness } t = 10 \text{ cms}$$

$$\text{Total load } p/\text{m}^2 \text{ surface} = 400 \text{ kgs}$$

Choosing the origin at the crown, the equation of the surface is given by :

$$z = \frac{1}{2r} (x^2 + y^2)$$

Noting that  $z = h$  for  $x = a$  and  $y = b$ , the radius of curvature of the surface is given by :

$$r = \frac{1}{2h} (a^2 + b^2) = \frac{1}{2 \times 5} (15^2 + 20^2) = 62.5 \text{ ms}$$

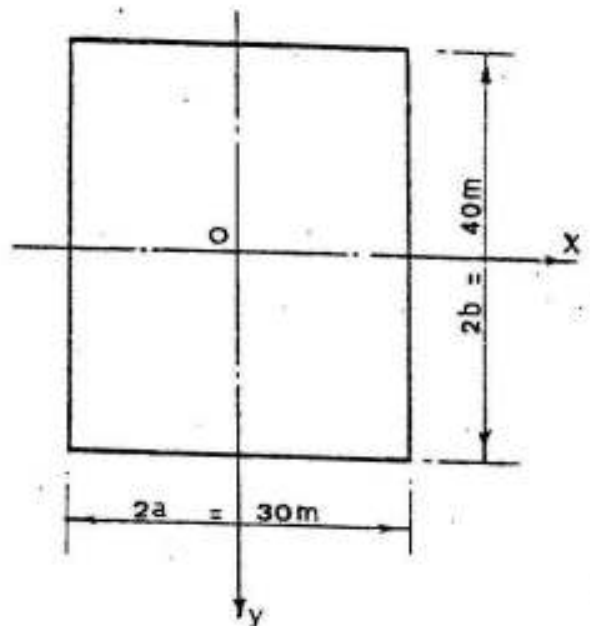


FIG. XII-104

The constants A, B & C of equations 45a, 45b and 45c can be calculated from the relations

$$(45a) \quad A b^2 = B a^2 \quad \text{or} \quad 20^2 A = 15^2 B \quad \text{i.e.} \quad B = 1.7778 A$$

$$(45b) \quad C - A a^2 - \frac{A b^4}{a^2} - 6 A b^2 = - p/4 r \quad \text{or} \quad C - 3336.1111A = - 1.6$$

$$(45c) \quad b^2 A - C = - pr/2 (a^2 + b^2) \quad \text{or} \quad -C + 400 A = - 20$$

Solving these three equations, we get :

$$A = 0.007356 \quad B = 0.013077 \quad C = 22.9424$$

The reduced internal forces are therefore given by :

$$n_x = 0.014712 x^4 + 0.156924 x^2 y^2 + 32.1130 x^2 - 35.3080 y^2 - 7970.22$$

$$n_y = 0.026154 y^4 + 0.088272 x^2 y^2 + 32.1130 y^2 - 35.3080 x^2 - 17030.24$$

$$n_{xy} = - 0.058848 x^3 y - 0.104616 x y^3 - 64.226 x y$$

Their values are as follows :

On the x - axis  $y = 0$  Fig. XII-105a

x	0	5	10	15	m
$-n_x$	7970	7158	4612	0	kg/m
$-n_y$	17030	17913	20560	24974	"
$-n_{xy}$	0				"

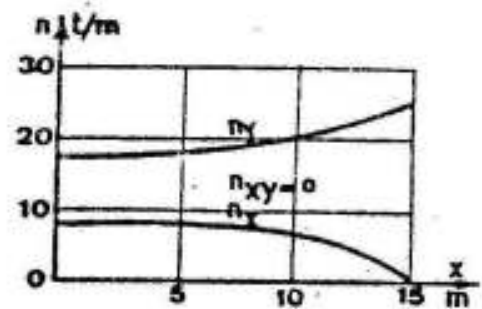


Fig. XII-105a

At the edge  $y=b/2=20m$  Fig. XII-105b

x	0	5	10	15	m
$-n_x$	22093	19712	12458	0	kg/m
$-n_{xy}$	0	12416	22391	35794	"
$-n_y$	0				"

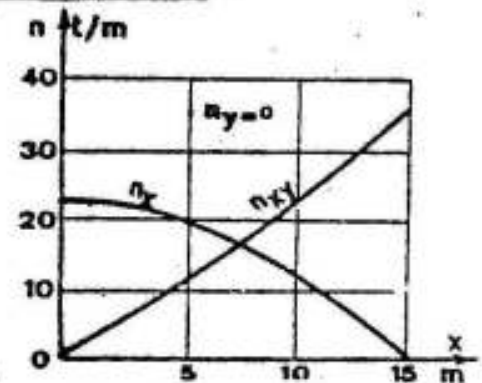


Fig. XII-105b

On the y - axis  $x = 0$  Fig. XII-105c

y	0	5	10	15	20	m
$-n_x$	7970	8853	11501	15914	22093	kg/m
$-n_y$	17030	16211	13557	8453	0	"
$-n_{xy}$	0					"

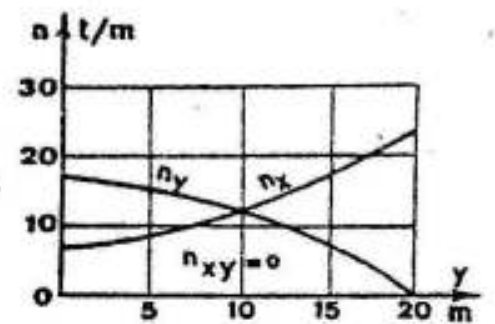


FIG. XII-105c

At the edge  $x=a/2=15m$  Fig. XII-105d

y	0	5	10	15	20	m
$-n_y$	24975	23659	19516	11956	0	kg/m
$-n_{xy}$	0	6006	13189	22726	35794	"
$-n_x$	0					"

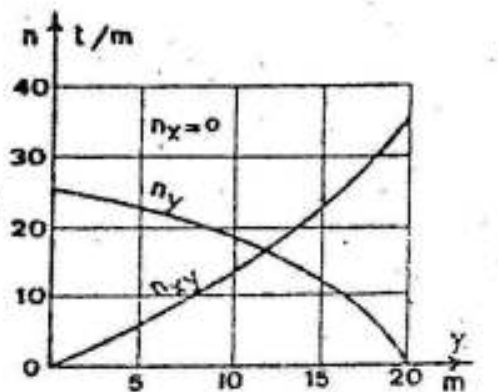


FIG. XII-105d

It is clear from the tables that the shell is subject to compressive stresses over its whole surface except at the corners where we have high shearing forces  $N_{xy} = 35794$  kg/m causing principal diagonal tensile forces  $N_1$  (normal to the bisector of the corner angle) and compressive forces  $N_2$  (in the direction of the bisector). The maximum magnitude of both  $N_1$  and  $N_2$  is equal to max.  $N_{xy}$  at the corner.

It is therefore recommended to increase the thickness of the shell at the corners to about 20 cms, and to resist the principal tensile forces  $N_1$  by top and bottom corner reinforcements arranged at  $45^\circ$  to the axes  $x$  and  $y$  normal to the bisector of the corner angle

Fig. XII-106 shows the general layout, main dimensions and details of reinforcements of two separate units of a series of double curved shell roofs of the elliptic paraboloid type constructed in Egypt near Cairo. Every two units are attached and supported on 6 main columns only. Each unit covers an area  $23.94 \times 24.75$  ms. The rises  $h_1$  and  $h_2$  of the shorter and longer diaphragms are approximately equal and each is 3 ms. The shell thickness within a horizontal radius of 10 ms is equal to 8 cms increased to 12 cms within a radius of 12.4 ms and to 24 cms at the four corners. The central part, 8 cms thick, is reinforced by one orthogonal mesh,  $6 \phi 8$  mm/m, the rest is reinforced by two meshes, each is composed of circular bars increasing from  $6 \phi 10$  mm/m, in the zone limited by the radii 10 and 12.4 ms, to  $8 \phi 13$  mm/m at the corners, and radial bars  $5 \phi 8$  mm/m arranged radially in the manner shown in figure. Each of the end diaphragms is an arch  $35 \times 55$  cms with a prestressed tie  $25 \times 25$  cms. The arch is reinforced by :  $8 \phi 19$  mm and the tie by  $4 \phi 16$  mm in addition to four Freyssinet cables 20 tons each.

The roof structure constructed according to this system adapts itself in an impressive, simple, easy and economic manner to rectangular areas of relatively big spans.





### 4-3 Conoid Shells

A conoid surface is originated when a straight line moves at one of its ends on a basic curve  $C$  (called directrix) and at the other end on a key line  $K$  in such a way that the straight line is always parallel to a vertical guide plane  $G$ . Accordingly, any vertical section between the basic curve  $C$  & the key line  $K$  has the same form and span as  $C$  but with a smaller rise  $h$ , it is called an affine curve. All sections parallel to the guide plane  $G$  are straight lines and are called the generators of the conoid. Fig. XII-107.

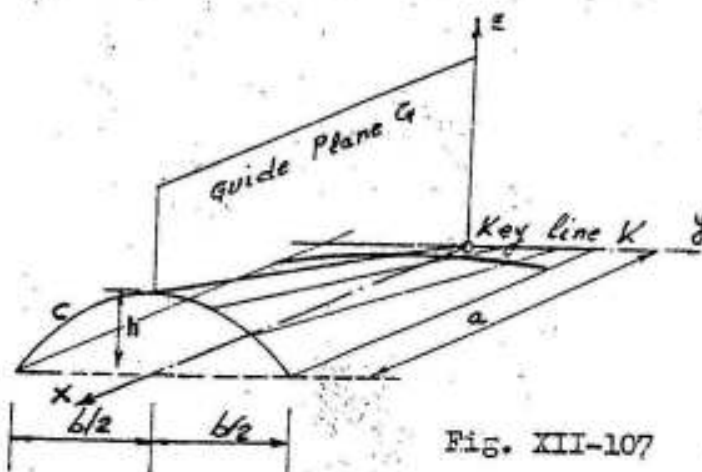


Fig. XII-107

A shell roof is generally a truncated conoid, bounded by two arches  $C$  and  $C'$  and two straight edges parallel to the guide plane  $G$ . Its formwork is very easy as it is constructed from straight planks.

Depending upon the curve used as the directrix, conoids are described as parabolic, circular ... etc. Of these, the parabolic conoid is by far most common.

The generators of the conoid surface being parallel to the vertical symmetry axis of the shell, they appear as parallel straight lines in the ground plan. Fig. XII-108.

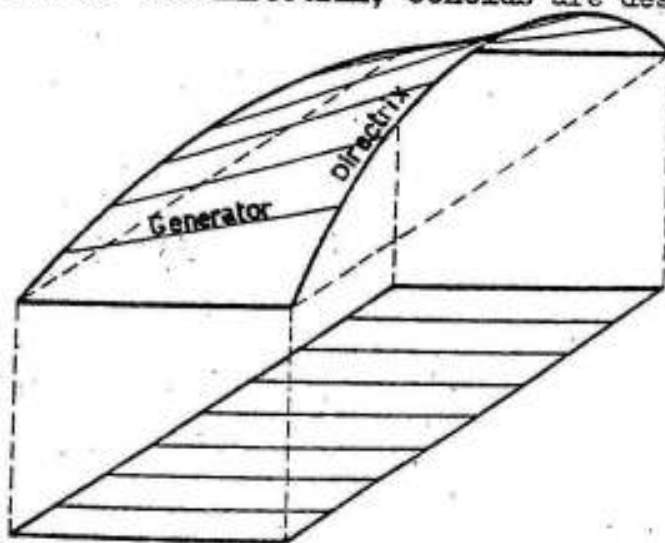


Fig. XII-108

The equation of the middle surface of a parabolic conoid shell is given by: (Fig. XII-109)

$$z = -\frac{h}{a}x \left(1 - \frac{4y^2}{b^2}\right) \quad (46)$$

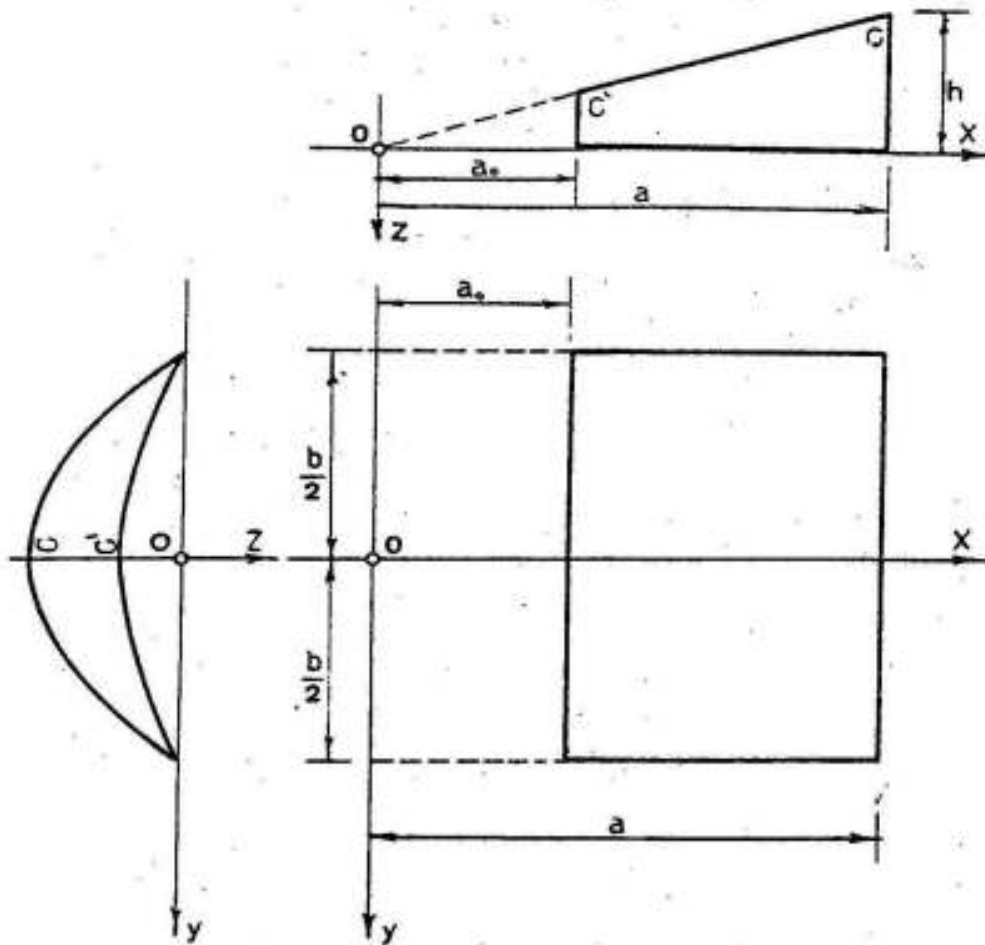


Fig. XIII-109 A parabolic conoid

The derivatives of this relation are given by:

$$\left. \begin{aligned} \frac{\partial z}{\partial x} &= -\frac{h}{a} \left(1 - \frac{4y^2}{b^2}\right) & \frac{\partial z}{\partial y} &= \frac{8hy}{ab^2} \\ \frac{\partial^2 z}{\partial x^2} &= 0 & \frac{\partial^2 z}{\partial x \partial y} &= \frac{8hy}{ab^2} & \frac{\partial^2 z}{\partial y^2} &= \frac{8hx}{ab^2} \end{aligned} \right\} (47)$$

In the following, the internal forces due to a vertical load  $\epsilon_z$  will be given.  $\partial^2 z / \partial x^2$  being equal to zero, the conditions of equilibrium, expressed by equations 12, can, in this case, be given in the form:

$$\left. \begin{aligned} \frac{\partial n_x}{\partial x} + \frac{\partial n_{yx}}{\partial y} &= 0 & \frac{\partial n_y}{\partial y} + \frac{\partial n_{xy}}{\partial x} &= 0 \\ n_y \frac{\partial^2 z}{\partial y^2} + 2 n_{xy} \frac{\partial^2 z}{\partial x \partial y} &= -\epsilon_z \end{aligned} \right\} (48)$$

It will be assumed also here that the edge arches can resist loads in their planes only and have no resistance to lateral forces so that the force components normal to them must be equal to zero, i.e.

$$\text{at } x = a_0 \quad \text{and} \quad x = a \quad n_x = 0 \quad (49a)$$

It is further known that in a conoid shell, symmetrical about the middle x-axis ( $y = 0$ ) subject to symmetrical vertical load  $\epsilon_z$ , we should have:

$$\text{for} \quad y = 0 \quad n_{xy} = 0 \quad (49b)$$

Due to a vertical distributed load  $g / m^2$  surface, we have:

$$\epsilon_z = g \left[ 1 + \frac{h^2}{2 a^2} \left( 1 - \frac{4 y^2}{b^2} \right)^2 + 32 \frac{h^2 x^2 y^2}{a^2 b^4} \right] \quad (50)$$

Satisfying the conditions of equilibrium (48), the edge conditions (49) and the relation between  $g$  and  $\epsilon_z$  given in (50), the reduced internal forces can be determined, according to Fischer<sup>±</sup> from the following relations:

$$\begin{aligned} n_x &= \frac{g h}{4 a b^2} \left\{ (b^2 - 6 y^2)(a - x) - \frac{16}{3} (a^3 - x^3) \right. \\ &\quad \left. - \frac{b^2 (a - a_0) - \frac{16}{3} (a^3 - a_0^3)}{a^5 - a_0^5} (a^5 - x^5) \right. \\ &\quad \left. + 6 \frac{a - a_0}{a^9 - a_0^9} g (a^9 - x^9) y^2 \right\} \\ n_y &= - \frac{g a b^2}{8 h x} \left[ 1 + \frac{h^2}{2 a^2} - \frac{32 h^2 x^2 y^2}{a^2 b^4} \right] + \frac{g h y^2}{2 a b^2} \left\{ \frac{5 x^3}{a^5 - a_0^5} \right. \\ &\quad \left. \left[ b^2 (a - a_0) - \frac{16}{3} (a^3 - x_0^3) \right] - \frac{18 y^2 x^7}{a^9 - a_0^9} - (a - a_0) \right\} \\ n_{xy} &= \frac{g h y}{4 a b^2} \left\{ b^2 - 2 y^2 - 16 x^2 - \frac{5 x^4}{a^5 - a_0^5} \left[ b^2 (a - a_0) - \right. \right. \\ &\quad \left. \left. - \frac{16}{3} (a^3 - a_0^3) \right] + \frac{18 y^2 x^8}{a^9 - a_0^9} (a - a_0) \right\} \end{aligned} \quad (51)$$

For the numerical calculations, it is recommended to replace  $x$  and  $y$  by  $\xi$  and  $\eta$  according to the following relations:

$$x = \xi a \quad (a_0 = \xi_0 a) \quad \text{and} \quad y = \frac{b}{2} \eta \quad (52)$$

So that the reduced internal forces can be given in the form:

$$\begin{aligned} n_x &= \frac{gh}{4ab^2} \left\{ b^2 a \left(1 - \frac{3\eta^2}{2}\right) (1-\xi) - \frac{16 a^3}{3} (1-\xi^3) - \frac{1-\xi^5}{1-\xi_0^5} \left[ b^2 a (1-\xi_0) \right. \right. \\ &\quad \left. \left. - \frac{16 a^3}{3} (1-\xi_0^3) \right] + \frac{3b^2 a}{2} (1-\xi_0) \eta^2 \frac{1-\xi^9}{1-\xi_0^9} \right\} \\ n_y &= - \frac{gb^2}{8h\xi} \left[ 1 + \frac{h^2}{2a^2} - \frac{8h^2}{b^2} \xi^2 \eta^2 \right] + \frac{gh\eta^2}{8a} \left\{ \frac{5 \xi^3}{a(1-\xi_0^5)} \left[ b^2 (1-\xi_0) - \right. \right. \\ &\quad \left. \left. - \frac{16 a^2}{3} (1-\xi_0^3) \right] - \frac{9}{2} \frac{b^2 \eta^2 \xi^7 (1-\xi_0)}{a (1-\xi_0^9)} \right\} \\ n_{xy} &= \frac{gh}{8 a b} \left\{ b^2 \left(1 - \frac{\eta^2}{2}\right) - 16 a^2 \xi^2 - \frac{5 \xi^4}{1-\xi_0^5} \left[ b^2 (1-\xi_0) - \right. \right. \\ &\quad \left. \left. - \frac{16 a^2}{3} (1-\xi_0^3) \right] + \frac{9}{2} \frac{b^2 \eta^2 \xi^8}{(1-\xi_0^9)} (1-\xi_0) \right\} \end{aligned} \quad (53)$$

Having determined the reduced internal forces  $n_x$ ,  $n_y$  and  $n_{xy}$ , the actual internal forces  $N_x$ ,  $N_y$  and  $N_{xy} = n_{xy}$  can be calculated using relations 3 & 4 and the principal forces  $N_1$  and  $N_2$  using conditions 5 & 6.

Fig. XII-110 shows the general layout, main dimensions and details of a conoid shell solved by Fischer<sup>\*</sup> for the following data:

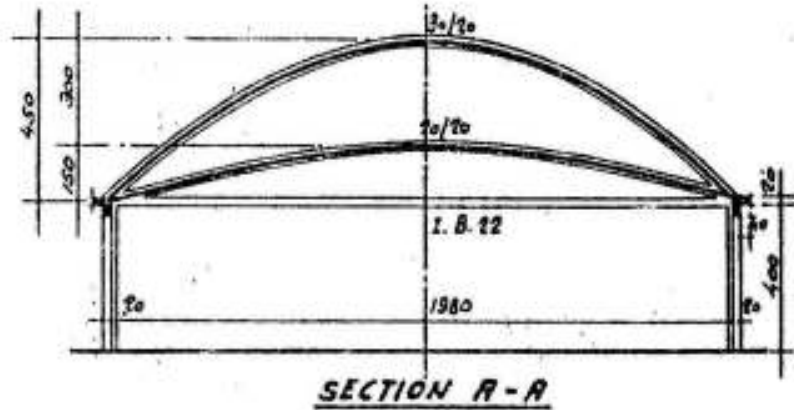
Theoretical length  $a = 12.00$  m , Actual length =  $a - a_0 = 8.00$  m  
 Breadth .....  $b = 20.00$  m , Max. rise .....  $h = 4.50$  m  
 Shell thickness  $t = 10$  cms , Load/m<sup>2</sup> surface  $\xi = 300$  kg/m<sup>2</sup>  
 $\xi_0 = \frac{a_0}{a} = \frac{4}{12} = 0.3333$  ;  $\xi_0^3 = 0.03703$  ;  $\xi_0^5 = 0.004115$  and  $\xi_0^9 = 0.000051$

Introducing these values in equation 53 of the reduced internal forces, it is easy to prove that:

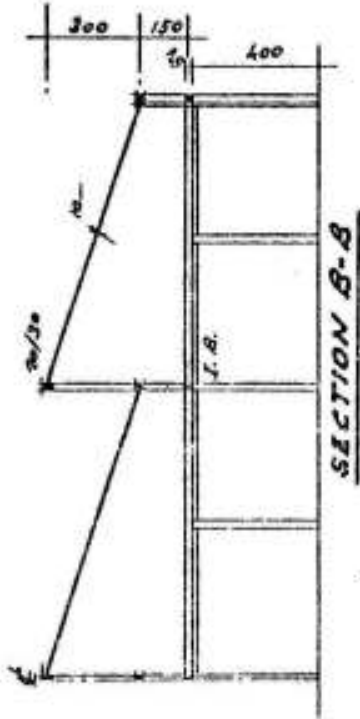
---

\* Fischer " Theorie und Praxis der Schalenkonstruktionen". Published by Wilhelm Ernst und Sohn. Berlin und Lünchen. 1967

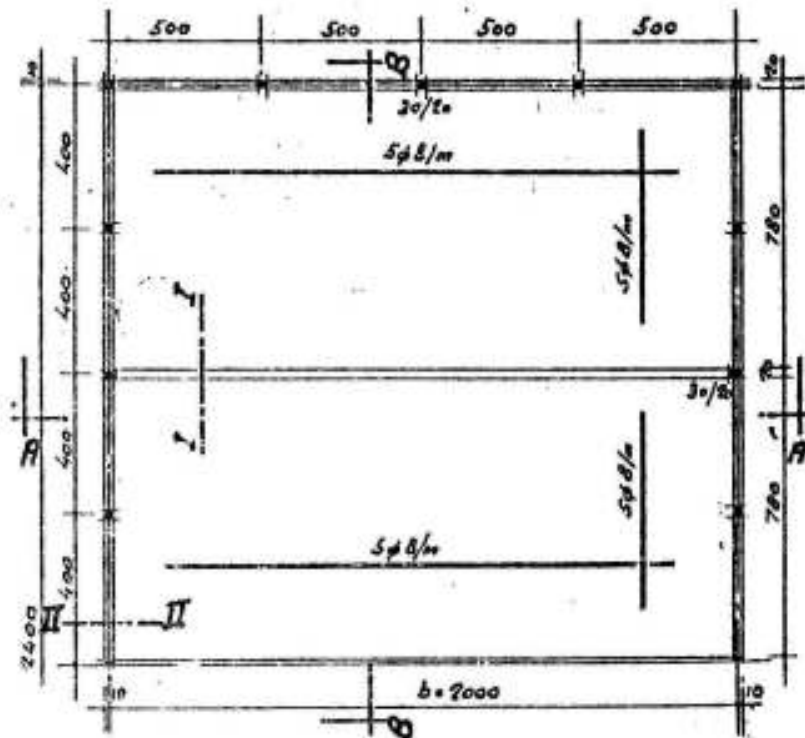
**DETAILS  
OF  
A CONOID ROOF**



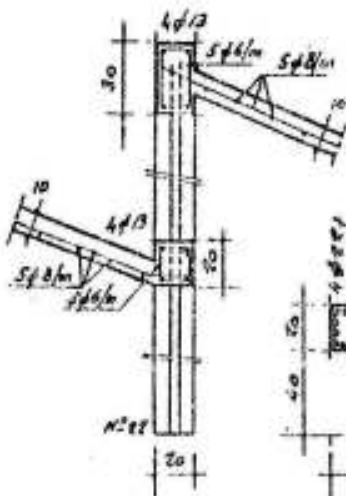
**SECTION A-A**



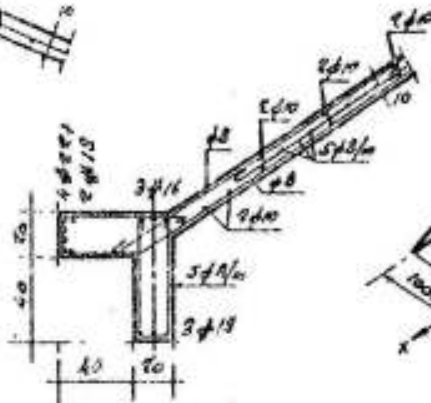
**SECTION B-B**



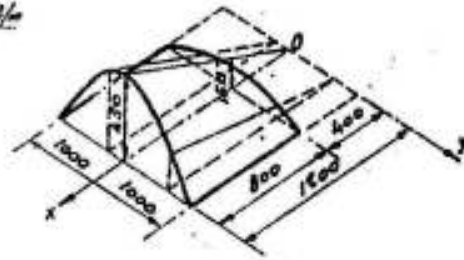
**HALF PLAN**



**SECTION I-I**



**SECTION II-II**



**LAYOUT**

$$n_x = 0.3375 (1-\xi)(1-\frac{3\eta^2}{2}) - 0.6480 (1-\xi^3) + 0.4006 (1-\xi^5) + 0.3375 \eta^2 (1-\xi^9)$$

$$n_y = \frac{1}{5} (-3.5675 + 1.3500 \eta^2 \xi^2 - 2.7823 \eta^2 \xi^4 - 1.4063 \eta^4 \xi^8)$$

$$n_{xy} = \eta \left\{ 0.2813 (1-\frac{\eta^2}{2}) - 1.6200 \xi^2 + 1.6694 \xi^4 + 0.8438 \eta^2 \xi^8 \right\}$$

The real internal forces  $N_x$ ,  $N_y$  and  $N_{xy}$  are, according to equation 3, given by:

$$N_x = n_x \cos \beta / \cos \alpha, \quad N_y = n_y \cos \alpha / \cos \beta \quad \text{and} \quad N_{xy} = n_{xy}$$

Knowing further that

$$\tan \alpha = \frac{\partial z}{\partial x} = \frac{h}{a} (1 - \frac{4y^2}{b^2}) = \frac{h}{a} (1 - \eta^2)$$

and

$$\tan \beta = \frac{\partial z}{\partial y} = \frac{8 h x y}{a b^2} = \frac{4 h}{b} \xi \eta$$

then  $\alpha$  and  $\beta$ , and the corresponding cos-values required for calculating  $N_x$  and  $N_y$  can be easily determined.

The calculated internal forces in the shell are as shown in Fig.

XII-111.

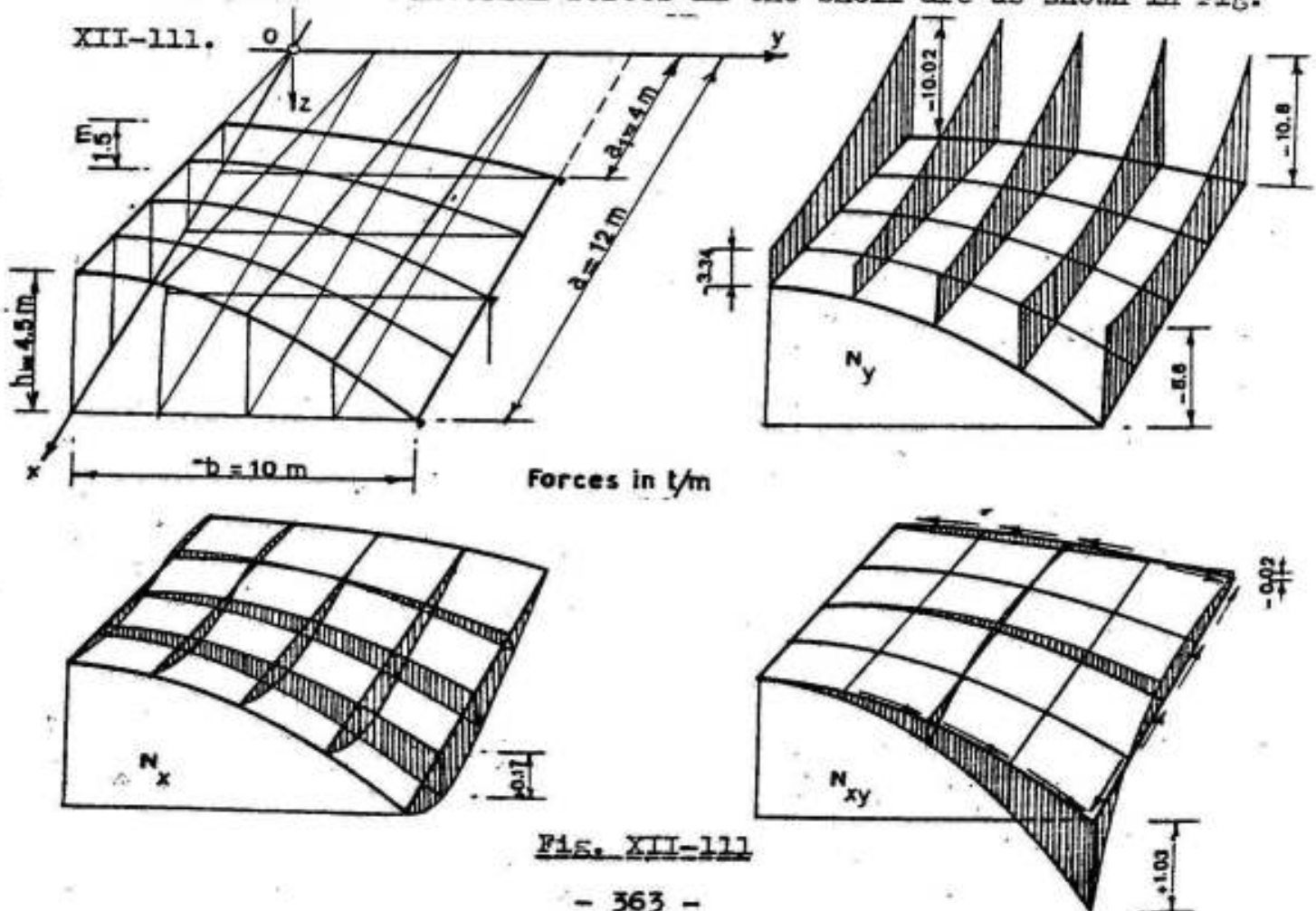


Fig. XII-111

The longitudinal beams at the straight edges of the conoid (Fig. XII-112) carry the components of the normal forces  $N_y$ . The vertical continuous beam (spans 4 ms) carries the vertical component  $V$  of the normal force  $N_y$ ,

where 
$$V = n_y \tan \beta.$$

The horizontal beams ( spans 8 ms ) carry the horizontal component  $H$  of the normal force  $N_y$  ;

where 
$$H = n_y.$$

The shearing force  $N_{xy} = n_{xy}$  acting along the straight edge

of the shell is small and may be neglected.

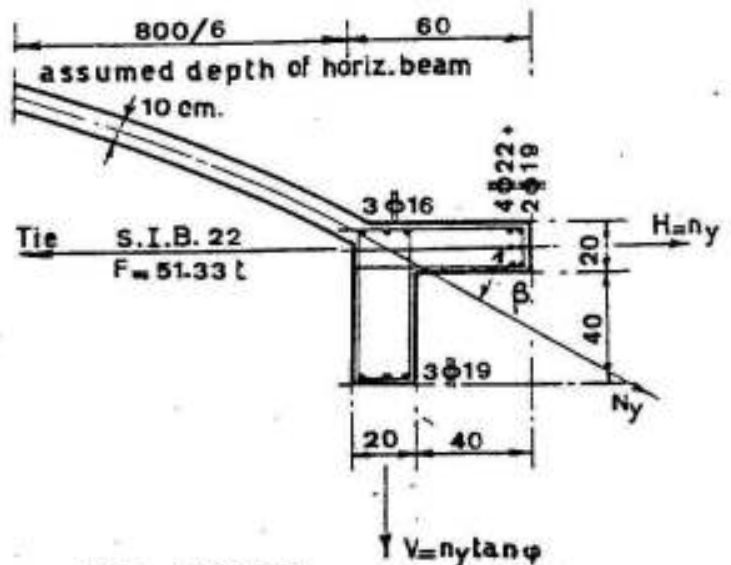


Fig. XII-112

The reactions of the horizontal beam will be resisted by the tie of the arches.

The diaphragm of the conoid is composed of two arches with a tie. The shearing forces transmitted to the flat arch are very small and hence, it does not need any design. The deep arch with the tie (Fig. XII-113) carries its own weight + weight of flat arch and tie  $G$  + the shearing forces  $N_{xy} = n_{xy}$  transmitted to it from the shell (components  $H$  and  $V$ ).

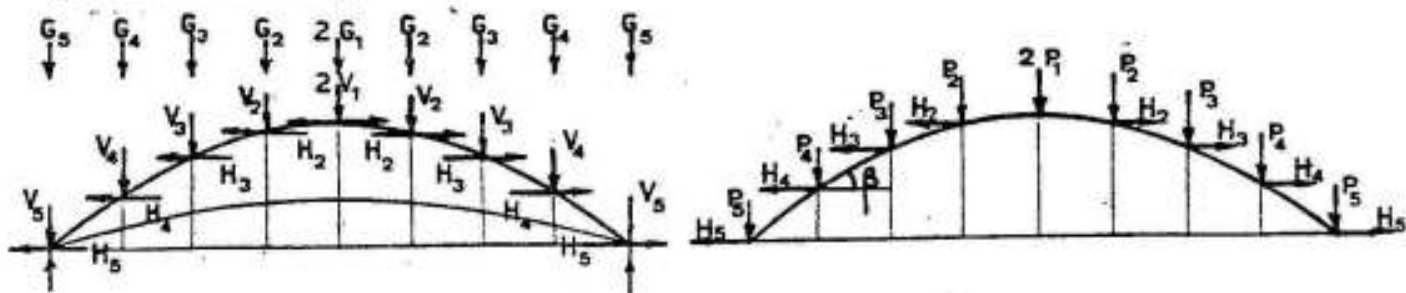
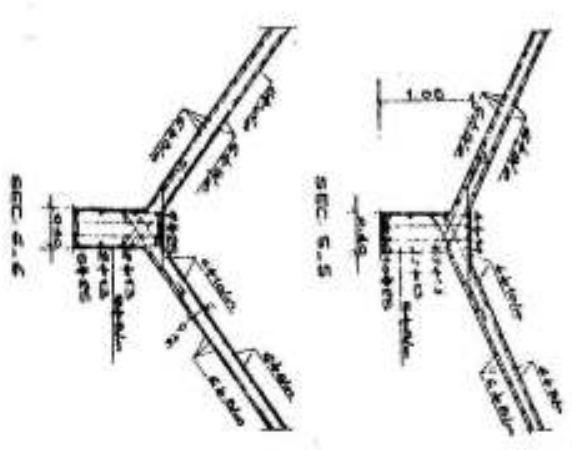
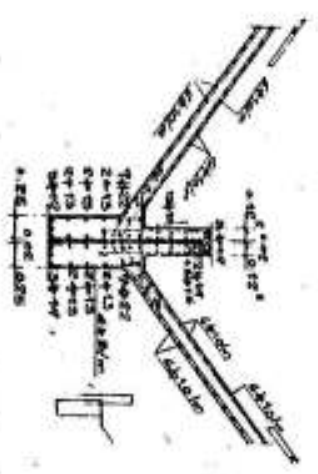
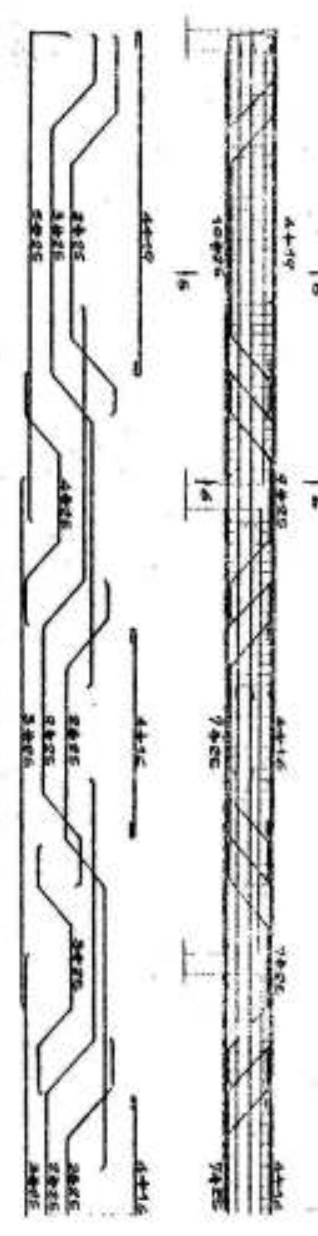
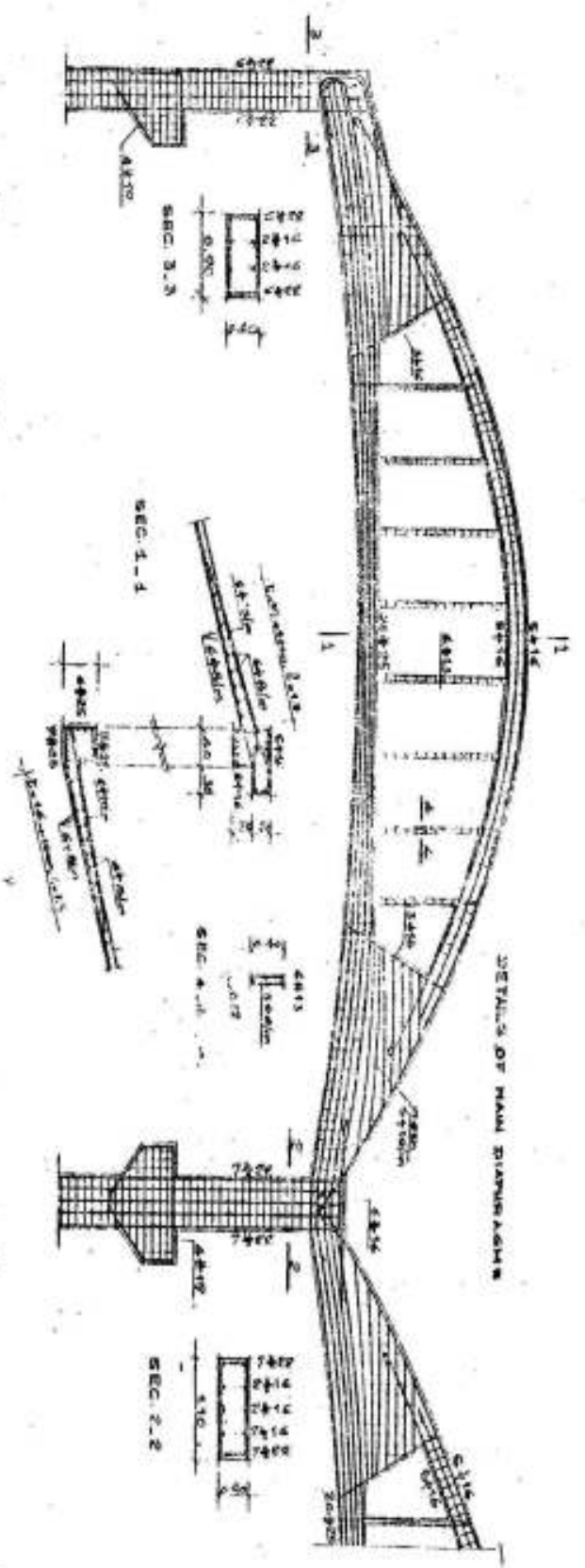


Fig. XII-113

The bending moments and normal forces in the deep arch are generally small that light arches are normally sufficient. The statically indeterminate thrust is also very small that the force in the tie







is approximately equal to the reaction of the horizontal beam only.

Fig. XII-114 shows the general layout and main dimensions of a part of the main stores of El-Nasr Pipes and Fittings Company at Helwan. The main part of these stores is  $\sim 92$  ms wide and  $\sim 108$  ms long with one longitudinal and three transverse expansion joints, so that the store is divided into six blocks each  $46$  ms ( $2 \times 23$  ms)  $\times 36$  ms ( $4 \times 9$  ms). It consists of two floors: a ground floor  $\sim 4.5$  ms high and a top floor  $\sim 9$  ms high.

The ground floor is used as store for the fittings and the small light products, while the top floor is used for storing the main product of the company, the pipes.

The live load on the first floor is prescribed to be  $6 \text{ ton/m}^2$ . For this reason, it has been chosen of the solid flat slab type  $\sim 4.5 \times 4.5$  ms. The slab thickness is chosen  $25$  cms and provided with a  $10$  cms thick drop panel  $2.25 \times 2.25$  ms. The typical intermediate columns are  $50 \times 50$  cms and provided with column heads  $140 \times 140$  cms.

The top floor of each block is covered by continuous two-bay conoids having a breadth  $b = 23$  ms and a span ( $a - a_0$ ) =  $9$  ms. The conoid is bounded by two arched diaphragms, one deep having a rise  $h = 4.5$  ms and one very flat having a rise of  $1.0$  m only. No horizontal tie is arranged, and the flat arch acts as a tie for the deep arch.

The thickness of the conoid slab is  $10$  cms increased to  $16$  cms at the outside edges. It is reinforced by one bottom mesh  $6\phi 8$  mm/m except at the free straight edge where it is increased to  $6\phi 10$  mm/m. All edges are however reinforced by another top mesh  $6\phi 10$  mm/m. The top arch is  $40 \times 45$  cms reinforced by  $10\phi 16$  mm, the lower arch is  $40 \times 45$  cms at the crown; its top surface is chosen horizontal for architectural requirements and reinforced by  $20\phi 25$  mm high grade steel. The details of their reinforcements are shown in Fig. XII-115.

This interesting structure is still under construction.

4-4 The Hyperbolic Paraboloid

Figure XII-116 shows a shell formed according to a hyperbolic paraboloid surface. Its equation with respect to the orthogonal

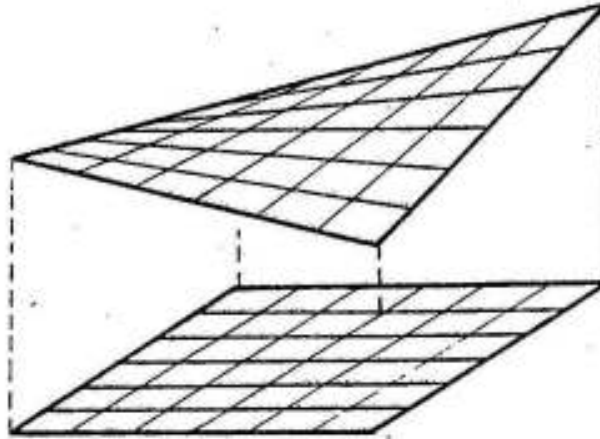


FIG. XII-116

system of axes  $x, y, z$  shown in figure XII - 117 is given by :

$$z = x y / c \quad (54)$$

in which

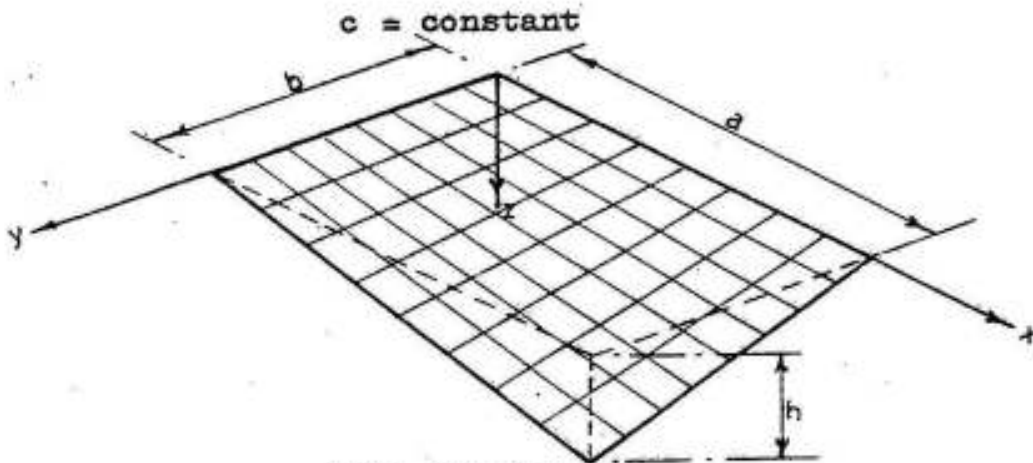


FIG. XII-117

It is easy to see that the  $z$  - co - ordinate of any point is  $h x y / a b$ . Hence, the equation of the surface can be given in the form :

$$z = \frac{h}{a b} x y \quad (55)$$

which means that

$$c = a b / h \quad (56)$$

A hyperbolic paraboloid may be regarded as a warped surface formed

by elevating or depressing one corner of a rectangle by a certain amount ( h ) while the other three corners remain in their original level. The surface shown in figures XII-116 and 117 is formed by two sets of straight line generators lying entirely on the surface . The plan projections on the x - y plane of these generators constitute two families of parallel lines which are the characteristic lines of the surface.

This surface being determined by two intersecting systems of straight lines, its formwork requires only straight wood joist generators. The smooth warped surface may be secured merely by covering these joists with flexible plywood sheathing.

The hyperbolic paraboloid shells have been successfully used in many different ways to form roofs giving a striking appearance needed in such diverse structures such as banks, churches, restaurants, exhibition and assembly halls... etc. Some of these possibilities are given by Ramaswamy<sup>¶</sup> and shown in figure XII-118 a to h .

The derivatives of equation (66) are :

$$\left. \begin{aligned} \frac{\partial z}{\partial x} &= y/c & \text{and} & & \frac{\partial z}{\partial y} &= x/c \\ \frac{\partial^2 z}{\partial x^2} &= 0 & \frac{\partial^2 z}{\partial x \partial y} &= 1/c & \frac{\partial^2 z}{\partial y^2} &= 0 \end{aligned} \right\} (57)$$

Inserting these values in the membrane condition of equilibrium expressed by equation (12), we get

$$\underline{n_x} = 0 \quad , \quad \underline{n_y} = 0 \quad \text{and} \quad \underline{n_{xy}} = - g c/2. (58)$$

In shallow shells the load p/m<sup>2</sup> surface is approximately equal to the projected load g so that, we may write also

$$\underline{n_{xy}} = - p a b / 2 h \quad (59)$$

Thus we arrive at the important conclusion :

" A shallow hyperbolic paraboloid submitted to the action of dead loads develops a state of pure shear, constant over the whole surface, and

¶ Ramaswamy : " Design and Construction of Concrete Shell Roofs."

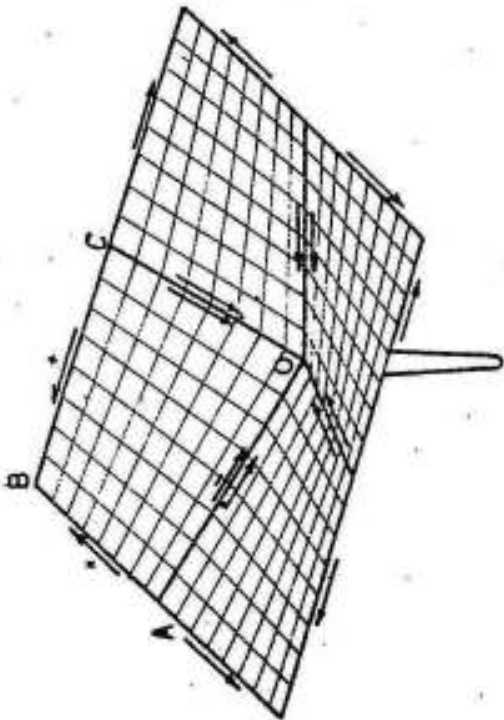


FIG. a

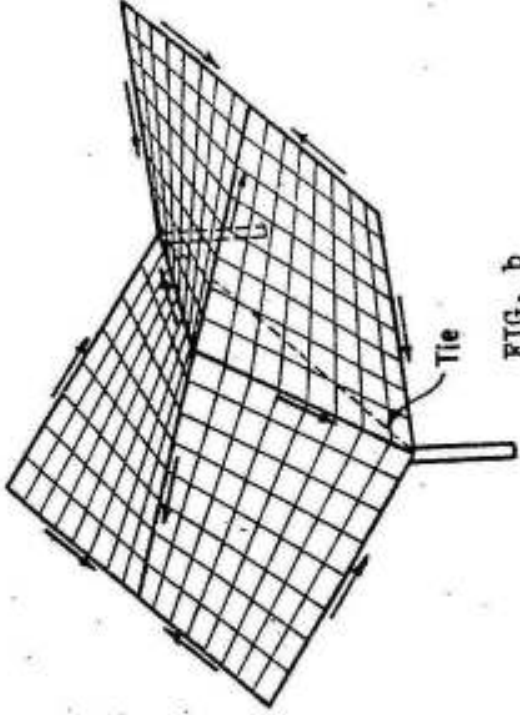


FIG. b

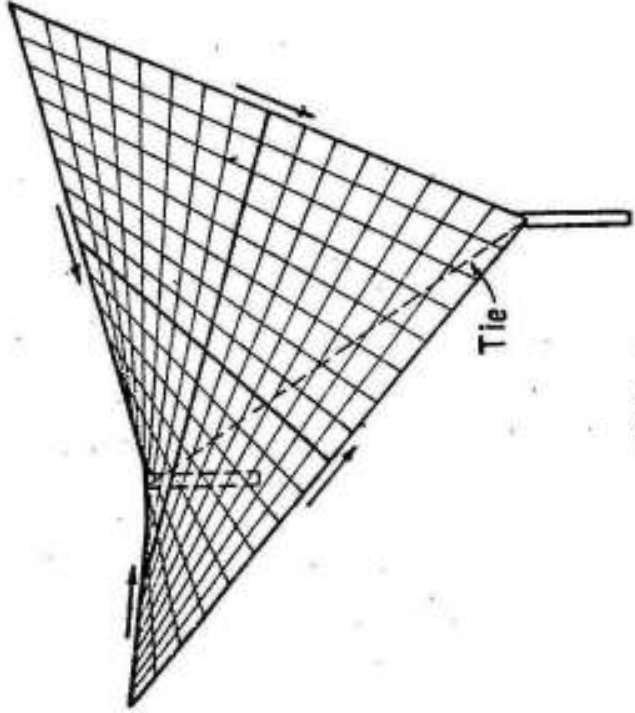


FIG. c

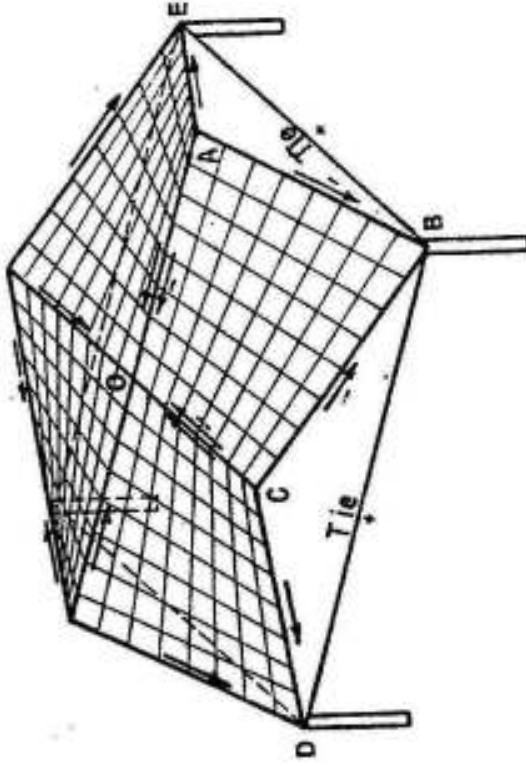


FIG. d

FIG. XII-118  
a to d

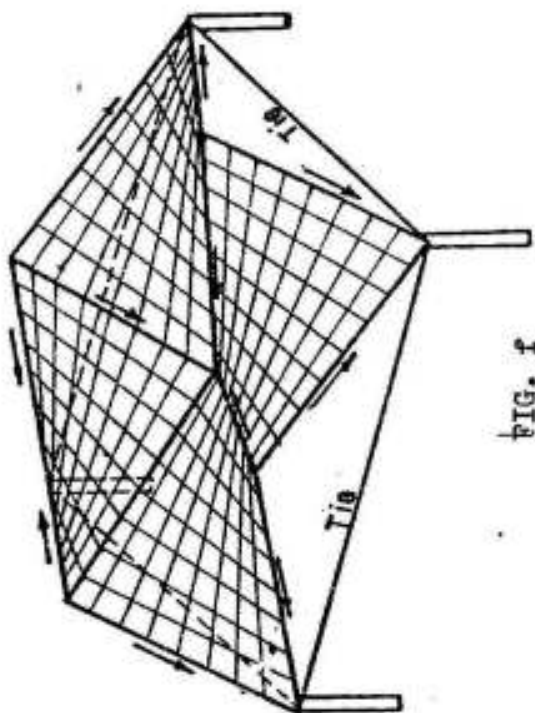


FIG. f

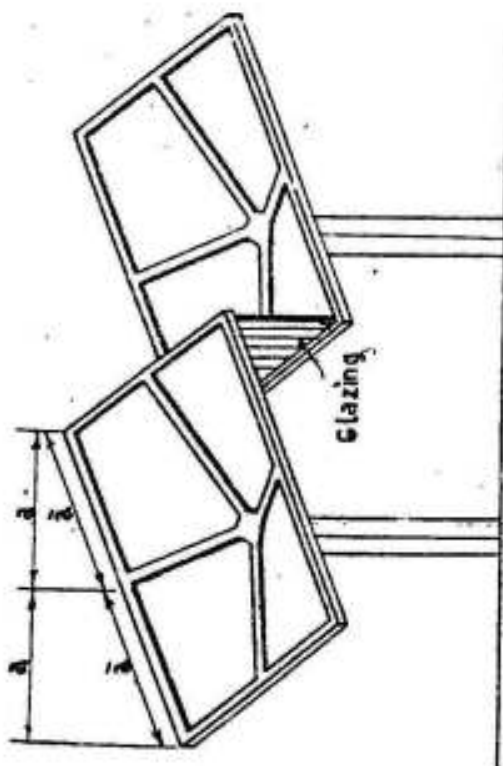


FIG. h

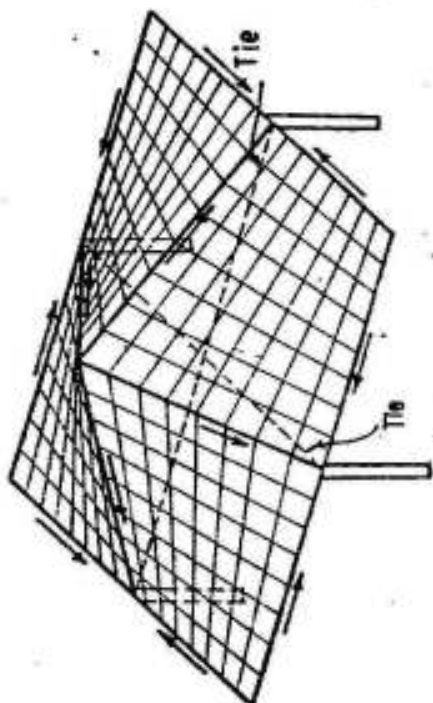


FIG. e

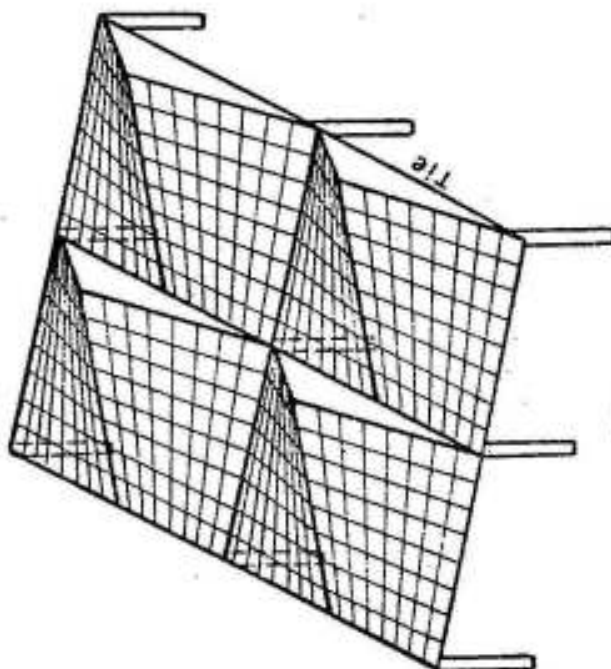


FIG. g

FIG. XII-118  
e to h

unaccompanied by normal stresses ". Due to this state of stresses , the shell will be subject to principal tensile and compressive forces along the vertical sections forming an angle of  $45^\circ$  with the directions  $x$  and  $y$ , in the arch - like fibers, there will be compression while in the inverted arches tension will arise. Fig. XII-119. The absolute value of the principal tensile and compressive forces is equal to the absolute value of the shearing force. This means  $n_1 = -n_2 = n_{xy}$  and  $N_1 = -N_2 = N_{xy}$  .

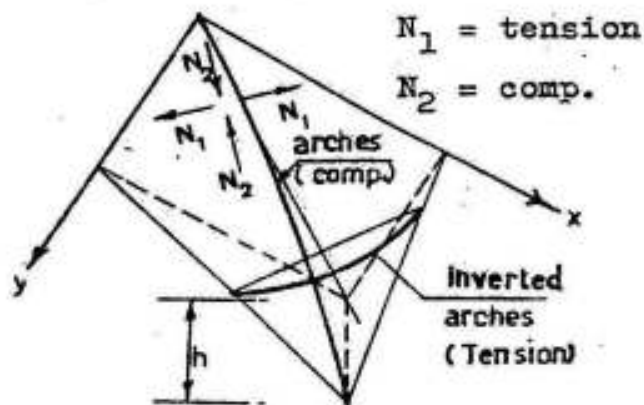


FIG. XII-119

We consider now the arrangement of the umbrella roof formed by four hyperbolic paraboloids resting on four triangular frames (fig.XII-118d) along their edges. Taking any one of the hyperbolic paraboloids, say  $O A C B$ , it abuts against the adjacent hyperbolic paraboloids along the edges  $OA$  and  $OB$ . Along the two remaining edges  $AC$  and  $BC$ , it is supported on frames which are stiff in their plane only. Each of the edges is subject to axial forces that may be found by summing up the shears transferred to them by the shell, their magnitude varies from zero at the free end and increases gradually to its maximum value  $H$  at the supported end. So that

$$H = n_{xy} \cdot l \quad (60)$$

in which  $l$  ( $= a$  or  $b$ ) is the projected length of the edge beam under consideration.

The sense of the forces  $H$  depends on the relative height of the corner points of any of the units of the hyperbolic paraboloid roof (Fig. XII-120). If one of the four corner points is situated lower (or higher) than the other three, then the resultant of the shearing forces will act from the higher corner points towards the lower ones.

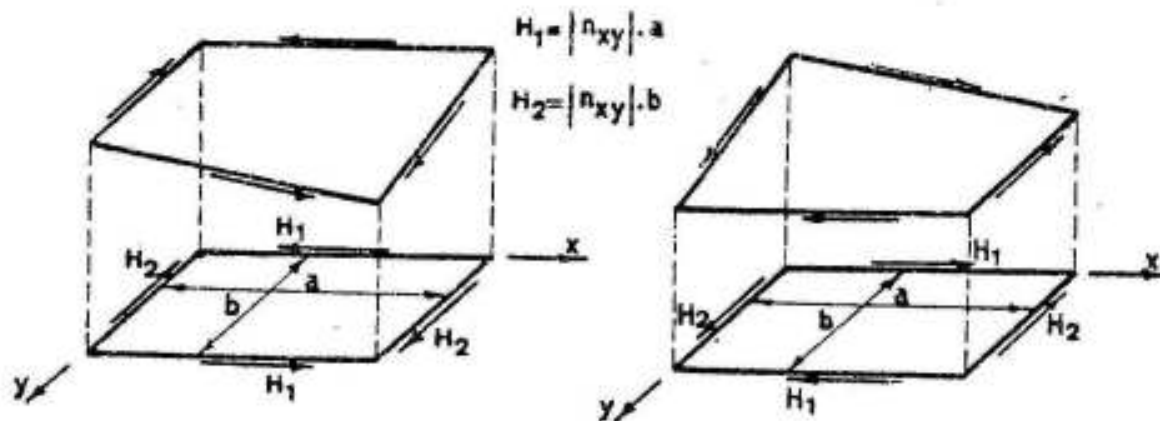


FIG. XII-120

Reverting again to the umbrella roof of figure XII-118d and according to the given principles, we find that the corner B is lower than the other three corners C, O and A and hence the forces in the edge beams A B and C B are directed downwards from A and C towards B. Since the supporting column lies at B, then :

Axial forces in A B and C B are compressive, zero at A and C and increase gradually to their maximum values at B. Axial forces in C O and A O are opposite in direction to those in A B and C B and since they are free at C and A and supported at O then the forces in the two beams are compressive, zero at C and A and increase gradually to their maximum values at O. Each of these two edge beams carries the axial forces transmitted to it from two adjacent hyperbolic paraboloids.

If we examine the forces acting in the edge beams of the inverted umbrella shown in figure XII-118a, we find that the forces in A O and C O are compressive, zero at A and C and maximum at O. Each of the two edge beams carries the forces from two adjacent elements of the roof. The forces in A B and B C are tensile, zero at B and maximum at A and C.

The forces acting in the edge beams tend to distort the frame formed by them. In order to prevent this, ties joining the supporting columns as shown in figure XII-118b to g are to be arranged.



Since  $n_x$  and  $n_y$  are equal to zero, the own weight of the ridge beams cannot be resisted by the shell. Therefore, it is necessary that the ridge beams take care of themselves and sustain their own weight as beams supported at the gables.

In order to illustrate the calculations, the statical investigation of some simple forms will be shown in the following examples.

Example 1

In this example a hyperbolic paraboloid shell supported on four corner columns, of the form shown in figure XII-121 is presented. The geometrical data of the shell are the following :

$$a = 12.0 \text{ m} \quad b = 9.0 \text{ m} \quad h = 6.4 \text{ m.}$$

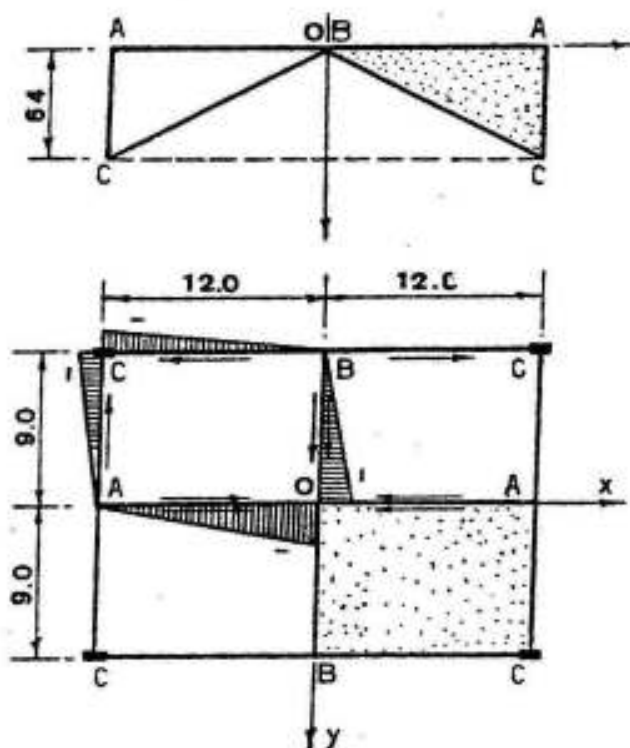
The specific value of the load acting on the shell is

$$g = 400 \text{ kg/m}^2$$

The shearing force arising in the shell due to this loading is

$$n_{xy} = - \frac{a b g}{2 h} = - \frac{12 \times 9 \times 400}{2 \times 6.4} = -3375 \text{ kg/m}$$

FIG. XII-121



The rib B C is subject to compression, zero at B and maximum at C. The horizontal projection of the compressive force at C is given by  $H_1 = n_{xy} \cdot a = 3375 \times 12 = 40500 \text{ kgs.}$

Similarly, the horizontal projection of the compressive force in A C at C is  $H_2 = n_{xy} \cdot b = 3375 \times 9 = 30375 \text{ kgs.}$

Each of the ribs A O and B O carry two elements of the roof. Hence  
 Max. horizontal projection of compression in AO at O =  $2 \times 40500 = 81000 \text{ kgs}$   
 " " " " " " BO at O =  $2 \times 30375 = 60750$

The tensile forces in the tie rods C B C and C A C are of the same

magnitude as  $H_1 = 40500$  kgs and  $H_2 = 30375$  kgs. The dimensions of the edge beams must be sufficient to resist the acting compressive forces and the bending moments due to their own weight.

Example 2

Umbrella roof supported on a single column at the center. (Fig. XII-122).

$a = 6.0$  m     $b = 4.5$  m     $h = 3.2$  m.

Assume specific value of load :

$$g = 320 \text{ kg/m}^2$$

The shearing force in the shell is given by :

$$n_{xy} = - \frac{a b g}{2 h} = - \frac{6 \times 4.5}{2 \times 3.2} \times 320 = -1350 \text{ kg/m}$$

Max. horizontal projection of tensile force in AO	at O	=	$1350 \times 6 \times 2 = 16200$	kgs
" " " " " " " "	BO	at O	=	$1350 \times 4.5 \times 2 = 12150$
" " " " comp. " "	CB	at B	=	$1350 \times 6.0 = 8100$
" " " " " " " "	CA	at A	=	$1350 \times 4.5 = 6075$

Example 3

For the inverted umbrella roof with O below A,C and B and having the same specific load and dimensions (Fig. XII-123), the forces in the edge beams will be of the same magnitude but opposite in sense. Hence

$$n_{xy} = 1350 \text{ kg/m}$$

The reduced forces in A O and

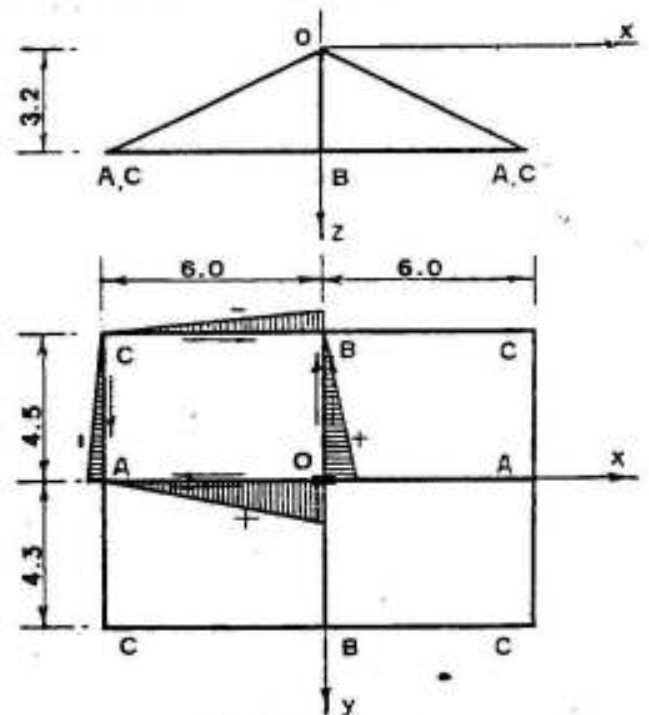


FIG. XII-122

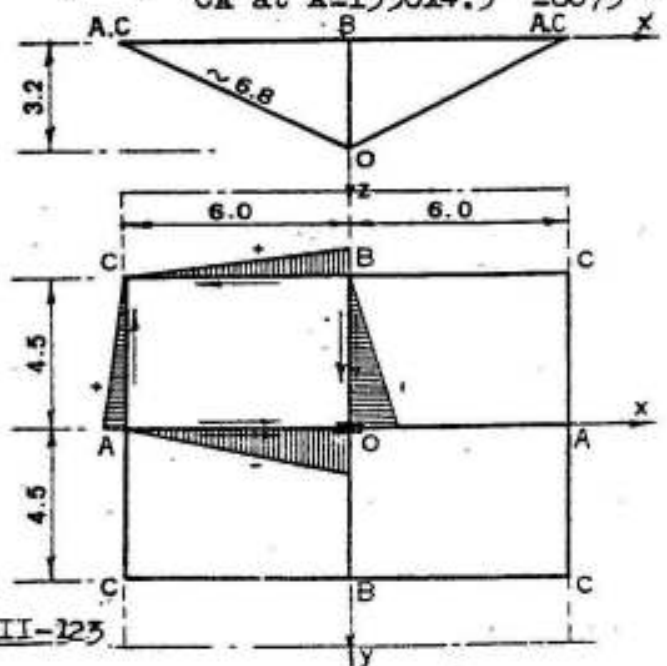


FIG. XII-123

B O are compressive, with maximum values of 16200 kg and 12150 kg at O respectively. The reduced forces in C B and C A are tensile, with maximum values of 8100 kgs at B and 6075 kgs at A .

The actual shearing force in the shell slab  $N_{xy}$  being equal to the reduced value  $n_{xy}$  , then the actual principal forces  $N_1$  and  $N_2$  are also equal to  $\pm n_{xy}$  . Hence the max. concrete compressive stress is given by

$$\sigma_c = n_{xy} / A_c \quad (63)$$

$\sigma_c$  is generally very low and the minimum executable thickness sufficient to protect the steel reinforcement from rusting ( 6 - 8 cms ) is sufficient.

The area of the steel reinforcement if it is arranged diagonally is :

$$A_s = n_{xy} / \sigma_s \quad (64)$$

For normal dimensions of hyperbolic paraboloid roofs  $A_s$  is low and it is recommended, in such cases, to arrange the reinforcements parallel to the edge beams in which case

$$A_s = n_{xy} / \sqrt{2} \sigma_s \quad (64a)$$

Assuming the thickness of the shell slab of example 1 is 6 cms, then:

$$\sigma_c = 3375/100 \times 6 = 5.63 \text{ kg/cm}^2$$

and the area of the required reinforcement if arranged parallel to the sides is

$$A_s = 3375 / \sqrt{2} \times 1400 = 1.69 \text{ cm}^2/\text{m}$$

chosen  $5 \phi 8 \text{ mm/m}$

The actual forces in the edge beams are equal to

$$H / \cos \alpha$$

in which H is the horizontal projection of the force in the beam and  $\alpha$  is the angle between the edge beam and its horizontal projection .

The ribs must further be checked for bending moments caused by their own weight, unsymmetrical live loads and the eccentricity of the

load. ( the compressive force is applied through the shell slab at the lower edge of the beam ).

In order to give an idea about the order of these moments, the internal forces acting on the intermediate rib A O of example 3 will be shown.

Actual max. compressive force in rib A O at O =  $16200 \times 6.8 = 18360$  kgs.

Assuming the cross-section of beam A O at O is as shown in figure XII-124 and decreases to zero at A,

then average own weight =  $\frac{1}{2} \times 1 \times \frac{0.4}{2} \times 2.5 = 0.25$  t/m. acting at

$\sim \frac{1}{3}$  a from O .

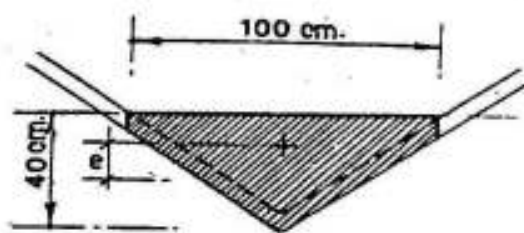


FIG. XII-124

Bending moment due to own weight =  $0.25 \times 6^2/3 = 3.0$  m t.

The bending moment due to unsymmetrical live load on C C B B is, according to Parme, given by ( T.h ) in which T is the maximum tension in the edge beam C B due to live load and h is the height of the paraboloid.

Assuming the live load =  $50 \text{ kg/m}^2$  and h being 3.2 ms, then maximum  $T = 8100 \times 50/320 = 1.256$  tons.

Bending moment due to unsymmetrical load =  $1.265 \times 3.2 = 4.05$  m t

If the shell is continuous as shown dotted, one may assume that half the bending moment is resisted by the adjacent shells and the other half is resisted by the beam A O.

The shearing forces are transmitted to the beam through the shell slab

Assuming the average depth of the beam is 25 cms; the bending moment due to eccentricity of force =  $18.36 \times \frac{0.25}{2} = 2.42$  m t. The total bending moment for one single shell :

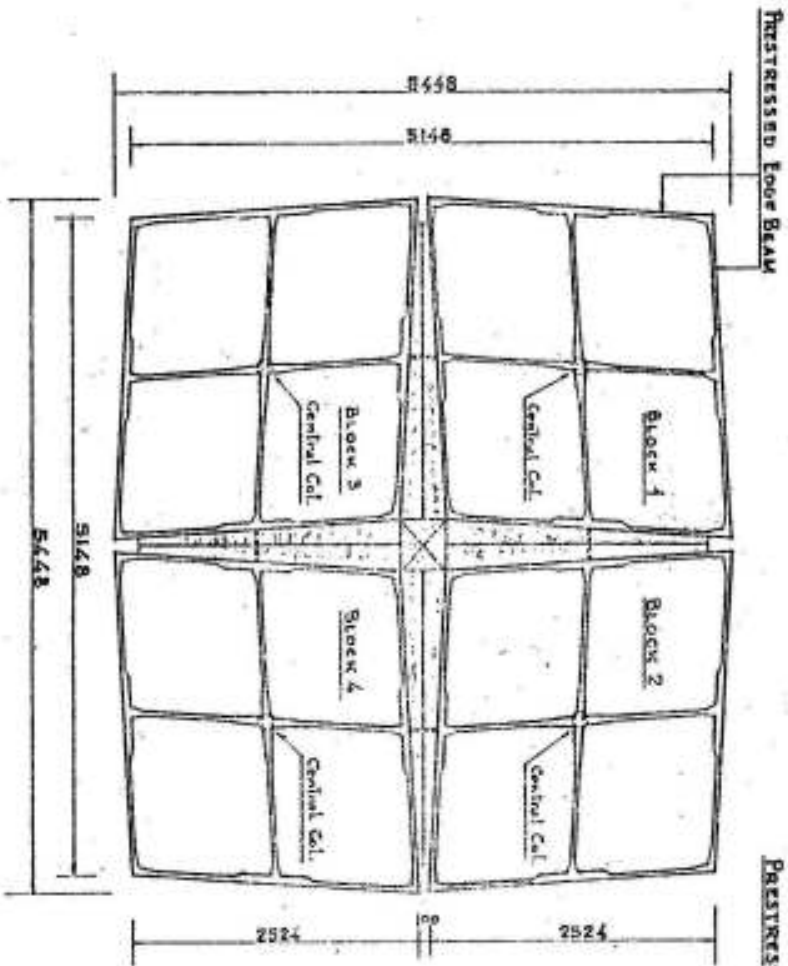
$$\text{total } M = 3.0 + 4.05 + 2.42 = 9.47 \text{ m t}$$

The edge beams C B are to be calculated for a max. tensile force at O = 8100 kgs plus a bending moment equal to this force multiplied by

the eccentricity from the center of shell slab to the center of the edge beam.

Figs. XII-125 and 126 give the general layout, main dimensions and details of reinforcements of the national exhibition halls at El Nasr city, Cairo. The roof of the halls is composed of a series of hyperbolic paraboloids of the inverted-umbrella type. Each unit of the series is 25 x 25 ms supported on a single column at the middle. In order to reduce the bending moments in the intermediate beams, its cantilevering arms were connected together by a tie. Prestressing was used both in the ties and in the tension edge beams.

PLAN



CROSS SECTION

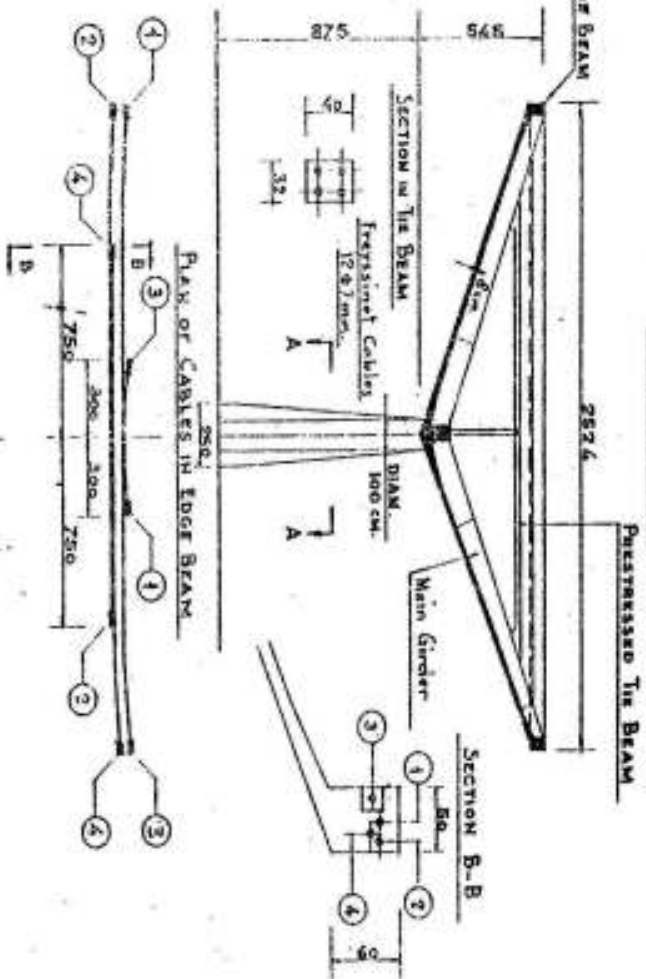


FIG. VII-125

CAIRO INTERNATIONAL FAIR  
EL-NABSE CITY  
NATIONAL EXHIBITION HILLS 1964



Printed and bound in Egypt by Zamzam Presses